Synthesis, Structure and Coordination Chemistry of New Mono- and Bipodal *N*-acyl(aroyl)thiocarbamic-*O*-alkyl esters and *N*-acyl(aroyl)-*N'*,*N'*-dialkylureas with Ni(II), Pd(II), Pt(II) and Cu(II).

Gavin Blewett

Dissertation presented for the degree of Doctor of Philosophy at the University of Stellenbosch

Promoter: Professor Klaus R. Koch
Co-promoter: Dr Martin W. Bredenkamp

December 2006

I, the undersigned, hereby declare that the work contained in this dissertation is my own original work and that I have not previously in its entirety or in part submitted it at any other university for a degree.

Signature: Date: 17/10/06

Abstract

N-acyl(aroyl)-*N'*,*N'*-dialkylthioureas have resulted in a number of potential industrial and analytical applications within the platinum group metals (PGM) industry. *N*-acyl(aroyl)thiocarbamic-*O*-alkyl esters and *N*-acyl(aroyl)-*N'*,*N'*-dialkylureas are remarkably similar in connectivity and molecular geometry to the *N*-acyl(aroyl)-*N'*,*N'*-dialkylthioureas and are therefore of interest as structural analogues.

A systematic study was made of the influence of variation of the *N*-acyl(aroyl) moiety, as well as the *O*-alkyl moiety of *N*-acyl(aroyl)thiocarbamic-*O*-alkyl esters, on the coordination geometry of this class of ligand to nickel(II), palladium(II) and platinum(II). Numerous single crystal X-ray analyses were undertaken on both the non-coordinated ligands as well as the resultant complexes in order to elucidate the effect these variations have on the molecular structures and the overall crystal lattices. Particular attention was paid to the effect that these variations have in the solid state on the carbon-nitrogen bond lengths within the non-coordinated ligands as well as the derived metal complexes. A systematic study was also undertaken of the steric and electronic influences of electron rich substituents introduced onto the aroyl moiety of the *N*-acyl(aroyl)thiocarbamic-*O*-alkyl esters on the metal-oxygen bond lengths within the derived *O*-alkyl-*N*-aroyl-thiocarbamato complexes.

A parallel investigation was carried out on a series of *N*-acyl(aroyl)-*N'*,*N'*-dialkylureas to elucidate the effect of the variation from bidentate (*S*,*O*)-donor atoms sets to the (*O*,*O'*)-donor atom sets. The molecular structures of several *N*-acyl(aroyl)-*N'*,*N'*-dialkylureas as well as several copper(II) complexes thereof were determined and used to investigate the steric and electronic influences the *N'*,*N'*-dialkyl and *N*-acyl(aroy) variations within this series have on the coordination of this class of ligand. The resultant scarcity of *trans*- or *anti*-(*O*,*O'*) chelates was also investigated from an electronic and steric perspective of the ligands and their coordination mode to the metals investigated. The first example of a *trans*- or *anti*-(*O*,*O'*) copper complex of this class of ligand was successfully isolated and fully characterised.

Furthermore, the theme has been expanded to incorporate the preparation and characterisation of bipodal equivalents to the simple monopodal *N*-acyl(aroyl)thiocarbamic-*O*-alkyl esters. These bipodal compounds potentially add a 'supramolecular' and 'self assembly' dimension to the *N*-acyl(aroyl)thiocarbamic-*O*-alkyl ester motif. The first crystal structures of this type are reported and include an interesting case of polymorphism. The coordination of this class of bipodal ligand to several platinum group metals as well as copper was investigated.

Uittreksel

N'-asiel(aroïel)-*N',N'*-Dialkieltioureums toon potensiaal in verskeie bedryfs en analitiese toepassings in die platinumgroep (PGM) metaalbedryf. *N*-Asiel(aroïel)tiokarbamaat *O*-alkiel esters is aansienlik eenders in konnektiwiteit en molekulêre struktuur aan *N*-asiel(aroïel)-*N,N*-dialkieltioureums en is om daardie rede van belang as strukturele analoë van die relatief welbestudeurde en –bekende *N*-asiel(aroïel)-*N',N'*-dialkieltioureums.

'n Sistematiese ondersoek na die invloed van die variëring van die *N*-asiel(aroïel)-groep is ondergaan, asook die *O*-alkiel groep van *N*-asiel(aroïel)tiokarbamaat *O*-alkiel esters, op die ko-ordinerings geometrie van hierdie klas van ligande aan nikkel(II), palladium(II) en platinum(II). Verskeie enkelkristal X-straal analises is onderneem op beide die ongeko-ordineerde ligande sowel as die gevolglike komplekse, om vas te stel wat die uitwerking is van die veranderlikes op molekulêre struktuur asook die kristal roosters in die geheel. Spesifieke aandag is geskenk aan die effek wat die veranderlikes het in die vaste toestand op die koolstof-stikstof bindingslengtes in die ongeko-ordineerde ligandes asook die metaalkompleks afgeleides. 'n Sistematiese studie is ook onderneem van die steries en elektroniese invloed van elektronryk substituente wat aan die aroïel groep van die *N*-asiel(aroïel)tiokarbamaat *O*-alkiel esters aangebring is op die metal-suurstof-bindingslengte in die afgeleide *O*-alkiel-*N*-aroïeltiokarbamato-komplekse.

'n Paralelle ondersoek is uitgevoer op 'n reeks *N*-asiel(aroïel)-*N',N'*-dialkielureums om die uitwerking van die variasie van die bidentate (*S,O*)-donoratoom stelle na (*O,O*)-donoratoom stele te bepaal. Die molekulêre strukture van verskeie *N*-asiel(aroïel)-*N',N'*-dialkielureums asook verskeie koper(II)-komplekse van hulle was onderneem en gebruik om die steriese en elektroniese invloed wat die *N',N'*-dialkiel- en *N*-asiel(aroïel)-veranderlikes binne die reeks het of die ko-ordinasie van hierdie klas van ligand. Die gevolglike tekort van die *trans*- of *anti*-(*O,O'*)-chelate is ook ondersoek vanuit 'n steriese en elektroniese perspektief van die ligande en hulle tipe ko-ordinasie aan die metale wat ondersoek is. Die eerste voorbeeld van 'n *trans*- of *anti*-(*O,O'*)-koperkompleks van hierdie ligande klas is met welslae geïsoleer en ten volle gekarakteriseer.

Die tema is verdermeer uitgebrei om die bereiding en karakterisering van due bipodale ekwivalente van die eenvoudige monopodale *N*-asiel(aroïel)tiokarbamaat *O*-alkiel esters in te sluit. Hierdie bipodale verbindings het die potensiaal om 'n 'supramolekulêre' en 'self-samestellende' dimensie aan die *N*-asiel(aroïel)tiokarbamaat *O*-alkiel esters motief te verleen. Die eerste kristalstrukture van hierdie tipe word hier vermeld en sluit 'n interessante geval van polimorfisme in. Die ko-ordinasie van hierdie klas van bipodale ligand aan verskeie platinumgroep metale asook koper is ondersoek.

"One of the continuing scandals in the physical sciences is that it remains in general impossible to predict the structure of even the simplest crystalline solids from a knowledge of their chemical composition."[1]

"What would the properties of materials be if we could really arrange the atoms the way we want them?"[2]

[1] J. Maddox, *Nature* 1988, ***335***, 201.
[2] R. Feynman, *Eng. Sci. 1960* 1960, 22-36.

Acknowledgements

I would sincerely like to thank the following people without whom none of this work would have materialised:

- To Jesus Christ, my Lord and God for carrying me through many difficult and trying times, guiding me and grooming me for what lies ahead.....
- My Mom, Dad, Grant and Kathy for the continued love and unfailing support, I know it wasn't easy
- Jane, for your never ending love, support, faith and encouragement no matter what
- My supervisor, Prof Klaus Koch for his energetic guidance, help, inspiration and enthusiasm
- My co-supervisor, Dr Martin Bredenkamp for the fruitful discussions and valuable comments, not to mention the much needed 'nitpicking' and proof reading of the final manuscript
- Dr Dave Robinson for his valuable and much appreciated alternative insights and ideas
- Mrs Milani for her encouragement, support and many interesting and welcome discussions
- The technical staff of the chemistry department for their assistance over the last couple of years
- The Stellenbosch University, NRF, THRIP and Anglo Platinum for financial assistance

....to all of you, my sincere thanks and gratitude.

Thank you one and all!

List of symbols and abbreviations

Å	Angstrom unit, 10^{-10} m
H(L-*S,O*) H_2(L-*S,O*)	Protonated ligand
L	deprotonated ligand
M^{n+}	Metal cation
T	temperature
ν	frequency
δ	chemical shift (NMR)
λ	wavelength
ppm	Parts per million (NMR)

Bu	butyl
Et	ethyl
Me	methyl
Ph	phenyl

DMSO-d_6	deuterated dimethylsulfoxide
$CDCl_3$	deuterated chloroform
DMF	dimethylformamide
ESMS	electron spray mass spectrometry
HPLC	high performance liquid chromatography
MS	mass spectrometry
UV-vis	ultra violet - visible

Ligand and complex notation

H(L^x-*S,O*): indicates ligand **L^x** containing one dissociable proton and potential sulphur and oxygen ligator atoms.

H(L^x-*O,O'*): indicates ligand **L^x** containing one dissociable proton and two potential oxygen ligator atoms.

H_2(L^x-*S,O*): indicates ligand **L^x** containing two dissociable protons and potential sulphur and oxygen ligator atoms.

M(L^x-*S,O*)$_2$: indicates a deprotonated ligand **L^x** coordinated to the metal M [M = Ni(II), Pd(II) and Pt(II)] in a bis bidentate fashion through sulphur and oxygen ligator atoms.

M(L^x-*O,O'*)$_2$: indicates a deprotonated ligand **L^x** coordinated to the metal M [M = Cu(II)] in a bis bidentate fashion through both oxygen ligator atoms.

The use of *cis*- or *trans*-(*S,O*) notation indicates that the coordination of the ligand to the respective metal has occurred in a bis *cis* or a bis *trans* fashion with respect to the sulphur and oxygen ligator atoms i.e. the sulphur (or oxygen) atoms are either *cis* or *trans* relative to each other.

Work Previously Presented

Parts of the work contained within this thesis have been presented either in the form of an oral presentation or a poster presentation at the following: -

- 1st European Chemistry Congress, Budapest Hungary, 27 – 31August 2006. ***Poster presentation.***
- 37th International Conference on Coordination Chemistry, International Convention Centre Cape Town 13 – 18 August 2006. ***Poster presentation.***
- 3rd Cape Organometallic Symposium, Breakwater Lodge, Cape Town Waterfront, 21 October 2005. ***Oral Presentation.***
- 2nd Cape Organometallic Symposium, Breakwater Lodge, Cape Town Waterfront, Thursday 28 October 2004. ***Poster presentation.***
- 37th National Convention of the South African Chemical Institute: "Chemistry for a better life" 4 to 9 July 2004 at the CSIR International Convention Centre, Pretoria. ***Oral Presentation.***
- SACI INORGANIC '03 NATIONAL CONFERENCE, Roode Vallei Country Lodge Pretoria, June 8-11, 2003. ***Oral Presentation.***
- 1st Cape Organometallic Symposium, Morgenhof Wine Estate Stellenbosch 2003. ***Poster Presentation.***
- 36th Convention of the South African Chemical Institute, University of Port Elizabeth, 1-5 July 2002. ***Poster Presentation - Best poster prize awarded.***
- 1st Binational RSC/SACI International Conference Organic Chemistry. University of Cape Town, 7 – 11 January 2001. ***Poster Presentation.***

Parts of the work contained within this thesis have also already appeared in the following publications:

- G. Blewett, M. W. Bredenkamp, K. R. Koch, *Acta Crystallogr., Sect. C: Cryst. Struct. Commun.* 2005, ***C61***, o469-o472.
- G. Blewett, C. Esterhuysen, M. W. Bredenkamp, K. R. Koch, *Acta Crystallogr., Sect. C: Cryst. Struct. Commun.* 2004, ***C60***, o862-o864.
- G. Blewett, C. Esterhuysen, M. W. Bredenkamp, K. R. Koch, *Acta Crystallogr., Sect. E: Struct. Rep. Online* 2006, ***E62***, m420-m422.
- G. Blewett, C. Esterhuysen, M. W. Bredenkamp, K. R. Koch, *Acta Crystallogr., Sect. E: Struct. Rep. Online* 2005, ***E61***, o4042-4044.

Three full papers are currently 'under construction' for publication in the near future in such journals as the 'New Journal of Chemistry' and the 'Journal of Molecular Structure'. One paper will cover the coordination of the *N*-acyl(aroyl)thiocarbamic-*O*-alkyl esters specifically to Pt(II) while a second paper will cover the coordination of this class of ligands to Ni(II) and Pd(II). A third paper will detail the work contained in this thesis concerning the *N*-acyl(aroyl)-*N'*,*N'*-dialkylureas and the coordination of these ligands with Cu(II).

Index: Chapter I

Index: Chapter II

Index: Chapter III

1. Introduction.

Index: Chapter IV

Index: Chapter V

Index: Chapter VI

Index: Chapter I

1. Introduction and scope of research

1.1 Thiourea moiety commonality within relevant sulphur containing ligand systems

Both the monopodal and bipodal *N*-aroylthiocarbamic-*O*-esters, as well as the *N*-aroyl(acyl)-*N'*,*N'*-dialkylureas, are remarkably similar in connectivity and molecular geometry to the analogous *N*-aroyl(acyl)-*N'*,*N'*-dialkylthioureas (Scheme 1). In turn, the *N*-aroyl(acyl)-*N'*,*N'*-dialkylthioureas are similar in connectivity and molecular geometry to dithio- and monothio-β-diketones and dithiobiurets, all of which contain the basic thiourea moiety as building blocks. The similarities in these ligand systems warrant a short discussion of each ligand system as well as the general coordination chemistry of each.

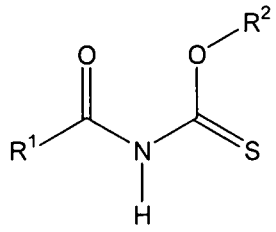

N-aroylthiocarbamic-*O*-esters

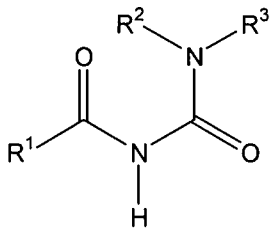

N-aroyl(acyl)-*N'*,*N'*-dialkylurea

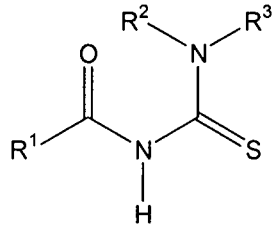

N-aroyl(acyl)-*N'*,*N'*-dialkylthiourea

Scheme 1 *N*-aroylthiocarbamic-*O*-ester, *N*-aroyl(acyl)-*N'*,*N'*-dialkylurea, N-aroy(acyl)-*N'*,*N'*-dialkylthiourea.

1.1.1 Thiourea, $[(NH_2)_2C(=S)]$, (L^i)

A commonality, amongst others, in all the ligand systems described above, apart from the *N*-aroyl(acyl)-*N'*,*N'*-dialkylurea class of ligand, is that they contain the basic thiourea moiety, $[(NH_2)_2C(=S)]$. Thiourea moieties are important chemical building blocks and have been identified as having numerous chemical and pharmaceutical applications[1-3]. The many potential uses of the thiourea moiety have led to numerous reports in the literature describing synthetic approaches used in the preparation of thioureas and substituted thioureas. These various methods will not be discussed here and reports describing these approaches, such as one by Katritzky *et al.*, should be consulted as required[4].

In general, thiourea, $[(H_2N)_2C(=S)$ $(\mathbf{L^i})]$, acts as a unidentate or mono-dentate ligand forming strong complexes with *(b)*-class metal ions‡, e.g. Cu^I, Ag^I, Au^I and Hg^{II}. However, Cu^{II} is reduced to Cu^I, Au^{III} to Au^I, Pt^{IV} to Pt^{II} and Te^{IV} to Te^{II} when complexed with thiourea thereby forming complexes in the lower oxidation state[5, 6]. The coordination of the thiourea to the metal ions varies from square planar (e.g. $[\mathbf{Pd(L^i)_2Cl_2}]$) to tetrahedral (e.g. $[\mathbf{Cd(L^i)_2Cl_2}]$) to octahedral (e.g. $[\mathbf{Te(L^i)_4Cl_2}]$)[5]. Thiourea, like many other sulphur donor ligands, has a high *trans* effect. This *trans* effect of the thiourea forms the basis of the Kurnakov test for distinguishing between *cis* and *trans* isomers of dihalogendiamineplatinum(II). The Kurnakov test relies on the *trans* effect of the following ligands in the decreasing order: $\mathbf{L^i} > Cl > NH_3$ [5, 7].

1.1.2 Dithiobiuret ($\mathbf{HL^{ii}}$)

Another potentially chelating form of thiourea, is dithiobiuret ($\mathbf{HL^{ii}}$), a molecule which contains two thiourea moieties. Dithiobiuret, by loss of a proton from its iminothiol tautomer (see Scheme 2), forms neutral complexes ($[\mathbf{M(L^{ii})_2}]$ with M = Ni^{II}, Pd^{II}, Pt^{II}, Cu^{II}, Cd^{II})[5]. In complexes with metals such as palladium(II), the dithiobiuret is arranged such that the four sulphur atoms are in a square planar geometry around the palladium ion[5].

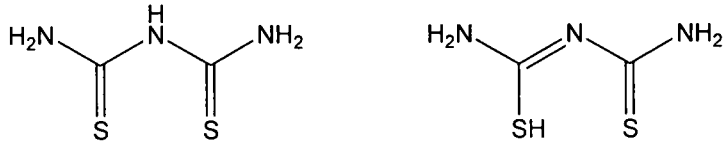

Scheme 2 Dithiobiuret and its iminothiol tautomer.

1.1.3 Monothio-β-diketones ($\mathbf{HL^{iii}}$).

Although the first metal complexes of acetylacetone were reported as early as 1887 by Coombes[5], it was only in 1964 that three groups independently initiated work on the synthesis and properties of monothio-*β*-diketones and their metal complexes[8-11]. To date, the work done on the preparation of monothio-*β*-diketones has yielded predominately two methods of synthesis, both affording yields in excess of 50%. The first involves the passage of H_2S through a dilute solution of the *β*-diketone in ethanol followed by the passage of HCl at -70° C through the solution. The second method involves the Claisen-type condensation of ketones with thionic esters, RC(S)OMe, or dithionic esters, RC(S)SMe, in diethyl ether in the presence of sodium amide[5]. Monothio-*β*-diketones have two possible isomeric forms (see I and II in Scheme 3). IR, UV-visible and NMR spectra, as well as X-ray diffraction studies, have shown that monothio-*β*-diketones exist predominantly in the thienol form (I in Scheme 3)[5]. Furthermore, studies of the dissociation constants, pK_D, of a number of monothio-*β*-diketones in dioxane-water, indicate that monothio-*β*-diketones are stronger acids than conventional *β*-diketones[5].

---

‡ Class (b) metals :Elements such as Au, Hg, Pb, Pd, Pt, Rh which form soft acids. They form stable complexes with soft bases and form stable compounds by π bonding.
Class (a) metals : Elements such as Al, Ca, Fe, lanthanides, Na, Ti which form hard acids. They form stable complexes with hard bases (including F^- and ligands containing O and N).

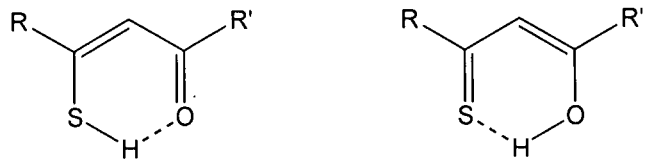

(I) (II)

Scheme 3 Isomeric forms of monothio-ß-diketones.

Several reviews can be found in the literature concerning monothio-*β*-diketones and their metal complexes[5, 12-14]. Monothio-*β*-diketones (**HL^{iii}**) generally form stable complexes [**M^{n+}(L^{iii})$_n$**] with (b)-class metal ions (M = Rh^{III}, Ni^{II}, Pd^{II}, Pt^{II}, Hg^{II} and Pd^{II}). Relatively few complexes of monothio-*β*-diketone complexes with (a) class metals have been reported; nevertheless complexes of Cr^{III}, Mn^{III}, Ga^{III} and In^{III} are known[5, 13]. Although α-alkyl-substituted monothio-*β*-diketones form complexes with Ni^{II} and Co^{III}, attempts to prepare complexes of Pd^{II}, Pt^{II}, Cu^{II}, Zn^{II} and Hg^{II} generally resulted in the oxidation of the ligand to the disulfide[5, 14-16].

Stability constant determinations have been made on a range of monothio-*β*-diketonato complexes in dioxane-water solutions. The results indicate that (b) class metal ions generally form more stable complexes with monothio-*β*-diketones than with *β*-diketones. The stability sequence in monothio-β-diketonato complexes has been reported as being Cu^{II} > Ni^{II} > Zn^{II} > Cd^{II} > Pd^{II} [5]. Generally, with few exceptions, Ni^{II} complexes of *β*-diketones are green, octahedral and paramagnetic, whereas Ni^{II} complexes of monothio-*β*-diketones are reported as being brown, square planar and diamagnetic. The determination of the dipole moments of over 200 monothio-*β*-diketone complexes showed that the Ni^{II}, Pd^{II}, Pt^{II} and Cu^{II} complexes are *cis* square-planar[5, 17-19]. Some Cu^{II} complexes of monothio-*β*-diketones were reported as having configurations between square-planar and tetrahedral[17-19]. Monothio-*β*-diketones are reported as having a *facial (cis)* octahedral coordination with Cr^{III}, Fe^{III}, Ru^{III}, Co^{III} and Ru^{III} [5].

The preference of monothio-*β*-diketones for the *cis* and *facial* octahedral structures, or configurations, has been explained in the literature as arising from strong d_π-d_π bonding between the metal and sulphur atoms[5]. Transition metal ions can form two π-bonds at 90° and consequently, in possible isomeric *cis* and *trans* structures, wherein only the two sulphur atoms of the four donor atoms can form d_π-d_π bonds, the *cis* isomer is more stable.

1.1.4 Dithio-β-diketone (HL^{iv})

Similar to the monothio-ß-diketones, the dithio-*β*-diketone (**HL^{iv}**) in general forms complexes of the type [**M(L^{iv})$_2$**] (e.g. M = Co^{II}, Ni^{II}, Pd^{II}, Pt^{II}, Zn^{II} Cd^{II} and Hg^{II}. Complexes of the type **M(L^{iv})$_3$** with M = Cr^{III}, Fe^{III}, Ru^{III}, Os^{III}, Co^{III}, Rh^{III} and Ir^{III} have been reported[5, 20, 21]. The deeply coloured complexes

are reported as being soluble in most organic solvents and air stable[20]. The Ni complexes of this sort are also reported as being diamagnetic and deep brown in colour[20, 21].

1.1.5 *N*-acyl(aroyl)-*N'*,*N'*-dialkylthiourea (HL^v)

A related member to the above family of compounds is the *N*-acyl(aroyl)-*N'*,*N'*-dialkylthiourea, $\mathbf{HL^v}$ (Scheme 1). Resemblance of the coordination chemistry of *N*-acyl(aroyl)-*N'*,*N'*-dialkylthioureas to simple, unsubstituted thioureas $[(NH_2)_2C{=}S]$ $\mathbf{HL^i}$ is limited. The coordination of *N*-acyl(aroyl)-*N'*,*N'*-dialkylthioureas is obviously far more varied. The metal complexes of *N*-acyl(aroyl)-*N'*,*N'*-dialkylthioureas, as well as the *N*-acyl(aroyl)-*N'*,*N'*-dialkylthioureas themselves, have some favourable physiochemical properties which have resulted in numerous potential technical and analytical applications with particular reference to the platinum group metals (PGM) industry[22-26]. Further to the PGM industry, this class of complex and ligand has found application in several medicinal areas due to their potential anticancer, antifungal and antimalarial properties[27-30]. These potential applications in a number of fields have stimulated the growth of investigation into this class of complex and ligand resulting in the properties and coordination chemistry of these ligands to be comparatively well understood and well documented.

Interest in this class of ligands with regard to their coordination chemistry and potential applications dates back to the pioneering work of Hoyer and Beyer[31] of the 1970's who reviewed the coordination chemistry of *N*-acyl-thioureas with particular reference to second row transition metals Ni^{II}, Cu^{I}, Cu^{II}, Co^{III}, Zn^{II}, Pd^{II}, Ag^{I} and Cd^{II} as well as Pb^{II} and Hg^{II} [32]. In 1985, König and co-workers reported that *N*-benzoyl-*N'*,*N'*-dialkylthioureas showed a pronounced selectivity towards the platinum group metals which resulted in effective solvent extraction of these metals[22]. Vest and co-workers reported in 1989 that *N*-benzoyl-*N'*,*N'*-dialkylthioureas were found to be more efficient extractants than the *N*-benzoyl-*N'*-alkylthioureas (Scheme 4)[23]. Several studies can be found in the literature which highlight the separation and trace determination of PGM's by high performance thin layer chromatography (HPTLC) after the complexation of the PGM metal ions with *N*-aroyl(acyl)-*N'*,*N'*-dialkylthioureas[33-35]. Koch *et al.* recently reported the use of reversed-phase high performance liquid chromatography (RP-HPLC) in the trace determination of Pd(II), Pt(II) and Rh(II) after complexing these metals with suitable *N*-acyl-*N'*,*N'*-dialkylthioureas[36]. However, to date, a review of the literature yields limited detailed structure and solution coordination chemistry of particularly Ni^{II}, Pd^{II} and Pt^{II} with this class of ligand[26].

In general, *N*-acyl(aroyl)-*N'*,*N'*-dialkylthioureas are prepared in a relatively simple two step one-pot synthesis from readily available inexpensive starting materials in high yields[31, 37]. The *N*-aroyl-*N'*,*N'*-dialkylthiourea ligands ($\mathbf{HL^v}$) are stable hydrophobic substances with one dissociable proton on the acidic amido –C(O)NHC(S)- moiety, while the corresponding *N*-acyl(aroyl)-*N'*-alkylthiourea ($\mathbf{H_2L^v}$) contains two dissociable protons (Scheme 4). The structure of the $\mathbf{HL^v}$ and $\mathbf{H_2L^v}$ ligands, as determined by X-ray diffraction, shows the significant influence of intramolecular hydrogen bonding within the non-coordinated ligand which in turn results in substantial differences between the preferred

conformations of $\mathbf{H_2L^v}$ and $\mathbf{HL^v}$. Consequently, this difference in the preferred conformation of $\mathbf{H_2L^v}$ and $\mathbf{HL^v}$, results in significant differences in the coordination of the two ligands to various transition metals. An intramolecular hydrogen bond between the thiourea –C(S)NHR moiety and the oxygen atom of the amidic group 'locks' the –C(O)NHC(S)NHR unit of $\mathbf{H_2L^v}$ into a planar six-membered structure. By comparison, the $\mathbf{HL^v}$ molecule assumes a 'twisted' conformation in the solid state, with the sulphur and oxygen atoms pointing approximately in opposite directions. The preferred conformations of $\mathbf{H_2L^v}$ and $\mathbf{HL^v}$ are illustrated in Scheme 4[38, 39].

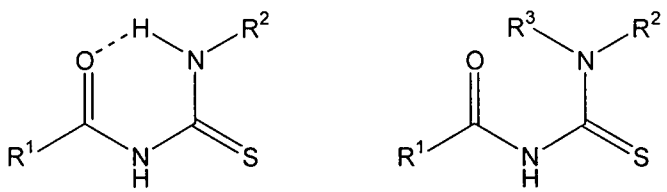

$\mathbf{H_2L^v}$ $\mathbf{HL^v}$

Scheme 4 The general structure of $\mathbf{H_2L^v}$ and $\mathbf{HL^v}$ as determined by X-ray diffraction.

A further significant feature of these ligands, as confirmed by X-ray crystallography, is that the amidic (O)C-NH and the thioamide NH-C(S), (S)C-N(R/H)$_2$ carbon nitrogen bonds are shorter than the average single carbon-nitrogen bond length of 1.472(5)Å[40]. Furthermore, a trend has been identified in the average bond C-N distances, the lengths increasing in the order (S)C-N(R/H)$_2$, 1.327(±0.006) < (O)C-NH 1.374(±0.011) NH-C(S) 1.409(±0.016)Å[26]. The partial double bond character of the (S)C-N(R/H) bond is clearly reflected in the NMR spectra of these molecules by the restricted rotation around this bond in solution on the NMR time scale. Separate ^{1}H and ^{13}C resonances are observed for the two methylene groups of the (S)CN(CH$_2$)$_2$- moiety in the ^{1}H and ^{13}C-NMR spectra at room temperature[26]. Consequently, *E/Z* configurational isomerism is observed in solution for unsymmetrically *N',N'*-dialkyl substituted $\mathbf{HL^v}$ molecules. This *E/Z* isomerism of the unsymmetrically *N',N'*-dialkyl substituted $\mathbf{HL^v}$ molecules is carried through into the complexes of these molecules[26, 38]. This *E/Z* isomerism of the complex has been confirmed in the literature for ***cis*-[Pt(L^v)$_2$]**, $\mathbf{HL^v}$ = *N*-benzoyl-*N'*-methyl-*N'*-(*n*-butyl)thiourea[38]. In the case of $\mathbf{H_2L^v}$ ligands in solution, this *E/Z* isomerism is not observed, probably as a result of the aforementioned intramolecular hydrogen bond which 'locks' the $\mathbf{H_2L^v}$ molecules into planar six-membered rings. Nonetheless, the carbon-nitrogen bond lengths of interest, as discussed for the $\mathbf{HL^v}$ class of ligands, are virtually indistinguishable from those of $\mathbf{H_2L^v}$[26].

From a review of the available literature of the coordination of *N*-acyl(aroyl)-*N',N'*-dialkylthioureas, $\mathbf{HL^v}$ with d^8 transition metals, it is evident that the predominant mode of coordination of $\mathbf{HL^v}$ ligands is the formation of bidentate chelates of type ***cis*-[M(L^v-*S,O*)$_2$]**[26, 32]. To date, only one *trans* structure of the type **[M(L^v-*S,O*)$_2$]** has been isolated and characterized crystallographically with $\mathbf{HL^v}$ = *N*-naphthoyl-*N',N'*-di(n-butyl)thiourea[41]. The absence of any other example of a ***trans*-[M(L^v-*S,O*)$_2$]** type structure is striking despite numerous attempts to prepare such a complex. Until recently, it was suggested in a review of the coordination chemistry of *N*-acyl(aroyl)-*N'*-alkyl- and *N*-acyl(aroyl)-

N',N'-dialkylthioureas that the *trans* Pt^{II} complexes ***trans*-[Pt(L^v-*S*,*O*)$_2$]**) can only be isolated for bulky electron rich *N*-aroylthiourea ligands[26]. It was speculated in this report that electron releasing aroyl groups enhance the relative 'softness' of the amidic oxygen donor atom in **HL^v** type ligands thus stabilizing a *trans* complex[26]. However, Koch *et al.* recently reported that the *cis/trans* isomerism of ***cis*-[M(L^v-*S*,*O*)$_2$]** type complexes (with M = Pd^{II}, Pt^{II}; **HL^v** = *N*-3,4,5-trimethoxybenzoyl-*N',N'*-diethyl-thiourea) is photo-induced and reversible. The resultant ***trans*-[M(L^v-*S*,*O*)$_2$]** complex cleanly reverts back to the initial *cis* complex, at a rate dependent upon the solution temperature, indicating that the reverse isomerism is a thermally controlled process[42].

Finally, the coordination chemistry of the **H_2L^v** ligands derived from the mono-alkyl amines differs significantly to the coordination chemistry of **HL^v**, due to the intramolecular hydrogen bond illustrated in Scheme 4 which results in the coordination chemistry of **H_2L^v** resembling that of simple thioureas, which generally coordinate through the sulphur atom to the metal ions in question in a mono-dentate fashion[26, 43]. As a result, complexes of the type ***cis/trans*-[M(H_2L^v-*S*)$_2X_2$]** are formed with the d^8 transition metals Pt^{II} and Pd^{II}. The ratio of the *cis* versus the *trans* isomer of the complex has been reported to be dependant on both M (M = Pd^{II}, Pt^{II}) and X (X = Cl^-, Br^-)[44-46].

1.2.1 Monopodal *N*- acyl(aroyl)thiocarbamic-*O*-esters.

N-acyl(aroyl)thiocarbamic-*O*-esters (Scheme 1) are remarkably similar in connectivity and molecular geometry to the analogous *N*-aroyl(acyl)-*N',N'*-dialkylthioureas. The similarities between the *N*-aroyl(acyl)-*N',N'*-dialkylthioureas and *N*-acyl(aroyl)thiocarbamic-*O*-esters stimulated our investigation into the fundamental coordination chemistry of *N*-acyl(aroyl)thiocarbamic-*O*-esters to Ni^{II}, Pd^{II} and Pt^{II}. However, like the *N*-acyl(aroyl)-*N',N'*-dialkylthioureas, the synthesis and characterization of the *N*-acyl(aroyl)thiocarbamic-*O*-esters and their complexes with transition metals turned out to be less straight forward.

To date, the study of the coordination of the *N*-acyl(aroyl)thiocarbamic-*O*-esters to transition metal elements has not been extensively explored and even less so with reference to the platinum group metals. Available literature in this area can be described as sporadic at best. Previously it was reported that *N*-benzoylthiocarbamic-*O*-esters have potential as `collectors' in ore froth-flotation[47-49] and more recently, *N*-benzoylthiocarbamic-*O*-esters have also been proposed as intermediates for regio- and chemoselective deoxygenation of primary and secondary alcohols[50]. A survey of the literature yields very little detailed structural and solution coordination chemistry of *N*-acyl(aroyl)thiocarbamic-*O*-esters to transition metals[51]. The only crystal structures listed on the Cambridge Structural Database (CSD)[52] similar to the molecular structures of the series of *N*-acyl(aroyl)thiocarbamic-*O*-esters reported in this thesis, are those of *O*-isopropyl *N*-(2-furoyl)thiocarbamate, and *O*-benzyl *N*-(2-furoyl)thiocarbamate[51, 53].

The preparation and detailed characterization of a series of *N*-acyl(aroyl)thiocarbamic-*O*-esters ligands and their resultant nickel(II), palladium(II) and platinum(II) complexes with the general formula

$[M(RC(O)NC(S)OR')_2]$ was investigated and is described in chapter 2 and chapter 3 of this thesis. Within the series of *N*-acyl(aroyl)thiocarbamic-*O*-esters and *N*-acyl(aroyl)thiocarbamic-*O*-ester complexes prepared, both the metal center of the complexes, as well as the R-substituents of the *N*-acyl(aroyl)thiocarbamic-*O*-ester ligands, were systematically varied in an attempt to investigate the influence these R-substituents and metal centers have on the coordination geometry of the *N*-acyl(aroyl)thiocarbamic-*O*-esters. The molecular structure of several of these *N*-acyl(aroyl)thiocarbamic-*O*-ester ligands and their resultant Ni^{II}, Pd^{II} and Pt^{II} complexes have been determined by X-ray crystal structure analysis.

1.2.2 Bipodal *N*-phenylenethiocarbamic-*O*-esters

Symmetrical bipodal analogues of the *N',N'*-dialkylthioureas, 3,3,3',3'-tetraalkyl-1,1'-phenylenedicarbonylbis(thioureas), **(H_2L)**, (Scheme 5) have been shown to contain a 'pre-programming' of self assembly to form 2:2 and 3:3 metallomacrocyclic complexes in high yield with the general structure ***cis*-[M(L-*S*,*O*)]$_n$** [n = 2 and 3, and M = Pt^{II}; n = 2, and M = Pd^{II} and Ni^{II}][54-56]. The Ni^{II} metallomacrocyclic complexes also show some interesting host-guest chemistry[56]. The relative points of substitution (*para* vs *meta*) of the phenylene spacer moiety in the ligand (Scheme 5) is critical in determining the geometry and metal:ligand (M:L) ratio of the resultant complex. Ligands derived from the *para*-substituted terephthalic acid give exclusively 3:3 (M:L) metallamacrocycles, while those derived from the meta-substituted isophthalic acid give rise to only 2:2 (M:L) complexes[54, 55]. 2:2 and 3:3 M:L metallamacrocycles of this sort have generally been reported for the group ten metals Ni^{II}, Pd^{II} and Pt^{II} [54-57].

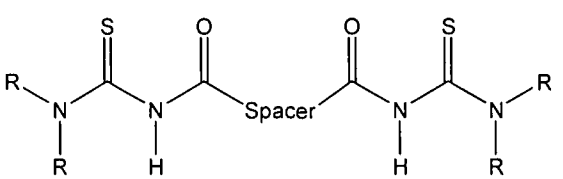

Bipodal N',N',N''',N'''-tetraalkyl-*N,N''*-aroylbis(thioureas)

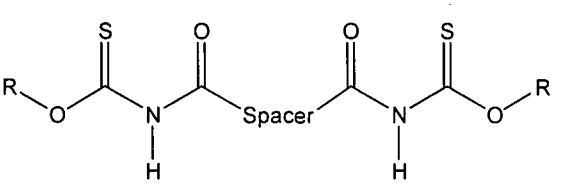

Bipodal *N*-phenylenethiocarbamic-*O*-esters

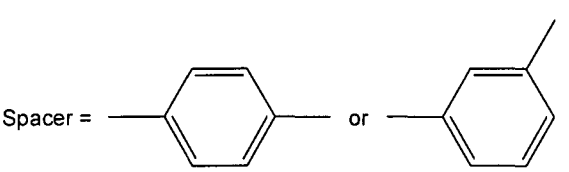

R = alkyl

Scheme 5 *N',N',N''',N'''*-tetraalkyl-*N,N''*-aroylbis(thioureas) and bipodal *N,N'*-phenylenebis(carbonylthiocarbamic-*O*-esters).

In this context, the bipodal *N,N'*-phenylenebis(carbonylthiocarbamic-*O*-esters) were of interest as potential structural analogues to the bipodal *N',N''',N''',N'''*-tetraalkyl-*N,N''*-aroylbis(thioureas). A survey of the literature reveals that there are no molecular structures of bipodal *N,N'*-phenylenebis(carbonylthiocarbamic-*O*-esters) listed on the Cambridge Structural Database (CSD)[52].

Therefore, further to the structural characterization of the series of monopodal *N*-acyl(aroyl)thiocarbamic-*O*-esters described above, a series of bipodal *N,N'*-phenylenebis(carbonylthiocarbamic-*O*-esters) were prepared and several of these molecular structures were determined by X-ray crystallography[58, 59].

1.2.3 *N*-acyl(aroyl)-*N'*,*N'*-dialkylureas

Acylchalcogenourea derivatives (Scheme 6) have been used in analytical applications since their coordinating properties were initially published[25, 34, 60]. This broad class of compound has been identified as having several potential industrial uses such as the determination of traces of transition metals by means of normal phase chromatography[35]. Acylchalcogenourea derivatives have also shown to selectively extract metals [typically of the 4th, 5th and 6th period of the periodic table e.g. Cu(II)] in the form of stable metal chelates[61]. Despite the potential application of these uses, a survey of the literature shows that very little has been published concerning the coordination chemistry and structure of the acylchalcogenourea ligands and their related metal complexes[60].

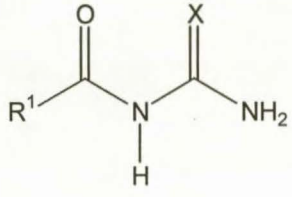

X = O, S, Se, Te

Scheme 6 General acylchalcogenourea motif.

A number of patents pertaining to acylchalcogenourea compounds have been filed due to the numerous potentially useful biological activities exhibited by compounds in which a urea group has been acylated on one or both of the nitrogens[62]. The biologically active acylchalcogenourea containing compounds include very simple structures such as the anticonvulsant phenacemide[63], through to more complex acylurea derivatives such as the hypnotic barbiturates[64], the anticonvulsant/antiepileptic hydantoin[65], and the spirohydantoin aldose reductase enzyme inhibitor[66].

Some work has been published concerning the thermochemical behaviour of the chalcogenourea derivatives and their Cu(II) complexes with O_4 or O_2S_2 donor atom sets thereby studying the influence of the donor atoms on the energies of the metal ligand binding[67]. Interest in the energetics of metal-to-oxygen bonds of the chalcogen complexes, has included some solution calorimetric studies, dealing with the acid strengths of ligands and the stability constants of the corresponding metal complexes[68]. The chalcogen chelate-type complexes constitute an important class of this type of compound, and among these, certainly, the β-diketonates are the most important and widely studied. A large number of papers on the thermochemistry of metal-*β*-diketonates has been published[69]. However very little of this work has focused on the structurally related *N*-aroyl(acyl)-*N'*,*N'*-dialkylurea chelates. Some calorimetric studies dealing with the acid strengths of acylchalcogenourea ligands and the stability

constants of the corresponding metal complexes have been published by Dietze *et al.*[68]. It has previously been shown that the difference in mass spectroscopy fragmentations of the free and coordinated acylchalcogenourea ligands is preferentially caused by the different stabilities of the ligand-metal bonding. It has been reported that for the *S,O*-donor atom chelates, such as in the case of the *N*-acyl(aroyl)-*N',N'*-dialkylthioureas, the oxygen-metal bonding fragments considerably easier under mass spectroscopy conditions than the sulphur-metal bonding[70].

The chemistry of tetrathiafulvalene (TTF)[71] and ferrocene has received a considerable amount of attention over the last 25 years regarding the development of redox-active supramolecules for potential advanced material applications. This has resulted in considerable effort being directed towards the production of highly organised single crystals[72] and thin films[73]. During this aforementioned study, work covering *N*-acyl ureas was reported, as these *N*-acyl ureas were identified as side products which formed during the activation of carboxyl groups with *N,N'*-dicyclohexylcarbodiimide (DCC)[74]. It was the use of triphenylene building blocks in dichloromethane or THF during the aforementioned study that resulted in the rearrangement of the *O*-acyl urea formed during the initial reaction of carboxy-derivatives with DCC, to *N*-acyl urea derivatives. These resultant unwelcome *N*-acylurea derivative byproducts prevented the formation of the target TTF-triphenylenes.

N-aroyl(acyl)-*N',N'*-dialkylureas, like *N*-acyl(aroyl)thiocarbamic-*O*-esters, (Scheme 1) are similar in connectivity and molecular geometry to the comparatively well studied and well documented analogues *N*-aroyl(acyl)-*N',N'*-dialkylthioureas. These similarities stimulated the investigation into the preparation, characterization and fundamental coordination chemistry of a series of *N*-aroyl(acyl)-*N',N'*-dialkylureas described here. A series of *N*-aroyl(acyl)-*N',N'*-dialkylureas was prepared, characterized and complexed with copper(II). By studying the coordination chemistry of this series of ligands, it was hoped that the influence of variation from the bidentate *S,O*-donor atom sets of the *N*-aroyl(acyl)-*N',N'*-dialkylthiourea ligands to the *O,O'*-donor atom sets of the *N*-aroyl(acyl)-*N',N'*-dialkylurea ligands would become evident. With this objective in mind, the molecular structure of several *N*-aroyl(acyl)-*N',N'*-dialkylureas, as well as that of several of copper(II) complexes thereof, were determined by single crystal X-ray diffraction.

2. Aims and Objectives

This thesis describes the preparation and characterization of three classes of ligand, as well as their coordination chemistry to several transition metals. These three classes of ligand are all variations of the basic motif of the *N*-aroyl(acyl)-*N'*,*N'*-dialkylthiourea class of ligand and can be categorized into the following three classes:

- Monopodal *N*-aroyl(acyl)thiocarbamic-*O*-esters (chapters 2 and 3)
- Bipodal *N*,*N'*-phenylenebis(carbonylthiocarbamic-*O*-esters) (chapter 4)
- *N*-aroyl(acyl)-*N'*,*N'*-dialkylureas (chapter 5).

The synthesis and coordination chemistry of each of the ligand systems listed in Table 1 were explored in detail in an attempt to elucidate the effect that a variation of motif, as well as variation of the metal centre, has on the overall coordination chemistry. Several crystal structures of both the ligands and complexes of each category were determined. In each case, numerous intra- and intermolecular hydrogen bonds, contacts and electrostatic interactions were observed and evaluated in order to identify overall differences in the coordination chemistry of the categories of compounds investigated. Detailed aims and objectives associated with each category of compound are given in more detail in the introduction to the relevant chapter.

An investigation into the preparation of complexes of the symmetrical bipodal analogues of thiocarbamic esters with Ni(II), Pd(II) and Pt(II) was undertaken. Complexes were in fact prepared, however these could not be easily characterized fully presumably due to their 'polymeric' and resultant insoluble nature. Therefore, complexes of the bipodal ligands prepared in chapter 4 are not listed in Table 1, nor are they discussed in detail in chapter 4.

Chapter 2 and Chapter 3

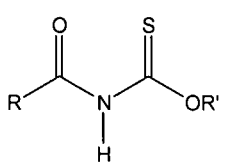

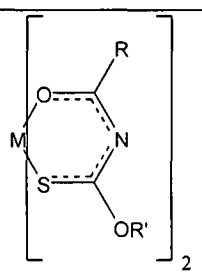

R	R'		M
= phenyl	= ethyl	**H(L^1-*S,O*)**	Ni(II), Pd(II), Pt(II)
= phenyl	= benzyl	**H(L^2-*S,O*)**	Ni(II), Pd(II), Pt(II)
= phenyl	= methyl	**H(L^3-*S,O*)**	Ni(II), Pd(II), Pt(II)
= phenyl	= butyl	**H(L^4-*S,O*)**	Ni(II), Pd(II), Pt(II)
= phenyl	= isopropyl	**H(L^5-*S,O*)**	Ni(II), Pd(II), Pt(II)
= phenyl	= dodecyl	**H(L^6-*S,O*)**	Pt(II)

...Table continued P.T.O.

= 4-methoxy phenyl	= ethyl	**H(L^{7}-*S,O*)**	Ni(II), Pd(II), Pt(II)
= 3,5-dimethoxy phenyl	= ethyl	**H(L^{8}-*S,O*)**	Ni(II), Pd(II), Pt(II)
= 3,4,5-trimethoxy phenyl	= ethyl	**H(L^{9}-*S,O*)**	Ni(II), Pd(II), Pt(II)

Chapter 4

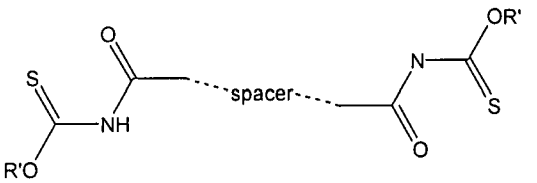

R'	spacer	
= methyl	*p*-phenylene	**H_2(L^{15}-*S,O*)**
= ethyl	*p*-phenylene	**H_2(L^{16}-*S,O*)**
= butyl	*p*-phenylene	**H_2(L^{17}-*S,O*)**
= methyl	*m*-phenylene	**H_2(L^{18}-*S,O*)**
= ethyl	*m*-phenylene	**H_2(L^{19}-*S,O*)**
= butyl	*m*-phenylene	**H_2(L^{20}-*S,O*)**
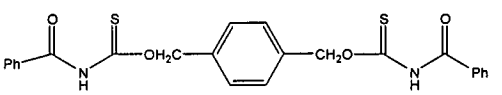		**H_2(L^{21}-*S,O*)**

Chapter 5

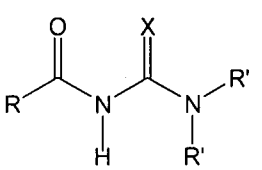

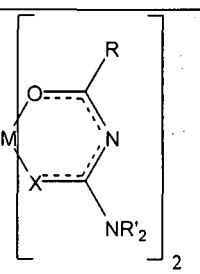

R	R'	X		M
= *tert*-butyl	= ethyl	= O	**H(L^{1}-*O,O*)**	Cu(II)
= *tert*-butyl	= methyl	= O	**H(L^{2}-*O,O*)**	Cu(II)
= 3,4,5-trimethoxy phenyl	= ethyl	= O	**H(L^{3}-*O,O*)**	Cu(II)
= *tert*-butyl	= ethyl	= S	**H(L^{4}-*O,O*)**	Cu(II), Ni(II)

Table 1 Ligand systems and complexes investigated.

3. Intermolecular and Intramolecular interactions.

In the single crystal X-ray analysis of the various ligands and complexes discussed in this thesis, numerous intra- and intermolecular hydrogen bonds, contacts and electrostatic interactions were observed. In many cases, these interactions and contacts were found to dictate the overall packing of the molecules in the unit cell. Apart from the 'traditional' hydrogen bonds observed, many non-classical weak hydrogen interactions, (H...X-atom), were also observed. For this reason some discussion of traditional hydrogen bonding as well as weaker non-classical hydrogen interactions is warranted.

The hydrogen bond is the most important of all directional intermolecular interactions. It is operative in determining molecular conformation, molecular aggregation and function of a vast number of inorganic and biological systems[75]. Research into the nature of the hydrogen bond continues due to the fundamental importance of hydrogen bonding in the areas of mineralogy, material science, supramolecular chemistry, biochemistry, molecular medicine and pharmacology to name but a few. Consequently the complexity of the hydrogen bond phenomena has increased dramatically and the general description or definition of what a hydrogen bond is has been refined over the years[75].

It is now accepted that the hydrogen bond is a much broader phenomenon than that which is traditionally sketched by interactions described by X-H...A resulting from interaction of strong polar groups $X^{\delta-}$-$H^{\delta+}$ (donor group) on the one side, and $A^{\delta-}$ (acceptor group) on the other (with X= O, N, halogen and A = O, N, S halide etc.). Furthermore, the H...A distance in all hydrogen bonds is not always shorter than the sum of the van der Waals radii. For an X-H group to be able to form hydrogen bonds, X does not need to be very electronegative, it is only necessary that X-H is at least slightly polar. This therefore includes groups such as C-H and P-H. In turn, the acceptor counterpart A does not need to be a particularly electronegative atom or anion, but only has to supply a sterically accessible concentration of negative charge[75].

Conventional 'strong and directional' hydrogen bonds, such as O-H...O, N-H...O and O-H...N, have long been recognized as being of fundamental importance in determining the supramolecular structure of organic solids[76]. In molecules lacking these hydrogen bond donors and acceptors, other types of weak and less directional forces, such as C-H...O, C-H...π and π-π interactions become important in generating supramolecular architectures[77, 78].

One of the major goals of modern 'crystal engineering' is targeted at the predictable assembly of molecular species into extended architectures. The most intriguing of this is the notion of being able to manipulate not only the features of specific molecules, but also the bulk, intermolecular characteristics and the properties of the entire crystalline aggregate[79]. The growth of crystal engineering has also coincided with advances in the understanding of intermolecular interactions and supramolecular chemistry as well as the realization that several aspects of solid-state chemistry of increasing relevance can only be resolved with a better and more detailed understanding of structure-function relationships.

As a result, advances in supramolecular chemistry have influenced the manner in which chemists view the existence of single crystals and, perhaps even more importantly, the design of new crystalline phases[80]. One of the necessary tasks of current research is the fabrication of supramolecular self-assembly organized by covalent or noncovalent interactions.[81] Hydrogen bonds of both the classical and non-classical type, fall into the category of the 'structure directing' non-covalent interactions and hence allow speculation on their application in crystal design[82]. Following from this, π-π interactions have increasingly been studied for the fine tuning of the topography of crystal structures[81] and it has been reported that this π-π interaction can contribute up to 10 kJ.mol^{-1} as intermolecular attractive energy through the well known face-to-face and C-H...π/edge-to-face interactions[83]. In studies concerning the benzene dimer, it has been shown that the edge-to-face (T-shaped) dimer is slightly more stable than the displaced face-to-face (displaced stacked) dimer, which in turn is more stable than the face-to-face (stacked) dimer interactions[84].

Early work by Schmidt emphasized that the physical and chemical properties of crystalline solids are as critically dependent upon the distribution of molecular components within the crystal lattice, as the properties of its individual molecular components[85]. Therefore, crystal engineering has implications that extend well beyond materials science into areas as diverse as pharmaceutical development and synthetic chemistry. The seminal work by Desiraju and Etter in solid-state organic chemistry afforded the concept of *supramolecular synthons*[86] and led to hydrogen bonds being perhaps the most widely exploited of the noncovalent interactions in the context of crystal engineering. Their research programs addressed the use of hydrogen bonding as a design element in crystal design and delineated the nature (strength and directionality) of the interaction. It is now readily accepted that these forces include weak hydrogen-bonding interactions such as C-H···X and CH···π interactions. In a recent literature example of supramolecular networks of $[\{Mn(bpp)_3Cl_2\}(H_2O)_2]_n$ (bpp = 1,3-bis (4-pyridyl) propane), C-H...π interactions were reported to stabilize the extended solid state structure formed by π-π interactions. The C-H...π interactions were reported as having a C-H...π angular range of 124.01-137.60° and a C...π distance range of 3.634-3.753Å[81].

It is now well recognized that C-H groups can act as weak hydrogen bond donors[87, 88]. The C-H donor strength of these groups depends on the carbon atom hybridisation in the order C(sp)-H > C(sp^2)-H > C(sp^3)-H, with some crystallographic data suggesting donor potential even for weakly polarized methyl groups[89]. Statistical database surveys demonstrate that mean C...O distances in C-H...O contacts correlate convincingly well with C-H acidities. Mean H...O distances of methyl donor groups R-CH_3, have been found to depend on the nature of the R group[89]. All these studies indicate that most kinds of C-H groups can participate in weak hydrogen bonds. Published theoretical calculations[90] estimate C-H...O hydrogen bond energies to be around 0.5 to 1 kcal mol^{-1}. Despite this wealth of experimental and theoretical work, the concept of the C-H...O hydrogen bond, and that of the weak hydrogen bond in general, is persistently questioned. It has even been claimed that the typical C-H...O/N hydrogen bond represents 'nothing more than a classical van der Waals interaction'[91]. This claim was refuted in the work of Steiner and Desiraju[89]. In this publication, hydrogen bonds were described as being inherently

directional with linear, or close to linear geometries favoured over bent ones, while the van der Waals contacts were described as being isotropic with interaction energies being independent of the contact angle[89]. In this context, a statistical analysis of structural data from the Cambridge Structural Database (CSD)[52] was done in an attempt to obtain a description of angular preferences, or lack thereof, of the hydrogen bond[89].

In summary, the findings of this statistical analysis showed

- Conventional hydrogen bonds, C(sp^3)-O-H...O=C, had a mean C-H..O contact angle θ of 154.0(4)° with a mean H...Y distance of 2.837(4)Å
- For the acidic ethynyl donors a mean CCH..O=C contact angle θ of 152(2)° was observed with a mean H...Y distance of 2.36(4)Å with the angular distribution between 100-180° being only slightly wider than that observed for the conventional hydrogen bond illustrated above.
- For vinyl donors, $C=CH_2$...O=C, the mean C-H..O contact angle θ falls to 143(1)° with a mean H...Y distance of 2.67(1)Å coupled with the angular distribution widening considerably over 100-180°.
- For the weakly polarized methyl donor, CH_2-CH_3...O=C, the mean contact angle θ falls further to 137.1(7)°, with a mean H...Y distance widening to 2.761(6)Å. The corresponding angular distribution between 100-180° is softened considerably, but still shows directional behavior with linear contact geometries being favoured.

Therefore, since C-H...O interactions of alkyl groups are not isotropic, even at the long distance cut off of 3.0Å, they should definitely not be classified as mere van der Waals contacts[89]. Furthermore, the differences in directionality behavior between any kind of C-H...O hydrogen bond and the van der Waals interaction, is a consequence of fundamentally different distance and angle fall-off characteristics of these interactions[89]. It must be noted that weak hydrogen bonds encompass a wide scale of strengths, just as do C-H group acidities, and it is therefore misleading to consider all kinds of C-H...O hydrogen bonds exactly alike[89]. It is also misleading to assign hydrogen bond character only to a certain class of C-H...O contacts and to consider the rest as nothing more than classical van der Waals interactions, since a C-H...O interaction does not become a van der Waals contact just because it crosses some arbitrary threshold[89]. However, not every C-H...O contact of a methyl group is 'automatically' a hydrogen bond.

Due to the high acidity and hence strong donor potential of terminal alkynes, coupled with their robust suitability for vibrational spectroscopic experiments, terminal alkynes are amongst the best suited donors of C-H...O type hydrogen bonds[88, 92]. Terminal alkynes have been reported as having hydrogen bonds with H...O separations in the range of 2.1-2.6Å with a mean value of 2.37(4)Å[88, 93]. However, very little is known about long C-H...O (and more generally long D-H...A) contacts. Hence an open question is: '*To which distances can C-H...O interactions be elongated before losing their hydrogen bond character?*[94]. The consensus in the literature is that no clear distance limits can be given, and that

for increasing H...O and C...O separations, there is a gradual transition from hydrogen bond interactions to 'nothing'[88]. Long C-H...O hydrogen bonds with H...O distances of 2.92Å (C-H distance of 1.08Å) and C...O distances of 3.71Å, with the C-H...O contact angle bent far from linearity at 130° have been reported in the literature for $[Cr(CO)_3\{\eta^6\text{-}[7\text{-}exo\text{-}(CCH)C_7H_7]\}]$[94]. Despite the significant deviation of the C-H...O contact angle from linearity, this long C-H...O hydrogen interaction was conclusively identified experimentally by Steiner *et al.* as a formal hydrogen bond using crystallography in conjunction with vibrational spectra. This work supports the long range nature of C-H...O interactions and clearly disfavours the view that hydrogen bond character stops at the sum of van der Waals radii. The experimental findings of Steiner *et al.* showed that since the alkynyl CC-H donor is a stronger donor than most C-H groups, C-H...O contacts of similar geometries with less acidic C-H groups will be correspondingly weaker, but nonetheless may still constitute a hydrogen bond[94].

Weak hydrogen bonds, such as the non-classical C-H...O hydrogen bond, can play a crucial role in the overall structure stabilisation of the molecules. An example of such, is the reported structural characterisation of two β-cyclodextrin compounds. In one the C-H...O hydrogen bond was found to stabilize the molecule in a similar fashion to that observed in the second isostructural compound of β-cyclodextrin which contained the classical N-H...O hydrogen bond as opposed to the C-H...O hydrogen bond[95]. The general conclusion from structural investigations of large molecular assemblies and even macromolecular systems, was that in the formation and stabilization of such systems, interactions, such as the C-H...O hydrogen bond, may tip the scales in a subtle balance of weak interactions which may determine whether a molecular assembly is ordered or not[95].

The statement *'Not all short C-H...O contacts are hydrogen bonds'* has been critically investigated by Steiner[96]. The systems investigated where hydrogen contacts did not constitute hydrogen bonds, despite favorably short contact distances, were all of the C-H...$O^{\delta+}$ type. Examples of systems of this type include H_3O^+, and $X{=}OH^+$. In the latter case, the positive charge need not be localized on the O-atom, but charge delocalization with substantial contribution of the resonance form $X{=}OH^+$ should be sufficient. Examples are systems like $P{=}OH^+ \Leftrightarrow P^+\text{-}OH$, $N\text{-}C{=}OH^+ \Leftrightarrow N^+{=}C\text{-}OH$ etc. The $N\text{-}C{=}OH^+ \Leftrightarrow N^+{=}C\text{-}OH$ system is relevant to the case of a protonated urea skeleton as illustrated in Scheme 7.

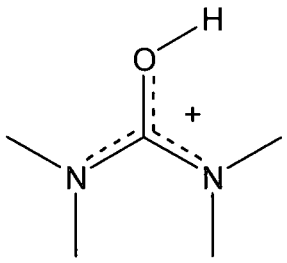

Scheme 7

The system illustrated in Scheme 7, is of particular interest in the context of the *N*-acyl(aroyl) substituted urea type ligands discussed in chapter 5 of this thesis. However, all the *N*-acyl(aroyl) substituted urea type ligands that were characterized by single crystal X-ray diffraction analysis were found not to be in the protonated form as illustrated in Scheme 7. Therefore, the special case of the C-H...$O^{\delta+}$ type systems, which do not constitute hydrogen bonding, does not warrant further discussion here.

The above discussion regarding classical and non-classical hydrogen bonding should be taken into account when evaluating the discussions of the crystal structures of the various ligand systems and metal complexes contained within this work, as many examples of non-classical hydrogen interactions have been identified in these systems. In turn, these interactions have often been identified as the interactions which largely dictate the overall packing of molecules within the respective unit cells.

4. References.

[1] C. R. Rasmussen, F. J. J. Villani, B. E. Reynolds, J. N. Plampin, A. R. Hood, L. R. Hecker, S. O. Nortey, A. Hanslin, M. J. Constanzo, R. M. J. Howse, A. J. Molinari, *Synthesis* 1988, 460-466.

[2] J. C. Manimala, E. V. Anslyn, *Tetrahedron Lett.* 2002, ***43***, 565-567.

[3] J. C. Manimala, E. V. Anslyn, *Eur. J. Org. Chem.* 2002, 3909.

[4] A. R. Katritzky, N. Kirichenko, B. V. Rogovoy, J. Kister, H. Tao, *Synthesis* 2004, ***11***, 1799-1805.

[5] *Comprehensive coordination chemistry: the synthesis, reactions, properties & applications of coordination compounds*, 1 ed., Oxford: Pergamon Press, **1987**.

[6] S. E. Livingstone, *Rev., Chem. Soc.* 1965, ***19***, 386.

[7] N. S. Kurnakov, *J. Prakt. Chem.* 1894, ***50***, 483.

[8] A. J. Aarts, H. O. Desseyn, M. A. Herman, *Transition Met. Chem.* 1980, ***5***, 10-14.

[9] E. Uhlemann, G. Klose, H. Muller, *Z. Naturforsch.* 1964, ***19b***, 962-964.

[10] A. Yokoyama, H. Tanaka, *Chem. Pharm. Bull.* 1964, ***12***, 683-689.

[11] A. Yokoyama, K. Ashida, H. Tanaka, *Chem. Pharm. Bull.* 1964, ***12***, 690-695.

[12] L. P. Eddy, J. W. Hayes, S. E. Livingstone, H. L. Nigam, D. V. Radford, *Aust. J. Chem.* 1971, ***24***, 1071-1074.

[13] S. E. Livingstone, *Coord. Chem. Rev.* 1971, ***7***, 59-80.

[14] E. Uhlemann, H. Mueller, P. Thomas, *Z. Chem.* 1971, ***11***, 401-409.

[15] R. K. Y. Ho, S. E. Livingstone, T. N. Lockyer, *Aust. J. Chem.* 1965, ***18***, 1927-1932.

[16] E. Uhlemann, U. Eckelmann, *Z. Anorg. Allg. Chem.* 1971, ***383***, 321-327.

[17] M. Das, *Inorg. Chim. Acta* 1979, ***36***, 79-83.

[18] M. Das, *Inorganic and Nuclear Chemistry Letters* 1980, ***16***, 529-533.

[19] M. Das, S. E. Livingstone, S. W. Filipczuk, J. W. Hayes, D. V. Radford, *J. Chem. Soc., Dalton Trans.* 1974, ***13***, 1409-1415.

[20] T. N. Lockyer, R. L. Martin, *Prog. Inorg. Chem.* 1980, ***27***, 223-324.

[21] H. Hartmann, E. Uhlemann, W. Huebner, E. Ludwig, L. Beyer, M. Walter, E. Hoyer, *Z. Chem.* 1981, ***21***, 271.

[22] K. H. König, M. Schuster, B. Steinbrech, G. Schneeweis, R. Schlodder, *Fresenius Z. Anal. Chem.* 1985, ***321***, 457-460.

[23] P. Vest, M. Schuster, K. H. Koenig, *Fresenius Z. Anal. Chem.* 1989, ***335***, 759-763.

[24] P. Vest, M. Schuster, K. H. Koenig, *Fresenius' Journal of Analytical Chemistry* 1991, ***339***, 142-144.

[25] P. Vest, M. Schuster, K. H. Köning, *Fresenius' Journal of Analytical Chemistry* 1991, ***341***, 566-568.

[26] K. R. Koch, *Coord. Chem. Rev.* 2001, ***216-217***, 473-488.

[27] C. Sacht, M. S. Datt, *Polyhedron* 2000, ***19***, 1347-1354.

[28] E. Rodriguez-Fernandez, E. Garcia, M. R. Hermosa, A. Jimenez-Sanchez, M. M. Sanchez, E. Monte, J. J. Criado, *Journal of Inorganic Biochemistry* 1999, ***75***, 181-188.

[29] T. J. Egan, K. R. Koch, P. L. Swan, C. Clarkson, D. A. Van Schalkwyk, P. J. Smith, *J. Med. Chem.* 2004, ***47***, 2926-2934.

[30] R. del Campo, J. J. Criado, E. Garcia, M. R. Hermosa, A. Jimenez-Sanchez, J. L. Manzano, E. Monte, E. Rodriguez-Fernandez, F. Sanz, *Journal of Inorganic Biochemistry* 2002, ***89***, 74-82.

[31] L. Beyer, R. Widera, E. Hoyer, *Z. Chem.* 1981, ***21***, 415.

[32] L. Beyer, E. Hoyer, J. Liebscher, H. Hartman, *Z. Chem.* 1981, ***21***, 81-91.

[33] K. H. Koenig, M. Schuster, G. Schneeweis, B. Steinbrech, *Fresenius Z. Anal. Chem.* 1984, ***319***, 66-69.

[34] M. Schuster, B. Kugler, K. H. Koenig, *Fresenius' Journal of Analytical Chemistry* 1990, ***338***, 717-720.

[35] M. Schuster, *Fresenius' Journal of Analytical Chemistry* 1992, ***342***, 791-794.

[36] A. N. Mautjana, J. D. S. Miller, A. Gie, S. A. Bourne, K. R. Koch, *J. Chem. Soc., Dalton Trans.* 2003, ***10***, 1952-1960.

[37] I. B. Douglass, F. B. Dains, *J. Am. Chem. Soc.* 1934, ***56***, 1408-1409.

[38] K. R. Koch, C. Sacht, T. Grimmbacher, S. Bourne, *S. Afr. J. Chem.* 1995, ***48***, 71-77.

[39] K. R. Koch, C. Sacht, S. Bourne, *Inorg. Chim. Acta* 1995, ***232***, 109-115.

[40] F. H. Allen, O. Kennard, D. G. Watson, L. Brammer, A. G. Orpen, R. Taylor, *J. Chem. Soc., Perkin Trans. 2* 1987, ***12***, S1-S19.

[41] K. R. Koch, J. du Toit, M. R. Caira, C. Sacht, *J. Chem. Soc., Dalton Trans.* 1994, 785-786.

[42] D. Hanekom, J. M. McKenzie, N. M. Derix, K. R. Koch, *Chem. Commun.* 2005, ***6***, 767-769.

[43] *Comprehensive coordination chemistry: the synthesis, reactions, properties & applications of coordination compounds, Vol. 5*, 1 ed., Oxford: Pergamon, **1987**.
[44] S. Bourne, K. R. Koch, *J. Chem. Soc., Dalton Trans.* 1993, ***13***, 2071-2072.
[45] A. Irving, K. R. Koch, M. Matoetoe, *Inorg. Chim. Acta* 1993, ***206***, 193-199.
[46] K. R. Koch, Y. Wang, A. Coetzee, *J. Chem. Soc., Dalton Trans.* 1999, ***6***, 1013-1016.
[47] Azizyan L. V., V. I. Ryaboi, *Obogashch. Rud (Leningrad)* 1989, ***2***, 21-24.
[48] V. A. Konev, V. I. Ryaboi, *Obogashch. Rud (Leningrad)* 1971, ***16***, 10-14.
[49] L. Quas, U. Schröder, B. Schröder, F. Dietze, L. Beyer, *Solvent Extr. Ion Exch.* 2000, ***18***, 1167-1177.
[50] M. Oba, K. Nishiyama, *Synthesis* 1994, 624-627.
[51] A. D. Morales, H. N. de Armas, N. M. Blaton, O. M. Peeters, C. J. D. Ranter, H. Márquez, R. P. Hernández, *Acta Crystallogr., Sect. C: Cryst. Struct. Commun.* 2000, ***C56***, 1042-1043.
[52] F. H. Allen, *Acta Crystallogr., Sect. B: Struct. Sci.* 2002, ***B58***, 380-388.
[53] L. A. Montiel-Ortega, S. Rojas-Lima, E. Otazo-Sanchez, R. Villagómez-Ibarra, *J. Chem. Crystallogr.* 2004, ***34***, 89-93.
[54] K. R. Koch, S. A. Bourne, A. Coetzee, J. Miller, *J. Chem. Soc., Dalton Trans.* 1999, 3157-3161.
[55] K. R. Koch, O. Hallale, S. A. Bourne, J. Miller, J. Bacsa, *J. Mol. Struct.* 2001, ***561***, 185-196.
[56] S. A. Bourne, O. Hallale, K. R. Koch, *Cryst. Growth Des.* 2005, ***5***, 307-312.
[57] R. Richter, J. Sieler, R. Koehler, E. Hoyer, L. Beyer, L. K. Hansen, *Z. Anorg. Allg. Chem.* 1989, ***578***, 191-197.
[58] G. Blewett, C. Esterhuysen, M. W. Bredenkamp, K. R. Koch, *Acta Crystallogr., Sect. C: Cryst. Struct. Commun.* 2004, ***C60***, o862-o864.
[59] G. Blewett, M. W. Bredenkamp, K. R. Koch, *Acta Crystallogr., Sect. C: Cryst. Struct. Commun.* 2005, ***C61***, o469-o472.
[60] M. A. V. Ribeiro da Silva, M. D. M. C. Ribeiro da Silva, L. C. M. Silva, *J. Chem. Thermodynamics* 2000, ***32***, 1113-1119.
[61] K. H. Köning, M. Schuster, G. Schneeweis, B. Steinbrech, *Fresenius Z. Anal. Chem.* 1985, ***325***, 621.
[62] http://www.cas.org/SCIFINDER/SCHOLAR, SciFinder Scholar, 2004
[63] M. A. Spielman, A. O. Geizler, W. J. Close, *J. Am. Chem. Soc.* 1948, ***70***, 4189.
[64] D. Lednicer, L. A. Mitscher, *The Organic Chemistry of Drug Synthesis*, J. Wiley & Sons, New York, **1977**.
[65] H. R. Henze, United States, **1946**.
[66] R. Sarges, R. C. Schnur, J. L. Belletire, M. J. Peterson, *J. Med. Chem.* 1988, ***31***, 230.
[67] M. A. V. Ribeiro da Silva, M. D. M. C. Ribeiro da Silva, L. C. M. da Silva, F. Dietze, E. Hoyer, *Thermochemica Acta* 2001, ***378***, 45-50.
[68] F. Dietze, J. Lerchner, S. Schmidt, L. Beyer, R. Köhler, *Z. Anorg. Allg. Chem.* 1991, ***600***, 37-46.
[69] M. A. V. Ribeiro da Silva, M. L. C. C. H. Ferao, *Pure Appl. Chem.* 1988, ***60***, 1225-1234.
[70] V. R. Herzschuh, B. Birner, L. Beyer, F. Dietze, E. Hoyer, *Z. Anorg. Allg. Chem.* 1980, 159-168.
[71] J. Garin, *Adv. Heterocycl. Chem.* 1995, ***62***, 249-304.
[72] M. R. Bryce, *J. Mater. Chem.* 1995, ***5***, 1481-1496.
[73] M. R. Bryce, *Chem. Soc. Rev.* 1991, ***29***, 355-390.
[74] T. Toniolo, G. Valle, M. Crisma, V. Morretto, J. Izbedski, J. Pelka, C. H. Schnieder, *Helv. Chim. Acta* 1990, ***73***, 626-633.
[75] T. Steiner, *Angew. Chem., Int. Ed. Engl.* 2002, ***41***, 48-76.
[76] G. R. Desiraju, T. Steiner, *The Weak Hydrogen Bond in Sructural Chemistry and Biology*, Oxford University Press, **1999**.
[77] M. J. Calhorda, *Chem. Commun.* 2000, 801-809.
[78] V. T. Yilmaz, C. Kazak, C. Kirilmis, M. Koca, F. W. Heinemann, *Acta Crystallogr., Sect. C: Cryst. Struct. Commun.* 2005, ***C61***, o438-o441.
[79] R. Robson, *J. Chem. Soc., Dalton Trans.* 2000, 3735-3744.
[80] B. Moulton, M. J. Zaworotko, *Chem. Rev.* 2001, ***101***, 1629-1658.
[81] A. K. Ghosh, D. Ghoshal, T.-H. Lu, G. Mostafa, C. N. Ray, *Cryst. Growth Des.* 2004, ***4***, 851-857.
[82] G. R. Desiraju, *J. Chem. Soc., Dalton Trans.* 2000, 3744-3751.
[83] I. G. Dance, *The Crystals as a Supramolecular Entity*, John Wiley, Chichester, **1996**.

[84] E. C. Lee, B. H. Hong, J. Y. Lee, J. C. Kim, D. Kim, Y. Kim, P. Tarakeshwar, K. S. Kim, *J. Am. Chem. Soc.* 2005, ***127***, 4530-4537.
[85] G. M. J. Schmidt, *Pure Appl. Chem.* 1971, ***27***, 647-678.
[86] G. R. Desiraju, *Angew. Chem., Int. Ed. Engl.* 1995, ***34***, 2311-2327.
[87] G. R. Desiraju, *Acc. Chem. Res.* 1991, ***24***, 290-296.
[88] T. Steiner, *Chem. Commun.* 1997, 727-734.
[89] T. Steiner, G. R. Desiraju, *Chem. Commun.* 1998, 891-892.
[90] J. J. Novoa, B. Tarron, M.-H. Whangbo, J. M. Williams, *J. Chem. Phys.* 1991, ***95***, 5179-5186.
[91] F. A. Cotton, L. M. Daniels, G. T. Jordan IV, C. A. Murillo, *Chem. Commun.* 1997, 1673-1674.
[92] G. R. Desiraju, *Acc. Chem. Res.* 1996, ***29***, 441449.
[93] G. R. Desiraju, *J. Chem. Soc., Chem. Commun.* 1990, 454-455.
[94] T. Steiner, B. Lutz, J. van der Maas, A. M. M. Schreurs, J. Kroon, T. Matthias, *Chem. Commun.* 1998.
[95] T. Steiner, G. Koellner, K. Gessler, W. Saenger, *J. Chem. Soc., Chem. Commun.* 1995, ***511-513***.
[96] T. Steiner, *Chem. Commun.* 1999, 313-314.

Index: Chapter II

1. Introduction

In general, *N*-acyl(aroyl)thiocarbamic-*O*-esters have not been as well reported in the literature as the comparable *N*-acyl(aroyl)-*N'*,*N'*-dialkylthioureas despite the first reports of *N*-benzoylthiocarbamic-*O*-esters appearing as early as 1874[1] and being identified as early as 1895 by Augustus E. Dixon[2]. The lack of investigation into the properties and coordination chemistry of *N*-acyl(aroyl)thiocarbamic-*O*-esters is even more surprising if one considers the structural similarities in terms of connectivity and molecular geometry between *N*-acyl(aroyl)thiocarbamic-*O*-esters and *N*-acyl(aroyl)-*N'*,*N'*-dialkylthioureas (Scheme 1). This lack of investigation is highlighted even further in context of the numerous reported potential technical and analytical applications of the analogous *N*-acyl(aroyl)-*N'*,*N'*-dialkylthioureas both in the medicinal and platinum group metals (PGM) industries[3-11].

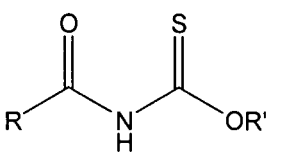

N-acyl(aroyl)thiocarbamic-*O*-ester

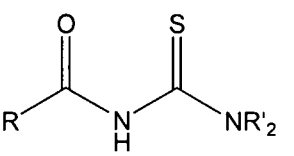

N-acyl(aroyl)-*N'*,*N'*-dialkylthioureas

R = alkyl , aryl
R' = alkyl

Scheme 1

N-aroylthiocarbamic-*O*-esters were reported as useful in heterocyclic chemistry synthesis in the 1960's[12] and as having potential application as 'collectors' in ore froth flotation processing[13, 14]. *N*-aroylthiocarbamic-*O*-esters have also been reported as being highly efficient in the extraction of silver(I) from aqueous solutions[15, 16]. Oba *et al.* recently proposed *N*-aroylthiocarbamic-*O*-esters as intermediates in regio- and chemoselective deoxygenation of primary and secondary aliphatic alcohols[17]. The first reference to the coordination properties of *N*-aroylthiocarbamic-*O*-esters are from U. Schröder *et al.* as recently as 1995[18]. More recently, reports have appeared concerning the thermochemical behaviour of *N*-aroylthiocarbamic-*O*-ester anions in solution[19] and Ribeiro da Silva *et al.* calculates the molar enthalpies of formation of three *N*-benzoylthiocarbamic-*O*-esters in the crystalline and gaseous phases as derived from molar enthalpies of combustion and molar enthalpies of sublimation[20].

Despite these sporadic reports, *N*-aroylthiocarbamic-*O*-esters seem to have been generally overlooked as chelating agents despite the relatively simple 'one pot' synthesis required to prepare these ligands. Nor does it appear as if a systematic study has been undertaken on the coordination chemistry of this class of compound. To date, only one *N*-aroylthiocarbamic-*O*-ester complex has been listed on the Cambridge Structural Database (CSD)[21], that of bis(*O*-ethyl-*N*-benzoylthiocarbamato)nickel(II) reported by U. Schröder *et al.*[18]

A series of *N*-benzoylthiocarbamic-*O*-alkyl esters, as listed in Figure 1, were prepared and fully characterised.

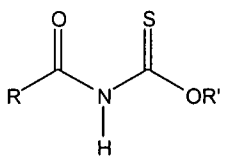

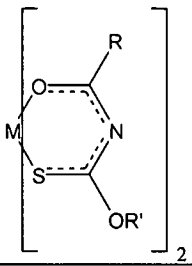

R	R'		M
= phenyl	= ethyl	H(L^1-*S,O*)	Ni(II), Pd(II), Pt(II)
= phenyl	= benzyl	H(L^2-*S,O*)	Ni(II), Pd(II), Pt(II)
= phenyl	= methyl	H(L^3-*S,O*)	Ni(II), Pd(II), Pt(II)
= phenyl	= butyl	H(L^4-*S,O*)	Ni(II), Pd(II), Pt(II)
= phenyl	= isopropyl	H(L^5-*S,O*)	Ni(II), Pd(II), Pt(II)
= phenyl	= dodecyl	H(L^6-*S,O*)	Pt(II)

Figure 1 Series of ligands and complexes described in chapter 2.

The coordination chemistry of these ligands with the d^8 transition metals nickel(II), palladium(II) and platinum(II) was then studied. Firstly, the alkoxy substituent on the *N*-benzoylthiocarbamic-*O*-alkyl esters was systematically varied in an attempt to elucidate the effect, if any, this substituent has on the coordination of these ligands to the metal(II) ions. Secondly, by varying the d^8 metal(II) ion from nickel(II) to palladium(II) to platinum(II), while keeping the alkoxy substituent constant, it was hoped that the effect due to the variation of the complexation metal alone, if any, would be illustrated.

The molecular structures of the following ligands and complexes were determined by single crystal X-ray diffraction in order to monitor the effects of variation of the alkoxy substituent and metal centre on both the coordination chemistry and the crystal structures:

H(L^1-*S,O*), H(L^2-*S,O*)

Ni(L^1-*S,O*)$_2$, Pd(L^1-*S,O*)$_2$, Pt(L^1-*S,O*)$_2$

Ni(L^3-*S,O*)$_2$

Ni(L^4-*S,O*)$_2$

Pt(L^6-*S,O*)$_2$

Ni(L^2-*S,O*)$_2$, Pd(L^2-*S,O*)$_2$

2. Results and Discussion

2.1 General preparation of ligands H(L^{1-5}-*S,O*)

Ligands **H(L^{1-5}-*S,O*)** were generally prepared according to a method illustrated in Scheme 2 which is based upon the method initially described by Douglass and Dains used for the preparation of the analogous *N*-acyl(aroyl)-*N'*,*N'*-dialkylthioureas[18, 22, 23]. **H(L^{1-5}-*S,O*)** were prepared under an inert anhydrous atmosphere in a two step 'one-pot' synthesis. Benzoyl chloride was reacted with an equimolar ratio of potassium isothiocyanate in anhydrous acetone followed by the addition of a two fold molar equivalent of the appropriate alcohol. The crude reaction products were initially recovered by extraction and further purified by crystallization. All ligands were obtained in good yields (> 66%) and a high degree of purity.

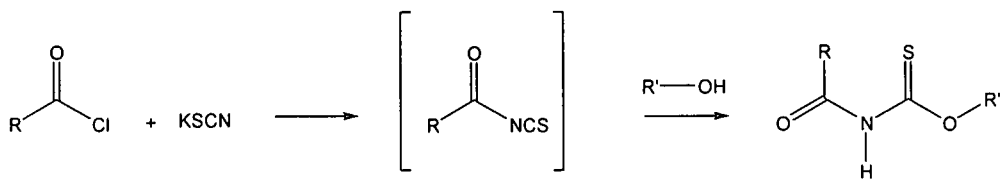

R = phenyl
R' = alkyl, benzyl

Scheme 2 Method of synthesis of *N*-benzolthiocarbamic-*O*-alkyl esters.

2.2 General preparation of complexes M(L^{1-5}-*S,O*)$_2$, M = Ni(II), Pd(II) and Pt(II)

Complexes **M(L^{1-5}-*S,O*)$_2$** were prepared by the dropwise addition of a 1:1 (v/v) acetonitrile water solution of nickel acetate tetrahydrate, potassium tetrachloropalladate or potassium tetrachloroplatinate to a constantly stirred solution made up of a two fold molar equivalent of the *N*-aroylthiocarbamic-*O*-ethyl ester ligand dissolved in a 1:1 (v/v) acetonitrile water solution (containing an equimolar equivalent of sodium acetate in the case of potassium tetrachloropalladate or potassium tetrachloroplatinate). The crude target complexes were isolated by centrifugation, washed with a cool 1:1 (v/v) acetonitrile water solution and dried under high vacuum. Where possible, crystals suitable for single crystal X-ray diffraction analysis were generally obtained from various binary solvent combinations. Apart from the complexes of *N*-benzoylthiocarbamic-*O*-benzyl ester, which were obtained in moderate yields (47-58%) and high purity, the remaining complexes were all obtained in high yields (> 74%) and a high degree of purity.

2.3 NMR Spectroscopy

Due to the availability of several NMR spectroscopic 'handles', the ^{1}H and ^{13}C NMR spectra can be used for the characterisation of the uncoordinated *N*-benzoylthiocarbamic-*O*-alkyl ester ligands **H(L^{1}-*S,O*)**, **H(L^{2}-*S,O*)**, **H(L^{3}-*S,O*)**, **H(L^{4}-*S,O*)** and **H(L^{5}-*S,O*)**. The monitoring of these spectroscopic 'handles', coupled with ^{195}Pt NMR where appropriate, affords a means by which the coordination of the ligands to the respective metals can be monitored.

The ^{1}H and ^{13}C NMR spectra of the metal complexes **M(L$^{1\text{-}5}$-*S,O*)$_2$**, upon initial inspection, resemble those of the uncoordinated ligands. However, there are small distinct changes that occur in the ^{1}H and ^{13}C NMR spectra upon coordination of the ligands to the metal that are indicative of a bis bidentate-(*S,O*) coordination of the *N*-benzoylthiocarbamic-*O*-alkyl ester ligands to the metal. These changes are comparable to those reported for the coordination of the structurally related *N*-benzoyl-*N'*,*N'*-dialkylthioureas to Ni(II), Pd(II) and Pt(II)[7, 11, 19, 24-26].

The most significant change that occurs in the ^{1}H NMR spectra upon the coordination of the *N*-benzoylthiocarbamic-*O*-alkyl ester ligands to the respective metals, is the disappearance of the distinctive N-H singlet in the 9.1 – 9.3 ppm region. This confirms that the coordination of the ligand to the metal has occurred in a deprotonated fashion.

The carbonyl and thiocarbonyl signals in the ^{13}C NMR spectra provide one of the more significant spectroscopic 'handles' by which the uncoordinated ligands can be characterised, which offer a valuable means by which the coordination of the ligands to the respective metals can be monitored as there is a significant upfield and downfield shift in the ^{13}C signals of the thiocarbonyl and carbonyl carbons respectively. These upfield and downfield shifts are characteristic of a bidentate-(*S,O*) coordination of the *N*-benzoylthiocarbamic-*O*-alkyl ester ligands to the respective metal ions. In the uncoordinated ligand, the thiocarbonyl peak appears downfield consistently at 189.3 – 190.3ppm while the carbonyl peak is observed consistently at 162.6 – 163.5ppm both regardless of the *O*-alkyl substituent used [**H(L^{1}-*S,O*)** C(S) 189.4ppm C(O) 162.7ppm; **H(L^{2}-*S,O*)** C(S) 189.4ppm C(O) 163.5ppm; **H(L^{3}-*S,O*)** C(S) 190.3ppm C(O) 162.6ppm; **H(L^{4}-*S,O*)** C(S) 189.7ppm C(O) 162.6ppm; **H(L^{5}-*S,O*)** C(S) 189.3ppm C(O) 163.3ppm]. In general, the intensities of carbonyl and thiocarbonyl resonances in ^{13}C NMR spectra are weak due to the long relaxation time associated with the carbon atoms of these moieties. In order to enhance these signals, ^{13}C spectra of both the uncoordinated ligands as well as the resultant Ni(II), Pd(II) and Pt(II) complexes were acquired using a 1 second pulse delay.

Upon coordination of the *N*-benzoylthiocarbamic-*O*-alkyl ester to metal ions, a substantial upfield shift is observed in the ^{13}C NMR signal of the thiocarbonyl peak and a downfield shift for the carbonyl peak. This observed 'cross-over' pattern of the carbonyl and thiocarbonyl ^{13}C NMR signals of the *N*-aroylthiocarbamic-*O*-alkyl esters upon coordination with metal ions is also observed for the complexation of the structurally analogous *N*-aroyl(acyl)-*N'*,*N'*-dialkylthioureas with Ni(II), Pd(II) and Pt(II)[7, 27-31]. The ^{13}C NMR signals of the C(O) and C(S) groups of the resultant **M(L-*S,O*)$_2$** [M = Ni(II), Pd(II) and Pt(II)] complexes are close together and separated by a maximum of 8.3ppm compared to the corresponding signals of the non-coordinated *N*-aroylthiocarbamic-*O*-alkyl esters which are separated by ±27ppm (see Table 1).

Furthermore, an interesting trend is observed in the relative upfield and downfield displacements of the thiocarbonyl and carbonyl resonances on going from the uncoordinated ligands to the respective complexes. These displacements are defined as :

- $\Delta^1 = (|\delta^{13}C(S)_{complex} - \delta^{13}C(S)_{ligand}|)$
- $\Delta^2 = (|\delta^{13}C(O)_{complex} - \delta^{13}C(O)_{ligand}|)$

The displacements Δ^1 and Δ^2 are listed in Table 1. The displacements of the thiocarbonyl resonances (Δ^1) for the various platinum complexes, **Pt(L^x-*S,O*)$_2$**, are larger than that of the corresponding palladium(II) complexes, **Pd(L^x-*S,O*)$_2$**, which are in turn larger than the displacement of the thiocarbonyl resonance observed for the corresponding nickel(II) complexes, **Ni(L^x-*S,O*)$_2$**. The reverse is true for the displacements of the resonance of the carbonyl moieties (Δ^2) where the displacement observed for the carbonyl moieties of the platinum(II) complexes, **Pt(L^x-*S,O*)$_2$**, are smaller than those observed for the corresponding palladium(II) complexes, **Pd(L^x-*S,O*)$_2$**, which are in turn smaller than those observed for the corresponding nickel (II) complexes, **Ni(L^x-*S,O*)$_2$**. Thus the trend observed for the displacement of the thiocarbonyl moiety follows the order Pt(II) > Pd(II) > Ni(II) while the trend observed for the displacement observed for the carbonyl moiety follows the order Ni(II) > Pd(II) > Pt(II). These trends are clearly seen by the values of the displacements give in Table 1. Given that the thiocarbonyl and carbonyl moiety are bonded to the metals directly through the sulphur and oxygen donor atoms respectively, it may be speculated that the displacements reflect the order of the HSAB[32] of 'softness' in the order Pt(II) > Pd(II) > Ni(II). A similar trend has been reported in the literature for a series of Pt(II), Pd(II) and Rh(II) complexes derived from *N*-acyl-*N'*,*N'*-dialkylthioureas[31].

Despite the clear ^{1}H and ^{13}C and NMR spectral evidence of a bidentate-(*S,O*) coordination and deprotonation of the *N*-benzoylthiocarbamic-*O*-alkyl ester ligands **H(L^1-*S,O*)**, **H(L^2-*S,O*)**, **H(L^3-*S,O*)**, **H(L^4-*S,O*)** and **H(L^5-*S,O*)** to Ni(II), Pd(II) and Pt(II), it was still necessary to confirm the 2:1 ligand to metal ratio in the resultant complexes by means of C, H, N, S analysis. (see experimental section 3.6).

	$H(L^x\text{-}S,O)$		$Ni(L^x\text{-}S,O)_2$				$Pd(L^x\text{-}S,O)_2$				$Pt(L^x\text{-}S,O)_2$			
	C(S)	C(O)	C(S)	Δ^1	C(O)	Δ^2	C(S)	Δ^1	C(O)	Δ^2	C(S)	Δ^1	C(O)	Δ^2
$H(L^1\text{-}S,O)$	189.4	162.7	178.1	11.3	186.2	23.5	177.5	11.9	184.7	22.0	173.8	15.6	180.7	18.0
$H(L^2\text{-}S,O)$	189.4	163.5	179.3	10.1	187.0	23.5	177.6	11.8	184.5	21.0	174.7	14.7	179.7	16.2
$H(L^3\text{-}S,O)$	190.3	162.6	178.3	12.0	186.6	24.0	177.7	12.6	185.2	22.6	178.3	12.0	186.6	24.0
$H(L^4\text{-}S,O)$	189.7	162.6	178.1	11.6	186.4	23.8	177.5	12.2	184.9	22.3	174.5	15.2	180.0	17.4
$H(L^5\text{-}S,O)$	189.3	163.3	178.0	11.3	185.7	22.4	177.3	12.0	184.3	21.0	174.3	15.0	179.5	16.2

Table 1 ^{13}C NMR shifts of the carbonyl and thiocarbonyl moieties of ligands $H(L^1\text{-}S,O)$, $H(L^2\text{-}S,O)$, $H(L^3\text{-}S,O)$, $H(L^4\text{-}S,O)$ and $H(L^5\text{-}S,O)$ as well as the derived Ni(II), Pd(II) and Pt(II) complexes. Displacements Δ^1 and Δ^2 are defined as $\Delta^1 = (|\delta^{13}C(S)_{complex} - \delta^{13}C(S)_{ligand}|)$; $\Delta^2 = (|\delta^{13}C(O)_{complex} - \delta^{13}C(O)_{ligand}|)$.

2.4 Mass Spectrometry

Ligands **H(L^1-*S,O*)**, **H(L^2-*S,O*)**, **H(L^3-*S,O*)**, **H(L^4-*S,O*)** and **H(L^5-*S,O*)** as well as the resultant Ni(II), Pd(II) and Pt(II) complexes were all further characterised by mass spectrometry. Only electron impact mass spectrometry (EI-MS) and limited electron spray mass spectrometry (ESMS) techniques were available. The appropriate *e/z* value for M^+ was identified for all ligands as well as complexes **M(L^1-*S,O*)$_2$**, **M(L^3-*S,O*)$_2$**, **M(L^4-*S,O*)$_2$**, M = Ni(II), Pd(II), Pt(II) and **M(L^5-*S,O*)$_2$** M = Ni(II) and Pd(II). The appropriate M^+ signals of complexes **M(L^2-*S,O*)$_2$**, M = Ni(II), Pd(II), Pt(II) and **Pt(L^5-*S,O*)$_2$** were not observed for EI-MS. In each case only *e/z* signals corresponding to fragments of the complex were observed. Signals pertaining to ligand fragments, comparable to those observed in the mass spectra of the uncoordinated ligands **H(L^2-*S,O*)** and **H(L^5-S,O)** were also observed. However, an electron spray mass spectrum (ESMS) signal *e/z* = 640.78 for **Pt(L^5-*S,O*)$_2$** could be observed (calculated for **[Pt(L^5-*S,O*)$_2$.H]$^+$** *e/z* = 640.9).

2.5 Infrared Spectroscopy

A characteristic feature of the infrared spectrum of the thiocarbamic ester ligands is the very broad band observed at ±3200cm^{-1} attributed to the N-H stretch of the uncoordinated ligand. The broadness of the stretching vibration of this group can be attributed to this group being involved in extensive intra- and intermolecular hydrogen bonding networks[33]. This was confirmed in the single crystal structure analysis of **H(L^1-*S,O*)** and **H(L^2-*S,O*)** (see sections 2.7.1 and 2.7.2). The broad stretch attributed to the N-H moiety disappears upon coordination of the ligand to the respective metals thereby confirming that the coordination of the ligand occurs in a deprotonated fashion.

The positions of several other characteristic infrared absorption bands representing the same modes of vibration of the uncoordinated ligand differ significantly from those of the coordinated ligands involved in the resultant metal complexes. A sharp stretch in the 1697 cm^{-1} – 1717 cm^{-1} region assigned to the carbonyl stretch in the uncoordinated ligands, shifts to the 1408 cm^{-1} – 1438 cm^{-1} region in the complexes. The signal changes from an intense sharp signal in the uncoordinated ligands to a significantly weaker and slightly broader signal in the complexes. A similar shift in the stretch assigned to the thiocarbonyl group is observed upon coordination to a metal, but to a much lesser degree. The stretch assigned to the thiocarbonyl moiety in the uncoordinated ligand occurs in the 1208 cm^{-1} – 1291 cm^{-1} region and shifts to the 1189 cm^{-1} – 1201 cm^{-1} region in the respective metal complexes. These shifts observed in the carbonyl and thiocarbonyl stretch are consistent with a weakening of the carbonyl and thiocarbonyl double bonds in the uncoordinated ligand coupled upon the formation of a six-membered chelate ring with the metal and extensive electron delocalisation through the chelation ring. This electron delocalisation through the metal chelate ring is supported by the observation of the downfield shift in the NMR spectra of the carbonyl moieties and a significant upfield shift in the thiocarbonyl moieties from ±162 ppm and ±189 ppm respectively in the uncoordinated ligand to ±180 – 185 ppm and 174 – 178 ppm respectively in the resultant metal complexes.

2.6 Computational Considerations

Complexes with tetracoordinated nickel(II) are mostly planar and more rarely tetrahedral. The tetracoordinated nickel(II) complexes are either paramagnetic or diamagnetic[34, 35]. Chelation of bidentate ligands such as **H(L^1-*S,O*)**, **H(L^2-*S,O*)**, **H(L^3-*S,O*)**, **H(L^4-*S,O*)** and **H(L^5-*S,O*)** to nickel(II) can adopt either a square planar conformation or a tetrahedral conformation, while tetrahedral conformations of nickel(II) result in the complexes generally exhibiting paramagnetic behaviour[34-38]. This can easily be rationalized by simple ligand field theory which allows for both low-spin as well as high-spin nickel(II) complexes. However in the case of square planar complexes, the spin-pairing energy is normally smaller than term splitting energy which generally results in square planar complexes of Ni(II) being diamagnetic[32, 34, 39, 40]. The paramagnetic versus diamagnetic nature of a nickel(II) complex is often used to distinguish between a tetrahedral coordination geometry and a square planar geometry of a ligand(s) around nickel(II) respectively.

It has also been reported that the paramagnetic tetrahedral isomer may exist in solution, yet the diamagnetic square planar isomer dominates in the solid state[34, 35]. The interchange between the two isomers in solution, i.e. planar ⇆ tetrahedral, has also been shown to often be dependent upon such conditions as ligand steric and/or electronic properties, temperature and solvent type[41, 42]. Some reports indicate that the occurrence of isomerisation between the square planar and tetrahedral conformations of some nickel(II) complexes in solution is time dependant and occurs only after several days[43].

The ^{1}H NMR spectra of **Ni(L^1-S,O)$_2$**, **Ni(L^4-S,O)$_2$** and **Ni(L^5-S,O)$_2$** indicated that these complexes exhibited partial paramagnetic character. These ^{1}H NMR spectra contained the required resonance signals, however the resonance signals were broad and did not exhibit the required coupling. Despite the partial paramagnetic nature of complexes **Ni(L^1-S,O)$_2$**, **Ni(L^4-S,O)$_2$** and **Ni(L^5-S,O)$_2$**, it was still possible to obtain suitable ^{13}C NMR spectra. The ^{1}H NMR spectra of **Ni(L^1-S,O)$_2$**, **Ni(L^4-S,O)$_2$** and **Ni(L^5-S,O)$_2$** were re-acquired after the original NMR samples were allowed to stand at ambient room temperature for 48 hours. The re-acquired ^{1}H spectra all contained the required resonances as well as the required coupling. However, the ^{1}H spectra of freshly prepared samples of **Ni(L^2-S,O)$_2$** and **Ni(L^3-S,O)$_2$** didn't exhibit any paramagnetic behaviour and showed no change when the ^{1}H spectra were re-acquired 48 hours later.

Computational DFT (density functional theory) calculations have been carried out by M. Burger of the Platinum Group Chemistry Research Group at Stellenbosch University in an attempt to calculate the energy pathway involved for the conversion of the square planar *cis*-Ni(L-*S,O*)$_2$ complex of a *N*-acetyl-*N'*,*N'*-dimethylthiourea (HL) to the equivalent square planar *trans*-Ni(L-*S,O*)$_2$ complex[44]. The DFT calculations indicate that the conversion of the square planar *cis*-Ni(L-*S,O*)$_2$ complex to the square planar *trans* equivalent most likely involves a spin triplet paramagnetic tetrahedral intermediate[44]. These DFT calculations offer further support for the tentative speculation that the partial paramagnetic behaviour exhibited in the ^{1}H spectra of complexes **Ni(L^1-S,O)$_2$**, **Ni(L^4-S,O)$_2$** and **Ni(L^5-S,O)$_2$** is

possibly due to the existence of tetrahedral or *pseudo*-tetrahedral isomers of these complexes to be present in solution[39, 40].

2.7 Single Crystal X-ray Diffraction Analysis of *N*-benzoylthiocarbamic-*O*-alkyl esters, H(L-*S,O*)

Only two molecular structures of *N*-aroylthiocarbamic-*O*-esters have previously been listed in the Cambridge Structural Database (CSD)[21], that of *N*-(2-furoyl)thiocarbamic-*O*-isopropyl ester[45] and *N*-(2-furoyl)thiocarbamic-*O*-benzyl ester[46]. Consequently, the molecular structure of *N*-benzoylthiocarbamic-*O*-ethyl ester [**H(L^1-*S,O*)**] and *N*-benzoylthiocarbamic-*O*-benzyl [**H(L^2-*S,O*)**] ester were determined and are reported here for the comparison in an attempt to identify any trends or similarities. Structural features of these ligands were compared to the trends that have previously been identified for the structurally analogous *N*-acyl(aroyl)-*N*',*N*'-dialkylthioureas[7, 29].

2.7.1 *N*-benzoylthiocarbamic-*O*-ethyl ester, H(L^1-*S,O*)

The molecular structure of *N*-benzoylthiocarbamic-*O*-ethyl ester, **H(L^1-*S,O*)**, is illustrated in Figure 2 showing the numbering scheme used. Selected bond lengths, bond angles and torsion angles are listed in Table 2. **H(L^1-*S,O*)** is orthorhombic, space group $Pna2_1$ with the *S,O*-donor atom sets essentially *cis* relative to each other.

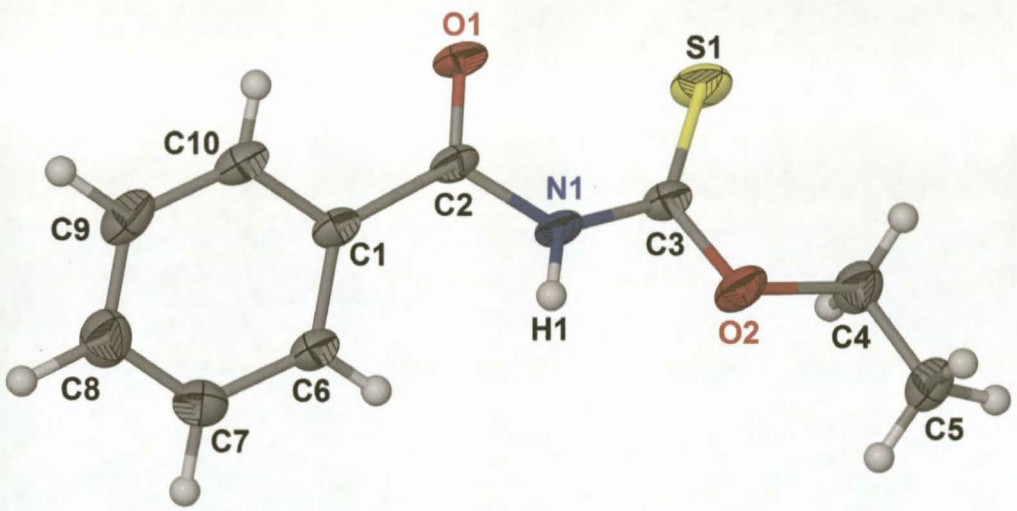

Figure 2 The molecular structure of **H(L^1-*S,O*)**, showing the atomic numbering scheme used. Displacement ellipsoids are drawn at the 50% probability level.

C1-C2	1.564(2)	N1-C3	1.437(2)
C2-O1	1.168(2)	C3-S1	1.587(2)
C2-N1	1.369(2)	C3-O2	1.273(2)
C10-C1-C2	121.8(2)	C6-C1-C2	124.5(2)
S1-C3-C2-O1	-17.9(1)		

Table 2 Selected bond lengths (Å), bond angles (°) and torsion angles (°) of **H(L^1-*S,O*)**.

In 1995 U. Schröder *et al.* reported that the C-N bonds of *N*-benzoylthiocarbamic-*O*-alkyl esters have partial double-bond character, which gives rise to hindered rotation around these bonds[18]. This results in four possible conformations of the benzoylthiocarbamic-*O*-alkyl esters namely, *E,Z', E,E', Z,E'* and *Z,Z'* as illustrated in Figure 3. Based on ^{1}H NMR spectroscopy, mass spectrometry and infrared spectrometric studies, as well as molecular modelling force field calculations, U. Schröder *et al.* suggested that *N*-benzoyl-thiocarbamic-*O*-alkyl esters prefer the *E,Z'*-conformation in solution[18].

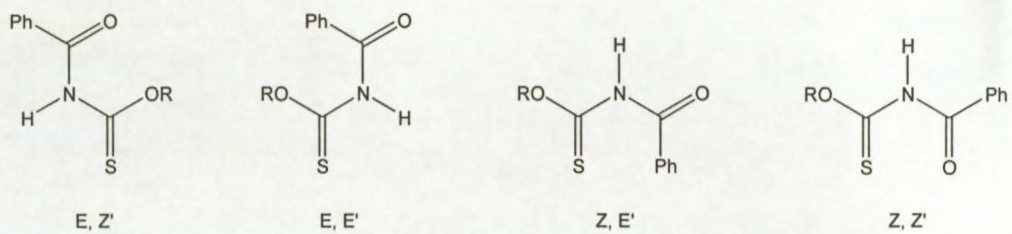

Figure 3 Possible conformations of *N*-benzoylthiocarbamic-*O*-alkyl esters as proposed by U. Schröder et al[18].

The preferred E,Z' conformation of *N*-benzoylthiocarbamic-*O*-alkyl esters, as proposed by U. Schröder *et al.*, is not consistent with that which was found for *N*-benzoylthiocarbamic-*O*-ethyl ester, **H(L^1-*S,O*)**, in the solid state (Figure 3). The ligand crystallized in the *Z,Z'*-conformation resulting in an essentially *cis-S,O* orientation. The O1-C2-N1-C3-S1 moiety deviates from absolute planarity with a S1-C3-C2-O1 improper torsion angle of -17.9(1)°. Furthermore, the phenyl ring is twisted away from the plane defined by the potential chelation ring, O1-C2-N1-C3-S1, resulting in the C1/C6/C7/C8/C9/C10 least-squares plane intersecting the O1/C2/N1/C3/S1 least-squares plane at 28.4(1)°. The twisting of the phenyl ring from the potential *S,O*-chelation moiety, in conjunction with the S1-C3-C2-O1 torsion angle of -17.9(1)°, results in a significant overall deviation from planarity of the molecule as a whole. This is further illustrated by the fact that the S1/C3/O2/C4/C5 least-squares plane intersects the C1/C6/C7/C8/C9/C10 least-squares plane at 35.9(1)°.

The C2-N1 bond of 1.369(2)Å is significantly shorter than the accepted average carbon-nitrogen single bond length of 1.472(5)Å[7, 47]. This suggests that the electron lone pair of nitrogen is delocalised to a degree into the N1-C2 bond. The N1-C3 bond of 1.437(2)Å is only fractionally shorter than the accepted carbon-nitrogen single bond length, indicating that both the C2-N1 and N1-C3 bonds have partial double bond character resulting in partially restricted rotation around these bonds. The C3-O2 bond distance of 1.273(2)Å is also shorter than the average carbon-oxygen single bond [Csp^2-OCsp^3] of 1.35(2)Å[47]. Consequently, we have a π-π conjugation along the O1-C2-N1 and S1-C3-O2 bond systems. Proposed resonance structures of **H(L^1-*S,O*)** are illustrated in Scheme 3. Based on the relative degree of partial double bond order identified in the C2-N1, N1-C3 and C3-O2 bonds, it is proposed that resonance structures (I), (II), (IV) and (V) are the principal resonance structures contributing to the overall structure of **H(L^1-*S,O*)**.

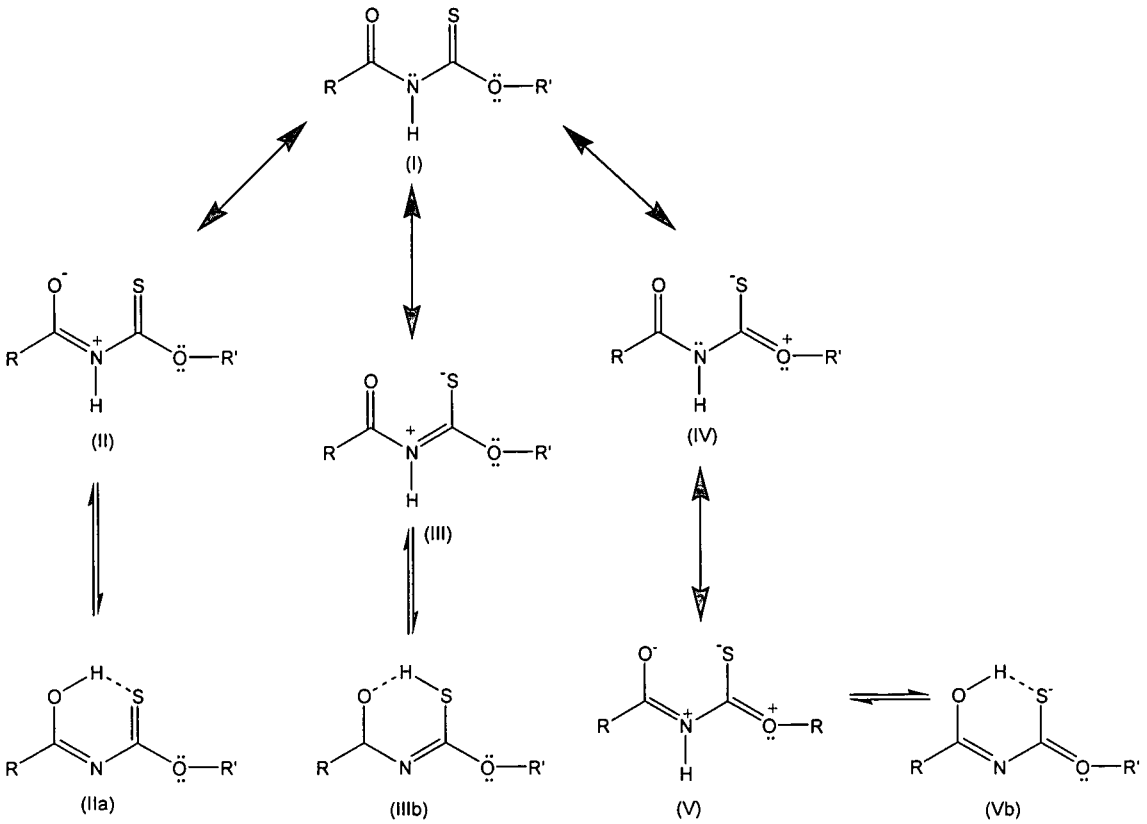

Scheme 3 Possible resonance structures of **H(L^1-*S,O*)**.

An asymmetry is observed in the C10-C1-C2 and C6-C1-C2 bond angles of **H(L^1-*S,O*)** [C10-C1-C2 121.8(2)°; C6-C1-C2 124.5(2)°]. This asymmetry may be a result of an attraction in the C10-H10...O1 system [C10-H10...O1 2.63Å, 103°, C10...O1 2.954(2)Å] and a repulsion in the C6-H6...H1 system [C6...N1 3.059(2)Å, C6...H1 2.69(3)Å]. A similar asymmetry was observed in the angles around the *ipso*-carbon of the furan ring of *N*-(2-furoyl)thiocarbamic-*O*-isopropyl ester[45].

A single classical intermolecular hydrogen bond as well as two non-classical intermolecular hydrogen contact interactions are observed in the crystal structure of **H(L^1-*S,O*)** between adjacent molecules (Table 3). An intermolecular hydrogen bond is observed between N1-H1...O1^i [N1-H1...O1^i 1.99(2)Å 165(2)°; symmetry code (i) x-½, ½-y, z] which cause the molecules of **H(L^1-*S,O*)** to link as one dimensional molecular chains parallel to (100). The N1-H1...O1^i intermolecular hydrogen bond is further stabilised by the C6-H6...O1^i and C6-H6...S1^i bifurcated intermolecular hydrogen contact [C6-H6...O1^i 2.58Å 128(2)°; C6-H6...S1^i 2.79(2)Å 135(2)° symmetry code (i) x-½, ½-y, z]. The bifurcated C6-H6...S1^i intermolecular hydrogen contact possibly also contributes to the *cis-S,O* or Z,Z' conformation that is observed for **H(L^1-*S,O*)**. The packing of the molecules within the unit cell of **H(L^1-*S,O*)** is illustrated in Figure 4.

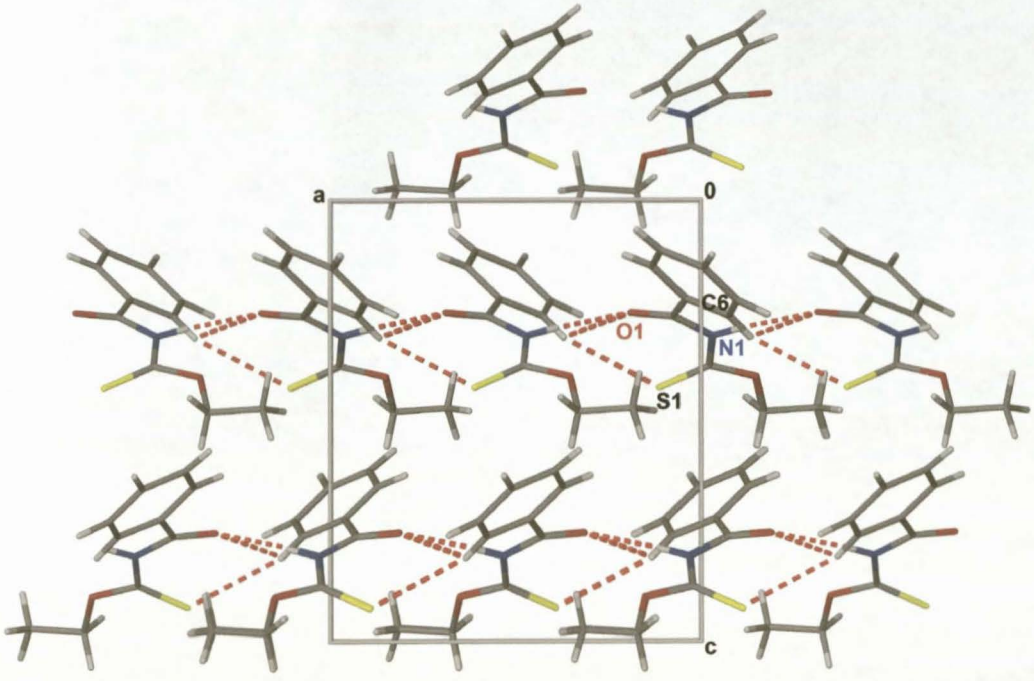

Figure 4 Extended packing diagram of **H(L^1-*S,O*)** as viewed along (010) showing the N1-H1...O1^i intermolecular hydrogen bonding and C6-H6...O1^i and C6-H6...S1^i intermolecular hydrogen contacts. Symmetry code (i) x-½, ½-y, z.

	Type	D-H...A	D-H (Å)	H...A (Å)	D...A (Å)	D-H...A (°)
H(L^1-*S,O*)	Inter	N1---H1...O1^i	0.83	1.99(2)	2.805(2)	165(2)
	Inter	C6-H6...O1^i	0.90	2.58(2)	3.222(2)	128(2)
	Inter	C6-H6...S1^i	0.90	2.79(2)	3.485(2)	135(2)

Table 3 Intermolecular hydrogen bonding and hydrogen contact geometry for **H(L^1-*S,O*)** as identified by XSeed[48, 49] and Platon[50] with s.u.s of the donor...acceptor (D...A) distances (Å) in parenthesis. Symmetry code (i) x-½, ½-y, z.

2.7.2 *N*-benzoylthiocarbamic-*O*-benzyl ester, H(L^2-*S,O*)

The molecular structure of *N*-benzoylthiocarbamic-*O*-benzyl ester, HL^2, is illustrated in Figure 5 showing the numbering scheme used. Selected bond lengths, bond angles and torsion angles are listed in Table 4. H(L^2-*S,O*) crystallizes orthorhombic, space group Iba2, with an *E,Z'* or essentially *trans-S,O* conformation.

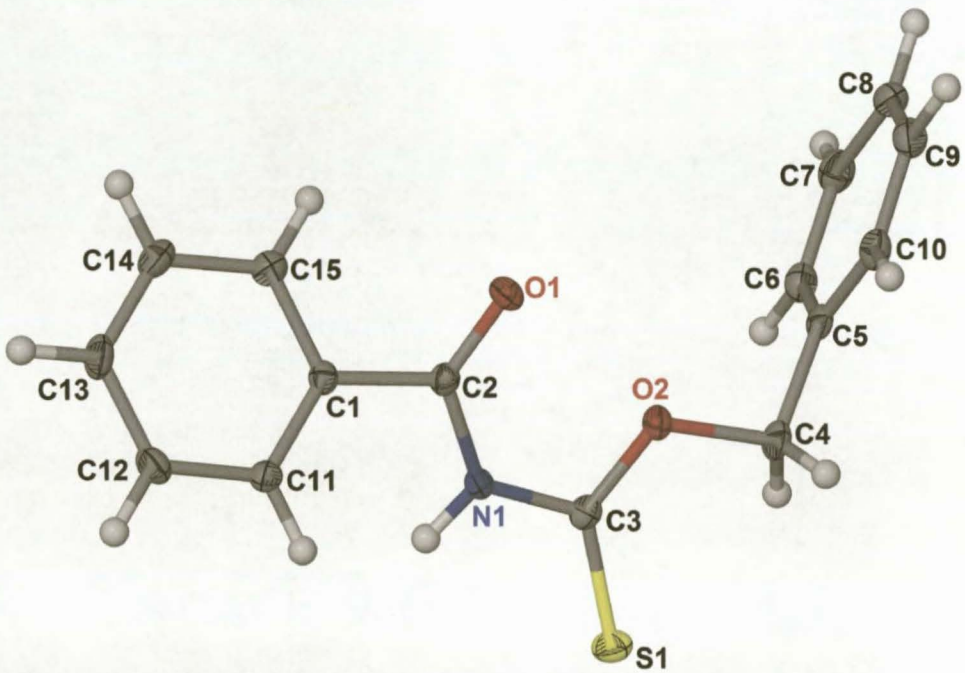

Figure 5 Molecular structure of HL^2 showing the numbering scheme used. Displacement ellipsoids are drawn at the 50% probability level.

C1-C2	1.493(2)	N1-C3	1.380(2)
C2-O1	1.214(2)(2)	C3-S1	1.653(2)
C2-N1	1.391(2)	C3-O2	1.320(2)
C15-C1-C2	116.4(2)	C11-C1-C2	123.6(1)
O1-C2-N1-C3	2.6(3)	C2-N1-C3-S1	174.7(1)
S1-C3-C2-O1	174.0(2)		

Table 4 Selected bond lengths (Å), bond angles (°) and torsion angles (°) of H(L^2-*S,O*).

The C2-N1 and N1-C3 bond lengths of 1.393(2)Å and 1.377(2)Å respectively are comparable and both shorter than the accepted average carbon-nitrogen single bond length of 1.472(5)Å[7, 47]. This indicates that these bonds have a partial double bond character thus giving rise to hindered rotation around these bonds. The C3-O2 bond length of 1.320(2)Å is comparable to the average carbon-oxygen bond length of 1.35(2)Å for a Csp^2-$OCsp^3$ moiety[47]. Consequently there is a π-π conjugation along the S1-C3-N1 and O1-C2-N1 bond systems but not along the S1-C3-O2 bond system as observed in the molecular

structure of **H(L^1-*S,O*)**. The observed *E,Z'* conformation of **H(L^2-*S,O*)** (Figure 5), in this case corresponds with the proposal of U. Schröder *et al.* that the preferred conformation of *N*-benzoylthiocarbamic-*O*-alkyl esters in solution is *E,Z'*[18]. For the structurally analogous *N*-acyl(aroyl)-*N',N'*-dialkylthioureas[29, 51, 52], the corresponding bond to C2-N1 in **H(L^2-*S,O*)** is usually shorter than the corresponding bond to N1-C3, which is closer in length to a carbon nitrogen single bond length. This results in a π-π conjugation along the corresponding O1-C2-N1 bond system of the *N*-acyl(aroyl)-*N',N'*-dialkylthioureas[29, 51, 52] and not along the corresponding S1-C3-N1 bond system as is the case in **H(L^2-*S,O*)**. This trend is also consistent for that which was observed for the structurally related *N*-acyl(aroyl)-*N',N'*-dialkylureas discussed in chapter 5[53].

The *anti* conformation of the O1-C2-N1-C3-S1 moiety of **H(L^2-*S,O*)** is essentially planar as illustrated by both the O1-C2-C3-O2 improper torsion *angle* of 174.0(2)° as well as the O1-C2-N1-C3 and C2-N1-C3-S1 torsion angles of 2.6(3)° and 174.7(1)° respectively. The greatest deviation from the least-squares plane defined through the C(S)NHC(O) moiety is C3 by a mere 0.039(1)Å while O2 deviates from this plane by 0.142(2)Å. The relative *anti* orientation of the carbonyl and thiocarbonyl groups observed for **H(L^2-*S,O*)** is parallel to the general trend that was observed for the thiocarbonyl and carbonyl moieties in the structurally related *N*-acyl(aroyl)-*N',N'*-dialkylthiourea ligands in the solid state[29, 51, 52].

The phenyl ring of the benzoyl group is twisted away from the plane defined through the C(S)NHC(O) moiety with the O1/C2/N1/C3/S1 least-squares plane intersecting the C1/C11-C15 least-squares plane at 27.0(1)°. Furthermore, the phenyl ring of the benzyl group is also twisted away from the plane defined through the C(S)NHC(O) moiety with the C5-C6-C7-C8-C9-C10 and O1/C2/N1/C3/S1 least-squares planes intersecting at 82.0(1)°. This results in the benzoyl and benzyl rings being almost perpendicular to each another with the least-squares planes defined through each of the phenyl rings intersecting at 88.3(1)°.

The asymmetry in the bond angles around the *ipso*-carbon of the phenyl ring of the benzoyl group of **H(L^2-*S,O*)** is similar to that in the molecular structure of **H(L^1-*S,O*)** (bond angles of C15-C1-C2 and C11-C1-C2 are 116.4(2)° and 123.6(2)° respectively). This asymmetry may be due to a repulsion in the C11-H11...H1-N1 [N1...C11 2.930(2)Å] system and an attraction in the C15-H15...O1 bond system [C15-H15...O1 2.69Å, 96.7°; C15...O1 2.795(2)Å]. This asymmetry is comparable to that which was observed in the molecular structure of *N*-(2-furoyl)thiocarbamic-*O*-isopropyl ester reported by Morales *et al.*[45]

In the crystal structure, adjacent molecules of **H(L^2-*S,O*)** are linked through a classic N1-H1...O1^{ii} intermolecular hydrogen bond [N1-H1...O1^{ii} 2.05Å, 149.4°; symmetry code (ii) x, -y, ½+z] which results in the formation of one dimensional molecular chains of **HL^2** parallel to [001] as illustrated in Figure 6. The N1-H1...O1^{ii} intermolecular hydrogen bond appears to be stabilized by a non-classical intermolecular C11-H11...O1^{ii} hydrogen contact [C11-H11...O1^{ii} 2.64Å, 104.0°]. A second

intramolecular hydrogen contact is observed, C4-H41...S1 [C4-H41...S1 2.60Å, 99.6°]. However, the intramolecular C4-H41...S1 contact appears to have little effect on the packing of the molecules of **H(L^2-*S,O*)** within the unit cell. The inter- and intramolecular hydrogen bonding and hydrogen contact geometries identified for **H(L^2-*S,O*)** is listed in Table 5.

	Type	D-H...A	D-H (Å)	H...A (Å)	D...A (Å)	D-H...A (°)
H(L^2-*S,O*)	Inter	N1-H1...O1^{ii}	0.88	2.05	2.838(2)	149.4
	Inter	C11-H11...O1^{ii}	0.95	2.64	3.013(2)	104.0
	Inter	C13-H13...Cg1^{iii}	0.95	2.59	3.496	159.6
	Intra	C4-H41...S1	0.99	2.69	3.022(2)	99.6

Table 5 Inter- and intramolecular hydrogen bonding and hydrogen contact geometry for **H(L^2-*S,O*)** as identified by XSeed[48, 49] and Platon[50] with s.u.s of the donor...acceptor (D...A) distances (Å) in parenthesis. Symmetry codes (ii) x, -y, ½+z; (iii) ½+x, y-½, ½+z.

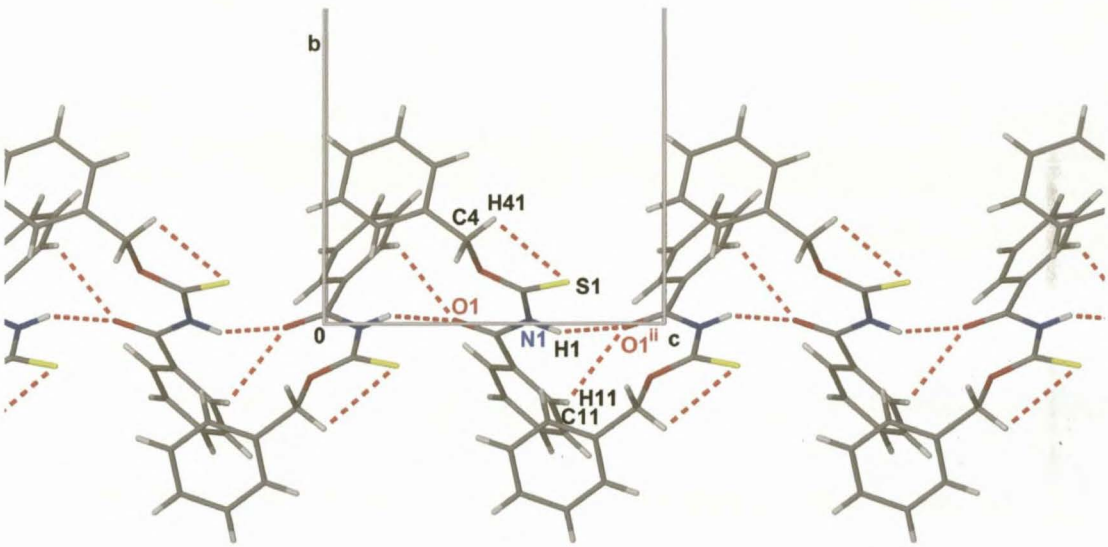

Figure 6 N1-H1...O1^{ii} intermolecular hydrogen bonding and C11-H11...O1^{ii} intermolecular hydrogen contact as viewed along [100] resulting in molecules extending as one dimensional chains parallel to the crystallographic *c*-axis. Intramolecular C4-H41...S1 hydrogen contacts have also been indicated. Symmetry code (ii) x, -y, ½+z.

A further intermolecular hydrogen interaction is observed which influences the packing of molecules of **H(L^2-*S,O*)** within the unit cell. An edge-to-face C-H...π intermolecular interaction is observed for C13-H13...Cg1^{iii}, where Cg1^{iii} is the centroid of the C5-C10 phenyl ring [C13-H13...Cg1^{iii} 2.59Å, 159.2°; symmetry code (iii) ½+x, y-½, ½+z]. This C-H...π interaction causes the one dimensional molecular chains which extend parallel to [001], as illustrated in Figure 6, to form two dimensional sheets alternatively interlocking along [111] and [$\bar{1}\,\bar{1}\,\bar{1}$]. These two dimensional sheets are illustrated in Figure 7 and are coloured blue and green respectively. The formation of the C13-H13...Cg1^{iii} interaction is clearly illustrated by the use of van der Waals radii in Figure 8.

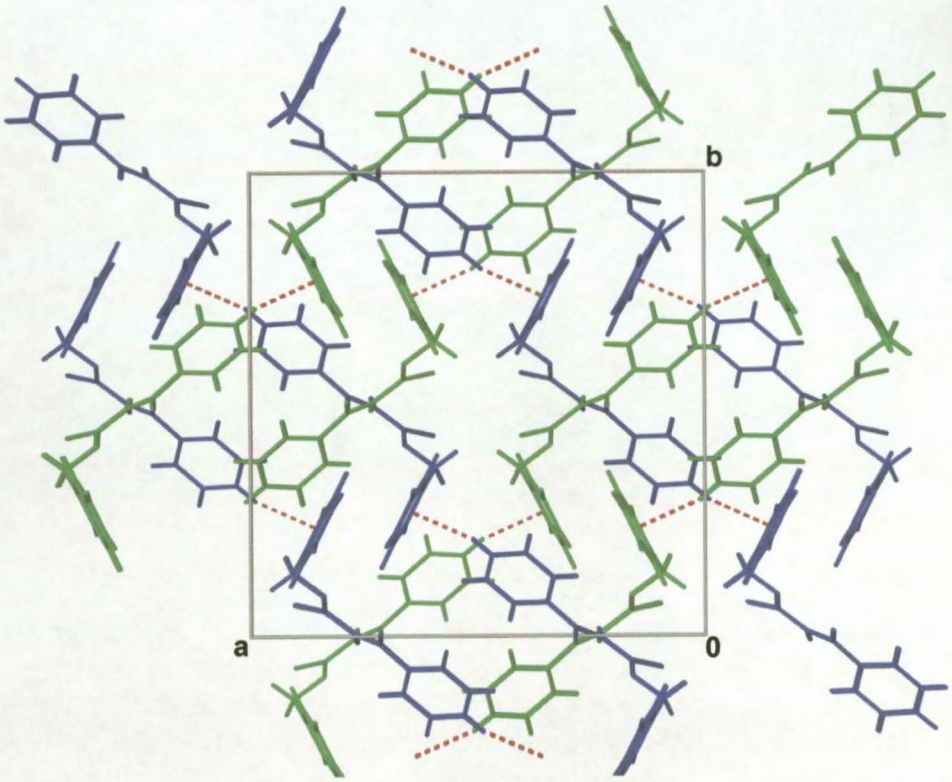

Figure 7 Extended packing diagram of H(L^2-*S,O*) as viewed along [001]. The alternate two dimensional sheets along [1 1 1] and [$\bar{1}$ $\bar{1}$ $\bar{1}$] resulting from the C-H...π interaction [C13-H13...Cg1^{iii}] have been indicated in blue and green respectively. Symmetry code (iii) ½+x, y-½, ½+z.

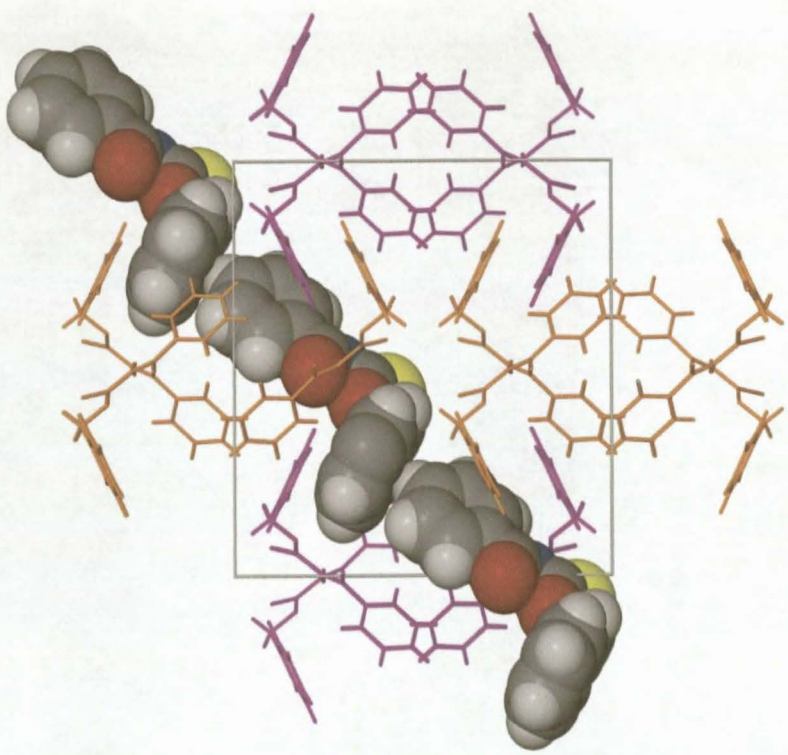

Figure 8 Extended packing diagram of H(L^2-*S,O*) as viewed along [001]. The C-H...π interaction [C13-H13...Cg1^{iii}] is indicated using a space filling model based on van der Waals radii. Symmetry code (iii) ½+x, y-½, ½+z.

The C-H…π interaction, as observed in **H(L^2-*S,O*)**, has been identified in the literature as a type of non-classical intermolecular hydrogen interaction which often dictates the overall packing of aromatic molecules in the unit cells of crystals[54]. The C-H…π interaction of **H(L^2-*S,O*)** has a centre-to-centre distance of 4.849Å [*Cg1…Cg1*^{iii}] which compares well with the C-H…π interactions reported for three benzoylfuran-2-yl ketone derivatives[55], the distance of 4.96Å between the centres of mass for the gas-phase benzene dimer reported by Arunan and Gutowsky[56], the ab initio calculated C-H…π interactions of the benzene dimer[57], as well as with the 5.05Å mean distance between phenyl ring centroids for interacting side chains in proteins[58].

2.7.3 Comparison of bond lengths of interest for H(L^1-*S,O*), H(L^2-*S,O*), *N*-(*2*-furoyl)thiocarbamic-*O*-isopropyl ester[45] and *N*-(*2*-furoyl)thiocarbamic-*O*-benzyl ester[46].

At the time of this research into the preparation and characterisation of *N*-aroylthiocarbamic-*O*-alkyl esters commencing, there was only one comparative structure listed on the Cambridge Structural Database (CSD)[21, 59], that being the structure of *N*-(*2*-furoyl)thiocarbamic-*O*-isopropyl ester[45]. Recently the molecular structure of *N*-(*2*-furoyl)thiocarbamic-*O*-benzyl ester[46] was also reported in the literature. It may then be instructive to compare the bond lengths of interest and the relative *S,O*-conformation of **H(L^1-*S,O*)** and **H(L^2-*S,O*)** with the comparable bond lengths and relative *S,O*-conformations reported for *N*-(*2*-furoyl)thiocarbamic-*O*-isopropyl ester[45] and *N*-(*2*-furoyl)thiocarbamic-*O*-benzyl ester[46] (see Table 6). The relative *cis/trans S,O*-conformations of each structure is compared by quoting the respective S-C-C-O improper torsion angle of the *S,O*-moiety. It must be noted that in the case of the molecular structure of *N*-(*2*-furoyl)thiocarbamic-*O*-benzyl ester by Montiel-Ortega *et al.*[46], both the *syn-S,O* and *anti-S,O* isomers were isolated, in which the *cis* and *trans* isomers of *N*-(*2*-furoyl)thiocarbamic-*O*-benzyl ester co-crystallized.

Several trends can be identified in the bond lengths as listed in Table 6. In all cases, both the amidic C(O)-N and the thiocarbamate HN-C(S) bond lengths are shorter than the accepted average single C-N bond length of 1.472(5)Å[7, 47]. With two exceptions, the trend appears to be that the C(O)-NH bond length is comparable in length to the HN-C(S) bond length. In the case of **H(L^1-*S,O*)**, the thiocarbamate HN-C(S) bond of 1.437(2)Å is significantly longer than the amidic C(O)-NH bond of 1.369(2)Å, while in the case of the *trans*-isomer of *N*-(*2*-furoyl)thiocarbamic-*O*-benzyl ester, the HN-C(S) bond of 1.381Å is significantly shorter than the C(O)-NH bond of 1.410Å. This is in contrast to a trend that was reported for the structurally analogous *N*-aroyl(acyl)-*N'*,*N'*-dialkylthioureas[7]. The amidic C(O)-NH, thioamide HN-C(S) and C(S)-NR_2 bonds of *N*-aroyl(acyl)-*N'*,*N'*-dialkylthioureas were all identified as being shorter than a C-N single bond and a trend within these bonds of increasing bond length in the order C(S)-NR_2 < C(O)-NH < HN-C(S) was identified[7].

	H(L^1-*S,O*)	H(L^2-*S,O*)	*N*-(2-furoyl)thiocarbamic-*O*-isopropyl ester[45]	*N*-(2-furoyl)thiocarbamic-O-benzyl ester[#46]	
Relative *S,O*-conformation	*cis/syn*	*trans/anti*	*trans/anti*	*cis/syn*	*trans/anti*
C=O	1.168(2)	1.214(2)	1.194(6)	1.220	1.201
C=S	1.587(2)	1.653(2)	1.636(5)	1.633	1.628
RC(O)-NH	1.369(2)	1.391(2)	1.387(6)	1.372	1.410
HN-C(S)OR	1.437(2)	1.380(2)	1.387(6)	1.379	1.381
C(S)-OR	1.273(2)	1.320(2)	1.290(6)	1.331	1.308
S-C-C-O	-17.9(1)	174.0(2)	180.0[*]	15.8[*]	149.5[*]

Table 6 Comparison of bond lengths (Å) of interest and relative *S,O*-conformations (°) within the molecular structures of H(L^1-*S,O*), H(L^2-*S,O*), *N*-(2-furoyl)thiocarbamic-O-isopropyl ester[45] and *N*-(2-furoyl)thiocarbamic-O-benzyl ester[46].

If the bond lengths of the *N*-aroylthiocarbamic-*O*-alkyl esters as listed in Table 6 are compared, it is clear that the bond lengths of both the carbonyl (C=O) and thiocarbonyl (C=S) bonds of **H(L^1-*S,O*)** [C2-O1 1.168(2), C3-S1 1.587(2)] are significantly shorter than the comparable bonds in the other structures listed. Furthermore, **H(L^1-*S,O*)** is the only molecule that was individually isolated in the solid state in the *cis-S,O* conformation. All the other *N*-aroylthiocarbamic-*O*-alkyl esters were isolated either in the *trans-S,O* conformation, or as a mixture of molecules in *cis* and *trans* conformations.

2.7.4 Comparison of important bond lengths of *N*-aroyl-*N'*-alkylthioureas and *N*-aroyl-*N',N'*-dialkylthioureas to the comparable bond lengths of H(L^1-*S,O*) and H(L^2-*S,O*).

Searches carried out on the Cambridge Structural Database (CSD)[21] for structures which contain the moieties A, B, C, and D as listed in Table 7, where A corresponds to the *N*-benzoyl-*N'*-alkylthiourea motif, B to the *N*-benzoyl-*N',N'*-dialkylthiourea motif, while C and D correspond to the motif contained within the *N*-benzoylthiocarbamic-*O*-alkyl esters **H(L^1-*S,O*)** and **H(L^2-*S,O*)**. A, B, C and D are depicted in Table 7 using the bond order notation and connectivity as used when carrying out structural searches on the CSD. The number of structural matches found on the CSD for A and B as well as for fragments C and D have been indicated as 'hits'. The maximum and minimum bond lengths, as well as the average bond length of each bond motif as obtained from this search are listed for A, B, C and D. The specific bond lengths of the comparable bond motifs of **H(L^1-*S,O*)** and **H(L^2-*S,O*)** are also listed. Table 7 thus allows the comparison of bond lengths of interest within fragments A, B, C and D to those of **H(L^1-*S,O*)** and **H(L^2-*S,O*)**.

[#] The bond lengths of interest were not reported by Montiel-Ortega *et al.* in the J. Chem. Crystallogr. article itself. The bond lengths were obtained from the Cambridge Structural Database (CSD), s.u values of these bonds are thus not quoted.

[*] These improper torsion angles were not quoted in the literature by Morales *et al.* and Montiel-Ortega *et al.* These values were obtained from the Cambridge Structural Database (CSD), s.u value are thus not quoted.

In general, the bond length of the carbonyl (C=O) and thiocarbonyl (C=S) moieties of **H(L^1-*S,O*)** are considerably shorter than the average determined for the comparable bonds of both the analogous *N*-benzoyl-*N'*-alkylthioureas [A in Table 7] and the *N*-benzoyl-*N',N'*-dialkylthioureas [B in Table 7]. Conversely, the N-C(S) bond length of **H(L^1-*S,O*)** is longer than the average determined for the comparative bond lengths of the *N*-benzoyl-*N'*-alkylthiourea and the *N*-benzoyl-*N',N'*-dialkylthiourea [A and B in Table 7]. Furthermore, the C(S)-O bond length of **H(L^1-*S,O*)** is slightly shorter than the average determined for the comparable bond length of fragments C and D. The bond lengths of interest for **H(L^2-*S,O*)** appear to be comparable in length to the average bond lengths determined for the corresponding bonds of interest in A, B, C and D. Furthermore, for A and B in Table 7, the average carbon-nitrogen bond lengths of interest follow with increasing bond length C(S)-N'HR/N'R_2 < C(O)-N < N-C(S), while the comparable bonds of fragment D follows with increasing bond length C(S)-O < C(O)-N ≈ N-C(S). Of further interest, is the average bond length of C(S)-NHR/NR_2 for A and B is similar to the average bond length of C(S)-OC for D. These trends offer further evidence that resonance structures (I), (II), (IV) and (V), as illustrated in Scheme 3, are the predominant resonance structures contributing to the overall molecular structure of **H(L^1-*S,O*)**.

		A 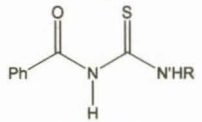 50 hits	B 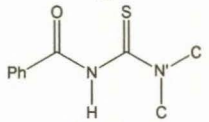 31 hits	C 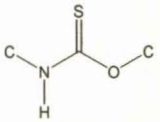 44 hits	D 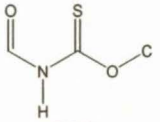 5 hits	H(L^1-*S*,*O*)	H(L^2-*S*,*O*)
C=O	min	1.198	1.197		1.194	1.168(2)	1.214(2)
	max	1.260	1.290	n/a	1.226		
	ave	1.222(1)	1.236(4)		1.212(4)		
C=S	min	1.623	1.653	1.625	1.628	1.587(2)	1.653(2)
	max	1.721	1.783	1.704	1.638		
	ave	1.673(2)	1.693(5)	1.660(2)	1.635(1)		
C(O)-N	min	1.341	1.305	1.372	1.372	1.369(2)	1.391(2)
	max	1.423	1.411	1.560	1.410		
	ave	1.379(2)	1.362(4)	1.439(5)	1.387(5)		
N-C(S)	min	1.349	1.306	1.297	1.376	1.437(2)	1.380(2)
	max	1.428	1.448	1.391	1.391		
	ave	1.385(2)	1.392(5)	1.333(3)	1.382(2)		
C(S)-N'/O	min	1.273	1.304	1.290	1.290	1.273(2)	1.320(2)
	max	1.391	1.374	1.368	1.344		
	ave	1.326(3)	1.333(2)	1.333(2)	1.323(7)		

Table 7 Comparison of bond lengths of interest (Å) within the analogous *N*-aroyl-*N'*-alkylthioureas **[A]**, *N*-aroyl-*N',N'*-dialkylthiourea **[B]** and the comparative moieties common to the *N*-benzoyl-thiocarbamic-*O*-alkyl esters **H(L^1-*S*,*O*)** and **H(L^2-*S*,*O*) [C and D]** as determined from the CSD version 5.27 Nov 2005, update Jan 2006.

2.8 Single Crystal X-ray Diffraction Analysis of Bis(*O*-alkyl-*N*-benzoylthiocarbamato)metal(II) complexes.

The molecular and crystal structures of the following complexes were determined by single crystal X-ray diffraction:

Ni(L^1-*S,O*)$_2$, Pd(L^1-*S,O*)$_2$, Pt(L^1-*S,O*)$_2$

Ni(L^2-*S,O*)$_2$, Pd(L^2-*S,O*)$_2$

Ni(L^3-*S,O*)$_2$

Ni(L^4-*S,O*)$_2$

Pt(L^6-*S,O*)$_2$

2.8.1 Bis(*N*-benzoyl-*O*-ethyl-thiocarbamato)nickel(II), Ni(L^1-*S,O*)$_2$.

Ni(L^1-*S,O*)$_2$ crystallizes in the monoclinic crystal system in space group Cc. The molecular structure of **Ni(L^1-*S,O*)$_2$** is illustrated in Figure 9 showing the numbering scheme used. **Ni(L^1-*S,O*)$_2$** has crystallised in a square planar bidentate *cis*-(*S,O*) fashion, similar to that which is observed in all cases, barring one, in the molecular structures of the *bis* complexes of d^8 transition metals of the *N*-aroyl-*N'*-alkyl- and *N*-aroyl-*N',N'*-dialkylthioureas[7, 27, 60].

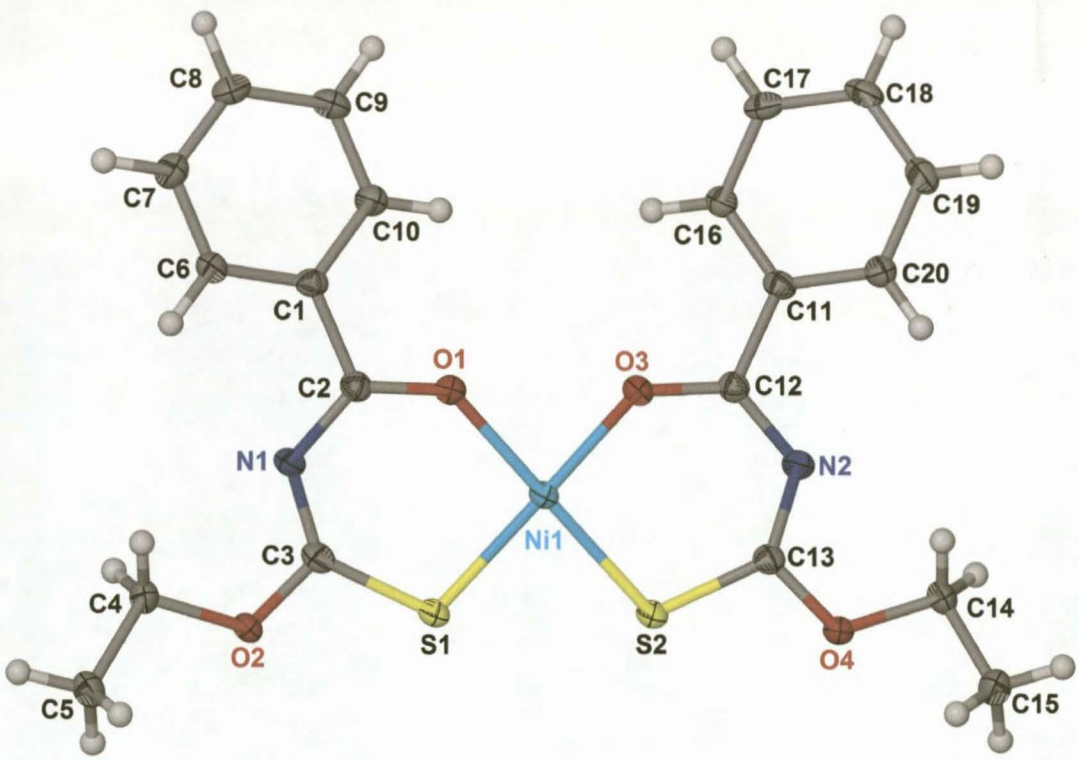

Figure 9 Molecular structure of **Ni(L^1-*S,O*)$_2$** showing the numbering scheme used. Displacement ellipsoids are shown at the 50% probability level.

When viewed side-on in the crystal structure, the overall shape of the **Ni(L^1-*S,O*)$_2$** complex can be described as being slightly bent or 'cup-shaped' (Figure 10). The least-squares plane of each of the

phenyl rings intersect each other at 31.2(1)°, while the least-squares plane as defined through each of the chelation rings intersect at 5.9(1)°. Furthermore, the C1/C6-C10 least-squares plane intersects the O1/C2/N1/C3/S1 least squares plane at 15.1(1)° while the C11/C16-C20 least-squares plane intersects the O3/C12/N2/C13/S2 least-squares plane at 12.7(1)°. Despite the overall 'cup-shaped' nature of the **Ni(L^1-*S,O*)$_2$** complex, each six membered chelate ring (NiSCNCO) in the complex is essentially planar, the greatest deviation from the O1/C2/N1/C3/S1 and O3/C12/N2/C13/S2 least-squares planes being C3 and C13 by 0.029(1)Å and 0.036(1)Å respectively.

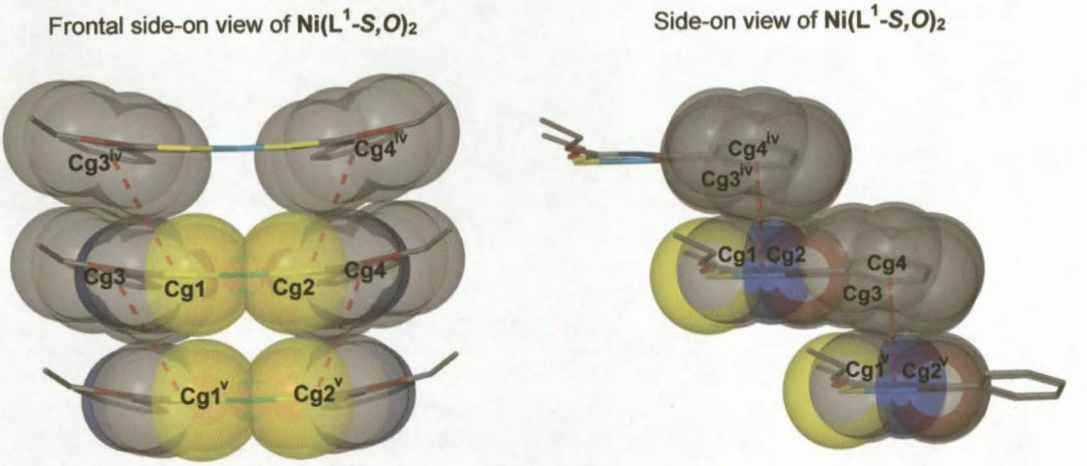

Figure 10 Observed intermolecular π…π interactions between Cg1…Cg3^{iv} and Cg3…Cg1^{v} as well as between Cg2…Cg4^{iv} and Cg4…Cg2^{iv} of adjacent molecules of **Ni(L^1-*S,O*)$_2$**. Hydrogen atoms have been excluded for clarity. Symmetry code (iv) 1+x, y, z; (v) x-1, y, z.

As shown in Figure 11, it is proposed that the phenyl rings are assisted in being brought into close coplanarity with the adjacent chelation rings by a non-classical 1-5 intramolecular hydrogen contact between each *ortho*-hydrogen of the phenyl ring and the adjacent oxygen or nitrogen atom of the neighbouring chelation ring. The intermolecular hydrogen contacts observed are C6-H6…N1 [C6-H6…N1 2.49Å, 99.0°], C10-H10…O1 [C10-H10…O1 2.46Å, 97.5°] as well as C16-H16…O3 [C16-H16…O3 2.46Å, 97.8°] and C20-H20…N2 [C20-H20…N2 2.49Å, 99.0°]. In each case, the H…A distances of the intramolecular hydrogen contacts, as listed in Table 8, are significantly shorter than the sum of the van der Waals radii of hydrogen and oxygen [2.72Å] or nitrogen [2.75Å]. These non-classical 1,5 intramolecular hydrogen contacts are illustrated in Figure 12 where the overlap of the van der Waals radii of the respective hydrogen and oxygen or nitrogen atoms is shown.

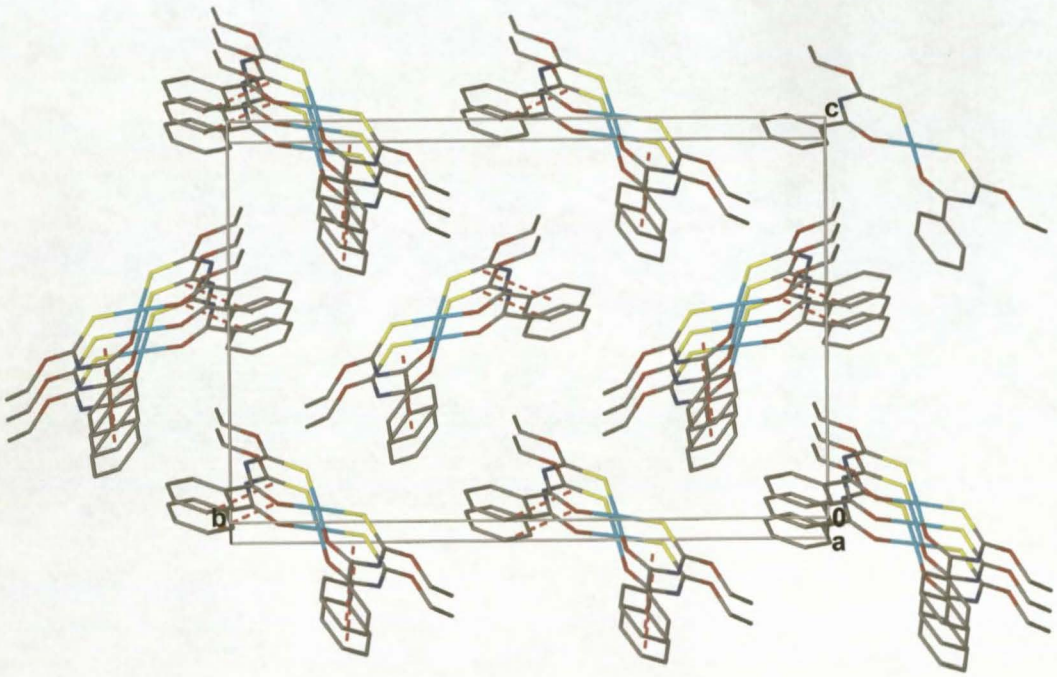

Figure 11 Extended packing diagram of **Ni(L^1-*S,O*)$_2$** as viewed across the *b-c* plane illustrating the herring bone arrangement of the molecules presumably resulting from the π...π interactions as indicated. Hydrogen atoms have been omitted for clarity.

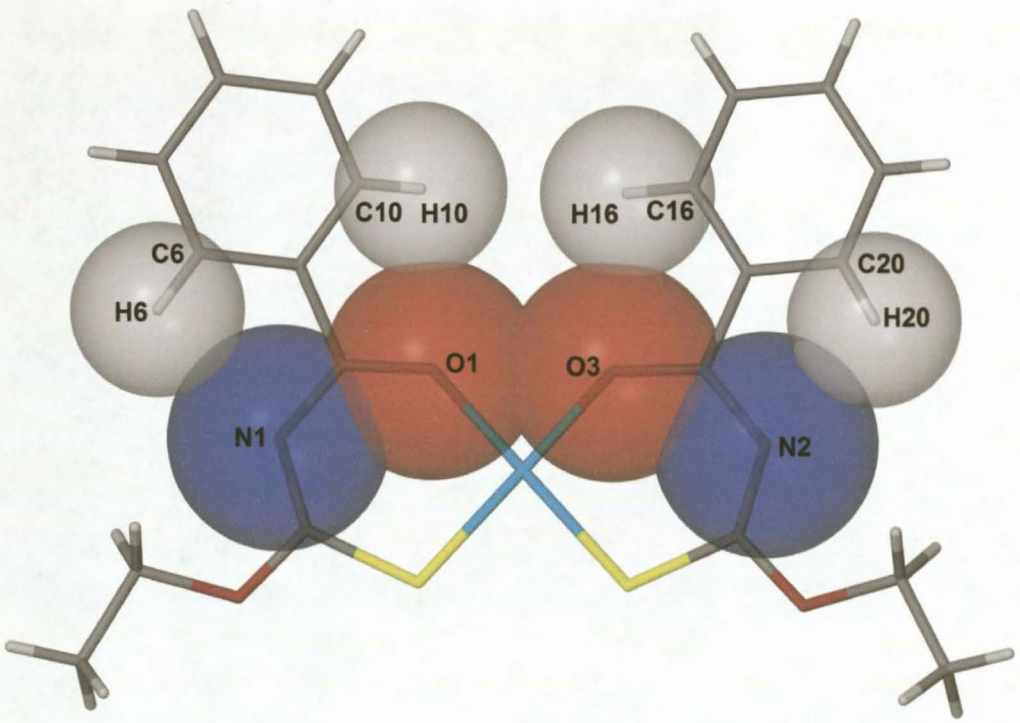

Figure 12 C6-H6...N1, C10-H10...O1 and C16-H16...O3, C20-H20...N2 intramolecular 1-5 hydrogen contacts indicated using the van der Waals radii of the respective hydrogen, nitrogen and oxygen atoms.

It is acknowledged that the values of the intermolecular hydrogen contacts quoted above may have more 'value' if the respective hydrogen atoms were found/located and not placed/calculated during the solving and refining of the molecular structure of **Ni(L^1-*S,O*)$_2$**. It is possible to locate these hydrogen atoms in the Fourier transform diffraction map and then calculate the resulting 1-5 intramolecular hydrogen contacts by using SHELXL[61]. However, the values of the resulting 1-5 intramolecular hydrogen contact distances and angles do not change significantly. The values of the intramolecular hydrogen contact distances and angles for both the found/located hydrogen atoms as well as the placed/calculated hydrogen atoms have been tabulated in Table 8. In general, the differences in these values fall well within the experimental error (s.u) and can thus be considered as comparable.

method	D-H...A	D-H (Å)	H...A (Å)	D...A (Å)	D-H...A (°)
calculated	C6---H6...N1	0.95	2.49	2.802(2)	99.0
located		0.97(2)	2.51(2)	2.802(3)	97(2)
calculated	C10---H10...O1	0.95	2.46	2.746(2)	97.5
located		0.88	2.48(2)	2.748(3)	98(2)
calculated	C16-H16...O3	0.95	2.46	2.753(2)	97.8
located		1.02(2)	2.46(2)	2.752(3)	96(1)
calculated	C20-H20...N2	0.95	2.49	2.800(3)	99.0
located		0.95(3)	2.47(3)	2.798(3)	101(2)

Table 8 1-5 intramolecular hydrogen contact geometry for **Ni(L^1-*S,O*)$_2$** as determined for placed/calculated hydrogens as well as for found/located hydrogens as identified by XSeed[48, 49] and Platon[50] with s.u.s in parenthesis.

The extended packing diagram of **Ni(L^1-*S,O*)$_2$** as viewed across the *b-c* plane is shown in Figure 11. The molecules of **Ni(L^1-*S,O*)$_2$** pack in a twin herringbone fashion. No classical intermolecular hydrogen bonds or contacts are observed. However, due to the observed relative coplanarity of the phenyl rings and chelate rings, several intermolecular π...π type interactions are observed between the phenyl rings and the chelation rings of adjacent molecules. These intermolecular π...π interactions appear to largely dictate the overall packing of the molecules of **Ni(L^1-*S,O*)$_2$** within the unit cell. π...π interactions are observed between Cg1...Cg3^{iv} and Cg3...Cg1^{v} [Cg1...Cg3^{iv} 4.179Å; Cg3...Cg1^{v} 4.179Å; where Cg1 is the centroid of the O1-C2-N1-C3-S1-Ni1 chelation ring and Cg3 is the centroid of the C1-C6-C7-C8-C9-C10 phenyl ring; symmetry code (iv) 1+x, y, z, (v) x-1, y, z]. Further π...π type interactions are observed between Cg2...Cg4^{iv} and Cg4...Cg2^{v} [Cg2...Cg4^{iv} 3.950Å; Cg4...Cg2^{v} 3.950Å where Cg2 is the centroid of the O3-C12-N2-C13-S2-Ni1 chelation ring and Cg4 is the centroid of the C11-C16-C17-C18-C19-C20 phenyl ring].

The intermolecular π...π interactions observed in the unit cell of **Ni(L^1-*S,O*)$_2$** are clearly indicated by the overlap of the van der Waals radii of adjacent molecules as illustrated in Figure 10.

2.8.2 Bis(*N*-benzoyl-*O*-ethyl-thiocarbamato)palladium(II), Pd(L^1-*S,O*)$_2$.

The complex **Pd(L^1-*S,O*)$_2$** shown in Figure 13 crystallizes monoclinic in space group Cc with four formula units per unit cell. Complex **Pd(L^1-*S,O*)$_2$** is essentially isostructural to **Ni(L^1-*S,O*)$_2$**.

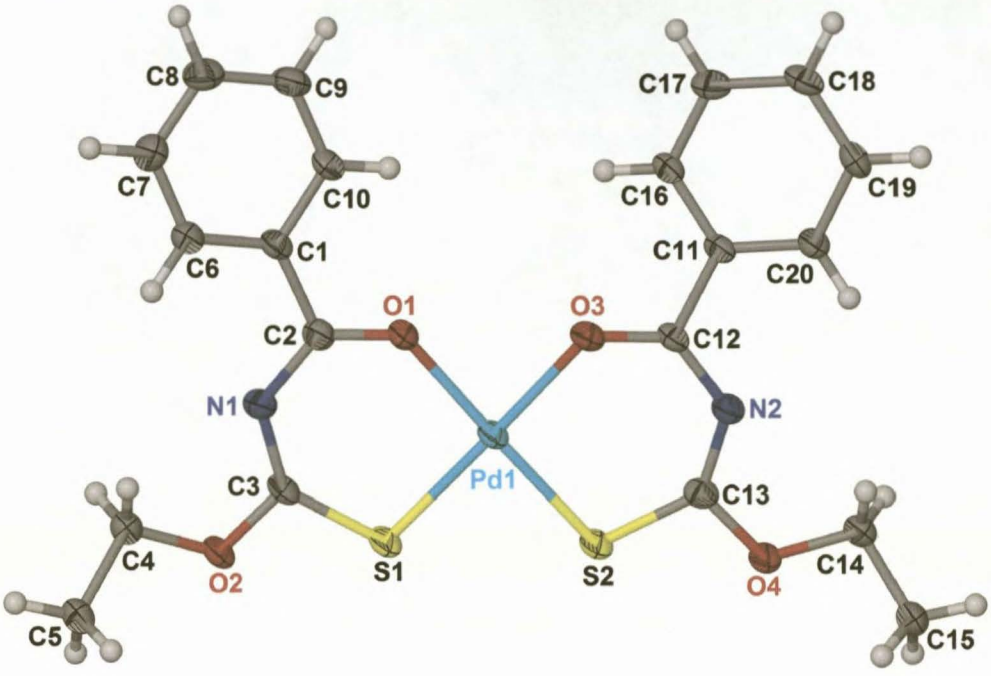

Figure 13 Molecular structure of **Pd(L^1-*S,O*)$_2$** showing the numbering scheme used. Displacement ellipsoids are drawn at the 50% probability level.

Complex **Pd(L^1-*S,O*)$_2$** is relatively planar with the greatest deviation from planarity in each of the least-squares planes of the chelate rings, O1/C2/N1/C3/S1/Pd1 and O3/C12/N2/C13/S2/Pd1 being C3 and C13 by 0.031(2)Å and 0.035(2)Å respectively. The phenyl rings, C1-C6-C7-C8-C9-C10 and C11-C16-C17-C18-C19-C20, are twisted towards each other to a small degree with the respective least-squares planes intersecting at 28.8(2)°. Nonetheless, each of the phenyl rings of **Pd(L^1-*S,O*)$_2$** remain in close coplanarity to the chelation rings [the O1/C2/N1/C3/S1/Pd1 and C1/C6/C7/C8/C9/C10 least-squares plane intersect at 15.4(2)° while the O3/C12/N2/C13/S2/Pd1 and C11/C16/C17/C18/C19/C20 least-squares planes intersect at 13.3(2)°]. As illustrated in Figure 14, complex **Pd(L^1-*S,O*)$_2$** is slightly bent in a similar fashion to that which was observed for complex **Ni(L^1-*S,O*)$_2$**. Several non-classical 1-5 intramolecular hydrogen contacts, comparable to that which was observed in the molecular structure of **Ni(L^1-*S,O*)$_2$** [see Figure 12], were observed between C6-H6…N1 [C6-H6…N1 2.52Å, 98.4°], C10-H10…O1 [C10-H10…O1 2.45Å 97.2°], C16-H16…O3 [C16-H16…O3 2.44 97.7] and C20-H20…N2 [C20-H2-…N2 2.50Å 98.8°] as listed in Table 9. The intramolecular hydrogen contact distances and angles, as determined when the respective hydrogens are placed/calculated, are similar to the hydrogen contact distances and angles determined when the respective hydrogens are found/located during the solving and refining process of the molecular structure of **Pd(L^1-*S,O*)$_2$**.

method	D-H...A	D-H (Å)	H...A (Å)	D...A (Å)	D-H...A (°)
calculated	C6---H6...N1	0.95	2.52	2.819(5)	98.4
located		0.84(5)	2.55(5)	2.822(5)	100(4)
calculated	C10---H10...O1	0.95	2.45	2.739(4)	97.2
located		0.97	2.45(3)	2.737(4)	97(2)
calculated	C16-H16...O3	0.95	2.44	2.733(4)	97.7
located		0.91(5)	2.51(4)	2.733(4)	94(3)
calculated	C20-H20...N2	0.95	2.50	2.808(5)	98.8
located		0.96(4)	2.48(5)	2.808(5)	100(3)

Table 9 Non-classical 1-5 intramolecular hydrogen contact geometry observed for **Pd(L^1-*S,O*)$_2$** as determined for placed/calculated hydrogens as well as for found/located hydrogens as identified by XSeed[48, 49] and Platon[50] with s.u.s in parenthesis.

In addition to the non-classical hydrogen contacts observed, several intermolecular π...π type interactions were observed. Intermolecular π...π type interactions were observed between Cg1...Cg3^{vi} and Cg3...Cg1^{vii} [Cg1...Cg3^{vi} 4.211Å, Cg3...Cg1^{vii} 4.211Å, where Cg1 is the centroid of the O1-C2-N1-C3-S1-Pd1 ring and Cg3 is the centroid of the C1-C6-C7-C8-C9-C10 ring; symmetry code (vi) 1+x, y, z; (vii) x-1, y, z]. Further π...π type interactions were observed between Cg2...Cg4^{vi} and Cg4...Cg2^{vii} [Cg2...Cg4^{vi} 3.936Å, Cg4...Cg2^{vii} 3.936Å, where Cg2 is the centroid of the O3-C12-N2-C13-S2-Pd1 ring and Cg4 is the centroid of the C11-C16-C17-C18-C19-C20 ring; symmetry code (vi) 1+x, y, z; (vii) x-1, y, z]. These intermolecular π...π interactions are illustrated in Figure 14 with the aid of van der Walls radii.

Frontal side-on view of **Pd(L^1-*S,O*)$_2$** Side view of **Pd(L^1-*S,O*)$_2$**

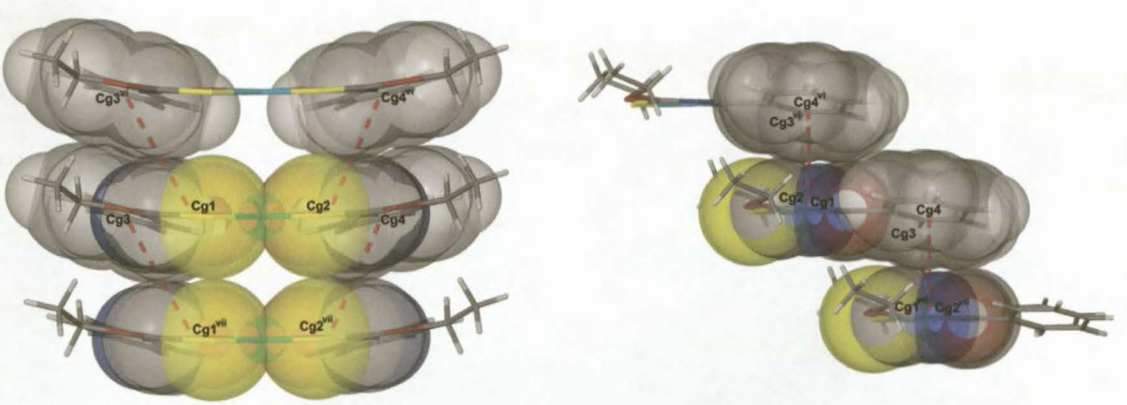

Figure 14 Intermolecular π...π interactions observed between Cg1...Cg3^{vi} and Cg2...Cg4^{vi} as well as between Cg3...Cg1^{vii} and Cg4...Cg2^{vii} of adjacent molecules of **Pd(L^1-*S,O*)$_2$**.

No classical intermolecular hydrogen contacts or bonds were observed between molecules in the unit cell of **Pd(L^1-*S,O*)$_2$**. Therefore, it is proposed that the intermolecular π...π type interactions, as described, largely dictate the packing of the molecules in the unit cell of **Pd(L^1-*S,O*)$_2$** which can be described as essentially packing in a twin herring bone fashion as illustrated in Figure 15.

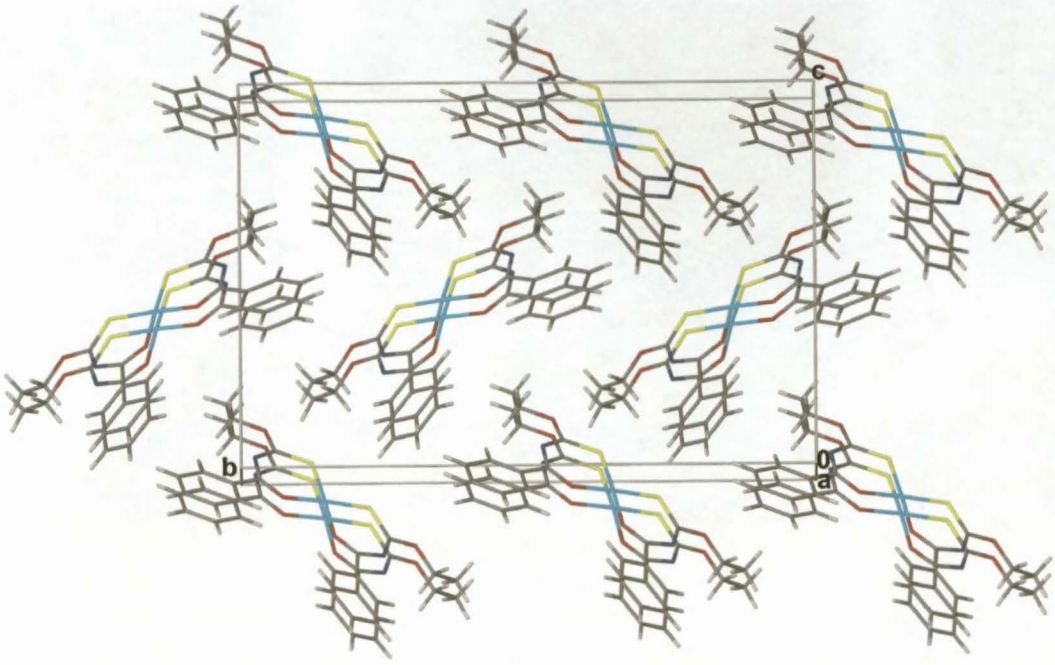

Figure 15 An extended packing diagram of **Pd(L^1-*S,O*)$_2$** as viewed along (100).

2.8.3 Bis(*N*-benzoyl-*O*-ethyl-thiocarbamato)platinum(II), Pt(L^1-*S,O*)$_2$.

Pt(L^1-*S,O*)$_2$ crystallizes monoclinic in space group Cc with four formula units per unit cell. The molecular structure of **Pt(L^1-*S,O*)$_2$** is illustrated in Figure 16 showing the numbering scheme used. Complex **Pt(L^1-*S,O*)$_2$** is isostructural to complex **Ni(L^1-*S,O*)$_2$** and complex **Pd(L^1-*S,O*)$_2$**.

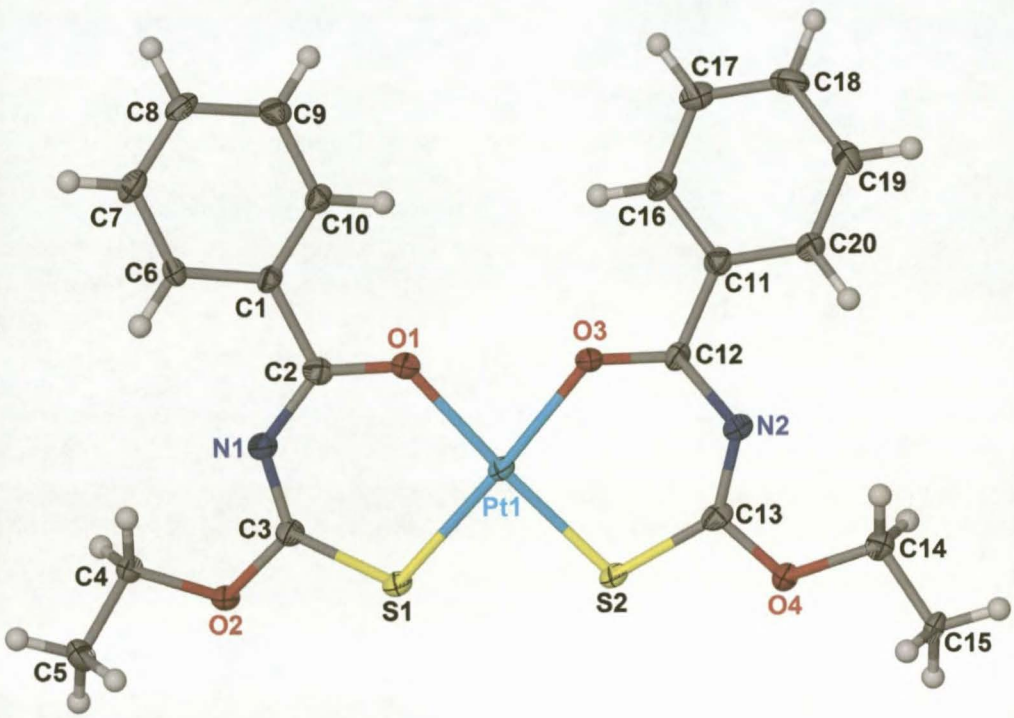

Figure 16 Molecular structure of **Pt(L^1-*S,O*)$_2$** showing the numbering scheme used. Displacement ellipsoids are drawn at the 50% probability level.

Similar to that illustrated in Figure 10 and Figure 14 for complexes **Ni(L^1-*S,O*)$_2$** and **Pd(L^1-*S,O*)$_2$** respectively, complex **Pt(L^1-*S,O*)$_2$** is 'cup-shape' when viewed side on in the crystal lattice. The chelation rings in **Pt(L^1-*S,O*)$_2$** are twisted to a slightly greater degree than the comparable chelation rings in **Pd(L^1-*S,O*)$_2$**, but to a lesser degree than the comparable chelation rings in **Ni(L^1-*S,O*)$_2$**.

No classical intra- or intermolecular hydrogen bonds were observed in the molecular structure of **Pt(L^1-*S,O*)$_2$**. However, as observed in the molecular structure of **Ni(L^1-*S,O*)$_2$** [see Figure 12] and **Pd(L^1-*S,O*)$_2$**, several non-classical 1-5 intramolecular hydrogen contacts between C6-H6…N1 [C6-H6…N1 2.53Å, 98.6°] and C10-H10…O1 [C10-H10…O1 2.42Å 98.3°) as well as between C16-H16…O3 [C16-H16…O3 2.43Å 97.6°] and C20-H20…N2 [C20-H20…N2 2.51Å 98.9°] as listed in Table 10 were observed.

In the case of the molecular structures of **Ni(L^1-*S,O*)$_2$** and **Pd(L^1-*S,O*)$_2$**, the hydrogen atoms that were involved in the 1-5 intramolecular hydrogen contacts could be both located/found or calculated/placed

during the refinement process. In both cases, the differences in these hydrogen contact distances and angles were negligible and well within experimental error. However, in the case of the molecular structure of **Pt(L^1-*S,O*)$_2$**, the hydrogen atoms involved in the proposed 1-5 intramolecular contacts could only be calculated/placed and not located/found.

D-H...A	D-H (Å)	H...A (Å)	D...A (Å)	D-H...A (°)
C6-H6...N1	0.95	2.52	2.819(5)	98.4
C10-H10...O1	0.95	2.45	2.739(4)	97.2
C16-H16...O3	0.95	2.44	2.733(4)	97.7
C20-H20...N2	0.95	2.50	2.808(5)	98.8

Table 10 Intermolecular hydrogen contact geometry observed in **Pt(L^1-*S,O*)$_2$** as determined for placed/calculated hydrogen atoms identified by XSeed[48, 49] Platon[50] with s.u.s of the donor...acceptor (D...A) distances (Å) in parenthesis.

The intramolecular 1-5 hydrogen contacts, coupled with the close coplanarity of the phenyl rings with the adjacent chelation rings observed in the molecular structure of **Pt(L^1-*S,O*)$_2$**, allows the formation of intermolecular π...π type interactions between Cg1...Cg3^{viii} and Cg3...Cg1^{ix} [Cg1...Cg3^{viii} 3.915Å, Cg3...Cg1^{vi} 3.915Å, where Cg1 is the centroid of the O1-C2-N1-C3-S1-Pt1 ring and Cg3 is the centroid of the C1-C6-C7-C8-C9-C10 ring; symmetry code (viii) x-1, y, z; (vii) 1+x, y, z]. Further intermolecular π...π type electrostatic interactions were observed between Cg2...Cg4^{viii} and Cg4...Cg2^{ix} [Cg2...Cg4^{viii} 4.175Å, Cg4...Cg2^{ix} 4.175Å, where Cg2 is the centroid of the O3-C12-N2-C13-S2-Pt1 ring and Cg4 is the centroid of the C11-C16-C17-C18-C19-C20 ring; symmetry code (viii) x-1, y, z; (vii) 1+x, y, z].

It is proposed that the intermolecular π...π interactions described above, largely dictate the packing of molecules within the unit cell of **Pt(L^1-*S,O*)$_2$**. The molecules pack in twin herring bone fashion comparable to that which was observed for the molecular packing of **Ni(L^1-*S,O*)$_2$** and **Pd(L^1-*S,O*)$_2$** (see figures Figure 11 and Figure 15).

2.8.4 *Bis*(*N*-benzoyl-*O*-methyl-thiocarbamato)nickel(II), Ni(L^3-*S,O*)$_2$.

Ni(L^3-*S,O*)$_2$ crystallizes monoclinic space group $P2_1/n$ with four formula units per unit cell. Complex **Ni(L^3-*S,O*)$_2$** has crystallised in a square planar bidentate *cis*-(*S,O*) fashion as illustrated in Figure 17 with C2 and S2 deviating from the O1/C2/N1/C3/S1/Ni1 and O3/C11/N2/C12/S2/Ni1 least-squares planes by 0.049(1)Å and -0.0903(8)Å respectively.

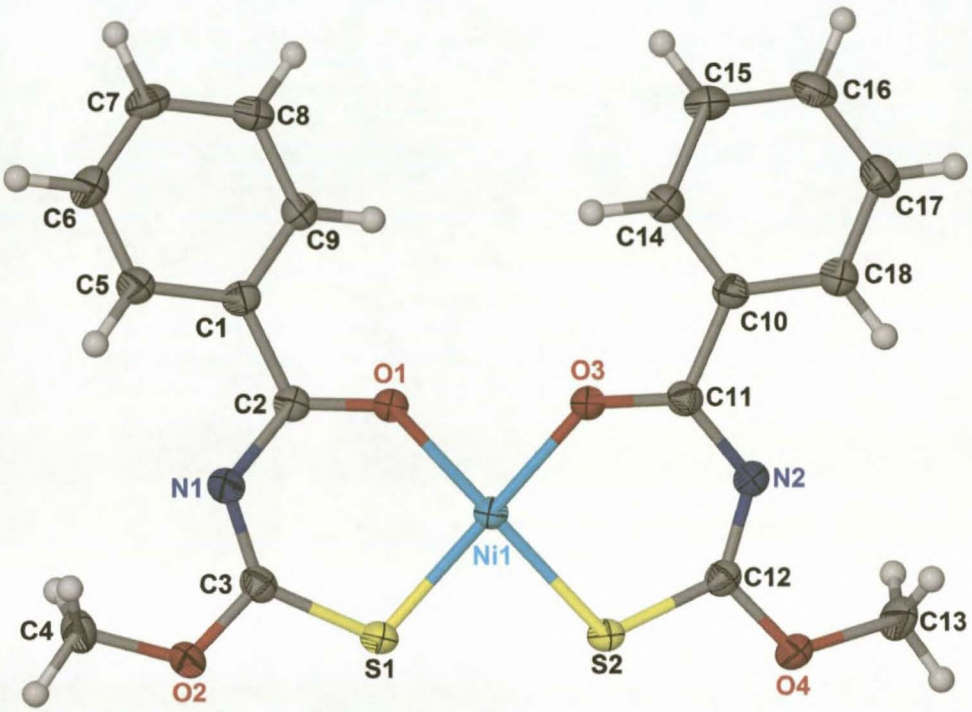

Figure 17 Molecular structure of **Ni(L^3-*S,O*)$_2$** showing the numbering scheme used. Displacement ellipsoids are drawn at the 50% probability level.

Complex **Ni(L^1-*S,O*)$_2$** and complex **Ni(L^3-*S,O*)$_2$** differ only in that **Ni(L^1-*S,O*)$_2$** contains an ethoxy substituent where **Ni(L^3-*S,O*)$_2$** has a methoxy substituent. As previously described, complex **Ni(L^1-*S,O*)$_2$** can be described as being 'cup-shaped' when viewed side-on in the crystal lattice [see **Error! Reference source not found.**] however, **Ni(L^3-*S,O*)$_2$** is more planar in nature when viewed from the same angle.

The C1-C5-C6-C7-C8-C9 phenyl ring is angled away from the O1-C2-N1-C3-S1-Ni1 chelation ring by 14.61(8)°. However, the C10-C14-C15-C16-C17-C18 phenyl ring is essentially coplanar with the O3-C11-N2-C12-S2-Ni1 chelation ring with the least-squares plane of each intersecting at 6.95(8)°.

No classical intra- or intermolecular hydrogen bonds were observed in the molecular structure of **Ni(L^3-*S,O*)$_2$**. However, 1-5 non-classical intramolecular hydrogen contacts, C5-H5…N1, C9-H9…O1, C14-H14…O3 and C18-H18…N2 were observed, which are comparable to those observed in the

molecular structure of **Ni(L^1-*S,O*)$_2$** [C5-H5...N1 2.49Å 98.8°, C9-H9...O1 2.44Å 98.6°, C14-H14...O3 2.43Å 98.6° and C18-H18...N2 2.48Å 99.3° – in Table 11]. In each case, the H...A distances of the intramolecular hydrogen contacts are significantly shorter than the sum of the van der Waals radii of hydrogen and oxygen [2.72Å] or nitrogen [2.75Å]. It is possible to locate/find each of the hydrogen atoms involved in these 1-5 hydrogen contacts during the crystal structure refinement process as opposed to calculating the positions of these hydrogen atoms. In each case the 1-5 intramolecular hydrogen contact distances and angles are similar.

method	D-H...A	D-H (Å)	H...A (Å)	D...A (Å)	D-H...A (°)
calculated	C5---H5...N1	0.95	2.49	2.793(2)	98.8
located		0.93(2)	2.50(2)	2.794(2)	98.4(14)
calculated	C9---H9...O1	0.95	2.44	2.749(2)	98.6
located		0.95(2)	2.39(2)	2.749(2)	101.8(14)
calculated	C14-H14...O3	0.95	2.43	2.734(2)	98.6
located		0.94(2)	2.40(2)	2.735(2)	100.7(14)
calculated	C18-H18...N2	0.95	2.48	2.795(2)	99.3
located		0.96(2)	2.45(2)	2.795(2)	101.1(13)

Table 11 1-5 intramolecular hydrogen contact geometry of **Ni(L^3-*S,O*)$_2$** as determined for placed/calculated hydrogens as well as for found/located hydrogens as identified by XSeed[48, 49] and Platon[50] with s.u.s in parenthesis.

Two intermolecular hydrogen contacts were observed in the molecular structure of Ni(L^3-*S,O*)$_2$ as listed in Table 12 which result in the formation of one dimensional molecular chains parallel to [100] [C7-H7...S1^{xviii} 2.96Å 131.8°; C15-H15...O4 2.79Å 152.3°; symmetry code (xviii) 1+x, y, z]. Intermolecular π...π type interactions were observed between Cg1...Cg2^{xx} and between Cg2...Cg1^{xx} [Cg1...Cg2^{xx} 3.55Å, Cg2...Cg1^{xx} 3.55Å where Cg1 is the centroid of the O1-C2-N1-C3-S1-Ni1 chelation ring while Cg2 is the centroid of the O3-C11-N2-C12-S2-Ni1 chelation ring; symmetry code (xx) 2-x, 2-y, -z]. The intermolecular π...π type interactions result in the molecules packing in a twin herringbone fashion when the unit cell is viewed along [100] as illustrated in Figure 18. The molecules involved in each twin herring bone arrangement are further cross-linked by an intermolecular C-H...π interaction [C6-H6...Cg2^{xxi} 2.97Å; symmetry code (xxi) 5/2-x, 1/2+y, 1/2-z].

method	D-H...A	D-H (Å)	H...A (Å)	D...A (Å)	D-H...A (°)
calculated	C7---H7...S1^{xviii}	0.95	2.95	3.666(2)	131.8
located		0.97(2)	2.94(2)	3.664(2)	132(1)
calculated	C15---H15...O4^{xviii}	0.95	2.79	3.662(2)	152.3
located		0.952(2)	2.83(2)	3.663(3)	152(2)

Table 12 Intermolecular hydrogen contact geometry of **Ni(L^3-*S,O*)$_2$** as determined for placed/calculated hydrogens as well as for found/located hydrogens as identified by XSeed[48, 49] and Platon[50] with s.u.s in parenthesis. Symmetry code (xviii) 1+x, y, z

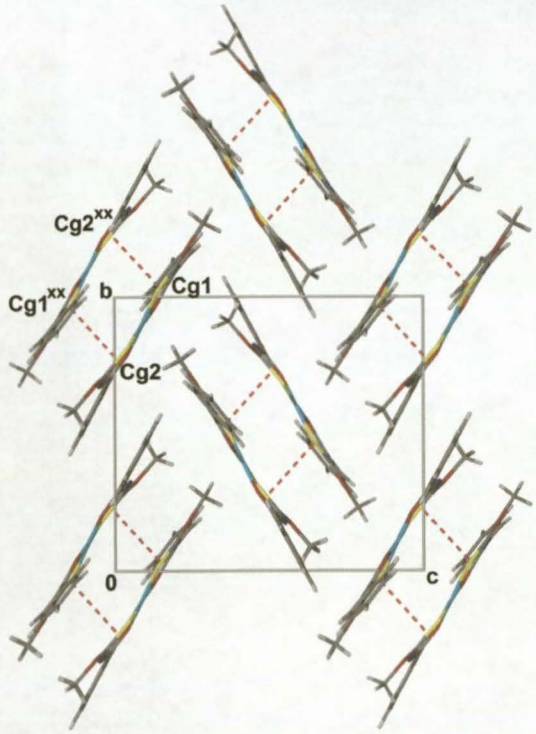

Figure 18 Extending packing diagram of Ni(L^3-*S,O*)$_2$ showing the twin herring bone arrangement of molecules within the unit cell when viewed along [100] resulting from the Cg1…Cg2^{xx} and Cg2…Cg1^{xx} interactions. Symmetry code (xx) 2-x, 2-y, -z.

2.8.5 *Bis*(*N*-benzoyl-*O*-butyl-thiocarbamato)nickel(II), Ni(L^4-*S,O*)$_2$.

Ni(L^4-*S,O*)$_2$ crystallizes monoclinic, space group *C*2/*c* with the asymmetric unit consisting of half a molecule. The complete molecule is generated with the symmetry operator –x, y, 1/2-z. The molecular structure of **Ni(L^4-*S,O*)$_2$** is illustrated in Figure 19 showing the numbering scheme used.

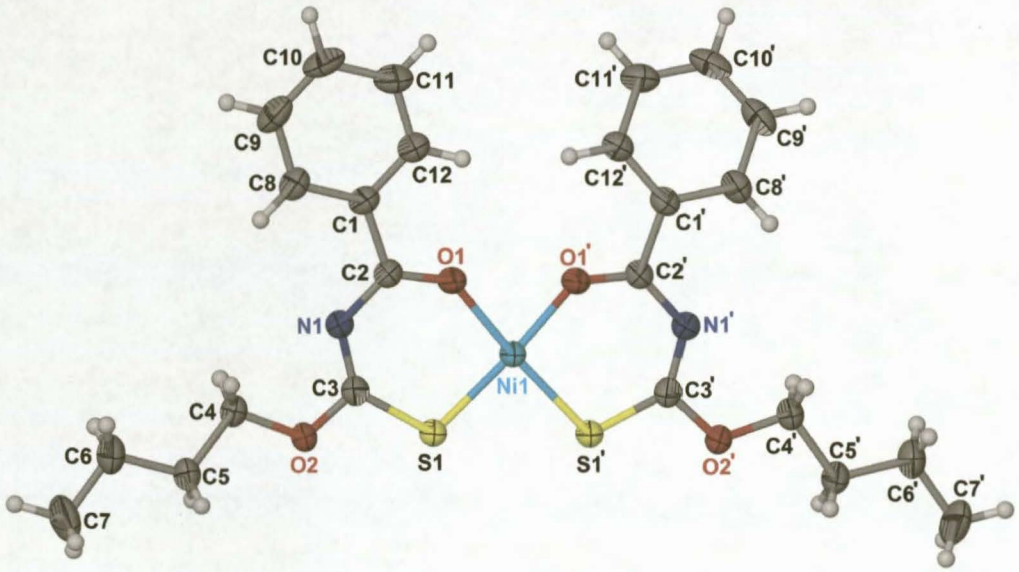

Figure 19 Molecular structure of **Ni(L^4-*S,O*)$_2$** showing the numbering scheme used. Displacement ellipsoids are drawn at the 50% probability level. Accented atoms are generated by the symmetry operator –x, y, ½-z.

Ni(L^4-*S,O*)$_2$ is isostructural to complexes **Ni(L^1-*S,O*)$_2$** and **Ni(L^3-*S,O*)$_2$**. Two non-classical 1-5 intermolecular hydrogen contacts are observed in the molecular structure of **Ni(L^4-*S,O*)$_2$**. Again, the positions of the hydrogen atoms involved in the intramolecular 1-5 hydrogen contacts can be both located/found as well as calculated/placed during the refinement process. In each case, the determined hydrogen contact geometry, as illustrated in Table 13, are similar.

method	D-H...A	D-H (Å)	H...A (Å)	D...A (Å)	D-H...A (°)
calculated	C8-H8...N1	0.95	2.52	2.823(2)	98.7
located		0.89(2)	2.53(2)	2.824(2)	100(1)
calculated	C12-H12...O1	0.95	2.39	2.703(2)	98.5
located		0.97(2)	2.38(2)	2.703(2)	99(2)
calculated	C10-H10...O2^{xxi}	0.95	2.61	3.517(2)	160.6
located		0.90(2)	2.64(2)	3.519(2)	165(2)

Table 13 Inter- and intramolecular hydrogen contact geometry of **Ni(L^4-*S,O*)$_2$** as determined for placed/calculated hydrogens as well as for found/located hydrogens as identified by XSeed[48, 49] and Platon[50] with s.u.s in parenthesis. [symmetry code (xxi) x,1+y, z].

A greater degree of overall planarity is observed in the molecular structure of **Ni(L^4-*S,O*)$_2$** than that observed in the molecular structures of **Ni(L^1-*S,O*)$_2$** and **Ni(L^3-*S,O*)$_2$**. The overall planarity of **Ni(L^4-*S,O*)$_2$** is shown in the extended packing diagram of **Ni(L^4-*S,O*)$_2$**, as viewed along [010], illustrated in Figure 20 and confirmed by torsion angles O1-C2-C1-C12, N1-C2-O1-Ni1, N1-C3-S1-Ni1 and N1-C3-O2-C4 of -10.1(2)°, -3.3(3)°, -0.8(2)° and 2.4(2)° respectively. Furthermore, the C1/C8/C9/C10/C11/C12 and O1/C2/N1/C3/S1/Ni1 least-squares planes intersect at 9.44(2)°. This essential coplanarity of the phenyl and chelate rings is possibly assisted by the C8-H8...N1 and C12-H12...O1 1-5 intramolecular hydrogen contacts listed in Table 13. Unlike that observed in complexes **M(L^1-*S,O*)$_2$** [M = Ni(II), Pd(II), Pt(II)] and **Ni(L^3-*S,O*)$_2$**, the alkoxy substituent of **Ni(L^4-*S,O*)$_2$** is largely coplanar with the O1-C2-N1-C3-S1-Ni1 chelate ring, with the O2/C4/C5/C6/C7 and O1/C2/N1/C3/S1/Ni1 least-squares planes intersecting at 4.04(2)°.

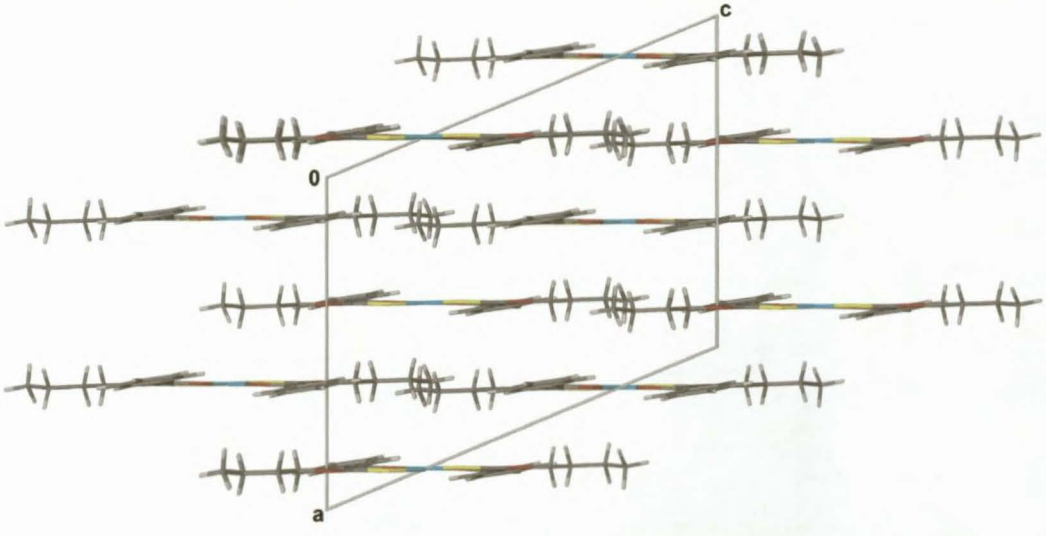

Figure 20 Extended packing diagram of **Ni(L^4-*S,O*)$_2$** as viewed along [010].

The observed intermolecular hydrogen bond, C10-H10...O2[xxi] [C10-H10...O2[xxi] 2.61Å, 160.6°], results in one dimensional molecular strings of **Ni(L^4-*S,O*)$_2$** extending parallel to [010]. It appears as though these one dimensional molecular strings are not cross linked to each other by any π...π or C-H...π type interactions. The absence of such intermolecular electrostatic interactions is in stark contrast to that observed in all the other bis(*N*-benzoyl-*O*-alkyl-thiocarbamato)metal(II) complexes of chapter 2.

2.8.6 *Bis*(*N*-benzoyl-*O*-dodecyl-thiocarbamato)platinum(II), Pt(L^6-*S,O*)$_2$.

Pt(L^6-*S,O*)$_2$ was received as a gift from Dr. U Schröder and was prepared according to methods already published[18]. Complex **Pt(L^6-S,O)$_2$** is illustrated in Figure 21 and crystallizes orthorhombic space group P*ccn* with four formula units per unit cell. The asymmetric unit consists of half a molecule of **Pt(L^6-S,O)$_2$** with the complete molecule being generated by the symmetry operator ½-x, ½-y, z. The bond lengths and torsion angles of interest in the molecular structure of **Pt(L^6-S,O)$_2$** are listed in Table 14.

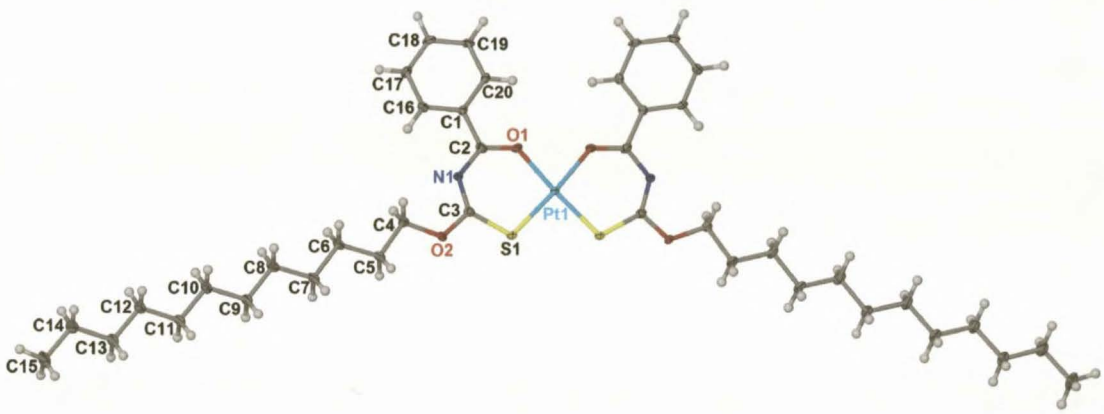

Figure 21 Molecular structure of **Pt(L^6-S,O)$_2$** showing the numbering scheme used. Displacement ellipsoids are drawn at the 50% probability level. The unlabeled atoms are generated by the symmetry operator ½-x, ½-y, z.

Complex **Pt(L^6-S,O)$_2$** is isostructural to the previous Ni(II), Pd(II) and Pt(II) complexes of the *N*-benzoylthiocarbamic-*O*-alkyl esters described in chapter 2. Despite the flexible dodecoxy substituent, the molecular structure of **Pt(L^6-S,O)$_2$** remains remarkably planar as illustrated by the torsion angles listed in Table 14. Both the phenyl ring as well as the dodecoxy substituent of **Pt(L^6-S,O)$_2$** are in close coplanarity with the Pt1-O1-C2-N1-C3-S1 chelate ring. The least-squares planes defined through the phenyl ring and the dodecoxy substituent intersect the least-squares plane of the chelate ring at 8.8(2)° and 6.1(2)° respectively. The close coplanarity of the phenyl and O1-C2-N1-C3-S1-Pt1 chelate ring is possibly assisted by the non-classical intramolecular 1-5 hydrogen contacts C16-H16...N1 and C20-H20...O1 [C16-H16...N1 2.49Å 99.3°; C20-H20...O1 2.39Å 98.4°].

C1-C2	1.485(6)	C3-S1	1.709(4)
C2-O1	1.259(5)	C3-O2	1.343(5)
C2-N1	1.351(5)	Pt1-O1	2.013(3)
N1-C3	1.310(5)	Pt1-S1	2.225(1)
O1-C2-C1-C12	-5.8(7)	N1-C3-O2-C4	-0.7(6)
N1-C3-S1-Pt1	4.4(6)	N1-C2-O1-Pt1	4.8(8)

Table 14 Bond lengths (Å) and torsion angles observed in **Pt(L^6-*S,O*)$_2$**.

The positions of the hydrogen atoms involved in the intramolecular 1-5 hydrogen contacts observed in **Pt(L^6-S,O)$_2$** can be both located/found as well as calculated/placed. In each case, the values of the distances and angles determined for the placed/calculated hydrogen atoms are comparable to the values determined for the located/found hydrogen atoms. These hydrogen contact distances and angles are listed in Table 15.

method	D-H...A	D-H (Å)	H...A (Å)	D...A (Å)	D-H...A (°)
calculated	C16---H16...N1	0.95	2.49	2.801(6)	99.3
located		0.93(7)	2.53(6)	2.800(6)	97(4)
calculated	C20---H20...O1	0.95	2.39	2.693(5)	98.4
located		0.95(5)	2.36(5)	2.694(6)	100(4)
calculated	C18-H18...O2^{xxii}	0.95	2.63	3.315(6)	129.2
located		0.91(5)	2.66(5)	3.316(6)	130(4)
Calculated	C18-H18...S1^{xxii}	0.95	2.96	3.691(5)	135.2
located		0.91(5)	2.93(5)	3.694(5)	143(4)

Table 15 Inter- and intramolecular hydrogen contact geometry of **Pt(L^6-*S,O*)$_2$** as determined for placed/calculated hydrogens as well as for found/located hydrogens as identified by XSeed[48, 49] and Platon[50] with s.u.s in parenthesis. [symmetry code (xxii) x, 3/2-y, 1/2+z].

Two non-classical intermolecular hydrogen bonds are observed in the unit cell of **Pt(L^6-*S,O*)$_2$** [C18-H18...O2^{xxii} 2.63Å 129.2° and C18-H18...S1^{xxii} 2.96Å 135.2°; symmetry code (xxii) x, 3/2-y, 1/2+z], which link the individual molecules of **Pt(L^6-*S,O*)$_2$** into one dimensional molecular chains extending parallel to [001]. Observed Cg1...Cg1^{xxiii} π...π type interactions form one dimensional molecular chains extending parallel to [010] which expands the one dimensional molecular chains extending parallel to [001] into two dimensional molecular sheets [Cg1...Cg1^{xxiii} 3.598Å where Cg1 is the centroid of the O1-C2-N1-C3-S1-Pt1 chelation ring; symmetry operator (xxiii) 1/2-x, 3/2-y, z]. An extended packing diagram of **Pt(L^6-*S,O*)$_2$**, as viewed along [010], is illustrated in Figure 22.

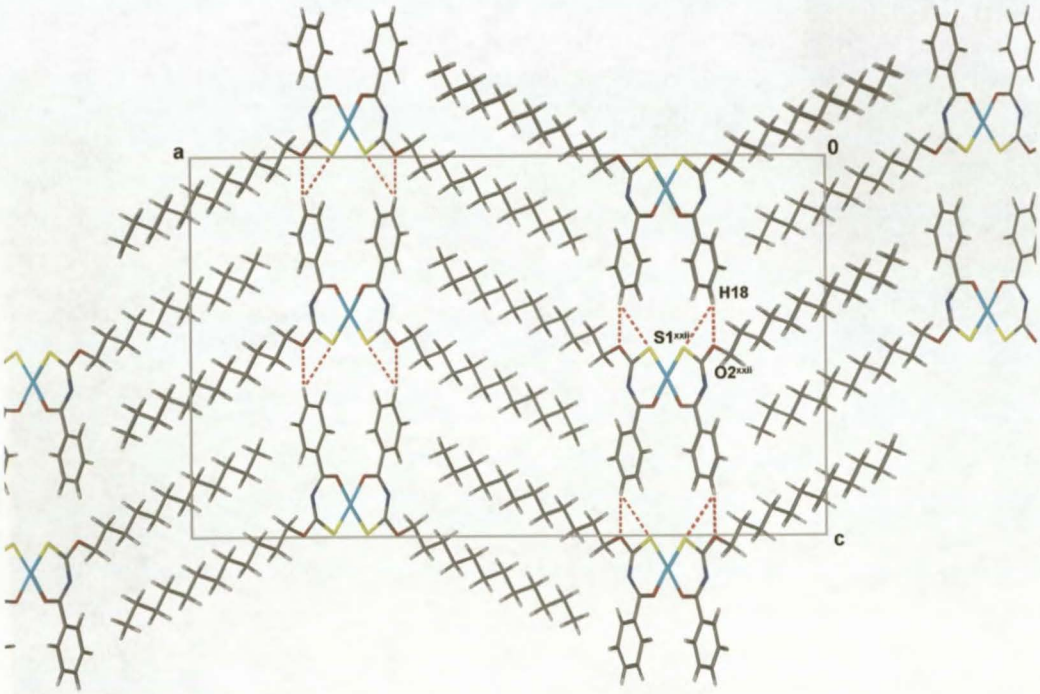

Figure 22 Extended packing diagram of **Pt(L^6-*S,O*)$_2$** showing the *a*-*c* plane. The C18-H18...O2^{xxii} and C18-H18...S1^{xxii} intermolecular interactions are indicated. Symmetry code (xxii) x, 3/2-y, 1/2+z.

A small void was identified by Platon[50] within the unit cell of **Pt(L^6-*S,O*)$_2$** which was further studied with Connolly software[62] using a probe radius of 1.20Å and determined as having a total volume of 28.7Å^3 (0.7% of the unit cell volume). The voids are essentially located between the phenyl rings of adjacent molecules and are flanked by the sulphur atoms in the [001] direction as illustrated in Figure 23 as red spheres.

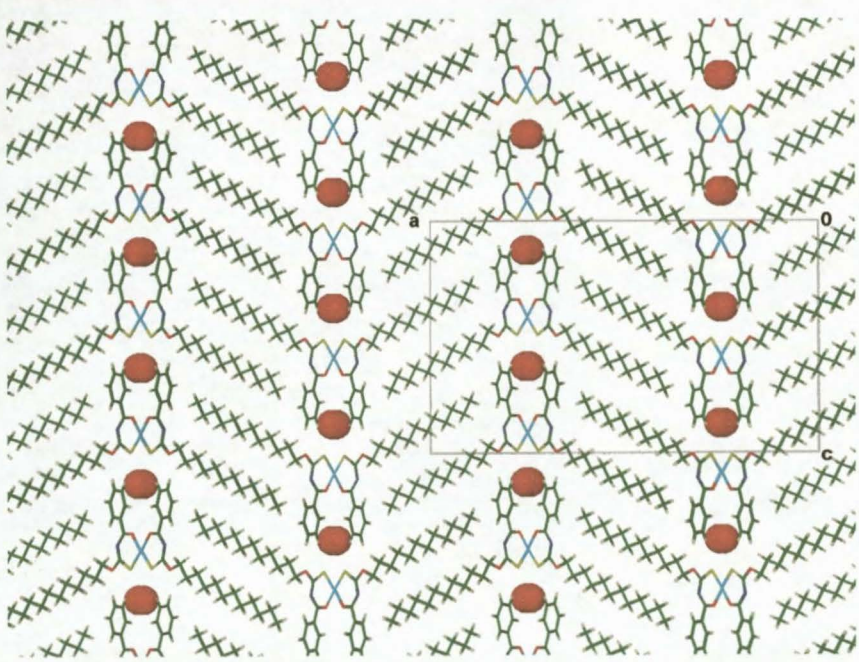

Figure 23 An extended packing diagram of **Pt(L^6-*S,O*)$_2$** as viewed along [010]. Voids identified within the unit cell are indicated as red spheres.

2.8.7 *Bis*(*N*-benzoyl-*O*-benzyl-thiocarbamato)nickel(II), Ni(L^2-*S,O*)$_2$.

Ni(L^2-*S,O*)$_2$ crystallizes orthorhombic space group $P2_12_12$ with four formula units per unit cell. The asymmetric unit consists of half a molecule of Ni(L^2-*S,O*)$_2$, with the complete molecule being generated by the symmetry operator 1-x, 1-y, z; illustrated in Figure 24 showing the numbering scheme used. The ligand is again coordinated to the nickel in a square planar bidentate *cis*-(*S,O*) fashion, the chelate rings of Ni(L^2-*S,O*)$_2$ being planar, C3 deviating from the O1/C2/N1/C3/S1/Ni1 least squares plane by 0.050(3)Å.

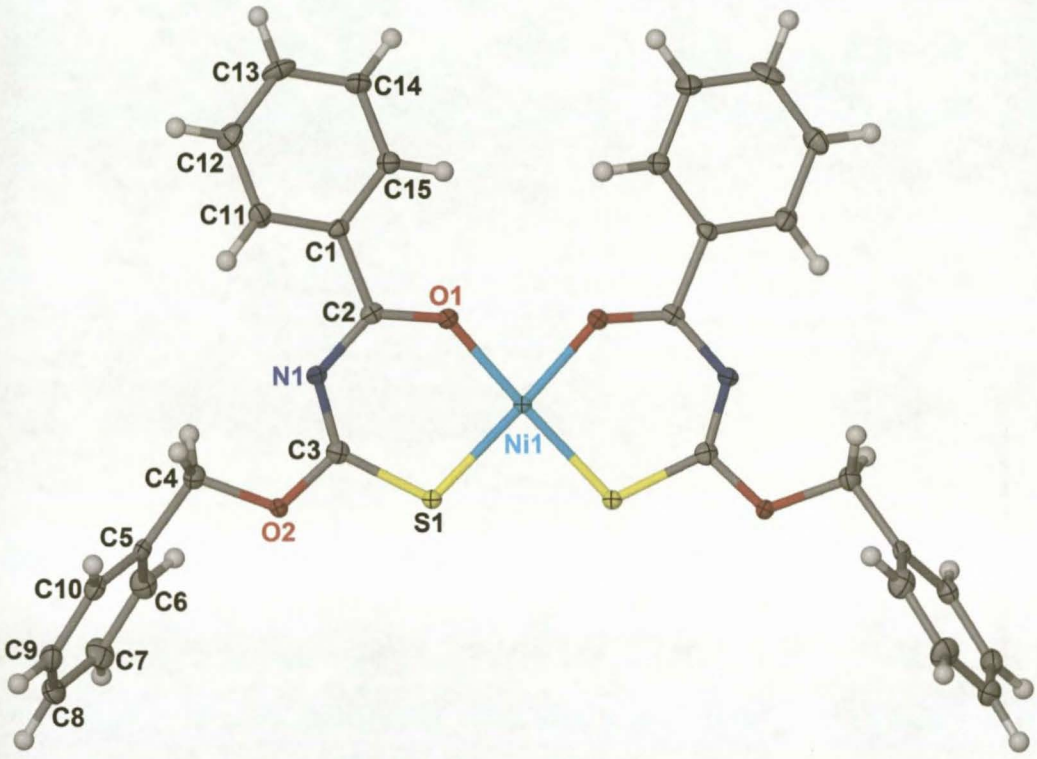

Figure 24 Molecular structure of Ni(L^2-*S,O*)$_2$ showing the numbering scheme used. Displacement ellipsoids are drawn at the 50% probability level. Unlabelled atoms are generated by the symmetry operator (1-x, 1-y, z).

The phenyl ring of the benzoyl moiety in the uncoordinated ligand H(L^2-*S,O*) is twisted away from the least-squares plane defined through the O1-C2-N1-C3-S1 moiety by 27.0(1)° with the benzoyl and benzyl rings being almost perpendicular to each other. The least-squares planes defined through the benzoyl and benzyl rings intersect at 88.3(1)°. In the molecular structure of Ni(L^2-*S,O*)$_2$, the benzoyl and benzyl moieties are twisted to a significantly lesser degree out of plane with respect to each other with the C1/C11/C12/C13/C14/C15 and C5/C6/C7/C8/C9/C10 planes intersecting at 61.8(1)°.

bond/torsion	**H(L_2-*S,O*)**	**Ni(L^2-*S,O*)$_2$**
S1-C3	1.653(2)	1.718(4)
O1-C2	1.214(2)	1.251(4)
C2-N1	1.391(2)	1.350(5)
N1-C3	1.380(2)	1.309(4)
C1-C2	1.492(2)	1.489(5)
C3-O2	1.320(2)	1.338(4)
Ni1-O1	n/a	1.859(2)
Ni1-S1	n/a	2.143(1)
O1-C2-N1-C3	-2.6(3)	-2.8(6)
C2-N1-C3-S1	174.7(1)	6.6(6)
C15-C1-C2-O1	25.2(2)	-11.2(5)
C3-O2-C4-C5	160.9(2)	171.4(3)

Table 16 Comparison of selected bond lengths (Å) and torsion angles (°) of **H(L^2-*S,O*)** and **Ni(L^2-*S.O*)$_2$** with s.u.s in parenthesis.

In **H(L^2-*S,O*)** coordinating with nickel, there has been a significant lengthening of the C2-O1 and C3-S1 bonds [**H(L^2-*S,O*)** O1-C2 1.214(2)Å, C3-S1 1.653(2)Å; **Ni(L^2-*S,O*)$_2$** O1-C2 1.251(4)Å, C3-S1 1.718(4)Å] accompanied by a shortening of the C2-N1 and C3-N1 bonds [**H(L^2-*S,O*)** C2-N1 1.391(2)Å, C3-N1 1.380(2)Å; **Ni(L^2-*S,O*)$_2$** C2-N1 1.350(5)Å, C3-N1 1.309(4)Å]. This is consistent with the loss of the amidic proton and extensive electron delocalization through the chelation ring.

In **Ni(L^2-*S,O*)$_2$**, the C1/C11/C12/C13/C14/C15 least-squares plane intersects the O1/C2/N1/C3/S1/Ni1 least-squares plane at 13.9(1)°. The relative close coplanarity of the C1-C11-C12-C13-C14-C15 phenyl ring and the O1-C2-N1-C3-S1-Ni1 chelation ring appears to be assisted by two non-classical 1-5 intramolecular hydrogen interactions as listed in Table 17 [C11-H11...N1 2.50Å 98.8°; C15-H15...O1 2.42Å 98.6°.].

D-H...A	D-H (Å)	H...A (Å)	D...A (Å)	D-H...A (°)
C11---H11...N1	0.95	2.50	2.810(5)	98.8
C15---H15...O1	0.95	2.42	2.726(4)	98.6

Table 17 Non-classical 1-5 intramolecular hydrogen contact geometry observed in **Ni(L^2-*S,O*)$_2$** as identified by XSeed[48, 49] and Platon[50] with s.u.s of the donor...acceptor (D...A) distances (Å) in parenthesis.

A non-classical intermolecular hydrogen bond is observed C13-H13...O2^x [C13-H13...O2^x 2.68Å 143.9° symmetry code (x) x, y, 1+z] which results in the formation of one dimensional molecular strings of **Ni(L^2-*S,O*)$_2$** extending parallel to [001] as illustrated in Figure 25.

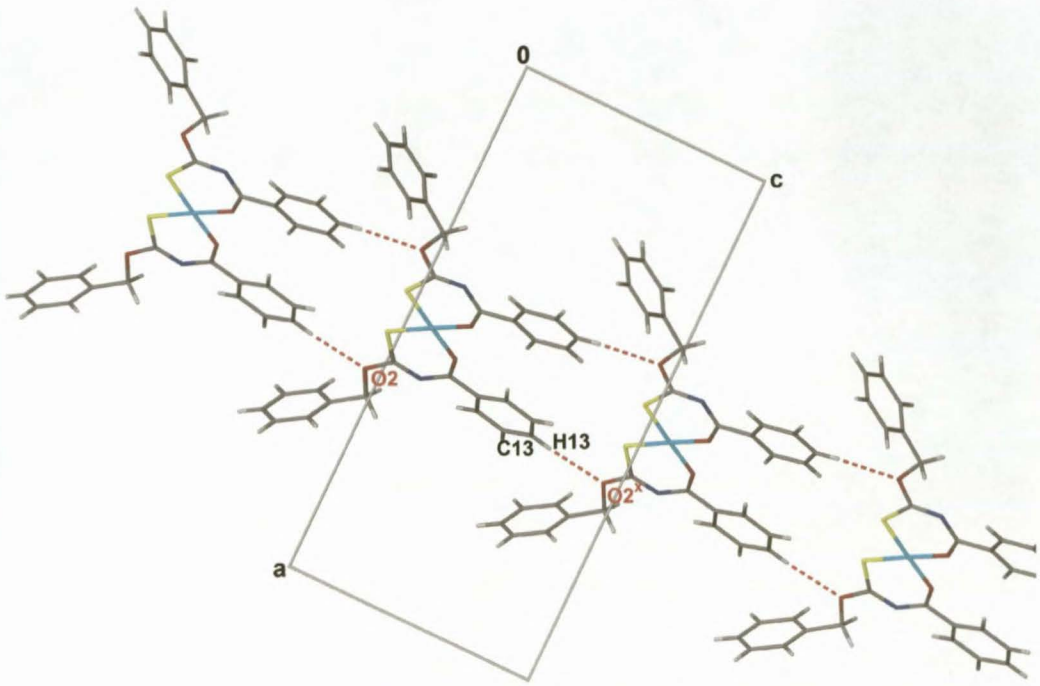

Figure 25 C13-H13...O2^{x} intermolecular hydrogen interactions as viewed along [010] which result in one dimensional molecular strings extending parallel to [001]. [C13-H13...O^{x} 2.68Å, 143.9°; symmetry code (x) x, y, 1+z].

D-H...A	D-H (Å)	H...A (Å)	D...A (Å)	D-H...A (°)
C13-H13...O2^{x}	0.95	2.68	3.488(5)	143.9
C10-H10...S1^{xi}	0.95	2.99	3.861(4)	153.0
C10-H10...O2^{xi}	0.95	2.91	3.796(5)	156.5

Table 18 Non-classical intermolecular hydrogen bonding observed in **Ni(L^{2}-*S,O*)$_2$** as identified by XSeed[48, 49] and Platon[50] with s.u.s of the donor...acceptor (D...A) distances (Å) in parenthesis. Symmetry codes (x) x, y, 1+z; (xi) x, 1+y, z.

A non-classical intermolecular hydrogen bond is observed, C10-H10...S1^{xi} [C1-H10...S1^{xi} 2.99Å 153.0°; symmetry code (xi) x, 1+y, z], causes the one dimensional molecular strings, which extend parallel to [001], to propagate into two dimensional sheets parallel to the *b-c* plane. The C10-H10...S1^{xi} intermolecular hydrogen bond is further supported by the non-classical C10-H10...O2^{xi} intermolecular hydrogen interaction [C10-H10...O2^{xi} 2.91Å 156.5°] which results in H10 being involved in a bifurcated intermolecular interaction. These two hydrogen interactions are further stabilized by an intermolecular π...π type interaction, Cg1...Cg1^{xii} [Cg1...Cg1^{xii} 3.561Å where Cg1 is the centroid of the O1-C2-N1-C3-S1-Ni1 chelation ring; symmetry code (xii) 1-x, 2-y, z]. This π...π type interaction cross links the two dimensional sheets resulting from the C10-H10...S1^{xi} and C10-H10...O2^{xi} interactions into a three dimensional array. The cross linking of the two dimensional sheets into a three dimensional array is further complemented by a C-H...π interaction; C8-H8...Cg2^{xiii} [C8-H8...Cg2^{xiii} 2.95Å 136.7° where Cg2 is the centroid of the C5-C6-C7-C8-C9-C10 phenyl ring,

symmetry operator (xiii) 3/2-x, 1/2+y, -z]. The three dimensional array of molecules resulting from these interactions, cause the molecules to pack in a herring bone fashion when the unit cell of **Ni(L^2-*S,O*)$_2$** is viewed along [001] as illustrated in Figure 26.

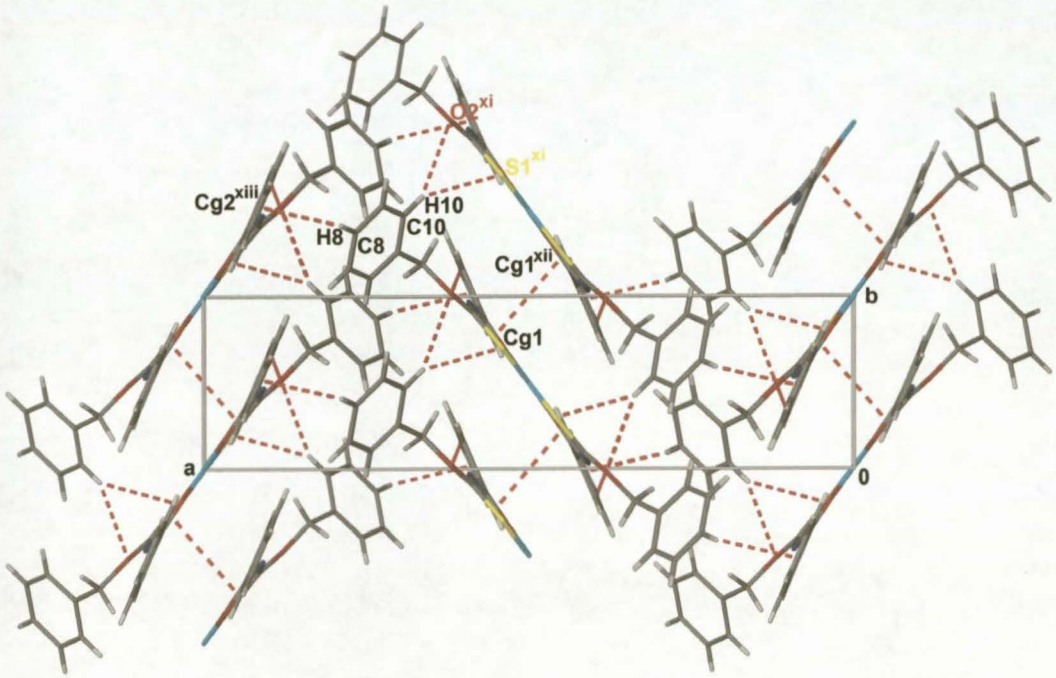

Figure 26 Extended packing diagram of **Ni(L^2-*S,O*)$_2$** as viewed along [001]. The C10-H10...S1^{xi}, C10-H10...O2^{xi}, Cg1...Cg1^{xii} and C8-H8...Cg2^{xiii} interactions are indicated using hashed lines. Symmetry codes (xi) x, y+1,z; (xii) 1-x, 2-y, z; (xiii) 3/2-x, 1/2+y, -z

2.8.8 *Bis* (*N*-benzoyl-*O*-benzyl-thiocarbamato)palladium(II), Pd(L^2-*S,O*)$_2$.

Pd(L^2-*S,O*)$_2$ crystallises orthorhombic space group P*ccn* with four formula units per unit cell as illustrated in Figure 27 showing the numbering scheme used. Similar to **Ni(L^2-*S,O*)$_2$**, the asymmetric unit consists of only half a molecule of **Pd(L^2-*S,O*)$_2$**, with the complete molecule being generated by the symmetry operator 1/2-x, 3/2-y, z.

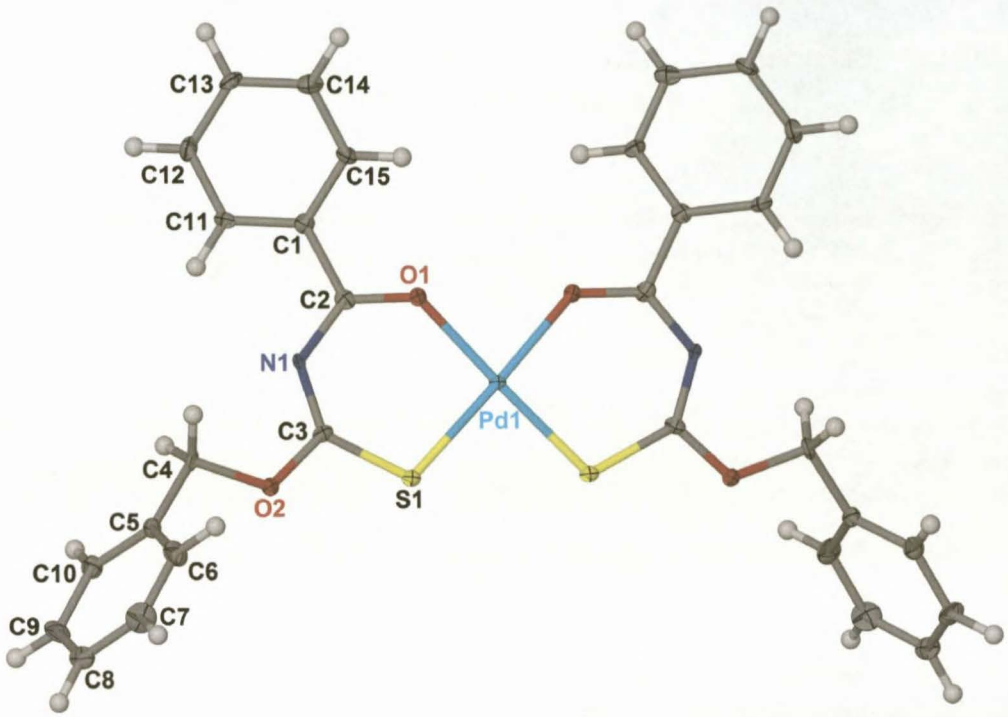

Figure 27 Molecular structure of **Pd(L^2-*S,O*)$_2$** showing the numbering scheme used. Displacement ellipsoids are drawn at the 50% probability level. Unlabelled atoms are generated by the symmetry operator 1/2-x, 3/2-y, z.

If the changes in bond lengths of interest in **H(L^2-*S,O*)** are compared with the comparable bonds in **Pd(L^2-*S,O*)$_2$**, these changes are consistent with the loss of the amidic proton coupled with extensive electron delocalization through the chelation ring [see Table 19]. The O1-C2 and S1-C3 bond lengths of **H(L^2-*S,O*)** have increased significantly [**H(L^2-*S,O*)** O1-C2 1.214(2)Å S1-C3 1.653(2)Å; **Pd(L^2-*S,O*)$_2$** O1-C2 1.261(6)Å S1-C3 1.718(5)(2)Å] accompanied by a shorting of C2-N1 and N1-C3 bond lengths upon coordination with the palladium [**H(L^2-*S,O*)** C2-N1 1.391(2)Å N1-C3 1.380(2)Å; **Pd(L^2-*S,O*)$_2$** C2-N1 1.350(6)Å N1-C3 1.309(6)Å].

Bond/torsion	$H(L^2\text{-}S,O)$	$Pd(L^2\text{-}S,O)_2$
S1-C3	1.653(2)	1.718(5)
O1-C2	1.214(2)	1.261(6)
C2-N1	1.391(2)	1.350(6)
N1-C3	1.380(2)	1.309(6)
C1-C2	1.492(2)	1.488(7)
C3-O2	1.319(2)	1.336(6)
Pd1-O1	n/a	2.014(3)
Pd1-S1	n/a	2.234(1)
O1-C2-N1-C3	-2.6(3)	-4.8(8)
C2-N1-C3-S1	174.7(1)	-7.5(8)
C15-C1-C2-O1	25.2(2)	-8.9(7)
C3-O2-C4-C5	160.9(2)	166.2(4)

Table 19 Comparison of selected bond lengths (Å) and torsion angles (°) of HL^2 and $Pd(L^2\text{-}S.O)_2$ with s.u.s in parenthesis.

The C1-C11-C12-C13-C14-C15 phenyl ring is relatively coplanar with the O1-C2-N1-C3-S1-Pd1 chelate ring with the least-squares plane defined through each intersecting at 13.2(2)°. This is similar to that which was observed in the molecular structure of $Ni(L^2\text{-}S,O)_2$ where the respective least-squares planes of the benzoyl and chelate rings intersected at 13.9(1)°. Two non-classical 1-5 intramolecular hydrogen interactions were observed C11-H11...N1 and C15-H15...O1 which presumably assist in bringing the phenyl ring of the benzoyl moiety into relative close coplanarity with the chelation ring of $Pd(L^2\text{-}S,O)_2$ [C11-H11...N1 2.50Å, 98.9°; C15-H15...O1 2.42Å 98.6°, see Table 20]. The benzoyl rings and benzyl rings in $Pd(L^2\text{-}S,O)$ are twisted at 58.7(2)° relative to each other in comparison to the comparable phenyl rings of $Ni(L^2\text{-}S,O)_2$ which are twisted at 61.8(1)° relative to each other. It is proposed that this has a significant influence on the overall arrangement of molecules in the unit cell of $Pd(L^2\text{-}S,O)_2$ which differ significantly to the overall arrangement of molecules in the unit cell of $Ni(L^2\text{-}S,O)_2$.

D-H...A	D-H (Å)	H...A (Å)	D...A (Å)	D-H...A (°)
C11---H11...N1	0.95	2.50	2.810(5)	98.8
C15---H15...O1	0.95	2.42	2.726(4)	98.6

Table 20 Non-classical 1-5 intramolecular hydrogen contact geometry observed in $Pd(L^2\text{-}S,O)_2$ as identified by XSeed[48, 49] and Platon[50] with s.u.s of the donor...acceptor (D...A) distances (Å) in parenthesis.

A non-classical intermolecular C13-H13...S2^{xiv} bond [C13-H13...O2^{xiv} 2.77Å 129.1°; symmetry code (xiv) x, 5/2-y, z-1/2] is observed in the crystal lattice of $Pd(L^2\text{-}S,O)_2$. This interaction results in the formation of one dimensional molecular strings of $Pd(L^2\text{-}S,O)_2$, as illustrated in Figure 28, extending along [001] comparable to that observed in $Ni(L^2\text{-}S,O)_2$. The orientation of the molecules in the one dimensional string of $Pd(L^2\text{-}S,O)_2$ differ significantly to the arrangement of molecules in the comparable one dimensional string of $Ni(L^2\text{-}S,O)_2$ [Figure 25].

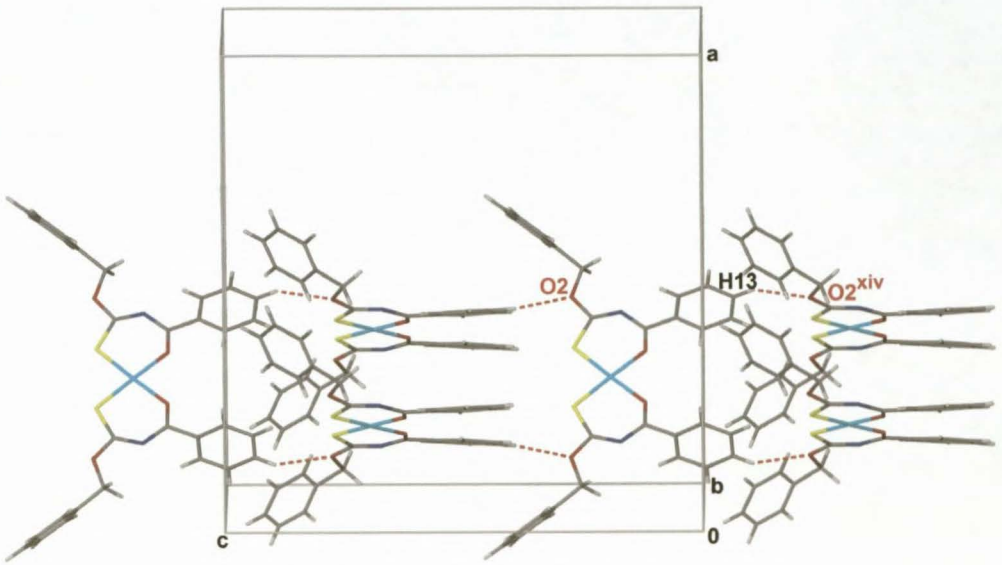

Figure 28 C13-H13...O2^{xiv} intermolecular hydrogen bond resulting in the formation of one dimensional molecular strings extending along [001]. [C13-H13...O^{xiv} 2.77Å, 129.1°; symmetry code (xiv) x, 5/2-y, z-1/2].

Two non-classical intermolecular hydrogen interactions were observed, C10-H10...O2^{xv} and C10-H10...S1^{xv} [C10-H10...O2^{xv} 3.20Å 161.7°, C10-H10...S1^{xv} 3.15Å 151.7°, symmetry code (xv) x, 1+y, z; see Table 21], which extend the one dimensional molecular strings in Figure 28 into two dimensional molecular sheets running parallel to the *b*-*c* plane.

D-H...A	D-H (Å)	H...A (Å)	D...A (Å)	D-H...A (°)
C13-H13...O2^{xiv}	0.95	2.77	3.450(6)	129.1
C10-H10...S1^{xv}	0.95	3.15	4.007(6)	151.7
C10-H10...O2^{xv}	0.95	3.20	4.116(6)	161.7

Table 21 Non-classical Intermolecular hydrogen bonding and hydrogen contact geometry observed in **Pd(L^2-*S,O*)$_2$** as identified by XSeed[48, 49] and Platon[50] with s.u.s of the donor...acceptor (D...A) distances (Å) in parenthesis. Symmetry codes (xiv) x, 5/2-y, z-1/2; (xv) x, 1+y, z.

The two dimensional sheets resulting from the hydrogen interactions listed in Table 21 are further cross linked into a three dimensional network via π...π type interactions, Cg1...Cg1^{xvi} and Cg3...Cg3^{xvi} [Cg1...Cg1^{xvi} 3.616Å, Cg3...Cg3^{xvi} 3.959Å; Cg1 is the centroid of the O1-C2-N1-C3-S1-Pd1 chelation ring and Cg3 is the centroid of the C1-C11-C12-C13-C14-C15 phenyl ring; symmetry code (xvi) 1/2-x, 5/2-y, z]. The three dimensional network of molecules is further complemented by a non-classical intermolecular C-H...π interaction, C8-H8...Cg3^{xvii} [C8-H8...Cg3 2.94Å 144.23°; symmetry code (xvii) 1-x, ½+y, ½-z].

The molecules of **Pd(L^2-*S,O*)$_2$** are arranged into a herring bone when the unit cell of **Pd(L^2-*S,O*)$_2$** is viewed along [001] similar to that which was observed in the unit cell of **Ni(L^2-*S,O*)$_2$** [see Figure 26]. However, as a result of the Cg3…Cg3^{xvi} and C8-H8…Cg3^{xvii} interactions, when the unit cell of **Pd(L^2-*S,O*)$_2$** is viewed along [010], as illustrated in Scheme 4, the molecules are linked into a parallel 'transverse wave-like' pattern extending across the *a-c* plane.

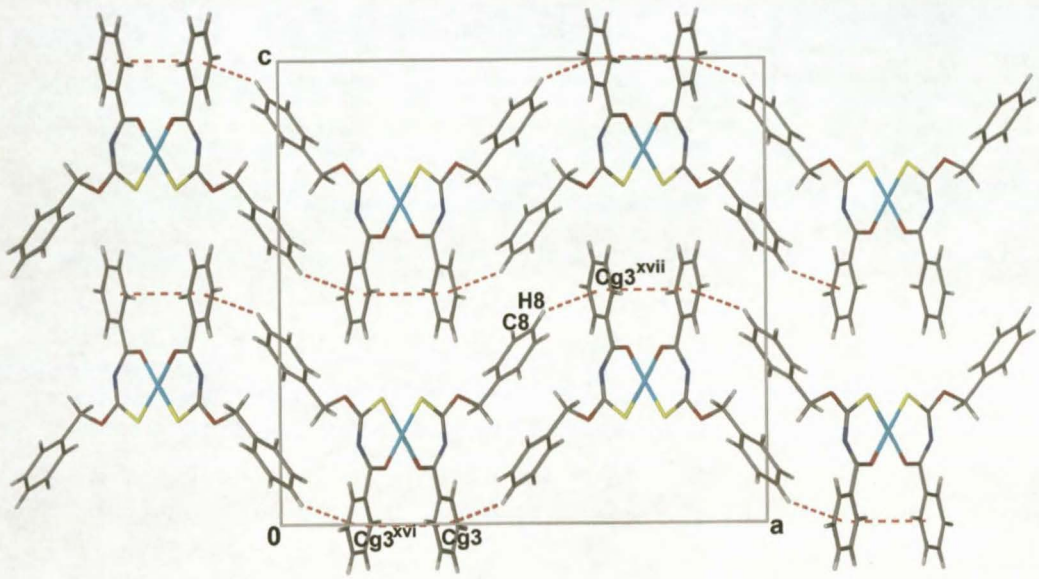

Scheme 4 An extended packing diagram of **Pd(L^2-*S,O*)$_2$** as viewed along [010] indicating the C8-H8…Cg3^{xvii} and Cg3…Cg3^{xvi} interactions which link the molecules in parallel 'transverse waves' across the *a-c* plane of the unit cell. Symmetry code (xvi) 1/2-x, 5/2-y, z; (xvii) 1-x, ½+y, ½-z.

The bond lengths and torsion angles of interest of **H(L^2-*S,O*)**, **Ni(L^2-*S,O*)$_2$** and **Pd(L^2-*S,O*)$_2$** are listed in Table 22 for comparison purposes. There has been a comparable shortening of the C2-N1 and N1-C3 bonds, accompanied by a comparable lengthening of the S1-C3 and O1-C2 bonds of **H(L^2-*S,O*)** upon coordination with Ni(II) and Pd(II) [**H(L^2-*S,O*)** C2-N1 1.391(2)Å N1-C3 1.380(2)Å S1-C3 1.653(2)Å O1-C2 1.214(2)Å; **Ni(L^2-*S,O*)$_2$** C2-N1 1.350(5)Å N1-C3 1.309(4)Å S1-C3 1.718(4)Å O1-C2 1.251(4)Å; **Pd(L^2-*S,O*)$_2$** C2-N1 1.350(6)Å N1-C3 1.309(6)Å S1-C3 1.718(5)Å O1-C2 1.261(6)Å] indicating that there is a similar degree of charge delocalization through these bonds in **Ni(L^2-*S,O*)$_2$** and **Pd(L^2-*S,O*)$_2$** respectively.

bond/torsion	H(L_2-*S,O*)	Ni(L^2-*S,O*)$_2$	Pd(L^2-*S,O*)$_2$
S1-C3	1.653(2)	1.718(4)	1.718(5)
O1-C2	1.214(2)	1.251(4)	1.261(6)
C2-N1	1.391(2)	1.350(5)	1.350(6)
N1-C3	1.380(2)	1.309(4)	1.309(6)
C1-C2	1.492(2)	1.489(5)	1.488(7)
C3-O2	1.319(2)	1.338(4)	1.336(6)
M-O1	n/a	1.859(2)	2.014(3)
M-S1	n/a	2.143(1)	2.234(1)
O1-C2-N1-C3	-2.6(3)	-2.8(6)	-4.8(8)
C2-N1-C3-S1	174.7(1)	6.6(6)	-7.5(8)
C15-C1-C2-O1	25.2(2)	-11.2(5)	-8.9(7)
C3-O2-C4-C5	160.9(2)	171.4(3)	166.2(4)

Table 22 Selected bond lengths (Å) and torsion angles (°) of H(L^2-*S,O*), Ni(L^2-*S,O*)$_2$ and Pd(L^2-*S,O*)$_2$ with s.u.s in parenthesis for comparative purposes.

Of greater significance, is the existence of voids in the unit cell of the crystal lattice of **Pd(L^2-*S,O*)$_2$**. Voids were not found in the unit cell of **Ni(L^2-*S,O*)$_2$**. These voids were initially identified by Platon[50] and were further determined as having a potential total volume of 46.4 Å^3 by using Connolly software[62] with a probe radius of 1.20Å. Each individual void, as illustrated in Scheme 5, was calculated as having an individual volume of 14.84Å^3. The voids are essentially located between four benzyl moieties and flanked by sulphur. As in the case of the crystal lattices of **Ni(L^2-*S,O*)$_2$** and **Pd(L^2-*S,O*)$_2$**, it has been recently reported that isostructural compounds can have significant differences in overall molecular arrangement solely due to a variance of the coordinated metal which in turn often has a significant impact on the existence, size and shape of voids that result within the respective unit cells[63].

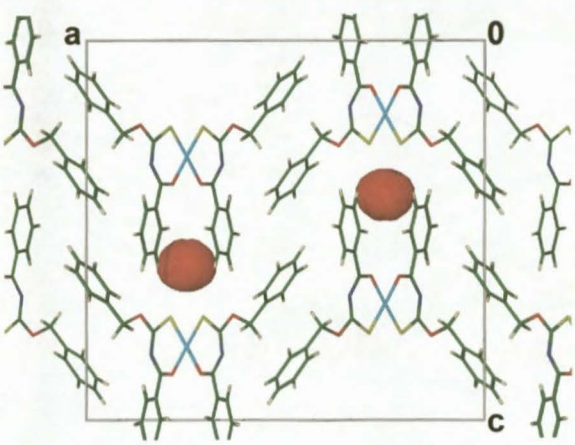

Scheme 5 Voids identified in the crystal lattice of **Pd(L^2-*S,O*)$_2$** as viewed along [010]. The voids are illustrated as red spheres.

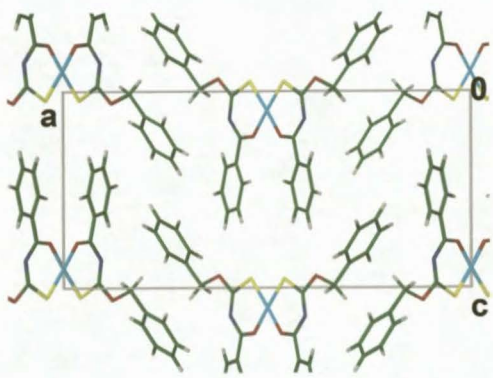

Scheme 6 Comparative view of Ni(L^2-*S,O*)$_2$ along [010]. Voids were not identified in the crystal lattice of Ni(L^2-*S,O*)$_2$.

2.8.9 Crystallization product of Pt (L^2-*S,O*)$_2$: benzamide

The ^{1}H and ^{13}C NMR data, as well as the infrared spectroscopy data, obtained for the purified and isolated amorphous yellow powder in the attempted synthesis of **Pt(L^2-*S,O*)$_2$** indicate that the target compound **Pt(L^2-*S,O*)$_2$** was in fact synthesized in high yield and a high degree of purity [see experimental section 3.6.6]. However, it is suggested that this compound is relatively unstable in solution at room temperature for extended periods. Whenever solutions of **Pt(L^2-*S,O*)$_2$** were allowed to stand in an attempt to obtain crystals suitable for single crystal X-ray diffraction analysis, only crystals of benzamide were obtained. It is proposed that benzamide is the product of hydrolysis of **Pt(L^2-*S,O*)$_2$**. The molecular structure of benzamide has been listed several times on the CSD[21]. Furthermore a crystallographic discussion of the molecular structure of benzamide is undertaken in the appendix of chapter 5 and consequently not included here.

3. Experimental

3.1 Methods and instrumentation

All reagents and solvents were commercially available and unless otherwise stated were used without further purification. Acetone was rendered anhydrous and degassed by distillation under argon over sodium carbonate. Benzene was prepared by distillation under argon over sodium metal with benzophenone as indicator. All alcohols used were rendered anhydrous by the methods described by Furness *et al.*[64] Dichloromethane was pre-dried over 4Å molecular sieves and distilled over either sodium hydride or calcium chloride under an inert atmosphere just prior to use. ^{1}H and ^{13}C NMR spectra (25°C) were recorded in deuterated chloroform using either a Varian INOVA 600 MHz spectrometer operating at 600 MHz or 151 MHz respectively, or a Varian VXR 300 MHZ spectrometer operating at 300 MHz or 76 MHz respectively. ^{1}H chemical shifts are quoted relative to the residual $CDCl_3$ solvent resonance at 7.26ppm. The ^{13}C chemical shifts are quoted relative to the $CDCl_3$ triplet at 77.7ppm. ^{195}Pt NMR spectra (30°C) were recorded in chloroform-*d* using the Varian INOVA 600 MHz spectrometer operating at 128 MHz. All ^{195}Pt chemical shifts are quoted relative to external H_2PtCl_6 (500 mg ml^{-1} in 30% v/v D_2O/1 M HCl), and are estimated to be accurate to ±2 ppm. UV-visible spectrophotometric experiments were carried out on an Agilent 8453E UV-visible spectrophotometer (Agilent Technologies). Elemental analyses were performed using a Carlo Erba EA 1108 elemental analyser in the microanalytical laboratory of the University of Cape Town, South Africa

3.2 General preparation of ligands H(L^1-*S,O*), H(L^2-*S,O*), H(L^3-*S,O*), H(L^4-*S,O*) and H(L^5-*S,O*).

Ligands **H(L^1-*S,O*)**, **H(L^2-*S,O*)**, **H(L^3-*S,O*)**, **H(L^4-*S,O*)** and **H(L^5-*S,O*)** were generally prepared according to a method based upon the method initially described by Douglass and Dains used for the preparation of the analogous *N*-acyl(aroyl)-*N'*,*N'*-dialkylthioureas[18, 22, 23]. The series of ligands were prepared under an inert anhydrous atmosphere in a two step 'one-pot' synthesis. Benzoyl chloride was reacted with an equimolar ratio of potassium isothiocyanate in anhydrous acetone followed by the addition of a two fold molar equivalent of the appropriate alcohol. The crude reaction products were initially recovered by extraction and further purified by crystallization. All ligands were obtained in good yields (> 66%) and a high degree of purity.

3.3 General preparation of complexes M(L^{1-5}-*S*,*O*)$_2$, M = Ni(II), Pd(II) and Pt(II)

The complexes reported here were generally prepared in a similar fashion to the reported literature methods used for the synthesis of palladium(II) and platinum(II) complexes derived from *N*-aroyl(acyl)-*N'*,*N'*-dialkylthioureas[30].

An acetonitrile water solution containing 0.25 mmol quantities of the appropriate nickel acetate tetrahydrate, potassium tetrachloropalladate or potassium tetrachloroplatinate was added dropwise to a constantly stirred ligand solution, made from 0.5 mmol equivalent of the *N*-aroylthiocarbamic-*O*-alkyl ester ligand dissolved in an acetonitrile water solution (containing 0.5 mmol of sodium acetate in the case of potassium tetrachloropalladate or potassium tetrachloroplatinate). The final solvent composition was 50%(v/v) water–acetonitrile. The reaction mixture was gently warmed to 60°C and stirred for two hours, after which the solution was cooled to room temperature and stirred overnight. An equivalent volume of water was then added and the solution cooled to ± 4°C for several hours. The crude product was isolated by centrifugation, washed with a cool acetonitrile water solution and dried under high vacuum. Where possible, crystals suitable for single crystal X-ray diffraction analysis were generally obtained from various binary solvent combinations.

3.4 Crystallography and structure refinement.

Crystals suitable for single crystal X-ray analysis were mounted on a thin glass fibre and data was collected on a Bruker Nonius SMART Apex diffractometer or a Nonius Kappa CCD diffractometer, both using graphite monochromated Mo-Kα radiation (λ = 0.7107 Å). Data integration and reduction were undertaken using SAINT[65] and space group determination using XPREP[65]. Multi-scan derived corrections were made to the data using SADABS[66]. The structures were solved using SHELXS-97[61] and refined using SHELXL-97[61] with the aid of the interface software XSEED[48, 49]. XSEED[48, 49] was also used to generate the molecular graphics as the GUI to POV-Ray[67]. In each structure, all non-hydrogen atoms were modelled anisotropically. Hydrogen atoms were placed in geometrically calculated positions, with C-H = 0.99 for $-CH_2-$, 0.98 for $-CH_3$ or 0.95 for phenyl and 0.88 Å for N-H. These were refined using a riding model with U_{iso}(H) = 1.2U_{eq}(parent) (for $-CH_2-$, phenyl and N-H) and 1.5U_{eq}(parent) (for $-CH_3$). Crystal structure interpretation was performed with the aid of XSEED[48, 49], PLATON[50] and MERCURY[68].

3.5 Computational Details

All calculations were performed with the Amsterdam Density Functional suite of programs (ADF)[69, 70], release 2004.01 and 2005.01. For the restricted ground state and spin-unrestricted triplet calculations, which included geometry optimizations, linear conformational scans and IRC calculations, the following procedures were selected:

Use was made of the local density approximation (LDA) functional of Volko-Wilk-Nusair (VWN)[71], argumented with the nonlocal gradient correction PW91 from Perdew and Wang[72]. Relativistic effects have been taken into account using the scalar relativistic (SR) zero-order regular approximation

(ZORA)[73]. The ZORA basis sets used were of triple ζ plus polarization Slater type function (STO) quality (basis TZP in ADF).

3.6 Preparative methods of ligands H(L^1-*S,O*), H(L^2-*S,O*), H(L^3-*S,O*), H(L^4-*S,O*) and H(L^5-*S,O*).

3.6.1 *N*-benzoylthiocarbamic-*O*-ethyl ester, H(L^1-*S,O*)

Benzoyl chloride (30.00mmol, 4.368g) dissolved in 70ml of anhydrous acetone was added dropwise with magnetic stirring to a solution of KSCN (30.00mmol, 2,915g). The solution was brought to a gentle reflux for 1 hour, cooled to room temperature and ethanol (60.00mmol, 3.49ml) dissolved in 50ml of anhydrous acetone was added dropwise with magnetic stirring. The reaction mixture was warmed to 60°C for one hour, cooled to room temperature and stirred overnight. 200ml of water was added to the reaction mixture to fully dissolve the precipitate. The crude reaction product was recovered by extraction with 3 x 25ml of chloroform. The combined organic extracts were washed with 3 x 25ml portions of cold water. The target produced was recovered from the organic fractions under reduced pressure to yield a pale yellow amorphous powder. The crude product was further purified by crystallisation from a mixture of ethanol and water.

Yield: 67.5% (based on benzoyl chloride).

NMR : δ_H (600 MHz, solvent $CDCl_3$) 9.21 (1H, br s, NH), 7.80 (2H, d, phenyl CH), 7.59 (1H, tr, phenyl CH), 7.43 (2H, tr, phenyl CH), 4.66 (2H, qu, CH_2), 1.44 (3H, tr, CH_3).

δ_C (151 MHz, solvent $CDCl_3$) 189.4 (C(S)), 162.7 (C(O)), 133.1, 128.6, 127.7 (Ph) 132.0 (*ipso*-Ph), 69.4 (OCH_2), 13.7 (CH_3).

FT-IR : (KBr disks) 3277 (br, NH), 1696vs, 1524vs, 1293vs cm^{-1}.

Mass spectrum (EI 70eV) *m/z* 209 (M^+, 8.8%), 165 (3.4%), 121 (4.7%), 105 (100%), 76 (47.3%), 51 (17.6%), 32 (10.8%), 28 (43.2%).

Found C 57.65; H 5.81; N 6.75; S 15.32; $C_{10}H_{11}NO_2S$ required C 57.39; H 5.30; N 6.69; S 15.29.

Melting point: 74.0 – 74.8°C

3.6.2 *N*-benzoylthiocarbamic-*O*-benzyl ester, H(L^2-*S,O*)

H(L^2-*S,O*) was prepared using a method analogous to that which was used to prepare *N*-benzoylthiocarbamic-*O*-ethyl ester, **H(L^1-*S,O*)** using a two fold molar excess of benzyl alcohol as the appropriate starting reagent.

Yield: 71.3% (based on benzoyl chloride)

NMR : δ_H (600 MHz, solvent $CDCl_3$) 9.36 (1H, br s, NH), 7.82 (2H, d, phenyl CH), 7.57 (1H, tr, phenyl CH), 7.46-7.48 (4H, m, phenyl CH), 7.38 (1H, tr, phenyl CH), 7.35 (2H, tr, phenyl CH), 5.63 (2H, s, CH_2).

δ_C (151 MHz, solvent $CDCl_3$) 189.4 (C(S)), 163.5 (C(O)), 135.0 (*ipso* phenyl), 133.5 (*ipso* phenyl), 133.8, 132.7, 129.6, 129.3, 128.7, 128.4 (Ph), 74.8 (CH_2).

FT-IR : (KBr disks) 3247 (br, NH), 1694vs, 1521vs, 1271vs cm^{-1}.

Mass spectrum (EI 70eV) *m/z* 271 (M^+, 3.4%), 212 (2.0%), 180 (2.7%), 150 (3.4%), 122 (6.8%), 108 (22.3%), 105 (100%), 91 (31.1%) 77 (51.4%) 51 (13.5%).

Found C 66.02; H 4.77; N 4.95; S 10.98; $C_{15}H_{13}NO_2S$ required C 66.40; H 4.83; N 5.16; S 11.82.

Melting point: 113.0 – 114.5°C

3.6.3 *N*-benzoylthiocarbamic-*O*-methyl ester, H(L^3-*S,O*)

H(L^3-*S,O*) was prepared using a method analogous to that which was used to prepare *N*-benzoylthiocarbamic-*O*-ethyl ester, **H(L^1-*S,O*)** using a two fold molar excess of methanol as the appropriate starting reagent.

Yield: 82.6% (based on benzoyl chloride).

NMR : δ_H (300 MHz, solvent $CDCl_3$) 9.29 (1H, br s, NH), 7.84 (2H, d, phenyl CH), 7.59 (1H, tr, phenyl CH), 7.49 (2H, tr, phenyl CH), 4.19 (3H, s, CH_3).

δ_C (76 MHz, solvent $CDCl_3$) 190.3 (C(S)), 162.6 (C(O)), 133.2, 129.0, 127.7 (Ph) 132.8 (*ipso*-Ph), 57.2 (CH_3).

FT-IR : (KBr disks) 3299 (br, NH), 1717vs, 1449vs, 1208vs cm^{-1}.

Mass spectrum (EI 70eV) *m/z* 195 (M^+, 16.9%), 105 (100%), 76 (64.2%), 51 (17.6%), 32 (6.8%), 28 (25.7%).

Found C 55.55; H 4.64; N 7.07; S 16.23; $C_9H_9NO_2S$ required C 55.37; H 4.65; N 7.17; S 16.42.

Melting point: 97.5 – 98.2°C

3.6.4 *N*-benzoylthiocarbamic-*O*-butyl ester, H(L^4-*S,O*)

H(L^4-*S,O*) was prepared using a method analogous to that which was used to prepare *N*-benzoylthiocarbamic-*O*-ethyl ester, **H(L^1-*S,O*)** using a two fold molar excess of butanol as the appropriate starting reagent.

Yield: 66.7% (based on benzoyl chloride).

NMR : δ_H (600 MHz, solvent $CDCl_3$) 9.17 (1H, br s, NH), 7.83 (2H, d, phenyl CH), 7.59 (1H, tr, phenyl CH), 7.49 (2H, tr, phenyl CH), 4.60 (2H, tr, OCH_2), 1.81 (2H, pt, CH_2), 1.49 (2H, st, CH_2), 0.91 (3H, tr, CH_3).

δ_C (151 MHz, solvent $CDCl_3$) 189.7 (C(S)), 162.6 (C(O)), 133.1, 129.0, 127.7 (Ph) 133.0 (*ipso*-Ph), 73.5 (CH_2), 30.2 (CH_2), 19.1 (CH_2), 13.7 (CH_3).

FT-IR : (KBr disks) 3252 (br, NH), 1696vs, 1533vs, 1291vs cm^{-1}.

Mass spectrum (EI 70eV) *m/z* 237 (M^+, 12.4%), 180 (6.2%), 164 (2.1%), 121 (13.1%), 105 (100%), 77 (57.9%), 44 (2.8%), 28 (77.9%).

Found C 60.81; H 6.50; N 5.48; S 13.05; $C_{12}H_{15}NO_2S$ required C 60.73; H 6.37; N 5.90; S 13.51.

Melting point: 52.3 – 53.6°C

3.6.5 *N*-benzoylthiocarbamic-*O*-isopropyl ester, H(L^5-*S,O*)

H(L^5-*S,O*) was prepared using a method analogous to that which was used to prepare *N*-benzoylthiocarbamic-*O*-ethyl ester, **H(L^1-*S,O*)** using a two fold molar excess of 2-propanol as the appropriate starting reagent.

Yield: 73.7% (based on benzoyl chloride).

NMR : δ_H (300 MHz, solvent $CDCl_3$) 9.16 (1H, br s, NH), 7.84 (2H, d, phenyl CH), 7.61 (1H, tr, phenyl CH), 7.51 (2H, tr, phenyl CH), 5.66 (1H, m, OCH), 1.44 (6H, d, CH_3).

δ_C (76 MHz, solvent $CDCl_3$) 189.3 (C(S)), 163.2 (C(O)), 133.5, 129.4, 128.1 (Ph) 132.4 (*ipso*-Ph), 78.1 (OCH), 21.3 (CH_3).

FT-IR : (KBr disks) 3265 (br, NH), 1696vs, 1508vs, 1276vs cm^{-1}.

Mass spectrum (EI 70eV) *m/z* 223 (M^+, 13.1%), 209 (15.7%), 193 (18.6%), 180 (12.4%), 164 (24.8%), 121 (89.0%), 105 (100%), 77 (75.2%) 32 (6.9%), 28 (21.4%)..

Found C 60.27; H 5.79; N 6.30; S 12.89; $C_{11}H_{13}NO_2S$ required C 59.17; H 5.87; N 6.27; S 14.36.

Melting point: 61.0 – 62.3°C

3.7 Preparative methods of complexes M(L^{1-5}-*S,O*)$_2$, M = Ni(II), Pd(II) and Pt(II)

3.7.1 Bis(*N*-benzoyl-*O*-ethyl-thiocarbamato)nickel(II), Ni(L^1-*S,O*)$_2$.

N-benzoylthiocarbamic-*O*-ethyl ester ($1x10^{-3}$mol) was dissolved in 15ml of acetonitrile and further diluted with 15ml of water. Nickel acetate tetrahydrate ($0.5x10^{-3}$mol) dissolved in 15ml of water and further diluted with 15ml of acetonitrile was added dropwise to the reaction mixture at room temperature over a period of ±10 minutes. The reaction mixture was warmed with stirring to 50°C for 1 hour, cooled to room temperature and stirred for a further 12 hours. 60ml of water was added and the reaction mixture was cooled to 4°C for 3-4 hours. The precipitate of the crude product was recovered by centrifugation. The isolated product was further purified by washing with a cold 1:1 mixture of acetonitrile and water and dried under high vacuum. Crystals suitable for single crystal X-ray diffraction analysis were obtained from a solution of chloroform.

Yield: quantitative (based on $Ni(CH_3COO)_2.4H_2O$).

NMR : δ_H (600 MHz, solvent $CDCl_3$) 8.16 (4H, d, phenyl *ortho*-CH), 7.56 (2H, tr, phenyl *para*-CH), 7.42 (4H, tr, *meta*-phenyl CH), 4.55 (4H, qu, OCH_2), 1.40 (6H, tr, CH_3).

δ_C (151 MHz, solvent $CDCl_3$) 186.2 (C(O)), 178.1 (C(S)), 133.3, 129.9, 128.4 (Ph) 135.1 (*ipso*-Ph), 66.7 (OCH_2), 14.3 (CH_3).

FT-IR : (KBr disks) 1520vs, 1418vs, 1202vs cm^{-1}.

Mass spectrum (EI 70eV) *m/z* 474 (M^+, 18.9%), 376 (5.4%), 343 (5.4%), 267 (30.4%), 209 (21.6%), 178 (7.4%), 105 (100%), 76 (79.1%), 28 (78.4%).

Found C 49.38; H 4.03; N 5.59; S 12.75; $C_{20}H_{20}N_2NiO_4S_2$ required C 50.55; H 4.24; N 5.89; S 13.50.

Melting point: 159.5 – 160.4°C

3.7.2 Bis(*N*-benzoyl-*O*-ethyl-thiocarbamato)palladium(II), Pd(L^1-*S,O*)$_2$.

N-benzoylthiocarbamic-*O*-ethyl ester ($1x10^{-3}$mol) was dissolved in 15ml of acetonitrile to which a solution of sodium acetate ($1.1x10^{-3}$mol) dissolved in 15ml of water was added dropwise and stirred at room temperature for 10 minutes. Potassium tetrachloropalladate ($0.5x10^{-3}$mol) dissolved in 15ml of water and further diluted with 15ml of acetonitrile was added dropwise to the above reaction mixture at room temperature over ±10 minutes. The reaction mixture was warmed with stirring to 50°C, cooled to room temperature and stirred for a further 12 hours. 60ml of water was added and the reaction mixture was cooled to 4°C for 3-4 hours. The precipitate of the crude product was recovered by centrifugation. The isolated product was further purified by repeated washing with a cold 1:1 mixture of acetonitrile and water and dried under high vacuum. Crystals suitable for single crystal X-ray diffraction analysis were obtained from a 1:1 (v/v) solution of chloroform and pentane.

Yield: 96.8% (based on K_2PdCl_2)

NMR : δ_H (300 MHz, solvent $CDCl_3$) 8.30 (4H, d, phenyl *ortho*-CH), 7.60 (2H, tr, phenyl *para*-CH), 7.47 (4H, tr, *meta*-phenyl CH), 4.59 (4H, qu, OCH_2), 1.41 (6H, tr, CH_3).

δ_C (76 MHz, solvent $CDCl_3$) 184.7 (C(O)), 177.5 (C(S)), 134.3, 131.3, 129.3 (Ph) 136.2 (*ipso*-Ph), 67.7 (OCH_2), 14.8 (CH_3).

FT-IR : (KBr disks) 1525vs, 1410vs, 1196vs cm^{-1}.

Mass spectrum (EI 70eV) *m/z* 522 (M^+, 1.4%), 105 (100%), 77 (75.7%), 52 (21.6%).

Found C 46.15; H 3.65; N 5.38; S 11.68; $C_{20}H_{20}N_2O_4PdS_2$ required C 45.94; H 3.85; N 5.36; S 12.26.

Melting point: 168.8 – 169.4°C

3.7.3 Bis(*N*-benzoyl-*O*-ethyl-thiocarbamato)platinum(II), Pt(L^1-*S,O*)$_2$.

Pt(L^1-*S,O*)$_2$ was prepared in an analogous method to that used for the preparation of **Pd(L^1-*S,O*)$_2$** using $0.5x10^{-3}$mol potassium tetrachloroplatinate as well as $1.1x10^{-3}$ mol of sodium acetate to ensure the complete deprotonation of the *N*-benzoylthiocarbamic-*O*-ethyl ester.

Yield: 97.7% (based on K_2PtCl_2)

NMR : δ_H (600 MHz, solvent $CDCl_3$) 8.32 (4H, d, phenyl *ortho*-CH), 7.64 (2H, tr, phenyl *para*-CH), 7.47 (4H, tr, *meta*-phenyl CH), 4.59 (4H, qu, OCH_2), 1.45 (6H, tr, CH_3).

δ_C (151 MHz, solvent $CDCl_3$) 180.7 (C(O)), 173.8 (C(S)), 133.1, 130.0, 128.7 (Ph) 136.1 (*ipso*-Ph), 66.8 (OCH_2), 14.3 (CH_3).

δ_{Pt} (128 MHz, solvent $CDCl_3$) -2544.6.

FT-IR : (KBr disks) 1508vs, 1418vs, 1201vs cm^{-1}.

Mass spectrum (EI 70eV) *m/z* 667 (M^+, 1.0%), 225 (6.7%), 147 (12.8%), 105 (100%), 77 (43.9%), 32 (14.9%).

Found C 38.07; H 3.06; N 4.46; S 9.95; $C_{20}H_{20}N_2O_4PtS_2$ required C 39.28; H 3.30; N 4.58; S 10.49.

3.7.4 Bis(*N*-benzoyl-*O*-benzyl-thiocarbamato)nickel(II), Ni(L^2-*S,O*)$_2$.

Ni(L^2-*S,O*)$_2$ was prepared in an analogous method to that used for the preparation of **Ni(L^1-*S,O*)$_2$** using *N*-benzoylthiocarbamic-*O*-benzyl ester, **H(L^2-*S,O*)**, as the ligand.

Yield: 51.3% (based on $Ni(CH_3COO)_2.4H_2O$).

NMR : δ_H (300 MHz, solvent $CDCl_3$) 8.19 (4H, d, phenyl *ortho*-CH), 7.59 (2H, tr, phenyl *para*-CH), 7.35 – 7.47 (14H, m, *meta*-phenyl CH and CH of benzyl), 5.54 (4H, s, OCH_2).

δ_C (76 MHz, solvent $CDCl_3$) 187.0 (C(O)), 179.3 (C(S)), 134.2, 130.8, 129.5, 129.3, 129.3, 129.0 (Ph) 136.2, 135.9 (*ipso*-Ph), 72.5 (OCH_2).

FT-IR : (KBr disks) 1524vs, 1439vs, 1191vs cm^{-1}.

Mass spectrum (EI 70eV) *m/z* M^+ of 598 not observed. 329 (0.7%), 270 (3.4%), 246 (1.4%), 214 (8.8%), 147 (35.1%), 123 (13.4%), 105 (100%), 91 (94.3%), 77 (77.7%), 65 (19.1%), 51 (33.8%).

Found C 59.51; H 4.04; N 4.69; S 11.47; $C_{30}H_{24}N_2NiO_4S_2$ required C 60.12; H 4.04; N 4.67; S 10.70.

Melting point: 189.0 – 190.7°C.

3.7.5 Bis(*N*-benzoyl-*O*-benzyl-thiocarbamato)palladium(II), Pd(L^2-*S,O*)$_2$.

Pd(L^2-*S,O*)$_2$ was prepared in an analogous method to that used for the preparation of **Pd(L^1-*S,O*)$_2$** using *N*-benzoylthiocarbamic-*O*-benzyl ester, **H(L^2-*S,O*)**, as the ligand.

Yield: 47.4% (based on K_2PdCl_2).

NMR : δ_H (300 MHz, solvent $CDCl_3$) 8.30 (4H, d, phenyl *ortho*-CH), 7.62 (2H, tr, phenyl *para*-CH), 7.48 (4H, tr, *meta*-phenyl CH), 7.36 – 7.43 (10H, m, phenyl), 5.57 (4H, s, OCH_2).

δ_C (76 MHz, solvent $CDCl_3$) 184.5 (C(O)), 177.6 (C(S)), 134.4 131.4 129.4 129.5 129.3 129.0 (Ph) 136.2, 136.1 (*ipso*-Ph), 72.9 (OCH_2).

FT-IR : (KBr disks) 1530vs, 1440vs, 1184vs cm^{-1}.

Mass spectrum (EI 70eV) *m/z* M^+ of 646 not observed. 270 (4.5%), 214 (7.1%), 147 (38.5%), 123 (13.5%), 105 (100%), 91 (64.1%), 77 (78.2%), 51 (37.8%), 28 (44.9%), 18 (80.1%).

Found C 53.67; H 3.28; N 4.34; S 9.51; $C_{30}H_{24}N_2O_4PdS_2$ required C 55.68; H 3.74; N 4.33; S 9.91.

3.7.6 Bis(*N*-benzoyl-*O*-benzyl-thiocarbamato)platinum(II), Pt(L^2-*S,O*)$_2$.

Pt(L^2-*S,O*)$_2$ was prepared in an analogous method to that used for the preparation of **Pt(L^1-*S,O*)$_2$** using *N*-benzoylthiocarbamic-*O*-benzyl ester, **H(L^2-*S,O*)**, as the ligand.

Yield: 58.7% (based on K_2PtCl_2)

NMR : δ_H (600 MHz, solvent $CDCl_3$) 8.33 (4H, d, phenyl *ortho*-CH), 7.65 (2H, tr, phenyl *para*-CH), 7.48 (4H, tr, phenyl *meta*-CH), 7.44 (4H, d, phenyl *ortho*-CH), 7.38 (4H, tr, phenyl *meta*-CH), 7.35 (2H, tr, phenyl *para*-CH) 5.58 (4H, s, OCH_2).

δ_C (151 MHz, solvent $CDCl_3$) 179.7 (C(O)), 174.7 (C(S)), 133.9, 130.7, 129.4, 129.3, 129.2, 128.8(Ph) 136.7, 136.0 (*ipso*-Ph), 74.6 (OCH_2).

δ_{Pt} (128 MHz, solvent $CDCl_3$) -2537.6

FT-IR : (KBr disks) 1510vs, 1451vs, 1188vs cm^{-1}.

Mass spectrum (EI 70eV) *m/z* of 735 not observed. 361 (0.7%), 270 (1.3%), 211 (3.8%), 147 (23.1%), 105 (70.5%), 91 (33.3%), 77 (59.6%), 51 (25.6%), 28 (34.6%), 18 (100%).

Found C 46.43; H 2.87; N 3.66; S 9.44; $C_{30}H_{24}N_2O_4PtS_2$ required C 48.97; H 3.29; N 3.81; S 8.72.

3.7.7 Bis(*N*-benzoyl-*O*-methyl-thiocarbamato)nickel(II), Ni(L^3-*S,O*)$_2$.

Ni(L^3-*S,O*)$_2$ was prepared in an analogous method to that used for the preparation of **Ni(L^1-*S,O*)$_2$** using *N*-benzoylthiocarbamic-*O*-methyl ester, **H(L^3-*S,O*)**, as the ligand.

Yield: 89.5% (based on $Ni(CH_3COO)_2.4H_2O$).

NMR : δ_H (600 MHz, solvent $CDCl_3$) 8.19 (4H, d, phenyl *ortho*-CH), 7.57 (2H, tr, phenyl *para*-CH), 7.43 (4H, tr, *meta*-phenyl CH), 4.06 (6H, s, OCH_3).

δ_C (151 MHz, solvent $CDCl_3$) 186.6 (C(O)), 178.3 (C(S)), 133.4, 129.9, 128.4 (Ph) 135.0 (*ipso*-Ph), 57.3 (OCH_3).

FT-IR : (KBr disks) 1522vs, 1410vs, 1205vs cm^{-1}.

Mass spectrum (EI 70eV) *m/z* 474 (M^+, 26.3%), 414 (3.2%), 361 (3.9%), 329 (7.1%), 253 (5.8%), 105 (100%), 77 (61.5%), 51 (17.9%) 28 (7.1%).

Found C 48.18; H 3.36; N 6.20; S 14.01; $C_{18}H_{16}N_2NiO_4S_2$ required C 48.35; H 3.61; N 6.26; S 14.34.

Melting point: 202.6 – 203.1°C

3.7.8 Bis(*N*-benzoyl-*O*-methyl-thiocarbamato)palladium(II), Pd(L^3-*S,O*)$_2$.

Pd(L^3-*S,O*)$_2$ was prepared in an analogous method to that used for the preparation of **Pd(L^1-*S,O*)$_2$** using *N*-benzoylthiocarbamic-*O*-methyl ester, **H(L^3-*S,O*)**, as the ligand.

Yield: 94.6% (based on K_2PdCl_2).

NMR : δ_H (300 MHz, solvent $CDCl_3$) 8.32 (4H, d, phenyl *ortho*-CH), 7.61 (2H, tr, phenyl *para*-CH), 7.48 (4H, tr, *meta*-phenyl CH), 4.08 (6H, s, OCH_3).

δ_C (76 MHz, solvent $CDCl_3$) 185.2 (C(O)), 177.7 (C(S)), 134.4, 131.4, 129.3 (Ph) 136.0 (*ipso*-Ph), 58.1 (OCH_3).

FT-IR : (KBr disks) 1531vs, 1410vs, 1197vs cm^{-1}.

Mass spectrum (EI 70eV) *m/z* 494 (M^+, 2.5%), 195 (3.8%), 105 (100%), 77 (92.4%), 51 (29.3%), 28 (17.2%), 18 (41.4%).

Found C 43.80; H 2.83; N 5.68; S 12.54; $C_{18}H_{16}N_2O_4PdS_2$ required C 43.69; H 3.26; N 5.66; S 12.96.

3.7.9 Bis(*N*-benzoyl-*O*-methyl-thiocarbamato)platinum(II), Pt(L^3-*S,O*)$_2$.

Pt(L^3-*S,O*)$_2$ was prepared in an analogous method to that used for the preparation of **Pt(L^1-*S,O*)$_2$** using *N*-benzoylthiocarbamic-*O*-methyl ester, **H(L^3-*S,O*)**, as the ligand.

Yield: quantitative (based on K_2PtCl_2).

NMR : δ_H (600 MHz, solvent $CDCl_3$) 8.35 (4H, d, phenyl *ortho*-CH), 7.57 (2H, tr, phenyl *para*-CH), 7.34 (4H, tr, phenyl *meta*-CH), 4.09 (6H, s, OCH_3).

δ_C (151 MHz, solvent $CDCl_3$) 186.6 (C(O)), 178.3 (C(S)), 133.2, 130.0, 128.7 (Ph) 136.0 (*ipso*-Ph), 57.3 (OCH_2).

δ_{Pt} (128 MHz, solvent $CDCl_3$) -2537.7.

FT-IR : (KBr disks) 1508vs, 1458vs, 1200vs cm^{-1}.

Mass spectrum (EI 70eV) *m/z* 583 (M^+ 3.8%), 360 (1.0%), 195 (4.5%), 147 (15.3%), 105 (100%), 77 (52.2%), 51 (12.7%).

Found C 34.83; H 2.64; N 4.75; S 10.47; $C_{18}H_{16}N_2O_4PtS_2$ required C 37.05; H 2.76; N 4.80; S 10.99.

3.7.10 Bis(*N*-benzoyl-*O*-butyl-thiocarbamato)nickel(II), Ni(L^4-*S,O*)$_2$.

Ni(L^4-*S,O*)$_2$ was prepared in an analogous method to that used for the preparation of **Ni(L^1-*S,O*)$_2$** using *N*-benzoylthiocarbamic-*O*-butyl ester, **H(L^4-*S,O*)**, as the ligand.

Yield: 95.9% (based on $Ni(CH_3COO)_2.4H_2O$).

NMR : δ_H (600 MHz, solvent $CDCl_3$) 8.17 (4H, d, phenyl *ortho*-CH), 7.57 (2H, tr, phenyl *para*-CH), 7.43 (4H, tr, phenyl *meta*-CH), 4.50 (4H, tr, OCH_2) 1.83 (4H, m, CH_2), 1.47 (4H, m, CH_2), 0.97 (6H, m, CH_3).

δ_C (151 MHz, solvent $CDCl_3$) 186.4 (C(O)), 178.1 (C(S)), 133.2, 129.9, 128.6 (Ph) 135.1 (*ipso*-Ph), 70.6 (OCH_2), 30.7 (CH_2), 19.1 (CH_2), 13.8 (CH_3).

FT-IR : (KBr disks) 1522vs, 1421vs, 1199vs cm^{-1}.

Mass spectrum (EI 70eV) *m/z* 523 (M^+ 56.1%), 403 (7.0%), 327 (7.0%), 295 (16.6%), 271 (12.1%), 222 (11.5%), 146 (5.1%), 105 (100%), 77 (63.1%), 32 (100%), 28 (100%).

Found C 53.09; H 5.22; N 4.98; S 11.42; $C_{24}H_{28}N_2NiO_4S_2$ required C 54.25; H 5.31; N 5.27; S 12.07.

Melting point: 143.7 – 144.5°C.

3.7.11 Bis(*N*-benzoyl-*O*-butyl-thiocarbamato)palladium(II), Pd(L^4-*S,O*)$_2$.

Pd(L^4-*S,O*)$_2$ was prepared in an analogous method to that used for the preparation of **Pd(L^1-*S,O*)$_2$** using *N*-benzoylthiocarbamic-*O*-butyl ester, **H(L^4-*S,O*)**, as the ligand.

Yield: 88.1% (based on K_2PdCl_2).

NMR : δ_H (300 MHz, solvent $CDCl_3$) 8.30 (4H, d, phenyl *ortho*-CH), 7.61 (2H, tr, phenyl *para*-CH), 7.48 (4H, tr, phenyl *meta*-CH), 4.53 (4H, tr, OCH_2), 1.77 (4H, m, CH_2), 1.46 (4H, m, CH_2), 0.95 (6H, m, CH_3).

δ_C (76 MHz, solvent $CDCl_3$) 184.9 (C(O)), 177.5 (C(S)), 134.2, 131.1, 129.3 (Ph), 136.3 (*ipso*-Ph), 71.7 (OCH_2), 31.3 (CH_2), 19.7 (CH_2), 14.3 (CH_3).

FT-IR : (KBr disks) 1522vs, 1435vs, 1190vs cm^{-1}.

Mass spectrum (EI 70eV) *m/z* 578 (M^+ 1.0%), 147 (3.2%), 123 (3.8%), 105 (100%), 77 (53.5%), 51 (22.9%), 28 (8.3%).

Found C 48.02; H 4.67; N 4.88; S 11.02; $C_{24}H_{28}N_2O_4PdS_2$ required C 49.78; H 4.87; N 4.84; S 11.08.

3.7.12 Bis(*N*-benzoyl-*O*-butyl-thiocarbamato)platinum(II), Pt(L^4-*S,O*)$_2$.

Pt(L^4-*S,O*)$_2$ was prepared in an analogous method to that used for the preparation of **Pt(L^1-*S,O*)$_2$** using *N*-benzoylthiocarbamic-*O*-butyl ester, **H(L^4-*S,O*)**, as the ligand.

Yield: 92.3% (based on K_2PtCl_2).

NMR : δ_H (600 MHz, solvent $CDCl_3$) 8.33 (4H, d, phenyl *ortho*-CH), 7.64 (2H, tr, phenyl *para*-CH), 7.47 (4H, tr, phenyl *meta*-CH), 4.53 (4H, tr, OCH_2), 1.80 (4H, m, CH_2), 1.49 (4H, m, CH_2), 0.98 (6H, tr, CH_3).

δ_C (151 MHz, solvent $CDCl_3$) 180.0 (C(O)), 174.5 (C(S)), 133.8, 130.6, 129.3 (Ph), 136.8 (*ipso*-Ph), 71.4 (OCH_2), 31.4 (CH_2), 19.9 (CH_2), 14.4 (CH_3).

δ_{Pt} (128 MHz, solvent $CDCl_3$) -2541.8.

FT-IR : (KBr disks) 1508vs, 1449vs, 1219vs cm^{-1}.

Mass spectrum (EI 70eV) *m/z* 667 (M^+ 1.0%), 225 (6.7%), 147 (12.8%), 105 (100%), 77 (43.9%), 32 (14.9%).

Found C 40.24; H 3.68; N 4.09; S 10.19; $C_{24}H_{28}N_2O_4PtS_2$ required C 43.17; H 4.23; N 4.20; S 9.60.

3.7.13 Bis(*N*-benzoyl-*O*-isopropyl-thiocarbamato)nickel(II), Ni(L^5-*S,O*)$_2$.

Ni(L^5-*S,O*)$_2$ was prepared in an analogous method to that used for the preparation of **Ni(L^1-*S,O*)$_2$** using *N*-benzoylthiocarbamic-*O*-isopropyl ester, **H(L^5-*S,O*)**, as the ligand.

Yield: 74.2% (based on $Ni(CH_3COO)_2.4H_2O$).

NMR : δ_H (600 MHz, solvent $CDCl_3$) 8.16 (4H, d, phenyl *ortho*-CH), 7.56 (2H, tr, phenyl *para*-CH), 7.44 (4H, tr, phenyl *meta*-CH), 5.58 (2H, m, OCH) 1.39 (12H, d, CH_3).

δ_C (151 MHz, solvent $CDCl_3$) 185.7 (C(O)), 178.0 (C(S)), 133.2, 129.8, 128.4 (Ph), 135.3 (*ipso*-Ph), 74.7 (OCH), 21.8 (CH_3).

FT-IR : (KBr disks) 1520vs, 1432vs, 1201vs cm^{-1}.

Mass spectrum (EI 70eV) *m/z* 502 (M^+ 49.0%), 400 (11.5%), 359 (7.6%), 298 (15.3%), 271 (43.3%), 222 (45.9%), 147 (14.6%), 105 (100%), 77 (79.0%), 51 (27.4%), 32 (33.1%), 28 (54.8%), 18 (6.4%).

Found C 52.51; H 4.81; N 4.91; S 12.66; $C_{22}H_{24}N_2NiO_4S_2$ required C 52.50; H 4.81; N 5.57; S 12.74.

Melting point: 162.5 – 163.7°C.

3.7.14 Bis(*N*-benzoyl-*O*-isopropyl-thiocarbamato)palladium(II), Pd(L^5-*S,O*)$_2$.

Pd(L^5-*S,O*)$_2$ was prepared in an analogous method to that used for the preparation of **Pd(L^1-*S,O*)$_2$** using *N*-benzoylthiocarbamic-*O*-isopropyl ester, **H(L^5-*S,O*)**, as the ligand.

Yield: 80.9% (based on K_2PdCl_2).

NMR : δ_H (300 MHz, solvent $CDCl_3$) 8.28 (4H, d, phenyl *ortho*-CH), 7.60 (2H, tr, phenyl *para*-CH), 7.48 (4H, tr, phenyl *meta*-CH), 5.60 (2H, m, OCH) 1.40 (12H, d, CH_3).

δ_C (76 MHz, solvent $CDCl_3$) 184.3 (C(O)), 177.3 (C(S)), 131.2, 131.1, 129.3 (Ph), 136.4 (*ipso*-Ph), 75.7 (OCH), 22.4 (CH_3).

FT-IR : (KBr disks) 1525vs, 1438vs, 1193vs cm^{-1}.

Mass spectrum (EI 70eV) *m/z* 550 (M^+ 1.0%), 361 (1.0%), 319 (1.0%), 222 (1.9%), 180 (3.8%), 147 (16.6%), 105 (100%), 77 (89.8%), 51 (40.1%), 32 (7.0%), 28 (26.1%), 18 (31.8%).

Found C 41.17; H 3.74; N 4.90; S 11.09; $C_{22}H_{24}N_2O_4PdS_2$ required C 41.31; H 3.78; N 4.38; S 10.03.

3.7.15 Bis(*N*-benzoyl-*O*-isopropyl-thiocarbamato)platinum(II), Pt(L^5-*S,O*)$_2$.

Pt(L^5-*S,O*)$_2$ was prepared in an analogous method to that used for the preparation of **Pt(L^1-*S,O*)$_2$** using *N*-benzoylthiocarbamic-*O*-isopropyl ester, **H(L^5-*S,O*)**, as the ligand.

Yield: 89.1% (based on K_2PtCl_2).

NMR : δ_H (600 MHz, solvent $CDCl_3$) 8.31 (4H, d, phenyl *ortho*-CH), 7.64 (2H, tr, phenyl *para*-CH), 7.47 (4H, tr, phenyl *meta*-CH), 5.62 (2H, m, OCH) 1.44 (12H, d, CH_3).

δ_C (151 MHz, solvent $CDCl_3$) 179.5 (C(O)), 174.3 (C(S)), 133.7, 130.6, 129.4 (Ph), 137.0 (*ipso*-Ph), 75.5 (OCH), 22.4 (CH_3).

FT-IR : (KBr disks) 1508vs, 1437vs, 1200vs cm^{-1}.

Mass spectrum (EI 70eV) *m/z* 639 of M^+ not observed. 147 (21.0%), 121 (18.5%), 105 (100%), 77 (77.7%), 51 (29.3%), 41 (22.9%), 18 (33.8%).

ESMS : *m/z* 640.78, calculated for [**Pt(L^5-*S,O*)$_2$.H**]$^+$ *m/z* = 640.9.

Found C 45.17; H 3.74; N 4.90; S 12.09; $C_{22}H_{24}N_2O_4S_2Pt$ required C 47.96; H 4.39; N 5.08; S 11.64.

3.7.16 Bis(*N*-benzoyl-*O*-dodecyl-thiocarbamato)platinum(II), Pt(L^6-*S,O*)$_2$.

Pt(L^6-*S,O*)$_2$ was received as a gift from U. Schröder and was prepared according to methods already published[18].

NMR : δ_H (600 MHz, solvent $CDCl_3$) 8.36 (4H, d, phenyl *ortho*-CH), 7.67 (2H, tr, phenyl *para*-CH), 7.51 (4H, tr, phenyl *meta*-CH), 4.56 (4H, tr, OCH_2) 1.85 (4H, pt, CH_2), 1.46 (4H, m, CH_2), 1.30 (16H, m CH_2), 0.92 (3H, tr, CH_3).

δ_C (151 MHz, solvent $CDCl_3$) 180.1 (C(O)), 174.5 (C(S)), 133.7, 130.7, 129.3 (Ph), 136.9 (*ipso*-Ph), 71.7 (OCH), 32.6, 30.3, 30.3, 30.3, 30.2, 30.0, 30.0, 29.4, 26.6, 23.4 (CH_2), 14.8 (CH_3).

FT-IR : (KBr disks) cm^{-1}.

Mass spectrum (EI 70eV) *m/z* 891 (M^+ 2.4%), 605 (1.2%), 518 (1.2%), 478 (2.4%), 349 (4.9%), 251 (4.9%), 225 (7.3%), 182 (22.0%), 167 (12.2%), 147 (13.2%), 121 14.6%), 105 (100%), 77 (80.5%), 51 (29.3%).

Found C 53.89; H 6.79; N 3.40; S 7.60; $C_{40}H_{60}N_2O_4S_2Pt$ required C 53.85; H 6.78; N 3.14; S 7.19.

Melting point: 115.0 – 116.7°C.

Appendix A:

Experimental crystal data, data collection and crystal refinement details.

Tables containing the experimental crystal data, data collection and crystal refinement details of the crystal structures of the non-coordinated ligands, as well as the complexes, can be found on the included compact disc of this thesis. An example of these tables for the crystal structure of **H(L^1-*S,O*)** is given below.

A.1 *N*-benzoylthiocarbamic-*O*-ethyl ester, H(L^1-*S,O*)

Crystal data

$C_{10}H_{11}NO_2S$
Mr = 209.26g.mol^{-1}
Orthorhombic, P*na*2$_1$
a = 9.41710(10) Å
b = 10.03670(10) Å
c = 11.1571(2) Å
V = 1054.53(2) Å^3
Z = 4
D_x = 1.318 Mg m^{-3}

Mo Kα radiation
λ = 0.71073 Å
Cell parameters from 1536 reflections
θ = 1.02 – 28.28°
μ = 0.280 mm^{-1}
T = 193 (2) K
Prism, Clear colorless
0.22 x 0.18 x 0.10 mm

Data collection

Nonius Kappa CCD diffractometer
φ and ω scans to fill Ewald sphere
Absorption correction: none

9131 measured reflections
2547 independent reflections

2242 reflections with I > 2σ(I)
R_{int} = 0.0441
θ_{max} = 28.00°
h = -12 → 12
k = -13 → 12
l = -14 → 14

Refinement

Refinement on F^2
$R[F^2 > 2\sigma(F^2)]$ = 0.0313
$wR(F^2)$ = 0.0806
S = 1.064
2160 reflections
164 parameters
H-atom parameters constr

$w = 1/[\sigma^2(F_o^2) + (0.00406P)^2 + 0.0483P]$
where $P = (F_o^2 + 2F_c^2)/3$
$(\Delta/\sigma)_{max}$ = 0.015
$\Delta\rho_{max}$ = 0.173 e Å^{-3}
$\Delta\rho_{min}$ = -0.254 e Å^{-3}

4. References

[1] L. Lössner, *J. Prakt. Chem.* 1874, ***10***, 235-261.

[2] A. E. Dixon, *J. Chem. Soc.* 1895, ***67***, 1040-1049.

[3] K. H. König, M. Schuster, B. Steinbrech, G. Schneeweis, R. Schlodder, *Fresenius Z. Anal. Chem.* 1985, ***321***, 457-460.

[4] P. Vest, M. Schuster, K. H. Koenig, *Fresenius Z. Anal. Chem.* 1989, ***335***, 759-763.

[5] P. Vest, M. Schuster, K. H. Koenig, *Fresenius' Journal of Analytical Chemistry* 1991, ***339***, 142-144.

[6] P. Vest, M. Schuster, K. H. Köning, *Fresenius' Journal of Analytical Chemistry* 1991, ***341***, 566-568.

[7] K. R. Koch, *Coord. Chem. Rev.* 2001, ***216-217***, 473-488.

[8] C. Sacht, M. S. Datt, *Polyhedron* 2000, ***19***, 1347-1354.

[9] E. Rodriguez-Fernandez, E. Garcia, M. R. Hermosa, A. Jimenez-Sanchez, M. M. Sanchez, E. Monte, J. J. Criado, *Journal of Inorganic Biochemistry* 1999, ***75***, 181-188.

[10] T. J. Egan, K. R. Koch, P. L. Swan, C. Clarkson, D. A. Van Schalkwyk, P. J. Smith, *J. Med. Chem.* 2004, ***47***, 2926-2934.

[11] R. del Campo, J. J. Criado, E. Garcia, M. R. Hermosa, A. Jimenez-Sanchez, J. L. Manzano, E. Monte, E. Rodriguez-Fernandez, F. Sanz, *Journal of Inorganic Biochemistry* 2002, ***89***, 74-82.

[12] M. Sakamoto, M. Tanaka, A. Fukuda, H. Aoyama, Y. Omote, *J. Chem. Soc., Perkin Trans. 1* 1988, ***6***, 1353-1355.

[13] L. V. Azizyan, V. I. Ryaboi, *Obogashch. Rud (Leningrad)* 1989, ***2***, 21-24.

[14] V. A. Konev, V. I. Ryaboi, *Obogashch. Rud (Leningrad)* 1971, ***16***, 10-14.

[15] L. Quas, U. Schröder, B. Schröder, F. Dietze, L. Beyer, *Solvent Extr. Ion Exch.* 2000, ***18***, 1167-1177.

[16] L. Quas, T. Ristau, U. Schröder, F. Dietze, L. Beyer, G. Heil, *Z. Anorg. Allg. Chem.* 2001, ***627***, 1909-1914.

[17] M. Oba, K. Nishiyama, *Synthesis* 1994, 624-627.

[18] U. Schröder, L. Beyer, F. Dietze, R. Richter, S. Schmidt, E. Hoyer, *J. Prakt. Chem.* 1995, ***337***, 184-188.

[19] B. Schröder, U. Schröder, F. Dietze, L. Beyer, *Inorg. Chem. Commun.* 2001, ***4***, 398-401.

[20] M. A. V. Ribeiro da Silva, L. M. N. B. F. Santos, B. Schröder, F. Dietze, L. Beyer, *J. Chem. Thermodyn.* 2004, ***36***, 491-495.

[21] F. H. Allen, *Acta Crystallogr., Sect. B: Struct. Sci.* 2002, ***B58***, 380-388.

[22] I. B. Douglass, F. B. Dains, *J. Am. Chem. Soc.* 1934, ***56***, 719-721.

[23] I. B. Douglass, F. B. Dains, *J. Am. Chem. Soc.* 1934, ***56***, 1408-1409.

[24] L. Beyer, R. Widera, E. Hoyer, *Z. Chem.* 1981, ***21***, 415.

[25] M. A. V. Ribeiro da Silva, M. D. M. C. Ribeiro da Silva, L. C. M. da Silva, J. R. B. Gomes, A. M. Damas, F. Dietze, E. Hoyer, *Inorg. Chim. Acta* 2003, ***356***, 95-102.

[26] R. Richter, J. Sieler, R. Koehler, E. Hoyer, L. Beyer, L. K. Hansen, *Z. Anorg. Allg. Chem.* 1989, ***578***, 191-197.

[27] K. R. Koch, J. du Toit, M. R. Caira, C. Sacht, *J. Chem. Soc., Dalton Trans.* 1994, 785-786.

[28] K. R. Koch, M. C. Matoetoe, *Magn. Reson. Chem.* 1991, ***29***, 1158-1160.

[29] K. R. Koch, C. Sacht, T. Grimmbacher, S. Bourne, *S. Afr. J. Chem.* 1995, ***48***, 71-77.

[30] A. Irving, K. R. Koch, M. Matoetoe, *Inorg. Chim. Acta* 1993, ***206***, 193-199.

[31] A. N. Mautjana, J. D. S. Miller, A. Gie, S. A. Bourne, K. R. Koch, *J. Chem. Soc., Dalton Trans.* 2003, ***10***, 1952-1960.

[32] G. L. Miesler, D. A. Tarr, *Inorganic Chemistry*, Prentice-Hall, **1991**.

[33] L. V. Sudha, D. N. Sathyanarayana, *J. Mol. Struct.* 1984, ***125***, 89-96.

[34] T. Froemmel, W. Peters, H. Wunderlich, W. Kuchen, *Angew. Chem., Int. Ed. Engl.* 1992, ***31***, 612-613.

[35] T. Froemmel, W. Peters, H. Wunderlich, W. Kuchen, *Angew. Chem., Int. Ed. Engl.* 1993, ***32***, 907-909.

[36] N. G. Zabirov, V. V. Brusko, A. Y. Verat, D. B. Krivolapov, I. A. Litvinov, R. A. Cherkasov, *Polyhedron* 2004, ***23***, 2243-2252.

[37] N. G. Zabirov, V. V. Brusko, A. Y. Verat, D. B. Krivolapov, I. A. Litvinov, R. A. Cherkasov, *Polyhedron*, ***In Press, Corrected Proof***.

[38] J. Csaszar, T. Szabo, G. Dombi, *Acta Chimica Academiae Scientiarum Hungaricae* 1976, ***88***, 1-11.

[39] M. Gerloch, R. C. Slade, *Journal of the Chemical Society: Inorganic, Physical, Theoretical* 1969, ***6***, 1012-1022.

[40] M. Gerloch, R. C. Slade, *Journal of the Chemical Society: Inorganic, Physical, Theoretical* 1969, ***6***, 1022-1028.

[41] G. N. La Mar, E. O. Sherman, *J. Am. Chem. Soc.* 1970, ***92***, 2691-2699.

[42] I. Bertini, D. Gatteschi, L. J. Wilson, *Inorg. Chim. Acta* 1970, ***4***, 629-631.

[43] R. Knorr, F. Ruf, *Angewandte Chemie* 1984, ***96***, 350-351.

[44] Research Group for Platinum Metals Chemistry; Stellenbosch University; *unpublished results.*

[45] A. D. Morales, H. N. de Armas, N. M. Blaton, O. M. Peeters, C. J. D. Ranter, H. Márquez, R. P. Hernández, *Acta Crystallogr., Sect. C: Cryst. Struct. Commun.* 2000, ***C56***, 1042-1043.

[46] L. A. Montiel-Ortega, S. Rojas-Lima, E. Otazo-Sanchez, R. Villagómez-Ibarra, *J. Chem. Crystallogr.* 2004, ***34***, 89-93.

[47] F. H. Allen, O. Kennard, D. G. Watson, L. Brammer, A. G. Orpen, R. Taylor, *J. Chem. Soc., Perkin Trans. 2* 1987, ***12***, S1-S19.

[48] L. J. Barbour, *Journal of Supramolecular Chemistry* 2001, ***1***, 189-191.

[49] J. L. Atwood, L. J. Barbour, *Cryst. Growth Des.* 2003, ***3***, 3-8.

[50] A. L. Spek, A Multipurpose Crystallographic Tool, University of Utrecht, Netherlands, **1999.**

[51] K. R. Koch, C. Sacht, S. Bourne, *Inorg. Chim. Acta* 1995, ***232***, 109-115.

[52] S. A. Bourne, O. Hallale, K. R. Koch, *Cryst. Growth Des.* 2005, ***5***, 307-312.

[53] G. Blewett, M. W. Bredenkamp, K. R. Koch, *Unpublished results* 2005.

[54] G. R. Desiraju, A. Gavezzotti, *J. Chem. Soc., Chem. Commun.* 1989, ***10***, 621-623.

[55] V. T. Yilmaz, C. Kazak, C. Kirilmis, M. Koca, F. W. Heinemann, *Acta Crystallogr., Sect. C: Cryst. Struct. Commun.* 2005, ***C61***, o438-o441.

[56] E. Arunan, H. S. Gutowsky, *J. Chem. Phys.* 1993, ***98***, 4294-4296.

[57] M. O. Sinnokrot, E. F. Valeev, C. D. Sherrill, *J. Am. Chem. Soc.* 2002, ***124***, 10887-10893.

[58] S. K. Burley, G. A. Petsko, *Science* 1985, ***229(4708)***, 23-28.

[59] Cambridge Crystallographic Data Centre, http://www.ccdc.cam.ac.uk

[60] L. Beyer, E. Hoyer, J. Liebscher, H. Hartman, *Z. Chem.* 1981, ***21***, 81-91.

[61] G. M. Sheldrick, SHELXS97 and SHELXL97, Programs for the Solution and Refinement of Crystal Structures, University of Göttingen, Institüt für Anorganische Chemie der Universität, Tammanstrasse 4, D-3400 Göttingen, Germany, 1997.

[62] M. L. Connolly, *Science* 1983, ***221***, 709-713.

[63] J. A. R. Navarro, E. Barea, J. M. Salas, N. Masciocchi, S. Galli, A. Sironi, C. O. Ania, J. B. Parra, *Inorganic Chemistry Communications* 2006, ***45***, 2397-2399.

[64] B. S. Furniss, A. J. Hannaford, P. W. G. Smith, A. R. Tatchell, *Vogel's Textbook of Practical Organic Chemistry*, 5th ed.

[65] Bruker, SMART, SAINT and XPREP, Area detector control and data integration and reduction software, Bruker Analytical X-ray Instruments Inc., Madison, WI, USA., 1995.

[66] G. M. Sheldrick, SADABS. Version 2.05, Empirical absorption correction program for area detector data, University of Göttingen, Germany., 2002.

[67] Pov-Ray, http://www.povray.org,

[68] I. J. Bruno, J. C. Cole, P. R. Edgington, M. Kessler, C. F. Macrae, P. McCabe, J. Pearson, R. Taylor, *Acta Crystallogr., Sect. B: Struct. Sci.* 2002, ***B58***, 389-397.

[69] G. Te Velde, F. M. Bickelhaupt, E. J. Baerends, C. Fonseca Guerra, S. J. A. Van Gisbergen, J. G. Snijders, T. Ziegler, *Journal of Computational Chemistry* 2001, ***22***, 931-967.

[70] E. J. Baerends, J. Autschbach, A. Bérces, Bo, C. *et al.*, *http://www.scm.com*.

[71] S. H. Vosko, L. Wilk, M. Nusair, *Canadian Journal of Physics* 1980, ***58***, 1200-1211.

[72] J. P. Perdew, J. A. Chevary, S. H. Vosko, K. A. Jackson, M. R. Pederson, D. J. Singh, C. Fiolhais, *Physical Review B: Condensed Matter and Materials Physics* 1992, ***44***, 6671-6687.

[73] E. van Lenthe, J. G. Snijders, E. J. Baerends, *J. Chem. Phys.* 1996, ***105***, 6505-6516.

Index: Chapter III

1. Introduction.

In chapter II, a series of ligands was prepared wherein the alkoxy substituent [-OR R = methyl, ethyl, butyl, isopropyl, dodecyl and benzyl] was systematically varied while the benzoyl moiety was kept consistent. These *N*-benzoylthiocarbamic-*O*-alkoxy ligands **H(L-*S,O*)** were complexed with the d^8 transition metal ions Ni(II), Pd(II) and Pt(II). In each case, the ligands formed ***cis*-M(L-*S,O*)$_2$** type complexes [M = Ni(II), Pd(II), Pt(II)] where the ligand was bound to the metal ions, upon the loss of a proton, in a square planar bidentate *cis*-(*S,O*) orientation. The equivalent ***trans*-M(L-*S,O*)$_2$** type complex was not observed spectroscopically, nor was the ***trans*-M(L-*S,O*)$_2$** complex isolated and characterised crystallographically. To date, no *trans*-(*S,O*) complexes of *N*-aroyl(acyl)thiocarbamic-*O*-esters have been reported in the literature.

N-aroyl-*N'*,*N'*-dialkylthioureas have long been known to form stable complexes with softer first row transition metal ions. This was initially demonstrated in the early investigations of Hoyer and Beyer[1-3] as well as those of König and Schuster[4-8]. In general, these *N*-aroyl-*N'*,*N'*-dialkylthioureas show an overwhelming tendency to coordinate to d^8 metal ions, upon the loss of a proton, in a *cis-S,O* mode of coordination as illustrated in Figure 1. In 1994, the first example of a *trans* complex of *N*-aroyl-*N'*,*N'*-dialkylthioureas was isolated and characterised by means of single crystal X-ray diffraction, namely *trans*-bis(*N*-naphthoyl-*N'*,*N'*-dibutylthioureato)platinum(II)[9]. This is one of only two examples of square planar *trans* complexes of this class of ligand currently listed on the Cambridge Structural Database (CSD)[10] and to date, *trans*-bis(*N*-naphthoyl-*N'*,*N'*-dibutylthioureato)platinum(II)[9] is still the only authenticated example of a square planar *trans* complex of this sort for the platinum group metals as characterised by single crystal X-ray diffraction. In the report of 1994 by Koch *et al.* it was proposed that the formation of *trans*-bis(*N*-naphthoyl-*N'*,*N'*-dibutylthioureato)platinum(II) was attributed to steric hindrance in the transition state of the reaction resulting from the relatively large *N*-naphthoyl moieties of the ligand.

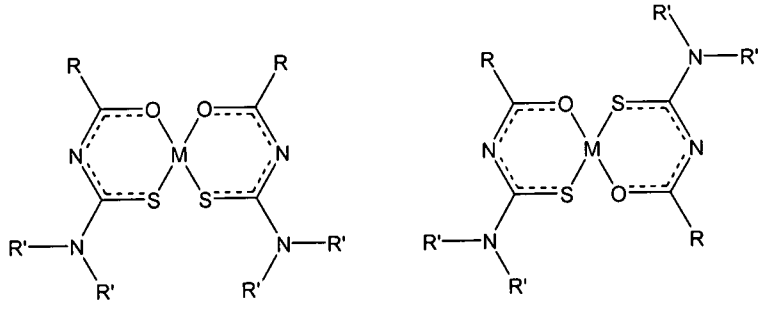

cis-M(L-*S,O*)$_2$ *trans*-M(L-*S,O*)$_2$

Figure 1 Possible modes of square planar coordination of *N*-aroyl-*N'*,*N'*-dialkylthioureas to d^8 transition metal ions.

Prior to the report of *trans*-bis(*N*-naphthoyl-*N'*,*N'*-dibutylthioureato)platinum(II) in 1994[9], a great degree of effort had been devoted by Koch *et al.* in attempts to produce and isolate *trans*-Pt(L-*S,O*)$_2$ complexes of the *N*-aroyl-*N'*,*N'*-dialkylthioureas by conventional synthetic routes[11]. Reports by Irving

et al. postulated that in the case of the square planar [Pt(L-*S,O*)$_2$] complexes, both the *cis*-(*S,O*) and *trans*-(*S,O*) configurations are possible, along with the corresponding protonated *cis/trans* $[Pt(LH)L]^+$ and $[Pt(LH)_2]^{2+}$ species as indicated in Scheme 1[12]. The existence of the protonated *cis/trans* $[Pt(LH)L]^+$ and $[Pt(LH_2)]^{2+}$ species was confirmed by Koch *et al.* in 1998 by means of ^1H and ^{195}Pt NMR studies of the protonation mediated interconversion of mono –(*S*) versus bidentate (*S,O*) coordination of Pt(II) by *N*-acyl-*N'*,*N'*-dialkylthioureas[13].

$$[PtCl_4]^{2-} + 2HL \rightarrow \textit{cis/trans}\text{-}[Pt(LH)_2]Cl_2 + 2Cl^-$$
$$[Pt(LH)_2]Cl_2 \rightarrow [Pt(LH)L]Cl + HCl$$
$$[Pt(LH)L]Cl \rightarrow [PtL_2] + HCl$$

Scheme 1

Further to the findings discussed above, *cis*- and *trans*-Pt(L-*S,O*)$_2$ complexes were obtained when *N*-(3,4,5-trimethoxybenzoyl)-*N'*,*N'*-di(*n*-butyl)thiourea as well as *N*-(3,4,5-trimethoxybenzoyl)-*N'*-morpholinothiourea were reacted with K_2PtCl_4[14]. The *cis*-(*S,O*) isomer predominated in all cases[14, 15]. These observations and assignments of the *cis* and *trans* isomers of Pt(L-*S,O*)$_2$ were solely based upon ^{195}Pt- and ^{13}C-NMR spectroscopy findings and were not verified by single crystal X-ray diffraction studies at the time[15]. In 2001 Koch published a speculative hypothesis in which it was proposed that the *trans*-Pt(L-*S,O*)$_2$ type complexes of *N*-aroyl-*N'*,*N'*-dialkylthiourea ligands could possibly be isolated if bulky, electron-rich *N*-aroylthiourea ligands were used[15]. It was speculated that the use of electron releasing aroyl groups may enhance the relative "softness" of the amidic oxygen donor atom and thereby stabilize the formation of the *trans*-Pt(L-*S,O*)$_2$ complex during synthesis[15].

A further variable that can be argued as being a contributing factor to the formation of the *cis* versus *trans* isomers of Pt(L-*S,O*)$_2$ complexes derived from *N*-aroyl-*N'*,*N'*-dialkylthioureas, is the method or mode of synthesis used. In general, platinum(II) complexes of *N*-aroyl-*N'*,*N'*-dialkylthioureas are prepared by adding equimolar amounts of a solution of K_2PtCl_4 dropwise to a constantly stirred solution of the appropriate *N*-aroyl-*N'*,*N'*-dialkylthiourea ligand (HL) in the presence of a mild base such as sodium acetate[16, 17]. However, work done on the complexation of *N*-aroyl-*N'*,*N'*-dialkylthioureas with platinum(II) has shown that the *cis*-Pt(L-S,O)$_2$ isomer is produced independently of whether the ligand solution was added to the metal solution, or whether the metal solution was added to the ligand solution while all experimental factors such as temperature, solvent type, reaction time and starting materials etc. were kept constant[14, 18, 19]. This apparent independence of the formation of the *cis*-isomer of the platinum(II) complexes of *N*-aroyl-*N'*,*N'*-dialkylthioureas from the reaction order used is consistent with that which was found in the preparation of the structurally analogous Ni(II), Pd(II) and Pt(II) complexes derived from *N*-aroylthiocarbamic-*O*-alkyl esters as described in chapter II of this thesis. A reversal in the mode of synthesis of these bis(*O*-alkyl-*N*-benzoylthiocarbamato)metal(II) complexes (i.e. addition of the ligand solution in the presence of a mild base to the metal solution, as opposed to the traditional method of the addition of the metal solution to the ligand solution in the presence of a mild base) didn't appear to affect the yields of the product

obtained, nor did there appear to be any spectroscopic indication of the formation of the equivalent *trans*-bis(*O*-alkyl-*N*-benzoylthiocarbamato)metal(II) complex.

In the series of *N*-benzoylthiocarbamic-*O*-alkyl ester ligands discussed in chapter II, the alkoxy substituent [-OR R = methyl, ethyl, butyl, isopropyl, dodecyl and benzoyl] was systematically varied while the benzoyl moiety was kept consistent. The Ni(II), Pd(II) and Pt(II) complexes of these ligands were essentially isostructural with each being square planar and having a *cis*-(*S,O*) orientation. As the alkoxy substituent and metal ion was varied, subtle differences were observed in the crystal structures. However, significant differences in the crystal structures of both the uncoordinated ligand [**H(L^2-*S,O*)**] and the complexes [**M(L^2-*S,O*)$_2$**, M = Ni(II), Pd(II)] were observed upon the introduction of the benzyl alkoxy moiety, presumably as a result of several intermolecular C-H…π and π…π type interactions.

Therefore, a second series of *N*-aroylthiocarbamic-*O*-alkyl ester ligands was prepared in which the alkoxy substituent was kept constant [-OR, R = ethyl), while the aroyl group was increasingly substituted with methoxy groups, as illustrated in Table 1, in order to investigate the effect the bulky, electron rich substituents on the aryl moiety have on the overall structure and coordination chemistry with Ni(II), Pd(II) and Pt(II). For this purpose, single crystal X-ray diffraction analysis was carried out on **Pt(L^7-*S,O*)$_2$**, **Pt(L^8-*S,O*)$_2$** and **Ni(L^9-*S,O*)$_2$**. Complexes bis[*N*-(3,5-dimethoxybenzoyl)-*N'*,*N'*-diethylureato]platinum(II) and bis[*N*-(3,4,5-trimethoxybenzoyl)-*N'*,*N'*-diethylureato]platinum(II) were also prepared and analyzed by means of single crystal X-ray diffraction analysis for comparison purposes.

N-(3-methoxy)thiocarbamic-*O*-ethyl ester, **H(L^7-*S,O*)**	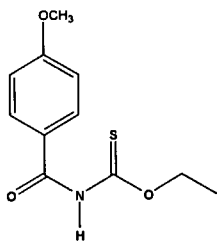	*N*-(3,5-dimethoxy)thiocarbamic-*O*-ethyl ester, **H(L^8-*S,O*)**	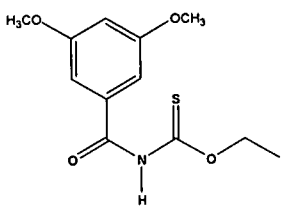
N-(3,4,5-trimethoxy)thiocarbamic-*O*-ethyl ester, **H(L^9-*S,O*)**	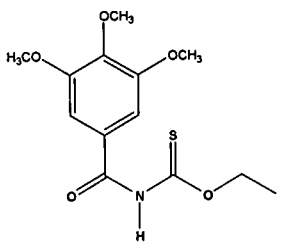		

Table 1 Series of *N*-aroylthiocarbamic-*O*-ethyl ester ligands prepared.

2. Results and Discussion.

2.1 General preparation of ligands H(L^7-*S,O*), H(L^8-*S,O*), H(L^9-*S,O*) and competing side reactions

The series of ligands listed in Table 1 were successfully prepared according to the method described in chapter II section 2.2, scheme 3 in yields exceeding 64%. Ligands *N*-(2,6-dimethoxybenzoyl)thiocarbamic-*O*-ethyl ester and *N*-(2,4-dimethoxybenzoyl)thiocarbamic-*O*-ethyl ester, as listed in Table 2, were also envisaged to form part of the series to be complexed with Ni(II), Pd(II) and Pt(II).

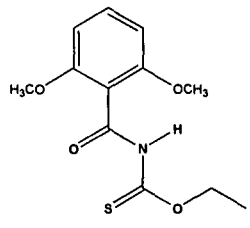	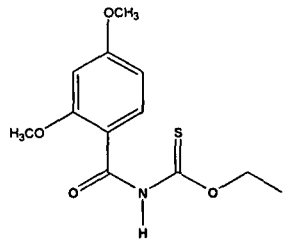
N-(2,6-dimethoxybenzoyl)thiocarbamic-*O*-ethyl ester	*N*-(2,4-diimethoxybenzoyl)thiocarbamic-*O*-ethyl ester

Table 2 Envisaged *N*-(dimethoxybenzoyl)thiocarbamic-*O*-alkyl esters for complexation with Ni(II), Pd(II) and Pt(II).

Despite there being spectroscopic evidence of *N*-(2,6-dimethoxybenzoyl)thiocarbamic-*O*-ethyl ester and *N*-(2,4-diimethoxybenzoyl)thiocarbamic-*O*-ethyl ester having being successfully synthesized, these compounds were not isolated in significant yields. In each case, the major reaction products isolated were found to be the corresponding benzoyl ethyl ester, namely ethyl 2,4-dimethoxybenzoate and ethyl 2,6-dimethoxybenzoate, and/or the corresponding carboxylic acid, namely 2,6-dimethoxybenzoic acid and 2,4-dimethoxybenzoic acid respectively.

The success of the synthetic procedure employed for the synthesis of the *N*-aroylthiocarbamic-*O*-ethyl esters requires the nucleophilic attack of the ethanol to occur primarily on the electrophilic thiocarbonyl carbon, and not on the electrophilic carbonyl carbon of the aroyl isothiocyanate intermediate indicated in Scheme 2 of chapter II. Both the carbonyl carbon and thiocarbonyl carbon of the aroyl isothiocyanate intermediate are in active competition for the nucleophilic ethanol attack. Nucleophilic attack by the ethanol on the carbonyl carbon of the aroyl isothiocyanate intermediate results in the elimination of the isothiocyanate moiety and formation of the aroyl ethyl ester as illustrated in Scheme 2. The *ortho*- and *para*-activating properties of the methoxy substituents on the 2,6-dimethoxybenzoyl isothiocyanate and 2,4-dimethoxybenzoyl isothiocyanate intermediates, result in the carbonyl carbon atom becoming the preferred site of nucleophilic attack by the ethanol. The corresponding carboxylic acid is presumably formed by the accepted mechanism of acid hydrolysis of the aroyl ester as illustrated in Scheme 3[20].

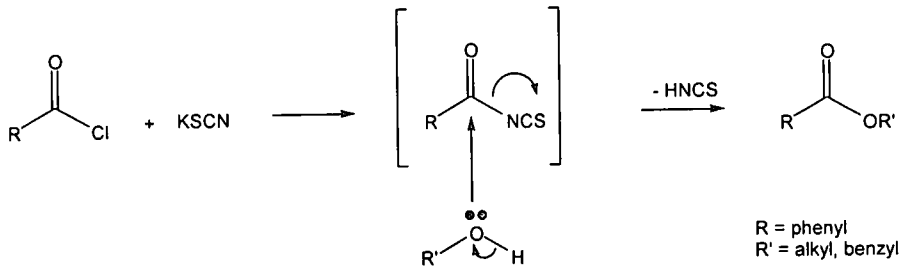

Scheme 2 Proposed mechanism of aroyl ester by-product formation.

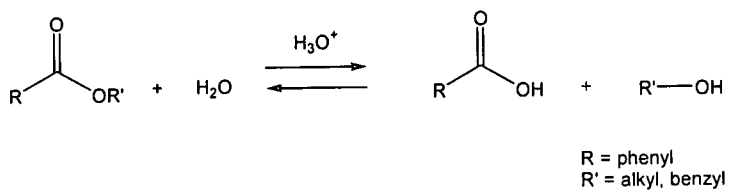

Scheme 3 Hydrolysis of the aroyl ester to the corresponding carboxylic acid.

An alternative mechanism proposed for the formation of the aroyl ethyl esters and corresponding carboxylic acids, as described above, is illustrated in Scheme 4. The proposed mechanism is illustrated using 2,6-dimethoxybenzoyl chloride, however the proposed mechanism is also applicable using 2,4-dimethoxybenzoyl chloride.

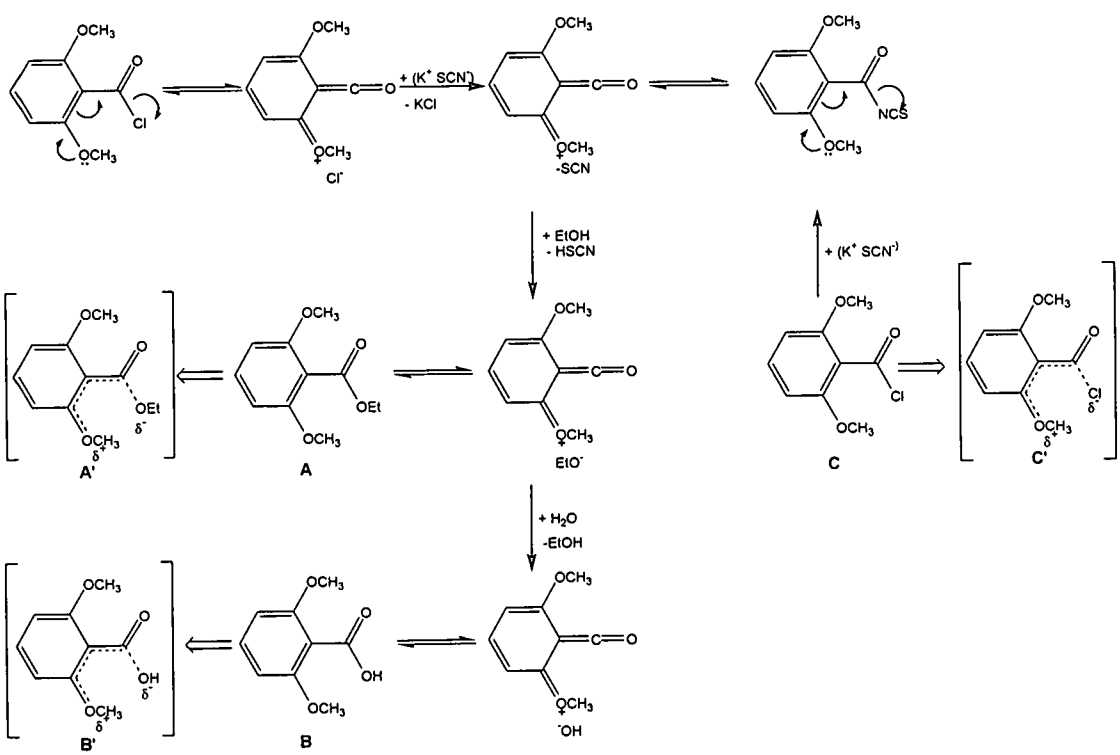

Scheme 4 Proposed alternative mechanism of aroyl ethyl ester (**A**) and corresponding carboxylic acid (**B**) formation.

Despite the *para* directing properties of 4-methoxybenzoyl chloride, the proposed reaction scheme illustrated in Scheme 4 is not applicable, as **A**, **B** and **C** in Scheme 4 are stabilised through delocalisation as a result of the *ortho* methoxy substituent forming **A'**, **B'** and **C'**. Therefore, in using 4-methoxybenzoyl chloride as the starting reagent, ligand **H(L^7-*S,O*)** is obtained and not the corresponding 4-methoxybenzoyl ethyl ester and carboxylic acid as per Scheme 4.

2.2 General Preparation of Complexes M(L^{7-9}-*S,O*)$_2$, M = Ni(II), Pd(II), Pt(II)

Complexes **M(L^{7-9}-*S,O*)$_2$**, M = Ni(II), Pd(II) and Pt(II) were prepared in reasonable yields and high purity according to the method described earlier in chapter II section 2.2[12].

2.3 Single Crystal X-ray Diffraction Analysis of Bis[*O*-ethyl-*N*-(methoxy-substitutedbenzoyl)thiocarbamato]metal(II) complexes of Ni(II), Pd(II) and Pt(II)

Single crystal X-ray diffraction analysis of **Pt(L^7-*S,O*)$_2$**, **Pt(L^8-*S,O*)$_2$** and **Ni(L^9-*S,O*)$_2$** were carried out. In these complexes, the ethoxy substituent is consistent with the alkoxy substituent used in complexes **Ni(L^1-*S,O*)$_2$**, **Pd(L^1-*S,O*)$_2$** and **Pt(L^1-*S,O*)$_2$**, the molecular structures of which were solved and fully described in chapter II. A direct comparison of the molecular structures of **Ni(L^1-*S,O*)$_2$**, **Pd(L^1-*S,O*)$_2$** and **Pt(L^1-*S,O*)$_2$** (as described in chapter II) with the molecular structures of **Pt(L^7-*S,O*)$_2$**, **Pt(L^8-*S,O*)$_2$** and **Ni(L^9-*S,O*)$_2$**, is therefore possible, which would elucidate any molecular and crystal structure differences resulting from the methoxy substituents introduced onto the benzoyl moieties. Furthermore, the effect of the introduction of these electron donating methoxy substituents on the oxygen-metal bond in complexes is evaluated.

Single crystal X-ray diffraction analysis was also carried out, in collaboration with D. Hanekom[19], of bis(*N*-(3,5-dimethoxybenzoyl)-*N',N'*-diethylthioureato)Pt(II), **Pt(L^{10}-*S,O*)$_2$**, and bis(*N*-(3,4,5-trimethoxybenzoyl)-*N',N'*-diethylthioureato)Pt(II), **Pt(L^{11}-*S,O*)$_2$** for comparative purposes. As yet, structures **Pt(L^{10}-*S,O*)$_2$** and **Pt(L^{11}-*S,O*)$_2$** are unpublished and are not listed on the CSD.

2.3.1 Bis[*O*-ethyl-*N*-(3-methoxybenzoyl)thiocarbamato]platinum(II), Pt(L^7-*S,O*)$_2$.

The molecular structure of **Pt(L^7-*S,O*)$_2$** is illustrated in Figure 2 and crystallises monoclinic, space group P21/c with 4 formula units per unit cell. Complex **Pt(L^7-*S,O*)$_2$** has crystallised in a square planar bidentate *cis*-(*O,S*) fashion comparable to that observed in the analogous Ni(II), Pd(II) and Pt(II) complexes described in chapter II. There is no significant twisting of either the phenyl or chelate rings.

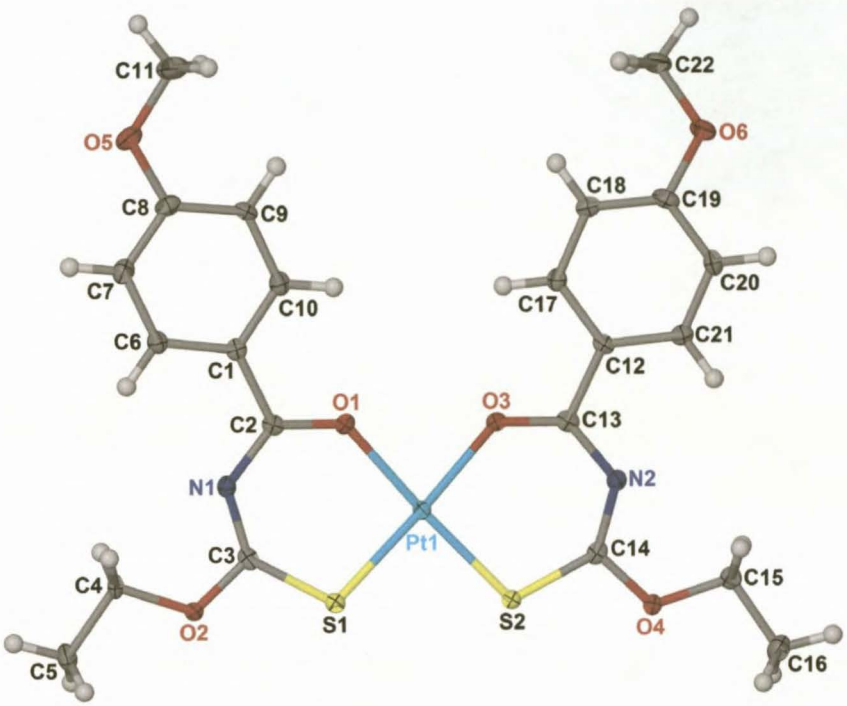

Figure 2 Molecular structure of **Pt(L^7-*S,O*)$_2$** showing the numbering scheme used. Displacement ellipsoids are drawn at the 50% probability level.

The bond lengths of the respective carbon-nitrogen bonds within each of the chelate rings are consistent with a partial double bond character due to electron delocalization through these bonds (see Table 3). Each of the chelation rings of **Pt(L^7-*S,O*)$_2$** are planar with the greatest deviation from the Pt1/O1/C2/N1/C3/S1 and Pt1/O3/C13/N2/C14/S2 least-squares planes being C3 and N2 by -0.025(3)Å and 0.022(3)Å respectively. Furthermore the chelate rings of **Pt(L^7-*S,O*)$_2$** are coplanar, with the least-squares planes defined through each intersecting at 1.5(1)°. Each of the phenyl rings of **Pt(L^7-*S,O*)$_2$** are essentially coplanar with the respective chelate rings, C1/C6/C7/C8/C9/C10 intersects Pt1/O1/C2/N1/C3/S1 at 3.0(1)° and C12/C17/C18/C19/C20/C21 intersects Pt1/O3/C13/N2/C14/S2 at a slightly steeper angle of 4.4(1)°. The overall planarity of the phenyl and chelate rings is also illustrated by the torsion angles listed in Table 3. The coplanarity of the phenyl rings with the adjacent chelate rings is possibly assisted by the non-classical 1-5 intramolecular hydrogen contacts C6-H6…N1, C10-H10…O1, C17-H17…O3 and C21-H21…N2 as listed in Table 4 and illustrated in Figure 3 [C6-H6…N1 2.49Å, C10-H10…O1 2.39Å, C17-H17…O3 2.38Å, C21-H21…N2 2.47Å]. In each case, the

contact distance is less than the sum of the van der Waals radii and are comparative to the 1-5 hydrogen contacts observed in the molecular structures of the bis(*O*-alkyl-*N*-benzoylthiocarbamato)metal(II) complexes of Ni(II), Pd(II) and Pt(II) described in chapter II.

Pt1-O1	2.021(3)	Pt1-O3	2.023(3)
Pt1-S1	2.230(1)	Pt1-S2	2.222(1)
C2-O1	1.266(5)	C13-O3	1.255(5)
C3-S1	1.712(4)	C14-S2	1.711(4)
C2-N1	1.357(5)	C13-N2	1.345(5)
N1-C3	1.311(2)	N2-C14	1.311(5)
C1-C2	1.473(5)	C13-C12	1.491(5)
C3-O2	1.333(4)	C14-O4	1.338(5)
O2-C4	1.454(4)	O4-C15	1.454(4)
O1-C2-C1-C10	-0.3(5)	O3-C13-C12-C17	-3.4(5)
Pt1-O1-C2-N1	-1.9(6)	Pt1-O3-C13-N2	1.7(6)
Pt1-S1-C3-N1	-4.8(4)	Pt1-S2-C14-N2	1.1(4)
N1-C3-O2-C4	-6.5(5)	N2-C14-O4-C15	4.4(5)

Table 3 Bond lengths (Å) and torsion angles (°) of interest observed in **Pt(L^7-*S,O*)$_2$**.

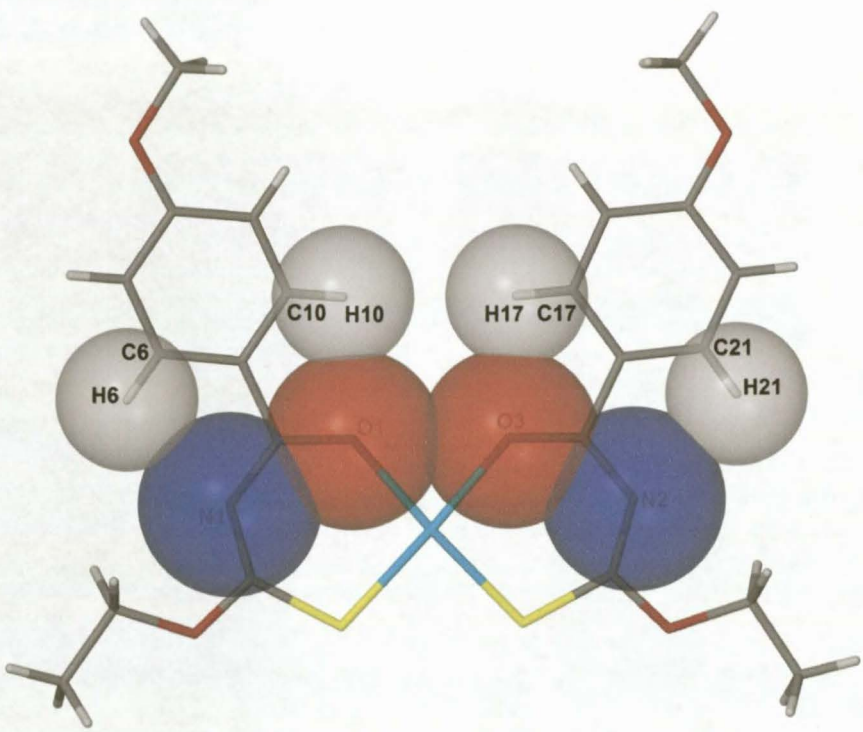

Figure 3 C6-H6...N1, C10-H10...O1, C17-H17...O3 and C21-H21...N2 intramolecular 1-5 hydrogen contacts as observed in **Pt(L^7-*S,O*)$_2$** illustrating the overlap of the van der Waals radii of the respective hydrogen, nitrogen and oxygen atoms.

method	D-H...A	D-H (Å)	H...A (Å)	D...A (Å)	D-H...A (°)
calculated	C6---H6...N1	0.95	2.49	2.813(6)	99.9
located		0.95(6)	2.51(6)	2.812(6)	98(4)
calculated	C10---H10...O1	0.95	2.39	2.706(5)	98.8
located		0.83(5)	2.39(5)	2.707(6)	104(4)
calculated	C17-H17...O3	0.95	2.38	2.702(5)	99.1
located		1.00(5)	2.39(5)	2.701(5)	97(3)
calculated	C21-H21...N2	0.95	2.47	2.749(6)	99.6
located		0.99(5)	2.55(5)	2.787(6)	93(3)

Table 4 1-5 intramolecular hydrogen contact geometry of **Pd(L^7-*S,O*)$_2$** identified by XSeed[21, 22] and Platon[23] with s.u.s in parenthesis. The various distances (Å) and angles (°) have been determined for both placed/calculated hydrogens and found/located hydrogens.

Each of the methoxy substituents on the benzoyl moieties of **Pt(L^7-*S,O*)$_2$** are also largely coplanar with the respective phenyl rings as illustrated by torsion angles C11-O5-C8-C9 and C22-O6-C19-C18 of -0.9(6)° and -2.(6)° respectively. Each of the methoxy substituents, while remaining coplanar with the respective phenyl rings, is angled inwards towards the adjacent phenyl moiety.

No classical intra- or intermolecular hydrogen bonds were observed in the crystal structure of complex **Pt(L^7-*S,O*)$_2$**. However, due to the overall planarity of the complex, two intermolecular π...π type interactions were observed, Cg1....$Cg4^i$ and Cg4...$Cg1^i$ [Cg1...$Cg4^i$ 3.67Å, Cg4...$Cg1^i$ 3.67Å where Cg1 is the centroid of the Pt1-O1-C2-N1-C3-S1 chelation ring and Cg4 is the centroid of the C12-C17-C18-C19-C20-C21 aromatic ring; symmetry code (i) -x, -y, -z] as illustrated in Figure 4 which result in a planar 'dimer type' arrangement of molecules when the unit cell is viewed along [010].

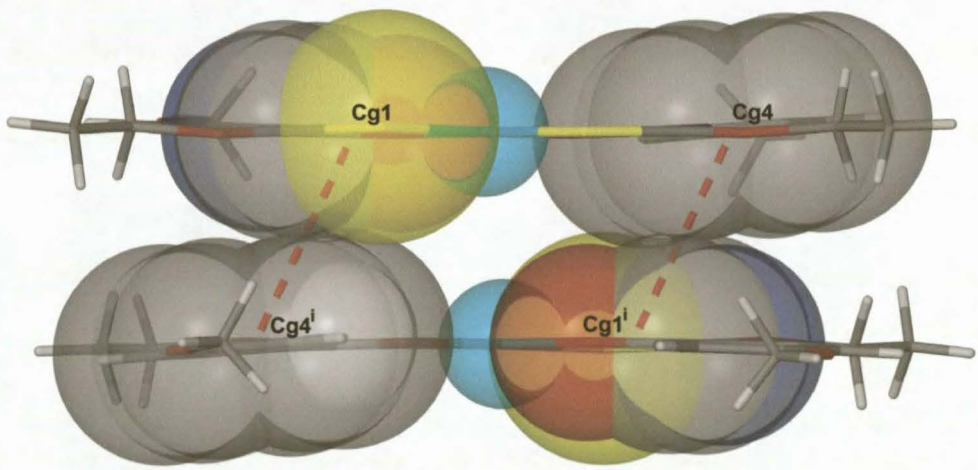

Figure 4 Intermolecular π...π type interactions observed between Cg1...$Cg4^i$ and Cg4...$Cg1^i$ in **Pt(L^7-*S,O*)$_2$**. Symmetry code (i) –x, -y, -z.

A non-classical intermolecular C-H...π interaction, C4-H41...$Cg4^{ii}$ [C4-H41...$Cg4^{ii}$ = 2.78Å; symmetry code (ii) -x, y-½, ½-z] expands the 'dimer-type' arrangement of molecules into one dimensional molecular strings extending parallel to [001] as illustrated in Figure 5.

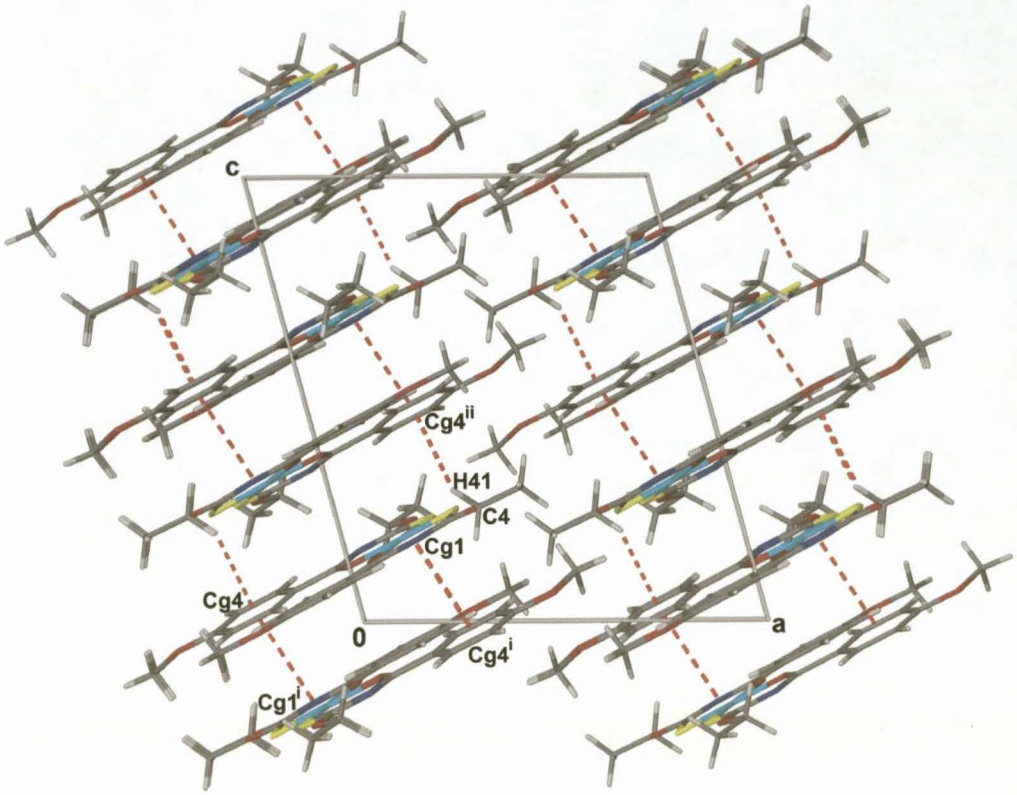

Figure 5 Extended packing diagram of **Pt(L^7-*S,O*)$_2$** as viewed along [010] showing the Cg1...Cg4^{i}, Cg4...Cg1^{i} and C4-H41...Cg4^{ii} interactions as identified by XSeed[21, 22] and Platon[23]. Symmetry code (ii) -x, y-½, ½-z.

2.3.2 Bis[*N*-(3,5-dimethoxybenzoyl)-*O*-ethyl-thiocarbamato]platinum(II), Pt(L^8-*S,O*)$_2$.

The molecular structure of complex **Pt(L^8-*S,O*)$_2$** is illustrated in Figure 6 and is essentially isostructural to complexes **Pt(L^1-*S,O*)$_2$** and **Pt(L^7-*S,O*)$_2$** despite the obvious increased steric hindrance resulting from the 3,5-dimethoxy substituents on the phenyl rings. Complex **Pt(L^8-*S,O*)$_2$** crystallises monoclinic, space group Cc with 4 formula units per unit cell. Bond lengths and torsion angles of interest for complex **Pt(L^8-*S,O*)$_2$** are listed in Table 5.

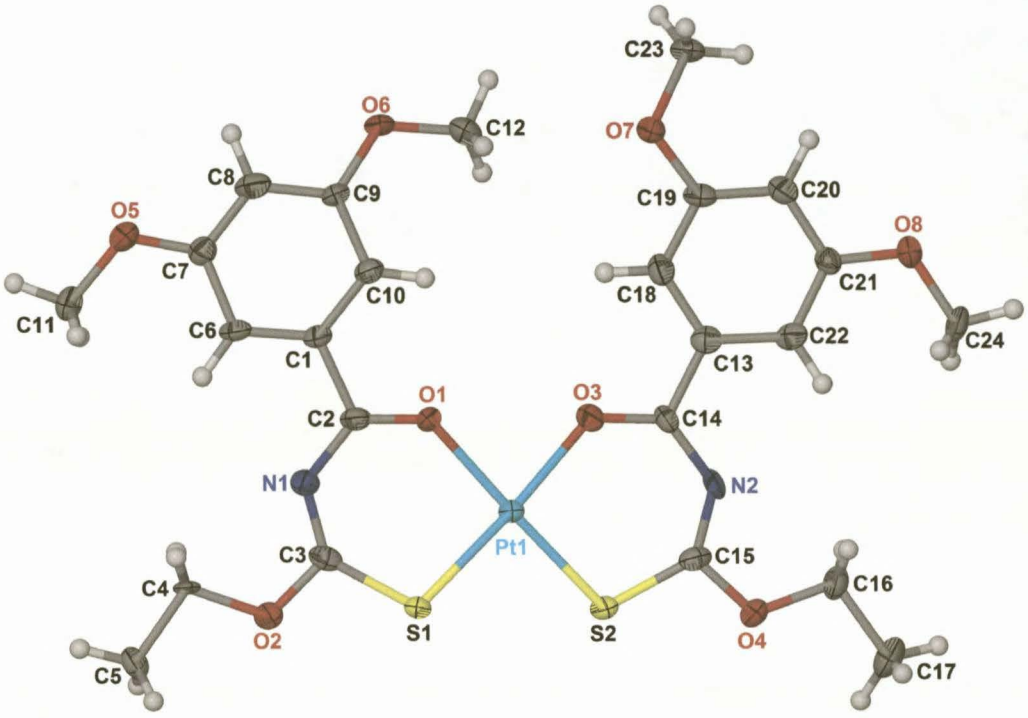

Figure 6 Molecular structure of **Pt(L^8-S,O)$_2$** showing the numbering scheme used. Displacement ellipsoids are drawn at the 50% probability level.

Pt1-O1	2.053(4)	Pt1-O3	2.031(5)
Pt1-S1	2.234(2)	Pt1-S2	2.233(2)
C2-O1	1.229(8)	C14-O3	1.270(8)
C3-S1	1.742(7)	C15-S2	1.719(7)
C2-N1	1.349(9)	C14-N2	1.335(9)
N1-C3	1.297(9)	N2-C15	1.278(9)
C1-C2	1.509(8)	C13-C14	1.472(9)
C3-O2	1.346(8)	C15-O4	1.329(8)
O2-C4	1.441(9)	O4-C16	1.445(9)
O1-C2-C1-C10	-0.3(5)	O3-C14-C13-C18	-3.4(5)
Pt1-O1-C2-N1	-1.9(6)	Pt1-O3-C14-N2	-0.7(11)
Pt1-S1-C3-N1	-4.8(4)	Pt1-S2-C15-N2	-2.4(8)
N1-C3-O2-C4	-6.5(5)	N2-C15-O4-C16	-4.4(9)
C11-O5-C7-C6	-1.3(11)	C12-O6-C9-C10	2.0(12)
C23-O7-C19-C20	4.8(10)	C24-O8-C21-C22	-4.5(10)

Table 5 Bond lengths (Å) and torsion angles (°) observed in **Pt(L^8-*S,O*)$_2$**.

The 3,5-dimethoxy electron releasing substituents on the phenyl rings of **Pt(L^8-*S,O*)$_2$** appear to have lengthened the Pt1-O1 and Pt1-O3 bond lengths [Pt-O1 2.053(4)Å; Pt-O3 2.031(5)Å] in comparison to the corresponding platinum-oxygen bond lengths bonds in complex **Pt(L^7-*S,O*)$_2$** [Pt1-O1 2.021(3)Å; Pt1-O3 2.023(5)Å] and complex **Pt(L^1-*S,O*)$_2$** [Pt1-O1 2.021(4)Å, Pt1-O3 2.012(4)Å] thereby effectively 'softening' the coordinating oxygen atoms in complex **Pt(L^8-*S,O*)$_2$**.

The phenyl rings of complex **Pt(L^8-*S,O*)$_2$** are coplanar with the least-squares plane defined through each intersecting at 0.9(3)°. The coplanarity of the phenyl rings with the adjacent chelate rings in complex **Pt(L^8-*S,O*)$_2$** is illustrated by torsion angles O1-C2-C1-C10 and O3-C14-C13-C18 of -0.3(5)° and -3.4(5)° respectively.

The methoxy substituents on the C1-C6-C7-C8-C9-C10 phenyl ring are both in plane with the phenyl ring [C11-O5-C7-C6 = -1.3(11)°, C12-O6-C9-C10 = 2.0(12)°] and are angled away from each other in towards the chelate ring. The C24-O8 methoxy substituent is coplanar with the C13-C18-C19-C20-C21-C22 phenyl ring [C24-O8-C21-C22 = -4.5(10)°] and angled in towards the chelate rings of **Pt(L^8-*S,O*)$_2$**, however, the C23-O7 methoxy substituent, while also being largely coplanar with C13-C18-C19-C20-C21-C22 phenyl ring [C23-O7-C19-C20 = 2.0(12)°], is angled away from the chelate ring possibly due to the steric crowding experienced between the two phenyl rings and methoxy substituent C12-O6.

Non-classical 1-5 intramolecular hydrogen contacts were observed in complex **Pt(L^8-*S,O*)$_2$** comparable to those observed in complex **Pt(L^7-*S,O*)$_2$** (see Figure 3). These intramolecular hydrogen contacts are

listed in Table 6. The hydrogen contact geometry has been determined for both calculated/placed and located/found hydrogens during the structure refinement process.

method	D-H...A	D-H (Å)	H...A (Å)	D...A (Å)	D-H...A (°)
calculated	C6---H6...N1	0.94	2.46	2.78(1)	99.8
located		1.04(6)	2.59(5)	2.787(7)	89(3)
calculated	C10---H10...O1	0.94	2.34	2.657(8)	99.1
located		0.96(7)	2.52(6)	2.671(7)	88(4)
calculated	C18-H18...O3	0.94	2.43	2.72(1)	98.0
located		0.86(6)	2.43(6)	2.732(8)	101(4)
calculated	C22-H22...N2	0.94	2.44	2.756(9)	99.3
located		1.01(5)	2.39(5)	2.751(8)	100(3)

Table 6 Non-classical 1-5 intramolecular hydrogen contact geometry observed for **Pd(L^8-*S,O*)$_2$** as determined for placed/calculated hydrogens as well as for found/located hydrogens as identified by XSeed[21, 22] and Platon[23] with s.u.s in parenthesis.

Two intermolecular π…π type interactions were observed in the extended packing diagram of complex **Pt(L^8-*S,O*)$_2$** namely Cg3…Cg4^{iii} and Cg4…Cg3^{iv} [Cg3…Cg4^{iii} 5.53Å, Cg4…Cg3^{iv} 3.53Å, here Cg3 is the centroid of the C1-C6-C7-C8-C9-C10 aromatic ring and Cg4 is the centroid of the C13-C18-C19-C20-C21-C22 aromatic ring; symmetry code (iii) ½+x, ½+y, z; (iv) x-½, y-½,z] which result in the formation of molecular strings extending diagonally across and parallel to the *a-b* plane of the unit cell as illustrated in Figure 7.

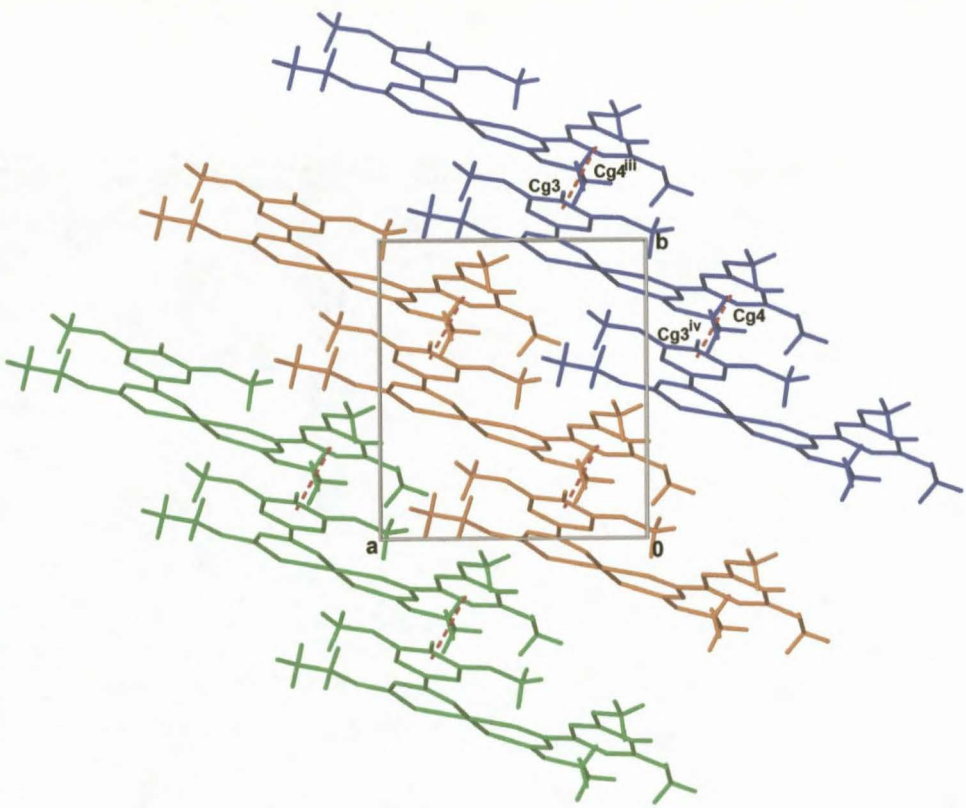

Figure 7 The molecular strings of **Pt(L^8-*S,O*)$_2$** that extend parallel to the *a-b* plane of the unit cell which result from the Cg3…Cg4^{iii} and Cg4…Cg3^{iv} interactions. The individual molecular strings are indicated in blue, brown and green respectively. Symmetry codes (iii) ½+x, ½+y, z; (iv) x-½, y-½,z.

The molecular strings of complex **Pt(L^8-*S,O*)$_2$** illustrated in Figure 7 are expanded into two dimensional molecular sheets by the observed non-classical intermolecular C4-H42…Cg2^{iii} and C24-H242…Cg1^{v} interactions [C4-H42…Cg2^{iii} 2.91Å 139.1°, C24-H242…Cg1^{v} 2.85Å 138.1°; where Cg1 is the centroid of the Pt1-O1-C2-N1-C3-S1 chelate ring and Cg2 is the centroid of the Pt1-O3-C14-N2-C15-S2 chelate ring; symmetry code (iii) ½+x, ½+y, z, (v) x-1, y, z].

2.3.3 Bis[*N*-(3,4,5-trimethoxybenzoyl)-*O*-ethyl-thiocarbamato]nickel (II), Ni(L^9-*S,O*)$_2$.

The molecular structure of complex **Ni(L^9-*S,O*)$_2$** is illustrated in Figure 8 and is isostructural to complex **Ni(L^1-*S,O*)$_2$** described in chapter II. Complex **Ni(L^9-*S,O*)$_2$** crystallises triclinic space group P$\bar{1}$ illustrated with two formula units per unit cell.

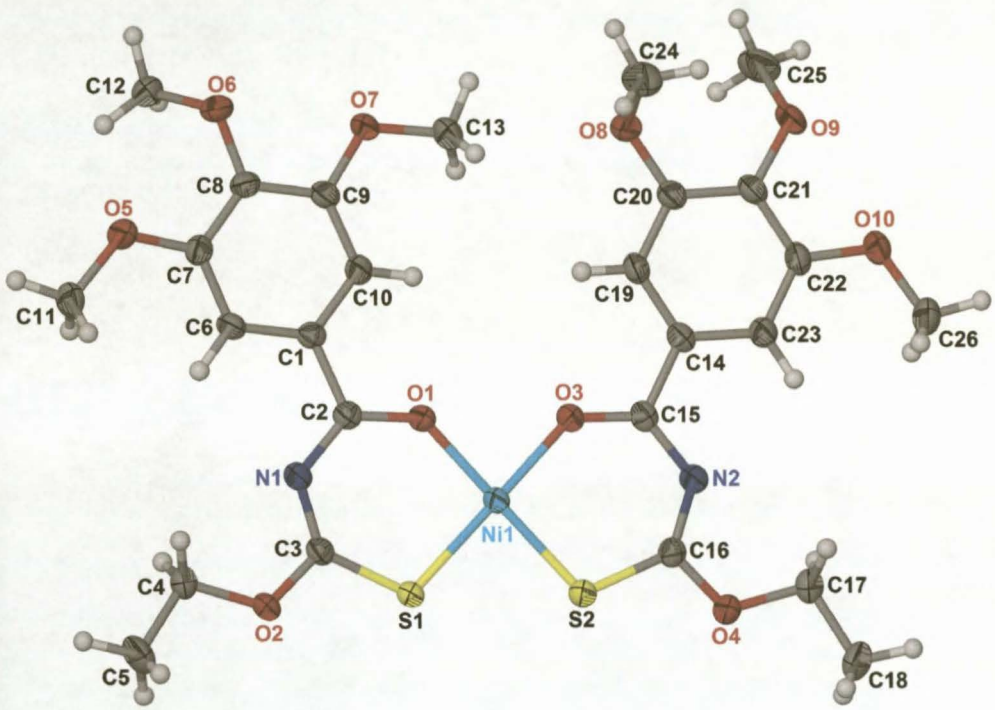

Figure 8 Molecular structure of **Ni(L^9-*S,O*)$_2$** showing the numbering scheme used. Displacement ellipsoids are drawn at the 50% probability level.

Bond lengths and torsion angles of interest in the molecular structure of complex **Ni(L^9-*S,O*)$_2$** are listed in Table 7. The bond lengths throughout each of the chelate rings of complex **Ni(L^9-*S,O*)$_2$** are consistent with extensive electron delocalization through each of the carbon-nitrogen, carbon-oxygen and carbon-sulphur bonds of the chelate rings.

Ni1-O1	1.864(1)	Ni1-O3	1.881(1)
Ni1-S1	2.1415(5)	Ni1-S2	2.1364(5)
C2-O1	1.272(2)	C15-O3	1.264(2)
C3-S1	1.721(2)	C16-S2	1.716(2)
C2-N1	1.342(2)	C15-N2	1.348(2)
N1-C3	1.305(2)	N2-C16	1.307(2)
C1-C2	1.477(3)	C14-C15	1.479(3)
C3-O2	1.327(2)	C16-O4	1.333(2)
O2-C4	1.464(2)	O4-C17	1.456(2)
O1-C2-C1-C10	3.5(3)	O3-C15-C14-C19	0.7(3)
Ni1-O1-C2-N1	0.4(3)	Ni1-O3-C15-N2	-1.6(4)
Ni1-S1-C3-N1	8.8(2)	Ni1-S2-C16-N2	7.8(2)
N1-C3-O2-C4	4.5(3)	N2-C16-O4-C17	5.6(3)
C11-O5-C7-C6	-11.2(3)	C12-O6-C8-C7	-56.1(3)
C13-O7-C9-C10	-2.7(3)	C24-O8-C20-C21	-71.0(3)
C25-O9-C21-C20	-54.7(3)	C26-O10-C22-C23	-5.8(3)

Table 7 Bond lengths (Å) and torsion angles (°) observed in **Ni(L^9-*S,O*)$_2$**.

Although complex **Ni(L^9-*S,O*)$_2$** has crystallized with a *cis*-(*S,O*) square planar arrangement of the ligator atoms, a significant degree of buckling is observed in each of the chelate rings of complex **Ni(L^9-*S,O*)$_2$** (see Figure 9) in comparison to complex **Ni(L^1-*S,O*)$_2$** (see Figure 10 chapter II) as indicated by torsion angles Ni1-S1-C3-N1 and Ni1-S2-C16-N2 of 8.8(2)° and 7.8(2)° respectively. The observed buckling of the chelate rings in the molecular structure of complex **Ni(L^9-*S,O*)$_2$** prevents the chelate rings from maintaining a similar degree of co-planarity to that observed in the molecular structures of complexes **Ni(L^1-*S,O*)$_2$**, **Pt(L^7-*S,O*)$_2$** and **Pt(L^8-*S,O*)$_2$**. The O1/C2/N1/C3/S1 and O3/C15/N2/C16/S2 least-squares planes defined through the chelate rings of complex **Ni(L^9-*S,O*)$_2$** intersect at the comparatively higher angle of 5.92(7)°.

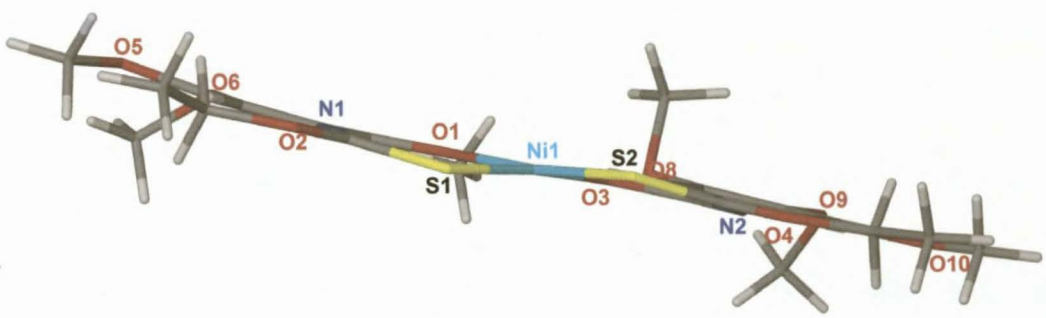

Figure 9 Side on view of **Ni(L^9-*S,O*)$_2$** illustrating the buckling of the chelation rings.

In spite of the observed comparative buckling of the chelate rings in complex **Ni(L^9-*S,O*)$_2$**, the phenyl rings remain essentially coplanar with the least-square planes defined through each intersecting at 3.92(8)°. The phenyl rings are in turn slightly twisted relative to the corresponding chelate rings, the C1/C6/C7/C8/C9/C10 and Ni1/O1/C2/N1/C3/S1 least-squares planes intersect at 6.46(7)°, while the C14/C19/C20/C21/C22/C23 and Ni1/O3/C15/N2/C16/S2 least-squares planes intersect at 4.20(7)°.

The comparative greater degree of distortion from overall planarity observed in the molecular structure of **Ni(L^9-*S,O*)$_2$** is most likely due to the increased steric hindrance that is experienced resulting from the 3,4,5-trimethoxy substituents on each of the phenyl rings. This steric hindrance is illustrated by the twisting of methoxy groups C12-O6, C24-O8 and C25-O9 out of the planes defined by each of the respective phenyl rings. The twisting out of plane of these methoxy groups is evident in the side on view of complex **Ni(L^9-*S,O*)$_2$** illustrated in Figure 9 and Figure 10 and is further illustrated by torsion angles C12-O6-C8-C7, C24-O8-C20-C21 and C25-O9-C21-C20 of -56.1(3)°, -71.0(3)° and -54.7(3)° respectively. Furthermore, each of the three hydrogens of atom C12 is disordered across two positions, each with a site occupancy factor of 50%.

The twisting of methoxy groups C24-O8 and C25-O9 out of the plane as defined by the C14-C19-C20-C21-C22-C23 phenyl ring appear to be stabilised by the observed non-classical intramolecular C24-H241…O9 and C25-H252…O8 contacts illustrated in Figure 10 [placed/calculated hydrogen positions: C24-H241…O9 2.51Å 120.3°; C25-H252…O8 2.57 101.2°; found/located hydrogen positions: C24-H241…O9 2.60Å 121(3)°; C25-H252…O8 2.58(4)Å 99(2)°].

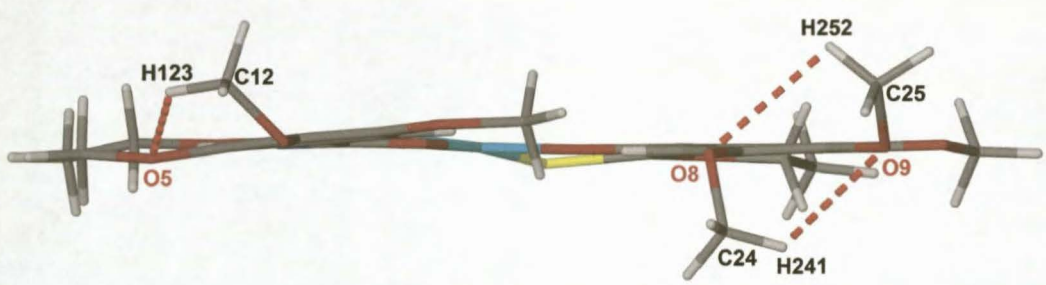

Figure 10 C24-H241…O9 and C25-H252…O8 electrostatic interactions observed in **Ni(L^9-*S,O*)$_2$** as identified by Platon[23].

Non-classical 1-5 intramolecular hydrogen contacts, comparable to those observed in the molecular structures of **Pt(L^7-*S,O*)$_2$** and **Pt(L^8-*S,O*)$_2$**, were observed between C6-H6…N1, C10-H10…O1 and C19-H19…O3 and C23-H23…N2 [see Table 8]. These non-classical intramolecular hydrogen interactions possibly minimise the degree as to which the phenyl rings would otherwise be twisted out of plane relative to the respective chelate rings due to the high degree of steric hindrance experienced by the phenyl rings.

Method	D-H...A	D-H (Å)	H...A (Å)	D...A (Å)	D-H...A (°)
calculated	C6---H6...N1	0.94	2.44	2.761(3)	100.1
located		0.86(2)	2.41(2)	2.763(3)	105(2)
calculated	C10---H10...O1	0.94	2.41	2.718(3)	98.7
located		1.00(2)	2.43(2)	2.716(3)	95(2)
calculated	C19-H19...O3	0.94	2.47	2.766(3)	98.3
located		0.97(3)	2.49(2)	2.765(3)	96(2)
calculated	C23-H23...N2	0.94	2.41	2.744(3)	100.7
located		0.88(2)	2.41(2)	2.744(3)	103(2)

Table 8 Non-classical 1-5 intramolecular hydrogen contact geometry observed for **Ni(L^9-*S,O*)$_2$** as determined for placed/calculated hydrogens as well as for found/located hydrogens as identified by XSeed[21, 22] and Platon[23] with s.u.s in parenthesis.

Two intermolecular π...π type interactions were observed, Cg3...Cg4^{vi} and Cg4...Cg3^{vii} [Cg3...Cg4^{vi} 3.63Å, Cg4...Cg3^{vii} 3.63Å where Cg3 is the centroid of the C1-C6-C7-C8-C9-C10 phenyl ring and Cg4 is the centroid of the C14-C19-C20-C21-C22-C23 phenyl ring; symmetry code (vi) x-1, y, z (vii) 1+x, y, z], which appear to dictate the overall packing of molecules of complex **Ni(L^9-*S,O*)$_2$** within the unit cell. These intermolecular π...π type interactions result in the formation of one dimensional molecular strings extending parallel to the *a*-axis of the unit cell as illustrated in Figure 11.

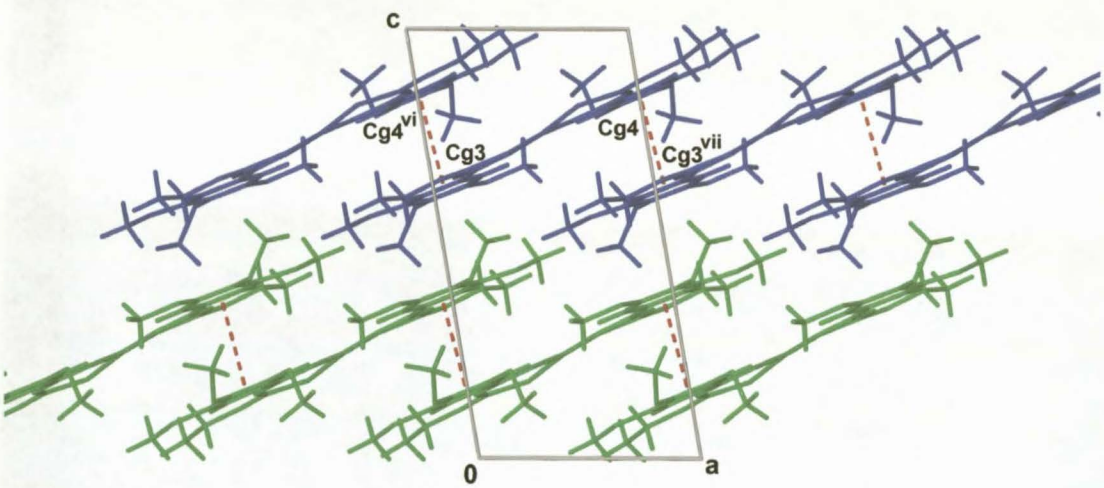

Figure 11 Extended packing diagram of **Ni(L^9-*S,O*)$_2$** as viewed along [010]. The one dimensional molecular strings extending parallel to the *a*-axis are indicated in blue and green respectively.

The one dimensional molecular strings indicated in Figure 11 are further cross-linked by non-classical intermolecular C-H...π interactions that expand the one dimensional strings into two dimensional molecular sheets extending parallel to the *a-b* plane [C4-H42...Cg3^{viii} 2.72Å, C17-H172...Cg1^{vii} 2.80Å; where Cg3 is the centroid of the C1-C6-C7-C8-C9-C10 phenyl ring and Cg1 is the centroid of the Ni1-O1-C2-N1-C3-S1 chelation ring; symmetry code (vii) x+1, y, z (viii) –x, 2-y, 1-z].

2.3.4 Evaluation of the effect of the methoxy substituents in complexes $M(L^{7-9}\text{-}S,O)_2$

Methoxy groups were incrementally substituted in the 4, 3 and 5, and 3,4,5 positions of the benzoyl groups of ligands **H(L^7-*S,O*)**, **H(L^8-*S,O*)** and **H(L^9-*S,O*)** respectively, while the alkoxy substituent of ligand each remained unchanged. These ligands were complexed with Ni(II), Pd(II) and Pt(II) with the objective of investigating the effect the methoxy substituents have on the molecular and crystal structures of the resultant complexes in comparison to the molecular and crystal structures of the series of complexes described in chapter II in which the alkyl substituents were systematically varied while the benzoyl moiety of each remained unchanged.

It was speculated that the electron rich methoxy substituents introduced onto the benzoyl moieties of ligands **H(L^7-*S,O*)**, **H(L^8-*S,O*)** and **H(L^9-*S,O*)** would

- increase the steric hindrance around the phenyl rings in the resultant complexes and
- possibly have an electronic influence on the coordinating carbonyl moiety in the resultant complexes due to the electronic releasing properties of the introduced methoxy substituents.

Complexes **Pt(L^7-*S,O*)$_2$** and **Pt(L^8-*S,O*)$_2$** are isostructural to the bis(*N*-benzoyl-*O*-ethylthiocarbamato)platinum(II) **Pt(L^1-*S,O*)$_2$** described in chapter II. The only difference in terms of substituents, is the methoxy and dimethoxy substituted benzoyl moieties of **Pt(L^7-*S,O*)$_2$** and **Pt(L^8-*S,O*)$_2$** in comparison to the unsubstituted benzoyl moiety of **Pt(L^1-*S,O*)$_2$**. This enables a direct comparison of the calculated difference in the average Pt-O and Pt-S bond lengths each complex , i.e. (|average (M-O) – average (M-S)|) in Table 9, and differences in these values may then be tentatively attributed to the methoxy substituents introduced in complexes **Pt(L^7-*S,O*)$_2$** and **Pt(L^8-*S,O*)$_2$**. The Pt-O and Pt-S bond lengths of the structurally analogous complexes *cis*-bis(*N*-benzoyl-*N'*,*N'*-diethylthioureato)platinum(II), **Pt(L^{12}-*S,O*)$_2$**[24], and *trans*-bis(*N*-naphthoyl-*N'*,*N'*-dibutylthioureato)platinum(II), **Pt(L^{13}-S,O)$_2$**[9] have been obtained from the CSD (Cambridge Structural Database)[10] and included in Table 9 for comparative purposes.

Bond	Pt(L^7-S,O)$_2$	Pt(L^8-S,O)$_2$	Pt(L^1-*S,O*)$_2$	Pt(L^{12}-S,O)[24]	*Pt(L^{13}-S,O)[9]
M-S	2.230(1)	2.234(2)	2.232(2)	2.231(2)	2.250
M-S	2.222(1)	2.233(2)	2.233(2)	2.233(2)	2.250
ave M-S	2.226(1)	2.234(1)	2.233(2)	2.232(1)	2.250
M-O	2.021(3)	2.053(4)	2.021(4)	2.018(5)	1.982
M-O	2.023(3)	2.031(5)	2.012(4)	2.023(6)	1.982
ave M-O	2.022(2)	2.042(3)	2.017(3)	2.021(4)	1.198
|(ave M-S)-(ave M-O)|	**0.204(2)**	**0.192(3)**	**0.216(4)**	**0.211(4)**	**0.268**

Table 9 Comparison of the Pt-O and Pt-S bond lengths of **Pt(L^7-*S,O*)$_2$**, **Pt(L^8-*S,O*)$_2$**, **Pt(L^1-*S,O*)$_2$**, **Pt(L^{12}-*S,O*)$_2$**[24] and **Pt(L^{13}-S,O)$_2$**[9].

* The value of the metal-oxygen and metal-sulphur bonds lengths of **Pt(L^{13}-*S,O*)$_2$** were obtained from the CSD and therefore esd values of these bonds are not quoted.

The difference in the average Pt-O and Pt-S bond lengths of the *cis* complexes **Pt(L^1-*S,O*)$_2$** and **Pt(L^{12}-*S,O*)$_2$** are comparable and substantially smaller than the difference in the average Pt-O and Pt-S bond lengths of ***trans*-Pt(L^{13}-S,O)$_2$**. Further to this, the methoxy and dimethoxy substituents of **Pt(L^8-*S,O*)$_2$** appear to have effectively lengthened the average Pt-O bond lengths in comparison to complex **Pt(L^1-*S,O*)$_2$** and thereby reduced the difference in the average Pt-O and Pt-S bonds in comparison to the differences in the average Pt-O and Pt-S bond lengths of complexes **Pt(L^1-*S,O*)$_2$**, **Pt(L^{12}-*S,O*)$_2$** and **Pt(L^{13}-*S,O*)$_2$**.

It is also possible to compare the difference in the average Ni-O and Ni-S bond lengths of **Ni(L^9-*S,O*)$_2$** with the difference in the average Ni-O and Ni-S bond lengths of **Ni(L^1-*S,O*)$_2$**. The Ni-O and Ni-S bond lengths of the structurally analogous Ni(II) complexes *cis*-bis(*N*-benzoyl-*N'*,*N'*-diethylthioureato)nickel(II)[25], **Ni(L^{12}-*S,O*)$_2$**, and *cis*-bis(*N*-naphthoyl-*N'*,*N'*-diethylthioureato)nickel(II)[26], **Ni(L^{14}-*S,O*)$_2$**, as obtained from the CSD[10], have been included in Table 10 for comparative purposes.

Bond	**Ni(L^9-*S,O*)$_2$**	**Ni(L^1-*S,O*)$_2$**	**Ni(L^{12}-*S,O*)$_2$**[25]	**Ni(L^{14}-*S,O*)$_2$**[26]
M-S	2.1415(1)	2.1400(5)	2.127	2.144
M-S	2.1364(5)	2.1420(6)	2.140	2.146
ave M-S	2.1390(5)	2.1410(4)	2.134	2.145
M-O	1.864(1)	1.867(1)	1.845	1.854
M-O	1.881(1)	1.869(1)	1.857	1.847
ave M-O	1.873(1)	1.868(1)	1.851	1.851
(ave M-S)-(ave M-O)	**0.266(5)**	**0.273(4)**	**0.283**	**0.294**

Table 10 Comparison of the Ni-O and Ni-S bond lengths of **Ni(L^9-*S,O*)$_2$**, **Ni(L^1-*S,O*)$_2$**, **Ni(L^{12}-*S,O*)$_2$**[25] and **Ni(L^{14}-*S,O*)$_2$**[26].

The difference in the average Ni-O and Ni-S bond lengths of complex **Ni(L^9-*S,O*)$_2$** is comparable to the differences in the average Ni-O and Ni-S bond lengths of complexes **Ni(L^1-*S,O*)$_2$** and **Ni(L^{12}-*S,O*)$_2$** but marginally smaller than the difference in the average Ni-O and Ni-S bonds length of complex **Ni(L^{14}-*S,O*)$_2$**. It can therefore be concluded that the electronic effect of the methoxy substituents on the Ni-O bond in complex **Ni(L^9-*S,O*)$_2$** is marginal at best.

The molecular structures of compounds bis(*N*-(3,5-dimethoxybenzoyl)-*N'*,*N'*-diethylthioureato)platinum(II), **Pt(L^{10}-*S,O*)$_2$**, and bis(*N*-(3,4,5-trimethoxybenzoyl)-*N'*,*N'*-diethylthioureato)platinum(II), **Pt(L^{11}-*S,O*)$_2$**, were determined in collaboration with D. Hanekom of the Research Group for Platinum Metals Chemistry at the Stellenbosch University[19]. Although these complexes did not form part of the greater investigation described in this thesis, these molecular structures are included here for comparative purposes, as they, as yet, are not published or listed on the

CSD[10]. The molecular structures of complexes **Pt(L^{10}-*S,O*)$_2$**, and **Pt(L^{11}-*S,O*)$_2$** are illustrated in Figure 12 and Figure 13 respectively.

In general, complexes **Pt(L^{10}-*S,O*)$_2$** and **Pt(L^{11}-*S,O*)$_2$** are isostructural to **Pt(L^{7}-*S,O*)$_2$**, **Pt(L^{8}-*S,O*)$_2$** and **Ni(L^{9}-*S,O*)$_2$** in that the respective *N*-(methoxy-substituted benzoyl)-*N'*,*N'*-diethylthiourea ligands are coordinated in a square planar *cis*-bis(*S,O*) fashion. Some disorder is observed in the O7-C28 methoxy substituent of **Pt(L^{10}-*S,O*)$_2$**. Both the oxygen and carbon atoms are disordered across two positions, each with a site occupancy factor of 50%. Carbon atoms C4 and C5 of complex **Pt(L^{11}-*S,O*)$_2$** are disordered across two positions, each with a site occupancy factor of 89% and 11% respectively while C21 and C22 are also disordered across two positions, each with a site occupancy factor of 66.5% and 33.5% respectively. The disorder observed in complexes **Pt(L^{10}-*S,O*)$_2$** and **Pt(L^{11}-*S,O*)$_2$** does not affect the Pt-O and Pt-S bond lengths used in comparison to the average Pt-O and Pt-S bond lengths of complexes **Pt(L^{7}-*S,O*)2**, **Pt(L^{8}-*S,O*)$_2$** and **Ni(L^{9}-*S,O*)$_2$**.

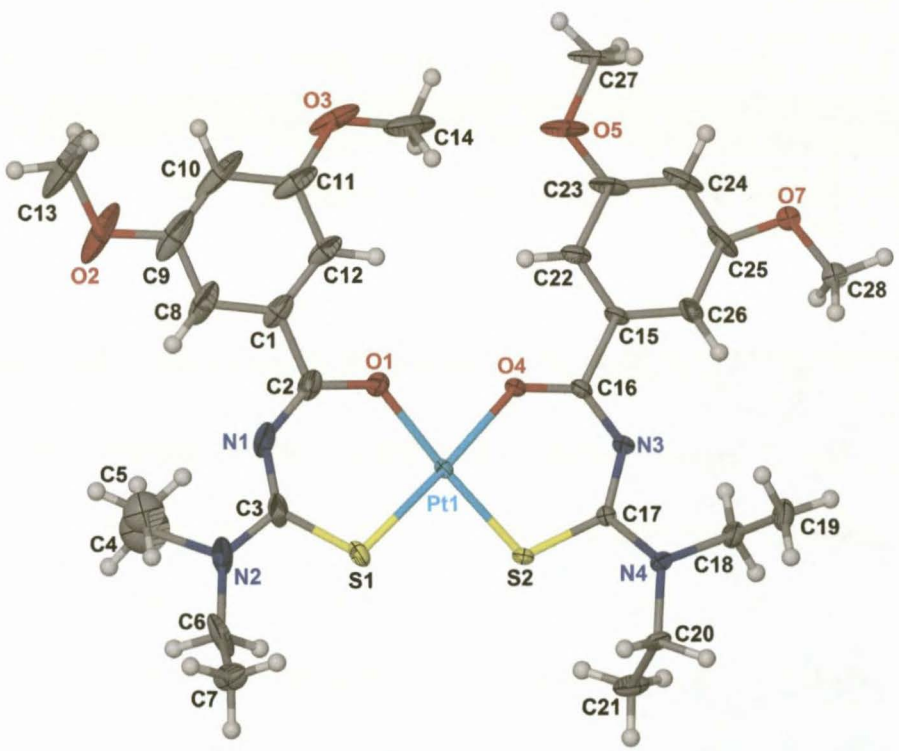

Figure 12 Molecular structure of complex **Pt(L^{10}-*S,O*)$_2$** showing the numbering scheme used. Displacement ellipsoids are drawn at the 50% probability level.

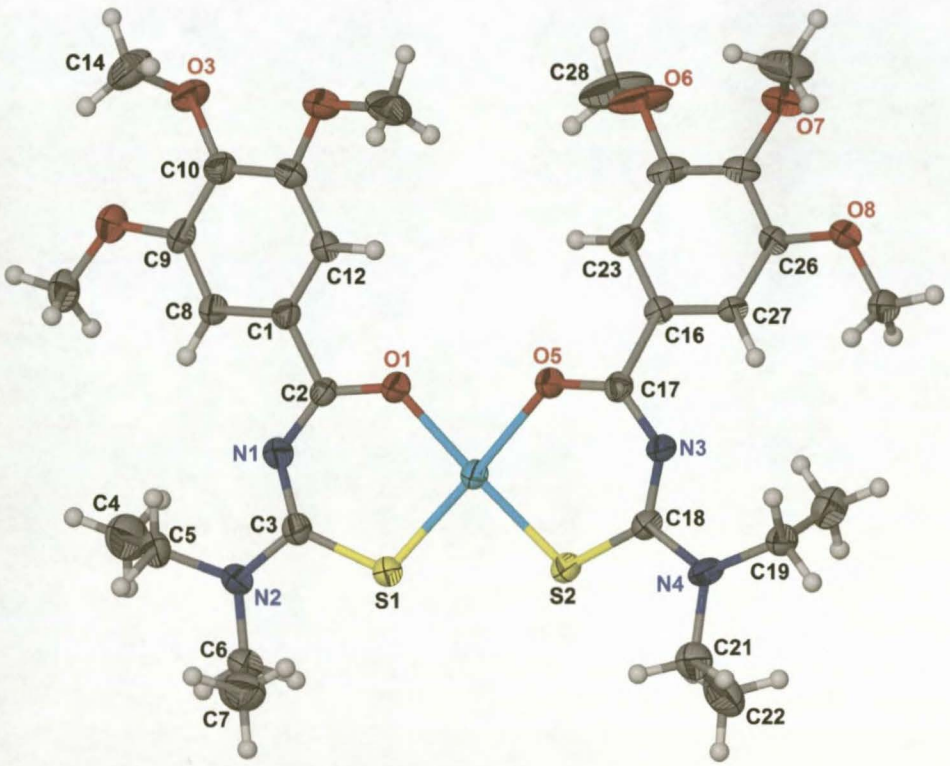

Figure 13 Molecular structure of complex **Pt(L^{11}-*S,O*)$_2$** showing the numbering scheme used. Displacement ellipsoids are drawn at the 50% probability level.

The Pt-O and Pt-S bond lengths of complexes **Pt(L^7-S,O)$_2$**, **Pt(L^8-S,O)$_2$**, **Pt(L^{10}-S,O)$_2$**, **Pt(L^{11}-S,O)$_2$** and **Pt(L^{12}-*S,O*)$_2$**[24] are listed in Table 11. The differences in the average Pt-O and Pt-S bond lengths of each complex, as listed in Table 11, can be used to monitor the effect that the methoxy substituents in each complex have on these bonds i.e. the smaller the difference in these bond lengths; the more the Pt-O bond length has been lengthened, presumably due electron rich properties of the methoxy substituents of the benzoyl rings.

Bond	Pt(L^7-S,O)$_2$	Pt(L^8-S,O)$_2$	Pt(L^1-*S,O*)$_2$	Pt(L^{10}-S,O)$_2$	Pt(L^{11}-S,O)$_2$	Pt(L^{12}-*S,O*)$_2$[24]
M-S	2.230(1)	2.234(2)	2.232(2)	2.236(9)	2.233(1)	2.231(2)
M-S	2.222(1)	2.233(2)	2.233(2)	2.231(9)	2.235(1)	2.233(2)
ave M-S	2.226(1)	2.234(1)	2.233(2)	2.234(6)	2.234(1)	2.232(1)
M-O	2.021(3)	2.053(4)	2.021(4)	2.010(2)	2.017(2)	2.018(5)
M-O	2.023(3)	2.031(5)	2.012(4)	2.014(2)	2.042(3)	2.023(6)
ave M-O	2.022(2)	2.042(3)	2.017(3)	2.012(3)	2.030(2)	2.021(4)
(ave M-S)-(ave M-O)	**0.204(2)**	**0.192(3)**	**0.216(4)**	**0.222(3)**	**0.204(2)**	**0.211(4)**

Table 11 M-O and M-S bond lengths of interest for compounds **Pt(L^7-S,O)$_2$**, **Pt(L^8-S,O)$_2$**, **Pt(L^1-S,O)$_2$**, **Pt(L^{10}-S,O)$_2$**, **Pt(L^{11}-S,O)$_2$** and **Pt(L^{12}-S,O)$_2$**[24].

The difference in the average Pt-O and Pt-S bond lengths of complex **Pt(L^8-*S,O*)$_2$** has effectively been reduced in comparison to the difference in the average Pt-O and Pt-S bond lengths of complex **Pt(L^1-*S,O*)$_2$**. However, in the case of complex **Pt(L^7-*S,O*)$_2$** the effect on the equivalent bonds is less. The difference in the Pt-O and Pt-S bonds in complex **Pt(L^{11}-*S,O*)$_2$** has also been effectively reduced relative to complex **Pt(L^{12}-*S,O*)$_2$**.

2.4 NMR Spectroscopy

The ^{1}H, ^{13}C and ^{195}Pt NMR spectra are valuable in the characterisation of complexes **M(L^7-*S,O*)$_2$**, **M(L^8-*S,O*)$_2$** and **M(L^9-*S,O*)$_2$**, [M = Ni(II), Pd(II) and Pt(II)], as several NMR "handles" are available in these spectra by which the coordination of the *N*-aroylthiocarbamic-*O*-ethyl ester to the respective metal ions can be monitored. ^{1}H, ^{13}C and ^{195}Pt NMR spectroscopy can also be used to confirm that the coordination of the *N*-aroylthiocarbamic-*O*-ethyl ester to the respective metal ions is in fact in a deprotonated bidentate-(*S,O*) fashion. The 2:1 ligand to metal ratio of the complexes was confirmed using C, H, N, S analysis.

The ^{1}H and ^{13}C NMR spectra of complexes **M(L^7-*S,O*)$_2$**, **M(L^8-*S,O*)$_2$** and **M(L^9-*S,O*)$_2$** [M = Ni(II), Pd(II) and Pt(II)] generally consist of resonance peaks which closely resemble those of the bis(*O*-alkyl-*N*-benzoylthiocarbamato)metal(II) complexes discussed in chapter II. The most significant and distinctive change that occurs in the ^{1}H NMR spectra of the uncoordinated ligands upon coordination to the respective metal ions, is the disappearance of the distinctive N-H singlet in the 9.1 – 9.2 ppm region. This confirms that the coordination of the ligand to the metal has occurred in a deprotonated fashion.

In order to enhance the characteristically weak ^{13}C resonance signals of the thiocarbonyl and carbonyl moieties, the ^{13}C spectra of both the uncoordinated ligands, as well as the complexes, were acquired using a 1 second pulse delay. In all the uncoordinated ligands, the thiocarbonyl peak appears furthest downfield consistently at 190 ppm, while the carbonyl peak is observed consistently at 163(±1)ppm, regardless of the *N*-aroyl substituent used [**H(L^7-*S,O*)** C(S) 190.9ppm C(O) 164.5ppm; **H(L^8-*S,O*)** C(S) 190.3ppm C(O) 163.3ppm; **H(L^9-*S,O*)** C(S) 190.6ppm C(O) 163.2ppm]. Due to the bidentate-(*S,O*) coordination of the *N*-aroylthiocarbamic-*O*-ethyl ester ligands to the respective metal ions, a substantial upfield shift is observed in the ^{13}C NMR signal of the C(S) group along with a substantial downfield shift in the signal for the C(O) group resulting in the thiocarbonyl signal of the complex now being more upfield relative to the carbonyl signal. This observed 'cross-over' pattern of the C(O) and C(S) ^{13}C NMR signals of the *N*-aroylthiocarbamic-*O*-ethyl esters upon coordination with the metal is comparable to that which has been widely reported for the complexation of the structurally analogous *N*-aroyl(acyl)-*N'*,*N'*-dialkylthioureas with Pd(II) and Pt(II)[9, 12, 15, 17, 27, 28]. The ^{13}C NMR signals of the C(S) and C(O) groups of the **M(L^{7-9}-*S,O*)$_2$** complexes are separated by 5 – 8ppm in comparison to the corresponding signals of the uncoordinated *N*-aroylthiocarbamic-*O*-ethyl esters, separated by ±26ppm.

An interesting trend is revealed in the relative upfield and downfield displacements of the thiocarbonyl and carbonyl resonances of the uncoordinated ligand **H(L^9-*S,O*)** upon complexation with the respective metal ions. These displacements are defined as follows and are listed in Table 12:

- $\Delta^1 = (|\delta^{13}C(S)_{complex} - \delta^{13}C(S)_{ligand}|)$
- $\Delta^2 = (|\delta^{13}C(O)_{complex} - \delta^{13}C(O)_{ligand}|)$

HL^9		Ni(L^9-*S,O*)$_2$				Pd(L^9-*S,O*)$_2$				Pt(L^9-*S,O*)$_2$			
C(S)	C(O)	C(S)	Δ^1	C(O)	Δ^2	C(S)	Δ^1	C(O)	Δ^2	C(S)	Δ^1	C(O)	Δ^2
190.6	163.2	178.5	12.1	186.7	23.5	176.8	13.8	184.3	21.1	174.1	16.5	181.4	18.2

Table 12 ^{13}C NMR shifts of thiocarbonyl and carbonyl moieties of **H(L^9-*S,O*)**, **Ni(L^9-*S,O*)$_2$**, **Pd(L^9-*S,O*)$_2$** and **Pt(L^9-*S,O*)$_2$**. Relative displacements $\Delta^1 = (|\delta^{13}C(S)_{complex} - \delta^{13}C(S)_{ligand}|$ and $\Delta^2 = (|\delta^{13}C(O)_{complex} - \delta^{13}C(O)_{ligand}|)$ are listed.

The relative displacement of the thiocarbonyl resonance (Δ^1) for the **Pt(L^9-*S,O*)$_2$** complex is larger than that of complex **Pd(L^9-*S,O*)$_2$**, which in turn is larger than that of complex, **Ni(L^9-*S,O*)$_2$**. The reverse is true for the relative displacements of the resonance of the carbonyl moieties (Δ^2), where the relative displacement of the carbonyl moiety (Δ^2) of complex **Ni(L^9-*S,O*)$_2$** is larger than that observed for complex **Pd(L^9-*S,O*)$_2$** which is in turn larger than that observed for complex, **Pt(L^9-*S,O*)$_2$**. Thus the trend observed for the displacement of the thiocarbonyl moiety follows the order Pt(II) > Pd(II) > Ni(II) while the trend observed for the displacement of the carbonyl moiety follows the order Ni(II) > Pd(II) > Pt(II). Given that the thiocarbonyl and carbonyl moieties are directly bonded to the metals through the sulphur and oxygen donor atoms respectively, it may be speculated that the displacements reflect the order of the HSAB[29] of 'softness' in the order Pt(II) > Pd(II) > Ni(II). A similar trend was observed for the series of *N*-benzoylthiocarbamic-*O*-alkyl ester ligands and complexes described in chapter II.

A small upfield shift in the order of 0.2 - 0.5ppm is observed in the ^{1}H signal of the methyl and methylene hydrogens of the ethoxy substituent of each of the uncoordinated ligands upon coordination with the respective metal ions. The upfield shift in the ^{13}C signals of the corresponding carbon atoms are a little more substantial and are in the order of 3 – 5 ppm. Comparable shifts are observed in the ^{1}H and ^{13}C signals of the *N*-aroyl substituents of the ligands upon coordination to the metal ions.

It has been widely reported that the ^{195}Pt nucleus is very sensitive to donor atom variation around the platinum nucleus as well as to variation in the coordination sphere of the platinum[30]. Much of the work that has been published concerning the characterisation of platinum(II) complexes, **Pt(L-*S,O*)$_2$**, derived from *N*-aroyl(acyl)-*N'*,*N'*-dialkylthioureas (**HL**), is primarily based upon ^{195}Pt NMR spectroscopy. It has been shown that for ***cis*-Pt(L-*S,O*)$_2$** type complexes of the *N*-aroyl-*N'*,*N'*-dialkylthioureas, where the two *N'*-alkyl groups are equivalent, the ^{195}NMR spectra consists of a single sharp resonance line in the ±-2700ppm region (in $CDCl_3$ relative to H_2PtCl_6 in 1.0M HCl)[13, 27]. In a report by Koch *et al.*, in

which the *trans* isomer of bis(*N*-naphthoyl-*N'*,*N'*-dibutylthioureato)platinum(II) was isolated, a consistent doubling of the peaks in both the ^{1}H and ^{13}C NMR spectra was observed[9]. This doubling of peaks was attributed to the presence of both the *cis* and the *trans* isomers of bis(*N*-naphthoyl-*N'*,*N'*-dibutylthioureato)platinum(II) in solution[9]. In work done by Grimmbacher on the structurally related bis(*N*-naphthoyl-*N'*-morpholinothioureato)platinum(II) complex, two distinct peaks were observed in the ^{195}Pt NMR spectrum, a major peak at -2708ppm and a minor peak at -3027ppm[31]. The major peak was assigned to the *cis*-[bis(*N*-naphthoyl-*N'*-morpholinothioureato)platinum(II)] complex, while the minor peak was assigned to the equivalent *trans* isomer[31].

A single sharp resonance signal was observed in each of the ^{195}Pt NMR spectra of **Pt(L^{7}-*S,O*)$_2$** and **Pt(L^{8}-*S,O*)$_2$** at -2570.1ppm and -2337.3ppm respectively [**Pt(L^{7}-*S,O*)$_2$** in $CDCl_3$, **Pt(L^{8}-*S,O*)$_2$** in DMSO with both ^{195}Pt shifts relative to an external standard of H_2PtCl_6 in 1.0M HCl]. However, two resonances were observed in ^{195}NMR spectrum of complex **Pt(L^{9}-*S,O*)$_2$**, a major signal at -2553.8ppm and minor signal upfield at -2686.4ppm as illustrated in Figure 14 [**Pt(L^{9}-*S,O*)$_2$** in $CDCl_3$, ^{195}Pt shifts relative to an external standard of H_2PtCl_6 in 1.0M HCl]. This second signal of -2686.4ppm suggests the possible existence of the ***trans*-Pt(L^{9}-*S,O*)$_2$** isomer. The existence of the ***trans*-Pt(L^{9}-*S,O*)$_2$** isomer, as suggested by the second resonance signal observed in the ^{195}Pt spectrum, was confirmed using RP-HPLC-ESMS analysis (see section 2.6). The relative integration in the ^{1}H NMR of **Pt(L^{9}-*S,O*)$_2$** suggests that the *cis*: *trans* isomer ratio of **Pt(L^{9}-*S,O*)$_2$** is 55.5 : 44.5.

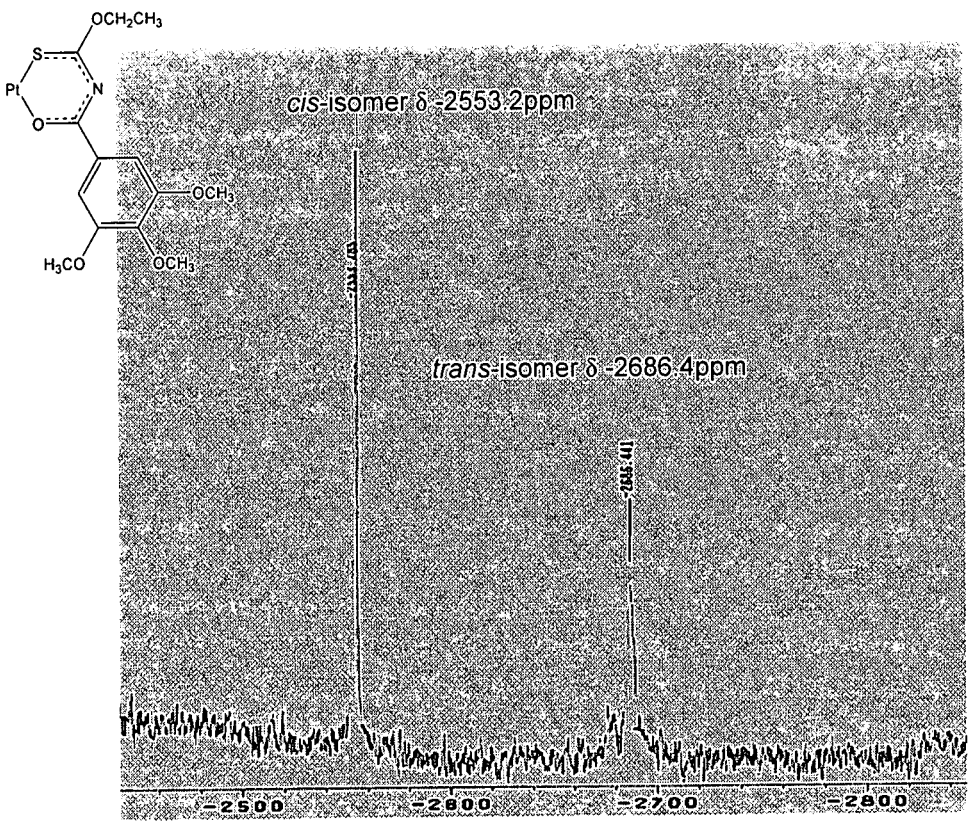

Figure 14 ^{195}Pt NMR spectra of **Pt(L^{9}-*S,O*)$_2$** indicating the two resonances that were observed.

Further to the ^{195}Pt NMR and HLPC-ESMS evidence of the *trans* isomer of **Pt(L^9-*S,O*)$_2$** having been prepared, a consistent doubling of peaks was also observed in the ^{1}H and ^{13}C NMR spectra of **Pd(L^7-*S,O*)$_2$**, **Pt(L^8-*S,O*)$_2$** and **Pt(L^9-*S,O*)$_2$**. An example of this is given in Figure 15 which shows the doubling of the carbonyl and thiocarbonyl resonances observed in the ^{13}C NMR spectra of **Pt(L^8-*S,O*)$_2$**. Only a single signal was observed in the ^{195}Pt spectra of **Pt(L^8-*S,O*)$_2$**, however, due to the poor solubility this complex, the signal to noise ratio was poor and it is possible that the second signal due the *trans* isomer was not observed as it was merely lost in the baseline "noise".

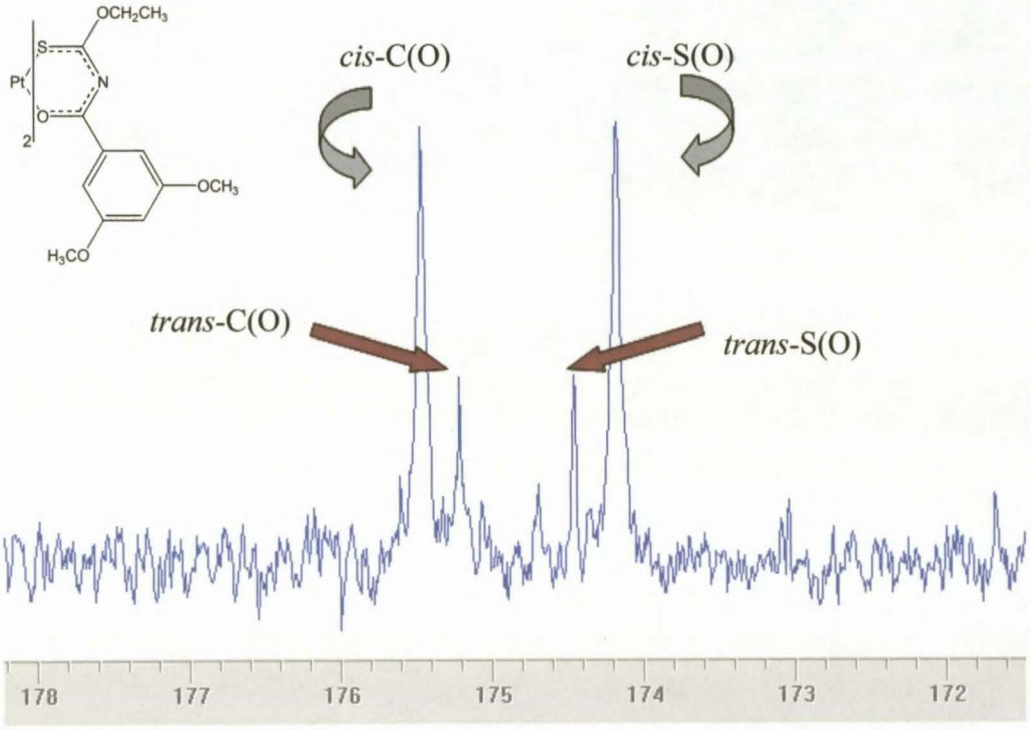

Figure 15 172-178ppm region of the ^{13}C NMR spectrum of **Pt(L^8-*S,O*)$_2$** showing the possible existence of both the cis and trans isomers in solution.

Complexes of tetracoordinated nickel(II) are mostly planar and more rarely tetrahedral. A bis chelation of bidentate ligands such as **H(L^7-*S,O*)**, **H(L^8-*S,O*)** and **H(L^9-*S,O*)** to nickel(II) can adopt either a square planar or a tetrahedral conformation. Square planar complexes of nickel(II) are generally diamagnetic while tetrahedral conformations of nickel(II) generally result in the complexes exhibiting paramagnetic behaviour[32-36]. This can easily be rationalized by simple ligand field theory which allows for both low-spin as well as high-spin nickel(II) complexes. However, in the case of square planar complexes, the spin-pairing energy is normally smaller than term splitting due to the field strength of the ligand as well as a possible lowering of the symmetry of the ligand field[29, 32, 37, 38]. The paramagnetic or diamagnetic nature of a nickel(II) complex is often used as a means to distinguish between a tetrahedral coordination geometry versus a square planar coordination geometry of a ligand(s) around the nickel(II).

It has been reported that a nickel(II) complex may be in the paramagnetic tetrahedral conformation in solution, yet the diamagnetic square planar isomer dominates in the solid state[32, 33]. The interchange between the two isomers in solution, i.e. square planar ⇆ tetrahedral, has also been reported to often be dependent upon such conditions as ligand steric and/or electronic properties, temperature and solvent type[39, 40]. Some reports indicate that the occurrence of isomerisation formation of some nickel(II) complexes in solution is time dependant and occurs only after several days[41].

The NMR spectra of **Ni(L^8-S,O)$_2$** indicated that this complex was paramagnetic. Only very broad poorly defined signals were observed in the ^{1}H NMR spectrum while no signals were observed in the ^{13}C NMR spectra. In contrast, complex **Ni(L^9-S,O)$_2$** only indicated partial paramagnetic character with comparatively distinct, yet broad non-coupled signals being observed in the ^{1}H NMR spectrum. A suitable ^{13}C spectrum of **Ni(L^9-S,O)$_2$** was obtained using an overnight run with a 1 second pulse delay. Complex **Ni(L^7-S,O)$_2$** was diamagnetic with typical ^{1}H and ^{13}C NMR spectra being obtained. The paramagnetic and partial paramagnetic behaviour exhibited in the ^{1}H and ^{13}C spectra of **Ni(L^8-*S,O*)$_2$** and **Ni(L^9-*S,O*)$_2$** respectively would suggest the possible existence of a tetrahedral or *pseudo*-tetrahedral isomer of **Ni(L^8-*S,O*)$_2$** and **Ni(L^9-*S,O*)$_2$** to be present in solution.

2.5 Mass Spectrometry

Ligands **H(L^7-*S,O*)**, **H(L^8-*S,O*)** and **H(L^9-*S,O*)**, as well as complexes **M(L^7-*S,O*)$_2$**, **M(L^8-*S,O*)$_2$** and **M(L^9-*S,O*)$_2$** [M = Ni(II), Pd(II) and Pt(II)], were all characterised by electron impact mass spectrometry [EI-MS]. The appropriate *m/z* value for M^+ was identified for ligands **H(L^7-*S,O*)**, **H(L^8-*S,O*)** and **H(L^9-*S,O*)** as well as for the nickel and palladium derived complexes thereof. The required *m/z* value for M^+ signals of **Pt(L^7-*S,O*)$_2$**, **Pt(L^8-*S,O*)$_2$** and **Pt(L^9-*S,O*)$_2$** were not observed. In each case only *m/z* signals corresponding to fragments of the respective platinum complexes were observed as well as signals pertaining to ligand fragments, similar to those observed in the mass spectra of the uncoordinated ligand.

2.6 High pressure liquid chromatographic (HPLC) and electron spray mass spectrometry (ESMS) analysis

Investigations into normal phase as well as reverse phase HPLC separation of the platinum group metal complexes derived from *N*-aroyl(acyl)-*N'*,*N'*-dialkylthioureas have been reported[17, 19, 42]. Normal phase HPLC separation of Pd(II) and Pt(II) complexes of *N*-benzoyl-*N'*,*N'*-dialkylthioureas result in extensive on-column complex decomposition presumably as a result of the inherent acidic nature of silica-based stationary phases, which interact strongly with metal complexes causing irreversible retention of polar analytes[17, 42]. The physiochemical properties of Pd(II) and Pt(II) complexes derived from *N*-aroyl(acyl)-*N'*,*N'*-dialkylthioureas make them suitable for reverse phase HPLC separation and determination[17]. Furthermore, Mautjana *et. al* reported that it is possible to detect the existence of the equivalent ***trans*-M(L-*S,O*)$_2$** complexes of *N*-aroyl(acyl)-*N'*,*N'*-dialkylthioureas by means of HPLC-ESMS analysis[17].

The consistent doubling of peaks observed in the ^{1}H and ^{13}C NMR spectra of complexes **Pd(L^{7}-*S,O*)$_2$**, **Pt(L^{8}-*S,O*)$_2$** and **Pt(L^{9}-*S,O*)$_2$** is comparable to the doubling of peaks observed in the ^{1}H and ^{13}C NMR spectra of bis(*N*-naphthoyl-*N'*,*N'*-dibutylthioureato)platinum(II) which was attributed to the existence of the equivalent *trans*-bis(*N*-naphthoyl-*N'*,*N'*-dibutylthioureato)platinum(II) isomer in solution[9]. Furthermore, the major and a minor signals observed in the ^{195}Pt NMR spectrum of **Pt(L^{9}-*S,O*)$_2$** are similar to the major and minor signals observed in the ^{195}Pt NMR spectrum of bis(*N*-naphthoyl-*N'*-morpholinothioureato)platinum(II) reported by Grimmbacher due to the equivalent *trans* isomer[31]. Consequently it was speculated that solutions of **Pd(L^{7}-*S,O*)$_2$**, **Pt(L^{8}-*S,O*)$_2$** and **Pt(L^{9}-*S,O*)$_2$** contained both the *cis* and *trans* isomers. To validate this speculation, RF-HPLC-ESMS analysis was required on solutions of **Pd(L^{7}-*S,O*)$_2$**, **Pt(L^{8}-*S,O*)$_2$** and **Pt(L^{9}-*S,O*)$_2$** using a 4.6 × 150 mm, 5 μm, Zorbax Eclipse XDB-C18 column with a acetonitrile-aqueous [90:10 (% v/v)] mobile phase comprising of an acetate buffer of pH ~ 6 prepared by mixing exactly 25 ml of 0.1 mol dm^{-3} acetic acid with 475 ml of 0.1 mol dm^{-3} sodium acetate solution[17, 43].

RP-HPLC analysis was initially carried out on samples of **H(L^{8}-*S,O*)**, **H(L^{9}-*S,O*)**, **Pt(L^{8}-*S,O*)$_2$** and **Pt(L^{9}-*S,O*)$_2$** to verify that both ligands and complexes remained intact under the conditions used as well as to test if more than one species was detected in samples **Pt(L^{8}-*S,O*)$_2$** and **Pt(L^{9}-*S,O*)$_2$**. Ligands **H(L^{8}-*S,O*)** and **H(L^{9}-*S,O*)** each produced chromatograms with single sharp peaks of high intensity with retention times of 1.65 – 1.75 minutes. Both a major and a minor peak were observed in the chromatograms of complexes **Pt(L^{8}-*S,O*)$_2$** and **Pt(L^{9}-*S,O*)$_2$** which eluted at 10.07 minutes and 32.61 minutes for **Pt(L^{8}-*S,O*)$_2$** and at 4.94 minutes and 24.57 minutes for **Pt(L^{9}-*S,O*)$_2$**. Complexes **Pt(L^{8}-*S,O*)$_2$** and **Pt(L^{9}-*S,O*)$_2$** were re-analysed using RP-HPLC-ESMS which indicated that the two peaks observed in the chromatograms of each complex were essentially of equal masses which conclusively shows that these second peaks corresponded to the equivalent *trans* isomers, [**Pt(L^{8}-*S,O*)$_2$** mH^+/z = 732.05 and 731.68 respectively, calculated for (**Pt(L^{8}-*S,O*)$_2$.H**)$^+$ = 732.10; **Pt(L^{9}-*S,O*)$_2$** mH^+/z = 791.90 and 792.02 respectively; calculated for (**Pt(L^{9}-*S,O*)$_2$.H**)$^+$ mH^+/z = 792.12]. Further signals of mH^+/z = 773.24 and 833.06 were also observed in the ESMS spectra of **Pt(L^{8}-*S,O*)$_2$** and **Pt(L^{9}-*S,O*)$_2$** respectively which correspond to the acetonitrile adducts of these platinum complexes [calculated for [**Pt(L^{8}-*S,O*)$_2$.CH$_3$CN.H**]$^+$ = 773.13 and calculated for [**Pt(L^{9}-*S,O*)$_2$.CH$_3$CN.H**]$^+$ = 833.15].

Subsequently to the work described in this chapter having be carried out, Hanekom *et. al* recently reported that ***cis*-M(L-*S,O*)$_2$** type complexes of Pt(II) and Pd(II) derived from *N*-(3,4,5-trimethoxy)benzoyl-*N'*,*N'*-diethylthiourea (**HL**) undergo reversible photoinduced isomerisation to the corresponding *trans* isomer upon irradiation with visible light in the 320–570 nm range[11]. Furthermore, they reported that in the dark, ***trans*-M(L-*S,O*)$_2$** cleanly reverts back to the *cis* complex at a rate dependent on the solution temperature[11].

Since the Ni(II), Pd(II) and Pt(II) complexes derived from *N*-aroylthiocarbamic-*O*-alkyl esters are essentially isostructural to the *N*-aroyl-*N'*,*N'*-dialkylthioureato complexes of nickel(II), palladium(II) and platinum(II), it is possible that the *trans* isomers of **M(L^{8}-*S,O*)$_2$** and **M(L^{9}-*S,O*)$_2$** [M = Pd(II) and

Pt(II)] as detected by ^{1}H, ^{13}C, ^{195}Pt NMR and RF-HPLC-ESMS resulted from photoinduced isomerism as a result of the ambient light to which the samples were exposed during sample preparation for analysis.

However, since HPLC/HPLC-ESMS analysis didn't form the basis of research into this class of compound, nor was the possible photoinduced isomerism known at this stage of the investigation, no further investigations regarding isomerism kinetics or isomerism mechanism etc. were carried out. Attempts were rather continued to isolate the equivalent *trans* isomers by means of traditional synthetic methodologies and ligand design of suitable steric and/or electronic properties.

2.7 Infrared Spectroscopy

A characteristic feature of the infrared spectra of ligands **H(L^{7}-*S,O*)**, **H(L^{8}-*S,O*)** and **H(L^{9}-*S,O*)** is the broad band observed at ±3200cm^{-1} attributed to the N-H group. The broadness of the stretching vibration of this group in the uncoordinated ligand can possibly be attributed to this group being involved in extensive intra- and intermolecular hydrogen bonding networks[44]. This broad stretching vibration of the N-H group at ±3200cm^{-1} disappears upon complexation with the metal ions which further confirms that the coordination of the ligand occurs in the deprotonated form.

A sharp stretch in the 1606cm^{-1} - 1725cm^{-1} region assigned to the carbonyl moiety in the non-coordinated ligand, shifts to the 1490cm^{-1}-1510cm^{-1} region in the resultant complexes. The signal changes from an intense sharp signal in the free ligand to a much weaker and slightly broader signal in the complex. In turn, the observed signals in the 1214cm^{-1}-1296cm^{-1} region assigned to the thiocarbonyl moiety stretch in the uncoordinated ligand shifts to the 1188cm^{-1}-1197cm^{-1} region in the resultant complexes. These shifts are comparable to the shifts observed in the infrared spectra of the *N*-benzoylthiocarbamic-*O*-alkyl esters and resultant d^{8} complexes described in chapter II. The infrared shifts observed in the carbonyl and thiocarbonyl stretches are consistent with a weakening of the carbonyl and thiocarbonyl double bond in the uncoordinated ligand coupled with extensive electron delocalisation through the resultant six-membered chelate ring with the metal. This electron delocalisation through the metal chelate ring is supported by the significant downfield shift in the ^{13}C NMR spectra signals of the C(O) groups with significant upfield shift in the signals of the C(S) groups from 163(±1)ppm and 190ppm respectively in the uncoordinated ligands to 180-185ppm and 174-178ppm respectively in the resultant complexes.

2.8 Concluding remarks

The introduction of methoxy substituents onto the phenyl ring in complexes **M(L^{7-9}-*S,O*)$_2$** [M = Ni(II), Pd(II) and Pt(II)] do not appear to have a significant effect on the overall molecular structure in the solid state, in that a *cis*-(*S,O*) coordination of the respective ligand to the metal ions in question is maintained. However, the methoxy substituents do appear to result in the overall molecular structure of the complexes conforming closer to absolute planarity in comparison to complexes **M(L^{1}-*S,O*)$_2$**, M = Ni(II), Pd(II) and Pt(II) (as described in chapter II) which adopt essentially a bent or 'cup-like' shape

when viewed side-on. However, the methoxy substituents of complexes **M(L^{7-9}-*S,O*)$_2$** [M = Ni(II), Pd(II) and Pt(II)] appear to influence the overall arrangement of molecules within the crystal lattice primarily due to inter- and intramolecular hydrogen interactions and contacts as well as the resultant increased steric hindrance caused by the methoxy substituents.

Furthermore, for the series of complexes described here in chapter III, signals attributed to the existence of the equivalent *trans*-(*S,O*) isomers in solution were detected by NMR spectroscopy. In contrast, *trans*-(*S,O*) isomers of the analogous complexes discussed in chapter II were not observed. The existence in solution of the *trans*-(*S,O*) isomers of complexes **Pt(L^{8}-*S,O*)$_2$** and **Pt(L^{8}-*S,O*)$_2$** was confirmed by RP-HPLC-ESMS.

Initially it was thought the existence of the *trans* isomers of complexes **M(L^{7-9}-*S,O*)$_2$** in solution (as detected by NMR and RP-HPLC ESMS spectrometry) were due to the electronic and steric properties of the methoxy substituents that had been introduced onto the phenyl moieties of these complexes in line with that which was speculated in the hypothesis of Koch in 2001 which proposed that *trans*-Pt(L-*S,O*)$_2$ type complexes derived from *N*-aroyl-*N',N'*-dialkylthiourea ligands could possibly be isolated if bulky, electron-rich *N*-aroylthiourea ligands were used[15]. As was demonstrated by single crystal X-ray diffraction analysis, the introduction of the electron rich methoxy substituents did in fact lengthen the M-O bond, thereby 'softening' the M-O bond, relative to the analogous non-methoxy substituted complexes described in chapter II. In some complexes however, this effect was marginal. Hanekom *et al.* recently reported that ***cis*-M(L-*S,O*)$_2$** type complexes of Pt(II) and Pd(II) derived from N-(3,4,5-trimethoxy)benzoyl-N',N'-diethylthiourea, **H(L-*S,O*)**, undergo reversible photoinduced isomerism to the corresponding *trans* isomer upon irradiation with visible light in the range 320 – 570nm[11]. Furthermore, it was reported that in the dark, *trans*-M(L-S,O)$_2$ cleanly reverts back to the *cis* complex at a rate determined by the solution temperature[11]. It is therefore possible that the detected *trans*-(*S,O*) isomers of complexes **M(L^{7-9}-*S,O*)$_2$** in fact resulted from a similar photoinduced isomerism due to the ambient light to which the samples were exposed. Nonetheless, it is clear that the cis-(*S,O*) isomers of complexes **M(L^{7-9}-*S,O*)$_2$** are more stable than the equivalent *trans*-(*S,O*) isomers.

3. Experimental

3.1 Methods and instrumentation

All reagents and solvents were commercially available and unless otherwise stated were used without further purification. Analytical grade potassium thiocyanate was thoroughly dried under heated vacuum. Acetone was rendered anhydrous and degassed by distillation under argon over sodium carbonate. Benzene was prepared by distillation under argon over sodium metal with benzophenone as indicator. All alcohols used were rendered anhydrous by the methods described by Furness *et al.*[45] Dichloromethane was pre-dried over 4Å molecular sieves and distilled over either sodium hydride or calcium chloride under an inert atmosphere just prior to use. ^{1}H and ^{13}C NMR spectra (25°C) were recorded in deuterated chloroform using either a Varian INOVA 600 MHz spectrometer operating at 600 MHz or 151 MHz respectively, or a Varian VXR 300 MHZ spectrometer operating at 300 MHz or 76 MHz respectively. ^{1}H chemical shifts are quoted relative to the residual $CHCl_3$ solvent resonance at 7.26ppm. ^{13}C chemical shifts are quoted relative to the $CDCl_3$ triplet at 77.7ppm. ^{195}Pt NMR spectra (30°C) were recorded in chloroform-*d* using the Varian INOVA 600 MHz spectrometer operating at 128 MHz. All ^{195}Pt chemical shifts are quoted relative to external H_2PtCl_6 (500 mg ml^{-1} in 30% v/v D_2O/1 M HCl), and are estimated to be accurate to ±2 ppm. Chromatographic analyses were carried out using a Waters 2690 'Alliance' fully automatic HPLC system equipped with automatic sample injection system and a Waters 996 photodiode array detector, using a 4.6 × 150 mm, 5 μm, Zorbax Eclipse XDB-C18 column. All eluents were filtered through a 0.45 μm (Microsep) nitrocellulose membrane and degassed by bubbling helium gas through eluent reservoirs for at least 1 hr prior to use. The column was conditioned with an acetonitrile-aqueous buffer mixture [90:10 (% v/v)], usually at 1 cm^3 min^{-1} for 15-30 min before commencing with sample (20 μl) injections. Acetate buffer of pH ~ 6 was prepared by mixing exactly 25 ml of 0.1 mol dm^{-3} acetic acid with 475 ml of 0.1 mol dm^{-3} sodium acetate solution. Elemental analyses were performed using a Carlo Erba EA 1108 elemental analyser in the microanalytical laboratory of the University of Cape Town

3.2 General Preparation of ligands H(L^7-*S,O*), H(L^8-*S,O*) and H(L^9-*S,O*)

All methoxy substituted benzoyl chlorides used were commercially available and used without further purification.

Ligands **H(L^7-*S,O*), H(L^8-*S,O*) and H(L^9-*S,O*)** were generally prepared under an anhydrous atmosphere of nitrogen according to a procedure based upon the method initially described by Douglass and Dains used for the preparation of the analogous *N*-acyl(aroyl)-*N'*,*N'*-dialkylthioureas[46, 47]. A similar method was reported in the literature by Schröder *et al.* in the preparation of several *N*-benzoyl-thiocarbamic-*O*-alkylesters[48]. The appropriate methoxy substituted benzoyl chloride (0.03mol) was dissolved in anhydrous acetone (60ml) and added dropwise with magnetic stirring to a solution of potassium thiocyanate (0.03mol) dissolved in anhydrous acetone (60ml). The reaction mixture was brought to a gentle reflux for 45 minutes to ensure the complete formation of the aroyl isothiocyanate. The reaction mixture was cooled to room temperature and the ethanol (0.06mol) dissolved in 60ml of anhydrous acetone was added over a period of ±10 minutes. After addition of the ethanol, the reaction

mixture was gently warmed to 60°C for 1 hour, allowed to cool to room temperature and stirred for a further 12 hours. 100 – 200ml of distilled water was added to the reaction mixture to ensure the complete solvation of the precipitate. The crude product was recovered by repetitive extraction with chloroform. The combined organic extracts were further washed several times with water. The crude reaction product was recovered under reduced pressure and further purified by crystallization from the diffusion of pentane into chloroform or from an acetone water mixture. If crystallization was not successful, the products were purified by column chromatography using Silica Gel as a stationary phase (± 1g product / 50g) with chloroform or a mixture of dichloromethane and acetone as the mobile phase.

3.3. General preparation of $M(L^{7-9}\text{-}S,O)_2$ M = Ni(II), Pd(II), Pt(II).

Complexes $M(L^{7-9}\text{-}S,O)_2$, M = Ni(II), Pd(II) and Pt(II) were prepared in reasonable yields and high purity according to the method described earlier in chapter II section 2.2[12].

An acetonitrile water solution containing 0.5 mmol quantities of the appropriate nickel acetate tetrahydrate, potassium tetrachloropalladate or potassium tetrachloroplatinate was added dropwise to a constantly stirred ligand solution, made from 1 mmol equivalent of the *N*-aroylthiocarbamic-*O*-ethyl ester ligand dissolved in an acetonitrile water solution (containing 1 mmol of sodium acetate in the case of potassium tetrachloropalladate or potassium tetrachloroplatinate). The final solvent composition was 50(v/v)% water–acetonitrile. The reaction mixture was warmed gently to 60°C and stirred for two hours, after which the solution was cooled to room temperature and stirred overnight. An equivalent volume of water was then added and the solution cooled to ± 4°C for several hours. The crude product was isolated by centrifugation, washed with a cool acetonitrile water solution and dried under high vacuum. Where possible, crystals suitable for single crystal X-ray diffraction analysis were generally obtained from various binary solvent combinations.

3.4 Crystallography and structure refinement

Crystals suitable for single crystal X-ray analysis were mounted on a thin glass fibre and data was collected on Bruker Nonius SMART Apex diffractometer using graphite monochromated Mo-Kα radiation (λ = 0.7107 Å). Data integration and reduction were undertaken using SAINT[49] and space group determination using XPREP[49]. Multi-scan derived corrections were made to the data using SADABS[50]. The structures were solved using SHELXS-97[51] and refined using SHELXL-97[51] with the aid of the interface software XSEED[21, 22]. XSEED[21, 22] was also used to generate the molecular graphics as the GUI to POV-Ray[52]. In each structure, all non-hydrogen atoms were modelled anisotropically. Hydrogen atoms were placed in geometrically calculated positions, with C-H = 0.99 for $-CH_2-$, 0.98 for $-CH_3$ or 0.95 for phenyl and 0.88 Å for N-H. These were refined using a riding model with $U_{iso}(H) = 1.2U_{eq}$(parent) (for $-CH_2-$, phenyl and N-H) and $1.5U_{eq}$(parent) (for $-CH_3$). Crystal structure interpretation was performed with the aid of XSEED[21, 22], PLATON[23] and MERCURY[53].

3.5 Preparative methods of uncoordinated ligands.

3.5.1 *N*-(4-methoxybenzoyl)thiocarbamic-*O*-ethyl ester, H(L^7-S,O)

ρ-Anisoyl chloride (28.75mmol, 4.904g) dissolved in 50ml of anhydrous acetone was added dropwise with magnetic stirring to a solution of KSCN (28.75mmol, 2,766g). The solution was brought to a gentle reflux for 1 hour, cooled to room temperature and ethanol (57.5mmol, 3.35ml) dissolved in 50ml of anhydrous acetone was added dropwise with magnetic stirring. The reaction mixture was warmed to 60°C for one hour, cooled to room temperature and stirred overnight. 200ml of water was added to the reaction mixture to fully dissolve the precipitate. The crude reaction product was recovered by extraction with 3 x 25ml of chloroform and in turn the combined organic extracts were washed with 3 x 25ml of water. The target product was recovered from the organic fractions under reduced pressure to yield a pale yellow amorphous powder. The crude produced was further purified by crystallisation from chloroform or a mixture of acetone and water.

Yield: 67.0% (based on ρ-Anisoyl chloride).

NMR : δ_H (300 MHz, solvent $CDCl_3$) 9.13 (1H, br s, NH), 7.81 (2H, d, phenyl CH), 6.96 (2H, d, phenyl CH), 4.65 (2H, qu, CH_2), 3.85 (3H, s, OCH_3), 1.42 (3H, tr, CH_3). δ_C (76 MHz, solvent $CDCl_3$) 190.8 (C(S)), 164.5 (C(O)), 162.7 130.7 115.0 (Ph) 125.8 (*ipso*-Ph), 70.0 (OCH_2), 56.2 (OCH_3), 14.2 (CH_3).

FT-IR : (KBr disks) 3392 (br, NH), 1717vs, 1505vs, 1214vs cm^{-1}.

Mass spectrum (EI 70eV) *m/z* 239 (M^+, 7.6%), 151 (17.2%), 135 (100%), 107 (11.5%), 92 (12.7%), 77 (17.8%), 64 (7.6%), 18 (10.2%).

Found C 55.45; H 5.40; N 5.55; S 12.90; $C_{22}H_{24}N_2NiO_6S_2$ required C 55.21; H 5.48; N 5.85; S 13.40.

Melting point: 75.0 – 76.8°C.

3.5.2 *N*-(3,5-dimethoxybenzoyl)thiocarbamic-*O*-ethyl ester, H(L^8-*S,O*)

H(L^8-*S,O*) was prepared in a method analogous to that which was used to prepare *N*-(4-methoxybenzoyl)thiocarbamic-*O*-ethyl ester, **H(L^7-*S,O*)**, using 3,5-dimethoxybenzoyl chloride as the aroyl chloride starting reagent.

Yield: 64.7% (based on 3,5-dimethoxybenzoyl chloride).

NMR : δ_H (300 MHz, solvent $CDCl_3$) 9.09 (1H, br s, NH), 6.91 (2H, s, *ortho*-phenyl CH), 6.63 (1H, d, *para*-phenyl CH), 4.64 (2H, qu, CH_2), 3.80 (6H, s, OCH_3), 1.42 (3H, tr, CH_3). δ_C (76 MHz, solvent $CDCl_3$) 190.3 (C(S)), 163.3 (C(O)), 162.1 (*meta*-phenyl C) 135.9 (*ipso*-phenyl C) 106.3 (*ortho*-phenyl C) 106.2 (*para*-phenyl C), 70.1 (OCH_2), 56.3 (OCH_3), 14.2 (CH_3).

FT-IR : (KBr disks) 3246m (br, NH), 1725vs 1518vs, 1296vs cm^{-1}.

Mass spectrum (EI 70eV) *m/z* 269 (M^+, 13.4%), 223 (7.6%), 181 (5.1%), 165 (100.0%), 137 (35.0%), 122 (35.7%), 107 (12.1%), 92 (5.7%) 63 (14.0%), 51 (8.3%), 18 (56.1%).

Found C 53.77; H 5.87; N 5.27; S 10.11; $C_{12}H_{15}NO_4S$ required C 53.52; H 5.61; N 5.20; S 11.91.

Melting point: 124.5 – 126.0°C.

3.5.3 *N*-(3,4,5-trimethoxybenzoyl)thiocarbamic-*O*-ethyl ester, H(L^9-*S,O*)

H(L^9-*S,O*) was prepared in a method analogous to that which was used to prepare *N*-(4-methoxybenzoyl)thiocarbamic-*O*-ethyl ester, **H(L^7-*S,O*)** using 3,4,5-trimethoxybenzoyl chloride as the aroyl chloride starting reagent.

Yield: 72.3% (based on 3,4,5-trimethoxybenzoyl chloride).

NMR : δ_H (300 MHz, solvent $CDCl_3$) 9.15 (1H, br s, NH), 7.01 (2H, s, *ortho*-phenyl CH), 4.65 (2H, qu, CH_2), 3.92 (3H, s, OCH_3), 3.89 (6H, s, OCH_3), 1.45 (3H, tr, CH_3). δ_C (76 MHz, solvent $CDCl_3$) 190.6 (C(S)), 163.2 (C(O)), 154.3 (*meta*-phenyl C), 143.3 (*ipso*-phenyl C), 128.8 (*para*-phenyl C), 106.6 (*ortho*-phenyl C), 70.1 (CH_2), 61.6 (OCH_3), 57.0 (OCH_3), 14.2 (CH_3).

FT-IR : (KBr disks) 3241m (br, NH), 1720vs, 1499vs 1240vs cm^{-1}.

Mass spectrum (EI 70eV) *m/z* 299 (M^+, 17.8%), 253 (8.3%), 211 (36.3%), 195 (100.0%), 152 (12.7%), 140 (10.2%), 109 (7.0%), 81 (8.3%) 28 (17.2%), 18 (94.3%).

Found C 52.82; H 5.73; N 4.48; S 9.13; $C_{13}H_{17}NO_5S$ required C 52.16; H 5.72; N 4.68; S 10.71.

3.6 Preparative methods of complexes.

3.6.1 Bis[*O*-ethyl-*N*-(4-methoxybenzoyl)thiocarbamato]nickel(II), Ni(L^7-*S,O*)$_2$.

N-(4-methoxybenzoyl)thiocarbamic-*O*-ethyl ester, **H(L^7-*S,O*)**, (1 x 10^{-3}mol) was dissolved in 15ml of acetonitrile and further diluted with 15ml of water. Nickel acetate tetrahydrate (0.5 x 10^{-3}mol) dissolved in 15ml of water and further diluted with 15ml of acetonitrile was added dropwise to the reaction mixture at room temperature over a period of ±10 minutes. The reaction mixture was stirred at room temperature for a further 12 hours after which time a further 60ml of water was added and the reaction mixture was cooled to 4°C for 3-4 hours. The precipitate of the crude product was recovered by centrifugation. The isolated product was further purified by washing with a cold 1:1 mixture of acetonitrile and water and dried under high vacuum.

The product appears to be sensitive to elevated temperature during the synthetic procedure. After the addition of the nickel acetate to the reaction mixture, the mixture was warmed to 50°C for one hour in an attempt to increase the overall reaction yield. However, during this time the reaction product precipitate initially produced darkens extensively. When isolated, the black/brown precipitate proves to be totally insoluble in conventional solvents. The remaining reaction mixture appears to contain various organic decomposition products as indicated by the ^1H and ^{13}C NMR spectra. No attempt was made to elucidate the structure of these products.

Yield: 14.3% (based on $Ni(CH_3COO)_2.4H_2O$).

NMR : δ_H (300 MHz, solvent $CDCl_3$) 8.14 (4H, d, phenyl CH), 6.91 (4H, d, phenyl CH), 4.51 (4H, qu, CH_2), 3.86 (6H, s, OCH_3), 1.36 (6H, tr, CH_3).

δ_C (76 MHz, solvent $CDCl_3$) 186.1 (C(O)), 178.6 (C(S)), 164.8 (*para*-phenyl C), 133.0 (*ortho*-phenyl C), 128.6 (*ipso*-phenyl C) 114.4 (*meta*-phenyl C) 67.0 (CH_2), 56.1 (OCH_3), 14.8 (CH_3).

FT-IR : (KBr disks) 1510vs, 1436vs 1197vs cm^{-1}.

Mass spectrum (EI 70eV) *m/z* 534 (M^+, 17.8%), 403 (0.6%), 304 (0.6%), 239 (1.3%), 178 (4.5%), 135 (100.0%), 107 (7.0%), 92 (13.4%), 77 (17.8%), 18 (9.6%).

Found C 49.42; H 4.73; N 5.48; S 12.02; $C_{22}H_{24}N_2NiO_6S_2$ required C 49.37; H 4.52; N 5.23; S 11.98.

3.6.2 Bis[*O*-ethyl-*N*-(4-methoxybenzoyl)thiocarbamato]palladium(II), Pd(L^7-*S,O*)$_2$.

N-(4-methoxybenzoyl)thiocarbamic-*O*-ethyl ester (1 x 10^{-3}mol) was dissolved in 15ml of acetonitrile to which a solution of sodium acetate (1.1 x 10^{-3}mol) dissolved in 15ml of water was added dropwise and stirred at room temperature for 10 minutes. Potassium tetrachloropalladate (0.5 x 10^{-3}mol) dissolved in 15ml of water and further diluted with 15ml of acetonitrile was added dropwise to the above reaction mixture at room temperature over ±10 minutes. The reaction mixture was stirred at room temperature for 12 hours after which time a further 60ml of water was added and the reaction mixture was cooled to 4°C for 3-4 hours. The precipitate of the crude product was recovered by centrifugation. The isolated product was further purified by washing with a cold 1:1 mixture of acetonitrile and water and dried under high vacuum.

Pd(L^7-*S,O*)$_2$ also proved to be sensitive to elevated temperatures during the synthesis process and any attempt to heat the reaction mixture in an attempt to increase the yield resulted in complete decomposition of the product over time.

Yield: 68.1% (based on K_2PdCl_4).

NMR : δ_H (300 MHz, solvent DMSO) 7.92 (4H, d, phenyl CH), 7.04 (4H, d, phenyl CH), 3.48 (4H, qu, CH_2), 3.32 (6H, s, OCH_3), 1.34 (6H, tr, CH_3).

A second minor set of ^{1}H NMR signals were obtained as follows:

δ_H (300 MHz, solvent DMSO) 7.88 (4H, d, phenyl CH), 7.00 (4H, d, phenyl CH), 4.16 (4H, qu, CH_2), 3.10 (6H, s, OCH_3), 1.25 (6H, tr, CH_3). Speculatively, these signals could possibly be assigned to the ***trans*-Pd(L^7-*S,O*)$_2$** complex.

δ_C (76 MHz, solvent DMSO) The solubility of the complex proved to be very low in most common NMR solvents. **Pd(L^7-*S,O*)$_2$** proved to be suitably soluble in DMSO to obtain a ^{1}H NMR spectrum, but not soluble enough to enable a ^{13}C NMR spectrum to be obtained with a good signal to noise ratio under standard data acquisition conditions.

FT-IR : (KBr disks) 1507vs, 1448vs 1193vs cm^{-1}.

Mass spectrum (EI 70eV) *m/z* 582 (M^+, 1.3%), 267 (1.3%), 238 (1.6%), 177 (5.1%), 135 (100.0%), 108 (7.6%), 92 (14.6.%), 77 (20.4%), 64 (9.6%), 28 (10.8%), 18 (22.3%).

Found C 45.42; H 4.73; N 4.93; S 11.13; $C_{22}H_{24}N_2O_6PdS_2$ required C 45.32; H 4.15; N 4.81; S 11.00.

3.6.3 Bis[*O*-ethyl-*N*-(4-methoxybenzoyl)thiocarbamato]platinum(II), Pt(L^7-*S,O*)$_2$.

Pt(L^7-*S,O*)$_2$ was prepared in an analogous method to that used for the preparation of **Pd(L^7-*S,O*)$_2$** using 0.5 x 10^{-3}mol potassium tetrachloroplatinate as well as 1.1 x 10^{-3} mol of sodium acetate to ensure the complete deprotonation of the *N*-(4-methoxybenzoyl)thiocarbamic-*O*-ethyl ester. The product proved

to be slightly sensitive to elevated temperatures during the synthesis procedure but the decomposition of **Pt(L^7-*S,O*)$_2$** didn't appear to be to the same degree as **Pd(L^7-*S,O*)$_2$**.

Yield: 59.9% (based on K_2PtCl_4).

NMR : δ_H (300 MHz, solvent $CDCl_3$) 8.28 (4H, d, phenyl CH), 6.95 (4H, d, phenyl CH), 4.53 (4H, qu, CH_2), 3.87 (6H, s, OCH_3), 1.39 (6H, tr, CH_3).

δ_C (76 MHz, solvent $CDCl_3$) 179.2 (C(O)), 174.4 (C(S)), 164.7 (*para*-phenyl C), 133.1 (*ortho*-phenyl C), 129.4 (*ipso*-phenyl C) 114.8 (*meta*-phenyl C) 67.1 (CH_2), 56.1 (OCH_3), 14.8 (CH_3).

δ_{Pt} (128 MHz, solvent $CDCl_3$ - external H_2PtCl_6 (500 mg ml^{-1} in 30% v/v D_2O/1 M HCl)) -2570.1.

FT-IR : (KBr disks) 1500vs, 1435vs 1196vs cm^{-1}.

Mass spectrum (EI 70eV) *m/z* M^+ of 671 was not observed. For the platinum complexes of *N*-aroylthiocarbamic-*O*-alkyl esters, M^+ peaks were generally not observed and the fragmentation signals observed were generally characteristic for further fragmentation ligand fractions as observed in other nickel and palladium complexes of the same ligand where an M^+ signal was observed. 285 (1.9%), 238 (3.2%), 177 (15.3%), 135 (100%), 107 (12.1%), 92 (24.8%), 77 (32.5%), 64 (13.4%), 18 (17.8%).

Found C 39.68; H 3.71; N 4.07; S 9.01; $C_{22}H_{24}N_2O_6PtS_2$ required C 39.34; H 3.60; N 4.17; S 9.55.

3.6.4 Bis[*N*-(3,5-dimethoxybenzoyl)-*O*-ethyl-thiocarbamato]nickel(II), Ni(L^8-*S,O*)$_2$.

Ni(L^8-*S,O*)$_2$ was prepared in an analogous method to that used for the preparation of **Ni(L^7-*S,O*)$_2$** using *N*-(3,5-dimethoxybenzoyl)thiocarbamic-*O*-ethyl ester as the ligand.

Yield: 43.8% (based on $Ni(CH_3COO)_2.4H_2O$).

NMR : **Ni(L^8-*S,O*)$_2$** was poorly soluble in the common NMR solvents, however a low concentration sample was prepared using DMSO. The NMR sample proved to be partially paramagnetic and only a very poor inconclusive ^1H NMR spectrum was obtained. No ^{13}C NMR signals were observed. Compound **Ni(L^8-*S,O*)$_2$** was characterised solely on IR and mass spectrometry as well as C,H,N,S analysis.

FT-IR : (KBr disks) 1494vs, 1450vs, 1196vs cm^{-1}.

Mass spectrum (EI 70eV) *m/z* 594 (M^+, 4.8%), 281 (5.1%), 207 (7.6%), 165 (100%), 137 (36.9%), 122 (32.5%), 77 (13.4%), 27 (38.9%), 18 (98.0%).

Found C 48.47; H 4.79; N 4.72; S 10.41; $C_{24}H_{28}N_2NiO_8S_2$ required C 48.42; H 4.74; N 4.71; S 10.77.

Melting point: 198.5 – 200°C.

3.6.5 Bis[*N*-(3,5-dimethoxybenzoyl)-*O*-ethyl-thiocarbamato]palladium(II), Pd(L^8-*S,O*)$_2$.

Pd(L^8-*S,O*)$_2$ was prepared in an analogous method to that used for the preparation of **Pd(L^7-*S,O*)$_2$** using *N*-(3,5-dimethoxybenzoyl)thiocarbamic-*O*-ethyl ester as the ligand.

Yield: 69.1% (based on K_2PdCl_4).

NMR : **Pd(L^8-*S,O*)$_2$** proved to be poorly soluble in the common NMR solvents. When DMSO was used as a solvent, decomposition of **Pd(L^8-*S,O*)$_2$** occurred. ^1H and ^{13}C NMR signals of **Pd(L^8-*S,O*)$_2$** were weak in relation to the signals of decomposition products. Compound **Pd(L^8-*S,O*)$_2$** was characterised solely on IR and mass spectrometry as well as C,H,N,S analysis.

FT-IR : (KBr disks) 1510vs, 1437vs, 1193vs cm^{-1}.

Mass spectrum (EI 70eV) *m/z* 642 (M^+, 1.3%), 376 (1.3%), 269 (2.5%), 207 (28.0%), 165 (100%), 137 (31.2%), 122 (28.7%), 77 (12.1%), 63 (12.1%), 28 (26.1%), 18 (57.3%).

Found C 44.40; H 3.82; N 4.04; S 9.96; $C_{24}H_{28}N_2O_8PdS_2$ required C 44.83; H 4.39; N 4.36; S 9.97.

3.6.6 Bis[*N*-(3,5-dimethoxybenzoyl)-*O*-ethyl-thiocarbamato]platinum(II), Pt(L^8-*S,O*)$_2$.

Pt(L^8-*S,O*)$_2$ was prepared in an analogous method to that used for the preparation of **Pt(L^7-*S,O*)$_2$** using *N*-(3,5-dimethoxybenzoyl)thiocarbamic-*O*-ethyl ester as the ligand. Yield: 68.8% (based on K_2PtCl_4).

NMR : Compound **Pt(L^8-*S,O*)$_2$** was poorly soluble in common NMR solvents. A sufficient degree of solubility in DMSO was obtained to allow suitable ^1H and ^{13}C and ^{195}Pt NMR spectra to be acquired. However, the standing of **Pt(L^8-*S,O*)$_2$** over periods of several hours in DMSO caused significant decomposition of the sample. The decomposition was evident visibly as a black precipitate which gradually settled out of solution as well as the growth of numerous signals over time in the NMR spectra. An obvious and consistent doubling of **Pt(L^8-*S,O*)$_2$** signals in the ^1H and ^{13}C NMR spectra was observed. The doubling of the signals is tentatively assigned to the presence of the ***trans*-Pt(L^8-*S,O*)$_2$** isomer. However, only a single ^{195}Pt signal was obtained. This signal was relatively weak and a second signal of the *trans* ***trans*-Pt(L^8-*S,O*)$_2$** isomer is possibly masked by the baseline due to the poor signal to noise ratio.

δ_H (300 MHz, solvent DMSO) 7.16 (4H, s, phenyl *ortho*-CH), 6.86 (2H, s, *para*-phenyl CH), 4.49 (4H, qu, CH_2), 3.79 (12H, s, OCH_3), 1.36 (6H, tr, CH_3).

δ_H of second **Pt(L^8-*S,O*)$_2$** isomer (300 MHz, solvent DMSO) 6.86 (4H, s, phenyl *ortho*-CH), 6.44 (2H, s, *para*-phenyl CH), 4.29 (4H, qu, CH_2), 3.77 (12H, s, OCH_3), 1.29 (6H, tr, CH_3).

δ_C (76 MHz, solvent DMSO) 181.4 (C(O)), 175.5 (C(S)), 160.8 137.4 108.2 (phenyl C), 136.3 (*ipso*-phenyl C) 67.0 (CH_2), 55.4 (OCH_3), 14.0 (CH_3).

δ_C of second **Pt(L^8-*S,O*)$_2$** isomer (76 MHz, solvent DMSO) 179.6 (C(O)), 174.3 (C(S)), 160.3 137.2 107.0 (phenyl C), 65.0 (CH_2), 54.9 (OCH_3), 13.9 (CH_3).

δ_{Pt} (128 MHz, solvent DMSO - external H_2PtCl_6 standard (500 mg ml^{-1} in 30% v/v D_2O/1 M HCl)) - 2337.3.

FT-IR : (KBr disks) 1511vs, 1435vs, 1199vs cm^{-1}.

Mass spectrum (EI 70eV) *m/z* M^+ of 731 was not observed. The resultant MS fragmentation pattern observed for **Pt(L^8-*S,O*)$_2$** is comparative to the MS fragmentation pattern observed for **Ni(L^8-*S,O*)$_2$** and **Pd(L^8-*S,O*)$_2$** apart for the respective M^+ signals of 594 of **Ni(L^8-*S,O*)$_2$** and 642 of **Pt(L^8-*S,O*)$_2$** which were in fact observed. The signals observed in the MS spectrum of **Pt(L^8-*S,O*)$_2$** are generally characteristic and comparable to MS fragmentation of ligand **HL^8**. 345 (1.9%), 297 (5.7%), 207 (40.7%), 165 (100%), 137 (33.8%), 122 (29.3%), 107 (14.6%), 77 (19.1%), 63 (14.0%), 28 (37.6%), 18 (66.2%).

Found C 39.50; H 3.74; N 3.82; S 8.66; $C_{24}H_{28}N_2O_8PtS_2$ required C 39.40; H 3.86; N 3.83; S 8.76.

Melting point: melts with decomposition 194.5 - 196.0°C.

3.6.7 Bis[*O*-ethyl-*N*-(3,4,5-trimethoxybenzoyl)thiocarbamato]nickel(II), Ni(L^9-*S,O*)$_2$.

Ni(L^9-*S,O*)$_2$ was prepared in an analogous method to that used for the preparation of **Ni(L^7-*S,O*)$_2$** using *N*-(3,4,5-trimethoxybenzoyl)thiocarbamic-*O*-ethyl ester as the ligand.

Yield: 27.8% (based on $Ni(CH_3COO)_2.4H_2O$). A significant degree of decomposition was observed during the synthesis as a black precipitate which was filtered off prior to the purification of **Ni(L^9-*S,O*)$_2$** which accounts for the low yield.

NMR: solubility of **Ni(L^9-*S,O*)$_2$** in $CDCl_3$ was not a problem, however, the sample appeared to be partially paramagnetic. As a result, the expected ^1H signals were obtained, but no coupling was observed. The required ^{13}C spectra signals were obtained in a good signal to noise ration using an overnight run.

δ_H (300 MHz, solvent $CDCl_3$) 7.60 (4H, phenyl CH), 4.68 (4H, OCH_2), 4.07 (6H, OCH_3), 4.02 (12H, OCH_3), 1.57 (6H, CH_3).

δ_H (300 MHz, solvent $CDCl_3$) Same sample as above left standing for 3 weeks at ambient temperature – a degree of coupling was now observed.

7.66 (4H, s, phenyl CH), 4.71 (4H, qu, OCH_2), 4.11 (6H, s, OCH_3), 4.06 (12H, s, OCH_3), 1.59 (6H, tr, CH_3).

δ_C (76 MHz, solvent $CDCl_3$) 186.7 (C(O)), 178.5 (C(S)), 153.8 (*meta*-phenyl C), 144.5 (*para*-phenyl C), 131.2 (*ipso*-phenyl C), 109.1 (*ortho*-phenyl C), 67.2 (CH_2), 61.5 (OCH_3), 57.3 (OCH_3), 14.7 (CH_3).

δ_C (76 MHz, solvent $CDCl_3$) Same sample as above left standing for 3 weeks at ambient temperature 186.7 (C(O)), 178.5 (C(S)), 153.8 (*meta*-phenyl C), 144.5 (*para*-phenyl C), 131.2 (*ipso*-phenyl C) 109.1 (*ortho*-phenyl C), 67.2 (CH_2), 61.6 (OCH_3), 57.3 (OCH_3), 14.8 (CH_3).

FT-IR : (KBr disks) 1494vs, 1377vs 1196vs cm^{-1}. Secondary peaks were observed 1498, 1440, 1368 which could possibly correlate with the existence of the ***trans*-Ni(L^9-*S,O*)$_2$**.

Mass spectrum (EI 70eV) *m/z* M^+ of 655 (6.7%), 584 (1.1%), 556 (2.2%), 425 (1.1%), 358 (1.7%), 312 (3.4%), 237 (14.6%), 195 (100%), 152 (15.%), 66 (13.5%), 44 (20.2%), 28 (44.9%).

Found C 45.31; H 4.92; N 3.75; S 8.45; $C_{26}H_{32}N_2NiO_{10}S_2$ required C 47.65; H 4.92; N 4.27; S 9.79.

Melting point: 178.0 – 179.6°C.

3.6.8 Bis[*O*-ethyl-*N*-(3,4,5-trimethoxybenzoylthiocarbamato]palladium(II), Pd(L^9-*S,O*)$_2$.

Pd(L^9-*S,O*)$_2$ was prepared in an analogous method to that used for the preparation of **Pd(L^7-*S,O*)$_2$** using *N*-(3,4,5-trimethoxybenzoyl)thiocarbamic-*O*-ethyl ester as the ligand.

Yield: 27.8% (based on K_2PdCl_4).

NMR : solubility of **Pd(L^9-*S,O*)$_2$** in $CDCl_3$ was not problematic. No secondary peaks where observed which would suggest the existence of a ***trans*-Pd(L^9-*S,O*)$_2$** isomer even after an overnight run of the ^{13}C spectra.

δ_H (300 MHz, solvent $CDCl_3$) 7.88 (4H, s, phenyl CH), 4.86 (4H, qu, OCH_2), 4.23 (6H, s, OCH_3), 4.19 (12H, s, OCH_3), 1.72 (6H, tr, CH_3).

δ_C (76 MHz, solvent $CDCl_3$) 184.3 (C(O)), 176.8 (C(S)), 153.8 (*meta*-phenyl C), 144.4 (*ipso*-phenyl C), 131.2 (*para*-phenyl C), 109.4 (*ortho*-phenyl C), 67.2 (CH_2), 61.6 (OCH_3), 57.1 (OCH_3), 14.7 (CH_3).

FT-IR : (KBr disks) 1497vs, 1361vs, 1188vs cm^{-1}.

Mass spectrum (EI 70eV) *m/z* M^+ of 702 (1.9%), 472 (0.6%), 327 (2.5%), 237 (26.1%), 195 (100%), 152 (12.1%), 66 (10.8%), 28 (23.6%), 18 (63.7%).

Found C 42.60; H 4.22; N 3.80; S 9.01; $C_{26}H_{32}N_2O_{10}PdS_2$ required C 44.41; H 4.59; N 3.98; S 9.12.

Melting point: product starts decomposing at 170.0°C and melts with total decomposition at 199.0 – 201°C.

3.6.9 Bis[*O*-ethyl-*N*-(3,4,5-trimethoxybenzoyl)thiocarbamato]platinum(II), Pt(L^9-*S,O*)$_2$.

Pt(L^9-*S,O*)$_2$ was prepared in an analogous method to that used for the preparation of **Pt(L^7-*S,O*)$_2$** using *N*-(3,4,5-trimethoxybenzoyl)thiocarbamic-*O*-ethyl ester as the ligand.

Yield: 56.5% (based on K_2PtCl_4).

NMR : solubility of **Pt(L^9-*S,O*)$_2$** in $CDCl_3$ was not problematic. Consistent secondary peaks where observed in both the ^1H and ^{13}C spectra which could tentatively suggest the existence of a ***trans*-Pt(L^9-*S,O*)$_2$** isomer still present even after an overnight run of the ^{13}C spectra. Two signals were also observed in the overnight ^{195}Pt spectra with the second signal tentatively assigned to the existence of the ***trans*-Pt(L^9-*S,O*)$_2$** isomer.

δ_H (300 MHz, solvent $CDCl_3$) 7.61 (4H, s, phenyl CH), 4.56 (4H, qu, OCH_2), 3.90 (6H, s, OCH_3), 3.86 (12H, s, OCH_3), 1.45 (6H, tr, CH_3).

δ_H of possible second **Pt(L^9-*S,O*)$_2$** isomer (300 MHz, solvent $CDCl_3$) 7.34 (4H, s, phenyl CH), 4.30 (4H, qu, OCH_2), 3.80 (6H, s, OCH_3), 3.64 (12H, s, OCH_3), 0.95 (6H, tr, CH_3).

δ_C (76 MHz, solvent $CDCl_3$) 179.9 (C(O)), 174.2 (C(S)), 154.0 (*meta*-phenyl C), 144.4 (*ipso*-phenyl C), 132.1 (*para*-phenyl C) 109.3 (*ortho*-phenyl C,) 67.3 (CH_2), 61.5 (OCH_3), 57.3 (OCH_3), 14.8 (CH_3).

δ_C of possible second **Pt(L^9-*S,O*)$_2$** isomer (76 MHz, solvent $CDCl_3$) 181.4 (C(O)), 174.1 (C(S)), 153.9 (*meta*-phenyl C), 142.5 (*ipso*-phenyl C), 131.9 (*para*-phenyl C), 108.6 (*ortho*-phenyl C), 66.0 (CH_2), 61.1 (OCH_3), 57.1 (OCH_3), 14.2 (CH_3).

δ_{Pt} (128 MHz, solvent DMSO - external H_2PtCl_6 standard [500 mg ml^{-1} in 30% v/v D_2O/1 M HCl]) -2553.8 with a second peak tentatively assigned to the ***trans*-Pt(L^9-*S,O*)$_2$** isomer observed at -2686.4.

FT-IR : (KBr disks) 1490vs, 1363vs, 1195vs cm^{-1}.

Mass spectrum (EI 70eV) *m/z* M^+ of 791 was not observed. The fragmentation signals that were in fact observed correlate well with several fragmentation signals that were observed in the MS spectrum of **Pd(L^9-*S,O*)$_2$** where the M^+ of 702 was observed.

m/z 327 (5.7%), 237 (19.1%), 222 (18.5%), 195 (57.3%), 166 (14.6%), 152 (7.0%), 137 (11.5%), 120 (8.9%), 81 (14.0%), 66 (9.6%), 28 (100%).

m/z (M+1) peak of 792.1 was observed using ES-MS

Found C 39.53; H 3.85; N 3.49; S 7.65; $C_{26}H_{32}N_2O_{10}PtS_2$ required C 39.44; H 4.07; N 3.54; S 8.10.

Melting point: product starts decomposing at 170.0oC and melts with total decomposition at 199.0 – 201°C.

Appendix B: ***Experimental crystal data, data collection and crystal refinement details.***

Tables containing the experimental crystal data, data collection and crystal refinement details of the crystal structures of the complexes discussed in chapter 3, can be found on the included compact disc of this thesis. An example of these tables for the crystal structure of **Pt(L^7-*S,O*)** is given below.

B.1 Bis[*O*-ethyl-*N*-(3-methoxybenzoyl)thiocarbamato]platinum(II), Pt(L^7-*S,O*)$_2$.

Crystal data

$C_{22}H_{24}N_2O_6PtS_2$
Mr = 671.64g.mol^{-1}
Monoclinic, P21/*c*
a = 12.3108(13) Å
b = 14.4398(16) Å
c = 14.0014(15) Å
β = 104.876(2)°
V = 2405.5(4) Å^3
Z = 4

D_x = 1.896 Mg m^{-3}
Mo Kα radiation
Cell parameters from 999 reflections
θ = 2.421 – 27.978°
μ = 6.044 mm^{-1}
T = 103 (2) K
prism, yellow
0.10 x 0.10 x 0.06 mm

Data collection

Bruker SMART APEX CCD diffractometer
ω scans
Absorption correction: multi-scan (SADABS[50, 54])
T_{min} = 0.5831
T_{max} = 0.7130
26778 measured reflections
5643 independent reflections

4940 reflections with I > 2σ(I)

R_{int} = 0.0439
θ_{max} = 28.25°

h = -16 → 16

k = -18 → 18
l = -18 → 18

Refinement

Refinement on F^2
$R[F^2 > 2\sigma(F^2)]$ = 0.0310
$wR(F^2)$ = 0.0645
S = 1.094
5643 reflections
302 parameters
H-atom parameters constrained

$w = 1/[\sigma^2(F_o^2) + (0.0309P)^2 + 2.6568P]$
where $P = (F_o^2 + 2F_c^2)/3$
$(\Delta/\sigma)_{max}$ = 0.001
$\Delta\rho_{max}$ = 1.698 e Å^{-3}
$\Delta\rho_{min}$ = -1.760 e Å^{-3}

4. References

[1] L. Beyer, E. Hoyer, J. Liebscher, H. Hartman, *Z. Chem.* 1981, ***21***, 81-91.
[2] L. Beyer, R. Widera, E. Hoyer, *Z. Chem.* 1981, ***21***, 415.
[3] P. Muehl, K. Gloe, F. Dietze, E. Hoyer, L. Beyer, *Z. Chem.* 1986, ***26***, 81-94.
[4] K. H. König, M. Schuster, B. Steinbrech, G. Schneeweis, R. Schlodder, *Fresenius Z. Anal. Chem.* 1985, ***321***, 457-460.
[5] K. H. Koenig, M. Schuster, G. Schneeweis, B. Steinbrech, *Fresenius Z. Anal. Chem.* 1984, ***319***, 66-69.
[6] M. Schuster, *Fresenius' Journal of Analytical Chemistry* 1992, ***342***, 791-794.
[7] M. Schuster, M. Schwarzer, *Analytica Chimica Acta* 1996, ***328***, 1-11.
[8] M. Schuster, M. Sandor, *Fresenius' Journal of Analytical Chemistry* 1996, ***356***, 326-330.
[9] K. R. Koch, J. du Toit, M. R. Caira, C. Sacht, *J. Chem. Soc., Dalton Trans.* 1994, 785-786.
[10] F. H. Allen, *Acta Crystallogr., Sect. B: Struct. Sci.* 2002, ***B58***, 380-388.
[11] D. Hanekom, J. M. McKenzie, N. M. Derix, K. R. Koch, *Chem. Commun.* 2005, ***6***, 767-769.
[12] A. Irving, K. R. Koch, M. Matoetoe, *Inorg. Chim. Acta* 1993, ***206***, 193-199.
[13] K. R. Koch, T. Grimmbacher, C. Sacht, *Polyhedron* 1998, ***17***, 267-274.
[14] J. Miller, PhD *thesis*, University of Cape Town, **2000**.
[15] K. R. Koch, *Coord. Chem. Rev.* 2001, ***216-217***, 473-488.
[16] K. R. Koch, Y. Wang, A. Coetzee, *Dalton Trans.* 1999, ***6***, 1013-1016.
[17] A. N. Mautjana, J. D. S. Miller, A. Gie, S. A. Bourne, K. R. Koch, *J. Chem. Soc., Dalton Trans.* 2003, ***10***, 1952-1960.
[18] Research Group for Platinum Metals Chemistry; Stellenbosch University; *unpublished results.*
[19] D. Hanekom, M.Sc *thesis*, Stellenbosch Univeristy, **2006**.
[20] T. W. G. Solomons, *Solomon's Organic Chemistry*, Fifth ed., John Wiley & Sons, INC, **1992**.
[21] L. J. Barbour, *Journal of Supramolecular Chemistry* 2001, ***1***, 189-191.
[22] J. L. Atwood, L. J. Barbour, *Cryst. Growth Des* 2003, ***3***, 3-8.
[23] A. L. Spek, A Multipurpose Crystallographic Tool, University of Utrecht, Netherlands, **1999.**
[24] C. Sacht, M. S. Datt, S. Otto, A. Roodt, *Dalton Trans.* 2000, ***5***, 727-733.
[25] R. del Campo, J. J. Criado, E. Garcia, M. R. Hermosa, A. Jimenez-Sanchez, J. L. Manzano, E. Monte, E. Rodriguez-Fernandez, F. Sanz, *Journal of Inorganic Biochemistry* 2002, ***89***, 74-82.
[26] U. Schröder, R. Richter, L. Beyer, J. Angulo-Cornejo, M. Lino-Pacheco, A. Guillen, *Z. Anorg. Allg. Chem.* 2003, ***629***, 1051-1058.
[27] K. R. Koch, M. C. Matoetoe, *Magn. Reson. Chem.* 1991, ***29***, 1158-1160.
[28] K. R. Koch, C. Sacht, T. Grimmbacher, S. Bourne, *S. Afr. J. Chem.* 1995, ***48***, 71-77.
[29] G. L. Miesler, D. A. Tarr, *Inorganic Chemistry*, Prentice-Hall, **1991**.
[30] P. S. Pregosin, *Coord. Chem. Rev.* 1982, ***44***, 247-291.
[31] T. Grimmbacher, PhD *thesis*, University of Cape Town, **1995**.
[32] T. Froemmel, W. Peters, H. Wunderlich, W. Kuchen, *Angew. Chem., Int. Ed. Engl.* 1992, ***31***, 612-613.
[33] T. Froemmel, W. Peters, H. Wunderlich, W. Kuchen, *Angew. Chem., Int. Ed. Engl.* 1993, ***32***, 907-909.
[34] N. G. Zabirov, V. V. Brusko, A. Y. Verat, D. B. Krivolapov, I. A. Litvinov, R. A. Cherkasov, *Polyhedron* 2004, ***23***, 2243-2252.
[35] N. G. Zabirov, V. V. Brusko, A. Y. Verat, D. B. Krivolapov, I. A. Litvinov, R. A. Cherkasov, *Polyhedron*, ***In Press, Corrected Proof***.
[36] J. Csaszar, T. Szabo, G. Dombi, *Acta Chimica Academiae Scientiarum Hungaricae* 1976, ***88***, 1-11.
[37] M. Gerloch, R. C. Slade, *Journal of the Chemical Society: Inorganic, Physical, Theoretical* 1969, ***6***, 1012-1022.
[38] M. Gerloch, R. C. Slade, *Journal of the Chemical Society: Inorganic, Physical, Theoretical* 1969, ***6***, 1022-1028.
[39] G. N. La Mar, E. O. Sherman, *J. Am. Chem. Soc.* 1970, ***92***, 2691-2699.
[40] I. Bertini, D. Gatteschi, L. J. Wilson, *Inorg. Chim. Acta* 1970, ***4***, 629-631.
[41] R. Knorr, F. Ruf, *Angewandte Chemie* 1984, ***96***, 350-351.
[42] M. Matoetoe, M.Sc *thesis*, University of Cape Town, **1989**.
[43] A. N. Mautjana, MSc *thesis*, University of Cape Town, **2000**.
[44] L. V. Sudha, D. N. Sathyanarayana, *J. Mol. Struct.* 1984, ***125***, 89-96.
[45] B. S. Furniss, A. J. Hannaford, P. W. G. Smith, A. R. Tatchell, *Vogel's Textbook of Practical Organic Chemistry*, 5th ed.
[46] I. B. Douglass, F. B. Dains, *J. Am. Chem. Soc.* 1934, ***56***, 719-721.

[47] I. B. Douglass, F. B. Dains, *J. Am. Chem. Soc.* 1934, ***56***, 1408-1409.
[48] U. Schröder, L. Beyer, F. Dietze, R. Richter, S. Schmidt, E. Hoyer, *J. Prakt. Chem.* 1995, ***337***, 184-188.
[49] Bruker, SMART, SAINT and XPREP, Area detector control and data integration and reduction software, Bruker Analytical X-ray Instruments Inc., Madison, WI, USA., 1995
[50] G. M. Sheldrick, SADABS. Version 2.05, Empirical absorption correction program for area detector data, University of Göttingen, Germany., 2002
[51] G. M. Sheldrick, SHELXS97 and SHELXL97, Programs for the Solution and Refinement of Crystal Structures, University of Göttingen, Institüt für Anorganische Chemie der Universität, Tammanstrasse 4, D-3400 Göttingen, Germany, 1997
[52] Pov-Ray, http://www.povray.org,
[53] I. J. Bruno, J. C. Cole, P. R. Edgington, M. Kessler, C. F. Macrae, P. McCabe, J. Pearson, R. Taylor, *Acta Crystallogr., Sect. B: Struct. Sci.* 2002, ***B58***, 389-397.
[54] R. Blessing, H., *Acta Crystallogr., Sect. A: Found. Crystallogr.* 1995, ***A51***, 33-38.

Index: Chapter IV

1. Introduction

As part of a broader investigation into the elucidation of the fundamental coordination chemistry of ligands based on the $RC(O)NHC(S)N(R')_2$ motif towards Pt(II) and Pd(II)[1], a series of symmetrical ligands based on the general structure illustrated in Scheme 1 has been reported[2-6]. A review of the literature reveals that research in this area can be traced back to 1986 where Köhler *et al.* reported the crystal structure of a Ni_3L_3 complex [L = 3,3,3',3'-tetraethyl-1,1'terephthaloylbis(thioureato) anion] as well as some less well characterized complexes of Cu(II), Zn(II), Hg(II) and Pd(II). The latter three complexes of Zn(II), Hg(II) and Pd(II) were reported as being polymeric $(ML)_n$ complexes of low solubility[7]. In 1987 König *et al.* reported some Ni(II), Cu(II), Pd(II) and Pt(II) complexes derived from a series of 3,3,3'3'-tetraalkyl-1,1'-alkanedicarbonyl-bis(thiourea) ligands, however no structural details were reported. The Pt(II) and Pd(II) complexes reported by König *et al.* that were derived from H_2L = 3,3,3',3'-tetraethyl-1,1'-adipoylbis(thiourea) were reported as having a stoichiometry of $Pt(H_2L)Cl_2$ and Pd_3L_3[8].

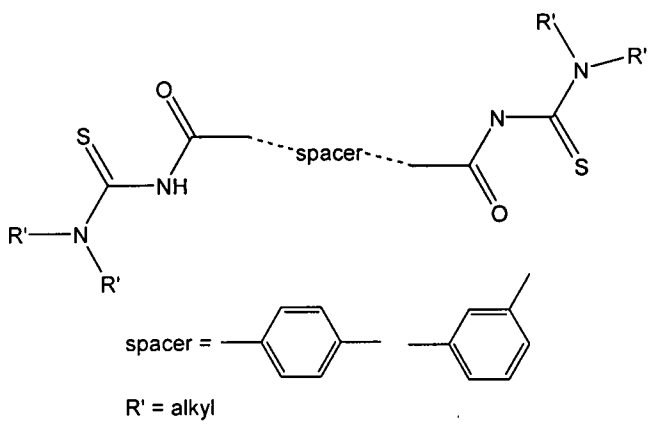

Scheme 1

It has been well demonstrated that bipodal 3,3,3',3'-tetralkyl-1,1'-phenylenebis(thioureas) may be used as "pre-programmed" chelating ligands to form metallomacrocyclic square planar d^8 metal complexes via self-assembly. The relative points of substitution (*para* vs. *meta*) of the phenylene spacer moiety in the ligand is critical in determining the geometry and M:L ratio of the resultant complex. Ligands derived from the *para*-substituted terephthalic acid give exclusively 3:3 (M:L) metallamacrocycles, while those derived from *meta*-substituted isophthalic acid give rise to only 2:2 (M:L) complexes [see Scheme 2][2, 3, 6]

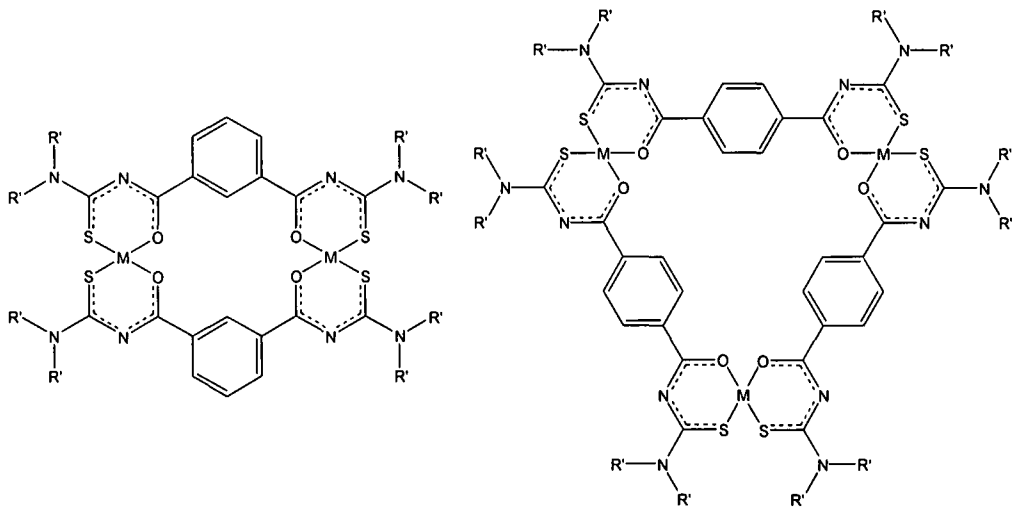

Scheme 2 2:2 and 3:3 (M:L) metallomacrocyclic square planar d^8 metal complexes derived from 3,3,3',3'-tetralkyl-1,1'-phenylenebis(thioureas).

The 'preprogrammed' nature of the 3,3,3',3'-tetralkyl-1,1'-phenylenebis(thioureas) to form single metallomacrocyclic products by self-assembly, suggests that by varying the structural design of these bipodal ligands, metal complexes with specifically designed structures and unique properties may be prepared. This methodology is analogous to the crystal engineering methodology where rational approaches are used for solid-state structural design based on the self-assembly of molecular components. This approach uses the concepts first developed by supramolecular chemistry in which hydrogen bonding, $\pi...\pi$ interactions and other weak interactions are used to generate and stabilize larger networks[9]. These weak interactions also include open framework structures that have been assembled using multifunctional organic ligands to link metals acting as nodes, as well as supramolecular structures constructed from discrete coordination-type units[4, 10, 11].

Bourne and Koch *et al.* reported that 3:3 and 2:2 Ni(II) metallomacrocyclic complexes derived from 3,3,3',3'-tetraethyl-1,1'terephthaloylbis(thiourea) and 3,3,3',3'-tetra(2-hydroxyethyl)-1,1'isothaloylbis(thiourea) respectively show some interesting host-guest chemistry[2, 4]. Bourne and Koch *et al.* further reported that the ability of the metallamacrocycles to act as host molecules in the crystal lattice is strongly dependent on the nature of the R-moieties as well as the coordinated metal[4]; i.e. longer chain alkyl substituents prevent the close packing of macrocyclic units and facilitate the capture of small organic guest molecules, while four-coordinate *cis*-[Ni(L-*S,O*)]$_2$ complexes readily form octahedral adducts with pyridine resulting in the formation of *cis*-[Ni(L-*S,O*)pyridine$_2$]$_2$ host-guest type structures. Similar host-guest type structures are not reported for the Pt(II) and Pd(II) analogue complexes[6].

Recent work in our laboratory has shown that aroyl(acyl)thioureas, RC(O)NHC(S)NR'$_2$, and their bipodal analogues, R'$_2$NC(S)NHC(O)RC(O)NHC(S)NR'$_2$ show some interesting inter- and intramolecular hydrogen-bonding interactions in the solid state[1, 4, 12-15]. In this context, bipodal *O*-alkyl-

N-benzoylthiocarbamic acid esters are of interest as potential structural analogues to the well studied bipodal 3,3',3'-tetralkyl-1,1'-phenylenebis(thioureas), which, to our knowledge, have received very little to no attention in the literature. In this context, the series of bipodal *O*-alkyl-*N*-benzoylthiocarbamic acid esters illustrated in Table 1 were envisaged, synthesized and fully characterized.

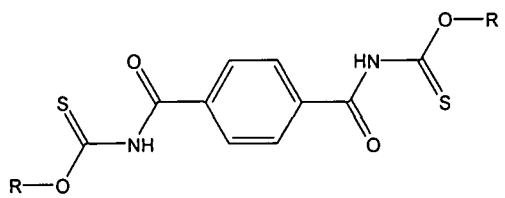

R =		
	$-CH_3$	$H_2(L^{15}\text{-}S,O)$
	$-CH_2CH_3$	$H_2(L^{16}\text{-}S,O)$
	$-(CH_2)_3CH_3$	$H_2(L^{17}\text{-}S,O)$

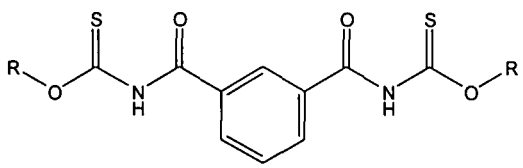

R =		
	$-CH_3$	$H_2(L^{18}\text{-}S,O)$
	$-CH_2CH_3$	$H_2(L^{19}\text{-}S,O)$
	$-(CH_2)_3CH_3$	$H_2(L^{20}\text{-}S,O)$

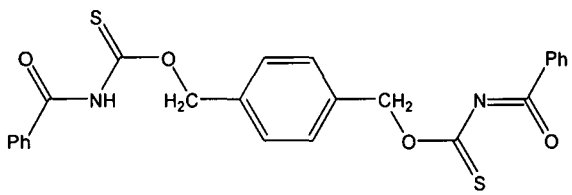

$H_2(L^{21}\text{-}S,O)$

Table 1 Series of bipodal thiocarbamic esters prepared and fully characterized.

The compounds listed in Table 1 were complexed with Ni(II), Pd(II) and Pt(II), however the physical characteristics of the resultant complexes unfortunately did not allow for adequate characterization. The complexes derived from the bipodal O-alkyl-N-benzoylthiocarbamicesters had an exceptionally poor solubility in most organic solvents thereby suggesting a polymeric-type product. This was verified in the case of the product resulting from the reaction of *O,O'*-dibutyl *N,N'*-(*p*-phenylene-dicarbonyl)bis(thiocarbamate) and copper(II) perchlorate [see section 2.7]. Since most of the complexes derived from the bipodal *O*-alkyl-*N*-benzoylthiocarbamic acid esters could not be fully characterized, they will not be discussed in any detail in this chapter.

A survey of the literature yields no detailed structural studies of bipodal O-alkyl-N-benzoylthiocarbamic acid acid esters. To date, apart from the structures reported in this thesis, namely *O,O'*-diethyl *N,N'*-(*p*-phenylene-dicarbonyl)bis(thiocarbamate)[16] and *O,O'*-dimethyl *N,N'*-(*m*-phenylenedicarbonyl)bis(thiocarbamate)[17], only two similar monopodal crystal structures of *N*-(2-furoyl)thiocarbamic-*O*-isopropyl ester[18] and *N*-(2-furoyl)thiocarbamic-*O*-benzyl ester[19] have been reported in the literature.

2. Results and Discussion

2.1 General preparation of bipodal *O*-alky-*N*-benzoylthiocarbamic esters

Compounds $H_2(L^{15\text{-}20}\text{-}S,O)$ [Table 1] were prepared according to the method illustrated Scheme 3 in a two step 'one-pot' synthesis under an inert anhydrous atmosphere.

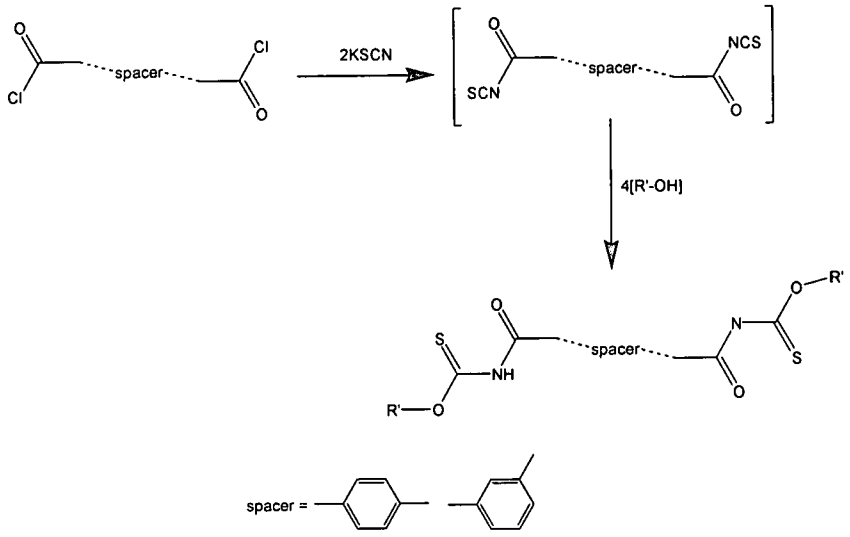

Scheme 3 Method of synthesis of bipodal *O,O'*-dialkyl-*N,N'*-(phenylene-dicarbonyl)bis(thiocarbamates).

Terephthaloyl or isophthaloyl dichloride was reacted with potassium isothiocyanate in anhydrous acetone followed by the addition of a four fold molar equivalent of the appropriate alcohol. The crude reaction products were initially recovered by extraction and further purified by either crystallization or column chromatography using silica gel as the stationary phase. During purification by column chromatography of $\mathbf{H_2(L^{19}\text{-}S,O)}$, an unexpected by-product was isolated and characterized crystallographically [see section 2.5.5]. All compounds were obtained in good yields (> 75%) and a high degree of purity, apart from compound $\mathbf{H_2(L^{21}\text{-}S,O)}$ which was obtained in only 38% yield but none the less high purity.

2.2 NMR Spectroscopy

The ^1H and ^{13}C NMR spectra of the bipodal *O,O'*-dialkyl-*N,N'*-(phenylene-dicarbonyl)bis(thiocarbamates) closely resemble the ^1H and ^{13}C NMR spectra observed for the equivalent monopodal *N*-aroylthiocarbamic-*O*-alkyl esters described in chapter II and chapter III (see Figure 1 as example).

All ^{13}C NMR spectra of compounds $\mathbf{H_2(L^{15\text{-}21}\text{-}S,O)}$ were acquired using a 1 second pulse delay in order to enhance the characteristically weak carbonyl and thiocarbonyl signals observed in the downfield region of the ^{13}C NMR spectra. In all cases the thiocarbonyl resonance signal is further down field (188.9 – 190.6ppm) relative to the carbonyl signal (161.5ppm – 170.1ppm) regardless of the spacer moiety or alkoxy substituent used [$\mathbf{H_2(L^{15}\text{-}S,O)}$ C(S) 189.7ppm C(O) 161.5ppm; $\mathbf{H_2(L^{16}\text{-}S,O)}$ C(S)

188.9ppm C(O) 161.9ppm; **$H_2(L^{17}$-*S,O*)** C(S) 189.2ppm C(O) 161.8ppm; **$H_2(L^{18}$-*S,O*)** C(S) 190.6ppm C(O) 170.1ppm; **$H_2(L^{19}$-*S,O*)** C(S) 189.9ppm C(O) 163.1ppm; **$H_2(L^{20}$-*S,O*)** C(S) 189.5ppm C(O) 162.2ppm; **$H_2(L^{21}$-*S,O*)** C(S) 190.6ppm C(O) 166.2ppm].

^{1}H NMR Spectrum

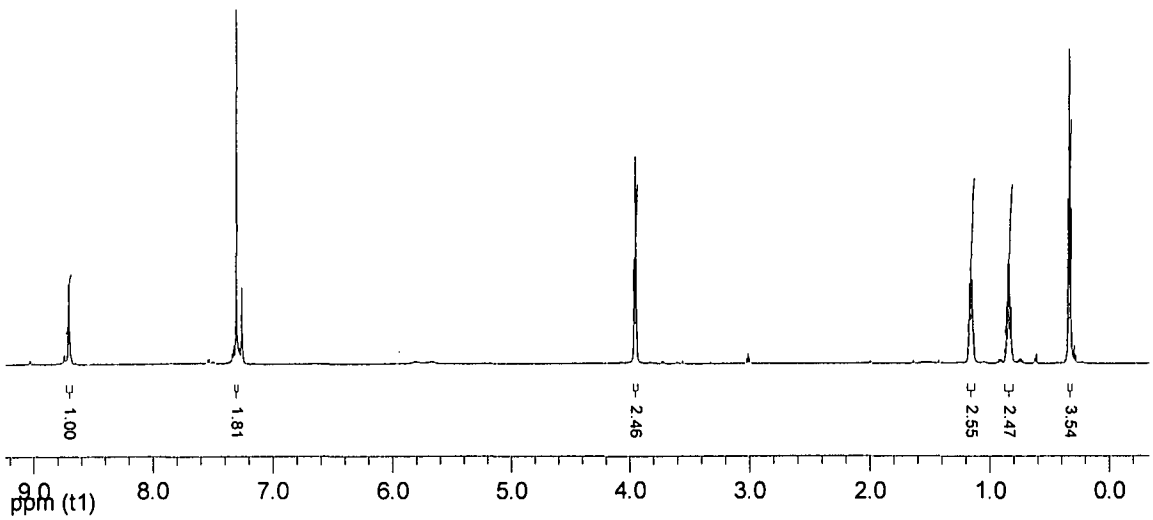

^{13}C NMR Spectrum

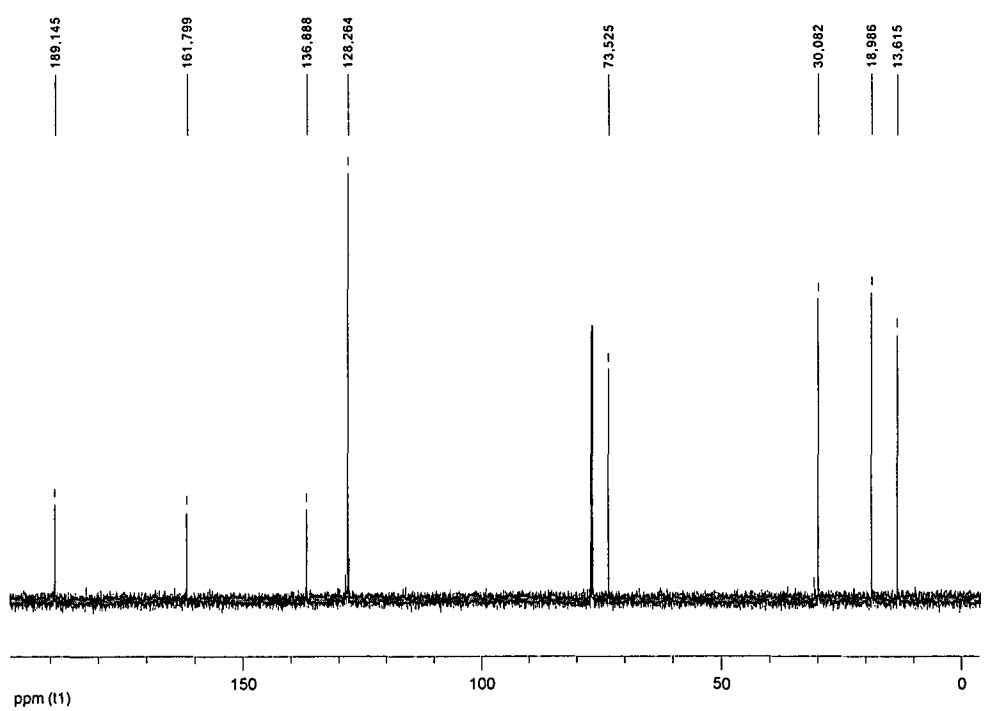

Figure 1 ^{1}H and ^{13}C NMR spectra of *O,O'*-dibutyl-*N,N'*-(*p*-phenylene-dicarbonyl)bis(thiocarbamate) in $CDCl_3$.

2.3 Mass Spectrometry

Apart from ^{1}H and ^{13}C NMR spectroscopy, compounds **$H_2(L^{15\text{-}21}$-*S,O*)** were further characterised by mass spectrometry. The appropriate m^+/z signal for the M^+ ion was obtained in all cases.

2.4 Infrared Spectroscopy

Similar to the structurally analogous *N*-aroylthiocarbamic-*O*-alkyl esters reported in chapter 2 and 3 of this thesis, the infrared spectra of the bipodal *O,O'*-dialkyl-*N,N'*-(phenylene-dicarbonyl)bis(thiocarbamates), **$H_2(L^{15\text{-}21}$-*S,O*)** all exhibit a broad band at ±3200cm^{-1} which can be attributed to the N-H stretch. The broadness of the stretching vibration of this group can partially be attributed to the N-H moiety being involved in extensive intra- and intermolecular hydrogen bonding networks[20]. This was confirmed in the single crystal structure analysis of **$H_2(L^{16}$-*S,O*)**, **$H_2(L^{18}$-*S,O*)**, **$H_2(L^{19}$-*S,O*)** and **$H_2(L^{21}$-*S,O*)**.

Sharp intense stretches are observed in the 1686 - 1702cm^{-1} and 1272 - 1300cm^{-1} regions which can be attributed to the carbonyl and thiocarbonyl moieties respectively. Characteristic stretches attributed to the C-N moiety of compounds **$H_2(L^{15\text{-}21}$-*S,O*)** are observed in the 1520 - 1542cm^{-1} region.

2.5 Single Crystal X-ray Diffraction Analysis of Bipodal *O,O'*-dialkyl-*N,N'*-(phenylene-dicarbonyl)bis(thiocarbamates).

Single crystal structure analysis was carried out on compounds **$H_2(L^{16}$-*S,O*)**, **$H_2(L^{18}$-*S,O*)**, **$H_2(L^{19}$-*S,O*)** and **$H_2(L^{21}$-*S,O*)**. To date, the only crystal structures of bipodal *O*-alkyl *N*-thiocarbamic esters that are listed on the CSD[21] are those reported here: *O,O'*-diethyl *N,N'*-(*p*-phenylene-dicarbonyl)bis(thiocarbamate)[16], **$H_2(L^{16}$-*S,O*)**, and *O,O'*-dimethyl *N,N'*-(*m*-phenylenedicarbonyl)bis(thiocarbamate)[17] **$H_2(L^{18}$-*S,O*)**. The aforementioned compound, **$H_2(L^{18}$-*S,O*)** crystallized in two forms and represents the first reported X-ray structure determination of isomers of this class of bipodal compound. The only other related crystal structures that are listed on the CSD are those of the monopodal *O*-isopropyl *N*-(2-furoyl)thiocarbamate[18] and *O*-benzyl *N*-(2-furoyl)thiocarbamate[19].

2.5.1 *O,O'*-diethyl *N,N'*-(*p*-phenylene-dicarbonyl)bis(thiocarbamate)[16], $H_2(L^{16}$-*S,O*).

$H_2(L^{16}$-*S,O*) crystallizes tetragonal, space group $P4_32_12$, in a *cis*-(*S,O*) fashion [Z,Z' conformation] with four formula units per unit cell. The molecular structure of $H_2(L^{16}$-*S,O*) illustrated in Figure 2 shows the numbering scheme used. Bond lengths, bond angles and torsion angles of interest are listed in Table 2.

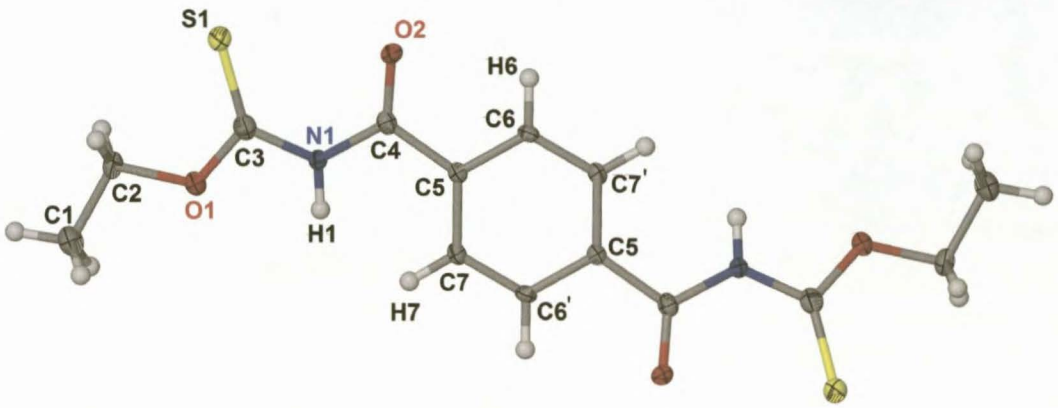

Figure 2 The molecular structure of $H_2(L^{16}$-*S,O*) showing the numbering scheme used. There is a twofold rotation axis passing through the centre of the phenylene ring. Accented atoms are generated by the symmetry code (i) 1+y, x-1, -z. Displacement ellipsoids are drawn at the 50% probability level.

S1-C3	1.638(3)	C5-C7	1.392(3)
O2-C4	1.213(3)	C5-C6	1.401(3)
N1-C3	1.383(3)	C5-C4	1.503(3)
N1-C4	1.384(3)	C7-C6'	1.377(4)
O1-C3	1.340(3)		
C7-C5-C4	124.6(2)	C6-C5-C4	116.1(2)
S1-C3-N1-C4	-1.6(4)	C3-N1-C4-O2	-5.8(4)

Table 2 Bond lengths (Å) and torsion angles (°) of interest observed in $H_2(L^{16}$-*S,O*). Symmetry code (i) 1+y, x-1, -z.

The planar conformation with a *cis*-(*S,O*) orientation of the carbonyl and thiocarbonyl groups observed in $H_2(L^{16}$-*S,O*) differs from the regularly reported *trans*-(*S,O*) orientation of the analogous monopodal and bipodal *N,N*-dialkyl- and *N*-alkyl-*N'*-aroyl(acyl)thioureas[1, 13, 22], as well as from the *trans*-(*S,O*) orientation observed for *O*-isopropyl *N*-(2-furoyl)thiocarbamate[18]. The essentially planar arrangement of atoms S1, C3, N1, C4 and O2 is illustrated by torsion angles S1-C3-N1-C4 and C3-N1-C4-O2 of -1.6(4)° and -5.8(4)°, respectively. As a result, the entire molecule of $H_2(L^{16}$-*S,O*) is effectively planar, in contrast to what is usually observed in the structurally related 3,3,3',3'-tetraalkyl-1,1'-terephthaloylbis(thioureas) which are generally significantly distorted from overall planarity[1, 15].

$H_2(L^{16}$-*S,O*) contains a twofold rotation axis located at the center of the phenylene ring and crystallizes in an *s-cisoid s-cisoid* conformation with respect to the C3-N1-C4 system. The two S/O groups are thus *anti* relative to one another, as a result of the twofold rotation axis. The *cis*-(*S,O*) orientation of **$H_2(L^{16}$-*S,O*)** results in a 1-4 N1-H1...O1 intramolecular hydrogen contact [N1-H1...O1 2.21Å, N1...O1 2.181(3)Å]. A further classical intermolecular hydrogen bond is observed between N1-H1...$O2^{ii}$ [N1-H1...$O2^{ii}$ 2.17Å 140°; symmetry code (ii) ½+y, ½-x, ¼+z]. Atom O2 in turn forms the reciprocal O2...H1-N1 intermolecular hydrogen bond (symmetry code ½-y, x-½, z-¼) with a second adjacent molecule which results in one molecule of **$H_2(L^{16}$-*S,O*)** being hydrogen bonded to four adjacent molecules as illustrated in Figure 3. The N1-H1...$O2^{ii}$ intermolecular hydrogen bond is further stabilized by a non-classical intermolecular C7-H7...$O2^{ii}$ interaction [C7-H7...$O2^{ii}$ 2.48Å 116°; symmetry code (ii) ½+y, ½-x, ¼+z]. Intra- and intermolecular hydrogen bonds and hydrogen contacts are listed in Table 3.

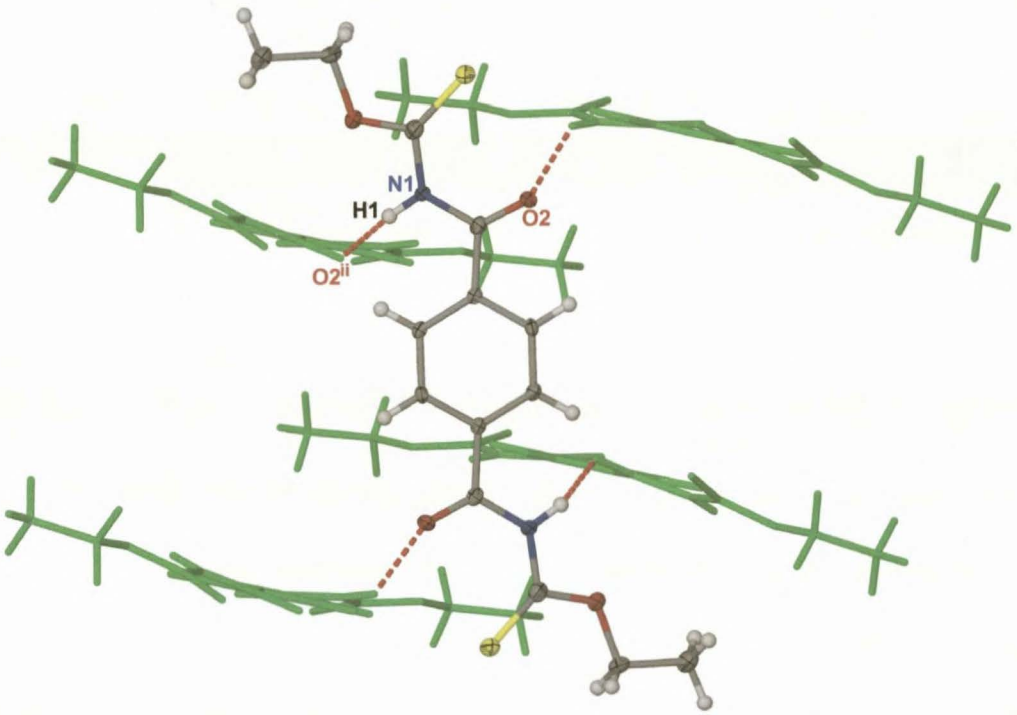

Figure 3 N1-H1...$O2^{ii}$ intermolecular hydrogen bond observed in **$H_2(L^{16}$-*S,O*)** symmetry code (ii) ½+y, ½-x, ¼+z. The four adjacent hydrogen molecules are indicated in green.

D-H...A	Type	D-H (Å)	H...A (Å)	D...A (Å)	D-H...A (°)
N1-H1...$O2^{ii}$	inter	0.88	2.17	2.895(3)	140.0
C7-H7...$O2^{ii}$	inter	0.95	2.48	3.020(3)	115.8
C6-H6...O2	intra	0.95	2.43	2.749(3)	99.6

Table 3 Inter- and intramolecular hydrogen bonding and hydrogen contact geometry as identified in **$H_2(L^{16}$-*S,O*)** by XSeed[23, 24] and Platon[25] with s.u.s in parenthesis.

The C3-N1 bond distance of 1.383(3)Å is shorter than that observed for the corresponding bipodal compounds 3,3,3',3'-tetraethyl-1,1'-terephthaloylbis(thiourea) [1.4173(16)Å][15] and 3,3,3',3'-tetraethyl-1,1'-isophthaloylbis(thiourea) [1.428 (4)Å][6] suggesting a greater degree of double-bond character in the C-N bond in question for **$H_2(L^{16}$-*S,O*)**. Moreover, the C4-N1 bond length of 1.384(3)Å is comparable in length to the corresponding bonds in the aforementioned bipodal *N',N',N''',N'''*-tetraalkyl-*N,N''*-aroylbis(thioureas). The partial double-bond character of the C-N bonds observed here is consistent with that suggested by Schröder *et al.* on the basis of spectroscopic studies[26].

The asymmetry of the C6-C5-C4 and C7-C5-C4 angles of 116.1(2)° and 124.6(2)° respectively is possibly caused by a repulsion between the N1-H1...H7-C7 system [N1...C7 = 2.923 (3)Å] and an attraction between the C6-H6...O2 system [C6-H6...O2 2.43Å, C6...O2 2.749(3)Å; see Table 3]. A similar asymmetry of bond angles around the carbonyl group relative to the furoyl group within the monopodal *O*-isopropyl *N*-(2-furoyl)thiocarbamate has been reported[18].

An extended packing diagram of **$H_2(L^{16}$-*S,O*)** is illustrated in Figure 4 showing the 'cubic-like' arrangement of molecules when the unit cell is viewed along [001].

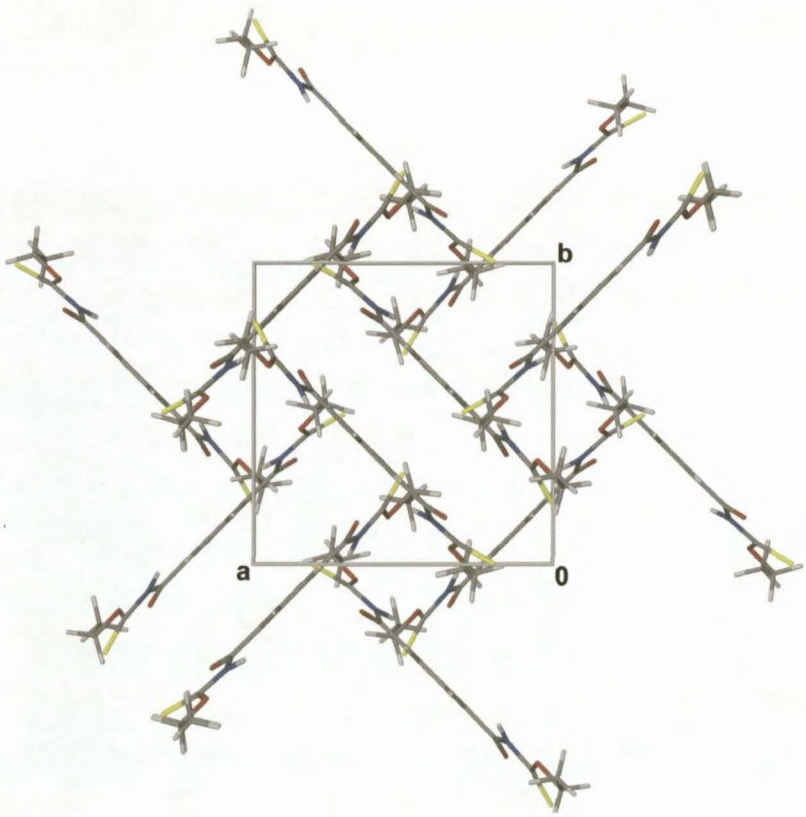

Figure 4 Extended packing diagram of **$H_2(L^{16}$-*S,O*)** showing the 'cubic' arrangement of molecules when viewed along [001].

2.5.2 *O,O'*-dimethyl *N,N'*-(*m*-phenylene-dicarbonyl)bis(thiocarbamate)[17], $H_2(L^{18}$-*S,O*).

Both a yellow and a white crystalline product were obtained in the crystallization of $H_2(L^{18}$-*S,O*), *anti-, anti-(S,O)* and *syn-, syn-(S,O)* polymorphs of *O,O'*-dimethyl *N,N'*-(*m*-phenylene-dicarbonyl)bis(thiocarbamate). These different crystals were identified under a microscope based on colour and were separated manually. The molecular structures of the white **(I)**, and yellow, **(II)** polymorphic, crystalline products of $H_2(L^{18}$-*S,O*) differ by the relative orientation of the thiocarbonyl moiety with respect to the aminocarbonyl groups. In **(I)**, the orientations of both thiocarbamate *O*-ester groups are *anti-* with respect to the aminocarbonyl moiety, while in **(II)**, one orientation is *anti* and the other is *syn*. Possible polymorphic forms of $H_2(L^{18}$-*S,O*) are illustrated in Scheme 4 which suggests a third polymorphic form of $H_2(L^{18}$-*S,O*), however **(III)** was not isolated.

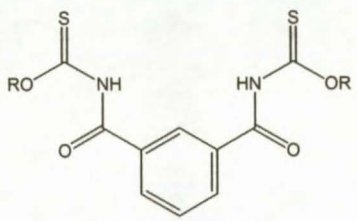

(I) *anti-, anti-(S,O)*

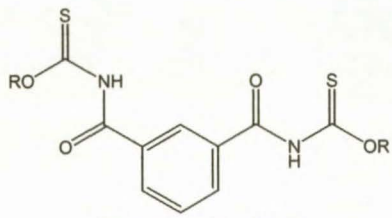

(II) *anti-, syn-(S,O)*

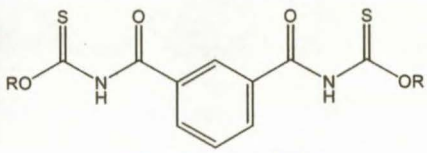

(III) *syn-, syn-(S,O)*

Scheme 4 Possible polymorphs of $H_2(L^{18}$-*S,O*).

The molecular structure of **(I)** is illustrated in Figure 5 while the molecular structure of **(II)** is illustrated in Figure 6. Selected bond lengths, bond angles and torsion angles of **(I)** and **(II)** are listed in Table 4 and Table 5 respectively

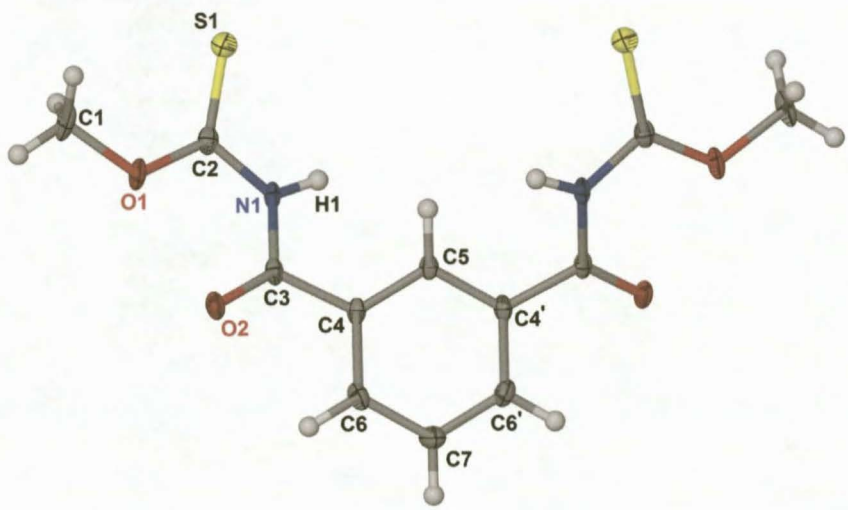

Figure 5 The molecular structure of $H_2(L^{18}$-*S,O*) **(I)** showing the numbering scheme used. Displacement ellipsoids are drawn at the 50% probability level. Accented atoms are generated by a two fold rotation axis which passes through atoms C5 and C7. [Symmetry code (vi) –x, y, ½-z].

S1-C2	1.637(2)	N1-C3	1.380(3)
O1-C2	1.318(2)	N1-C2	1.391(3)
O2-C3	1.220(2)		
C6-C4-C3	117.15(17)	C5-C4-C3	122.78(19)
C3-N1-C2-S1	164.72(16)	C2-N1-C3-O2	5.8(3)

Table 4 Bond lengths (Å), bond angles (°) and torsion angles (°) of interest observed in **(I)** of $H_2(L^{18}$-*S,O*) with s.u.s in parenthesis.

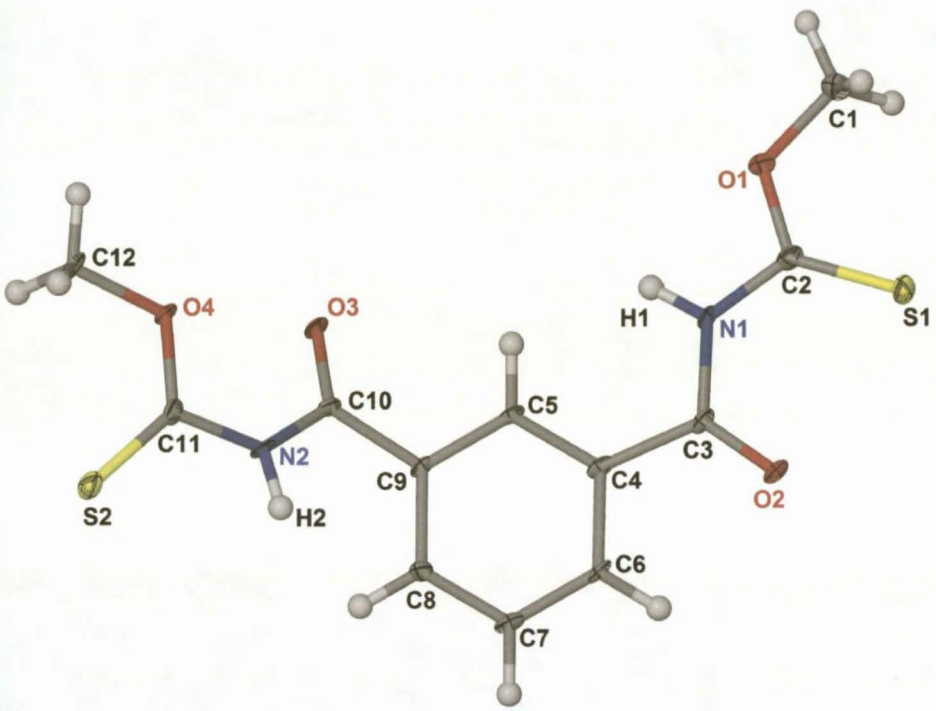

Figure 6 The molecular structure of $H_2(L^{18}$-*S,O*) **(II)** showing the numbering scheme used. Displacement ellipsoids are drawn at the 50% probability level.

S1-C2	1.634(4)	O3-C10	1.226(4)
S2-C11	1.639(4)	N1-C2	1.377(5)
O1-C2	1.343(4)	N1-C3	1.401(4)
O4-C11	1.327(4)	N2-C10	1.372(4)
O2-C3	1.212(4)	N2-C11	1.381(4)
C5-C4-C3	125.4(3)	C5-C9-C10	117.9(3)
C6-C4-C3	115.6(3)	C8-C9-C10	122.2(3)
C3-N1-C2-S1	0.3(6)	C2-N1-C3-O2	-8.4(6)
C10-N2-C11-S2	162.2(3)	C11-N2-C10-O3	-2.7(6)

Table 5 Bond lengths (Å), bond angles (°) and torsion angles (°) of interest observed in **(II)** of $H_2(L^{18}$-*S,O*) with s.u.s in parenthesis.

In **(I)**, both the thiocarbonyl and carbonyl moieties within the asymmetric unit are *anti* relative to one another, the complete molecule being generated by a twofold rotation axis passing through atoms C5 and C7 of the phenylene ring. The asymmetric unit of **(II)** consists of a complete molecule and, in contrast to **(I)**, does not contain internal symmetry. The relative orientations of the thiocarbonyl and carbonyl moieties, S1 and O2, are *syn* with respect to each other, while atoms O3 and S2 are *anti* relative to one another. The approximate *anti* orientation of the sulphur and oxygen atoms within the C(S)NHC(O) moieties of **(I)**, and of atoms O3 and S2 in **(II)**, is frequently observed in the closely related bipodal *N',N',N''',N'''*-tetraalkyl-*N,N''*-aroylbis(thioureas)[6, 15] and for the monopodal *N*-aroyl-*N'*-alkyl- and *N*-aroyl-*N',N'*-dialkylthioureas[13, 27-29]. The comparable uncommon *syn* orientation of the thiocarbonyl and carbonyl moieties (S1 and O2) observed in **(II)** was also observed in the structurally related *O,O'*-diethyl *N,N'*-(p-phenylenedicarbonyl)bis(thiocarbamate)[16] **$H_2(L^{16}$-*S,O*)** and *O,O'*-(*p*-xylene-α,α'diyl) *N,N'*-dibenzoyl bis(thiocarbamate), **$H_2(L^{21}$-*S,O*)** [see section 2.5.4].

The *anti- anti* and *syn- anti* conformations of **(I)** and **(II)** have a significant effect on their molecular packing in the crystal lattice. The *anti- anti* conformation in **(I)** results in intermolecular N1-H1…$O2^{viii}$ hydrogen bonds as well as non-classical bifurcated C5-H5…$O2^{viii}$ C5-H5…$O2^{ix}$ hydrogen contacts between adjacent molecules, causing molecules of **(I)** to pack in chains parallel to the *c*-axis as illustrated in Figure 7 [N1-H1…$O2^{viii}$ 2.08Å, C5-H5…$O2^{viii}$ 2.58Å, C5-H5…$O2^{ix}$ 2.58Å; symmetry codes (viii) x, 1-y, z-½; (ix) –x, 1-y, 1-z]. Further distinctive intermolecular C6-H6…$S1^{vii}$ hydrogen bond interactions in **(I)** cause these chains of molecules to extend as two dimensional sheets parallel to (100) [C6-H6…S^{vii} 2.76Å; symmetry code (vii) x, 1+y, z]. The intermolecular hydrogen interactions observed in **(I)** are listed in Table 6.

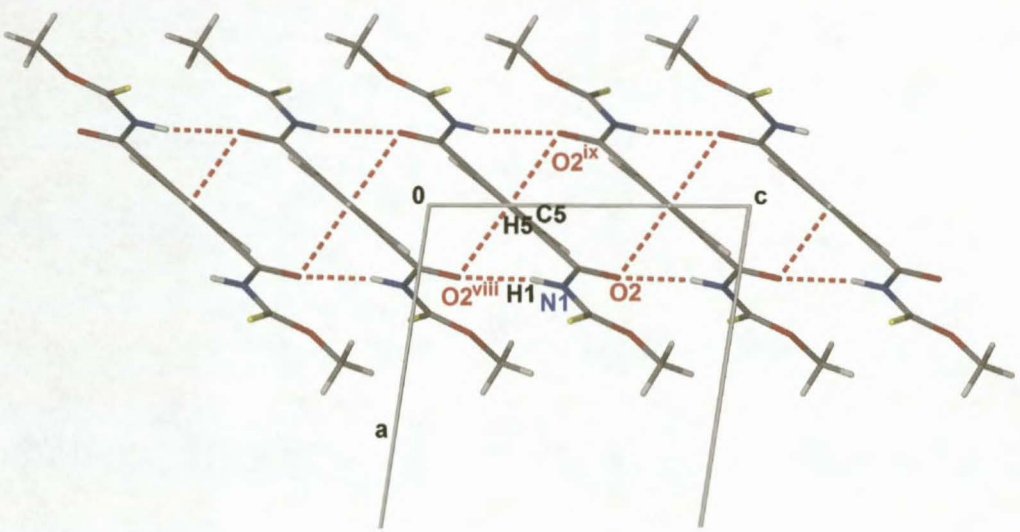

Figure 7 Molecules of **$H_2(L^{18}$-*S,O*) (II)** as viewed along [010] extending parallel to the *c*-axis resulting from the N1-H1…$O2^{viii}$ hydrogen bonds as well as bifurcated C5-H5…$O2^{viii}$ and C5-H5…O^{ix} hydrogen interactions between adjacent molecules; [symmetry codes (viii) x, 1-y, z-½; (ix) –x, 1-y, 1-z].

D-H...A	Type	D-H (Å)	H...A (Å)	D...A (Å)	D-H...A (°)
C6-H6...S1^{vii}	inter	0.95	2.76	3.525(2)	138.0
C5-H5...O2^{viii}	inter	0.95	2.58	3.068(2)	113.0
C5-H5...O2^{ix}	inter	0.95	2.58	3.068(2)	113.0
N1-H1...O2^{viii}	inter	0.88	2.08	2.948(2)	169.0

Table 6 Intermolecular hydrogen bonds and hydrogen contact geometry observed in the unit cell of **$H_2(L^{18}$-*S,O*) (II)** as identified by XSeed[23, 24] and Platon[25] with s.u.s in parenthesis. Symmetry codes (vii) x, 1+y, z; (viii) x, 1-y, z-½; (ix)) –x, 1-y, 1-z.

The *syn- anti* conformation of **(II)** results in these molecules packing with a network of bifurcated intermolecular N1-H1...O3^{x}, C5-H5...O3^{x}, N2-H2...O2^{xi} and N2-H2...S1^{xi} hydrogen interactions to adjacent molecules [N1-H1...O3^{x} 2.04Å, C5-H5...O3^{x} 2.32Å, N2-H2...O2^{xi} 2.55Å, N2-H2...S1^{xi} 2.57Å; symmetry codes: (x) -x, -y, 2-z; (xi) 1-x, 1-y, 2-z]. As a result, each molecule of **(II)** interacts with two adjacent molecules via a series of hydrogen interactions, producing two one-dimensional molecular chains per unit cell extending parallel to [110] as illustrated in Figure 8. The intermolecular hydrogen bond and contact geometry observed in **(II)** is listed in Table 7.

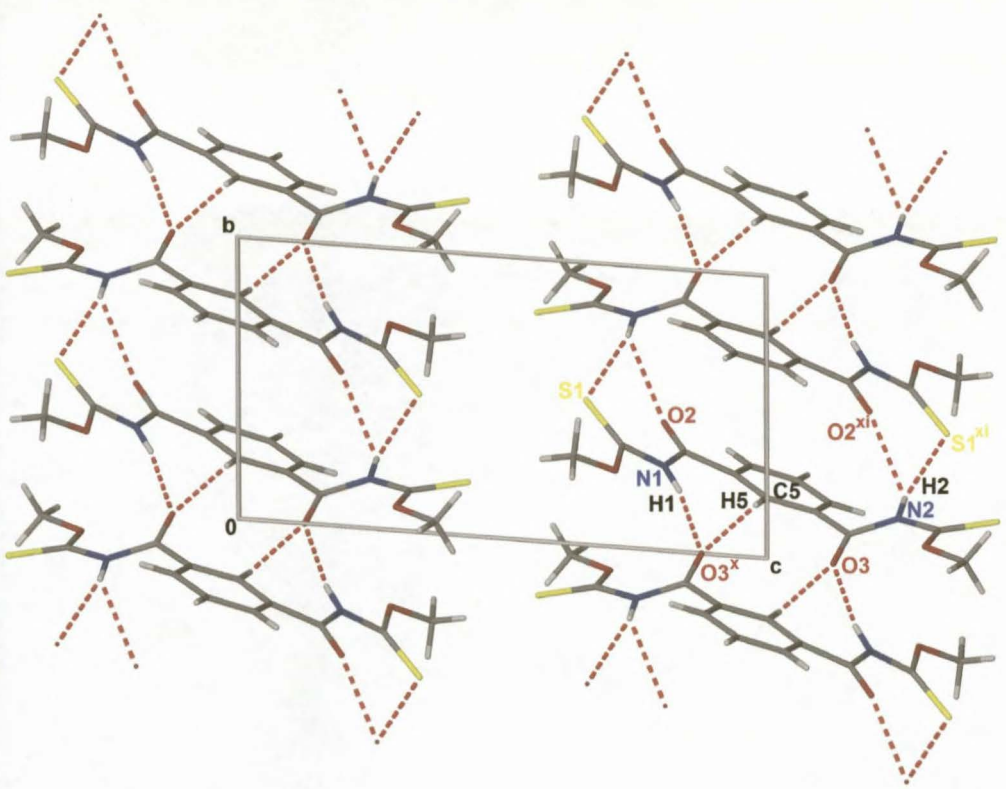

Figure 8 Extended packing diagram of **$H_2(L^{18}$-*S,O*) (II)** as viewed along [100] showing the intermolecular N1-H1...O3^{x}, N2-H2...S1^{xi}, N2-H2...O2^{xi} and C5-H5...O3^{x} hydrogen interactions [symmetry codes: (x) –x, -y, 2-z; (xi) 1-x, 1-y, 2-z].

D-H...A	Type	D-H (Å)	H...A (Å)	D...A (Å)	D-H...A (°)
N1-H1...O3^{x}	inter	0.88	2.04	2.913(4)	169.1
N2-H2...S1^{xi}	inter	0.88	2.57	3.421(3)	162.8
N2-H2...O2^{xi}	inter	0.88	2.55	2.949(4)	108.5
C5-H5...O3^{x}	inter	0.95	2.32	3.140(4)	144.7

Table 7 Intermolecular hydrogen bond geometry observed in $H_2(L^{18}$-*S,O*) **(II)** as identified by XSeed[23, 24] and Platon[25] with s.u.s in parenthesis. Symmetry codes (x) –x, -y, 2-z; (xi) 1-x, 1-y, 2-z.

The C2-N1 bonds in both **(I)** [C2-N1 1.391(3)Å] and **(II)** [C2-N1 1.377(5)Å], as well as C11-N2 in **(II)** [C11-N2 1.381(4)Å], are all shorter than the corresponding bonds in the bipodal compound 3,3,3',3'-tetraethyl-1,1'-terephthaloylbis-(thiourea)[15] [1.4173(16)Å] and in 3,3,3',3'-tetraethyl-1,1'-isophthaloylbis(thiourea)[6] [1.428(4)Å]. This fact indicates a greater degree of double-bond character in the C-N bonds in question in **(I)** and **(II)**. Correspondingly, the C3-N1 bond length of **(I)** [C3-N1 1.380(3)Å] and C10-N2 of **(II)** [C10-N2 1.372(4)Å] are somewhat longer than the corresponding C-N bond length for 3,3,3',3'-tetraethyl-1,1'-terephthaloylbis(thiourea)[15] [1.3606(17)Å]. The C3-N1 bond in **(II)** [C3-N1 1.401(4)Å] is significantly longer than the comparable C-N bonds in both 3,3,3',3'-tetraethyl-1,1'-terephthaloylbis(thiourea)[15] [1.3606(17)Å] and 3,3,3',3'-tetraethyl-1,1'-isophthaloylbis(thiourea)[6] [1.381(4)Å].

The conformations of the $C(O)NHC(S)OCH_3$ branches of **(I)** are remarkably planar, with atom O1 deviating from the C4/C3/N1/C2/O1/C1 least-squares plane by only 0.070(2)Å. Atoms O2 and S1 lie out of this plane by only -0.118(3)Å and -0.291(3)Å, respectively, in contrast to the situation observed for 3,3,3',3'-tetraethyl-1,1'-terephthaloylbis(thiourea)[15] and 3,3,3',3'-tetraethyl-1,1'-isophthaloylbis(thiourea)[6]. In **(I)**, the C4/C3/N1/C2/O1/C1 plane intersects the plane of the phenylene ring at an angle of 25.50(9)°. The *anti* coplanarity of S1 and O2 in **(I)** is illustrated by the torsion angles listed in Table 4.

Both $C(O)NHC(S)OCH_3$ branches of **(II)** are also remarkably planar. For the *syn* branch of **(II)**, atom C4 deviates from the C4/C3/N1/C2/O1/C1 least-squares plane by only 0.060(2)Å, while atoms O2 and S1 deviate from this plane by -0.085(7)Å and 0.185(8)Å respectively. The *syn* coplanarity of atoms S1 and O2 in **(II)** is illustrated by the torsion angles listed in Table 5. Furthermore, the *syn* coplanarity of atoms S1 and O2 in **(II)** is possibly assisted by the 1-4 intramolecular hydrogen contact observed N1-H1...O1 2.220Å. The C4/C3/N1/C2/O1/C1 plane intersects the plane of the phenylene ring at an angle of 16.5(3)°. Similarly, atoms C10, O3 and S2 deviate from the C9/C10/N2/C11/O4/C12 least-squares plane of the *anti* $C(O)NHC(S)OCH_3$ branch of **(II)** by only 0.147(3)Å, 0.458(5)Å and 0.230(6)Å respectively. The *anti* coplanarity of atoms S2 and O3 in **(II)** is illustrated by the torsion angles listed in Table 5.

The asymmetry of the C5-C4-C3 and C6-C4-C3 bond angles [C5-C4-C3 122.78(19)°, C6-C4-C3 117.15(17)°] in **(I)** may be the result of a repulsion in the N1-H1...H5-C5 system and an attraction in the C6-H6...O2 system. Similar observations pertain to **(II)**, with an asymmetry in the C5-C4-C3 and

C6-C4-C3 angles [C5-C4-C3 125.4(3)°, C6-C4-C3 115.6(3)°] due to a possible repulsion in the N1-H1...H5-C5 system and an attraction between the C6-H6...O2 system. For the *anti* branch in **(II)**, qualitatively similar interactions may be inferred from the asymmetry between the C5-C9-C10 and C8-C9-C10 angles [C5-C9-C10 117.9(3)°, C8-C9-C10 122.2(3)°] possibly as a result of repulsive interactions in the N2-H2...H8-C8 system and attractive interactions in the C5-H5...O3 system. Similar observations have been made for *O*-isopropyl *N*-(2-furoyl)-thiocarbamate[18].

As illustrated in Scheme 4, a third polymorphic form of **$H_2(L^{18}$-*S,O*)**, with a *cis- cis*-(*S,O*) orientation, **(III)**, exists. However, polymorph **(III)** was not isolated in the solid state. Crystallization and polymorphism are complex phenomena and an appreciation of polymorphism is fundamental to an understanding of the crystallization process itself[30]. It has been suggested that our understanding of polymorphism is, however, still far from complete and the occurrence of polymorphism cannot be safely predicted[31]. In many cases in the literature, the pattern of hydrogen bonds formed within a molecule studied is said to constitute the basis for polymorphism within those molecules[31]. It is possible that the hydrogen bonding observed in **(I)** and **(II)** contributes to the occurrence of the polymorphism observed. However, the overall packing of the molecules of **(I)** and **(II)** is undoubtedly dictated by a collection of subtleties, only some of which are the hydrogen-bond interactions observed.

2.5.3 *O,O'*-diethyl *N,N'*-(*m*-phenylene-dicarbonyl)bis(thiocarbamate), $H_2(L^{19}$-*S,O*).

$H_2(L^{19}$-*S,O*) crystallizes monoclinic space group *C*2/*c* with eight formula units per unit cell and has an *anti*-, *anti*-(*S,O*) orientation of the respective carbonyl and thiocarbonyl groups similar to that observed in polymorph **(I)** of **$H_2(L^{18}$-*S,O*)** [see Figure 5]. No other polymorphic forms of **$H_2(L^{19}$-*S,O*)** were isolated. The molecular structure of **$H_2(L^{19}$-*S,O*)** is illustrated in Figure 9. A molecule of acetonitrile co-crystallized with **$H_2(L^{19}$-*S,O*)**. Selected bond lengths, bond angles and torsion angles of interest are listed in Table 8.

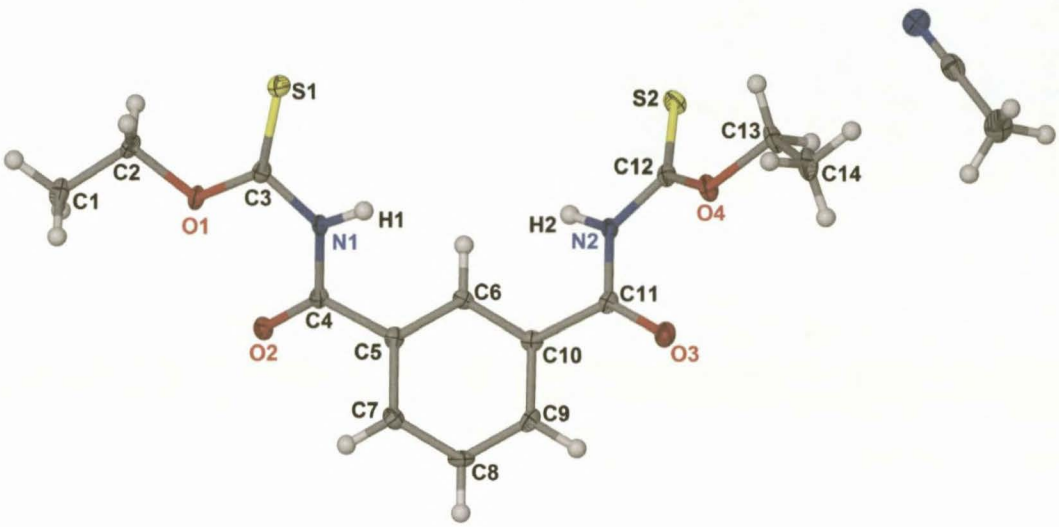

Figure 9 Molecular structure of **$H_2(L^{19}$-*S,O*)** showing the numbering scheme used. Displacement ellipsoids are drawn at the 50% probability level.

S1-C3	1.644(3)	S2-C12	1.646(3)
O2-C4	1.219(3)	O3-C11	1.215(3)
C4-N1	1.379(4)	C11-N2	1.389(3)
C3-N1	1.390(3)	C12-N2	1.377(3)
C3-O1	1.316(3)	C12-O4	1.317(3)
C6-C5-C4	122.9(2)	C6-C10-C11	122.6(2)
C7-C5-C4	117.4(2)	C9-C10-C11	117.7(3)
C4-N1-C3-S1	-175.8(2)	C11-N2-C12-S2	160.0(2)
C3-N1-C4-O2	-2.8(4)	C12-N2-C11-O3	-16.0(4)

Table 8 Bond lengths (Å), bond angles (°) and torsion angles (°) of interest observed in **$H_2(L^{19}$-*S,O*)** with s.u.s in parenthesis.

The thiocarbonyl moiety S1-C3 of **$H_2(L^{19}$-*S,O*)** is essentially *anti* coplanar with carbonyl moiety O2-C4 while thiocarbonyl moiety S2-C12 is essentially *anti* coplanar with carbonyl moiety O3-C11 as

illustrated by C4-N1-C3-S1 and C3-N1-C4-O2 torsion angles of -175.8(2)° and -2.8(4)° respectively and torsion angles C11-N2-C12-S2 and C12-N2-C11-O3 of 160.0(2)° and -16.0(4)° respectively.

A great degree of distortion from overall planarity is observed in $H_2(L^{19}$-*S,O*), with each of the $C(O)NHC(S)OCH_2CH_3$ branches of $H_2(L^{19}$-*S,O*) being twisted out of the plane defined by the phenylene spacer. The C5-C4-N1-C3-O1-C2-C1 branch of $H_2(L^{19}$-*S,O*) is remarkably planar with the greatest deviation from the least-squares plane being atom C2 by -0.085(3)Å. However a significantly greater degree of distortion from planarity is observed in the second $C(O)NHC(S)OCH_2CH_3$ branch of $H_2(L^{19}$-*S,O*), with atom C11 deviating from the C14/C13/O4/C12/N2/C11/C10 least-squares plane by 0.310(2)Å. In turn the C5/C4/N1/C3/O1/C2/C1 plane intersects the least-squares plane of the phenylene spacer at 27.0(1)° while the C14/C13/O4/C12/N2/C11/C10 plane intersects the same least-squares plane of the phenylene spacer at 54.0(1)°.

The asymmetry in the C6-C5-C4 and C7-C5-C4 bond angles [C6-C5-C4 122.9(2)°, C7-C5-C4 117.4(2)°] is possibly due to a repulsion in the N1-H1...C6-H6 system and an attraction in the C7-H7...O2 system [C7-H7...O2 2.59Å]. A similar asymmetry in the C6-C10-C11 and C9-C10-C11 bond angles [C6-C10-C11 = 122.6(2)°, C9-C10-C11 = 117.7(3)°] is possibly the result of a repulsion in the C6-H6...H2-N2 system and an attraction in the C9-H9...O3 system [C9-H9...O3 = 2.52Å]. Comparable observations were made in the molecular structures of $H_2(L^{16}$-*S,O*) and $H_2(L^{18}$-*S,O*) as well as the molecular structure of *O*-isopropyl *N*-(2-furoyl)-thiocarbamate[18].

The C(O)-N and C(S)-N bond lengths of 3,3,3',3'-tetraethyl-1,1'-terephthaloylbis(thiourea)[15], $H_2(L^{22}$-*S,O*), and 3,3,3',3'-tetraethyl-1,1'-isophthaloylbis(thiourea)[6], $H_2(L^{23}$-*S,O*), have been tabulated in Table 9 along with the bond lengths of the corresponding C-N bonds of $H_2(L^{18}$-*S,O*) and $H_2(L^{19}$-*S,O*) for comparative purposes. The C(S)-N bond lengths of $H_2(L^{19}$-*S,O*) [N1-C3 1.390(3)Å; N2-C12 1.377(3)Å] are shorter than the bond lengths of the comparable C(S)-N bonds in both $H_2(L^{22}$-*S,O*) and $H_2(L^{23}$-*S,O*). This fact indicates a greater degree of double bond character in the C-N bonds of $H_2(L^{19}$-*S,O*). Correspondingly, the C(O)-N bond lengths of $H_2(L^{19}$-*S,O*) [N1-C4 1.379(4)Å; N2-C11 1.389(3)Å] are longer than the equivalent C(O)-N bond lengths of $H_2(L^{22}$-*S,O*) [1.361(2)Å] but are comparable in length to the corresponding C(O)-N bonds of $H_2(L^{23}$-*S,O*) [1.381Å;].

Bond	$H_2(L^{18}$-*S,O*) (I)	$H_2(L^{18}$-*S,O*) (II)		$H_2(L^{19}$-*S,O*)		$H_2(L^{22}$-*S,O*)	$H_2(^{23}$-*S,O*)
C(O)-N	1.380(3)	1.401(4)	1.372(4)	1.379(4)	1.389(3)	1.361(2)	1.381(4)
C(S)-N	1.391(3)	1.377(5)	1.381(4)	1.390(3)	1.377(3)	1.417(2)	1.428(4)

Table 9 C(O)-N and C(S)-N bond lengths of $H_2(L^{18}$-*S,O*) and $H_2(L^{19}$-*S,O*) as well as those of 3,3,3',3'-tetraethyl-1,1'-terephthaloylbis(thiourea)[15], $H_2(L^{22}$-*S,O*), and 3,3,3',3'-tetraethyl-1,1'-isophthaloylbis(thiourea)[6], $H_2(L^{23}$-*S,O*).

An intermolecular π…π type interaction is observed between the phenylene spacer rings of adjacent molecules of **$H_2(L^{19}$-*S,O*)** as illustrated in Figure 10 [Cg1…Cg1^{xii} 3.618Å where Cg1 is the centroid of the C5-C7-C8-C9-C10-C6 phenylene ring; symmetry code (xii) –x, y, ½ –z].

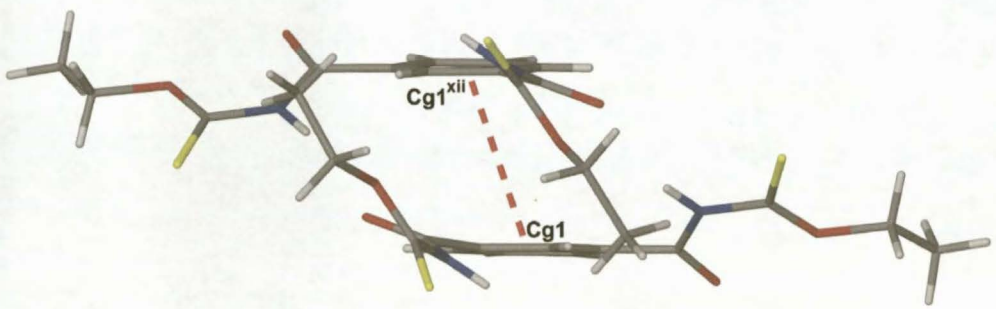

Figure 10 Electrostatic π…π type interactions observed between adjacent molecules of **$H_2(L^{19}$-*S,O*)** Symmetry code (xii) –x, y, ½-z.

Several intermolecular hydrogen bonds were observed in **$H_2(L^{19}$-*S,O*)** as listed in Table 10. A clear intermolecular hydrogen bond is observed between N1- H1…O3^{xiii} [N1- H1…O3^{xiii} 2.083Å] and between N2-H2…O2^{xiv} of an adjacent molecule [N2-H2…O2^{xiv} 1.986Å]. The N1- H1…O3^{xiii} and N2-H2…O2^{xiv} intermolecular hydrogen bonds result in the formation of one dimensional molecular chains of **$H_2(L^{19}$-*S,O*)** extending parallel to [001] as illustrated in Figure 11. These one dimensional molecular chains are further cross-linked via the non-classical intermolecular hydrogen bond C8-H8…S2^{xv} into two dimensional molecular sheets extending parallel to the *b-c* plane of the unit cell.

D-H…A	Type	D-H (Å)	H…A (Å)	D…A (Å)	D-H…A (°)
N1-H1…O3^{xiii}	inter	0.88	2.08	2.908(3)	155.6
N2-H2…O2^{xiv}	inter	0.88	1.99	2.836(3)	161.4
C8-H8…S2^{xv}	inter	0.95	2.81	3.691(3)	155.1

Table 10 Intermolecular hydrogen bond geometries observed in **$H_2(L^{19}$-*S,O*)** as identified by XSeed[23, 24] and Platon[25] with s.u.s in parenthesis. Symmetry codes (xiii) –x, y, ½-z; (xiv) -x, -y, -z; (xv) x, y-1, z.

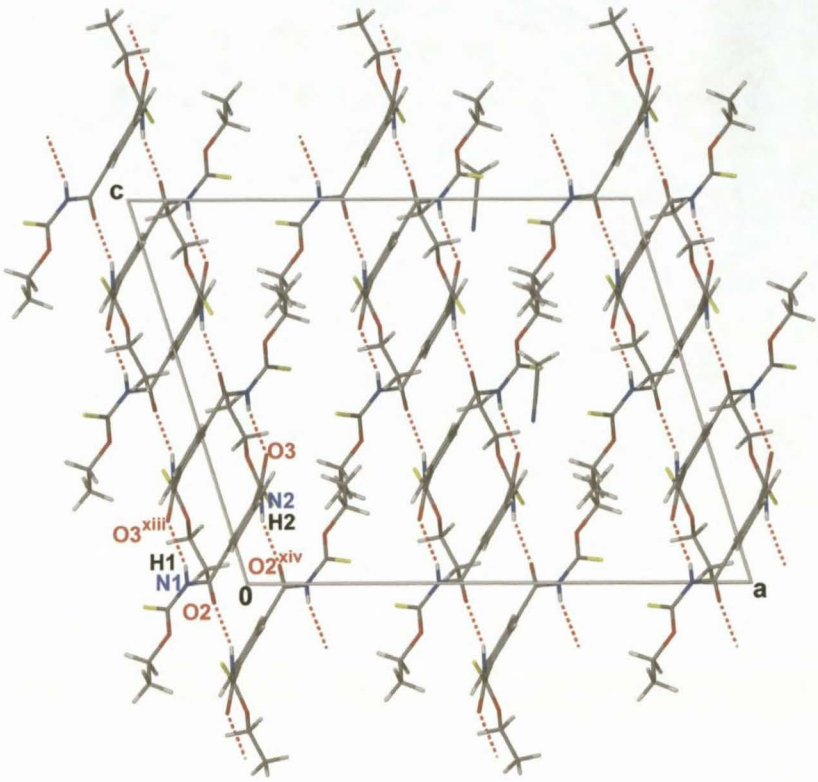

Figure 11 Extended packing diagram of $H_2(L^{19}$-*S,O*) as viewed along [010] showing the one dimensional molecular chains extending parallel to [001] resulting from the N1-H1…O3^{xiii} and N2-H2…O2^{xiv} intermolecular hydrogen bonds as indicated. The co-crystallized molecules of acetonitrile have been omitted for clarity. Symmetry codes (xiii) –x, y, ½-z; (xiv) –x, -y, -z.

2.5.4 *O,O'*-(*p*-xylene-α,α'diyl) *N,N'*-dibenzoyl bis(thiocarbamate), $H_2(L^{21}$-*S,O*).

$H_2(L^{21}$-*S,O*) was prepared in an attempt to effectively reverse the order of the thiocarbonyl and carbonyl moieties relative to the spacer molecule in order to observe the effect this moiety reversal has in the solid state in comparison to the traditional bipodal 3,3,3',3'-tetralkyl-1,1'terephthaloylbis(thioureas) reported in the literature and the *O,O'*-dialkyl *N,N'*-(phenylenedicarbonyl)bis(thiocarbamates) reported in this chapter. No crystal structures similar to that of **$H_2(L^{21}$-*S,O*)** are listed on the Cambridge Structural Database[21].

Compound **$H_2(L^{21}$-*S,O*)** crystallizes triclinic space group $P\bar{1}$ with two formula units per unit cell. The molecular structure of **$H_2(L^{21}$-*S,O*)** is illustrated in Figure 12 showing the numbering scheme used. A single inclusion molecule of dichloromethane co-crystallised with **$H_2(L^{21}$-*S,O*)** as indicated in Figure 12.

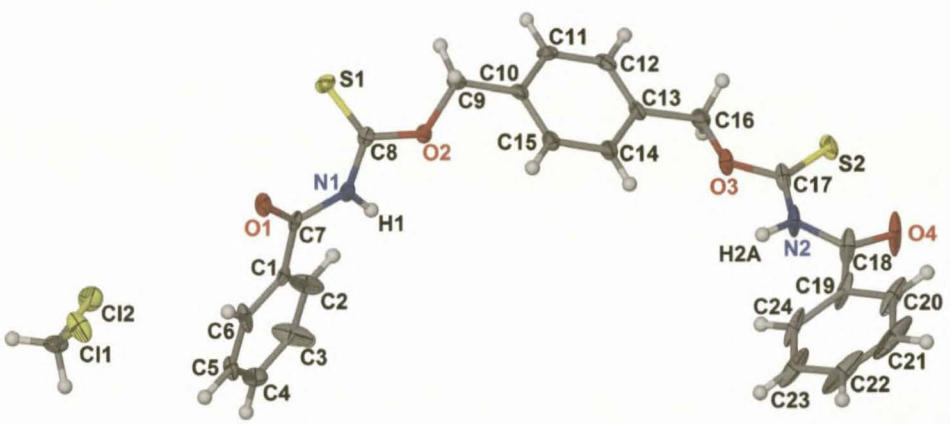

Figure 12 Molecular structure of **$H_2(L^{21}$-*S,O*)** showing the numbering scheme used. Displacement ellipsoids have been drawn at the 50% probability level.

The C19-C20-C21-C22-C23-C24 phenyl ring of **$H_2(L^{21}$-*S,O*)** shown in Figure 12, contains a high degree of dynamic disorder. This is illustrated by the fact that the Displacement ellipsoids of the C19-C20-C21-C22-C23-C24 phenyl ring are elongated to a large degree all in the same direction. It is suspected that there are at least three distinct positions for the carbon atoms of this ring. It is likely that the final R-factor of 8.1% could be reduced to around 6.0% if these positions were modelled. However, it was advised that this labour intensive task was not warranted for thesis publication purposes*. Bond lengths and torsion angles of interest observed in **$H_2(L^{21}$-*S,O*)** are listed in Table 11.

* Advice by Prof. L. Barbour, Department of Chemistry and Polymer Science, Stellenbosch University.

S1-C8	1.640(4)	S2-C17	1.642(4)
O1-C7	1.216(5)	O4-C18	1.212(5)
C7-N1	1.389(5)	C18-N2	1.388(6)
C8-N1	1.373(5)	C17-N2	1.368(6)
C8-O2	1.333(4)	C17-O3	1.342(5)
S1-C8-C7-O1	-26.1(3)	S2-C17-C18-O4	5.0(4)

Table 11 Bond lengths (Å) and torsion angles of interest observed in $H_2(L^{21}$–*S,O*).

The molecular structure of $H_2(L^{21}$–*S,O*) has a *syn*-, *syn*-(*S,O*) orientation similar to that observed in $H_2(L^{16}$–*S,O*). This planar arrangement of the two carbonyl and thiocarbonyl moieties is illustrated by the improper torsion angles S1-C8-C7-O1 and S2-C17-C18-O4 of -26.1(3)° and 5.0(4)° respectively. The relative planarity of the two carbonyl and thiocarbonyl moieties is possibly assisted by the two 1-4 intramolecular hydrogen contacts observed between N1-H1...O2 and N2-H2A...O3 [N1-H1...O2 2.189Å; N2-H2A...O3 2.218Å].

Several classical intermolecular hydrogen bonds were observed in the unit cell of $H_2(L^{21}$-*S,O*) as listed in Table 12.

D-H...A	Type	D-H (Å)	H...A (Å)	D...A (Å)	D-H...A (°)
N1-H1...O4^{iv}	inter	0.88	2.18	2.898(4)	138.8
N1-H1...S2^{iv}	inter	0.88	2.88	3.614(3)	142.09
N2-H2A...O1^{v}	inter	0.88	2.09	2.950(4)	166.0

Table 12 Intermolecular hydrogen bonding observed in the unit cell of $H_2(L^{21}$-*S,O*) as identified by XSeed[23, 24] and Platon[25] with s.u.s in parenthesis. [Symmetry codes (iv) 1-x, 2-y,-z; (v) 1-x, 1-y, -z].

Several non-classical intra- and intermolecular hydrogen interactions, as listed in Table 13, were observed in the crystal lattice of $H_2(L^{21}$-*S,O*).

D-H...A	Type	D-H (Å)	H...A (Å)	D...A (Å)	D-H...A (°)
C2-H2...O4^{iv}	inter	0.95	2.28	3.205(6)	163.7
C14-H14...O1^{v}	inter	0.95	2.53	3.419(5)	156.3
C24-H24...O1^{v}	inter	0.95	2.49	3.040(5)	117.1
C14-H14...O3	intra	0.95	2.35	2.698(5)	100.7
C15-H15...O2	intra	0.95	2.77	2.909(5)	88.9

Table 13 Non-classical inter- and intramolecular hydrogen bond and contact geometries observed in $H_2(L^{21}$-*S,O*) as identified by XSeed[23, 24] and Platon[25] with s.u.s in parenthesis. [Symmetry codes (iv) 1-x, 2-y,-z; (v) 1-x, 1-y, -z].

The various classical and non-classical intermolecular hydrogen bonds and interactions listed in Table 12 and Table 13 cause molecules of $H_2(L^{21}$-*S,O*) to be linked into molecular strings propagating parallel to the *b*-axis.

The C8-N1 and C7-N1 bond lengths [C8-N1 1.373(5)Å, C7-N11.389(5)Å], as well as the C17-N2 and C18-N2 bond lengths [C17-N2 1.368(6)Å, C18-N2 1.388(6)Å], of **$H_2(L^{21}$-*S,O*)** indicate that these bonds have a partial double bond character.

Unlike in the molecular structure of **$H_2(L^{16}$-*S,O*)**, the overall molecular structure of **$H_2(L^{21}$-*S,O*)** deviates extensively from planarity due to the 'twisting' out of plane of the two terminal benzoyl rings relative to the phenylene spacer ring. The C1/C2/C3/C4/C5/C6 least-squares plane intersects the C11/C12/C13/C14/C15/C16 least-squares plane at 72.9(1)° while the C19/C20/C21/C22/C23/C24 least-squares plane intersects the C11/C12/C13/C14/C15/C16 least-squares plane at 42.7(2)°. This 'twisting' of the phenyl rings, and resultant distortion from overall planarity within **$H_2(L^{21}$-*S,O*)**, allows the formation of two C-H…π interactions between adjacent molecules [C4-H4…$Cg1^{iii}$ = 2.78Å, where *Cg*1 is the centroid of the C1-C6 benzoyl rings; symmetry codes: (iii) –x, 2-y, -z]. This C-H…π interaction links two adjacent molecules of **$H_2(L^{21}$-*S,O*)** into a 'cubic-like' dimer arrangement of molecules in the unit cell when viewed along [010] as illustrated in Figure 13.

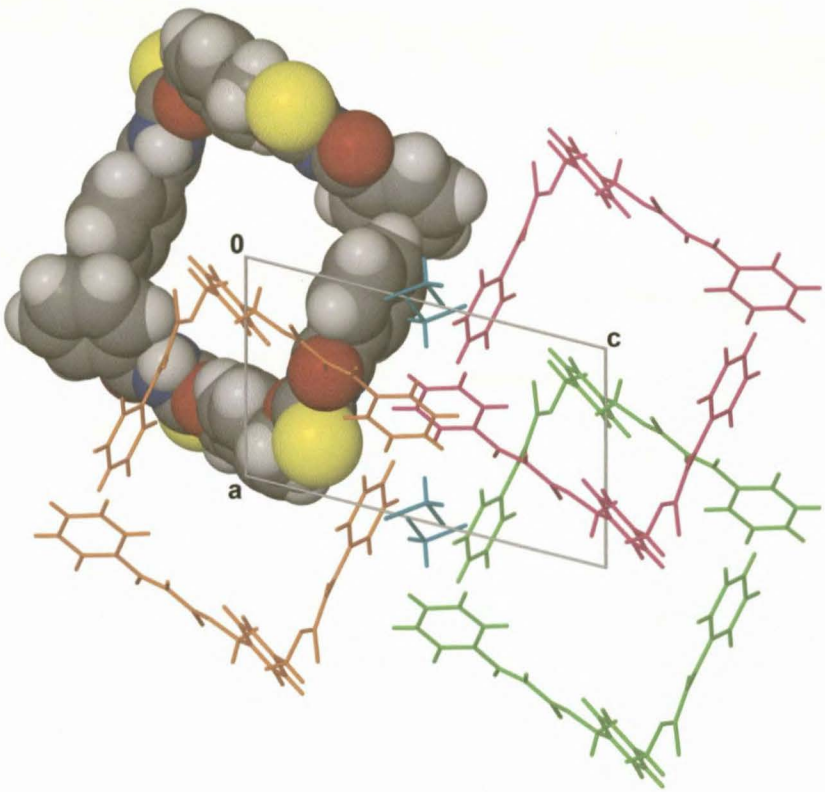

Figure 13 Extended packing diagram of **$H_2(L^{21}$-*S,O*)** as viewed along [010] indicating the 'cubic-like' arrangement of molecules resulting from the C-H…π interactions [C4-H4…$Cg1^{iii}$ = 2.78Å, symmetry codes: (iii) –x, 2-y, -z].

2.5.5 Trithiocyanuric acid, $TMTH_3$.

On several occasions the experimental procedure used for the preparation of the series of *O,O'*-dialkyl *N,N'*-(phenylene-dicarbonyl)bis(thiocarbamates) described in this chapter involved the use of column chromatography. One of the by-products produced during the synthesis of *O,O'*-diethyl *N,N'*-(*m*-phenylene-dicarbonyl)bis(thiocarbamate), $\mathbf{H_2(L^{19}\text{-}S,O)}$, was isolated by column chromatography and identified as 1,3,5-triazine-2,4,6-(1H,3H,5H)trithione.

1,3,5-Triazine-2,4,6-(1H,3H,5H)trithione, more commonly known as trithiocyanuric acid or 2,4,6-trimercaptone ($\mathbf{TMTH_3}$ adopted for this discussion), has the attributes of high symmetry and planarity, coupled with three hydrogen bond donors and three acceptors. This allows for varying degrees of deprotonation of $\mathbf{TMTH_3}$ and the resulting anion can function as a thiolate or amide ligand for metals. As a result, $\mathbf{TMTH_3}$ has been used in several research programs for the intended design of distinctive crystals via the incorporation of the metal complexes of $\mathbf{TMTH_3}$ into designed crystal assemblies. Consequently, the molecular structure of trithiocyanuric acid and several of its derivates have previously been determined and are listed on the Cambridge Structural Database (CSD)[21, 32]. In many of these listings on the CSD, trithiocyanuric acid is typically co-crystallized with 4,4'-bipyridine and toluene, 4,4'-bipyridine and xylene, 4,4'-bipyridine and anthracene or 4,4'-bipyridine and benzene[33]. In other listings of the CSD trithiocyanuric acid has been co-crystallized with acetone[34], 4,4'-bipyridine[34], pyridine[35] and hexamethylphosphoramide[36].

The molecular structure of $\mathbf{TMTH_3}$, isolated as an unexpected by-product during the synthesis of $\mathbf{H_2(L^{19}\text{-}S,O)}$, is illustrated in Figure 14. $\mathbf{TMTH_3}$ co-crystallized with an inclusion molecule of methanol.

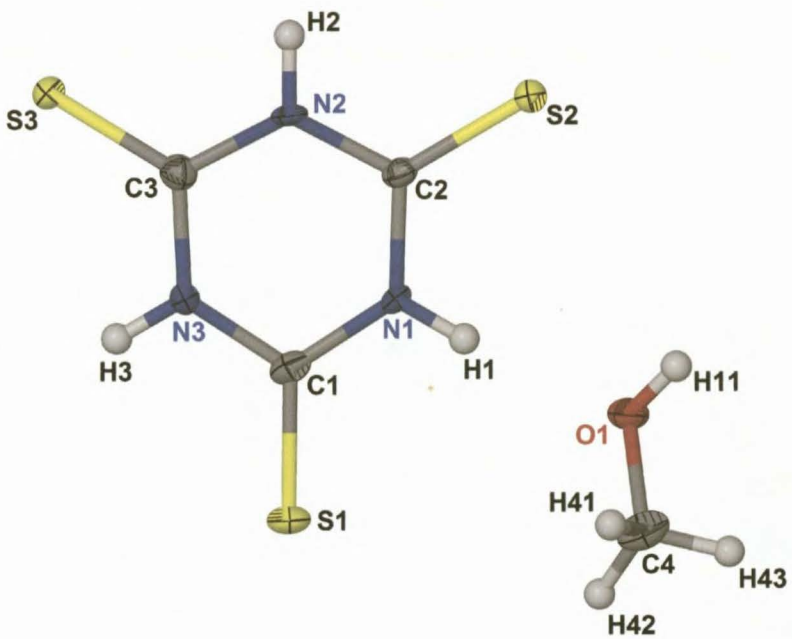

Figure 14 Molecular structure of $\mathbf{TMTH_3.CH_3OH}$ showing the numbering scheme used. Displacement ellipsoids are drawn at the 50% probability level.

Several intermolecular hydrogen bonds were observed in the molecular structure of **TMTH$_3$** as listed in Table 14. The asymmetric unit of **TMTH$_3$** is linked to two adjacent molecules of trithiocyanuric acid through N2-H2…S2^{xvi} and N3-H3…S3^{xvii} intermolecular hydrogen bonds [N2-H2…S2^{xvi} 2.45Å; N3-H3…S3^{xvii} 2.41Å; symmetry code (xvi) 3/2-x, 3/2-y, 1-z, (xvii) 1-x, -y, 1-z]. This results in the formation of stacked tapes of intermolecular hydrogen bonded **TMTH$_3$** molecules as illustrated in Figure 15. The one dimensional adjacent tapes of **TMTH$_3$** are angled differently across the *ac* plane such that they are inclined at 80.6(2)° relative to each other with methanol molecules located between adjacent one dimensional tapes.

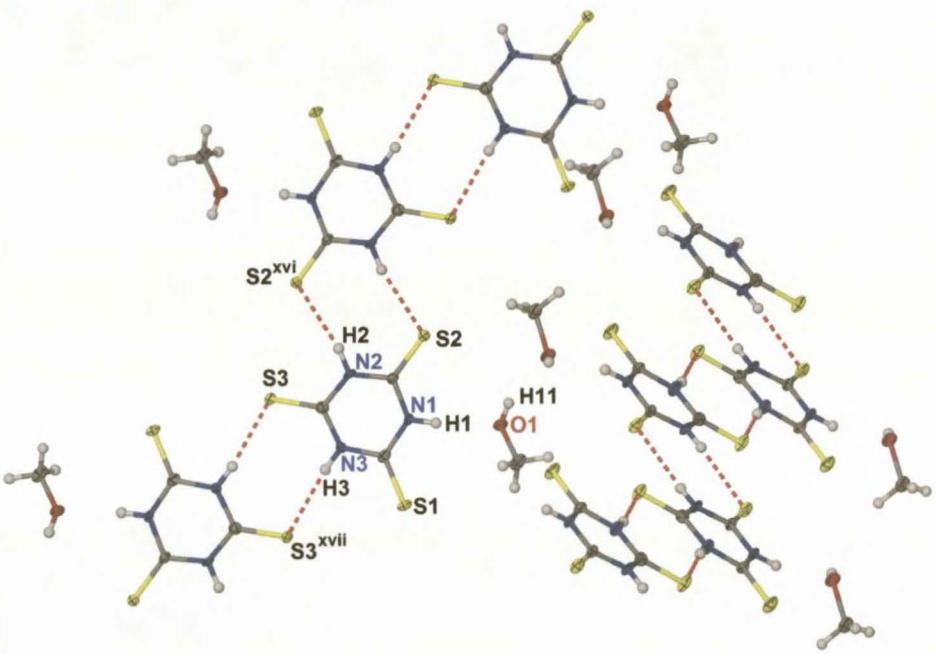

Figure 15 Two of the one dimensional molecular tapes of **TMTH$_3$** which result from the intermolecular N-H…S hydrogen bonds. The adjacent tapes are inclined at 80.6(2)° relative to each other and separated by methanol molecules.

The asymmetric unit of **TMTH$_3$** is hydrogen bonded to an adjacent molecule of co-crystallized methanol through the N1-H1…O1 intermolecular hydrogen bond [N1-H1…O1 1.98Å] illustrated in Figure 16. In turn, the methanol molecule of the asymmetric unit is further hydrogen bonded to a second adjacent molecule of methanol through the O1-H11…O1^{xviii} intermolecular hydrogen bond [O1-H11…O1^{xviii} 2.09Å; symmetry code (xviii) 3/2-x, 1/2+y, 3/2-z]. This O1-H11…O1^{xviii} intermolecular hydrogen bond creates an unusual continuous one dimensional molecular chain of methanol parallel to [010]. These molecular chains of methanol effectively form the 'backbone' within the unit cell by cross linking adjacent tapes of **TMTH$_3$** into a three dimensional intermolecular hydrogen bonded net as illustrated in Figure 17.

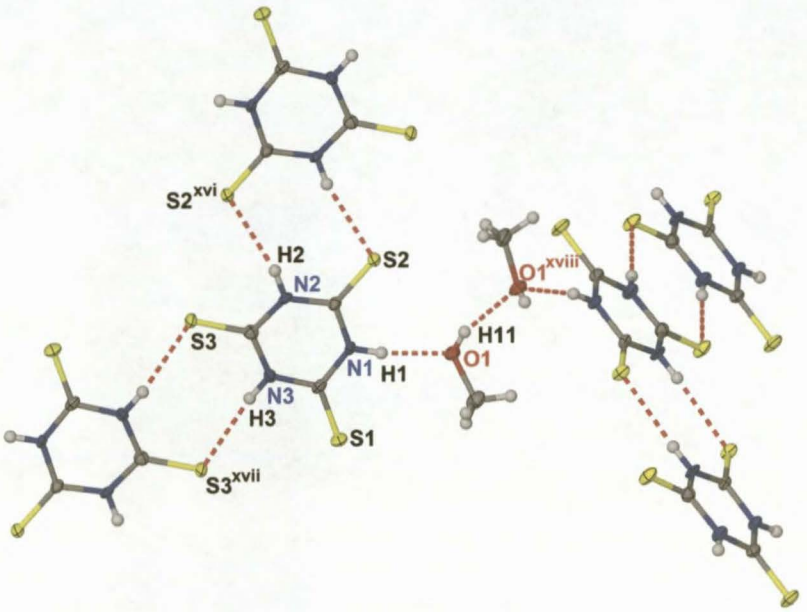

Figure 16 Adjacent one dimensional molecular tapes of **TMTH$_3$** cross linked by methanol molecules via the N1-H1...O1 and O1-H11...O1^{xviii} intermolecular hydrogen bonds [symmetry code (xvi) 3/2-x, 3/2-y, 1-z; (xvii) 1-x, -y, 1-z; (xviii) 3/2-x, 1/2+y, 3/2-z].

D-H...A	Type	D-H (Å)	H...A (Å)	D...A (Å)	D-H...A (°)
N2-H2...S2^{xvi}	inter	0.86	2.45	3.287(6)	164.5
N3-H3...S3^{xvii}	inter	0.86	2.41	3.259(6)	171.8
N1-H1...O1	inter	0.86	1.98	2.826(7)	168.4
O1-H11...O1^{xviii}	inter	0.76(5)	2.09(5)	2.818(6)	162(5)

Table 14 Intermolecular hydrogen bond geometry observed in **TMTH$_3$** as identified by XSeed[23, 24] and Platon[25] with s.u.s in parenthesis. Symmetry codes (xvi) 3/2-x, 3/2-y, 1-z; (xvii) 1-x, -y, 1-z; (xviii) 3/2-x, 1/2+y, 3/2-z.

At the time that the molecular structure of **TMTH$_3$** containing the 'backbone' of intermolecular hydrogen bonded methanol was determined, a survey of the CSD revealed that this phenomenon had never before been reported. However, subsequently to this work having been carried out, a similar molecular structure of trithiocyanuric acid co-crystallized with methanol, has been reported by Dean *et al.*[37]. The methanol solvated structure of trithiocyanuric acid reported by Dean *et al.* comprises of a hydrogen bonded net of one dimensional tapes of trithiocyanuric acid cross linked by chains of methanol comparable to that which was observed here for **TMTH$_3$**.

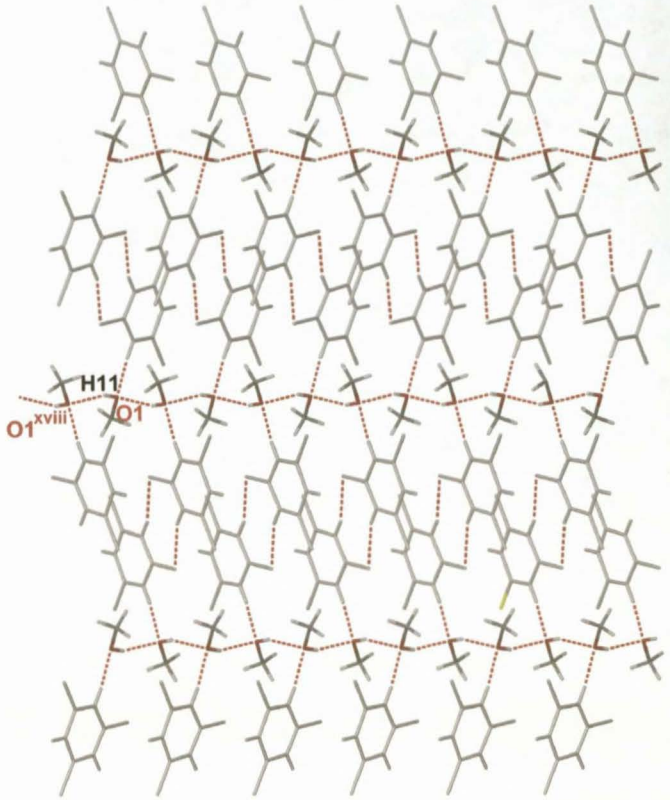

Figure 17 The unique one dimensional molecular chains of methanol resulting from the O1-H11...O1^{xviii} interaction extending parallel to [010]. Symmetry code (xviii) 3/2-x, 1/2+y, 3/2-z.

2.6 Ground-state molecular calculations.

O,O'-dimethyl *N,N'*-(*m*-phenylene-dicarbonyl)bis(thiocarbamate), **$H_2(L^{18}$-*S,O*)**, crystallized in two forms as a result of interesting *anti- anti* and *syn- anti* conformational isomerism of the thiocarbonyl and carbonyl moieties relative to one another. This represents the first reported X-ray structure determination of polymorphism of this class of bipodal compound[17]. The white form, *anti- anti*, **(I)**, crystallizes with the benzene ring lying about a twofold rotation axis, resulting in both the thiocarbonyl and carbonyl moieties being *anti* relative to each other. The yellow modification crystallizes as *syn-anti*, **(II)**, with one thiocarbonyl moiety *syn* and the other *anti* relative to the respective carbonyl groups.

Geometry optimizations were carried out to establish the minimum ground-state gas phase structures of polymorphs **(I)** and **(II)** of **$H_2(L^{18}$-*S,O*)**. For polymorph **(I)**, calculations were performed using C_1 as well as C_2 symmetry restrictions. Calculations for polymorph **(II)** were carried out using only C_1 symmetry. These ground-state calculations were carried out in order to allow for a comparison of the internal coordinates as determined from the density functional theory (DFT) calculations with the internal coordinates obtained from the single crystal structure determination of both **(I)** and **(II)**.

Frontal and side-on views of the C_1 and C_2 DFT geometrically optimized structures of **(I)**, as well as the single crystal structure of **(I)**, are illustrated in Figure 18 . Similarly, the frontal and side-on views of the C_1 DFT geometrically optimized structure of **(II)**, as well as the single crystal structure of **(II)**, are illustrated in Figure 19. Generally, the internal coordinates of the C_1 and C_2 calculated structures of **(I)** as well as the C_1 calculated structure of **(II)** compare well with those obtained from the single crystal structure determination. However, a few subtle differences are observed upon closer inspection. It is however possible that these subtle differences, as discussed below, are due to packing effects within the crystal lattice.

The thiocarbonyl moiety bond length of **(I)** [S1-C2 1.637(2)Å] is significantly shorter than the C_1 and C_2 DFT calculated bond lengths [1.662Å and 1.633Å respectively]. The single crystal structure carbonyl bond length of 1.218(2)Å compares favourably with the C_1 and C_2 DFT calculated carbonyl bond lengths of 1.221Å each. Both the O1-C2 and N1-C3 bond lengths of the crystal structure [O1-C2 1.317(2); N1-C3 1.30(3)Å] are also significantly shorter than the bond lengths of both DFT optimised structures [C_1 structure O1-C2 1.331Å, N1-C3 1.403Å; C_2 structure O1-C2 1.334Å, N1-C31.402Å]. Similar differences were observed in the bond lengths of the C_1 DFT geometrically optimized structure of **(II)** versus the bond lengths as determined crystallographically. The crystallographically determined bond length of the thiocarbonyl moiety S2-C2 of **(II)** [S2-C2 1.639(4)Å] is shorter than the DFT calculated bond length [S2-C2 1.663Å] while the N2-C10 bond length of the crystal structure [N2-C10 1.372Å] is also shorter than the comparable DFT calculated bond length [N2-C10 1.403Å].

A greater degree of *trans*-(*S,O*) orientation is observed in the C_1 and C_2 calculated structures of **(I)** [C_1 S1-C2-C3-O2 = -173.5°; C_2 S1-C2-C3-O2 = -171.3°] in relation to the single crystal structure of **(I)**

[S1-C2-C3-O2 = 161.5(2)°]. Similarly, a greater *anti*-(*S,O*) planarity is observed in the C_1 calculated structure of **(II)** [S2-C11-C10-O3 = -171.3°] in comparison to the crystal structure of **(II)** [S2-C11-C10-O3 = 150.9(3)°].

The relative energies of the gas phase calculated ground-states of **(I)** and **(II)** have been determined and listed in Table 17. The relative energies calculated for the C_1 and C_2 gas phase ground-state structures of polymorph **(I)** are comparable and differ by only 0.35862 kcal.mol^{-1}. The relative energy of the C_1 calculated structure of **(I)** is 0.91086 kcal.mol^{-1} lower in energy than the C_1 calculated structure of **(II)**. However the C_2 calculated structure of **(I)** is 1.26948 kcal.mol^{-1} lower in energy than the C_1 calculated ground state of **(II)**. The calculated relative energies of the single crystal structures of **(I)** and **(II)**, listed in Table 17, are also comparable indicating that there is probably no thermodynamic preference of one polymorph over the other.

Crystallographically determined structure (a)

C_1 restriction (b)

C_2 restriction (c)

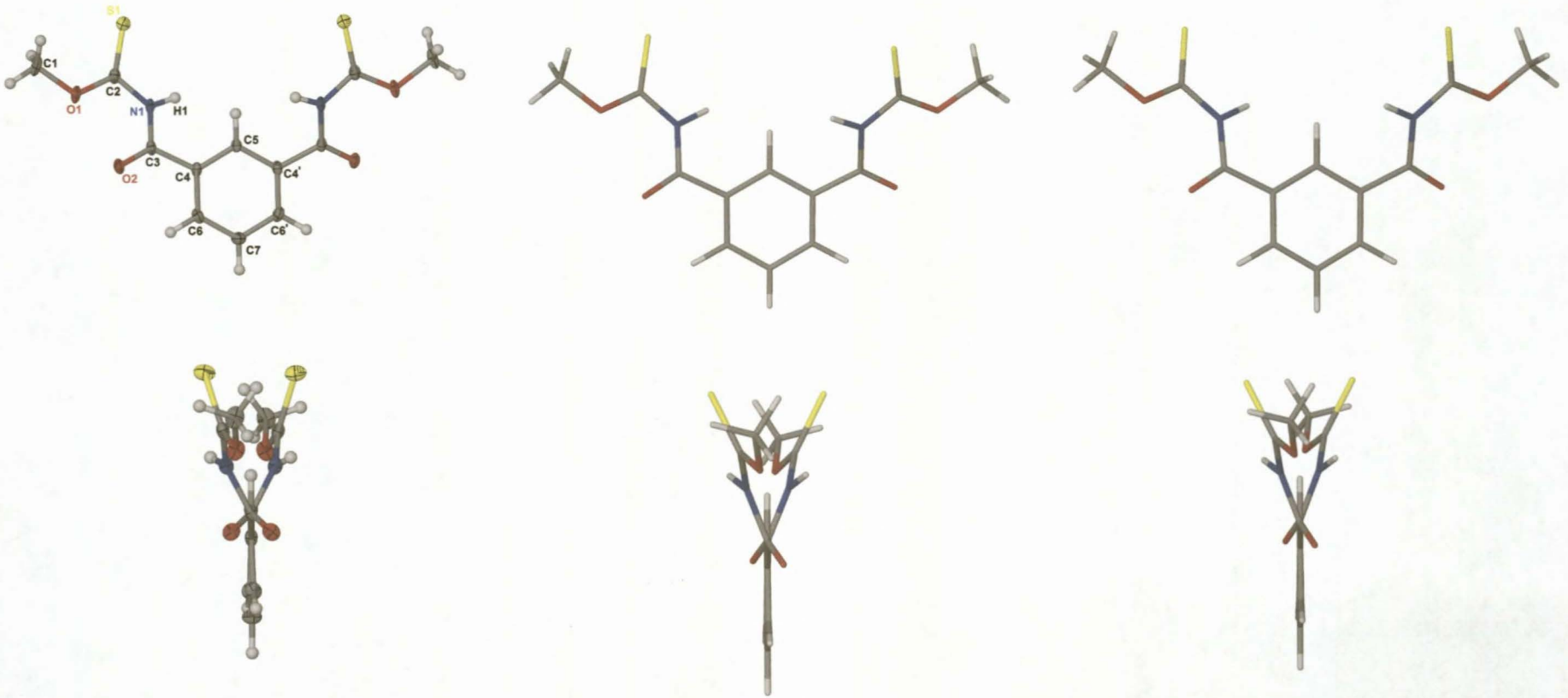

Figure 18 Frontal and side-on views of the molecular structure of polymorph **(I)** of $H_2(L^{18}$-***S,O***$)$ as determined (a) crystallographically (b) DFT calculated with C_1 symmetry restriction and (c) DFT calculated using C_2 symmetry restriction.

	Single Crystal structure (a)	DFT with C1 restriction (b)	DFT with C2 restriction (c)		Single Crystal structure (a)	DFT with C1 restriction (b)	DFT with C2 restriction (c)
S1 - C2	1.637(2)Å	*1.662Å*	*1.663Å*	N1 - C2	1.391(3)Å	*1.389Å*	*1.392Å*
S1' - C2'	n/a	*1.633Å*	*n/a*	N1' - C2'	n/a	*1.393Å*	*n/a*
O2 - C3	1.218(2)Å	*1.221Å*	*1.221Å*	N1 - C3	1.380(3)Å	*1.403Å*	*1.402Å*
O2' - C3'	n/a	*1.221Å*	*n/a*	N1' - C3'	n/a	*1.403Å*	*n/a*
O1 - C2	1.317(2)Å	*1.331Å*	*1.334Å*	C3 - C4	1.499(3)Å	*1.505Å*	*1.506 Å*
O1' - C2'	n/a	*1.333Å*	*n/a*	C3 - C4	n/a	*1.505Å*	*n/a*
C5 - C4 - C3	122.97(19)°	*123.87°*	*124.18*	C6 - C4 - C3	117.06(17)°	*116.81°*	*116.49°*
C5' - C4' - C3'	n/a	*124.28°*	*n/a*	C6' - C4' - C3'	n/a	*116.39°*	*n/a*
C6-H6...O2	2.542Å, 96.80°	*2.499Å, 96.54°*	*2.470Å, 96.87°*	C6'-H6'...O2'	n/a	*2.468Å, 96.8°*	*n/a*
C5-H5...H1-N1	2.155Å, 102.86°	*2.013Å, 104.96°*	*2.005Å, 104.88°*	C5'-H5'...H1'-N1'	n/a	*2.013Å, 104.75°*	*n/a*
S1-C2-N1-C3	164.79(16)°	*-176.7°*	*-175.1°*	C2-N1-C3-O2	5.8(3)°	*1.6°*	*1.6°*
S1'-C2'-N1'-C3'	n/a	*-176.8°*	*n/a*	C2'-N1'-C3'-O2'	n/a	*1.5°*	*n/a*
S1-C2-C3-O2	161.5(2)	*-173.5°*	*-171.3°*	S1'-C2'-C3'-O2'	n/a	*-173.9°*	*n/a*
O2-C3-C4-C6	28.8°	*21.8°*	*20.8°*	O2'-C3'-C4'-C6'	n/a	*21.6°*	*n/a*

Table 15 Selected bond lengths (Å), bond angles (°) and torsion angles (°) of the molecular structure of polymorph **(I)** of $H_2(L^{18}$-*S,O*) as determined (a) crystallographically (b) DFT calculated using C_1 symmetry restriction and (c) DFT calculated using C_2 symmetry restriction.

Crystallographically determined structure **(II)**

(a)

DFT optimised structure of **(II)**

(b)

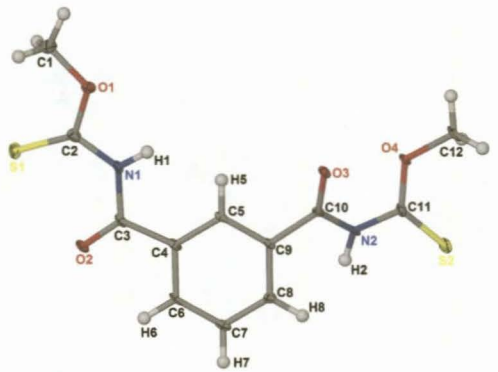

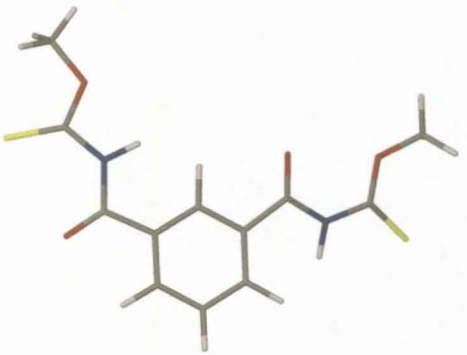

Figure 19 Frontal and side-on views of molecular structure of polymorph **(II)** of $H_2(L^{18}$-*S,O*) as determined (a) crystallographically (b) DFT calculated using C_1 symmetry restriction.

	Single crystal structure	*DFT with C_1 restriction*		Single crystal structure	*DFT with C_1 restriction*
S1 – C2	1.634(4)Å	*1.643Å*	N1 - C2	1.377(5)Å	*1.388Å*
S2 – C2	1.639(4)Å	*1.663Å*	N2 – C11	1.381(4)Å	*1.392Å*
O2 – C3	1.212(4)Å	*1.219Å*	N1 - C3	1.401(4)Å	*1.399Å*
O3 – C10	1.226(4)Å	*1.222Å*	N2 – C10	1.372(4)Å	*1.403Å*
O1 – C2	1.343(4)Å	*1.366Å*	C3 - C4	1.495(5)Å	*1.507Å*
O4 – C11	1.327(4)Å	*1.333Å*	C10 – C9	1.496(4)Å	*1.501Å*
C5 – C4 - C3	125.4(3)°	*124.42°*	C5 – C9 – C10	117.9(3)°	*115.89°*
C6 – C4 - C3	115.6(3)°	*116.43°*	C8 – C9 – C10	122.2(3)°	*124.75°*
C5 – H5...H1-N1	2.084Å, 111.77°	*1.921Å, 106.39°*	C8 – H8...N2 – N2	2.193Å, 99.73°	*2.037Å, 101.82°*
C5 – H5...O3 – C10	2.643Å, 94.88°	*2.418Å, 99.09°*	C6 – H6...O2 – C3	2.432Å, 98.85°	*2.428Å, 97.77°*
S1 – C2 - N1 - C3	0.3(6)°	*-5.8°*	S2 – C11 – N2 – C10	162.2(3)°	*-172.3°*
C2 – N1 - C3 - O2	-8.4(6)°	*-7.3°*	C11 – N2 – C10 – O3	-2.7(6)°	*-3.4°*
S1 – C2 – C3 – O2	-6.8(3)°	*-10.9°*	S2 – C11 – C10 – O3	150.9(3)°	*-171.3°*
O2 – C3 – C4 – C6	-11.0(5)°	*-10.6*	O3 – C10 – C9 – C8	-142.6(3)°	*-158.0°*
O2 – C3- C4 - C6	-11.0°	*-10.6°*	O3 - C10 - C9 - C5	38.°1	*22.1°*

Table 16 Selected bond lengths (Å), bond angles (°) and torsion angles (°) of the molecular structure of polymorph **(II)** of **$H_2(L^{18}$-*S,O*)** as determined (a) crystallographically (b) DFT calculated using C_1 symmetry restriction.

	Polymorph (I)				Polymorph (II)	
	C_1 restricted		C_2 restricted		C_1 restricted	
	a.u.	kcal.mol^{-1}	a.u.	kcal.mol^{-1}	a.u.	kcal.mol^{-1}
single crystal	-7.26638013	-4559.7245113	-7.26636578	-4559.7155066	-7.26230666	-4557.1683691
DFT struc.	-7.43391902	-4664.8568014	-7.43449052	-4665.2154232	-7.43246747	-4663.9459396

Table 17 Calculated relative energies of single crystal of polymorphs **(I)** and **(II)** as well the relative energies of the DFT optimised structures using C_1 and C_2 symmetry restrictions for **(I)** and C_1 symmetry restrictions for **(II)**.

2.7 Complexes of Bipodal *O,O'*-dialkyl-*N,N'*-(phenylene-dicarbonyl)bis(thiocarbamates).

As discussed in the introduction to this chapter, bipodal 3,3,3',3'-tetralkyl-1,1'-phenylenebis(thioureas) may be used as "pre-programmed" chelating ligands to form metallomacrocyclic square planar d^8 metal complexes via self-assembly. The relative points of substitution (*para* vs *meta*) of the phenylene space moiety in the ligand is critical in determining the geometry and M:L ratio of the resultant complex. Ligands derived from the *para*-substituted terephthalic acid give exclusively 3:3 (M:L) metallamacrocycles, while those derived from meta-substituted isophthalic acid give rise to only 2:2 (M:L) complexes [see Scheme 2][2, 3, 6].

In this context, bipodal *O*-alkyl-*N*-benzoylthiocarbamic acid esters are of interest as potential structural analogues to bipodal 3,3',3'-tetralkyl-1,1'-phenylenebis(thioureas). In this context, the series of bipodal *O*-alkyl-*N*-benzoylthiocarbamic acid esters illustrated in Table 1 were envisaged, synthesized, fully characterized and further complexed with Cu(II), Ni(II), Pd(II) and Pt(II). It was speculated that 2:2 or 3:3 (M:L) complexes, analogous to those derived from the bipodal 3,3,3',3'-tetralkyl-1,1'-phenylenebis(thioureas), would result. Unfortunately the physical characteristics of the resultant complexes derived from the bipodal *O*-alkyl-*N*-benzoylthiocarbamic esters did not allow for adequate characterization. These complexes had an exceptionally poor solubility in most organic solvents which suggested a polymeric-type product had been produced.

Small deep blue rectangular crystals of the reaction product of *O,O'*-dibutyl *N,N'*-(p-phenylene-dicarbonyl)bis(thiocarbamate) and copper(II) perchlorate were obtained from a solvent combination of benzene, ethanol and pyridine. These crystals diffracted poorly with a very low 2θ angle during single crystal X-ray diffraction analysis. Nevertheless, a molecular structure was determined which indicated that the ligand, *O,O'*-dibutyl *N,N'*-(p-phenylene-dicarbonyl)bis(thiocarbamate), had in fact hydrolysed under the reaction conditions used resulting in the polymeric product illustrated in Figure 20. The reaction product is made up of copper atoms linked into a one dimensional molecular chain by spacer molecules of deprotonated 1,4-benzenedicarboxylic and with a pyridine molecule coordinated in each of the axial positions of the copper. A guest molecule of benzene was observed along with a single

water molecule coordinated in the equatorial position to each of the copper atoms. Carbon atoms C11A and C12A [sof refined to 69(4)%] of the benzene guest are disordered across positions C11B and C12B [sof refined to 31(4)%] respectively.

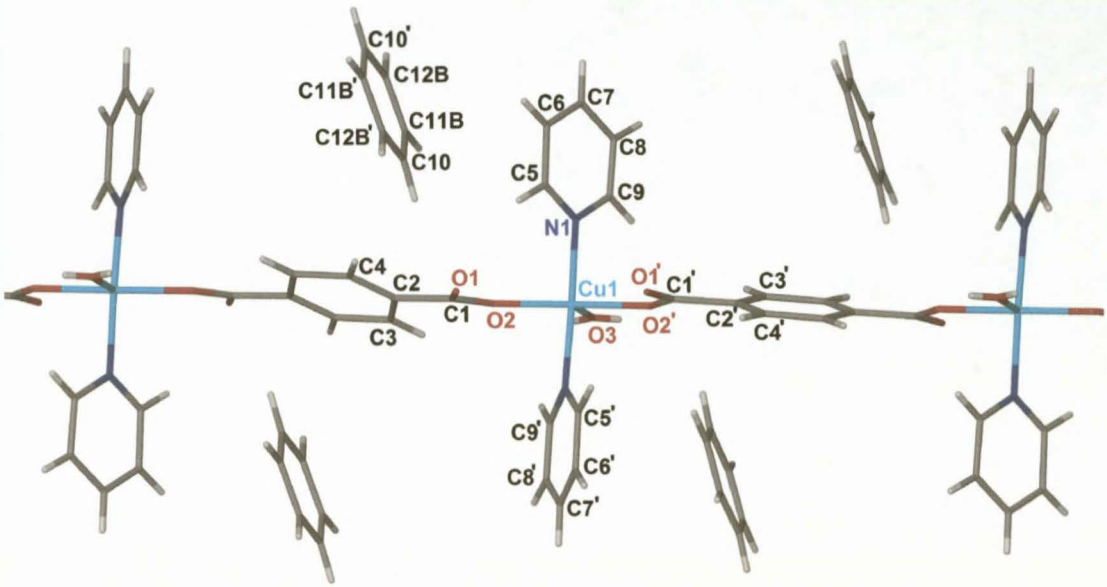

Figure 20 Molecular structure of the polymeric product resulting from the reaction of *O,O'*-dibutyl *N,N'*-(p-phenylene-dicarbonyl)bis(thiocarbamate) and copper(II) perchlorate. Accented atoms are generated by the symmetry operator 1-x, y, 3/2-z.

The poor quality of the X-ray diffraction data due to the poor diffraction properties of the product crystals doesn't allow the crystal structure to be refined with a R-factor lower than 10.2%. It is therefore not possible to describe the bond distances and bond angles of the molecular structure in any accurate detail. However, the data is of sufficient quality to verify the coordination motif and polymeric nature of the product obtained as illustrated in Figure 20. The two equatorially coordinated pyridine molecules are orientated approximately at 90° to the coordinating oxygen atoms [N1-Cu1-O2 = 91.3(3)°, N1-Cu1-O3 = 94.1(2)°] and are twisted at approximately 60.8(4)° relative to each other. The one dimensional strings extend parallel to and diagonally across the *a-c* plane of the unit cell as illustrated in Figure 21.

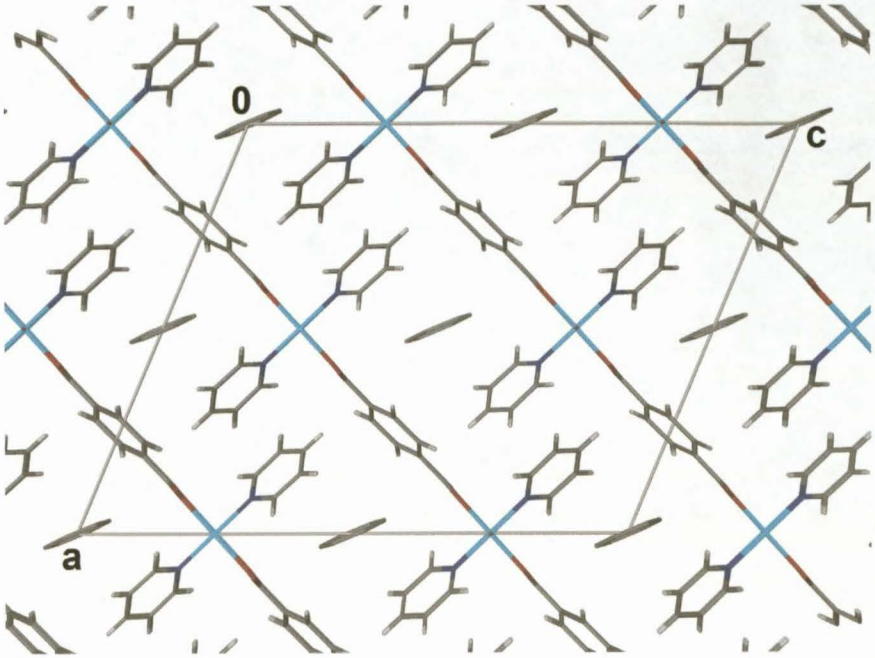

Figure 21 Unit cell of polymeric reaction product of *O,O'*-dibutyl *N,N'*-(p-phenylene-dicarbonyl)bis(thiocarbamate) and copper(II) perchlorate as viewed along [010].

3. Experimental

3.1 Methods and instrumentation

All reagents and solvents were commercially available and unless otherwise stated were used without further purification. The reagents *viz.* terephthaloyl dichloride, isophthaloyl dichloride and KSCN were used as supplied without further purification. Acetone was rendered anhydrous using calcium carbonate while ethanol was rendered anhydrous using magnesium and iodine. Both solvents were distilled under an inert atmosphere just prior to use. ^{1}H and ^{13}C NMR spectra (25°C) were recorded in deuterated chloroform using either a Varian INOVA 600 MHz spectrometer operating at 600 MHz or 151 MHz respectively, or a Varian VXR 300 MHZ spectrometer operating at 300 MHz or 76 MHz respectively. ^{1}H chemical shifts are quoted relative to the residual $CHCl_3$ solvent resonance at 7.26ppm. The ^{13}C chemical shifts are quoted relative to the $CHCl_3$ triplet at 77.7ppm. UV-visible spectrophotometric experiments were carried out on an Agilent 8453E UV-visible spectrophotometer (Agilent Technologies). Elemental analyses were performed using a Carlo Erba EA 1108 elemental analyser in the microanalytical laboratory of the University of Cape Town, South Africa.

3.2 General preparation of ligands

All reactions were carried out under a dry argon atmosphere using standard Schlenk and vacuum line techniques. Ligands, $\mathbf{H_2L}$[15-21], were prepared using a modification of the procedure initially reported by Douglas and Dains for the preparation of *N*-aroylthioureas[38, 39]. A similar method was reported in the literature by Schröder *et al.* in the preparation of several *N*-Acyl-thiocarbamic-*O*-alkylesters[26].

The appropriate terephthaloyl dichloride or isophthaloyl dichloride (0.03mol) dissolved in anhydrous acetone (60ml) was added dropwise with magnetic stirring to a solution of potassium thiocynate (0.06mol) dissolved in anhydrous acetone (60ml). The reaction mixture was brought to a gentle reflux for 1 hour. The reaction mixture was cooled to room temperature and the appropriate alcohol (1.2mol) dissolved in 60ml of anhydrous acetone was added dropwise over a period of ±10 minutes. After addition of the appropriate alcohol, the reaction mixture was gently warmed to 60°C for 1 hour, cooled to room temperature and stirred for a further 12 hours. 150ml of distilled water was added to the reaction mixture. The crude product was recovered by repetitive extraction with chloroform followed by washing of the organic phase with water. The crude reaction product was recovered under reduced pressure and further purified by crystallization. If crystallization was not successful and further purification was required, the products were purified by column chromatography using silica gel as a stationary phase (± 1g product / 50g) with chloroform or a mixture of dichloromethane and acetone as the mobile phase.

3.3 Crystallography and structure refinement

Crystals suitable for single crystal X-ray analysis were mounted on a thin glass fibre and data was collected on Bruker Nonius SMART Apex diffractometer using graphite monochromated Mo-Kα radiation (λ = 0.7107 Å). Data integration and reduction were undertaken using SAINT[40] and space group determination using XPREP[40]. Multi-scan derived corrections were made to the data using

SADABS[41]. The structures were solved using SHELXS-97[42] and refined using SHELXL-97[42] with the aid of the interface software XSEED[23, 24]. XSEED[23, 24] was also used to generate the molecular graphics as the GUI to POV-Ray[43]. In each structure, all non-hydrogen atoms were modelled anisotropically. Hydrogen atoms were placed in geometrically calculated positions, with C-H = 0.99 for $-CH_2-$, 0.98 for $-CH_3$ or 0.95 for phenyl and 0.88 Å for N-H. These were refined using a riding model with U_{iso}(H) = 1.2U_{eq}(parent) (for $-CH_2-$, phenyl and N-H) and 1.5U_{eq}(parent) (for $-CH_3$). Crystal structure interpretation was performed with the aid of XSEED[23, 24], PLATON[25] and MERCURY[32].

3.4 Computational Details

All calculations were performed with the ADF (Amsterdam Density Functional) suite of programs[44, 45], release 2004.01 and 2005.01.

Restricted ground-state calculations, including geometry optimizations, were performed with:

- Local density approximation (LDA) functional of Vosko-Wilk-Nusair (VWN)[46], augmented with the nonlocal gradient correction PW91 from Perdew and Wang[47].
- Relativistic effects have been taken into account using the scalar relativistic (SR) zero-order regular approximation (ZORA)[48].
- The ZORA basis sets used were of triple ζ plus polarization Slater type function (STO) quality (basis TZP in ADF).

3.5 Preparative methods of bipodal compounds

3.5.1 *O,O'*-dimethyl *N,N'*-(*p*-phenylene-dicarbonyl)bis(thiocarbamate), $H_2(L^{15}$-*S,O*).

Terephthaloyl dichloride (30.00mmol, 6.091g) dissolved in 60ml of anhydrous acetone was added to a solution of KSCN (60.00mmol, 5.850g) dissolved in 60ml of anhydrous acetone under an inert atmosphere. The reaction mixture was refluxed at 70°C for one hour, cooled to room temperature, after which an anhydrous solution of methanol (0.1200mol 6.989ml) dissolved in 60ml of anhydrous acetone was added dropwise with stirring to the reaction mixture. The mixture was gently warmed to 60°C for one hour, cooled to room temperature stirred for a further 12 hours. Water (150ml) was added to the reaction mixture followed by repetitive extraction with chloroform. The combined organic fractions were further washed with three 25ml portions of water. Removal of the solvent in vacuo resulted in a pale-yellow amorphous target product in high yield and a high degree of purity.

Yield: 74.7% (based on terephthaloyl dichloride).

NMR : δ_H (600 MHz, solvent $CDCl_3$) 9.22 (2H, br s, NH), 7.94 (4H, s, phenyl CH), 4.20 (6H, s, CH_3). δ_C (151 MHz, solvent $CDCl_3$) 189.7 (C(S)), 161.5 (C(O)), 136.9 (*ipso*-Ph), 128.3 (Ph), 59.6 (OCH_3).

Mass spectrum (EI 70eV) *m/z* 312 (M^+, 9.6%), 280 (14.0%), 222 (39.2%), 190 (100.0%), 163 (10.2%), 132 (26.8%), 104 (61.8%), 76 (34.5%), 50 (16.6%), 18 (22.3%).

Found C 45.87; H 3.82; N 8.90; S 19.93; $C_{12}H_{12}N_2O_4S_2$ required C 46.14; H 3.87; N 8.97; S 20.53.

3.5.2 *O,O'*-diethyl *N,N'*-(*p*-phenylene-dicarbonyl)bis(thiocarbamate), $H_2(L^{16}$-*S,O*).

$H_2(L^{16}$-*S,O*) was prepared using an analogous method to that described in the preparation of *O,O'*-dimethyl *N,N'*-(*p*-phenylene-dicarbonyl)bis(thiocarbamate), **$H_2(L^{15}$-*S,O*)** with ethanol as the appropriate alcohol.

Crystals suitable for single crystal X-ray diffraction analysis were obtained by crystallization from a 1:1 chloroform ethanol mixture.

Yield: 84.8% (based on terephthaloyl dichloride).

NMR : δ_H (600 MHz, solvent $CDCl_3$) 9.29 (2H, br s, NH), 7.93 (4H, s, phenyl CH), 4.65 (4H, qu, CH_2), 1.44 (6H, tr, CH_3). δ_C (151 MHz, solvent $CDCl_3$) 188.9 (C(S)), 161.9 (C(O)), 136.9 (*ipso*-Ph), 128.3 (Ph), 69.6 (CH_2), 13.7 (CH_3).

FT-IR: (KBr disks) 3260(s), 1697(s), 1542(s), 1281(s), 1186(s) cm^{-1}.

Mass spectrum (EI 70eV) *m/z* 340 (M^+, 1.9%), 294 (7.0%), 236 (18.2%), 190 (100.0%), 132 (19.1%), 104 (41.4%), 76 (29.3%), 46 (3.8%), 18 (22.3%).

Found C 50.10; H 4.74; N 8.60; S 17.64; $C_{14}H_{16}N_2O_4S_2$ required C 49.39; H 4.74; N 8.23; S 18.84.

Melting point: 137.2 – 138.1°C.

3.5.3 *O,O'*-dibutyl *N,N'*-(*p*-phenylene-dicarbonyl)bis(thiocarbamate), $H_2(L^{17}$-*S,O*).

$H_2(L^{17}$-*S,O*) was prepared using an analogous method to that described in the preparation of *O,O'*-dimethyl *N,N'*-(*p*-phenylene-dicarbonyl)bis(thiocarbamate), **$H_2(L^{15}$-*S,O*)** by using butanol as the appropriate alcohol.

Yield: 88.5% (based on terephthaloyl dichloride).

NMR : δ_H (600 MHz, solvent $CDCl_3$) 9.34 (2H, br s, NH), 7.94 (4H, s, phenyl CH), 4.59 (4H, tr, CH_2), 1.79 (4H, m, CH_2), 1.47 (4H, m, CH_2), 0.97 (6H, tr, CH_3). δ_C (151 MHz, solvent $CDCl_3$) 189.2 (C(S)), 161.8 (C(O)), 136.9 (*ipso*-Ph), 128.3 (Ph), 77.6 (CH_2), 30.1 (CH_2), 19.0 (CH_2), 13.7 (CH_3).

FT-IR: (KBr disks) 3260(s), 1694(s), 1538(s), 1292(s), 1190(s) cm^{-1}.

Mass spectrum (EI 70eV) *m/z* 396 (M^+, 1.3%), 337 (1.6%), 322 (2.5%), 267 (8.3%), 225 (5.1%), 205 (22.3%), 190 (54.8%), 148 (100.0%), 104 (39.5%), 56 (36.9%), 41 (22.9%).

Found C 54.58; H 6.13; N 7.00; S 15.98; $C_{18}H_{24}N_2O_4S_2$ required C 54.52; H 6.10; N 7.06; S 16.17.

3.5.4 *O,O'*-dimethyl *N,N'*-(*m*-phenylene-dicarbonyl)bis(thiocarbamate), $H_2(L^{18}$-*S,O*).

$H_2(L^{18}$-*S,O*) was prepared using an analogous method to that described in the preparation of *O,O'*-dimethyl *N,N'*-(*p*-phenylene-dicarbonyl)bis(thiocarbamate), **$H_2(L^{15}$-*S,O*)**. Isophthaloyl dichloride and methanol were used as the starting reagents.

Yield: 81.3% (based on isophthaloyl dichloride).

NMR : δ_H (600 MHz, solvent $CDCl_3$) 10.30 (2H, br s, NH), 8.62 (1H, s, phenyl CH), 8.13 (1H, d, phenyl CH), 8.11 (1H, d, phenyl CH), 7.56 (1H, tr, phenyl CH), 3.96 (6H, s, CH_3). δ_C (151 MHz, solvent $CDCl_3$) 190.6 (C(S)), 170.1 (C(O)), 134.1 (Ph), 134.0 (*ipso*-Ph), 130.4 (Ph), 127.3 (Ph), 68.4(CH_3).

FT-IR: (KBr disks) for polymorph **(I)** 3265(s), 1686(s), 1529(s), 1282(s) cm^{-1}.

FT-IR: (KBr disks) for polymorph **(II)** 3299(s), 1688(s), 1520(s), 1272(s) cm^{-1}.

Found C 45.98; H 3.92; N 8.96; S 19.44; $C_{12}H_{12}N_2O_4S_2$ required C 46.14; H 3.87; N 8.97; S 20.53.

3.5.5 *O,O'*-diethyl *N,N'*-(*m*-phenylene-dicarbonyl)bis(thiocarbamate), $H_2(L^{19}$-*S,O*).

$H_2(L^{19}$-*S,O*) was prepared using an analogous method to that described in the preparation of *O,O'*-dimethyl *N,N'*-(*p*-phenylene-dicarbonyl)bis(thiocarbamate), **$H_2(L^{15}$-*S,O*)**. Isophthaloyl dichloride and ethanol were used as the starting reagents. **$H_2(L^{19}$-*S,O*)** was also purified by column chromatography using silica gel as a stationary phase (± 1g product / 50g) and a mixture of chloroform (95% v/v) and methanol (5% v/v).

Yield: 90.5% (based on isophthaloyl dichloride).

NMR : δ_H (300 MHz, solvent $CDCl_3$) 9.50 (2H, br s, NH), 8.44 (1H, s, phenyl CH), 8.11 (1H, d, phenyl CH), 8.09 (1H, d, phenyl CH), 7.63 (1H, tr, phenyl CH), 4.60 (4H, qu, CH_2), 1.36 (6H, tr, CH_3). δ_C (151 MHz, solvent $CDCl_3$) 189.9 (C(S)), 163.1 (C(O)), 134.1 (Ph), 133.3 (Ph), 130.6 (Ph), 127.6 (Ph), 70.0(CH_2), 14.1 (CH_3).

Mass spectrum (EI 70eV) *m/z* 340 (M^+, 1.9%), 294 (7.0%), 236 (18.2%), 190 (100.0%), 132 (19.1%), 104 (41.4%), 76 (29.3%), 58 (7.6%), 46 (3.8%), 28 (7.3%).

FT-IR: (KBr disks) 3273(s), 1702(s), 1523(s), 1277(s) cm^{-1}.

Found C 50.03; H 4.56; N 8.32; S 17.43; $C_{14}H_{16}N_2O_4S_2$ required C 49.39; H 4.74; N 8.23; S 18.84.

3.5.6 *O,O'*-dibutyl *N,N'*-(*m*-phenylene-dicarbonyl)bis(thiocarbamate), $H_2(L^{20}$-*S,O*).

$H_2(L^{20}$-*S,O*) was prepared using an analogous method to that described in the preparation of *O,O'*-dimethyl *N,N'*-(*p*-phenylene-dicarbonyl)bis(thiocarbamate). Isophthaloyl dichloride and butanol were used as the starting reagents.

Yield: 87.3% (based on isophthaloyl dichloride).

NMR : δ_H (300 MHz, solvent $CDCl_3$) 9.73 (2H, br s, NH), 8.44 (1H, s, phenyl CH), 8.11 (1H, d, phenyl CH), 8.10 (1H, d, phenyl CH), 7.63 (1H, tr, phenyl CH), 4.56 (4H, qu, CH_2), 1.78 (4H, m, CH_2), 1.46 (4H, m, CH_2), 0.95 (6H, tr, CH_3). δ_C (76 MHz, solvent $CDCl_3$) 189.5 (C(S)), 162.2 (C(O)), 133.7 (Ph), 132.7 (Ph), 129.7 (Ph), 126.8 (Ph), 73.4 (CH_2), 30.2 (CH_2), 19.1 (CH_2), 13.7(CH_3).

Mass spectrum (EI 70eV) *m/z* 396 (M^+, 3.8%), 337 (2.5%), 322 (3.8%), 280 (7.6%), 264 (15.3%), 225 (5.7%), 208 (19.1%), 205 (17.1%), 190 (100.0%), 165 (22.3%) 148 (69.4%), 130 (14.0%), 104 (22.3%), 76 (21.7%), 28 (51.6%), 18 (6.4%).

Found C 55.03; H 6.18; N 7.41; S 15.75; $C_{18}H_{24}N_2O_4S_2$ required C 55.03; H 6.18; N 7.41; S 15.75.

3.5.7 *O,O'*-(*p*-xylene-α,α'diyl) *N,N'*-dibenzoyl bis(thiocarbamate), $H_2(L^{21}$-*S,O*).

Benzoyl chloride (3,6ml, 30mmol) dissolved in 60ml of anhydrous acetone was added to a solution of KSCN (2.915g, 30mmol) dissolved in 60ml of anhydrous acetone. 1,4-dimethanol benzene (2.073g, 15mmol) dissolved in 60ml of anhydrous acetone was added dropwise to the reaction mixture. The reaction mixture was refluxed for 1 hour, cooled to room temperature and stirred for a further 12 hours. 100ml of water was added to the reaction mixture and the crude product was extracted with 3 x 50ml of chloroform. The combined organic extracts were further washed with 3 x 50ml portions of water. The

product was isolated as a crystalline solid in a high degree of purity by removal of the solvent in vacuo. Crystals suitable for single crystal X-ray diffraction analysis were obtained from chloroform.

Yield: 37.9% (based on benzoyl chloride).

NMR : δ_H (300 MHz, solvent d_7-DMF) 12.16 (2H, br s, NH), 8.02-8.08 (m), 7.48-7.71 (m), 5.68 (4H, s, CH_2). δ_C (76 MHz, solvent d_7-DMF) 190.6 (C(S)), 166.2 (C(O)), 136.5 (Ph), 134.5 (Ph), 133.8 (Ph), 129.7 (Ph), 129.4 (Ph), 129.2 (Ph), 72.9 (CH_2).

FT-IR: (KBr disks) 3259(s), 1696(s), 1521(s), 1300(s), cm^{-1}.

Found C 62.28; H 4.30; N 6.17; S 12.45; $C_{24}H_{20}N_2O_4S_2$ required C 62.05; H 4.34; N 6.03; S 13.80.

Melting point: 153.6 – 154.2°C.

Appendix C: Chapter IV

Experimental crystal data, data collection and crystal refinement details.

Tables containing the experimental crystal data, data collection and crystal refinement details of the crystal structures of the non-coordinated ligands, as well as the complexes, can be found on the included compact disc of this thesis. An example of these tables for the crystal structure of $\mathbf{H_2(L^{16}\text{-}S,O)}$ is given below.

C.1 *O,O'*-diethyl *N,N'*-(*p*-phenylene-dicarbonyl)bis(thiocarbamate), $H_2(L^{16}\text{-}S,O)$.

Crystal data

$C_{14}H_{16}N_2O_4S_2$	Mo Kα radiation
Mr = 340.41g.mol^{-1}	Cell parameters from 1547 reflections
Tetragonal, $P4_32_12$	θ = 2.4 – 26.0°
a = 10.5794(4) Å	μ = 0.36 mm^{-1}
c = 14.0773(12)Å	T = 100 (2) K
V = 1575.58(16)Å^3	needle, colorless
Z = 4	0.43 x 0.06 x 0.06 mm
D_x = 1.435 Mg m^{-3}	

Data collection

Bruker SMART APEX CCD diffractometer	1448 reflections with I > 2σ(I)
ω scans	R_{int} = 0.050
Absorption correction: multi-scan (SADABS[41, 49])	θ_{max} = 26.0°
T_{min} = 0.975	h = -13 → 13
T_{max} = 0.979	
16377 measured reflections	k = -13 → 13
1547 independent reflections	l = -17 → 17

Refinement

Refinement on F^2	$w = 1/[\sigma^2(F_o^2) + (0.0605P)^2 + 0.9712P]$
$R[F^2 > 2\sigma(F^2)]$ = 0.041	where $P = (F_o^2 + 2F_c^2)/3$
$wR(F^2)$ = 0.104	$(\Delta/\sigma)_{max}$ = 0.002
S = 1.09	$\Delta\rho_{max}$ = 0.35 e Å^{-3}
1547 reflections	$\Delta\rho_{min}$ = -0.22 e Å^{-3}
96 parameters	Absolute structure: 598 Friedel pairs[50]
H-atom parameters constrained	Flack parameter = 0.08(15)

4. References

[1] K. R. Koch, *Coord. Chem. Rev.* 2001, ***216-217***, 473-488.
[2] O. Hallale, S. Bourne, K. R. Koch, *CrystEngComm* 2005, ***7***, 161-166.
[3] K. R. Koch, S. A. Bourne, A. Coetzee, J. Miller, *J. Chem. Soc., Dalton Trans.* 1999, 3157-3161.
[4] S. A. Bourne, O. Hallale, K. R. Koch, *Cryst. Growth Des.* 2005, ***5***, 307-312.
[5] A. N. Westra, S. A. Bourne, K. R. Koch, *Dalton Trans.* 2005, ***17***, 2916-2924.
[6] K. R. Koch, O. Hallale, S. A. Bourne, J. Miller, J. Bacsa, *J. Mol. Struct.* 2001, ***561***, 185-196.
[7] R. Koehler, R. Kirmse, R. Richter, J. Sieler, E. Hoyer, L. Beyer, *Z. Anorg. Allg. Chem.* 1986, ***537***, 133-144.
[8] K. H. Koenig, M. Kuge, L. Kaul, H. J. Pletsch, *Chemische Berichte* 1987, ***120***, 1251-1253.
[9] H. J. Schneider, *Angew. Chem., Int. Ed. Engl.* 1991, ***30***, 1417-1436.
[10] M. L. Kilkenny, L. R. Nassimbeni, *J. Chem. Soc., Dalton Trans.* 2001, ***20***, 3065-3068.
[11] L. R. Nassimbeni, M. L. Kilkenny, *J. Chem. Soc., Dalton Trans.* 2001, ***8***, 1172-1175.
[12] K. R. Koch, C. Sacht, S. Bourne, *Inorg. Chim. Acta* 1995, ***232***, 109-115.
[13] K. R. Koch, C. Sacht, T. Grimmbacher, S. Bourne, *S. Afr. J. Chem.* 1995, ***48***, 71-77.
[14] K. Ramadas, N. Srinivasan, N. Janarthanan, *Tetrahedron Lett.* 1993, ***34***, 6447-6450.
[15] D. Ugar, U. Flörke, N. Külcü, H. Arslan, *Acta Crystallogr., Sect. E: Struct. Rep. Online* 2003, ***E59***, o1345-o1346.
[16] G. Blewett, C. Esterhuysen, M. W. Bredenkamp, K. R. Koch, *Acta Crystallogr., Sect. C: Cryst. Struct. Commun.* 2004, ***C60***, o862-o864.
[17] G. Blewett, M. W. Bredenkamp, K. R. Koch, *Acta Crystallogr., Sect. C: Cryst. Struct. Commun.* 2005, ***C61***, o469-o472.
[18] A. D. Morales, H. N. de Armas, N. M. Blaton, O. M. Peeters, C. J. D. Ranter, H. Márquez, R. P. Hernández, *Acta Crystallogr., Sect. C: Cryst. Struct. Commun.* 2000, ***C56***, 1042-1043.
[19] L. A. Montiel-Ortega, S. Rojas-Lima, E. Otazo-Sanchez, R. Villagómez-Ibarra, *J. Chem. Crystallogr.* 2004, ***34***, 89-93.
[20] L. V. Sudha, D. N. Sathyanarayana, *J. Mol. Struct.* 1984, ***125***, 89-96.
[21] F. H. Allen, *Acta Crystallogr., Sect. B: Struct. Sci.* 2002, ***B58***, 380-388.
[22] K. H. König, M. Schuster, B. Steinbrech, G. Schneeweis, R. Schlodder, *Fresenius Z. Anal. Chem.* 1985, ***321***, 457-460.
[23] L. J. Barbour, *Journal of Supramolecular Chemistry* 2001, ***1***, 189-191.
[24] J. L. Atwood, L. J. Barbour, *Cryst. Growth Des.* 2003, ***3***, 3-8.
[25] A. L. Spek, A Multipurpose Crystallographic Tool, University of Utrecht, Netherlands, **1999.**
[26] U. Schröder, L. Beyer, F. Dietze, R. Richter, S. Schmidt, E. Hoyer, *J. Prakt. Chem.* 1995, ***337***, 184-188.
[27] A. D. Morales, S. Garcia-Granda, Y. R. Esteva, A. P. Stevens, G. A. A. Crespo, *Acta Crystallographica Section C* 1997, ***C53***, IUC9700019.
[28] A. D. Morales, H. N. de Armas, N. M. Blaton, O. M. Peeters, C. De Ranter, J., H. Márquez, R. P. Hernández, *Acta Crystallogr., Sect. C: Cryst. Struct. Commun.* 2000, ***C56***, 503-504.
[29] S. Shanmuga Sundara Raj, K. Puviarasan, D. Velmurugan, G. Jayanthi, H.-K. Fun, *Acta Crystallogr., Sect. C: Cryst. Struct. Commun.* 1999, ***C55***, 1318-1320.
[30] G. R. Desiraju, *Science* 1997, ***278***, 404-405.
[31] M. T. Kirchner, L. S. Reddy, G. R. Desiraju, R. K. R. Jetti, R. Boese, *Cryst. Growth Des.* 2004, ***4***, 701-709.
[32] I. J. Bruno, J. C. Cole, P. R. Edgington, M. Kessler, C. F. Macrae, P. McCabe, J. Pearson, R. Taylor, *Acta Crystallogr., Sect. B: Struct. Sci.* 2002, ***B58***, 389-397.
[33] A. Ranganathan, V. R. Pedireddi, S. Chatterjee, C. N. R. Rao, *J. Mater. Chem.* 1999, ***9***, 2407-2411.
[34] V. R. Pedireddi, S. Chatterjee, A. Ranganathan, C. N. R. Rao, *J. Am. Chem. Soc.* 1997, ***119***, 10867-10868.
[35] M. K. Krepps, S. Parkin, D. A. Atwood, *Cryst. Growth Des.* 2001, ***1***, 291-297.
[36] W. Clegg, J. E. Davies, M. R. J. Elsegood, E. Lamb, J. J. Longridge, J. M. Rawson, R. Snaith, A. E. H. Wheatley, *Inorg. Chem. Commun.* 1998, ***1***, 58-60.
[37] P. A. W. Dean, M. Jennings, T. M. Houle, D. C. Craig, I. G. Dance, J. M. Hook, M. L. Scudder, *CrystEngComm* 2004, ***6***, 543-548.
[38] I. B. Douglass, F. B. Dains, *J. Am. Chem. Soc.* 1934, ***56***, 1408-1409.
[39] I. B. Douglass, F. B. Dains, *J. Am. Chem. Soc.* 1934, ***56***, 719-721.
[40] Bruker, SMART, SAINT and XPREP, Area detector control and data integration and reduction software, Bruker Analytical X-ray Instruments Inc., Madison, WI, USA., 1995.

[41] G. M. Sheldrick, SADABS. Version 2.05, Empirical absorption correction program for area detector data, University of Göttingen, Germany., 2002.
[42] G. M. Sheldrick, SHELXS97 and SHELXL97, Programs for the Solution and Refinement of Crystal Structures, University of Göttingen, Institüt für Anorganische Chemie der Universität, Tammanstrasse 4, D-3400 Göttingen, Germany, 1997.
[43] Pov-Ray, http://www.povray.org,
[44] G. Te Velde, F. M. Bickelhaupt, E. J. Baerends, C. Fonseca Guerra, S. J. A. Van Gisbergen, J. G. Snijders, T. Ziegler, *Journal of Computational Chemistry* 2001, ***22***, 931-967.
[45] E. J. Baerends, J. Autschbach, A. Bérces, Bo, C. *et al.*, *http://www.scm.com*.
[46] S. H. Vosko, L. Wilk, M. Nusair, *Canadian Journal of Physics* 1980, ***58***, 1200-1211.
[47] J. P. Perdew, J. A. Chevary, S. H. Vosko, K. A. Jackson, M. R. Pederson, D. J. Singh, C. Fiolhais, *Physical Review B: Condensed Matter and Materials Physics* 1992, ***44***, 6671-6687.
[48] E. van Lenthe, J. G. Snijders, E. J. Baerends, *J. Chem. Phys.* 1996, ***105***, 6505-6516.
[49] R. H. Blessing, *Acta Crystallogr., Sect. A: Found. Crystallogr.* 1995, ***A51***, 33-38.
[50] H. D. Flack, *Acta Crystallogr., Sect. A: Found. Crystallogr.* 1983, ***A39***, 876-881.

Index: Chapter V

1. Introduction

As indicated in chapter I, *N*-acyl(aroyl)-*N'*,*N'*-dialkylureas-(*O*,*O'*) [Scheme 1, X = O], are a further variation to the *N*-acyl(aroyl)-*N'*,*N'*-dialkylthiourea-(*S*,*O*) motif [Scheme 1, X = S]. By studying the coordination chemistry of a series of *N*-acyl(aroyl)-*N'*,*N'*-dialkylureas-(*O*,*O'*) to Cu(II), it was hoped that the influence of variation from the bidentate *S*,*O*-donor atom sets to the *O*,*O'*-donor atom sets would become evident. With this objective in mind, the molecular structure of several *N*-aroyl(acyl)-*N'*,*N'*-dialkylureas, as well as that of several of copper(II) complexes thereof, were determined by single crystal X-ray diffraction.

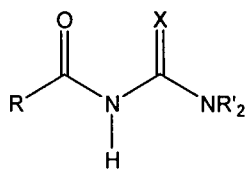

R = alkyl, phenyl
R' = alkyl
X = O, S

Scheme 1

Coordination Chemistry

It has previously been shown that with the acylchalcogenourea metal type complexes, in which the donor atom set changes from (*O*,*O*) of *N*-benzoyl-*N'*,*N'*-dialkylurea chelates to (*S*,*O*), to (*Se*,*O*) and further to (*S*,*S*) donor atom sets in related molecules, lead to an increase in stability of the 'softer' *b*-group metal ions (Ni^{2+}, Zn^{2+}, Cd^{2+}, Co^{2+}, Pb^{2+}, Tl^{2+}) as well as an increase in the acid strength of the coordinating agents[1]. Köning *et al.* however also reported that no complexation to Ni^{2+}, Zn^{2+}, Cd^{2+}, Co^{2+}, Pb^{2+}, Tl^{2+} metal ions occurred for the *N*-benzoyl-*N'*,*N'*-diethylurea-(*O*,*O*) ligands investigated under the conditions of potentiometric titration[1].

It might be expected that the coordination properties of the acylchalcogenoureas as ligands depend greatly on the number and the nature of the substituents on the terminal nitrogen atoms, as well as the substituents on the acyl or aroyl groups. For example, it has been found that, in changing from ethyl- to butyl-substitution at the carbamide side of the ligand, with constant chalcogen sites, leads to an increase of stability of the neutral chelate and to a decrease of the acidity of the ligands[1]. However, a literature review shows that little to no work has been published concerning how these aforementioned substituents influence the coordination of the chelate ligands to metal ions such as Cu^{2+} and Ni^{2+} in the solid state.

Synthesis methodologies reported in the literature

A survey of synthetic methods for the preparation of *N*-aroyl(acyl)ureas reported in the literature yielded a wide variety of methodologies dating as far back as 1938[2]. The general preparation of *N*-aroyl(acyl)ureas typically involves the reaction of substituted ureas with acyl chlorides at elevated

temperatures and often includes the use of expensive and exotic catalysts[3]. Other methods include the rather slow reaction of amides with isocyanates[4]. Recently, methods starting from the corresponding acyl isocyanate have been reported[5, 6].

Other synthetic routes reported involve the use of carboxylic acid chlorides as the starting materials with two plus equivalents of a strong base such as potassium hydride[7]. This method in particular is characterized by very low yields, a characteristic which appears to be typical of most methods reported in the literature. The method used to prepare *N*-benzoyl-*N'*,*N'*-dialkylureas, upon which a large percentage of the work that is reported in the literature appears to be based, is via the preparation of benzoylisocyanates reacted with the appropriate dialkyl amine[8]. As a result of investigations of the role played by acylureas and acylcarbamates in phytochemistry[9-11] and medicinal chemistry[12], an alternative method of synthesis involving the condensation of aroyl chlorides with synthesised sodium cyanate under varying solvent and catalytic conditions has been reported[13]. An alternative mild method for the synthesis of di- and trisubstituted *N*-acylureas on a solid support has recently been reported in the literature from investigations resulting from the fact that the *N*-acylurea substructure has several agrochemical[14] and medicinal applications. One such example thereof is the dopamine D2 agonist, Cabergoline[15], which was launched in 1993 as an anti-Parkinson's agent[16]. However, a solid support synthesis did not suite the requirements of the current study and was ruled out as a practical synthetic alternative. Consequently, none of the literature methods, primarily due to the required synthetic conditions and the less than suitable reported yields, appeared suitable.

Therefore, as part of a broader investigation of the coordination of bidentate chalcogenourea type ligands (including bidentate-(*O,S*) thiocarbamic esters: chapter 2 and chapter 3) to several transition metals, this work investigates alternate synthetic methods for the preparation and characterisation of a series of *N*-aroyl(acyl)–*N'*,*N'*-dialkylurea ligands-(*O,O'*), as illustrated in Figure 1, and their coordination to copper(II). The molecular structures of ligands **H(L$^{1\text{-}4}$-*S,O*)** were determined by single crystal X-ray diffraction analysis.

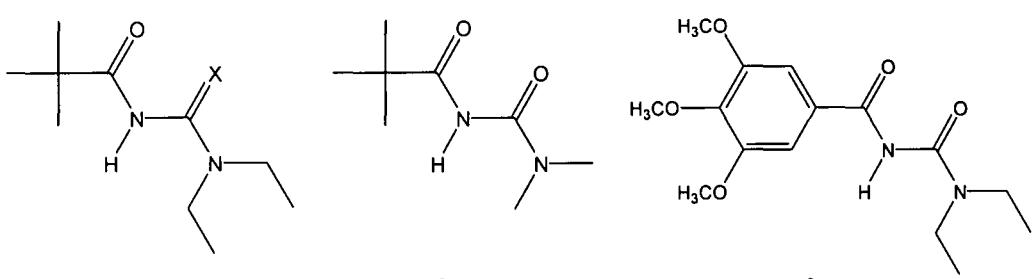

HL^1-(*O,O'*) (X = O)
HL^4-(*S,O*) (X = S)

HL^2-(*O,O'*)

HL^3-(*O,O'*)

Figure 1 *N*-aroyl(acyl)-*N'*,*N'*-dialkylchalcogenourea ligands **H(L$^{1\text{-}4}$-*X,O*)** (X = S/O) prepared and characterised by single crystal X-ray diffraction.

Copper complexes derived from *N*-aroyl(acyl)–*N'*,*N'*-dialkylureas characterised by single crystal X-ray structure determination are illustrated in Figure 2. 12 crystal structures are listed in the Cambridge Structural Database (CSD)[17, 18] of copper complexes of *N*-acyl(aroyl)thioureas, only one of which

reports a *trans* structure[19]. The remainder of the structures reported essentially conform to *cis*-*S,O* structures. The only metal complex of the *N*-acyl(aroyl)-*N'*,*N'*-dialkylurea type that is listed on the CSD is that of tris(*N*-benzoyl-*N'*,*N'*-diethylureato-*O,O'*)-chromium(III)[20]. Therefore, the structures of **Cu(L^2-*O,O*)$_2$** and **Cu(L^3-*O,O*)$_2$** reported here are the first copper complexes of this type that have been characterised by means of single crystal X-ray analysis.

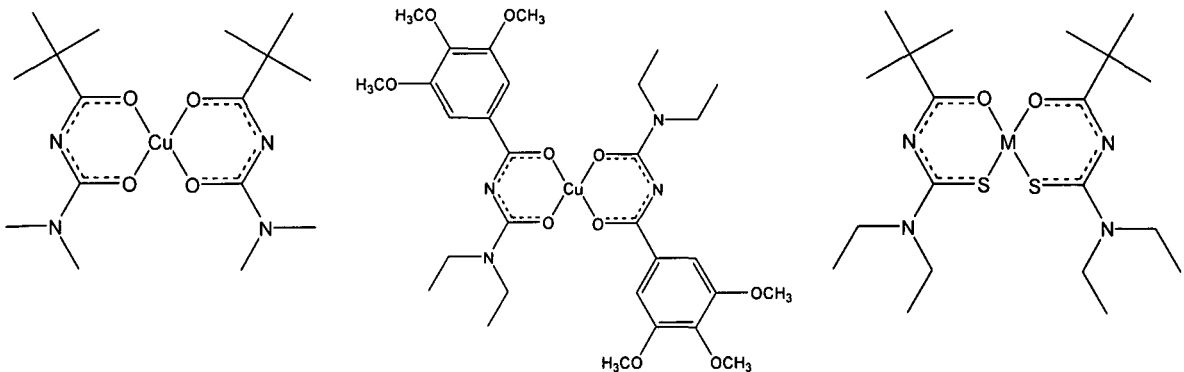

Figure 2 Bis(*N*-acyl(aroyl)-*N'*,*N'*-dialkylchalcogenureato)M(II) [M = Cu(II), Ni(II)] complexes characterised by means of single crystal X-ray diffraction.

Ligands **H(L$^{1\text{-}3}$-*O,O'*)** were prepared by the condensation of the appropriate aroyl(acyl)chloride in the presence of triethylamine with the appropriate *N,N*-dialkylurea under inert and anhydrous conditions. **H(L^4-*S,O*)** was prepared according to the method previously described by Douglass and Dains[21]. **Ni(L^4-*S,O*)$_2$** and **Cu(L^4-*S,O*)$_2$** were prepared from the dropwise addition of an acetonitrile/water (1:1 v/v) solution of the nickel or copper acetate to a solution of **H(L^4-*S,O*)** in the same solvent mixture. The products were recovered by filtration or extraction and re-crystallised from chloroform and ethanol or methanol. Several methods were investigated for the preparation of complexes **Cu(L$^{1\text{-}3}$-*O,O'*)$_2$** in an attempt to maximise the yields and minimise the formation of by-products. In most cases, the target product was only produced in small quantities in conjunction with high yields of copper hydroxide. The most successful method used in the preparation of complexes **Cu(L$^{1\text{-}3}$-*O,O'*)$_2$** in a high yield and a high degree of purity involved the addition of an aprotic solution of copper perchlorate to an aprotic solution of the appropriate ligand in the presence of the organic base, *N,N*-diisopropylethyl amine.

Some of the by-products that were isolated during the synthesis of compounds **H(L$^{1\text{-}3}$-*O,O'*)** and the complexation of these ligands with copper, included tetrakis(μ_2-2,2-dimethylpropanoato-*O,O'*)-bis(pyridine-*N*)-dicopper, $Cu_2(C_5H_9O_2)_4(C_5H_5N)_2$, Bis(di-$\mu$-ethoxo)-bis(*N*-pivaloyl-*N'*,*N'*-diethylureato)dicopper(II), $[Cu_2(L^1\text{-}O,O')_2(C_2H_5O)_2]$, 1,1-dibenzoyl-3,3-dimethylurea and benzamide.

2. Results and Discussion

2.1 Single crystal X-ray diffraction analysis.

The molecular structures of a series of *N*-acyl(aroyl)-*N'*,*N'*-dialkylurea ligands (Figure 1) and the resultant copper complexes (Figure 2) were determined by single crystal X-ray structural analysis in an attempt to compare how these ligands and resultant copper complexes compare with the comparatively well studied and well documented *N*-acyl(aroyl)-*N'*,*N'*-dialkylthiourea ligands and transition metal complexes thereof. At the time that the experimental work of Chapter V was carried out, the crystal structures of **H(L^4-*S,O*)** and **M(L^4-*S,O*)$_2$** [M = Ni, Cu], had not yet been listed on the Cambridge Structural Database (CSD)[17, 18] and were consequently determined for comparative purposes. However, these molecular structures have subsequently been reported by Ribeiro da Silva *et al*[22].

In the single crystal X-ray analysis of ligands **H(L^{1-4}-*S,O*)** and complexes **Cu(L^2-*O,O'*)$_2$**, **Cu(L^3-*O,O'*)$_2$**, **Cu(L^4-*S,O*)$_2$** and **Ni(L^4-*S,O*)$_2$**, numerous hydrogen bonds and contacts were observed. In many cases, these interactions and contacts were found to dictate the overall packing of the molecules in the unit cell. Apart from the traditional hydrogen bonds observed, many non-classical weak hydrogen interactions were also observed. A detailed discussion of hydrogen bonding as well as weaker non-classical hydrogen interactions is carried out in Chapter I in this thesis and is therefore not included here.

2.1.1 *N*-pivaloyl-*N'*,*N'*-diethylurea, H(L^1-*O*,*O'*)

H(L^1-*O*,*O'*) crystallizes in space group $P2_1/c$ with an essentially *anti* orientation of the (*O*,*O'*) donor atom sets. The O1-C2-N1-C3-O2 chelation moiety deviates extensively from planarity as illustrated in Figure 3. A list of selected bond lengths and torsion angles observed in **H(L^1-*O*,*O'*)** are listed in Table 2.

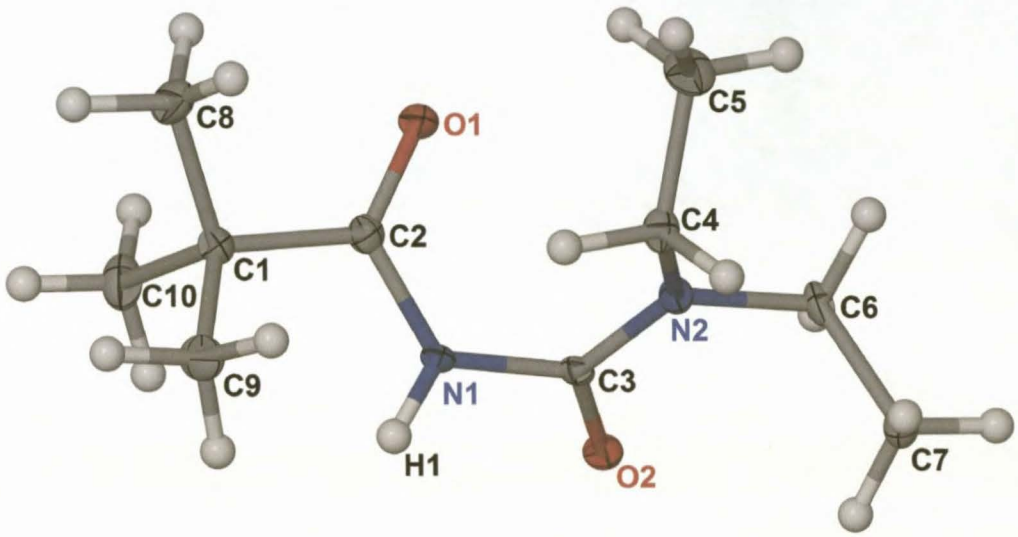

Figure 3 The molecular structure of **H(L^1-*O*,*O'*)**, showing the atomic numbering scheme used. Displacement ellipsoids are drawn at the 50% probability level.

The C2-N1 and C3-N2 bond lengths of **H(L^1-*O*,*O'*)** of 1.376(3)Å and 1.345(3)Å respectively, indicate that these bonds have a partial double bond character, as they are shorter than the accepted carbon-nitrogen single bond length of 1.472(5)[23, 24]. The C3-N1 bond length of 1.408(3)Å thus corresponds more closely to a C–N single bond. This indicates that there is a π-π conjugation along the O2-C3-N2 system and along the O1-C2-N1 system, but to a lesser extent along the O2-C3-N1 system. The C-N bond lengths in increasing bond order in **H(L^1-*O*,*O'*)**, N1-C3 [1.408(3)Å] < C2-N1 [1.376(3)Å] < C3-N2 [1.345(3)Å], correspond to the trend that was identified in the equivalent C-N bonds of interest in a series of several of the structurally related *N*-(aroyl)acyl-*N'*,*N'*-dialkyl- thioureas[23].

The potential coordinating CO moieties of **H(L^1-*O*,*O'*)** assume an essentially *anti* orientation, or otherwise can be described as being at obtuse angles relative to one another, which is parallel to the trend that was observed for the thiocarbonyl and carbonyl moieties in several of the structurally related *N*-acyl(aroyl)-*N'*,*N'*-dialkylthiourea ligands in the solid state[25, 26]. The orientation of the carbonyl moieties is illustrated by the torsion angles O1-C2-N1-C3, C2-N1-C3-O2 of 7.7(3)° and 118.1(2)° respectively, as well as by the improper torsion angle O1-C2…C3-O2 of -109.6(3)°. The relative *anti* orientation of the carbonyl moieties is possibly stabilised by the observed non-classical intramolecular hydrogen contact C5-H51…O1 [C5-H51…O1 2.42Å, 127.7°]. The O1-C2-N1-C3-O2 moiety of **H(L^1-**

***O,O'*)** also deviates extensively from planarity with the maximum deviation from the O1/C2/N1/C3/O2 least-squares plane being that of C3 and O2 by 0.391(2)Å and -0.298(2)Å respectively.

Several inter- and intramolecular hydrogen interactions are observed in **H(L^1-*O,O'*)** [Table 4]. **H(L^1-*O,O'*)** has a N1-H1…O2^i intermolecular hydrogen bond [N1-H1…O2^i 2.19Å, 141.3°; symmetry code (i) 1-x, 1-y, -z] to an adjacent molecule which in turn is hydrogen bonded back to the original molecule via the reverse intermolecular O2…H1^i-N1^i bond. A non-classical intermolecular hydrogen interaction, C4-H42…O2^{ii} is observed [C4-H42…O2 2.48Å, 168.5°; symmetry code (ii) x, ½-y, z-½] which links **H(L^1-*O,O'*)** to a second adjacent molecule and propagates the growth of one dimensional chains of **H(L^1-*O,O'*)** along [001] as illustrated in Figure 4.

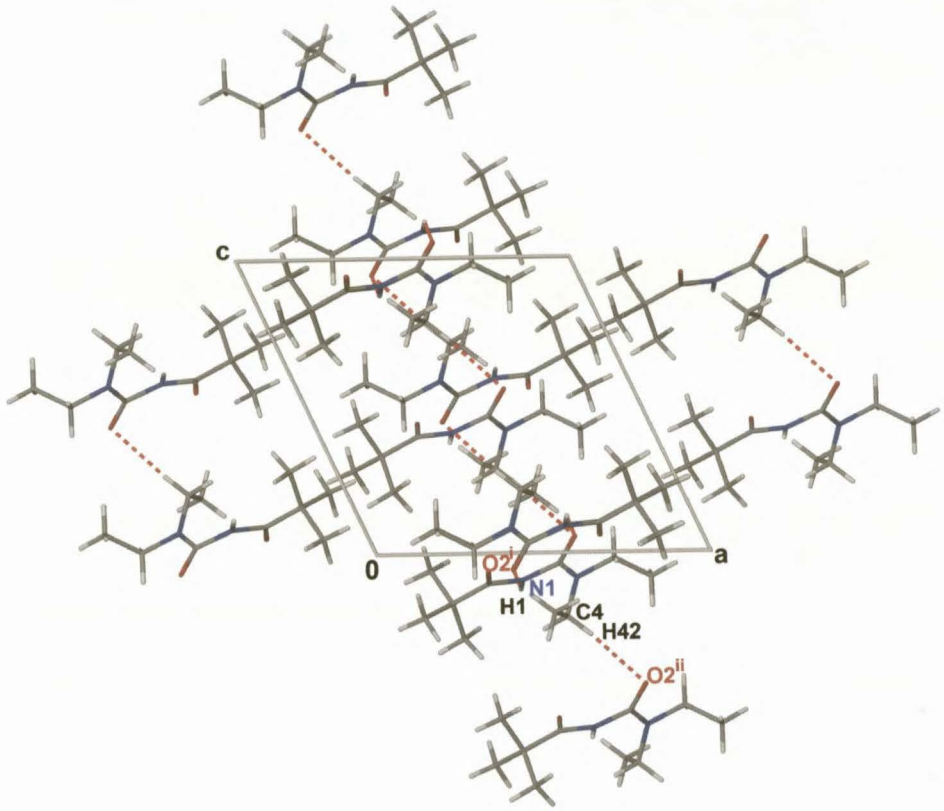

Figure 4 An extended packing diagram of **H(L^1-*O,O'*)** as viewed along [010]. The N1-H1…O2^i intermolecular hydrogen bond and non-classical intermolecular C4-H42…O^{ii} interaction have been indicated. Symmetry codes (i) 1-x, 1-y, -z; (ii) x, ½-y, z-½.

2.1.2 *N*-pivaloyl-*N'*,*N'*-dimethylurea, H(L^2-*O,O'*).

H(L^2-*O,O'*) crystallizes in the $P2_1/c$ space group with four independent molecules forming the asymmetric unit, denoted A, B, C and D in Figure 5, resulting in 16 formula units per unit cell. In all of the structures A, B, C and D, the bond order through the C-N bonds of interest are consistent with increasing bond order, NH-C(O)N'R_2 < RC(O)-NH < (O)C-N'R_2 as listed in Table 2. In all four molecules of **H(L^2-*O,O'*)**, there is a π-π conjugation along the (O)C-N'R_2 and the RC(O)-NH bonds of the (O)C-NH-C(O)-N'R_2 moieties but not along the NH-C(O)N'R_2 bonds.

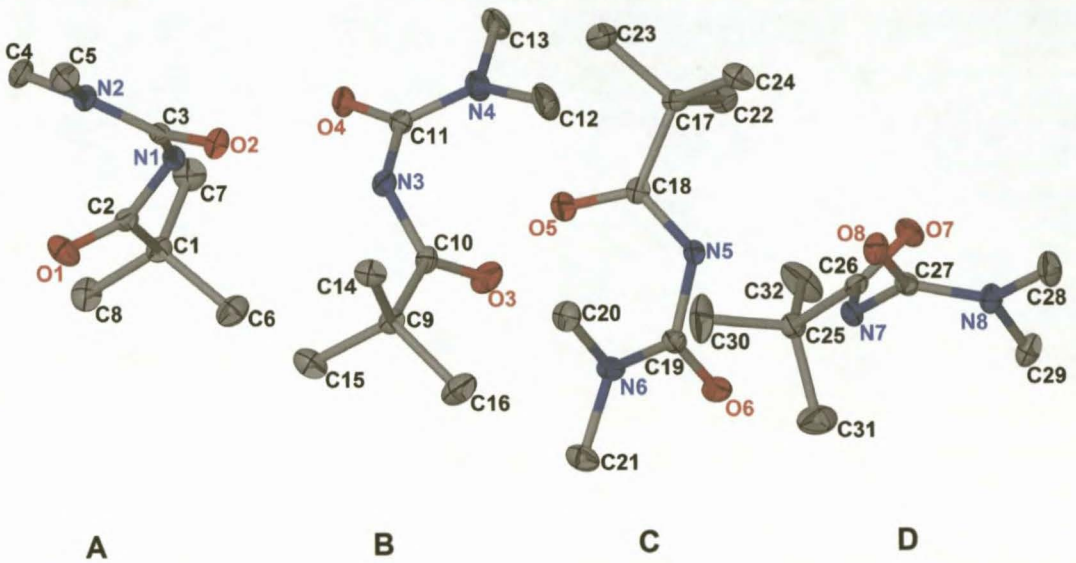

Figure 5 The molecular structure of **H(L^2-*O,O'*)** indicating molecules A, B, C, D in the asymmetric unit and showing the numbering scheme used. Displacement ellipsoids are drawn at the 50% probability level and hydrogen atoms have been excluded for clarity.

The potential coordinating CO moieties of the four independent molecules of **H(L^2-*O,O'*)** all assume an essentially *anti* or obtuse position relative to one another, similar to that observed in the crystal structure of **H(L^1-*O,O'*)**. The anti orientation of the CO moieties in each of the four molecules of **H(L^2-*O,O'*)** is clearly illustrated by the relevant torsion angles listed in Table 2. The C(O)-NH-C(O) chelation moieties in all four molecules deviate extensively from planarity.

As a result of the asymmetric unit of **H(L^2-*O,O'*)** consisting of four independent molecules, the resulting inter- and intramolecular hydrogen interactions are extensive. A complete list of all the inter- and intramolecular hydrogen bonds and contacts observed within the crystal lattice of **H(L^2-*O,O'*)** is listed in Table 4. Primarily, the four independent molecules of the asymmetric unit of **H(L^2-*O,O'*)** are arranged as two sets of 'dimers' held together by the hydrogen bonds formed between the N-H of the amide group and the oxygen of the urea group of an adjacent molecule. The dimers are formed between molecules A-B and C-D of the asymmetric unit as defined in Figure 5 [A-B: N1-H1…O4 2.09Å 146.1°; N3-H3…O2 2.08Å 146.8°; C-D: N5-H5…O8 2.13Å 138.5°; N7-H7…O6 2.10Å 146.1°]. The carbonyl group of the pivaloyl moiety plays no part in the hydrogen bond architecture that results in the formation of the two sets of 'dimers' A-B and C-D. The two sets of A-B and C-D 'dimers' are further cross linked into a three dimensional network of molecules of **H(L^2-*O,O'*)** via several classical and non-classical inter- and intramolecular hydrogen bonds and contacts as listed in Table 4.

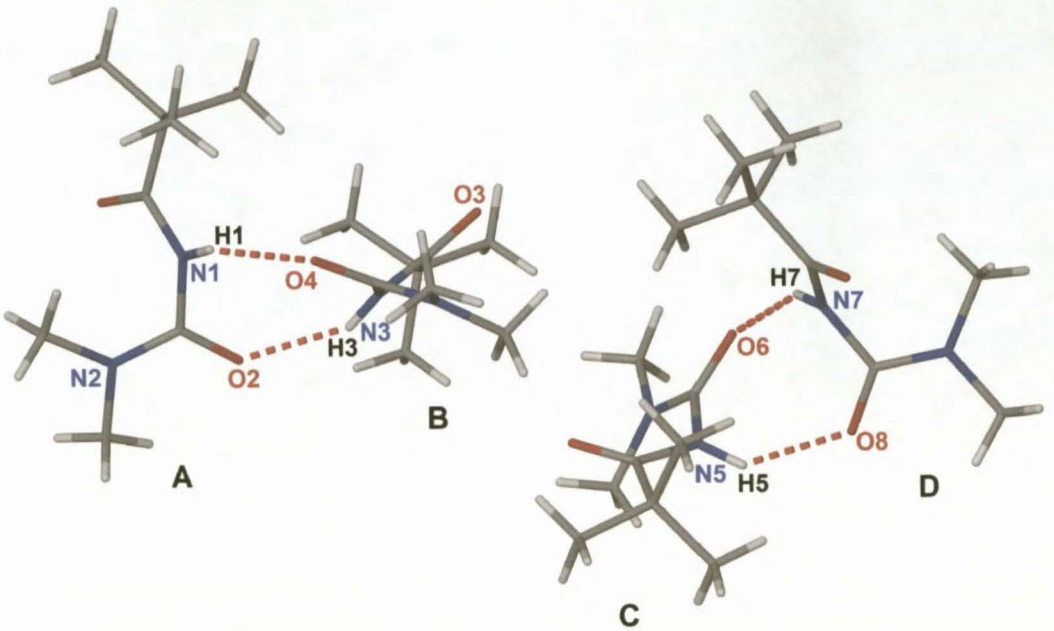

Figure 6 The 'dimer' arrangement, A-B and C-D, of molecules of **H(L^2-*O,O'*)** resulting from the N1-H1...O4, N3-H3...O2, N5-H5...O8 and N7-H7...O6 hydrogen bonds.

2.1.3 *N*-(3,4,5-trimethoxybenzoyl)-*N'*,*N'*-diethylurea, H(L^3-*O,O'*).

The molecular structure of **H(L^3-*O,O'*)** is illustrated in Figure 7 and selected bond lengths and torsion angles are listed in Table 4. Molecules of **H(L^3-*O,O'*)** crystallize monoclinic with space group $P2_1/n$ with 4 formula units per unit cell. The potential coordinating carbonyl groups of **H(L^3-*O,O'*)** are essentially *anti* or form an obtuse angle relative to one other, similar to that which was observed in the crystal structures of **H(L^1-*O,O'*)** and **H(L^2-*O,O'*)**. Carbons atoms, C6 and C7, of one of the ethyl groups of **H(L^3-*O,O'*)** are disordered across two positions labelled C8 and C9 respectively: the alternative chains are labelled C6 and C7 [sof refined to 53.7(7)%] and C8 and C9 [sof refined to 46.3(7)%] respectively.

The two methoxy substituents in the three and five positions on the benzoyl ring [C15-O3 and C17-O5] are essentially coplanar with the phenyl ring. Atoms O3 and C15 deviate from the least-squares plane defined through the phenyl ring by 0.005(3) Å and 0.072(4) Å respectively while atoms O5 and C17 deviate from this same least-squares plane by 0.017(3) Å and -0.144(3) Å respectively. This coplanarity of the methoxy groups in the 3 and 5 positions with the phenyl ring is further illustrated by torsion angles C15-O3-C11-C10 of 2.2(3)° and C17-O5-C13-C14 of 7.7(3)°. Methoxy groups C15-O3 and C17-O5 are angled outwards away from the C16-O4 methoxy substituent. Methoxy group C16-O4 is almost perpendicular to the benzoyl ring with torsion angle C16-O4-C12-C13 = 99.3(2)°. The geometrical arrangement of the methoxy groups on the benzoyl ring appears to be largely dictated by

steric interactions alone, since the only intermolecular hydrogen interaction observed involving the methoxy substituents, namely C17-H172...O1^{ix} [C17-H172...O1^{ix} 2.55Å, 138.9°; symmetry code (ix) x-½, ½-y, z-½], is a 'weak' non-classical hydrogen interaction and consequently does not appear to have any significant influence on the overall packing of molecules of **HL^3-*O,O'*)** in the unit cell.

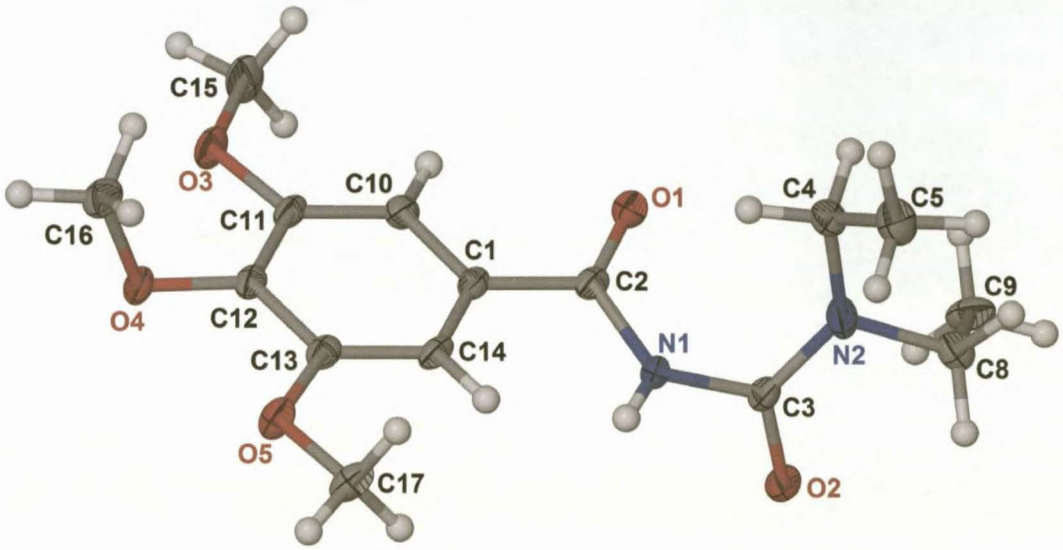

Figure 7 The molecular structure of **H(L^3-*O,O'*)** showing the numbering scheme used. Displacement ellipsoids are drawn at the 50% probability level. Disordered ethyl group positions C6 and C7 have been omitted.

The trend as observed for the bond lengths of the C-N bonds of interest in ligand **H(L^3-*O,O'*)** is comparable to that identified in ligands **H(L^1-*O,O'*)** and **H(L^2-*O,O'*)**, i.e. with increasing bond order N1-C3 [1.414(2)Å] < C2-N1 [1.381(2)Å] < C3-N2 [1.335(3)Å]. The C3-N2 and C2-N1 bond lengths of 1.335(3)Å and 1.381(2)Å respectively both indicate significant partial double bond character, while the bond length of N1-C3 of 1.414(2)Å is close to the accepted average C-N single bond length of 1.472(5)Å[23, 24]. This results in a π-π conjugation along the O2-C3-N2 system and along the O1-C2-N1 system, but to a lesser extent along the O2-C3-N1 system. This is schematically represented in Scheme 2 and is similar to that observed in the crystal structures of ligand **H(L^1-*O,O'*)** as well as to that observed in the four independent molecules of the asymmetric unit of ligand **H(L^2-*O,O'*)**.

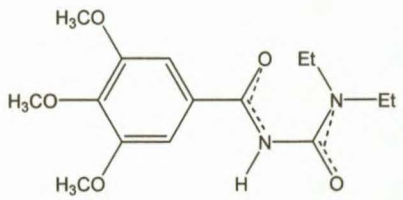

Scheme 2

The two potential coordinating CO moieties, C2-O1 and C3-O2, of **H(L^3-*O,O'*)** are *anti* forming an obtuse angle relative to one another similar to that which was observed for **H(L^1-*O,O'*)** and **H(L^2-*O,O'*)**, torsion angles O1-C2-N1-C3 = -8.6(3)° and C2-N1-C3-O2 = 120.1(2)°. The relative obtuse angled orientation of C2-O1 and C3-O2 is further illustrated by the improper torsion angle O1-C2…C3-O2 of -109.6(2)°. The C(O)-NH-C(O) coordinating moiety of **H(L^3-*O,O'*)** deviates extensively from planarity with the greatest deviation from the O1/C2/N1/C3/O2 least-squares plane being atom N1 and O1 by -0.547(2)Å and 0.531(1)Å respectively. The relative *anti* orientation of C2-O1 and C3-O2 is possibly stabilised by the observed non-classical hydrogen contacts C4-H41…O1 [C4-H41…O1 2.43Å 112.1°] and C4-H41…N1 [C4-H41…N1 2.40Å 106.8°].

The asymmetric unit of **H(L^3-*O,O'*)** is linked via a classical intermolecular hydrogen bond, N1-H1…O2^{viii} [N1-H1…O2^{viii} 2.16Å, 141.5° symmetry code (viii) 2-x, 1-y, 2-z], and weaker non-classical intermolecular hydrogen bond C14-H141…O2^{viii} [C14-H141…O2^{viii} 2.59Å, 130.1°] to an adjacent molecule while a third non-classical intermolecular hydrogen interaction C17-H172…O1^{ix} [C17-H172…O1^{ix} 2.55Å, 138.9° symmetry code (ix) x-½, ½-y, z-½] was observed. These interactions are indicated in Figure 8 of the unit cell of **H(L^3-*O,O'*)** as viewed along [100].

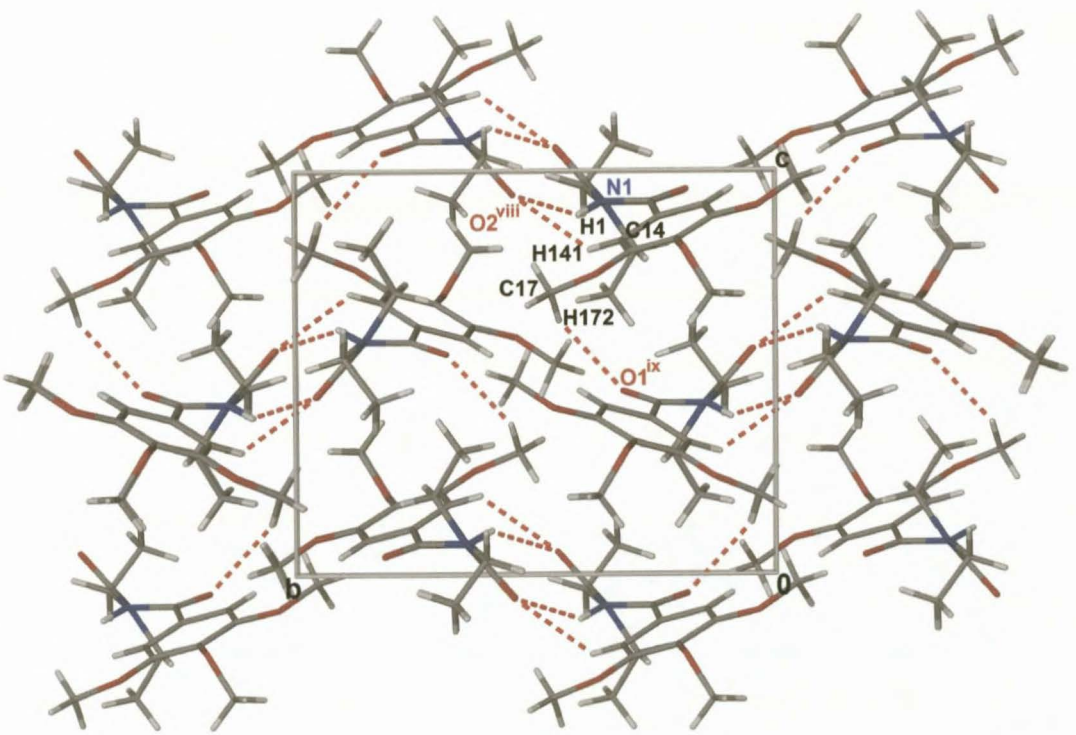

Figure 8 A perspective of the unit cell of **H(L^3-O,O')** as viewed along [100]. The N1-H1…O2^{viii} intermolecular hydrogen bond and non-classical intermolecular C14-H141…O2^{viii} and C17-H172…O1^{ix} interactions have been indicated.

2.1.4 *N*-pivaloyl-*N'*,*N'*-diethylthiourea, H(L^4-*S*,*O*).

By obtaining the crystal structure of **H(L^4-*S*,*O*)**, it allows a direct comparison to the crystal structure of **H(L^1-*O*,*O'*)** thereby indicating molecular and crystal lattice differences in the solid state that occur solely due to a variation of the potential bidentate-*O*,*O* coordination of **H(L^1-*O*,*O'*)** to the potential bidentate-*S*,*O* coordination of **H(L^4-*S*,*O*)** and not due to differences induced by differences in the *N*-acyl or *N'*,*N'*-dialkyl substituents since these groups in **H(L^1-*O*,*O'*)** and **H(L^4-*S*,*O*)** are identical.

H(L^4-*S*,*O*) crystallizes orthorhombic in a *Pbca* space group with eight molecules per unit cell. The molecular structure of **H(L^4-*S*,*O*)** is illustrated in Figure 9 showing the numbering scheme used.

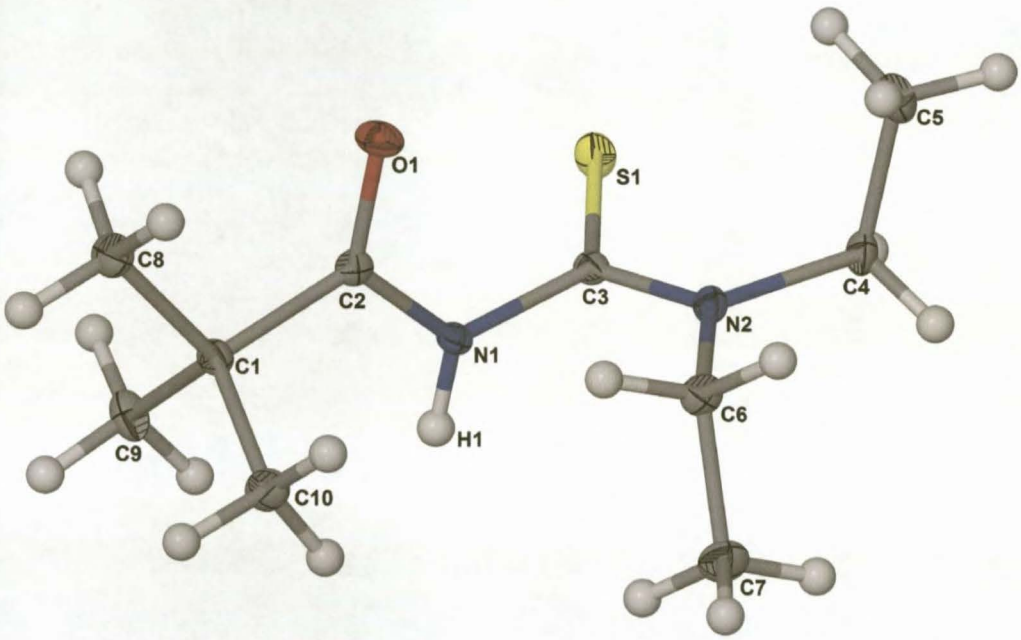

Figure 9 The molecular structure of **H(L^4-*S*,*O*)** showing the numbering scheme used. Displacement ellipsoids are drawn at the 50% probability level.

A partial double bond character is observed for all the C-N bonds of interest with the following increasing bond order C3-N1 [1.435(1)Å] < C2-N1 [1.352(2)Å] < C3-N2 [1.334(2)Å]. The bond length of C2-N1 [1.352(2)Å] of **H(L^4-*S*,*O*)** shows a greater degree of double bond character than the comparative C-N bonds of **H(L^1-*O*,*O'*)** [1.376(3)Å], **H(L^2-*O*,*O'*)** [1.374(3)Å, 1.375(3)Å, 1.372(3)Å, 1.382(3)Å] and **H(L^3-*O*,*O'*)** [1.381(2)Å], thereby indicating a greater degree of restricted rotation around this bond. In turn, the C3-N1 bond [1.435(1)Å] of **H(L^4-*S*,*O*)** is significantly longer than the equivalent bonds of **H(L^1-*O*,*O'*)** [1.408(3)Å], **H(L^2-*O*,*O'*)** [1.415(3)Å, 1.419(3)Å, 1.417(3)Å, 1.415(3)Å] and **H(L^3-*O*,*O'*)** [1.414(2)Å] and is the closest in length to the accepted average single C-N bond of 1.472(5)Å[23, 24]. Consequently a π-π conjugation is observed along the S1-C3-N2 and O1-C2-N1 moieties **H(L^4-*S*,*O*)** but to a lesser degree along the S1-C3-N1 moiety.

Bond	H(L^1-*O,O'*)	H(L^2-*O,O'*)				H(L^3-*O,O'*)	H(L^4-*S,O*)
		A	B	C	D		
C2-N1	1.376(3)	1.374(3)	1.375(3)	1.372(3)	1.382(3)	1.381(2)	1.352(2)
N1-C3	1.408(3)	1.415(3)	1.419(3)	1.417(3)	1.415(3)	1.414(2)	1.435(1)
C3-N2	1.345(3)	1.331(3)	1.335(3)	1.331(3)	1.377(3)	1.335(3)	1.334(2)

Table 1 Comparison of C-N bond lengths (Å) of interest for ligands H(L^1-*O,O'*), H(L^2-*O,O'*), H(L^3-*O,O'*) and H(L^4-*S,O*) as determined by single crystal X-ray structure determination.

The carbonyl and thiocarbonyl moieties of **H(L^4-*S,O*)** are almost perpendicular to one another with torsion angles C3-N1-C2-O1 = -0.28(17)° and C2-N1-C3-S1 = -84.49(13)°. The carbonyl and thiocarbonyl moieties can be described as being *syn* or forming an acute angle relative to one another, as illustrated by the improper torsion angle O1-C2...C3-S1 of -70.1(1)° as opposed the relative obtuse angle or *anti* orientation of the two structurally equivalent carbonyl moieties in ligands **H(L^1-*O,O'*)**, **H(L^2-*O,O'*)** and **H(L^3-*O,O'*)**. However, the *N*-aroyl-*N'*,*N'*-dialkylthiourea ligands reported in the literature generally assume a twisted conformation in the solid state, with the sulphur and oxygen atoms pointing approximately in opposite directions and can otherwise be described as being *anti* relative to each other[23]. In this regard, ligands **H(L^1-*O,O'*)**, **H(L^2-*O,O'*)** and **H(L^3-*O,O'*)** conform more to the general trend observed for *N*-aroyl-*N'*,*N'*-dialkylthiourea ligands vis-à-vis the relative obtuse angle or *anti* orientation of the carbonyl and thiocarbonyl moieties than what **H(L^4-*S,O*)** does.

Several classical and non-classical intermolecular hydrogen bonds and interactions were observed in the unit cell of **H(L^4-*S,O*)** as illustrated in Figure 10. The classical intermolecular hydrogen bond N1-H1...O1^x [N1-H1...O^x 2.00Å, 170.5°; symmetry code (x) x+½, y, ½-z.], supported by the non-classical C7-H73...O1^x and C9-H92...O1^x interactions [C7-H73...O^x 2.51, 169.4°; C9-H92...O^x 2.57Å, 150.8°] results in molecules of **H(L^4-*S,O*)** packing as two parallel one dimensional molecular chains extending along [100] as illustrated in Figure 10.

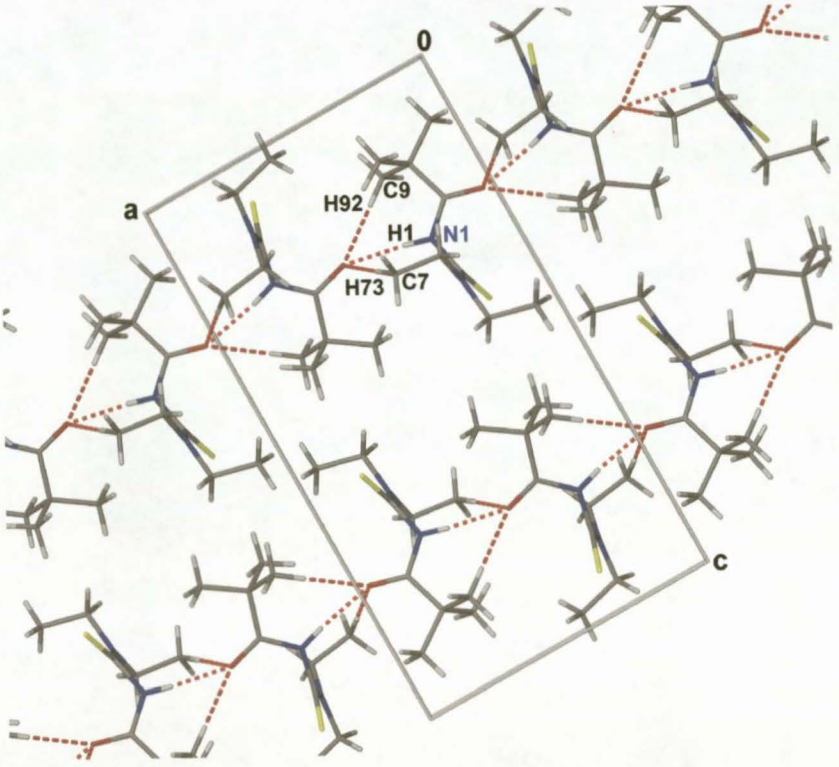

Figure 10 The extended packing diagram of **H(L^4-*S,O*)** as viewed along [010]. The N1-H1...$O1^x$ intermolecular hydrogen bond as well as the non-classical intermolecular hydrogen interactions C7-H73...$O1^x$ and C9-H92...$O1^x$ result in two one dimensional molecular strings of **H(L^4-*S,O*)** extending parallel to [100]. Symmetry code (x) x+½, y, ½-z.

2.1.5 *Bis*-(*N*-pivaloyl- *N'*,*N'*-dimethylureato)copper (II), Cu(L^2-*O*,*O'*)$_2$

The complex **Cu(L^2-*O*,*O'*)$_2$** forms monoclinic crystals in space group P2/c with two formula units per unit cell. The molecular structure of **Cu(L^2-*O*,*O'*)$_2$** reveals a square planar (*O*,*O'*)-bidentate coordination of two ligands to the copper atom as illustrated in Figure 11. The significant deviation from planarity of the C(O)-NH-C(O) chelation moiety observed in each of the four molecules of the asymmetric unit of the uncoordinated ligand, **H(L^2-*O*,*O'*)**, is lost upon complexation with the copper. Cu1 exhibits the greatest deviation from the C2/O1/Cu1/O2/C3 least-squares plane by 0.065(1)Å. In turn, the maximum deviation from the least-squares plane defined through the copper and the four co-ordinating oxygen atoms is Cu1 by 0.033(1)Å. The *N'*,*N'*-dimethyl carbon atoms are coplanar with the plane defined by the chelating oxygen atoms and the copper with atoms N2, C4, and C5 deviating from the C2/O1/Cu1/O2/C3 least-squares plane by -0.120(5)Å, -0.067(6)Å and -0.099(7)Å respectively. A large degree of thermal disorder was observed for the carbon atoms C7 and C8 as illustrated by the large displacement ellipsoids in Figure 11.

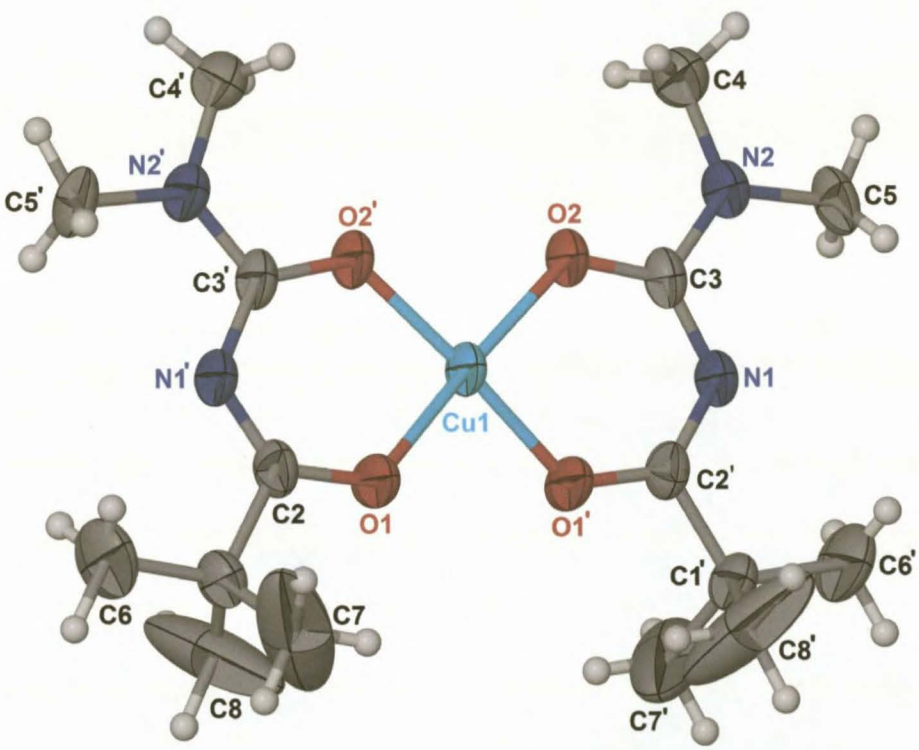

Figure 11 The molecular structure of **Cu(L^2-*O*,*O*)$_2$** showing the numbering scheme used. Displacement ellipsoids are drawn at the 50% probability level. Accented atoms are generated by the symmetry operator 1-x, y, ½-z.

In contrast to what was observed in the crystal structure of the four independent molecules A, B, C, and D of the un-coordinated ligand of **H(L^2-*O*,*O'*)**, few inter- and intramolecular hydrogen bonds or contact interactions were observed for **Cu(L^2-*O*,*O*)$_2$**. C7-H72 and C8-H83 both show intramolecular hydrogen contacts with O1 of the adjacent carbonyl moiety [C7-H72…O1 2.43Å, 99.9°; C8-H83…O1 2.52Å, 99.7°] as illustrated in Figure 12. The high degree of thermal disorder of C7 and C8 suggests that the C-

H...O interactions observed may represent an energy minimum and furthermore these C-H...O interactions may prevent the free rotation of the pivaloyl group around the C1-C2 bond. These intramolecular hydrogen interactions appear to have little to no effect on the overall packing of the molecules of **Cu(L^2-*O,O'*)$_2$** within the unit cell.

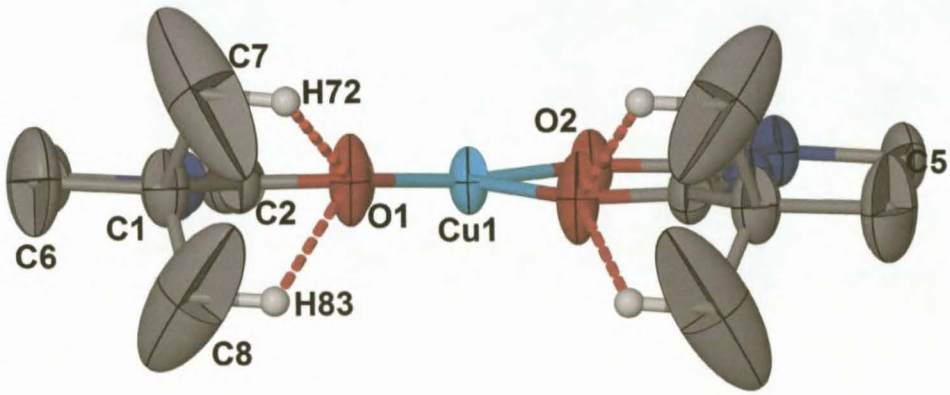

Figure 12 A side-on view of **Cu(L^2-*O,O'*)$_2$** showing the essentially square planar arrangement of the bidentate-*(O,O')* chelation of the two ligands around the copper metal centre. The C7-H72...O1 and C8-H83...O1 hydrogen contacts have been indicated.

By comparison to the structure of the four molecules in the asymmetric unit of the uncoordinated ligand, **H(L^2-*O,O'*)**, [A: C2-O1 1.215(3)Å, C3-O2 1.232(3)Å; B: C10-O3 1.214(3)Å, C11-O4 1.227(3)Å; C: C18-O5 1.213(3)Å, C19-O6 1.236(3)Å; D: C26-O7 1.216(3)Å, C27-O8 1.233(3)Å], the bond lengths of the carbonyl moieties in complex **Cu(L^2-*O,O'*)$_2$** are significantly longer [C2-O1 1.274(4)Å, C3-O2 1.271(4)Å]. The lengthening of these carbonyl bonds in **H(L^2-*O,O'*)**, in conjunction with the significant shortening of the C-N bonds in **H(L^2-*O,O'*)** [A: C2-N1 1.374(3) C3-N1 1.415(3)Å; B: C10-N3 1.375(3)Å, C11-N3 1.419(3)Å; C: C18-N5 1.372(3)Å, C19-N15 1.417(3)Å; D: C26-N7 1.382(3)Å, C27-N7 1.415(3)Å] upon complexation with copper in **Cu(L^2-*O,O'*)$_2$**, [C2-N1 1.297(5)Å, C3-N1 1.357(5)Å], indicates extensive electron delocalization through the chelation ring in Cu(L^2-*O,O'*)$_2$. Furthermore, the bond lengths of C2-O1 [1.274(4) Å] and C3-O2 [1.271(4) Å] in the complex, **Cu(L^2-*O,O'*)$_2$**, are of equal length, which suggests that there is an equal electron distribution through these carbonyl groups. Similarly, the Cu1-O1 [1.881(3)Å] and Cu1-O2 [1.902(3)Å] bond lengths are essentially of equal length indicating equal electron delocalisation through these bonds thereby suggesting that the *N*-pivaloyl and *N',N'*-dimethyl substituents on the chelate ring play similar roles in the metal oxygen bonding in **Cu(L^2-*O,O'*)$_2$**.

The length of the C(O)-NMe$_2$ bond in the four molecules of the asymmetric unit in the uncoordinated ligand **H(L^2-*O,O'*)** [A: C3-N2 1.331(3)Å; B: C11-N4 1.335(3)Å; C: C19-N6 1.331(3)Å; D: C27-N8 1.337(3)Å] remains largely unchanged upon complexation to the copper in **Cu(L^2-*O,O'*)$_2$** [C3-N2 1.339(5)Å] and the bond thus retains its partial double bond character and restricted rotation around this bond.

The essentially planar individual molecules of **Cu(L^2-*O,O'*)$_2$** stack in layers of alternating mirror images of each other such that the molecules of every alternate layer align with each other when the unit cell is viewed along [001] as illustrated in Figure 13

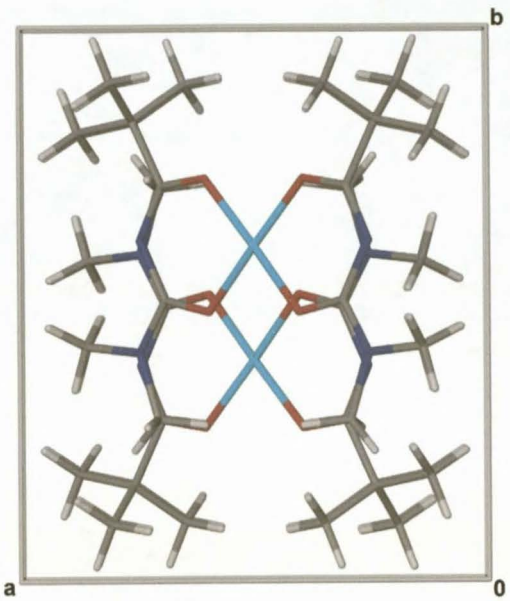

Figure 13 The unit cell of **Cu(L^2-*O,O*)$_2$** as viewed along [001] indicating the stacking of alternating mirror images of molecules with the molecules of each alternate layer aligning.

The overall alignment of the individual molecules of **Cu(L^2-*O,O*)$_2$** illustrated in Figure 13 results in atom Cu1 of one molecule aligning with O2 of the molecule immediately above and below with Cu1…$O2^{i}$ and Cu1…$O2^{ii}$ interatomic distances of 4.093(3)Å respectively [$O2^{i}$…Cu1…$O2^{ii}$ 152.5(1)°; symmetry codes (i) x, 1-y, z-½; (ii) 1-x, 1-y, 1-z]. Although this interatomic Cu…O distance is rather long, it possibly still allows for an electrostatic interaction between Cu1 and $O2^{i}$ and $O2^{ii}$, thereby giving the copper atom essentially a pseudo-octahedral coordination sphere. Similar intermolecular Cu(II)…O interactions have been reported in the literature[27-29] which include intermolecular Cu…O interaction distances of 4.034Å reported for the non-mesogenic bis(5-octyloxytropolonato)copper(II)[30] complex. The molecules of **Cu(L^2-*O,O*)$_2$** align in one dimensional 'molecular strings' parallel to [001] when viewed along [010] as illustrated in Figure 14.

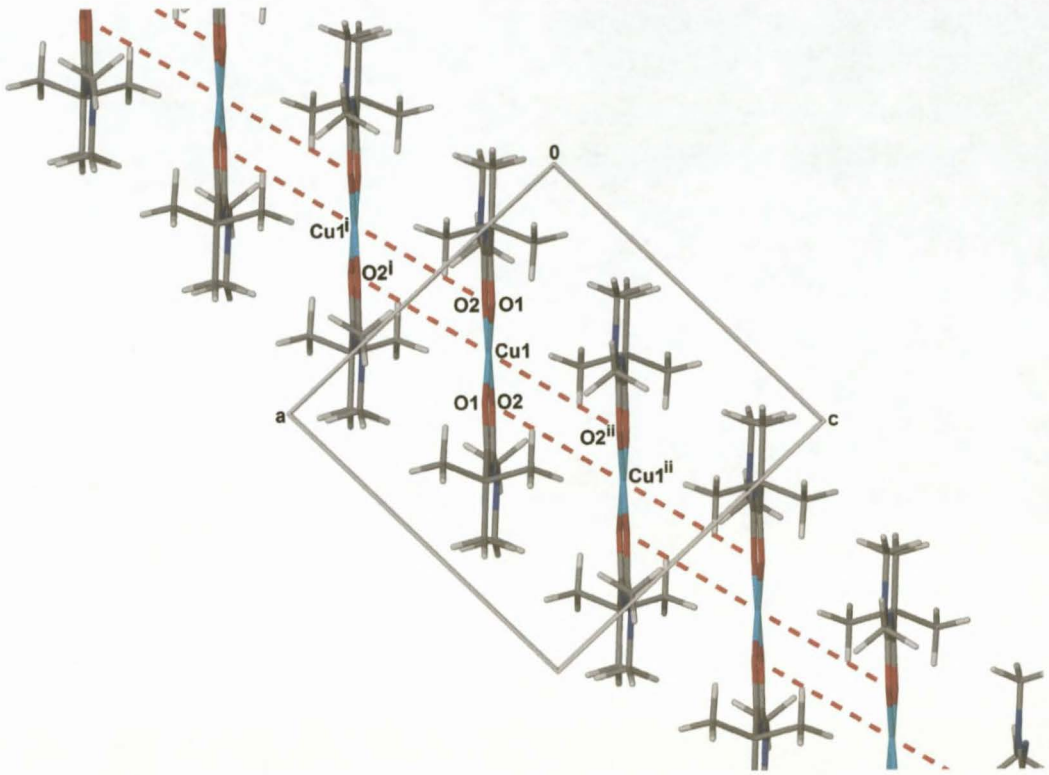

Figure 14 Extended packing diagram of **Cu(L^2-O,O)$_2$** as viewed along [010] showing the interatomic distances and alignment of O2^i...Cu...O2^{ii}. [Cu...O2^i, Cu...O2^{ii} 4.093(3)Å; O2^i...Cu1...O2^{ii} 152.46°] [Symmetry code: (i) x, 1-y, z-1/2; (ii) 1-x, 1-y, 1-z].

2.1.6 *Bis[N*-(3,4,5-trimethoxybenzoyl)-*N'*,*N'*-diethylureato]copper(II), Cu(L^3-*O,O'*)$_2$.

Complex **Cu(L^3-*O,O'*)$_2$** crystallizes monoclinic space group $P2_1/c$ with four formula units per unit cell. The molecular structure of **Cu(L^3-*O,O'*)$_2$** is square-planar bidentate-(*O,O'*) as illustrated in Figure 15. Disorder of carbons atoms C19 and C20 [sof refined to 85.6(1)%] as well as carbon atoms C23 and C24 [sof refined to 14.4(1)%] across positions C21 and C22 [sof refined to 14.4(1)%] and C25 and C26 [sof refined to 85.6(1)%] respectively, was observed. The significant deviation from planarity that was observed for the O1-C2-N1-C3-O2 chelation moiety of the uncoordinated ligand, **H(L^3-*O.O'*)** has been lost upon complexation to the copper, resulting in the chelation rings of **Cu(L^3-*O,O'*)$_2$** being remarkably planar.

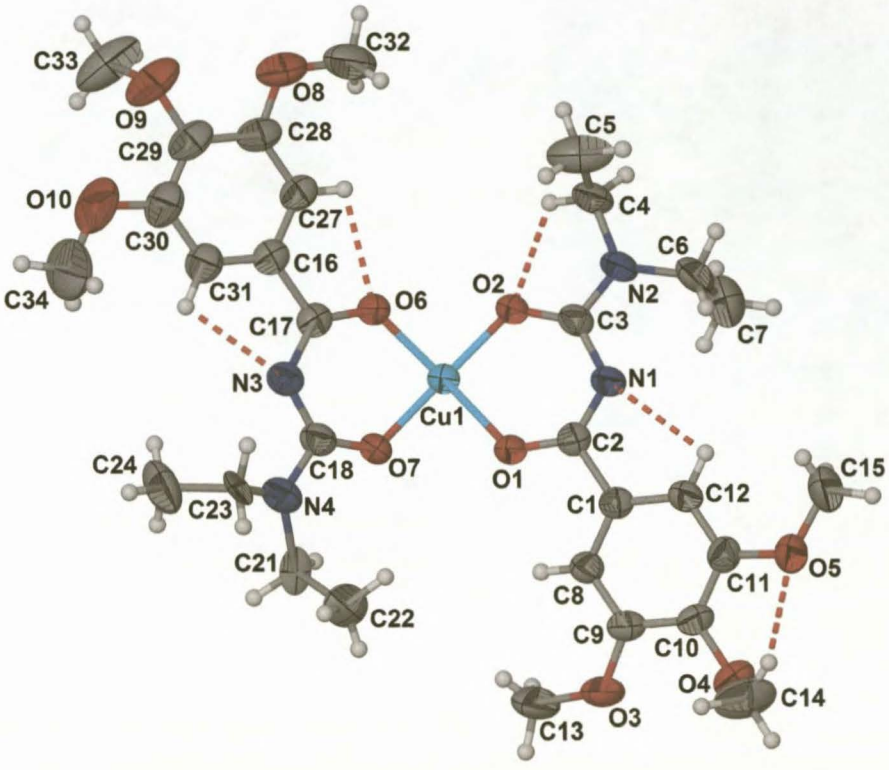

Figure 15 Molecular structure of **Cu(L^3-*O*,*O*)$_2$** showing the numbering scheme used. Displacement ellipsoids have been drawn at the 50% probability level. Intramolecular hydrogen contacts have been indicated. The observed disorder of groups C21 C22 and C23 C24 is not indicated.

The coordination around the copper atom is square-planar with copper deviating from the Cu1/O1/O2/O6/O7 least-squares plane by -0.101(1) Å. Each of the chelate rings are also planar, yet are twisted in towards the copper centre. The least-squares planes defined through O2/C3/N1/C2/O1 and O6/C17/N3/C18/O7 intersect the Cu1/O1/O2/O6/O7 least-squares plane at 9.43(0.1)° and 23.6(1)° respectively. The C16/C27-C31 and the C1/C8-C12 trimethoxy substituted phenyl rings are essentially coplanar with their respective C(O)NC(O) chelation moieties. However, both are twisted relative to the square planar coordination sphere of the copper by 9.4(1)° and 23.6(1)° respectively. The co-planarity of the two 3,4,5-trimethoxybenzoyl rings, C16/C27-C31 and C1/C8-C12, with the respective chelate rings is possibly assisted by the observed 1-4 intramolecular hydrogen contacts C12-H12...N1, C27-H27...O6, C31-H31...N3 [C12-H12...N1 2.43Å 100.3°, C27-H27...O6 2.41Å 99.6°, C31-H31...N3 2.44Å 100.2°] illustrated in Figure 15. The slightly greater degree of co-planarity of the C16/C27-C31 phenyl ring with the O6-C17-N3-C18 chelation moiety is possibly due to the second C27-H27....O6 hydrogen contact which was not observed between C8-H8 and O1.

The four *meta*-methoxy substituents are essentially co-planar with the respective aromatic rings as indicated by torsion angles C32-O8-C28-C27, C34-O10-C30-C31, C15-O5-C11-C12 and C13-O3-C9-C8 of 1.5(5)°, 7.4(6)°, 7.8(5)° and 5.3(5)° respectively. However, both *para*-methoxy substituents are almost perpendicular to the respective aromatic rings, C14-O4-C10-C11 = -81.7(4)°, C33-O9-C29-C30 = 85.3(5)°, presumably due to steric hindrance.

The four Cu-O bonds of **Cu(L^3-*O,O'*)$_2$** are essentially equivalent in length [Cu-O1 1.907(2)Å, Cu-O2 1.903(2)Å, Cu-O6 1.915(2)Å, Cu-O7 1.902(2)Å] thereby indicating that there is largely an equal degree of electron delocalization through these copper-oxygen bonds. The C3-N2 bond of the non-coordinated ligand, **H(L^3-*O,O'*)** [1.335(3)Å], remains largely unchanged in length upon complexation with the copper [C3-N2 1.337(3); C18-N4 1.340(4)Å] indicating that this bond retains a degree of partial double bond character and restricted rotation upon complexation.

Only one non-classical intermolecular hydrogen interaction C34-H343… $O4^{xi}$ is observed between molecules of **Cu(L^3-*O,O'*)$_2$** which results in molecules of **Cu(L^3-*O,O'*)$_2$** linking as one dimensional strings extending parallel to [100] as illustrated in Figure 16 [C34-H343… $O4^{xi}$ 2.57Å 142.3° symmetry code (xi) x-1, y, z]

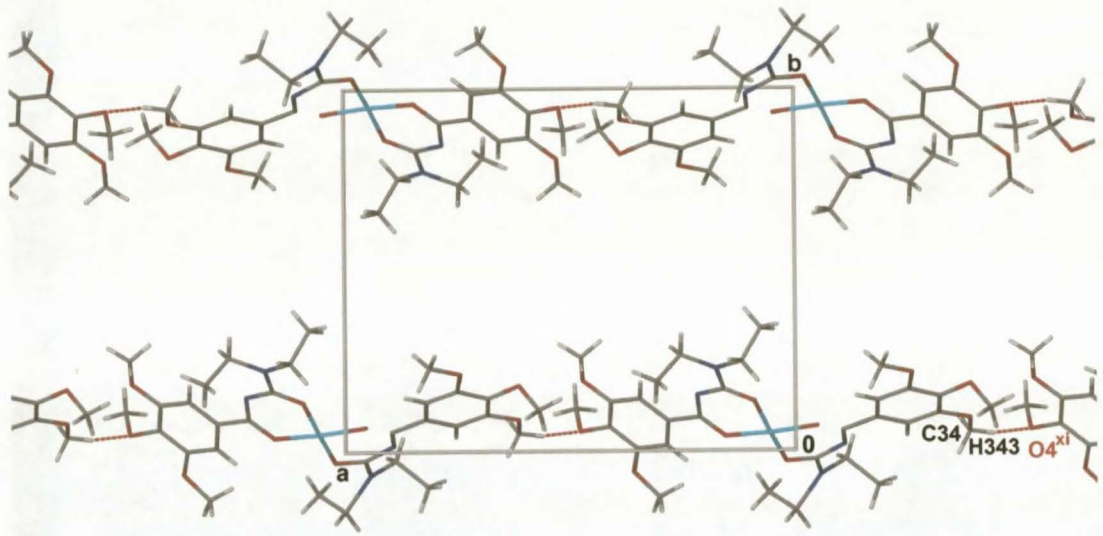

Figure 16 Partial unit cell of **Cu(L^3-*O,O'*)$_2$** as viewed along [001] illustrating the one dimensional chains extending parallel to [100] as a result of the non-classical intermolecular hydrogen contact C34-H343…$O4^{xi}$ [symmetry code (xi) x-1, y, z].

When viewed along [100], molecules of **Cu(L^3-*O,O'*)$_2$** pack in a twin herringbone fashion such that Cu1 of one molecule is aligned with $O6^{xii}$ [symmetry code (xii): -x, -y, -z] of an adjacent molecule, thereby allowing an intermolecular copper-oxygen electrostatic interaction, Cu1…$O6^{xii}$ 2.745(2)Å [Cu1…$Cu1^{xii}$ distance of 3.6804(7)Å], as illustrated in Figure 17. In turn, $Cu1^{xii}$ has the equivalent interaction with O6 of the original asymmetric unit. This copper-oxygen 'dimer' interaction results in the copper having a distorted pseudo-square pyramidal coordination sphere. This is possibly a contributing factor in the chelation rings of **Cu(L^3-*O,O'*)$_2$** being bent away from the 'dimer' partner as illustrated in Figure 18.

Interatomic copper(II)…oxygen interactions, such as those observed in **Cu(L^3-*O,O'*)$_2$** [Cu1…O6 2.745(2)Å], have been reported in the literature[27-29]. Intermolecular Cu-O…Cu linkages with intermolecular Cu…O2 distances of 3.311(2)Å were observed in the crystal lattice of bis(4-hexadecyloxytropolonato)copper(II)[30]. This interatomic interaction was determined as being a contributing factor to the occurrence of mesogenic versus non-mesogenic properties within a series of transition metal complexes investigated[30]. These intermolecular copper-oxygen interactions reported for bis(4-hexadecyloxytropolonato)copper(II) were also found to dominate the overall molecular packing[30] as appears to be the case for **Cu(L^3-*O,O'*)$_2$**.

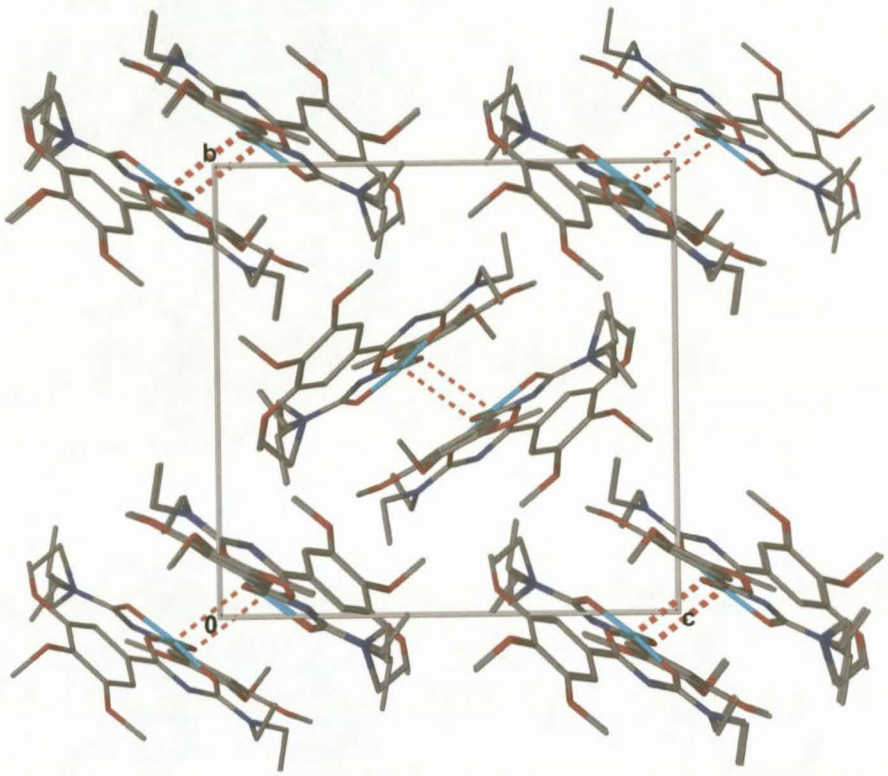

Figure 17 A perspective of the extended unit cell of **Cu(L^3-*O,O'*)$_2$** viewed along [100] illustrating the twin herring bone arrangement of the molecules as well as the intermolecular Cu1…O6^{xii} interactions [symmetry code (xii) -x, -y, -z]. All hydrogen atoms have been omitted for clarity.

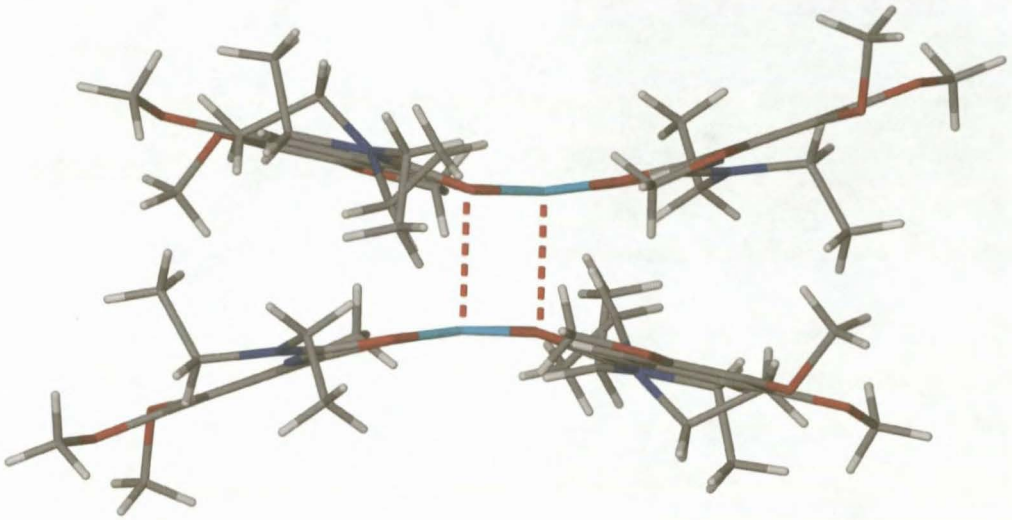

Figure 18 A side-on perspective of **Cu(L^3-*O,O*)$_2$** 'dimer' showing from the Cu1...O6 (symmetry code: -x, -y, -z) interactions. The resultant angling of the chelation ring away from the 'dimer' partner in towards the copper is clearly illustrated.

The most striking observation of **Cu(L^3-*O,O'*)$_2$**, by comparison to **Cu(L^1-*O,O'*)$_2$**, is the overall *trans*-(*O,O'*) or *anti*-(*O,O'*) orientation of the two ligands relative to one another. All copper(II) complexes reported in the literature derived from *N*-acyl(aroyl)thiourea ligands, barring one[19], are square-planar neutral bis chelates with essentially a *cis*-(*S,O*) arrangement of the ligator atoms around the copper atom[17, 18]. A single *trans*-(*S,O*) structure has been reported, *trans*-bis[*N,N*-diethyl-*N'*-(*p*-nitrobenzoyl)thioureato]copper(II)[19]. This preferred *cis*-(*S,O*) configuration for complexes derived from *N*-acyl(aroyl)thiourea chelates is also preferred by other metals such as nickel(II), palladium(II) and platinum(II)[17-19, 23] for which there is only one exception confirmed by X-ray structure analysis: *trans*-bis(*N*-naphthoyl-*N',N'*-dibutylthiourea)platinum(II) complex[31]. A comparable trend, with respect to the relative modes of coordination of ligands of the bis complexes of the *N*-acyl(aroyl)-*N, 'N'*-dialkylureas, can not be identified, as the only structure of this sort that has been characterised by means of single crystal X-ray structure analysis is that of tris-(*N*-benzoyl-*N',N'*-diethylureato)chromium(III)[20]. It is postulated that the relative *anti*-(*O,O'*) orientation of the ligands of **Cu(L^3-*O,O'*)$_2$** is thermodynamically more stable than the equivalent *syn*- or *cis*-(*O,O'*) complex due to the bulky nature of the three methoxy substituents on the benzoyl ring.

2.1.7 Bis(*N*-pivaloyl-*N'*,*N'*-diethylthioureato)copper(II), Cu(L^4-*S*,*O*)$_2$.

The single crystal structures of **Cu(L^4-*S*,*O*)$_2$** and **Ni(L^4-*S*,*O*)$_2$** have both recently been reported in the general literature, but the X-ray structure of **Cu(L^4-*S*,*O*)$_2$** and **Ni(L^4-*S*,*O*)$_2$** had not yet been reported in the literature at the time that the work reported on here was carried out. The X-ray structures of **Cu(L^4-*S*,*O*)$_2$** and **Ni(L^4-*S*,*O*)$_2$** reported by Hernández *et al.* were not the focus of the article nor were they discussed in any significant detail[18, 32]. Rather, the molar enthalpies of formation and sublimation were determined and used to derive the molar enthalpies of formation in the gaseous phase, which in turn were used to evaluate the difference between the mean metal–ligand and hydrogen-ligand bond dissociation enthalpies. For this reason, and for purposes of comparison to structures **Cu(L^2-*O*,*O*)$_2$** and **Cu(L^3-*O*,*O*)$_2$**, the X-ray crystal structures of **Cu(L^4-*S*,*O*)$_2$** and **Ni(L^4-*S*,*O*)$_2$** were determined and are reported here.

The coordination of the ligand to the metal in **Cu(L^4-*S*,*O*)$_2$** is in a *cis*-bis-(*S*,*O*) fashion as illustrated in Figure 19. The coordination around the copper is square planar with O1 deviating from the S1/O1/O2/S2/Cu1 least-squares plane by 0.162(2)Å. Each of the chelate moieties of the two ligands in **Cu(L^4-*S*,*O*)$_2$** are planar with the greatest deviation from planarity from the S1/C3/N1/C2/O1 and S2/C13/N3/C12/O2 least-squares planes being C2 and C13 by -0.119(3)Å and -0.131(2)Å respectively. However, in contrast to that observed for **Cu(L^2-*O*,*O*)$_2$** [see Figure 12], the molecule of **Cu(L^4-*S*,*O*)$_2$**, as a whole, is significantly distorted from overall planarity, with each ligand being twisted away from perfect square planarity in opposite directions relative to one another, as is evident when the molecule is viewed side-on as illustrated in Figure 20. This is further indicated by the fact that the S1/C3/N1/C2/O1 and S2/C13/N3/C12/O2 least-squares planes intersect each other at 16.4(2)°.

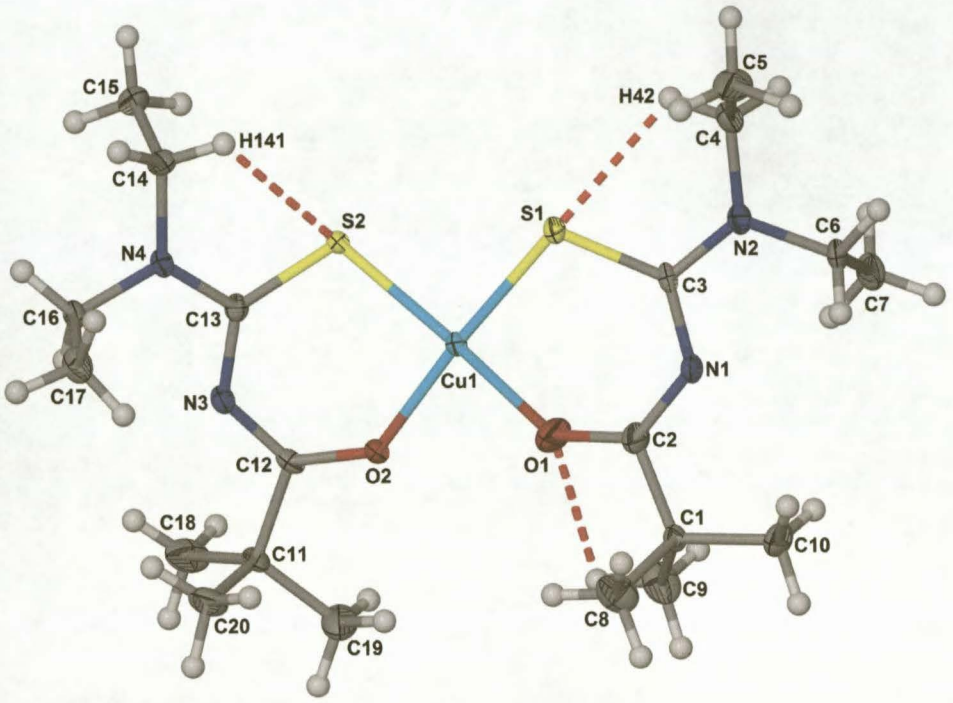

Figure 19 The molecular structure of **Cu(L^4-*S,O*)$_2$** showing with the numbering scheme used. Displacement ellipsoids are drawn at the 50% probability level. Intramolecular hydrogen contacts C4-H42...S1, C9-H91...O1 and C14-H141...S2 have been indicated.

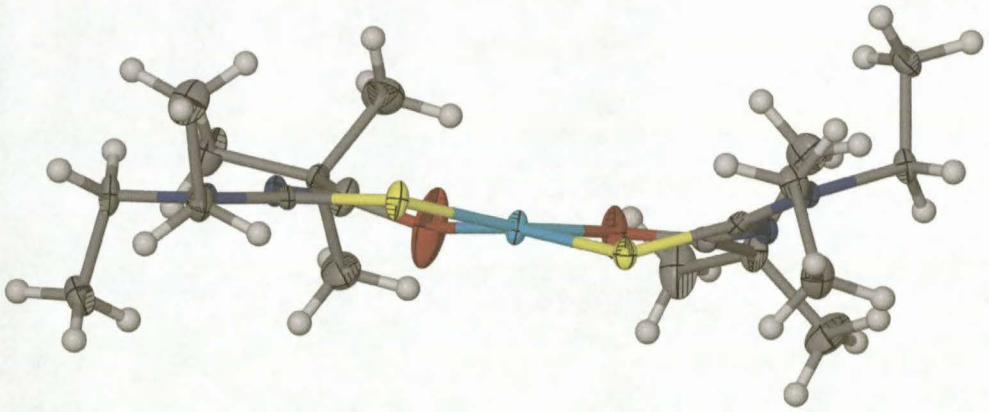

Figure 20 A side-on view of **Cu(L^4-*S,O*)$_2$** showing the significant twisting in opposite directions of each of the coordinating ligands.

All bond lengths, with particular reference to the C-N bonds of interest within the chelation ring of **Cu(L^4-*S,O*)$_2$** [C2-N1 1.296(5)Å, C3-N1 1.339(5)Å, C12-N3 1.331(5)Å, C13-N3 1.342(5)Å], appear to be within expected ranges typical of *N*-acyl-*N'*,*N'*-dialkyl thiourea complexes of this type. There has been a significant shortening in the length of bonds C2-N1 and N1-C3 as well as a lengthening of

bonds S1-C3 and O1-C2 of the uncoordinated free ligand **H(L^4-*S,O*)** upon deprotonation and complexation to the copper metal [**H(L^4-*S,O*)** C2-N1 1.352(2)Å, C3-N1 1.435(1)Å, S1-C3 1.662(1)Å, O1-C2 1.232(1)Å; **Cu(L^4-*S,O*)$_2$** C2-N1 1.296(5)Å, C3-N1 1.339(5)Å, C12-N3 1.331(5)Å, C13-N3 1.342(5)Å, S1-C3 1.754(3)Å, O1-C2 1.258(5)Å, C13-S2 1.746(4)Å, C12-O2 1.246(5)Å]. Clearly the bond orders of the thiocarbonyl and carbonyl bonds decrease upon complexation to the copper, together with a significant increase in the bond orders of the two C-N bonds of interest within the chelation ring, thereby confirming extensive electron delocalisation through the respective chelate rings of complex **Cu(L^4-*S,O*)$_2$**. Similar to that observed in the crystal structures of complexes **Cu(L^2-*O,O*)$_2$** and **Cu(L^3-*O,O*)$_2$**, the bond length of C2-N1 of **Cu(L^4-*S,O*)$_2$** [C2-N1 1.296(5)Å] remains significantly shorter upon complexation to copper than bond N1-C3 [1.339(5)Å], however, bonds C12-N3 and N3-C13 of **Cu(L^4-*S,O*)$_2$** are of comparative length [N3-C12 1.331(5)Å; N3-C13 (1.342(5)Å]. Furthermore, the bond length of bond C3-N2 in the uncoordinated ligand **H(L^4-*S,O*)** [C3-N2 1.334(2)Å] remains largely unchanged upon complexation to the copper [**Cu(L^4-*S,O*)$_2$** C3-N2 1.338(4)Å, C13-N4 1.331(5)Å] thereby retaining a degree of partial double bond character and a degree of restricted rotation around this bond.

No intermolecular hydrogen bonding was observed in the crystal lattice of complex **Cu(L^4-*S,O*)$_2$**. However three intramolecular hydrogen contacts were observed C4-H42…S1, C9-H91…O1 and C14-H141…S2 [C4-H42…S1 2.50Å 109.6°, C9-H91…O1 2.42Å 100.0° and C14-H141…S2 2.55Å 105.8°] It is proposed that the intramolecular hydrogen contacts C4-H42…S1 and C14-H141…S2 assist in bringing atoms C4 and C14 into closer coplanarity to the respective chelation rings. C4 and C14 deviate from the S1/C3/N1/C2/O1 and S2/C13/N3/C12 least-squares planes of the respective chelate rings by 0.457(7)Å and -0.682(6)Å respectively.

2.1.8 Bis(*N*-pivaloyl- *N'*,*N'*-diethylthioureato)nickel(II), Ni(L^4-*S,O*)$_2$

Complex **Ni(L^4-*S,O*)$_2$** crystallizes in monoclinic space group $P2_1$ with a *cis*-(*S,O*) arrangement of the ligature atoms as illustrated in Figure 21. The coordination of the two ligands is in a strict square planar fashion around the nickel centre with Ni1 deviating from the Ni1/S1/S2/O1/O2 least-squares plane by -0.0061(8)Å. The coordination around Ni1 conforms the closest to perfect planarity in comparison to complexes **Cu(L^2-*O,O*)$_2$**, **Cu(L^3-*O,O*)$_2$** and **Cu(L^4-*S,O*)$_2$**.

When **Ni(L^4-S,O)$_2$** is viewed side-on, as is illustrated in Figure 22, it is clearly illustrated that each of the ligands of **Ni(L^4-S,O)$_2$** are bent away in opposite directions from the coordination sphere of the nickel. The S1/C3/N1/C2/O1 and O1/O2/S2/S1 least-squares planes intersect at 10.2(1)° while the S2/C13/N3/C12/O2 and O1/O2/S2/S1 least-squares planes intersect at 19.4(1)°.

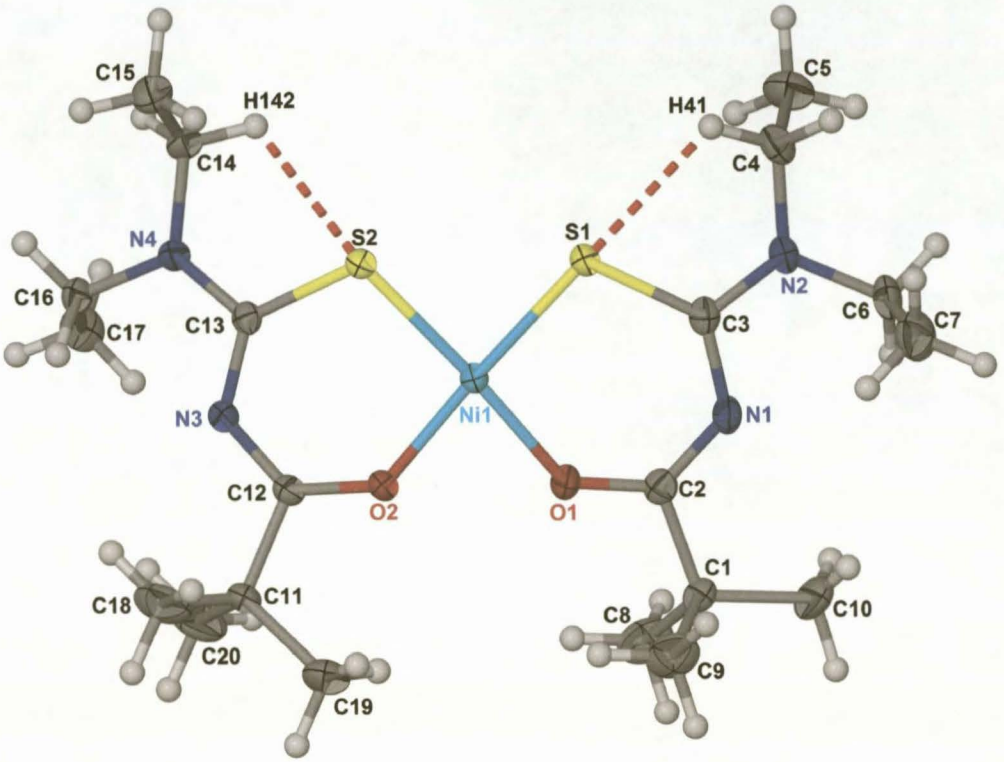

Figure 21 Molecular structure of complex **Ni(L^4-*S*,*O*)$_2$** showing the numbering scheme used. Displacement ellipsoids are drawn at the 50% probability level. Intramolecular hydrogen contacts C4-H41...S1 and C14-H142...S2 have been indicated.

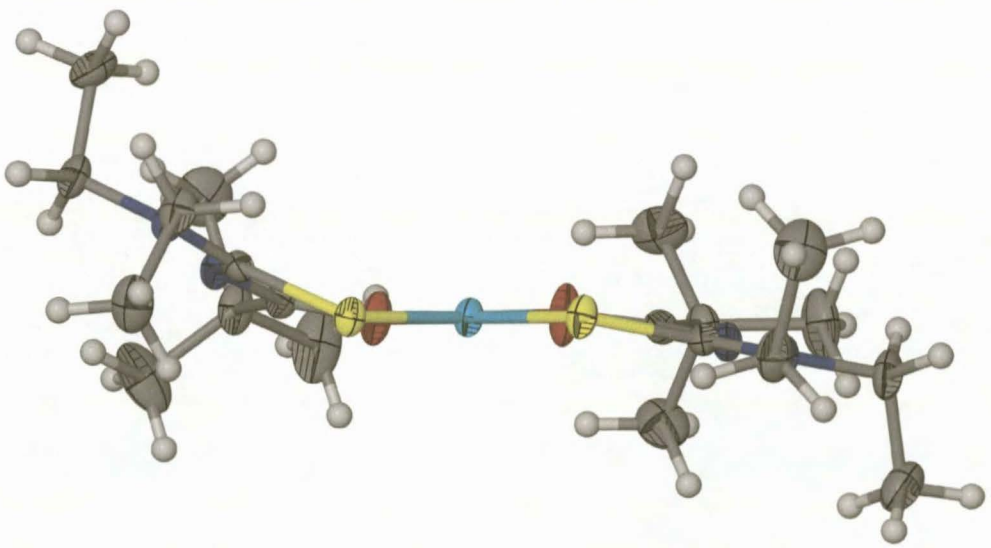

Figure 22 A side-on view of **Ni(L^4-*S*,*O*)$_2$** indicating how each of the ligands is bent away in opposite directions from the coordination sphere of the nickel.

All the bond lengths of interest in complex **Ni(L^4-*S,O*)$_2$** are in the expected ranges. There has been a significant shortening of bonds C2-N1 and C3-N1 of the non-coordinated ligand **H(L^4-*S,O*)** [C2-N1 1.352(2)Å; C3-N1 [1.435(1)Å)] upon complexation with the nickel [**Ni(L^4-*S,O*)$_2$** C2-N1 1.305(3)Å, C3-N1 1.344(3)Å and C12-N3 1.323(3)Å, C13-N3 1.333(3)Å] leading to the decrease of the bond orders of the thiocarbonyl and carbonyl groups [**H(L^4-S,O)** C3-S1 1.662(1)Å, C2-O1 1.232(1)Å; **Ni(L^4-*S,O*)$_2$** C3-S1 1.748(2)Å, C2-O1 1.259, C13-S2 1.751(2)Å C12-O2 1.252(3)Å]. The bond length of N1-C2 in **Ni(L^4-*S,O*)$_2$** is significantly shorter than N1-C3 [N1-C2 1.305(3)Å; N1-C3 1.344(3)Å], however, bond N3-C13 is comparable in length to N3-C12 [(N3-C13 1.333(3)Å; N3-C12 1.323(3)Å] similar to that observed in complex **Cu(L^4-*S,O*)$_2$**. The bond length of bond C3-N2 in the uncoordinated ligand **H(L^4-*S,O*)** [C3-N2 1.334(2)Å] remains largely unchanged upon complexation [**Ni(L^4-*S,O*)$_2$** C3-N2 1.332(3)Å, C13-N4 1.333(3)Å] thereby indicating the retention of its partial double bond character and the restricted rotation around this bond.

Intramolecular hydrogen contacts were observed between C4-H41...S1 and C14-H142...S2 [C4-H41...S1 2.52Å; C14-H142...S2 2.55Å] which appear to have little to no effect on the packing of the molecules of **Ni(L^4-*S,O*)$_2$** within the unit cell. The individual molecules of **Ni(L^4-*S,O*)$_2$** essentially pack in a herringbone fashion when viewed along [001] as illustrated in Figure 23. It is proposed that the C4-H41...S1 intramolecular contact assists in bringing atom C4 into closer coplanarity with the S1-C3-N1-C2-O1 chelation moiety thereby deviating from the S1/C3/N1/C2/O1 least-squares plane by -0.043(4)Å. However, despite the C14-H142...S2 hydrogen contact, atom C14 remains significantly out of plane with the S2-C13-N3-C12-O2 chelate moiety and deviates from the S2/C13/N3/C12/O2 least-squares plane by 1.154(3)Å.

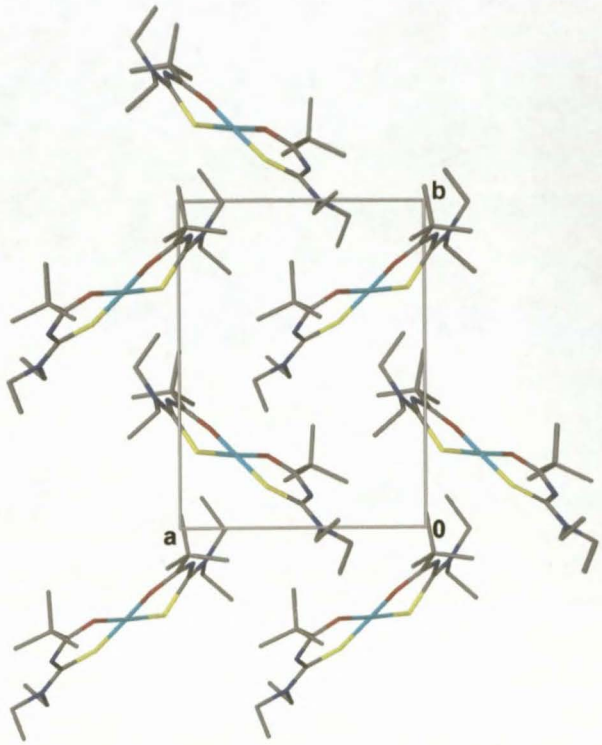

Figure 23 The unit cell of **Ni(L^4-*S,O*)$_2$** as viewed along [001]. All hydrogen atoms have been omitted for clarity.

H(L^1-*O,O'*)		**H(L^3-*O,O'*)**		**H(L^4-*S,O*)**	
C2-O1	1.219(3)	C2-O1	1.219(2)	C2-O1	1.2319(14)
C2-N1	1.376(3)	C2-N1	1.381(2)	C2-N1	1.3516(15)
N1-C3	1.408(3)	N1-C3	1.414(2)	N1-C3	1.4345(14)
C3-O2	1.240(3)	C3-O2	1.233(2)	C3-S1	1.6622(12)
C3-N2	1.345(3)	C3-N2	1.335(3)	C3-N2	1.3339(15)
Torsion Angles					
O1-C2-N1-C3	0.7(4)	O1-C2-N1-C3	-8.6(3)	O1-C2-N1-C3	-0.28(17)
C2-N1-C3-O2	-127.1(3)	C2-N1-C3-O2	-120.1(2)	C2-N1-C3-S1	-84.49(13)

H(L^2-*O,O'*)							
A		**B**		**C**		**D**	
C2-O1	1.215(3)	C10-O3	1.214(3)	C18-O5	1.213(3)	C26-O7	1.216(3)
C2-N1	1.374(3)	C10-N3	1.375(3)	C18-N5	1.372(3)	C26-N7	1.382(3)
N1-C3	1.415(3)	N3-C11	1.419(3)	N15-C19	1.417(3)	N7-C27	1.415(3)
C3-O2	1.232(3)	C11-O4	1.227(3)	C19-O6	1.236(3)	C27-O8	1.233(3)
C3-N2	1.331(3)	C11-N4	1.335(3)	C19-N6	1.331(3)	C27-N8	1.337(3)
Torsion Angles							
O1-C2-N1-C3	7.7(3)	O3-C10-N3-C11	5.9(3)	O5-C18-N5-C19	10.6(3)	O7-C26-N7-C27	1.1(3)
C2-N1-C3-O2	118.1(2)	C10-N3-C11-O4	119.3(2)	C18-N5-C19-O6	118.0(2)	C26-N7-C27-O8	120.4(2)

Table 2 Selected bond lengths and torsion angles for non-coordinated ligands **H(L^1-*O,O'*)**, **H(L^2-*O,O'*)**, **H(L^3-*O,O'*)** and **H(L^4-*S,O*)** as determined by single crystal X-ray structural analysis with s.u.s in parenthesis.

$Cu(L^1\text{-}O,O')_2$		$Cu(L^3\text{-}O,O')_2$				$Ni(L^4\text{-}S,O)_2$				$Cu(L^4\text{-}S,O)_2$			
C2-O1	1.274(4)	C2-O1	1.266(3)	C17-O6	1.267(3)	C2-O1	1.259(3)	C12-O2	1.252(3)	C2-O1	1.258(5)	C12-O2	1.246(5)
C2-N1	1.297(5)	C2-N1	1.304(3)	C17-N3	1.321(4)	C2-N1	1.305(3)	C12-N3	1.323(3)	C2-N1	1.296(5)	C12-N3	1.331(5)
N1-C3	1.357(5)	N1-C3	1.362(3)	N3-C18	1.360(3)	N1-C3	1.344(3)	N3-C13	1.333(3)	N1-C3	1.339(5)	N3-C13	1.342(5)
C3-O2	1.271(4)	C3-O2	1.263(3)	C18-O7	1.245(4)	C3-S1	1.748(2)	C13-S2	1.751(2)	C3-S1	1.754(3)	C13-S2	1.746(4)
C3-N2	1.339(5)	C3-N2	1.337(3)	C18-N4	1.340(4)	C3-N2	1.332(3)	C13-N4	1.333(3)	C3-N2	1.338(4)	C13-N4	1.331(5)
Cu-O1	1.881(3)	Cu-O1	1.9073(17)	Cu-O6	1.9149(17)	Ni-O1	1.8498(15)	Ni-O2	1.8621(15)	Cu-O1	1.898(3)	Cu-O2	1.925(3)
Cu-O2	1.902(3)	Cu-O2	1.9038(19)	Cu-O7	1.902(2)	Ni-S1	2.1486(15)	Ni-S2	2.1495(16)	Cu-S1	2.2354(10)	Cu-S2	2.2340(9)

Table 3 Selected bond lengths and torsion angles of complexes $Cu(L^1\text{-}O,O')_2$, $Cu(L^3\text{-}O,O')_2$, $Ni(L^4\text{-}S,O)_2$ and $Cu(L^4\text{-}S,O)_2$ as determined by single crystal X-ray structural analysis with s.u.s in parenthesis.

	Type	D-H...A	D-H (Å)	H...A (Å)	D...A (Å)	D-H...A (°)
H(L^1-*O,O'*)	Inter	N1---H1...O2^{i}	0.88	2.19	2.925(3)	141.3
	Inter	C4---H42...O^{ii}2	0.99	2.48	3.457(3)	168.5
	Intra	C5---H51...O1	0.98	2.42	3.112(3)	127.7
H(L^2-*O,O'*)	Inter	C4---H42...O1^{iii}	0.98	2.50	3.464(3)	169.8
	Inter	C12---H123...O7^{iv}	0.98	2.55	3.516(3)	168.9
	Inter	C21---H211...O1^{v}	0.98	2.56	3.419(3)	145.7
	Inter	C24---H241...O3^{vi}	0.98	2.43	3.414(3)	177.6
	Inter	C28---H282...O4^{vii}	0.98	2.58	3.517	159.0
	Intra	N1---H1...O4	0.88	2.09	2.862(2)	146.1
	Intra	N3-H3...O2	0.88	2.08	2.858(2)	146.8
	Intra	N5---H5...O8	0.88	2.13	2.851(2)	138.5
	Intra	N7---H7...O6	0.88	2.10	2.870(2)	146.1
	Intra	C30---H301...O6	0.98	2.57	3.500(3)	159.6
	Intra	C14---H142...O2	0.98	2.58	3.505(3)	157.8
	Intra	C14---H141...O5	0.98	2.50	3.444(3)	161.2
H(L^3-*O,O'*)	Inter	N1---H1...O2^{viii}	0.88	2.16	2.903(2)	141.5
	Inter	C14---H141...O2 ^{viii}	0.95	2.59	3.286(2)	130.1
	Inter	C17---H172...O1^{ix}	0.98	2.55	3.353(3)	138.9
H(L^4-*S,O*)	Inter	N1---H1...O1^{x}	0.86	2.00	2.8492(13)	170.5
	Inter	C7---H73...O1^{x}	0.96	2.51	3.4561(16)	169.4
	Inter	C9---H92...O1^{x}	0.96	2.57	3.4402(16)	150.8

Symmetry codes : (i) 1-x, 1-y, -z; (ii) x, ½-y, -½+z; (iii) 2-x, 2-y, -z; (iv) 1-x, ½+y, ½-z; (v) 1-x, 1-y, -z; (vi) x-1, y, z; (vii) x-1, y-1, z; (viii) 2-x, 1-y, 2-z; (ix) x-½, ½-y, z-½; (x) x+½, y, ½-z.

Table 4 Inter -and intramolecular hydrogen bonding and hydrogen contact geometry for non-coordinated ligands **H(L^1-*O,O'*)**, **H(L^2-*O,O'*)**, **H(L^3-*O,O'*)** and **H(L^4-*S,O*)** as identified by XSeed[33, 34] and Platon[35] with s.u.s of the donor...acceptor [D...A] distances (Å) in parenthesis.

	Type	D-H...A	D-H (Å)	H...A (Å)	D...A (Å)	D-H...A (°)
Cu(L^2-*O,O'*)$_2$	Intra	C7---H72...O1	0.96	2.43	2.759(9)	99.9
	Intra	C8---H83...O1	0.96	2.52	2.840(9)	99.7
Cu(L^3-*O,O'*)$_2$	Intra	C12---H12...N1	0.93	2.43	2.750(3)	100.3
	Intra	C27---H27...O6	0.93	2.41	2.721(3)	99.6
	Intra	C31---H31...N3	0.93	2.44	2.758(4)	100.2
	Intra	C4---H41...O2	0.97	2.33	2.683(4)	100.6
	Intra	C14---H141...O5	0.96	2.59	3.104(5)	113.7
	Inter	C34---H343...O4[xi]	0.96	2.57	3.385(5)	142.3
Cu(L^4-*S,O*)$_2$	Intra	C4---H42...S1	0.97	2.50	2.973(4)	109.6
	Intra	C9---H91...O1	0.96	2.42	2.757(6)	100.0
	Intra	C14---H141...S2	0.97	2.55	2.970(4)	105.8
Ni(L^4-*S,O*)$_2$	Intra	C4---H41...S1	0.99	2.52	2.981(3)	108.0
	Intra	C14---H142...S2	0.99	2.55	2.980(2)	105.8

Symmetry codes: (xi) x-1, y, z.

Table 5 Inter -and intramolecular hydrogen bonding and hydrogen contact geometry for structures **Cu(L^2-*O,O*)$_2$**, **Cu(L^3-*O,O*)$_2$**, **Cu(L^4-*S,O*)$_2$** and **Ni(L^4-*S,O*)$_2$** as identified by XSeed[33, 34] and Platon[35] with s.u.s of the donor...acceptor [D...A] distances (Å) in parenthesis.

2.1.9 Comparison of the crystal structures Cu(L^4-*S,O*)$_2$ and Ni(L^4-*S,O*)$_2$ with the literature reported crystal structures thereof.

When the work discussed in section 2.1 of chapter V commenced, the crystal structures of H(L^4-*S,O*), Cu(L^4-*S,O*)$_2$ and Ni(L^4-*S,O*)$_2$ had not yet been listed on the Cambridge Structural Database (CSD)[17, 18]. The crystal structures of H(L^4-*S,O*), Cu(L^4-*S,O*)$_2$ and Ni(L^4-*S,O*)$_2$ were obtained in order to allow a comparison of the molecular structures in the solid state of the non-coordinated ligand H(L^4-*S,O*), and the resultant complexes, Cu(L^4-*S,O*)$_2$ and Ni(L^4-*S,O*)$_2$ to the equivalent non-coordinated bidentate-*O,O* ligands H(L^1-*O,O'*), H(L^2-*O,O'*) and H(L^3-*O,O'*) and the resultant copper complexes Cu(L^2-*O,O*)$_2$ and Cu(L^3-*O,O*)$_2$. However, while the experimental work in this area was being conducted, the crystal structures of H(L^4-*S,O*), Cu(L^4-*S,O*)$_2$ and Ni(L^4-*S,O*)$_2$ were subsequently reported by Ribeiro da Silva *et al.*[22]. The reported values of interest are listed in Table 6 along with the values of the equivalent bond lengths as determined by ourselves.

Bond	H(L^4-*S,O*)	[i]HPVET[22]	Cu(L^4-*S,O*)$_2$	Ni(L^4-*S,O*)$_2$	[ii]Cu(PVET)$_2$[22]	[iii]Ni(PVET)$_2$[22]
C2-O1	1.232(1)	1.228(2)	1.258(5)	1.259(3)	1.243(4)	1.243(6)
C2-N1	1.352(2)	1.359(2)	1.296(5)	1.305(3)	1.322(5)	1.328(6)
N1-C3	1.435(1)	1.433(2)	1.339(5)	1.344(3)	1.337(4)	1.345(5)
C3-S1	1.662(1)	1.672(2)	1.754(3)	1.748(2)	1.742(3)	1.735(4)
C3-N2	1.334(2)	1.323(2)	1.338(5)	1.332(3)	1.339(4)	1.348(6)
C12-O2			1.246(5)	1.252(3)	1.232(5)	1.254(6)
C12-N3			1.331(5)	1.323(3)	1.299(5)	1.312(6)
N3-C13			1.342(5)	1.333(3)	1.352(5)	1.351(6)
C13-S2			1.746(4)	1.751(2)	1.736(4)	1.733(5)
C13-N4			1.331(5)	1.333(3)	1.355(4)	1.350(6)
Cu-O1			1.898(3)		1.928(3)	
Cu-O2			1.925(3)		1.899(3)	
Cu-S1			2.235(1)		2.236(1)	
Cu-S2			2.234(1)		2.228(1)	
Ni-O1				1.850(2)		1.870(3)
Ni-O2				1.862(2)		1.849(3)
Ni-S1				2.149(2)		2.151(1)
Ni-S2				2.150(2)		2.146(1)

Table 6 Comparison of observed bond lengths in the single crystal structures of H(L^4-*S,O*), Cu(L^4-*S,O*)$_2$ and Ni(L^4-*S,O*)$_2$ with the values of the equivalent bonds reported by Ribeiro *et al.*[22]. All bond lengths are in Angstrom units with s.u.s in parenthesis.

The values of the bond lengths of interest reported by Ribeiro da Silva *et al.* for H(L^4-*S,O*), Cu(L^4-*S,O*)$_2$ and Ni(L^4-*S,O*)$_2$ compare favourably with the values determined by ourselves.

[i] HPVET : *N*-pivaloyl-*N'*,*N'*-diethylthiourea
[ii] Cu(PVET)$_2$: bis(*N*-pivaloyl-*N'*,*N'*-diethylthiourea)copper(II)
[iii] Ni(PVET)$_2$: bis(*N*-pivaloyl-*N'*,*N'*-diethylthiourea)nickel(II)

2.1.10 Tetrakis(μ_2-2,2-dimethylpropanoato-κ^2 *O,O'*)-bis(pyridine-κ*N*)copper(II), $Cu_2(C_5H_9O_2)_4(C_5H_5N)_2$[36].

As part of the systematic investigation into the new class of *N*-acyl-*N'*,*N'*-dialkylurea ligands and their coordination chemistry to copper(II), the compound tetrakis(μ_2-2,2-dimethylpropanoato-κ^2 *O,O'*)-bis(pyridine-κ*N*)copper(II) $\mathbf{Cu_2(C_5H_9O_2)_4(C_5H_5N)_2}$, arose as an unexpected product from the bi-phasic reaction of copper(II) perchlorate hexahydrate with *N*-pivaloyl-*N'*,*N'*-dimethylurea in the presence of pyridine during an attempt to isolate crystals of $\mathbf{Cu(L\text{-}\mathit{O,O'})_2}$ (HL = *N*-pivaloyl-*N'*,*N'*-dimethylurea). The compound, $\mathbf{Cu_2(C_5H_9O_2)_4(C_5H_5N)_2}$ consists of centrosymmetric, binuclear cage units with four dimethylpropanato bridges linking the two Cu centres [Cu...Cu = 2.6229(9)Å]. The square pyramidal copper coordination is completed by a pyridine N atom at the apical site. A π...π stacking interaction between adjacent pyridine molecules helps to consolidate the crystal packing. Presumably this 'lantern-type' dimeric copper complex results from the hydrolysis of the *N*-pivaloyl-*N'*,*N'*-dimethylurea under the reaction conditions used (see section 3.5.10).

The first copper(II) carboxylate-bridge dimer was reported as early as 1953[37] and numerous related compounds have been synthesised and structurally characterised since[17]. The synthesis and structural characterisation of a significant number of copper(II) carboxylate monoadduct complexes[17, 38] of the type $[LCu(OOCR)_2]_2$ published in the literature largely resulted from an effort to determine the factors influencing the magnitude of intermolecular magnetic exchange interaction that occurs between the two copper atoms in compounds of this type[39]. A further area of research which resulted in the structural characterisation of copper(II) carboxylate dimers is the potential use of these compounds as building blocks in combination with linkage ligands for oligonuclear or polynuclear formation[40].

Early reports of X-ray studies of dimers of $[LCu(OOCR)_2]_2$, where L is a substituted pyridine ligand, suggested that the introduction of an α-substituent onto L (e.g. L = α-picoline and quinoline) noticeably affected the dimer structures[41]. The effect of the α-substituent onto L usually included a large displacement of the copper atoms from the basal planes containing the four oxygen atoms resulting in an increase in the Cu...Cu distances[41, 42]. It was further stated that a steric hindrance addition to one or more of the ligands, L, make the dimer 'lantern-type' structure $[LCu(OOCR)_2]_2$ more favourable/feasible than the monomeric or polymeric structures of the type $[L_2M(OOCR)_2]_n$[41, 43]. Kirillova *et al.* and Pasynskii *et al.* further stated that with an increase of electron density on M due to the presence of strong electron donor groups, such as R = *tert*-butyl groups, as substituents on the carboxylate ligand, the formation of $LM(OOCR)_2$ fragments rather than $L_2M(COOR)_2$ would be favoured[41, 44]. It appears that Kirillova *et al.* were only successful in obtaining the 'lantern-type' dimer of Cu(II) with R = *tert*-butyl when L = γ-picoline was used as ligand[41]. In summary, Kirillova *et al.* concluded that both the presence of α-substituents on the pyridine rings and the presence of electron donating groups on the carboxylato ligands were required as stabilizing factors for the formation of dimers of the type $[LCu(OOCR)_2]_2$[41].

The crystals of $Cu_2(C_5H_9O_2)_4(C_5H_5N)_2$ are triclinic, P$\bar{1}$, and contain only one molecule per unit cell. The binuclear cage units have four dimethylpropanato bridges linking the two copper centres. The coordination geometry around the copper atoms is slightly distorted square-pyramidal, with the four oxygen atoms of the bridging carboxylate groups in the basal plane and the nitrogen of the pyridine in the apical position. The molecular structure of $Cu_2(C_5H_9O_2)_4(C_5H_5N)_2$ is illustrated in Figure 24 showing the numbering scheme used. Selected bond lengths and bond angles are listed in Table 7.

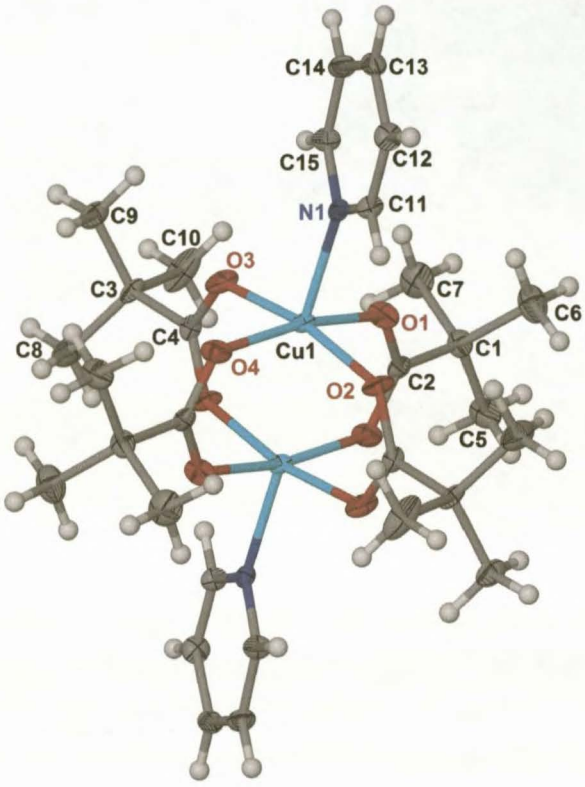

Figure 24 Molecular structure of $Cu_2(C_5H_9O_2)_4(C_5H_5N)_2$ showing 50% displacement ellipsoids as well as the numbering scheme used. The unlabelled atoms are generated by 1-x, 1-y, 1-z from the asymmetric atoms.

Of interest in the molecular structure of $Cu_2(C_5H_9O_2)_4(C_5H_5N)_2$ is the close proximity of the copper atoms [Cu1…Cu1[i] 2.6229(9)Å]. In comparative 'lantern-type' dimeric copper complexes, in which axial ligands are absent, such as $Cu_2(PhN_3Ph)_4$, a direct copper-copper bond of 2.44Å was observed[41, 45]. In the case of $Cu_2(PhN_3Ph)_4$, the axial positions are spatially blocked by the phenyl groups[41, 45]. The interatomic copper distance of 2.6229(9)Å observed for $Cu_2(C_5H_9O_2)_4(C_5H_5N)_2$ is significantly longer than the Cu…Cu' distance of 2.584(4)Å reported for $Cu_2(piv)_4(pyz)_2$ (Hpiv = pivalic acid, pyz = pyrazine)[46] but significantly shorter than the Cu…Cu' distance of 2.681(1)Å reported for $Cu_2(piv)_4(Et_3N)_2$[40]. The interatomic copper distance of $Cu_2(C_5H_9O_2)_4(C_5H_5N)_2$ of 2.6229(9)Å is also shorter than the values reported for several comparative neutral dimeric copper(II) carboxylate

[i] symmetry code (i) 1-x, 1-y, 1-z

compounds evaluated by Moreland and Doedens[39] who reported these compounds as having interatomic Cu...Cu distances in the range of 2.652 - 2.886Å[39, 41, 47]. Nevertheless, the longer Cu1...Cu1^{i} distance observed for **$Cu_2(C_5H_9O_2)_4(C_5H_5N)_2$** is similar to the average of 2.66(5)Å for the reported interatomic copper-copper distances of the 447 structures of dimeric copper (II) centres bridged by carboxylate ligands listed on version 5.26 of the Cambridge Structural Database (CSD)[17].

The copper atoms in **$Cu_2(C_5H_9O_2)_4(C_5H_5N)_2$** are displaced towards the pyridine molecules from the basal O1-O2-O3-O4 plane by 0.200(1)Å. As previously stated above, the degree of displacement of the copper atoms from the basal plane and the resulting interatomic copper-copper distances have previously been reported as being related to the degree of steric hindrance on both the apical substituents as well as the R-groups on the carboxylate bridges[40, 48]. The steric impact of the ligands in the apical positions of complexes of this type has been reported as being significant enough whereby the typical square-pyramidal coordination geometry around the copper can be distorted toward trigonal bipyramidal[48].

The Cu-N bond length [2.153(3)Å] in **$Cu_2(C_5H_9O_2)_4(C_5H_5N)_2$** is significantly shorter than the comparative Cu-N bond length of 2.360(3)Å reported for the structurally analogous tetrakis(μ_2-2,2-dimethylpropanoato-O,O')-bis(2,6-dimethylpyridine-N)-dicopper(II)[48]. Kirillova *et al.* proposed that in general an increase in electron density on the copper atoms, due to the electron releasing property of the *tert*-butyl groups on the carboxylate bridges, would most likely weaken the pyridine-copper donor-acceptor interaction. This hypothesis is supported by the copper-nitrogen bond lengths in [C_7H_8N-$Cu(OOCR)_2]_2$ which decreased from 2.224Å to 2.107Å on replacing R = CH_3 with CF_3 which was accompanied by an increase in the Cu...Cu distance from 2.652 to 2.886Å[41]. Interestingly in **$Cu_2(C_5H_9O_2)_4(C_5H_5N)_2$**, the Cu-N bond length remains relatively short despite the presence of the *tert*-butyl groups on the carboxylate bridges.

The chelation rings of the bridging carboxylate groups are almost planar, with Cu1 deviating from the C2/O1/O4 least-squares plane by -0.022(2)Å and from the C4/O3/O2 least squares plane by 0.0362(2)Å. In turn, the planar axial pyridine substituents are twisted away from these planes, with the N1/C11-C15 least-squares plane of the pyridine ring intersecting the C2/O1/O4 and the C4/O3/O2 least-squares planes by 66.1(2)° and 23.5(2)° respectively. The overall symmetry of the complex results in the Cu1-N1 bond being almost co-linear with the Cu1...Cu1^{i} axis [N1-Cu1...Cu1^{i} = 172.75(8)°].

No inter- or intramolecular hydrogen bonds or interactions were observed between molecules of **$Cu_2(C_5H_9O_2)_4(C_5H_5N)_2$** in the unit cell. However, a π-π stacking interaction between the pyridine rings of adjacent molecules is observed [*Cg*1...*Cg*1^{ii} 3.628Å, where Cg1 is the centroid of the N1-C11-C12-C13-C14-C15 pyridine ring, symmetry code (ii) 1-x, 1-y, 2-z]. This π-π interaction allows the molecules of **$Cu_2(C_5H_9O_2)_4(C_5H_5N)_2$** to extend as one-dimensional molecular chains along [001] as indicated in Figure 25.

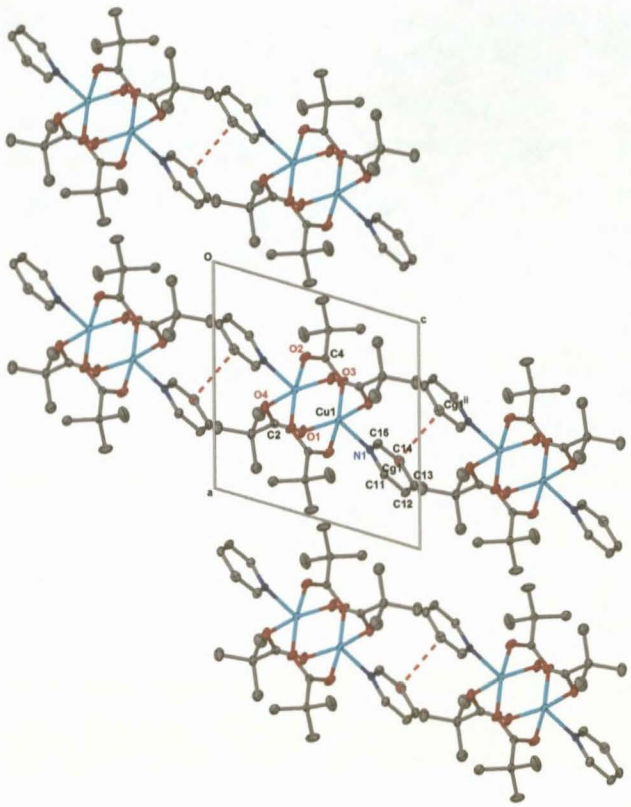

Figure 25 An extended packing diagram of $Cu_2(C_5H_9O_2)_4(C_5H_5N)_2$ as viewed along [010]. The pyridine π-π interaction has been indicated (Cg1...Cg1^{ii} 3.628Å, symmetry code (ii) 1-x, 1-y, 2-z). Hydrogen atoms have been omitted for clarity.

Cu1...Cu1^{i}	2.6229(9)	Cu1-O3	1.968(2)
Cu1-N1	2.153(3)	Cu1-O4	1.977(2)
O1-C2	1.262(4)	O3-C4	1.261(4)
O1-Cu1-O3	88.90(11)	O1-Cu1-N1	93.71(10)
O3-Cu1-N1	98.69(10)	C4-O3-Cu1	120.4(2)
C2-O1-Cu1	126.8(2)		

Table 7 Selected bond lengths and bond angles of $Cu_2(C_5H_9O_2)_4(C_5H_5N)_2$.

2.1.11 Bis(di-μ-ethoxo-bis(*N*-pivaloyl-*N'*,*N'*-diethylureato)dicopper(II), $[Cu_2(L^1\text{-}O,O')_2(C_2H_5O)_2]$. Attempts to obtain crystals of $Cu(L^1\text{-}O,O')_2$ suitable for crystal structure analysis (from crude reaction product prepared as described in experimental section 3.5.5) from a variety of solvents and solvent combinations (e.g. heptane, benzene, dichloromethane and chloroform) proved unsuccessful. However in an attempt to crystallize $Cu(L^1\text{-}O,O')_2$ from ethanol, crystals of bis(di-μ-ethoxo-bis(*N*-pivaloyl-*N'*,*N'*-diethylureato)dicopper(II), $[Cu_2(L^1\text{-}O,O')_2(C_2H_5O)_2]$ were unexpectedly isolated.

The asymmetric unit of $[Cu_2(L^1\text{-}O,O')_2(C_2H_5O)_2]$ is a dinuclear system in which the two copper(II) atoms are bridged by two μ_2-ethoxo ions. The coordination of the two copper(II) ions is completed by two oxygen atoms of the deprotonated *N*-pivaloyl-*N'*,*N'*-diethylurea ligands in an approximately square-planar environment. The compound $[Cu_2(L^1\text{-}O,O')_2(C_2H_5O)_2]$, crystallises in the centrosymmetric triclinic space group P$\bar{1}$ as shown in Figure 26. Selected bond distances, bond angles and torsion angles are listed in Table 8.

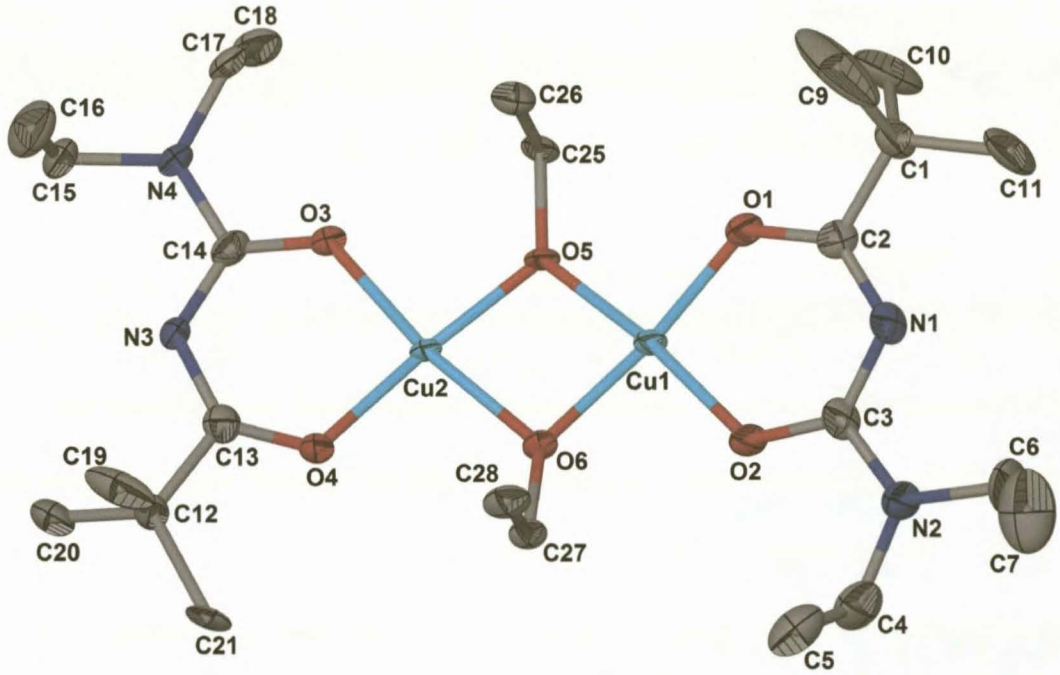

Figure 26 The molecular structure of $[Cu_2(L^1\text{-}O,O')_2(C_2H_5O)_2]$ showing the numbering scheme used. Displacement ellipsoids are drawn at the 50% probability level. Hydrogen atoms have been omitted for clarity.

The coordination around each of the two copper(II) atoms is essentially square planar with the maximum deviation from the Cu1/O1/O2/O5/O6 least-squares plane being atom O6 by 0.040(3)Å. However, the deviation from planarity around the second copper atom, Cu2, is more pronounced with the greatest deviation from the Cu2/O3/O4/O5/O6 least-squares plane being that of Cu2 by -0.105(2)Å.

Atoms Cu2 and O6 have a close proximity to atoms $Cu2^{i}$ and $O6^{i}$ of an adjacent $[Cu_2(L^1\text{-}O,O')_2(C_2H_5O)_2]$ molecule presumably allowing an electrostatic interaction between these atoms [$Cu2\ldots O6^{i}$ = 2.359(5)Å, $O6\ldots Cu2^{i}$ = 2.359(5)Å; symmetry code (i) 1-x, 1-y, z]. This $Cu2\ldots O6^{i}$ and $O6\ldots Cu2^{i}$ interaction effectively results in the coordination around Cu2 being a pseudo five coordinate square pyramid. It is proposed that this $Cu2\ldots O6^{i}$ and $O6\ldots Cu2^{i}$ interaction contributes to the deviation of atom Cu2 from planarity observed in the Cu2/O3/O4/O5/O6 least-squares plane. This intermolecular $Cu2\ldots O6^{i}$ interaction results in the formation of 'dimers' of $[Cu_2(L^1\text{-}O,O')_2(C_2H_5O)_2]$ as illustrated in Figure 27. Interestingly, this intermolecular pseudo square pyramid coordination, observed for Cu2 in $[Cu_2(L^1\text{-}O,O')_2(C_2H_5O)_2]$, is not uncommon for square planar complexes of copper(II) due to the characteristic Lewis acidity of copper[29]. Several examples of this can readily be found in the literature[17, 29, 49, 50].

Cu1-O1	1.907(5)	Cu2-O3	1.916(5)
Cu1-O2	1.902(4)	Cu2-O4	1.920(4)
Cu1-O5	1.885(4)	Cu2-O5	1.910(4)
Cu1-O6	1.954(4)	Cu2-O6	1.968(4)
O1-C2	1.289(8)	O3-C14	1.282(8)
C2-N1	1.321(9)	C14-N3	1.359(9)
N1-C3	1.377(9)	N3-C13	1.324(9)
C3-N2	1.359(9)	C14-N4	1.352(8)
$Cu2\ldots O6^{i}$	2.359(5)	$O6\ldots Cu2^{i}$	2.359(5)
O1-Cu1-O2	91.7(2)	O3-Cu2-O4	91.1(2)
O5-Cu1-O6	78.5(2)	O5-Cu2-O6	77.6(2)
Cu1-O5-Cu2	103.7(2)	Cu2-O6-Cu1	99.1(2)
O1-C2...C3-O2	-2.1(6)	O3-C14...C13-O4	-4.5(7)

Table 8 Selected bond lengths (Å), bond angles (°) and torsion angles (°) of $[Cu_2(L^1\text{-}O,O')_2(C_2H_5O)_2]$.

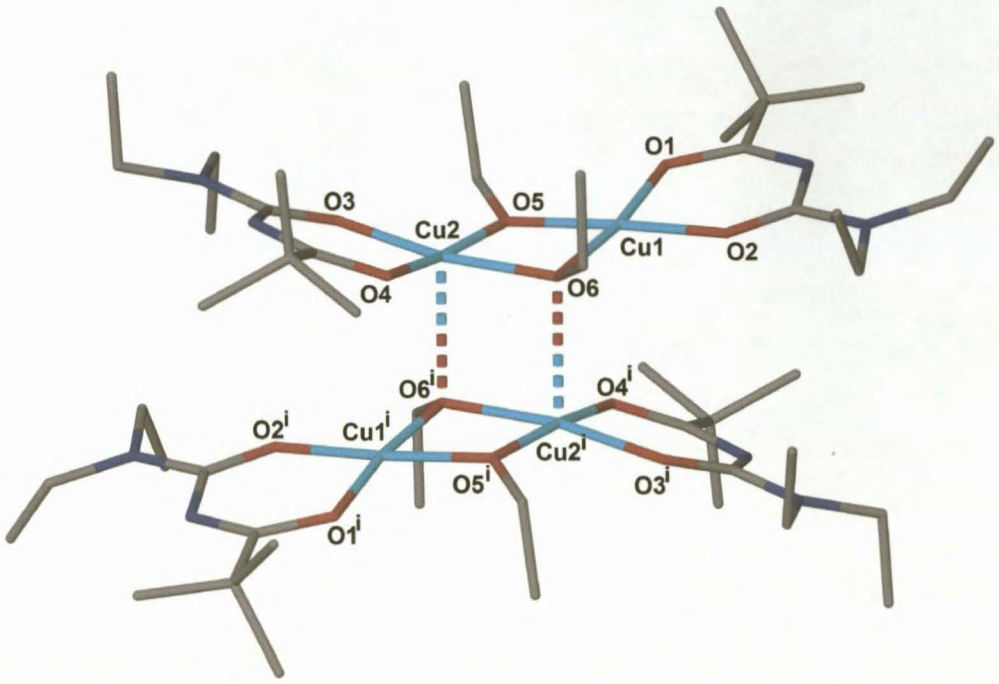

Figure 27 'Dimer' arrangement of molecules of **[$Cu_2(L^1$-*O,O'*$)_2(C_2H_5O)_2$]** resulting from the intermolecular Cu2...O6^i interaction [symmetry code (i) 1-x, 1-y, z]. Hydrogen atoms have been omitted for clarity.

The distance of the intermolecular Cu2...O6^i (2.359(5)Å) interaction observed for **[$Cu_2(L^1$-*O,O'*$)_2(C_2H_5O)_2$]**, compares well with a similar intermolecular Cu...O interaction reported in the crystal structure of a structurally related complex, bis(di-μ-ethoxo-bis(3,5-di-*tert*-butylsemiquinonato)dicopper(II) [Cu...O 2.342(5)Å][50]. Several instances are reported in the literature where such intermolecular Cu...O interactions are much longer than that observed for **[$Cu_2(L^1$-*O,O'*$)_2(C_2H_5O)_2$]**, such as in the case of tetrakis(μ_3-methoxy)tetrakis[1,1,1,5,5,5-hexafloro-2,4-pentanedionato)copper(II) [Cu...O = 2.547(4)Å] [29]. Longer, yet similar intermolecular Cu...O interactions were observed in the crystal structure of complex **Cu(L^3-*O',O'*$)_2$** [Cu...O 2.745(2)Å - see sections 2.3.8].

The bridging Cu_2O_2 group [Cu1-O5-Cu2-O6] of **[$Cu_2(L^1$-*O,O'*$)_2(C_2H_5O)_2$]** is planar and asymmetric. The greatest deviation from the Cu1/Cu2/O5/O6 least-squares plane is O5 by -0.070(2)Å. In turn, the Cu1-O5-Cu2 and Cu1-O6-Cu2 bond angles of the bridging ethoxo ligands are 103.7(2)° and 99.1(2)° respectively. Consequently, the Cu1-O5 and Cu2-O5 bond lengths [Cu1-O5 1.885(4)Å, Cu2-O5 1.910(4)Å] are shorter than the Cu1-O6 and Cu2-O6 bond lengths [Cu1-O6 1.954(4)Å, Cu2-O6 1.968(4)Å].

The coordination of each of the two deprotonated *N*-pivaloyl-*N'*,*N'*-diethylurea ligands to atoms Cu1 and Cu2 is planar. However, both of these ligands are 'bent' upwards resulting in the

O3/C14/N3/C13/O4 and the O1/C2/N1/C3/O2 least-squares planes intersecting the Cu1/O5/Cu2/O6 least-squares plane at 22.9(3)° and 7.0(3)° respectively. It is speculated that the 'bending up' of both of the bridging ethoxo ligands, away from the Cu1-O5-Cu2-O6 plane, blocks the potential sixth coordination site of the copper. The orientation of the pivaloyl groups as well as the diethyl groups of the *N*-pivaloyl-*N'*,*N'*-diethylurea ligands further restrict access to the potential sixth coordination site of the copper atoms. The blocking of this potential sixth coordination site of the copper possibly prevents the molecules of **[$Cu_2(L^1$-*O*,*O'*$)_2(C_2H_5O)_2$]** forming one dimensional chains that may otherwise have formed similar to that which is observed in the packing diagram of **Cu(L^2-*O*,*O'*$)_2$** illustrated in Figure 14. The side view and top view of the **$Cu_2(L^1$-*O*,*O'*$)_2(C_2H_5O)_2$]** dimer, illustrated in Figure 28, clearly shows the inaccessibility of the potential sixth coordination site of copper due to the orientation of both the ethoxy and *N*-pivaloyl-*N'*,*N'*-diethylurea ligands.

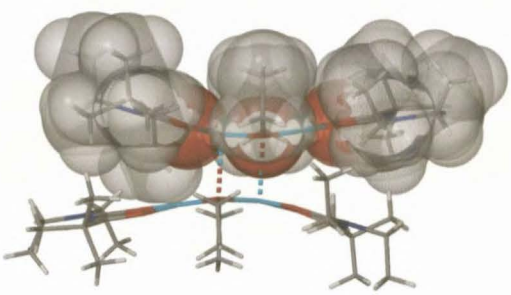

Side view of the **[$Cu_2(L^1$-*O*,*O'*$)_2(C_2H_5O)_2$]** dimer showing the Cu2...O6^{i} interaction. Semi transparent Van der Waals spheres have been overlaid on the asymmetric unit.

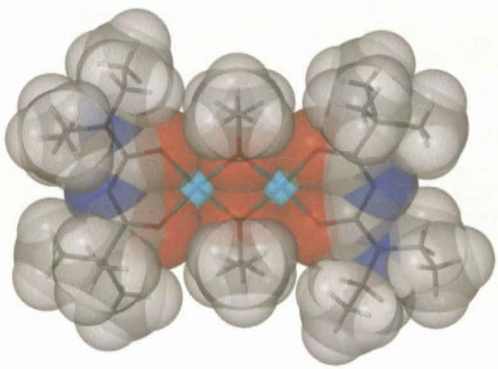

Top view of **[$Cu_2(L^1$-*O*,*O'*$)_2(C_2H_5O)_2$]** with an overlay of semi transparent Van der Waals spheres.

Figure 28 Side and top views of **[$Cu_2(L^1$-*O*,*O'*$)_2(C_2H_5O)_2$]** indicating how the potential six coordination site of copper is effectively blocked due to the orientation of both the bridging ethoxy and *N*-pivaloyl-*N'*,*N'*-diethylurea ligands.

2.2 Mass Spectrometry.

Ligands **H(L$^{1-3}$-*O,O'*)**, **H(L^4-*S,O*)** and complexes **Cu(L$^{1-3}$- *O,O'*)$_2$**, **Cu(L^4- *S,O*)$_2$** and **Ni(L^4- *S,O*)$_2$** were all characterised by mass spectroscopy with the appropriate *m/z* M^+ being identified in all cases. In the case of the mass spectrum of ligands **H(L^1-*O,O'*)**, **H(L^2-*O,O'*)** and **H(L^4-*S,O*)**, signals corresponding to products that may be the result of a fragmentation and rearrangement similar to the classical McLafferty type rearrangement, were identified. A peak of the corresponding product resulting from a McLafferty type rearrangement in the mass spectrum of **H(L^3-*O,O'*)** (*m/z* = 239) was not observed. Although the McLafferty rearrangement is typically observed in the mass spectra of alcohols that contain a hydrogen on the γ carbon, a fragmentation mechanism which involves the breaking of two covalent bonds, similar to the classical McLafferty type rearrangement, is proposed for ligands **H(L^1-*O,O'*)**, **H(L^2-*O,O'*)** and **H(L^4-*S,O*)** as illustrated in figure 3. The comparatively longer bond length of the C3-N1 bonds observed in the crystal structures of **H(L^1-*O,O'*)**, **H(L^2-*O,O'*)** and **H(L^4-*S,O*)**, when compared to the bond length of bonds C2-N1 and C3-N2 bonds, resulting in the C3-N1 bonds being the weaker bonds of the three C-N bonds of interest, may be a contributing factor for the fragmentation of this bond and the resulting rearrangement that occurs under electron impact MS conditions. A similar observation has been reported in the literature for the *N',N'*-disubstituted-*N*-ferrocenoylureas[51].

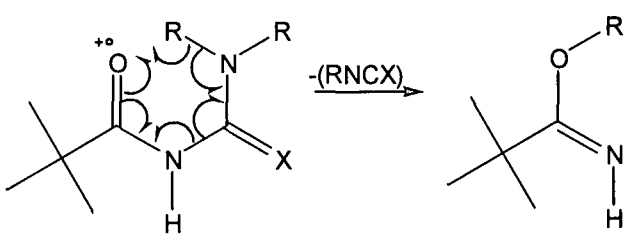

Figure 29 Proposed mechanism for the McLafferty type rearrangements observed for ligands **H(L^1-*O,O'*)**, **H(L^2-*O,O'*)** and **H(L^4-*S,O*)**. **H(L^1-*O,O'*)** R=Et, X=O'; **H(L^2-*O,O'*)** R=Me, X=O'; **H(L^4-*S,O*)** R=Et, X=S.

2.3 Infrared Spectroscopy.

A characteristic of the infrared spectra of the uncoordinated ligands **H(L$^{1-3}$-*O,O'*)** and **H(L^4-*S,O*)** is the very broad band observed in the 3213 – 3228cm^{-1} region attributed to the N-H group. The broadness of the stretching vibration of this group in the uncoordinated ligands can be attributed to this group being involved in extensive intra- and intermolecular hydrogen bonding networks[52]. The involvement of this N-H group in intermolecular hydrogen interactions was confirmed by single crystal X-ray analysis. In the case of ligands **H(L^1-*O,O'*)**, **H(L^2-*O,O'*)** and **H(L^3-*O,O'*)**, the nitrogen of the respective N-H groups was identified as acting as both a donor and acceptor in the hydrogen bonding network. In the case of **H(L^4-*S,O*)**, the N-H group participates in a single intermolecular hydrogen bond to an adjacent molecule where the nitrogen acts only as a donor atom. This comparatively limited involvement of the N-H group of **H(L^4-*S,O*)** in intermolecular hydrogen bonding is reflected in the infrared spectrum of **H(L^4-*S,O*)**, where the infrared N-H stretching vibration observed at 3228cm^{-1}, although still broad, is significantly more intense and sharper in shape than the comparable stretching vibrations of the N-H groups of **H(L^1-*O,O'*)**, **H(L^2-*O,O'*)** and **H(L^3-*O,O'*)**. The broad infrared absorption assigned to the N-

H amide stretching vibration at ±3200cm^{-1} in the uncoordinated ligands disappears upon complexation with the metal which is concurrent with the loss of this proton.

A sharp band in the 1648 – 1659cm^{-1} region assigned to the carbonyl group in the non-coordinated ligands shifts to the 1516 - 1598cm^{-1} region in the resultant complexes. The absorption changes from an intense sharp band in the uncoordinated ligand to a much weaker and slightly broader band in the complex. This shift is consistent with a weakening of the carbonyl double bond in the uncoordinated ligand and extensive electron delocalisation through the resultant six-membered chelate ring.

2.4 Chromophoric character of bis(*N*-pivaloyl-*N'*,*N'*-diethylureato)copper(II) Cu($\mathbb{L}^1$-*O*,*O*)$_2$, bis(*N*-pivaloyl-*N'*,*N'*-diethylthioureato)copper(II) Cu($\mathbb{L}^4$-*S*,*O*)$_2$ and bis(*N*-pivaloyl-*N'*,*N'*-diethylthioureato)nickel(II) Ni($\mathbb{L}^4$-*S*,*O*)$_2$.

It is well documented that transition metal complexes absorb in the visible region as well as the near infra-red and near ultraviolet regions resulting in their colour. The absorption bands in the visible region of these complexes are commonly characterised as being weak, for which ε_{max} (molar extinction coefficient) values fall in the range of 1-10^{-2} due to *d-d* transitions within the orbitals of the metal ion[53]. By comparison, these complexes often also exhibit much stronger absorption bands in the near ultraviolet and ultraviolet region with ε_{max} values in the order of 10^3 -10^4. These strong absorptions are attributed to charge-transfer transitions[53]. It is reported that frequently, for any series of structurally similar metal complexes which are alike with regards to having identical geometry and the same set of coordinating donor atoms to the metal, show similar absorption with respect to the number and the position of *d-d* absorption bands[54].

In this context, the physical appearance of the complexes **Cu($\mathbb{L}^1$-*O*,*O'*)$_2$**, **Cu($\mathbb{L}^4$-*S*,*O*)$_2$** and **Ni($\mathbb{L}^4$-S,O)$_2$** prepared in this study are examined, the occurrence of a chromophoric effect due to changes in metal centre (while the ligand remains the same), as well as a chromophoric effect due to changes in donor atoms (while metal centre remains the same), became clearly evident. **Cu($\mathbb{L}^4$-*S*,*O*)$_2$** and **Ni($\mathbb{L}^4$-*S*,*O*)$_2$** have the identical ligand system but different metal centres, while **Cu($\mathbb{L}^1$-*O*,*O'*)$_2$** and **Cu($\mathbb{L}^4$- *S*,*O*)$_2$** have the same metal centre but a different ligand system in terms of a difference in one set of donor atoms to the copper. **Cu($\mathbb{L}^1$-*O*,*O'*)$_2$** is blue in colour, **Cu($\mathbb{L}^4$-*S*,*O*)$_2$** is dark green, while **Ni($\mathbb{L}^4$-*S*,*O*)$_2$** is purple in colour. The UV/visible absorption spectra [Figure 32 and Figure 33] of **Cu($\mathbb{L}^1$-*O*,*O'*)$_2$**, **Cu($\mathbb{L}^4$-*S*,*O*)$_2$** and **Ni($\mathbb{L}^4$-*S*,*O*)$_2$**, as illustrated in Figure 30 confirm this. The spectra of **Cu($\mathbb{L}^4$-*S*,*O*)$_2$** and **Ni($\mathbb{L}^4$-*S*,*O*)$_2$** were compared to illustrate electronic changes solely due to variation in the metal centre of the respective complexes, while the ligand system remained the same. The spectra of **Cu($\mathbb{L}^1$-*O*,*O*)$_2$** and **Cu($\mathbb{L}^4$-*S*,*O*)$_2$** illustrate the electronic changes that occurred solely due to changes in one donor atom in the chelate ring of the ligand system while the metal centre remains the same [i.e. the sulphur atom of ligand **H($\mathbb{L}^4$-*S*,*O*)**, is exchanged with an oxygen atom in **H($\mathbb{L}^1$-*O*,*O'*)**]. The electronic spectra recorded for **Cu($\mathbb{L}^1$-*O*,*O'*)$_2$**, **Cu($\mathbb{L}^4$-*S*,*O*)$_2$** and **Ni($\mathbb{L}^4$-*S*,*O*)$_2$** were obtained as solutions in chloroform. The ε_{max} values at the respective wavelengths for the bands observed are listed in Table 9. The absorption bands at 243 and 342nm for **Cu($\mathbb{L}^1$-*O*,*O'*)$_2$**, at 262nm and 365nm for **Cu($\mathbb{L}^4$-*S*,*O*)$_2$** and at

260 and 301nm for **Ni(L^4-*S,O*)$_2$** correlate with bands that are attributed to charge-transfer transitions of copper(II) and nickel(II) complexes in the literature, while the bands observed at 617nm for **Cu(L^1-*O,O'*)$_2$**, at 584nm for **Cu(L^4-*S,O*)$_2$** and at 509nm for **Cu(L^4-*S,O*)$_2$** are ascribed to d-d transitions[53, 55].

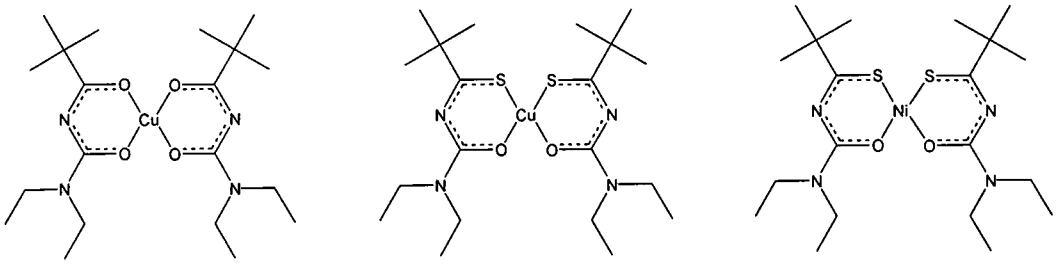

Figure 30 Complexes **Cu(L^1-*O,O*)$_2$**, **Cu(L^4-*S,O*)$_2$** and **Ni(L^4-*S,O*)$_2$** used for ultraviolet and visible spectral studies to illustrate the chromophoric effect due to donor atom variations and metal centre variations.

It is well known that the geometry of transition metal complexes have a marked effect on the electronic spectra of the complexes, not only with respect to the number and relative positions of the bands, but also their intensities[54]. This brings into consideration a further factor to which the differences observed in the UV/visible absorption spectra of **Cu(L^1-*O,'O*)$_2$**, **Cu(L^4-*S,O*)$_2$** and **Ni(L^4-*S,O*)$_2$** can be attributed: that being the possible occurrence of *trans* versus *cis* isomers of the complexes as illustrated in Figure 31.

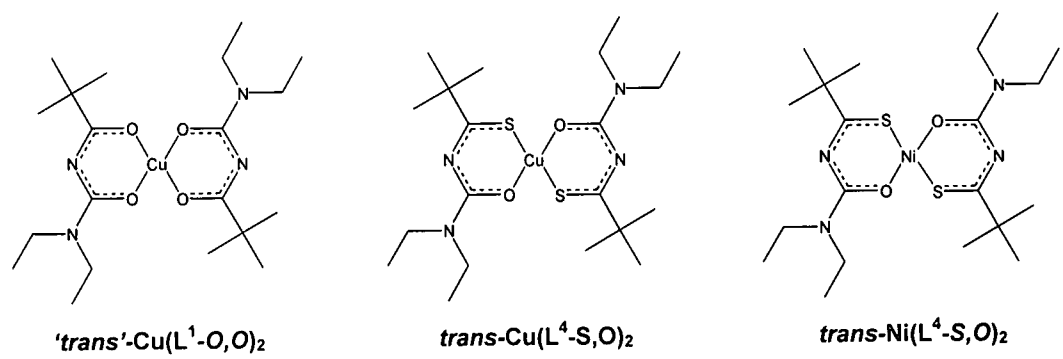

Figure 31 Possible *trans* confirmations of complexes **Cu(L^1-*O,O*)$_2$**, **Cu(L^4-*S,O*)$_2$** and **Ni(L^4-*S,O*)$_2$**.

However, the single X-ray crystal structure analysis of **Cu(L^4-*S,O*)$_2$** and **Ni(L^4-*S,O*)$_2$** further confirmed the structures to be isostructural with a *cis*-bis(*S,O*) arrangement of ligator atoms and square planar in geometry. The single crystal X-ray structure analysis of the structurally related complex **Cu(L^2-*O,O'*)$_2$** showed the complex to be isostructural in geometry to **Cu(L^4-*S,O*)$_2$** i.e. *cis*-bis(*O,O'*) square planar geometry around the copper metal centre. Although it is recognised that molecules in the solid state do are not necessarily representative of what occurs in solution, it is assumed for this comparison that the changes observed in the UV/visible absorption spectra of the complexes investigated here can be largely attributed to differences in donor atoms sets when comparing the spectra of **Cu(L^1-*O,O'*)$_2$** with

the spectra of **Cu(L^4-*S,O*)$_2$** and due to differences in metal centres when comparing the spectra of **Cu(L^4-*S,O*)$_2$** with the spectra of **Ni(L^4-*S,O*)$_2$**. Furthermore, as is evident from Table 9, complexes **Cu(L^1-*O,O'*)$_2$**, **Cu(L^4-*S,O*)$_2$**, **Ni(L^4-*S,O*)$_2$** all have comparable ε_{max} values in the visible region, thereby offering further support to the fact that the complexes are isostructural in solution with regards to their complex geometry[53].

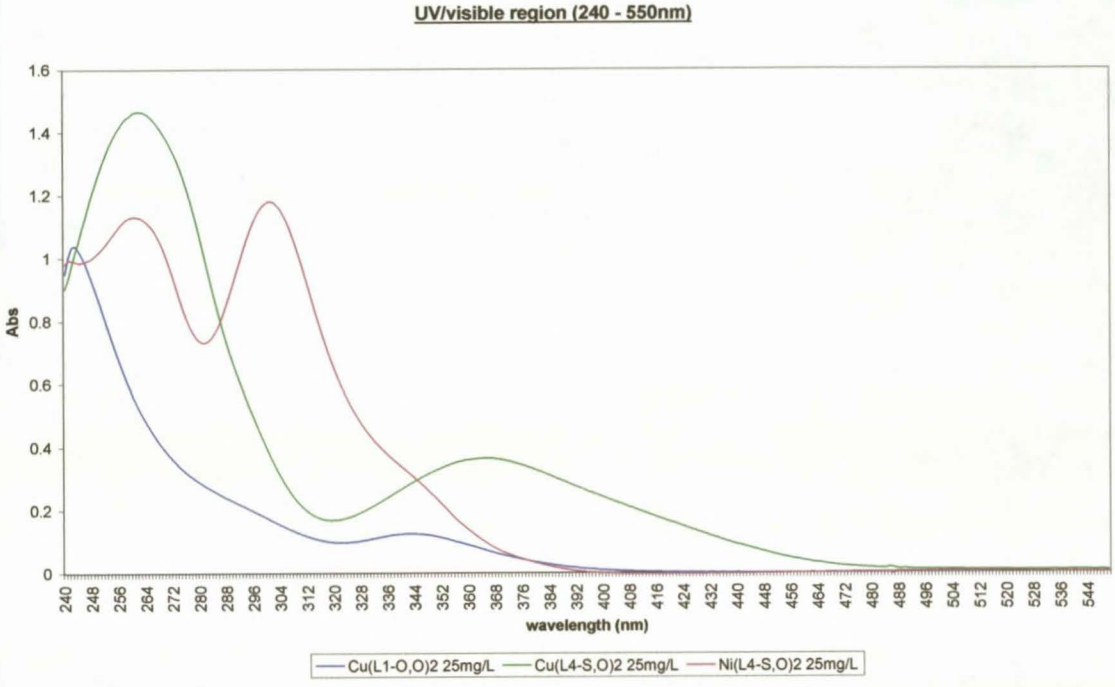

Figure 32 UV/visible absorption spectrum (240-550nm) of 25mg/L $CHCl_3$ solutions **Cu(L^1-*O,O*)$_2$**, **Cu(L^4-*S,O*)$_2$** and **Ni(L^4-*S,O*)$_2$**.

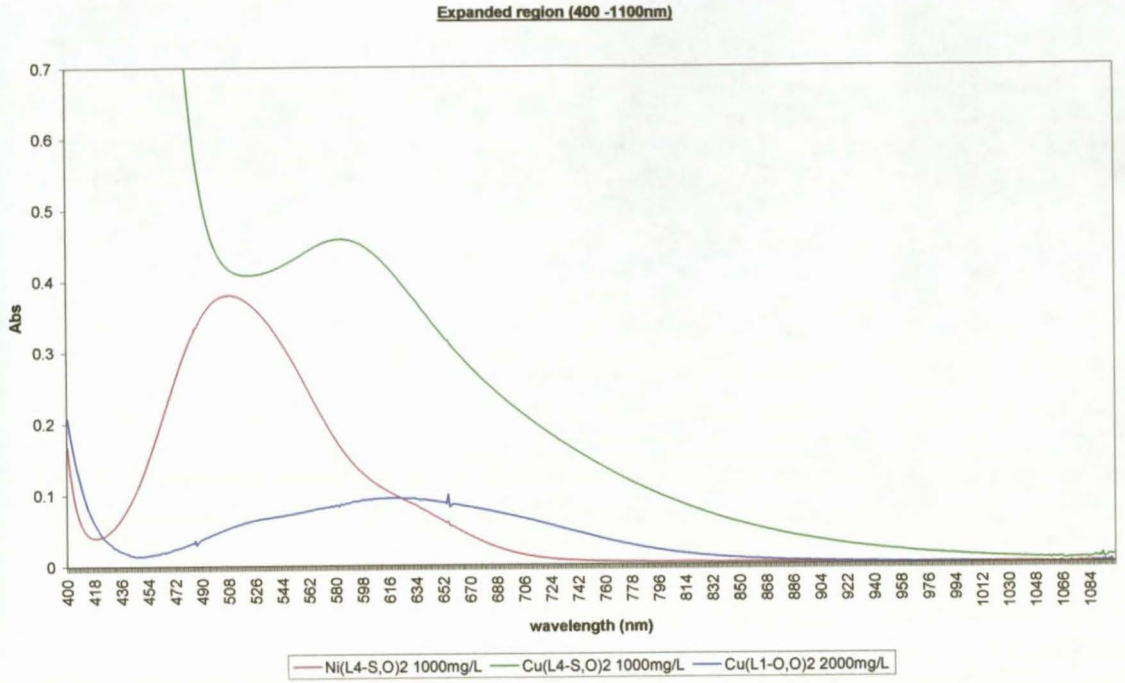

Figure 33 Expanded absorption spectrum (400-1100nm) of 2000mg/L $CHCl_3$ solution of **Cu(L^1-*O,O*)$_2$** and 2000mg/L $CHCl_3$ solutions of **Cu(L^4-*S,O*)$_2$** and **Ni(L^4-*S,O*)$_2$**.

Complex	Complex conc. (mol.dm^{-3})	Absorbance	Wavelength	Molar absorption coefficient (ε)
Cu(L^1-*O,O'*)$_2$	5.41E-05	1.0396	243	19 216
		0.12499	342	2 310
	4.33E-03	0.98481	617	228
Cu(L^4-*S,O*)$_2$	5.06E-05	1.4354	262	28 376
		0.34754	365	6 870
	2.02E-03	0.458418	584	227
Ni(L^4-*S,O*)$_2$	5.11E-05	1.1315	260	22 149
		1.1808	301	23 114
	2.04E-03	0.38038	509	186

Table 9 ε_{max} values for observed peaks of **Cu(L^1-*O,O'*)$_2$**, **Cu(L^4-*S,O*)$_2$** and **Ni(L^4-*S,O*)$_2$** in both the UV and visible regions.

3. Experimental

3.1 Methods and instrumentation

All reagents and solvents were commercially available and unless otherwise stated were used without further purification. Dichloromethane was pre-dried over 4Å molecular sieves and distilled over either sodium hydride or calcium chloride under an inert atmosphere just prior to use. ^{1}H and ^{13}C NMR spectra (25°C) were recorded in deuterated chloroform using either a Varian INOVA 600 MHz spectrometer operating at 600 MHz or 151 MHz respectively, or a Varian VXR 300 MHz spectrometer operating at 300 MHz or 76 MHz respectively. ^{1}H chemical shifts are quoted relative to the residual $CHCl_3$ solvent resonance at 7.26ppm. The ^{13}C chemical shifts are quoted relative to the $CDCl_3$ triplet at 77.7ppm. UV-visible spectrophotometric experiments were carried out on an Agilent 8453E UV-visible spectrophotometer (Agilent Technologies). Elemental analyses were performed using a Carlo Erba EA 1108 elemental analyser in the microanalytical laboratory of the University of Cape Town, South Africa.

3.2 General preparation of H(L^{1-3}-*O,O'*), H(L^{4}-*S,O*), Ni(L^{4}-*S,O*)$_2$ and Cu(L^{4}-*S,O*)$_2$.

Ligands, H(L^{1-3}-*O,O'*), were prepared by the condensation of the appropriate aroyl(acyl)chloride in the presence of triethylamine with the appropriate *N,N*-dialkylurea under inert and anhydrous conditions. H(L^{4}-*S,O*) was prepared according to the method previously described by Douglas *et al.*[21] Ni(L^{4}-*S,O*)$_2$ and Cu(L^{4}-*S,O*)$_2$ were prepared from the dropwise addition of an acetonitrile/water (1:1 v/v) solution of the nickel or copper acetate to a solution of H(L^{4}-*S,O*) in the same solvent mixture. The products were recovered by filtration or extraction into chloroform and re-crystallised from chloroform and ethanol or methanol.

3.3 General preparation of Cu(L^{1-3}-*O,O'*)$_2$.

Several methods were attempted in the preparation of Cu(L^{1-3}-*O,O'*)$_2$ in an attempt to maximise the yields and minimise the formation of by-products. The methods attempted included the use of copper(II) chloride as a starting material in a two phase system using chloroform and water as a reaction medium using a variety of inorganic and organic bases such as potassium hydroxide, potassium carbonate and pyridine. In all of these cases, the target product was produced only in small quantities with the major product being the copper hydroxide. The most successful method that was used to prepare the target copper complexes Cu(L^{1-3}-*O,O'*)$_2$ in a high yield and a high degree of purity involved the addition of an aprotic solution of copper perchlorate to an aprotic solution of the appropriate ligand in the presence of the organic base, *N,N*-diisopropylethylamine.

3.4 Crystallography and structure refinement

Crystals suitable for single crystal X-ray analysis were mounted on a thin glass fibre and data was collected on Bruker Nonius SMART Apex diffractometer using graphite monochromated Mo-Kα radiation (λ = 0.7107 Å). Data integration and reduction were undertaken using SAINT[56] and space group determination using XPREP[56]. Multi-scan derived corrections were made to the data using SADABS[57]. The structures were solved using SHELXS-97[58] and refined using SHELXL-97[58] with the

aid of the interface software XSEED[33, 34]. XSEED[33, 34] was also used to generate the molecular graphics as the GUI to POV-Ray[59]. In each structure, all non-hydrogen atoms were modelled anisotropically. Hydrogen atoms were placed in geometrically calculated positions, with C-H = 0.99 for $-CH_2-$, 0.98 for $-CH_3$ or 0.95 for phenyl and 0.88 Å for N-H. These were refined using a riding model with U_{iso}(H) = $1.2U_{eq}$(parent) (for $-CH_2-$, phenyl and N-H) and $1.5U_{eq}$(parent) (for $-CH_3$). Crystal structure interpretation was performed with the aid of XSEED[33, 34], PLATON[35] and MERCURY[18].

3.5 Preparative methods.

3.5.1 *N*-pivaloyl-*N'*,*N'*-diethylurea, H(L^1-*O*,*O'*).

Alternative name : ***N*-2,2-dimethylpropanoyl-*N'*,*N'*-diethylurea**

Triethylamine ($3.3x10^{-2}$ mol) dissolved in 10ml of anhydrous dichloromethane was added dropwise with stirring to a solution of $3.0x10^{-2}$ mol of pivaloylchloride dissolved in 40ml of anhydrous dichloromethane. After stirring at room temperature for 10minutes, the above reaction mixture was added to a solution of $3.0x10^{-2}$ mol of *N,N*-dimethylurea dissolved in 50ml of anhydrous dichloromethane. The solution was gently warmed to 60°C for 2 hours, cooled to room temperature and stirred overnight. 50ml of water was added and the crude product was extracted with 3 x 25ml of chloroform. The crude product was isolated as a white crystalline product under reduced pressure and further purified by crystallization from dichloromethane and pentane. Crystals suitable for single crystal X-ray analysis were identified and isolated. The trisubstituted by-product was identified in small quantities in the crude product.

Yield: 90.4% (based on pivaloyl chloride).

NMR : δ_H (300 MHz, solvent $CDCl_3$) 9.20 (1H, br s, NH), 4.41 (4H, qu, $2CH_2$), 2.29 (9H, s, $3CH_3$) 2.25 (6H, tr, $2CH_3$). δ_C (76 MHz, solvent $CDCl_3$) 178.1 (C(O)), 154.8 (C(O)), 42.5 (br, $2CH_2$), 40.2 (quaternary-C), 27.5 ($3CH_3$), 13.6 (br, $2CH_3$).

FT-IR : (KBr disks) 3225s (br, NH), 1705s, 1648vs, 1481s, 1287s cm^{-1}.

Mass spectrum (EI 70eV) *m/z* 200 (M^+, 10.2%), 143 (100%), 129 (1.0%), 115 (6.4%), 100 (19.1%), 72 (45.2%), 58 (17.8%), 57 (45%), 44 (5.7%), 41 (17.2%), 29 (13.4%).

Mp: 53.5-54.8°C.

Found C, 59.90; H, 10.43; 13.82; $C_{10}H_{20}N_2O_2$ required C, 59.97; H, 10.07; N, 13.99.

3.5.2 *N*-pivaloyl-*N'*,*N'*-dimethylurea, H(L^2-*O*,*O'*)

Alternative name : ***N*-2,2-dimethylpropanoyl-*N'*,*N'*-dimethylurea**

Triethylamine ($3.3x10^{-2}$ mol) was dissolved in 10ml of anhydrous dichloromethane was added dropwise to a solution of $3.0x10^{-2}$ mol of pivaloyl chloride dissolved in 40ml of anhydrous dichloromethane. After stirring at room temperature for 10 minutes, the above reaction mixture was added to a solution of $3.0x10^{-2}$ mol of *N,N*-dimethylurea dissolved in 50ml of anhydrous dichloromethane. The solution was gently warmed to 60°C for 2 hours, cooled to room temperature and stirred overnight. The white precipitate was dissolved into 50ml of water and the crude product was extracted with 3 x 25ml of chloroform. The crude product was recovered as a white crystalline product under reduced pressure and further purified by crystallization from ethyl acetate. The crystals were

washed with small portions of cold ethanol and dried under high vacuum. Crystals suitable for single crystal X-ray analysis were identified and isolated.

Yield : 64.5% (yield based on pivaloyl chloride).

NMR : δ_H (300 MHz, solvent $CDCl_3$) 8.37 (1H, br s, NH), 2.90 (6H, s, $2CH_3$), 1.16 (9H, s, $3CH_3$). δ_C (76 MHz, solvent $CDCl_3$) 178.0 (C(O)), 156.1 (C(O)), 40.2 (quaternary-C), 38.0 (br s, $2CH_3$), 27.6 ($3CH_3$).

FT-IR : (KBr disks) 3213s (br, NH), 1699s sh, 1659vs, 1498s, 1396 s, 1198s cm^{-1}.

Mass spectrum (EI 70eV) *m/z* 172 (M+, 43.0%), 129 (1.9%), 115 (100%), 88 (11.4%), 72 (91.1%), 57 (68.4%), 45 (38.0%), 29 (5.1%).

Mp: 104.0-105.0°C.

Found C, 55.67; H, 10.50; N, 16.20; $C_8H_{16}N_2O_2$ required C, 55.79; H, 9.36; N, 16.27.

3.5.3 *N*-(3,4,5-trimethoxybenzoyl)-*N'*,*N'*-diethylurea, H(L^3-*O*,*O'*)

Alternative name : **1,1-Diethyl-3-(3,4,5-trimethoxy-benzoyl)-urea**

Triethylamine ($3.3x10^{-2}$ mol) dissolved in 10ml of anhydrous dichloromethane was added dropwise to a solution of $3.0x10^{-2}$ mol of 3,4,5-trimethoxybenzoyl chloride dissolved in 40ml of anhydrous dichloromethane. After stirring at room temperature for 10minutes, the above reaction mixture was added to a solution of *N,N*-dimethylurea dissolved in 50ml of anhydrous dichloromethane. The solution was gently warmed to 60°C for 2 hours, cooled to room temperature and stirred overnight. The white precipitate was dissolved in 50ml of water and the crude product was extracted with 3 x 25ml of chloroform. The crude white crystalline product was isolated under reduced pressure and further purified by crystallization from dichloromethane and toluene. Crystals suitable for single crystal X-ray structural analysis were selected and analysed. When the reaction synthesis was carried out in the reverse order, i.e. the dichloromethane solution of *N,N*-diethylurea was added to the solution of triethylamine and 3,4,5-trimethoxybenzoyl chloride, the target product was isolated in a 13.0% yield.

Yield : 53.6% (yield based on mol 3,4,5-trimethoxybenzoyl chloride used)

NMR : δ_H (300 MHz, solvent $CDCl_3$) 9.25 (1H, br s, NH), 7.18 (2H, s, *ortho*-Ph), 3.90 (6H, s, *3,5*-OCH_3), 3.88 (3H, s, *4*-CH_3), 3.41 (4H, br m, $2CH_2$), 1.20 (6H, tr, $2CH_3$). δ_C (76 MHz, solvent $CDCl_3$) 166.6 (C(O)), 155.3 (C(O)), 153.7, 142.4 106.1 (Ph), 128.6 (*ipso*-Ph), 61.6 (*4*-OCH_3), 56.9 (*3,5*-OCH_3), 42.7 (v br, $2CH_2$), 13.8 and 13.9 ($2CH_3$).

FT-IR : (KBr disks) 3226s (br NH), 1683s sh, 1654vs, 1589s, 1429s, 1330s, 1223s, 1127s cm^{-1}.

Mass spectrum (EI 70eV) *m/z* 310 (M^+, 3.2%), 267 (10.8%), 237 (51.9%), 195 (88.0%), 166 (12.0%), 152 (9.5%), 109 (4.4%), 58 (20.3%), 32 (67.1%), 28 (100%).

Found C,57.98; H, 6.10; N, 9.51; $C_{15}H_{22}N_2O_5$ required C, 58.05; H, 7.15; N, 9.03.

3.5.4 *N*-pivaloyl-*N'*,*N'*-diethylthiourea, H(L^4-*S*,*O*)

Alternative name : ***N*-(2,2-dimethylpropanoyl)-*N'*,*N'*-diethylthiourea**

N-pivaloyl-*N,N*-diethylthiourea was prepared according to a modified method previously described by Douglass and Dains.[21]. A solution of pivaloyl chloride (30mmol) dissolved in 40ml of anhydrous acetone was added to a solution of potassium thiocyanate (30mmol) dissolved in 40ml of anhydrous

acetone. The solution was brought to gentle reflux for 1 hour and then cooled to room temperature. Diethylamine (30mmol) dissolved in 40ml of anhydrous acetone was added dropwise to the reaction mixture and brought to a gentle reflux for 1 hour. The mixture was cooled to room temperature and poured into 100ml of cold water. The reaction mixture was allowed to stand overnight at room temperature to allow the slow evaporation of the acetone. The crude product precipitate was recovered by filtration and further purified by recrystallization from a solution of acetone water. Crystals suitable for single crystal X-ray analysis were selected and analysed.

Yield : 71.2% (based on mol pivaloyl chloride used).

NMR : δ_H (300 MHz, solvent $CDCl_3$) 7.69 (1H, s, NH), 3.43 and 3.92 (4H, m, $2CH_2$), 1.26 (6H, s, $2CH_3$) 1.21 (9H, s, $3CH_3$). δ_C (76 MHz, solvent $CDCl_3$) 187.1 (C(S)), 172.1 (C(O)), 45.1 and 45.7 ($2CH_2$), 41.3 (*tert*-C), 28.2 ($3CH_3$), 12.5 and 12.9 ($2CH_3$).

FT-IR : (KBr disks) 3228s (br) (NH), 1648s (C(O)), 1507vs 1422s (CN), 1237s (C(S)) cm^{-1}.

Mass spectrum (EI 70eV) *m/z* 216 (M^+, 56.4%), 159 (41.0%), 145 (97.7%), 131 (10.3%), 116 (10.3%), 88 (10.3%), 72 (100%), 57 (48.7%), 44 (35.9%), 29 (15.4%).

Mp: 89-90°C.

Found C, 55.80; H, 10.19; N, 12.76; S, 14.66; $C_{10}H_{20}N_2SO$ required C, 55.52; H 9.32; N, 12.95; S, 14.82%.

3.5.5 *cis*-bis(*N*-pivaloyl-*N'*,*N'*-diethylureato)copper (II), $Cu(L^1\text{-}O,O')_2$

N,*N*-diisopropylethylamine (0.55mmol) dissolved in 10ml of acetonitrile was added dropwise to a solution of *N*-pivaloyl- *N'*,*N'*-diethylurea (0.5mmol) in 15 ml of acetonitrile and stirred at room temperature for several minutes. Copper perchlorate (0.5mmol) dissolved in 15ml of acetonitrile was added dropwise with stirring at room temperature. The reaction mixture was stirred for a further 12 hours. The crude product was extracted into 3 x 25ml portions of hexane, recovered under reduced pressure as a blue crystalline solid and dried under high vacuum. Crystals suitable for single crystal X-ray structure analysis were not obtained despite using a wide variety of solvents as well as several solvent combinations.

Yield: 97.8% (based on mol copper perchlorate used)

FT-IR : (KBr disks) 1541vs br, 1484s, 1452, 1427s, 1359, 1300 cm^{-1}.

Mass spectrum (EI 70eV) *m/z* 461 (M^+, 2.6%), 390 (2.6%), 347 (13.6%), 334 (4.5%), 317 (6.5%), 263 (16.2%), 143 (46.8%), 100 (44.2%), 72 (57 (100%), 43 (63.6%), 28 (77.3%).

Found C, 51.89; H, 8.29; N, 11.42; $C_{20}H_{38}CuN_4O_4$ required C, 51.98; H, 8.29; N, 12.12.

3.5.6 *cis*-bis(*N*-pivaloyl-*N'*,*N'*-dimethylureato)copper (II), $Cu(L^2\text{-}O,O')_2$

N,*N*-diisopropylethylamine (0.55mmol) dissolved in 10ml of acetonitrile was added dropwise to a solution of *N*-pivaloyl-*N'*,*N'*-dimethylurea (0.5mmol) in 15 ml of acetonitrile and stirred at room temperature for several minutes. Copper perchlorate (0.5mmol) dissolved in 15ml of acetonitrile was added dropwise with stirring at room temperature. The reaction mixture was stirred for a further 12 hours. The crude product was extracted into 3 x 25ml portions of hexane, recovered under reduced

pressure as a purple crystalline solid and dried under high vacuum. Crystals suitable for single crystal X-ray structure analysis were obtained from the slow crystallization from hexane.

Yield: 96.9% (based on mol copper perchlorate used)

FT-IR : (KBr disks) 1598s, 1543vs, 1485s, 1463s, 1403s cm^{-1}.

Mass spectrum (EI 70eV) *m/z* 405 (M^+, 16.2%), 398 (33.1%), 348 (28.6%), 291 (93.5%), 278 (13.6%), 271 (11.0%), 233 (42.9%), 220 (13.6%), 172 (81.2%), 151 (9.1%), 115 (100%), 87 (24.0%), 72 (100%).

Found C, 48.13; H, 7.73; N, 13.48; $C_{16}H_{30}CuN_4O_4$ required C, 47.34; H, 7.45; N, 13.80.

3.5.7 *cis*-bis(*N*-(3,4,5-trimethoxybenzoyl)-*N'*,*N'*-diethylureato)copper (II), $Cu(L^3\text{-}O,O')_2$

Copper perchlorate was dissolved in 10ml of methanol water (3:1 v/v) and added dropwise with stirring to a 10ml solution of *N*-(3,4,5-trimethoxybenzoyl)-*N'*,*N'*-diethylurea in the same solvent. After several minutes a solution of potassium carbonate dissolved in 10ml of water was added dropwise with stirring to the reaction mixture and stirred for a further 12 hours at room temperature. A further 10ml of water was added to ensure maximum precipitation of the crude product. The light blue crystalline precipitate was isolated by filtration, washed with several cold portions of a solution of methanol and water (3:1 v/v) and dried under high vacuum. Crystallisation from chloroform yielded crystals suitable for single crystal X-ray analysis.

Yield: 72.6% (based on mol copper perchlorate used).

FT-IR : (KBr disks) 1544vs br, 1465s, 1427s, 1376s, 1360s 1288w cm^{-1}.

Mass spectrum (EI 70eV) *m/z* 681 (M^+, 8%), 609 (1.9%), 536 (3.9%), 373 (9.1%), 309 (3.2%), 237 (29.9%), 222 (12.3%), 195 (66.2%), 178 (16.9%), 135 (11.7%), 118 (9.1%), 58 (35.7%), 32 (69.5%), 28 (100%).

Found C, 50.48; H, 6.14; N, 8.02; $C_{30}H_{42}CuN_4O_{10}$ required C, 52.82; H, 6.21; N, 8.21.

3.5.8 *cis*-bis(*N*-pivaloyl-*N'*,*N'*-diethylthioureato)copper(II), $Cu(L^4\text{-}S,O)_2$

A solution of copper acetate monohydrate (0.25mmol) dissolved in 30ml of methanol and water (1:1 v/v) and added to a solution of *N*-pivaloyl-*N'*,*N'*-diethylthiourea (0.5mmol) dissolved in 30 ml of methanol. The reaction mixture was stirred at room temperature for 1 hour after which a further 30 ml of water was added. The reaction mixture was then cooled overnight to allow a precipitate to settle out. The crude crystalline precipitate was recovered by filtration and washed with water. The product was further purified by recrystallization from methanol and dried under high vacuum. Very dark green crystals suitable for single crystal X-ray diffraction were obtained by slow crystallization from chloroform and ethanol or by slow crystallization from methanol. When crystallizing from a mixture of chloroform and ethanol, a lower yield of 63% was obtained and a co-crystallization of sulphur as S_8 crystals were also obtained.

Yield : 92.8% (yield based on copper(II) acetate monohydrate).

FT-IR : (KBr disks) 1516s, 1487vs, 1422vs, 1353s, 1255s cm^{-1}.

Mass spectrum (EI 70eV) *m/z* 493 (M^+ 34.1%), 311 (9.1%), 261 (6.8%), 259 (9.1%), 215 (100%), 159 (25.0%), 116 (20.5%), 72 (54.5%), 57 (40.9%).

Mp: 112.5-113.0°C

Found C, 47.6; H, 8.0; N, 11.4; S, 12.6; $C_{20}H_{38}CuN_4O_2S_2$ required C, 48.60; H, 7.75; N, 11.34; S, 12.98%.

3.5.9 *cis*-bis(*N*-pivaloyl-*N'*,*N'*-diethylthioureato)nickel(II), ($Ni(L^4\text{-}S,O)_2$

A solution of nickel(II)acetate tetrahydrate (0.25mmol) was dissolved in 40ml of acetonitrile and water (1:1 v/v) and added dropwise to a 40ml acetonitrile-water (1:1 v/v) solution of *N*-pivaloyl-*N'*,*N'*-diethylthiourea (0.5mmol). The reaction mixture was gently warmed to 50°C and stirred for 1 hour after which a further 80 ml of water was added. The reaction mixture was then cooled to 5°C overnight to allow a crude product precipitate to settle out. The crystalline precipitate was recovered by filtration, recrystallized from chloroform and ethanol and dried under high vacuum. Magenta crystals suitable for single crystal X-ray diffraction were obtained by slow crystallization from chloroform.

Yield: 64.8% (yield based on mol nickel(II) acetate tetrahydrate used).

NMR: δ_H (300 MHz, solvent $CDCl_3$) 3.66 and 3.61 (8H, m, $4CH_2$), 1.20 (6H, s, $2CH_3$), 1.10 (24H, s, $8CH_3$). δ_C (76 MHz, solvent $CDCl_3$) 179.5 (C(O)), 174.6 C(S)), 47.4 and 47.9 ($2CH_2$), 39.5 (quaternary-C), 26.9 ($3CH_3$), 11.4 and 13.1 ($2CH_3$).

FT-IR: (KBr disks) 1522s, 1493vs, 1421vs, 1353s, 1256 cm^{-1}.

Mass spectrum (EI 70eV) *m/z* 488 (M^+ 64.4%), 371 (17.8%), 274 (40.0%), 216 (22.2%), 159 (22.2%), 127 (40.0%), 117 (37.8%), 72 (86.7%), 57 (100%).

Mp: 146.5 - 147.2°C

Found C, 49.30; H, 8.0; N, 11.65; S, 13.2; $C_{20}H_{38}N_4NiO_2S_2$ required C, 49.09; H 7.83; N, 11.45; S, 13.11%.

3.5.10 Tetrakis(μ_2-2,2-dimethylpropanoato-κ^2O,O')-bis(pyridine-κN)copper(II), $Cu_2(C_5H_9O_2)_4(C_5H_5N)_2$.

Pyridine (0.55x10-3 mol) was added dropwise with stirring to a solution of *N*-pivaloyl-*N'*,*N'*-dimethylurea ($0.5x10^{-5}$ mol) dissolved in 20ml of chloroform. The reaction mixture was stirred at room temperature for 10 minutes. Copper perchlorate hexahydrate ($0.25x10^{-3}$ mol) dissolved in 20ml of water was added and the reaction mixture was allowed to stir at room temperature overnight. The two phases were separated and the aqueous phase was repeatedly extracted with small volumes of chloroform and ether (10ml). The organic fractions were combined and the crude product was recovered as a blue amorphous solid under reduced pressure and dried under high vacuum. The crude product was further purified by crystallization from a solution of chloroform. Hexane was added to a concentrated chloroform solution of the crude product until the solution became turbid. Upon standing at room temperature for several weeks, crystals suitable for single crystal X-ray diffraction were obtained and isolated manually under a microscope.

Yield 71% (based on mol copper perchlorate hexahydrate used)

Supplement A: ***Further synthesis products***

A.1 *N,N*-dibenzoyl-*N',N'*-dimethylurea (1,1-Dibenzoyl-3,3-dimethylurea)

It was attempted to prepare *N*-benzoyl-*N',N'*-dimethylurea, Scheme 4, as part of the series of *N*-acyl(aroy)-*N',N'*-dialkylurea ligands **H(L^1-*O,O'*)**, **H(L^2-*O,O'*)** and **H(L^3-*O,O'*)** as well as the series of complexes resulting from the coordination of these ligands with copper.

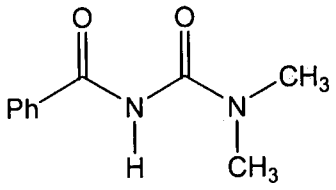

Scheme 3 *N*-benzoyl-*N',N'*-dimethylurea

However, in attempting to prepare *N*-benzoyl-*N',N'*-dimethylurea, from a method analogous to that used to prepare **H(L^1-*O,O'*)**, **H(L^2-*O,O'*)** and **H(L^3-*O,O'*)**, *N,N*-dibenzoyl-*N',N'*-dimethylurea, Scheme 4, was isolated as the primary product of crystallization[60]. The *N*-acylurea substructure has several agrochemical and medicinal applications[16, 61] and acylchalcogenourea derivatives have been increasingly used in analytical applications since their coordinating properties were first discovered[62]. As a result, a number of papers have been published concerning various methods of synthesis of these ligands[7, 16, 62] and the synthesis of *N,N*-dibenzoyl-*N',N'*-dimethylurea has previously been published[16, 63, 64].

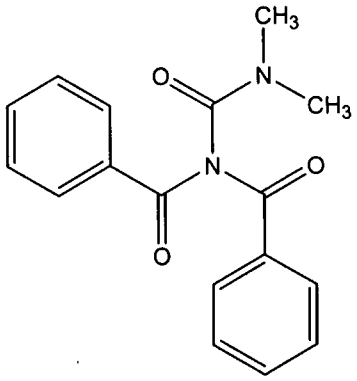

Scheme 4 *N,N*-dibenzoyl-*N',N'*-dimethylurea

The proposed mechanism by which *N,N*-dibenzoyl-*N',N'*-dimethylurea formed as the primary product of the reaction is outlined in Scheme 5. It is proposed that several factors contribute to the formation of *N,N*-dibenzoyl-*N',N'*-dimethylurea:

- there is a slight excess ($3x10^{-3}$ mol) of the strong base triethylamine in the initial reaction mixture which is most likely able to deprotonate the relatively acidic proton of the *N*-benzoyl-*N',N'*-dimethylurea

- the triethylammonium chloride of the benzoyltriethylammonium chloride intermediate indicated in Scheme 5 is a good leaving group
- the *N*-benzoyl-*N'*,*N'*-dimethylurea may still have a degree of nucleophilic character due to the lone pair located on the central nitrogen atom

It is further proposed that due to the factors listed above, the second nucleophilic attack on the benzoyltriethylammonium chloride intermediate may occur by either of two pathways.

1. The *N*-benzoyl-*N'*,*N'*-dimethylurea may carry out a nucleophilic attack directly on the benzoyltriethylammonium chloride intermediate by means of the lone pair located on the central nitrogen of the *N*-benzoyl-*N'*,*N'*-dimethylurea [reaction pathway (i)], or more likely,
2. the *N*-benzoyl-*N'*,*N'*-dimethylurea is first deprotonated by the excess triethylamine and the resulting deprotonated *N*-benzoyl-*N'*,*N'*-dimethylurea then carries out a nucleophilic attack on the benzoyltriethylammonium chloride intermediate [reaction pathway (ii)].

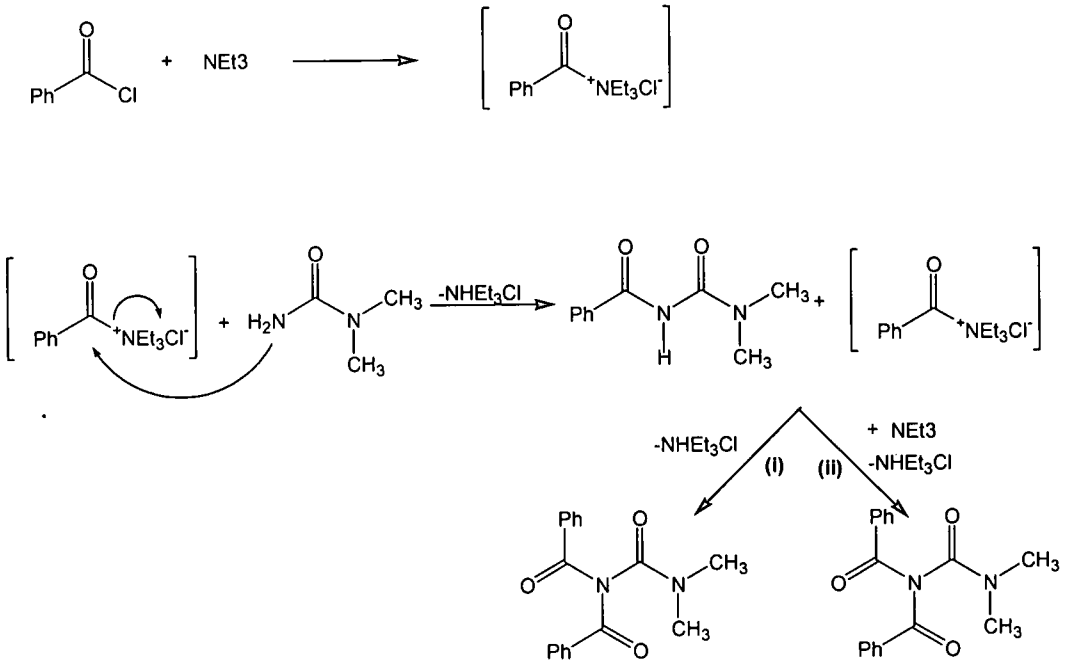

Scheme 5 Proposed mechanism of formation of *N*,*N*-dibenzoyl-*N'*,*N'*-dimethylurea

Although the synthesis of *N*,*N*-dibenzoyl-*N'*,*N'*-dimethylurea has previously been reported[16, 63, 64], a survey of the Cambridge Structural Database (CSD) showed that this structure has not yet been crystallographically characterized[17]. The crystals isolated in the reaction described were characterized by single crystal X-ray diffraction analysis. The molecular structure of *N*,*N*-dibenzoyl-*N'*,*N'*-dimethylurea is shown in Figure 34. Selected bond lengths and torsion angles are listed in Table 10. The molecules of *N*,*N*-dibenzoyl-*N'*,*N'*-dimethylurea interact through several C-H...O intermolecular

hydrogen bonds and hydrogen contacts as well as through several C-H...π interactions resulting in a three-dimensional network. The mean planes of the two benzoyl rings of *N*,*N*-dibenzoyl-*N'*,*N'*-dimethylurea intersect at 72.0(1)°. The observed overall non-planar nature of *N*,*N*-dibenzoyl-*N'*,*N'*-dimethylurea as illustrated in Figure 34 is to be expected due to the pyramidal sp^3 hybridization of the central nitrogen atom.

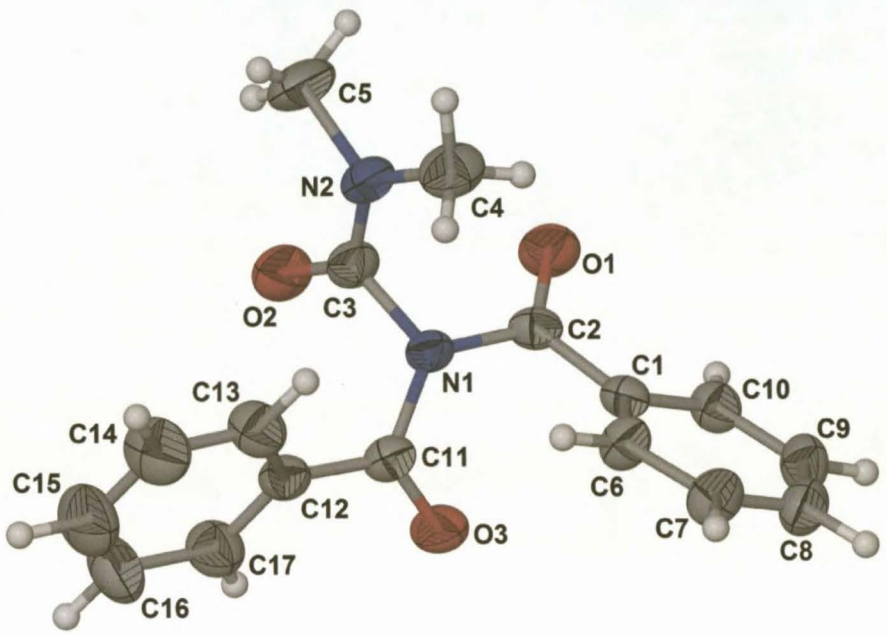

Figure 34 Molecular structure of ***N,N*-dienzoyl-*N'*,*N'*-dimethylurea**. Displacement ellipsoids are drawn at the 50% probability level.

N1-C11	1.416(3)	C1-C2	1.479(4)
N1-C2	1.422(3)	N2-C3	1.324(4)
N1-C3	1.454(4)	N2-C4	1.440(4)
O3-C11	1.203(3)	N2-C5	1.464(4)
O1-C2	1.205(3)	O2-C3	1.208(4)
C11-C12	1.486(4)		
O2-C3-C11-O3	84.3(4)	O1-C2-C11-O3	109.1(3)
O2-C3-C2-O1	76.8(3)		

Table 10 Selected bond lengths (A°) and torsion angles (°) of ***N,N*-dibenzoyl-*N'*,*N'*-dimethylurea**.

The C-N bond lengths C2-N1 (1.422(3)Å), N1-C3 (1.454(4)Å) and N1-C11 (1.416(3)Å) are all shorter than the accepted average C-N single bond length of 1.472(5)Å[24], however C3-N2 is significantly shorter at 1.324(4)Å, thereby indicating a significant partial double bond character and restricted rotation around this bond.

The carbonyl moiety, C3-O2, is orientated at an acute angle relative to the C11-O3 and C2-O1 carbonyl moieties, as illustrated by the pseudo-torsion angles O2-C3...C11-O3 of 84.3(4)° and O2-C3...C2-O1 76.8(3)°, while the carbonyl moiety C2-O1 is obtuse relative to carbonyl C11-O3 as illustrated by the pseudo-torsion angle O1-C2...C11-O3 109.1(3)°.

The crystal packing of *N*,*N*-dibenzoyl-*N'*,*N'*-dimethylurea is governed by the weak intermolecular hydrogen interactions as listed in Table 11, as well as through several face–to-edge C-H...π interactions. One-dimensional molecular chains of *N*,*N*-dibenzoyl-*N'*,*N'*-dimethylurea extend along [100] as a result of the C7-H7...O3^{i} intermolecular hydrogen bond [C7-H7...O3^{i} 2.47Å 153.1° symmetry code (i) x+1, y, z]. The molecular structure of *N*,*N*-dibenzoyl-*N'*,*N'*-dimethylurea is also stabilized by several intra- and intermolecular hydrogen contacts as listed in Table 12. The one-dimensional chains extending along [100] extend as two-dimensional sheets parallel to [010] due to the C9-H9...O1^{ii} and C5-H56...O3^{iii} hydrogen contacts [C9-H9...O1^{ii} 2.58Å 125.9°; C5-H56...O3^{iii} 2.58Å 128.2°, symmetry codes (ii) –x, ½+y, ½-z; (iii) x, y-1, z] The packing of the molecules of *N*,*N*-dibenzoyl-*N'*,*N'*-dimethylurea are further stabilized by the weak C4-H41...N1, C4-H42...O1 and C5-H51...O2 intramolecular hydrogen contacts.

D-H...A	D-H	H...A	D...A	D-H...A
C7-H7...O3^{i}	0.95	2.47	3.349(4)	153.1
C4-H46...O2^{i}	0.98	2.40	3.277(5)	149.0

Table 11 Hydrogen bond geometry of ***N*,*N*-dibenzoyl-*N'*,*N'*-dimethylurea** as identified by XSeed[33, 34] and Platon[35] with s.u.s of the donor...acceptor [D...A] distances (Å) in parenthesis.

D-H...A	D-H	H...A	D...A	D-H...A
C9-H9...O1^{ii}	0.95	2.58	3.226(4)	125.9
C5-H56...O3^{iii}	0.98	2.58	3.281(5)	128.2
C4-H41...N1	0.98	2.30	2.771(4)	108.4
C4-H42...O1	0.98	2.56	3.211(5)	123.5
C5-H51...O2	0.98	2.30	2.733(5)	106.0

Table 12 Hydrogen contact geometry of ***N*,*N*-dibenzoyl-*N'*,*N'*-dimethylurea** as identified by XSeed[33, 34] and Platon[35] with s.u.s of the donor...acceptor [D...A] distances (Å) in parenthesis.

Face-to-edge C-H...π interactions as illustrated in Figure 35 [C14-H14...*Cg*1^{iv} = 3.24Å, C17-H17...*Cg*1^{v} = 3.13Å, where *Cg*1 is the centroid of the C12-C17 benzoyl rings; symmetry codes: (iv) ½+x, -y-½, -z; (v) x-½, ½-y, -z] result in the formation layers of *N*,*N*-dibenzoyl-*N'*,*N'*-dimethylurea parallel to the (001) plane. A further C-H...π interaction, C9-H9...*Cg*2^{vi} = 3.49Å [*Cg*2 is the centroid of the C1/C6-C10 benzoyl ring; symmetry code: (vi) 1-x, ½+y, ½-z], was observed in *N*,*N*-dibenzoyl-*N'*,*N'*-dimethylurea.

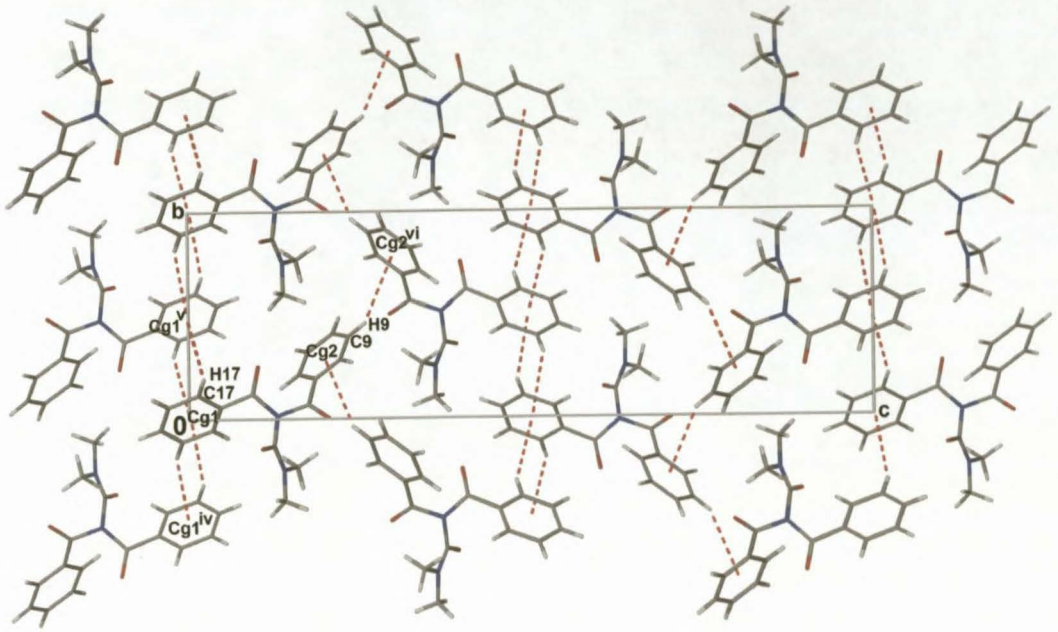

Figure 35 An extended packing diagram of ***N,N*-dibenzoyl-*N',N'*-dimethylurea** viewed along [100], indicating the C14-H14...*Cg1*^{iv}, C17-H17...*Cg1*^{v} and C9-H9...*Cg2*^{vi} interactions as dashed lines. *Cg1* and *Cg2* are the centroids of the C12-C17 and C1/C6-C10 rings respectively. [Symmetry codes: (iv) ½+x, -y-½, -z; (v) x-½, ½-y, -z; (vi) 1-x, ½+y, ½-z].

The C-H...π interactions observed here compare well with the C-H... π interactions that were observed for three benzoylfuran-2-yl ketone derivatives[65], as well as with the *ab initio* calculated C-H... π interactions reported by Sinnokrot et al.,[66] which in turn correlate well with the 5.05Å mean distance between phenyl ring centroids for interacting side chains in proteins reported by Burley and Petsko[67].

A.1.1 Experimental

Syntheses was carried out under a dry argon atmosphere using standard Schlenk and vacuum-line techniques. Triethylamine, ($3.3x10^{-2}$ mol) dissolved in 10ml of anhydrous dichloromethane, was added dropwise with stirring to a solution of $3.0x10^{-2}$ mol of benzoyl chloride dissolved in 20ml of anhydrous dichloromethane. After stirring at room temperature for 10 minutes, the above reaction mixture was added to a solution of $3.0x10^{-2}$ mol of *N,N*-dimethylurea dissolved in 60ml of anhydrous dichloromethane. The solution was gently warmed to 60°C for 1 hour, cooled to room temperature and stirred overnight. 30ml of water was added and the crude product was extracted with 3 x 25ml of chloroform. The combined organic layers were washed with 3 x 25ml of water, dried over $MgSO_4$, filtered and the crude product was isolated as a white crystalline product under reduced pressure and further purified by crystallization from ethyl acetate and dichloromethane. Crystals suitable for single crystal X-ray analysis were selected and isolated. [overall yield 24.6% (based on *N,N*- dimethylurea used).]

Elemental analysis calculated for $C_{17}H_{16}N_2O_3$ (296.32 $gmol^{-1}$): C 68.91, H 5.44, N 9.45; found 68.53, H 5.42, N 9.97%.

All hydrogen atoms were placed in geometrically calculated positions with C-H = 0.99Å (for $-CH_2-$), 0.98Å (for $-CH_3$) and 0.95Å (for phenyl) and refined using a riding model with $U_{iso}(H) = 1.2U_{eq}$ (parent) (for $-CH_2-$ and phenyl), or $U_{iso}(H) = 1.5U_{eq}$(parent) (for $-CH_3$). In the absence of significant anomalous scattering effects, Friedel pairs were merged.

A.1.2 Crystal data

$C_{17}H_{16}N_2O_3$
Mr = 296.32g.mol^{-1}
Orthorhombic, $P2_12_12_1$
a = 6.002 (3) Å
b = 8.822 (5) Å
c = 29.339 (15) Å
V = 1553.5 (14) $Å^3$
Z = 4
D_x = 1.267 Mg m^{-3}

Mo Kα radiation
Cell parameters from 8844 reflections
θ = 2.4–26.0°
μ = 0.09 mm^{-1}
T = 100 (2) K
Needle, colourless
0.30 x 0.10 x 0.05 mm

A.1.3 Data collection

Bruker SMART APEX CCD diffractometer
ω scans
Absorption correction: multi-scan (SADABS[57, 68])
T_{min} = 0.964, T_{max} = 0.996
8844 measured reflections
1803 independent reflections

1483 reflections with I > 2σ(I)

R_{int} = 0.036
θ_{max} = 26.0°

h = -7 → 3
k = -10 → 10
l = -32 → 36

A.1.4 Refinement

Refinement on F^2
$R[F^2 > 2\sigma(F^2)]$ = 0.048
$wR(F^2)$ = 0.105
S = 1.15
1803 reflections
201 parameters

H-atom parameters constrained
$w = 1/[\sigma^2(F_o^2) + (0.041P)^2 + 0.2226P]$
where $P = (F_o^2 + 2F_c^2)/3$
$(\Delta/\sigma)_{max}$ = 0.009
$\Delta\rho_{max}$ = 0.15 e $Å^{-3}$
$\Delta\rho_{min}$ = -0.14 e $Å^{-3}$

A.1.5 Data collection

SMART[69]; cell refinement: SAINT[70]; data reduction: SAINT[70]; program(s) used to solve structure: SHELXS97[58]; program(s) used to refine structure: SHELXL97[58]; molecular graphics: X-SEED[33, 34]; software used to prepare material for publication: X-SEED[33, 34].

A.2 Benzamide

A further by-product that was isolated during the synthesis of *N*-benzoyl-*N'*,*N'*-dimethylurea was crystalline benzamide. The benzamide presumably formed as a result of hydrolysis (Scheme 6) by adventitious water present during the initial synthesis or even possibly during the work-up of the crude reaction product as discussed in section 3.5 which included the use of water. An account of similar hydrolysis has been recorded in the recent literature where the attempted crystallization of the phosphinimide 2,3-diphenyl-2-(nitro-benzoylimido)-3,4-dihydro-2*H*-2$\sigma^4$2λ^5-naphtho[2,3-e][1,3,2]-oxaza-phosphorin-4-one from a solution of dichloromethane resulted in the formation of *p*-nitrobenzamide[71]. Other accounts have also been recorded in the literature where benzamide has been prepared directly from benzoyl chloride as the product of nitrogen fixation[72]. However, in such accounts, the use of transition metal complexes such as TiX_4-Li-TMSCl (X = Cl, $OCHMe_2$; TMS = trimethylsilyl) was necessary[72-74].

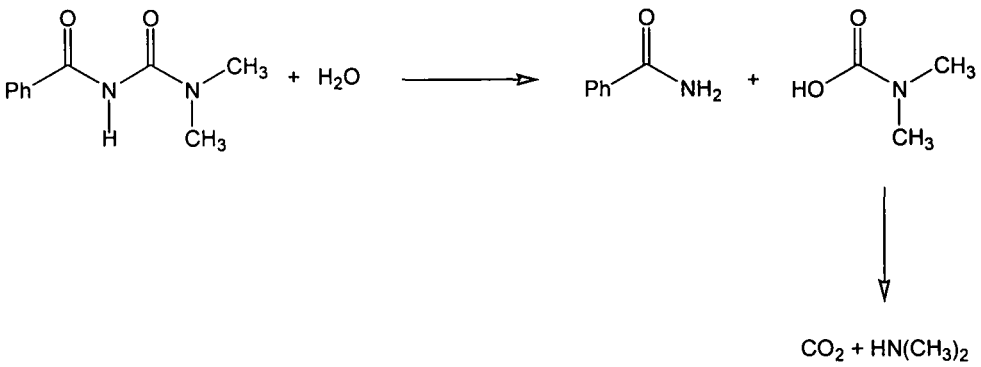

Scheme 6 Proposed formation of benzamide during the synthesis of *N*-benzoyl-*N'*,*N'*-dimethylurea

The molecular structure of benzamide was initially reported as early as 1959[75]. The molecular structure has been deposited a further five times with the CCDC (Cambridge Crystallographic Data Centre)[76-78], the most recent of which was in 2003[79]. Other structures of benzamide that can be found on the CSD[17] (Cambridge Structural Database) have the benzamide included in a structure of a more complex molecule[17]. The molecular structure of benzamide reported here compares well with the molecular structures of benzamide listed on the CSD[75-79] (see Table 13).

	Benzamide	CCDC[75]	CCDC[76]	CCDC[77]	CCDC[77]	CCDC[78]	CCDC[79]
Space group	$P2_1/c$	$P2_1/c$	$P2_1/c$	$P2_1/c$	$P2_1/c$	$P2_1/c$	$P2_1/c$
a =	5.533(2)	5.590(10)	5.607(2)	5.529(1)	5.549(1)	5.549(1)	5.566(0)
b =	5.029 (2)	5.010(10)	5.046(2)	5.033(1)	5.033(1)	5.033(1)	5.053(0)
c =	21.491(6)	21.930(50)	22.053(8)	21.343(3)	21.548(4)	21.548(4)	21.698(4)
α =	90.00	90.00	90.00	90.00	90.00	90.00	90.00
β =	90.863(5)°	90.75(17)	90.66(3)	88.73(1)	89.22(1)	89.22(1)	90.39(0)
γ =	90.00	90.00	90.00	90.00	90.00	90.00	90.00
R_{int} =	0.023	0.087	0.0680	0.040	0.0630	0.047	0.0376
D (g/cm^3) =	1.346 $^{-3}$	1.310	1.290	1.355	1.337	1.337	1.323
T (K) =	100 (2)	295	295	15	123	123	173

Table 13 Crystallographic data for benzamide as well as for the molecular structures of benzamide listed on the CSD.

Benzamide crystallizes monoclinic with space group $P2_1/c$. The molecular structure of benzamide is illustrated in Figure 36 showing the numbering scheme used. Selected bond lengths, bond angles and torsion angles are listed in Table 14. The amide group is rotated significantly out of the plane of the phenyl ring. This is illustrated by the fact that the C1/C3-C7 least-squares plane intersects the least-squares plane defined through C2/O1/N1 at 25.6(2)°. The non-planarity of the benzamide is further illustrated by the C7-C1-C2-O1 and the C3-C1-C2-O1 torsion angles of 25.0(3)° and -153.7(2)° respectively. An asymmetry of bond angles is observed in bond angles C1-C2-O1 (120.4(2)°) and N1-C2-O1 (122.2(2)°). This asymmetry may result from an attraction between H7 and O1 due to a weak hydrogen contact between C7-H7...O1 (2.57Å, 96.4°). Similar asymmetry of bond angles around the carbonyl group of *O,O'*-diethyl *N,N'*-(*p*-phenylene-dicarbonyl)bis(thiocarbamate) (C-H...O 2.42Å, 99.7°) due to comparable hydrogen contacts has been reported in the literature[80]. The observed asymmetry of bond angles around the carbonyl group of *N*-(2-furoyl)thiocarbamaic-*O*-isopropyl ester (C-H...O 2.96Å) has also been attributed to a comparable intramolecular hydrogen interaction[81]. The 'weak' intermolecular hydrogen contact C7-H7...O1 observed here appears to have little to no effect on the overall packing of the molecules of benzamide within the unit cell.

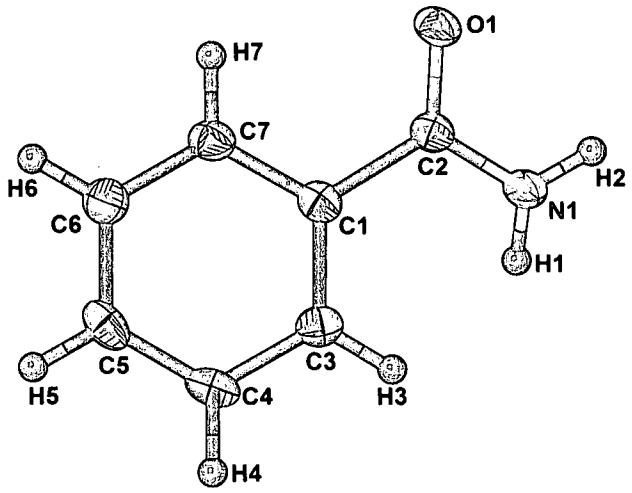

Figure 36 Molecular structure of benzamide showing the numbering scheme used. Displacement ellipsoids are drawn at the 70% probability level.

C1-C2	1.496(3)	C2-N1	1.332(2)
O1-C2	1.241(2)		
C7-C1-C2	118.6(2)	C3-C1-C2	122.1(2)
C1-C2-O1	120.4(2)	O1-C2-N1	122.2(2)
C7-C1-C2-O1	25.0(3)	C3-C1-C2-N1	25.6(3)
C3-C1-C2-O1	-153.7(2)		

Table 14 Selected bond lengths (Å), bond angles (°) and torsion angles (°) of benzamide.

The crystal packing of benzamide appears to be governed by a collection of intermolecular hydrogen bonds as well as by a face-to-edge C-H...π interaction. The molecules of benzamide are initially linked via two intermolecular hydrogen bonds to O1 [N1-H1...O1^{i} 2.04Å, 155.1°; N1-H2...O1^{ii} 2.05Å, 173.2° symmetry code (i) x, 1+y, z, (ii) 1-x, 1-y, -z] of two adjacent molecules which results in one dimensional molecular chains extending parallel to the *a-b* plane of the unit cell as illustrated in Figure 37.

D-H...A	D-H	H...A	D...A	D-H...A
N1-H1...O1^{i}	0.93	2.04	2.904(2)	155.1
N1-H2...O1^{ii}	0.88	2.05	2.932(2)	173.2 *
C7-H7...O1	0.95	2.57	2.840(2)	96.4

Table 15 Hydrogen bond and hydrogen contact geometry of benzamide as identified by XSeed[33, 34] and Platon[35] with s.u.s of the donor...acceptor [D...A] distances (Å) in parenthesis.

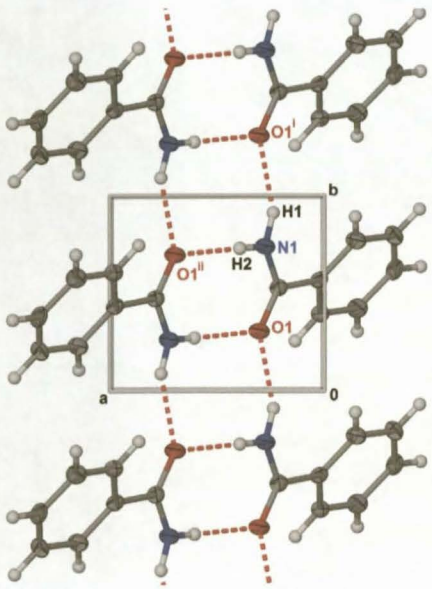

Figure 37 One dimensional chains of benzamide extending along the *a-b* plane resulting from the N1-H1...O1^{i} and N1-H2...O1^{ii} intermolecular hydrogen bonds as viewed along [001]. Symmetry codes: (i) x,1+y,z; (ii) 1-x,1-y,-z.

The alternate layers of one dimensional molecular chains are further cross linked via a face-to-edge C-H...π interaction [C6-H6...*Cg*1^{iii} 3.00Å, 143.23°, where *Cg*1^{iii} is the centroid of the C1/C3-C7 phenyl ring; symmetry code: (iii) –x, y-½, ½-z] which results in the formation of undulating three dimensional sheets. The face-to-edge C-H...π interaction is illustrated in Figure 38.

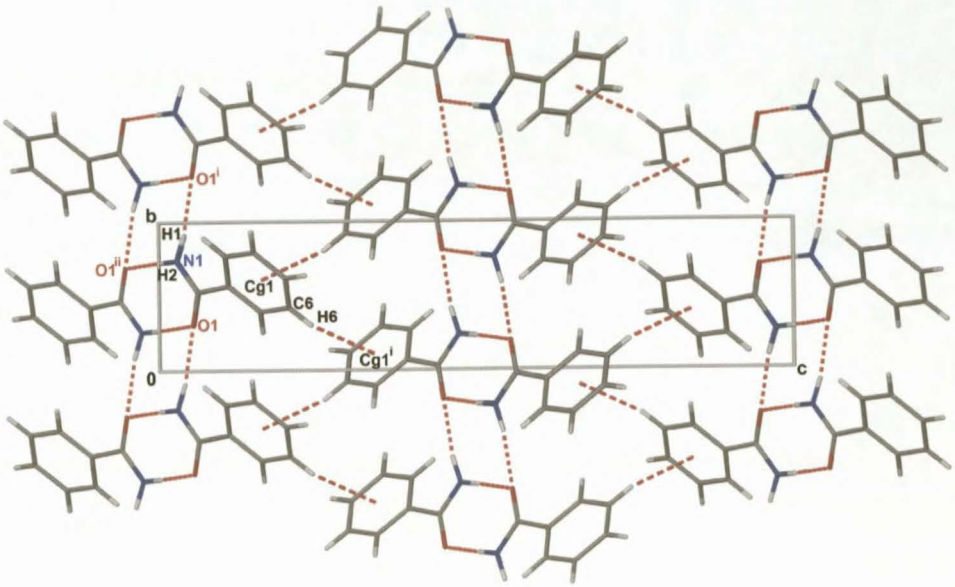

Figure 38 An extended packing diagram of benzamide as viewed along [100] indicating the undulating three dimensional sheets resulting from the face-on-edge C6-H6...Cg1^{iii} interactions as well as the N1-H1...O1^{i} and N1-H2...O1^{ii} intermolecular hydrogen bonds [Symmetry codes: (i) x, 1+y,z; (ii) 1-x, 1-y, -z; (iii) –x, y-½, ½-z].

A.2.1 Experimental

Syntheses was carried out under a dry argon atmosphere using standard Schlenk and vacuum-line techniques. Triethylamine, ($3.3x10^{-2}$ mol) dissolved in 10ml of anhydrous dichloromethane, was added dropwise with stirring to a solution of $3.0x10^{-2}$ mol of benzoyl chloride dissolved in 20ml of anhydrous dichloromethane. After stirring at room temperature for 10 minutes, the above reaction mixture was added to a solution of $3.0x10^{-2}$ mol of *N*,*N*-dimethylurea dissolved in 60ml of anhydrous dichloromethane. The solution was gently warmed to 60°C for 1 hour, cooled to room temperature and stirred overnight. 30ml of water was added and the crude product was extracted with 3 x 25ml of chloroform. The combined organic layers were washed with 3 x 25ml of water, dried over $MgSO_4$, filtered and the crude product was isolated as a white crystalline product under reduced vacuum and further purified by crystallization from ethyl acetate and dichloromethane. Crystals suitable for single crystal X-ray analysis were identified and isolated. [overall yield 35% (based on *N*,*N*- dimethylurea used).]

All hydrogen atoms were placed in geometrically calculated positions with C-H = 0.99Å (for $-CH_2-$), 0.98Å (for $-CH_3$) and 0.95Å (for phenyl) and refined using a riding model with $U_{iso}(H) = 1.2U_{eq}$ (parent) (for $-CH_2-$ and phenyl), or $U_{iso}(H) = 1.5U_{eq}$(parent) (for $-CH_3$). In the absence of significant anomalous scattering effects, Friedel pairs were merged.

A.2.2 Crystal data

C_7H_7NO
M_r = 121.14g.mol^{-1}
Monoclinic, $P2_1/c$
a = 5.533(2) Å
b = 5.029 (2) Å
c = 21.491 (6) Å
β = 90.863 (5)°
V = 597.8 (3) Å^3
Z = 4

D_x = 1.346 Mg m^{-3}
Mo Kα radiation
Cell parameters from 2507 reflections
θ = 3.68 – 25.98°
μ = 0.092 mm^{-1}
T = 100 (2) K
Plates, colourless
0.55 x 0.35 x 0.20 mm

A.2.3 Data collection

Bruker SMART APEX CCD diffractometer
ω scans
Absorption correction: multi-scan (SADABS[57, 68])
T_{min} = 0.9513, T_{max} = 0.9819
8844 measured reflections
1148 independent reflections

999 reflections with I > 2σ(I)

R_{int} = 0.023
θ_{max} = 25.98°

h = -6 → 6
k = -6 → 3
l = -26 → 25

A.2.4 Refinement

Refinement on F^2
$R[F^2 > 2\sigma(F^2)]$ = 0.0500
$wR(F^2)$ = 0.1227
S = 1.149
1148 reflections
84 parameters

H-atom parameters constrained
$w = 1/[\sigma^2(F_o^2) + (0.0506P)^2 + 0.4020P]$
where $P = (F_o^2 + 2F_c^2)/3$
$(\Delta/\sigma)_{max}$ = 0.000
$\Delta\rho_{max}$ = 0.250 e Å^{-3}
$\Delta\rho_{min}$ = -0.204 e Å^{-3}

A.2.5 Data collection

SMART[69]; cell refinement: SAINT[70]; data reduction: SAINT[70]; program(s) used to solve structure: SHELXS97[58]; program(s) used to refine structure: SHELXL97[58]; molecular graphics: X-SEED[33, 34]; software used to prepare material for publication: X-SEED[33, 34].

A.3 S_8 product resulting from the redox of $Cu(L^4\text{-}S,O)_2$.

During the re-crystallisation process of $Cu(L^4\text{-}S,O)_2$ (see section 3.5.8) from a solvent mixture of ethanol and chloroform, white cubic crystals were also isolated along with the dark green needles that were isolated, characterised and discussed in section 2.3.7. These white cubic crystals were identified by single crystal X-ray diffraction as being S_8 as illustrated in Figure 39. The S_8 presumably resulted from the oxidation of the ligand accompanied by the reduction of the copper(II). No speculation is made of the mechanism of the proposed redox of the $Cu(L^4\text{-}S,O)_2$ complex. Neither was any analysis made of the resulting compounds that remained in solution during the crystallization of S_8. The S_8 crystallized as monoclinic crystals in space group P*n*, and R = 1.2%. The asymmetric unit consists of two rings of S8 with 1.5 units per unit cell.

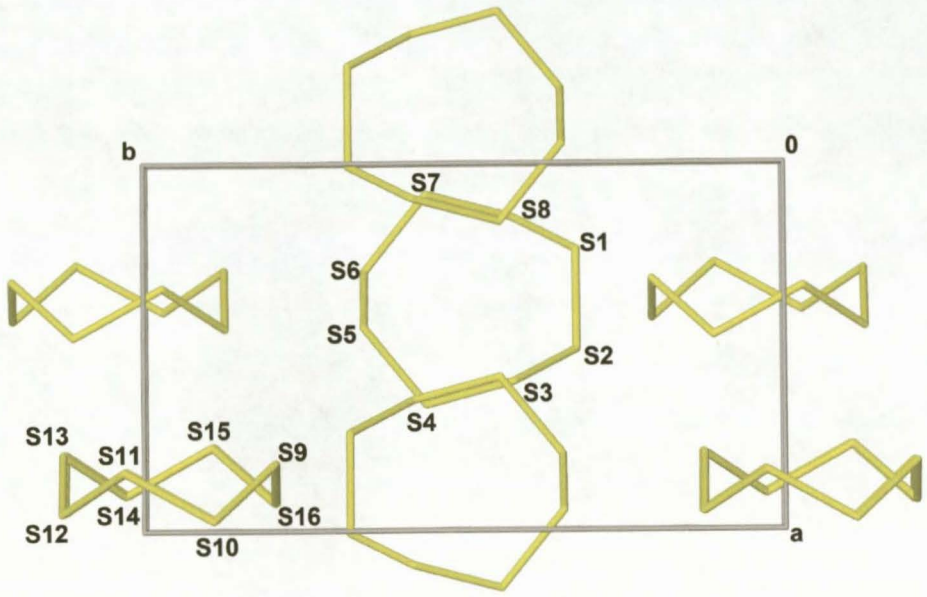

Figure 39 Unit cell of S_8 viewed along [001] showing the numbering scheme used.

A.3.1 Crystal data

S_8
M_r = 256.56g.mol^{-1}
Monoclinic, Pn
a = 8.1134(7) Å
b = 13.0380(12) Å
c = 8.3267(7) Å
β = 113.0250(10)°
V = 810.65(12) Å^3
Z = 4

D_x = 2.102 Mg m^{-3}
Mo Kα radiation
Cell parameters from 4826 reflections
θ = 2.97 – 28.28°
μ = 2.100 mm^{-1}
T = 100 (2) K
Rectangular plates, clear colourless
0.25 x 0.15 x 0.10 mm

A.3.2 Data collection

Bruker SMART APEX CCD diffractometer
ω scans
Absorption correction: multi-scan (SADABS[57, 68])
T_{min} = 0.692
T_{max} = 0.811
4826 measured reflections
3289 independent reflections

3138 reflections with I > 2σ(I)

R_{int} = 0.0122
θ_{max} = 28.28°

h = -10 → 9

k = -11 → 17
l = -10 → 10

A.3.3 Refinement

Refinement on F^2
$R[F^2 > 2\sigma(F^2)]$ = 0.0204
$wR(F^2)$ = 0.0496
S = 0.997
3289 reflections
145 parameters
H-atom parameters constrained

$w = 1/[\sigma^2(F_o^2) + (0.0235P)^2 + 0.4709P]$
where $P = (F_o^2 + 2F_c^2)/3$
$(\Delta/\sigma)_{max}$ = 0.078
$\Delta\rho_{max}$ = 0.443 e Å^{-3}
$\Delta\rho_{min}$ = -0.348 e Å^{-3}

Appendix D:

Experimental crystal data, data collection and crystal refinement details.

Tables containing the experimental crystal data, data collection and crystal refinement details of the crystal structures of the non-coordinated ligands and complexes described in Chapter V, can be found on the included compact disc of this thesis. An example of these tables for the crystal structure of **H(L^1-*O,O*)** is given below.

D.1 *N*-pivaloyl-*N'*,*N'*-diethylurea, H(L^1-*O,O*).

Crystal data

$C_{10}H_{20}N_2O_2$
Mr = 200.28g.mol^{-1}
Monoclinic, P21/*c*
a = 11.161(4) Å
b = 10.535(3) Å
c = 10.876(4) Å
β = 114.971(6)°
V = 1159.3(7) Å^3
Z = 4

D_x = 1.147 Mg m^{-3}
Mo Kα radiation
Cell parameters from 6019 reflections
θ = 2.01 – 28.27°
μ = 0.080 mm^{-1}
T = 100 (2) K
Needles, Clear colorless
0.20 x 0.30 x 0.10 mm

Data collection

Bruker SMART APEX CCD diffractometer
ω scans
Absorption correction: multi-scan (SADABS[57, 68])
T_{min} = 0.972
T_{max} = 0.992
6019 measured reflections
2441 independent reflections

1194 reflections with I > 2σ(I)

R_{int} = 0.0896
θ_{max} = 28.27°

h = -14 → 14

k = -10 → 13
l = -13 → 14

Refinement

Refinement on F^2
$R[F^2 > 2\sigma(F^2)]$ = 0.0637
$wR(F^2)$ = 0.0941
S = 0.807
2441 reflections
132 parameters
H-atom parameters constrained

$w = 1/[\sigma^2(F_o^2) + (0.0036P)^2 + 0.0000P]$
where $P = (F_o^2 + 2F_c^2)/3$
$(\Delta/\sigma)_{max}$ = 0.000
$\Delta\rho_{max}$ = 0.248 e Å^{-3}
$\Delta\rho_{min}$ = -0.273 e Å^{-3}

4. References

[1] K. H. König, H. J. Pletsch, M. Schuster, *Z. Anal Chem* 1986, ***325***, 621-624.
[2] F. F. Blicke, A. P. Centollela, *J. Am. Chem. Soc.* 1938, ***60***, 2923-2924.
[3] A. Padwa, J. P. Snyder, E. A. Curtis, S. M. Sheehan, K. J. Worsencroft, C. O. Kappe, *J. Am. Chem. Soc.* 2000, ***122***, 8155-8167.
[4] P. F. Wiley, *J. Am. Chem. Soc.* 1949, ***71***, 3746-3748.
[5] P. Kutschy, M. Dzurilla, V. Ficeri, D. Koscik, *Collect. Czech. Commun.* 1993, ***58***, 575-587.
[6] Z. Li, X. Wang, Y. Da, J. Chen, *Synth. Commun.* 2000, ***30***, 2635-2645.
[7] J. L. Belletire, M. M. Hiller, *Synth. Commun.* 1989, ***19***, 3543-3551.
[8] V. R. Herzschuh, B. Birner, L. Beyer, F. Dietze, E. Hoyer, *Z. Anorg. Allg. Chem.* 1980, 159-168.
[9] C. R. Worthing, S. B. Walker, in *The Pesticide Manual, 7th Edition*, The British Crop Protection Council, **1983**.
[10] C. C. Yu, R. J. Kuhr, *J. Agric. Food Chem.* 1976, ***24***, 134.
[11] Y. Nakagawa, K. Kitahawa, T. Nishiona, H. Iuramura, T. Fujita, *Pestic. Biochem. Physiol.* 1984, ***21***, 304.
[12] A. Goodman Gilman, L. S. Goodman, A. Gilman, *The Pharmacological Basis of Therapeutics 6th Edition*, Macmillan Publishing Co. Inc., **1980**.
[13] M.-Z. Deng, P. Caubere, *Tetrahedron* 1988, ***44***, 6079-6086.
[14] A. B. DeMilo, D. M. Ostromecky, S. C. Chang, R. E. Redfern, R. L. Fye, *J. Agric. Food Chem.* 1978, ***26***, 164-166.
[15] E. Brambilla, E. Di Salle, G. Briatico, S. Mantegani, A. Temperilli, *Eur. J. Med. Chem.* 1989, ***24***, 421-426.
[16] J. Ravn, M. Ankersen, M. Begtrup, J. F. Lau, *Tetrahedron Lett.* 2003, ***44***, 6931-6935.
[17] F. H. Allen, *Acta Crystallogr., Sect. B: Struct. Sci.* 2002, ***B58***, 380-388.
[18] I. J. Bruno, J. C. Cole, P. R. Edgington, M. Kessler, C. F. Macrae, P. McCabe, J. Pearson, R. Taylor, *Acta Crystallogr., Sect. B: Struct. Sci.* 2002, ***B58***, 389-397.
[19] W. Hernández, E. Spodine, A. Vega, R. Richter, J. Griebel, R. Kirmse, U. Schröder, L. Beyer, *Z. Anorg. Allg. Chem.* 2004, ***630***, 1381-1386.
[20] L. Golič, B. Heyn, L. Beyer, T. Hjonggwan, E. Hoyer, *Z. Chem.* 1986, ***26***, 213-214.
[21] I. B. Douglass, F. B. Dains, *J. Am. Chem. Soc.* 1934, ***56***, 719-721.
[22] M. A. V. Ribeiro da Silva, M. D. M. C. Ribeiro da Silva, L. C. M. da Silva, J. R. B. Gomes, A. M. Damas, F. Dietze, E. Hoyer, *Inorg. Chim. Acta* 2003, ***356***, 95-102.
[23] K. R. Koch, *Coord. Chem. Rev.* 2001, ***216-217***, 473-488.
[24] F. H. Allen, O. Kennard, D. G. Watson, L. Brammer, A. G. Orpen, R. Taylor, *J. Chem. Soc., Perkin Trans. 2* 1987, ***12***, S1-S19.
[25] K. R. Koch, C. Sacht, T. Grimmbacher, S. Bourne, *S. Afr. J. Chem.* 1995, ***48***, 71-77.
[26] K. R. Koch, C. Sacht, S. Bourne, *Inorg. Chim. Acta* 1995, ***232***, 109-115.
[27] G.-J. Xu, S.-P. Yan, D.-Z. Liao, Z.-H. Jiang, C. Peng, *Acta Crystallogr., Sect. E: Struct. Rep. Online* 2005, ***E61***, m933-m935.
[28] D. M. L. Goodgame, I. Hussain, A. J. P. White, D. J. Williams, *J. Chem. Soc., Dalton Trans.* 1999, 2899-2900.
[29] W. Bidell, V. Shklover, H. Berke, *Inorganic Chemistry* 1992, ***31***, 5561-5571.
[30] J. M. Elliott, J. R. Chipperfield, S. Clark, S. J. Teat, E. Sinn, *Inorganic Chemistry* 2002, ***41***, 293-299.
[31] K. R. Koch, J. du Toit, M. R. Caira, C. Sacht, *J. Chem. Soc., Dalton Trans.* 1994, 785-786.
[32] M. A. V. Ribeiro da Silva, M. D. M. C. Ribeiro da Silva, L. C. M. da Silva, J. R. B. Gomes, A. M. Damas, F. Dietze, E. Hoyer, *Inorganica Chemica Acta* 2005, ***356***, 95-102.
[33] L. J. Barbour, *Journal of Supramolecular Chemistry* 2001, ***1***, 189-191.
[34] J. L. Atwood, L. J. Barbour, *Cryst. Growth Des.* 2003, ***3***, 3-8.
[35] A. L. Spek, A Multipurpose Crystallographic Tool, University of Utrecht, Netherlands, **1999.**
[36] G. Blewett, C. Esterhuysen, M. W. Bredenkamp, K. R. Koch, *Acta Crystallogr., Sect. E: Struct. Rep. Online* 2006, ***E62***, m420-m422.
[37] J. N. Van Niekerk, F. R. L. Schoening, *Acta Crystallographica* 1953, ***6***, 227-232.
[38] M. Kato, Y. Muto, *Coord. Chem. Rev.* 1988, ***92***, 45-83.
[39] J. A. Moreland, R. J. Doedens, *J. Am. Chem. Soc.* 1975, ***97***, 508-513.
[40] M. Mikuriya, H. Azuma, R. Nukada, M. Handa, *Chem Lett.* 1999, ***1***, 57-58.
[41] N. I. Kirillova, Y. T. Struchkov, M. A. Porai-Koshits, A. A. Pasynskii, A. S. Antsyshkina, L. K. Minacheva, G. G. Sadikov, T. C. Idrisov, V. T. Kalinnikov, *Inorg. Chim. Acta* 1980, ***42***, 115-119.

[42] J. A. Moreland, R. J. Doedens, *J. Am. Chem. Soc.* 1972, ***97***, 508-513.

[43] A. A. Pasynskii, T. C. Idrisov, K. M. Suvorova, V. M. Novotortsev, V. T. Kalinnkov, *Koordinatsionnaya Khimiya* 1975, ***1***, 799-803.

[44] A. A. Pasynskii, T. C. Idrisov, V. M. Novotortsev, V. T. Kalinnikov, *Koordinatsionnaya Khimiya* 1975, ***1***, 1059-1060.

[45] C. M. Harris, B. F. Hoskins, R. L. Martin, *J. Chem. Soc.* 1959, 3728-3736.

[46] M. Mikuriya, R. Nukada, H. Morishita, M. Handa, *Chem Lett.* 1995, ***8***, 617-818.

[47] Y. A. Simonov, V. I. Ivanov, A. V. Ablov, L. N. Milkova, T. I. Malinovskii, *Zh. Strukt. Khim.* 1976, ***17***, 516-523.

[48] Y. Kani, M. Tsuchimoto, S. Ohba, H. Matsushima, T. Tokii, *Acta Crystallogr., Sect. C: Cryst. Struct. Commun.* 2000, ***C56***, 923-925.

[49] Cambridge Crystallographic Data Centre, http://www.ccdc.cam.ac.uk

[50] A. Bencini, A. Dei, C. Sangregorio, F. Totti, M. G. F. Vaz, *Inorganic Chemistry* 2003, ***42***, 8065-8071.

[51] B. Schetter, B. Speiser, *J. Organomet. Chem.* 2004, ***689***, 1472-1480.

[52] L. V. Sudha, D. N. Sathyanarayana, *J. Mol. Struct.* 1984, ***125***, 89-96.

[53] A. B. P. Lever, *Inorganic Electronic Spectroscopy*, second ed., Elsevier, **1984**.

[54] D. Sutton, *Electronic spectra of Transition Metal Complexes*, McGraw-Hill, London, **1968**.

[55] S. Dhar, D. Senapati, P. K. Das, P. Chattopadhyay, M. Nethaji, A. R. Chakravarty, *J. Am. Chem. Soc.* 2003, ***125***, 12118-12124.

[56] Bruker, SMART, SAINT and XPREP, Area detector control and data integration and reduction software, Bruker Analytical X-ray Instruments Inc., Madison, WI, USA., 1995.

[57] G. M. Sheldrick, SADABS. Version 2.05, Empirical absorption correction program for area detector data, University of Göttingen, Germany., 2002.

[58] G. M. Sheldrick, SHELXS97 and SHELXL97, Programs for the Solution and Refinement of Crystal Structures, University of Göttingen, Institüt für Anorganische Chemie der Universität, Tammanstrasse 4, D-3400 Göttingen, Germany, 1997.

[59] Pov-Ray, http://www.povray.org,

[60] G. Blewett, C. Esterhuysen, M. W. Bredenkamp, K. R. Koch, *Acta Crystallogr., Sect. E: Struct. Rep. Online* 2005, ***E61***, o4042-4044.

[61] A. J. Hill, W. M. Degnan, *J. Am. Chem. Soc.* 1940, ***62***, 1595-1596.

[62] M. A. V. Ribeiro da Silva, M. D. M. C. Ribeiro da Silva, L. C. M. Silva, *J. Chem. Thermodynamics* 2000, ***32***, 1113-1119.

[63] W. Schroth, R. Krieg, H. Kluge, M. Gäbler, *Z. Chem.* 1985, ***25***, 398-399.

[64] W. Schroth, H. Kluge, *Z. Chem.* 1986, ***26***, 295-297.

[65] V. T. Yilmaz, C. Kazak, C. Kirilmis, M. Koca, F. W. Heinemann, *Acta Crystallogr., Sect. C: Cryst. Struct. Commun.* 2005, ***C61***, o438-o441.

[66] M. O. Sinnokrot, E. F. Valeev, C. D. Sherrill, *J. Am. Chem. Soc.* 2002, ***124***, 10887-10893.

[67] S. K. Burley, G. A. Petsko, *Science* 1985, ***229(4708)***, 23-28.

[68] R. H. Blessing, *Acta Crystallogr., Sect. A: Found. Crystallogr.* 1995, ***A51***, 33-38.

[69] Bruker, SMART. Version 5.625, Bruker AXS Inc., Madison, Wisconsin, USA, 2001

[70] Bruker, SAINT. Version 6.36a, Bruker AXS Inc., Madison, Wisconsin, USA, 2002

[71] P. G. Jones, H. Thönnessen, R. Schmutzler, A. K. Fischer, *Acta Crystallogr., Sect. E: Struct. Rep. Online* 2002, ***E58***, o1436-o1438.

[72] M. Mori, K. Hori, M. Akashi, M. Hori, Y. Sato, M. Nishida, *Angew. Chem., Int. Ed. Engl.* 1998, ***37***, 636-637.

[73] M. Mori, Y. Uozumi, M. Shibasaki, *Tetrahedron Lett.* 1987, ***28***, 6187-6190.

[74] M. Kawaguchi, S. Hamaoka, M. Mori, *Tetrahedron Lett.* 1993, ***34***, 6907-6910.

[75] B. R. Penfold, J. C. B. White, *Acta Crystallographica* 1959, ***12***, 130.

[76] C. C. F. Blake, R. W. H. Small, *Acta Crystallogr., Sect. B: Struct. Sci.* 1972, ***28***, 2201.

[77] Q. Gao, G. A. Jeffrey, J. R. Ruble, R. K. McMullan, *Acta Crystallogr., Sect. B: Struct. Sci.* 1991, ***47***, 742.

[78] J. R. Ruble, A. Galvao, *Acta Crystallogr., Sect. B: Struct. Sci.* 1995, ***51***, 835.

[79] K. Kobayashi, A. Sato, S. Sakamoto, K. Yamaguchi, *J. Am. Chem. Soc.* 2003, ***125***, 3035-3045.

[80] G. Blewett, C. Esterhuysen, M. W. Bredenkamp, K. R. Koch, *Acta Crystallogr., Sect. C: Cryst. Struct. Commun.* 2004, ***C60***, o862-o864.

[81] A. D. Morales, H. N. de Armas, N. M. Blaton, O. M. Peeters, C. J. D. Ranter, H. Márquez, R. P. Hernández, *Acta Crystallogr., Sect. C: Cryst. Struct. Commun.* 2000, ***C56***, 1042-1043.

Index: Chapter VI

1. Concluding Remarks

The work in this thesis illustrates that several variations of the basic *N*-acyl(aroyl)-*N'*,*N'*-dialkylthiourea motif have been made successfully. A series of compounds of each motif variation was prepared, fully characterised and in turn were successfully complexed to nickel(II), copper(II), palladium(II) and platinum(II).

The *O*-alkyl-*N*-aroylthiocarbamic esters were found to exclusively coordinate in a *cis*-bis(*S,O*) bidentate fashion in the solid state. It was illustrated that a variation to both the *O*-alkyl substituent as well as the *N*-aroyl substituent, did not significantly affect the coordination mode of these ligands to the respective metals used. However, variation of these substituents had a significant influence on the packing of the molecules within the crystal lattice. In the case of the un-coordinated ligands, the packing of the molecules within the unit cell appeared to be largely dictated by intermolecular hydrogen bonding while the packing of the molecules of the metal complexes was primarily dictated by C-H...π and π...π type interactions as well as other weak non-classical intermolecular interactions.

It was further illustrated that the introduction of bulky electron rich methoxy groups onto the *N*-aroyl moiety of the *O*-alkyl-*N*-aroylthiocarbamic ester complexes did lengthen, or otherwise 'soften', the metal-oxygen bond as initially proposed. However, this effect was marginal in most cases and the equivalent *trans*-(*S,O*) metal complex was only detected spectroscopically and not isolated in the solid state. It has subsequently been reported by Hanekom *et al.* that the *cis-trans* isomerism of the structurally analogous *N*-aroyl-*N'*,*N'*-dialkylthiourea complexes is in fact photoinduced[1, 2] and it is suspected that the same would be true for metal complexes derived from *O*-alkyl-*N*-aroylthiocarbamic esters. However, it is suspected that both steric hindrance as well as electronic factors also play a role this regard and should be brought into consideration.

A variation of the *S,O*-coordinating atoms of *N*-aroylthiocarbamic-*O*-alkyl esters to the *O,O'*-coordinating atoms of *N*-acyl(aroyl)-*N'*,*N'*-dialkylureas had a pronounced effect on the coordinating properties of these compounds as well as to the susceptibility of these compounds and resultant copper(II) complexes to hydrolysis. Several unexpected compounds and complexes were produced, isolated and characterised[3, 4] in the attempted synthesis of the non-coordinated *N*-acyl(aroyl)-*N'*,*N'*-dialkylureas as well as the complexed copper(II). One example of a *trans*- or *anti*-(*O,O'*) copper complex was successfully isolated in the solid state and characterised crystallographically. Since both the coordinating atoms of the compounds within this series are essentially equivalent, it is speculated that the *cis-trans* isomerism is chiefly controlled by steric and subtle electronic considerations as initially proposed.

The *N*-acyl(aroyl)-thiocarbamic-*O*-alkyl ester variation to the *N*-acyl(aroyl)-*N'*,*N'*-dialkylthiourea motif was further successfully extended to a series of bipodal *N*-benzoylthiocarbamic-*O*-alkyl esters. Several of these structures represent the first reported single crystal X-ray structures of this type of compound. Furthermore, an interesting case of *syn- anti*-(*S,O*) and *anti- anti*-(*S,O*) polymorphism was

observed for *O,O'*-dimethyl *N,N'*-(*m*-phenylenedicarbonyl)-bis(thiocarbamate) which represents the first reported X-ray crystallographic structure determination of isomers of this class of bipodal ligand[5]. However, the envisaged 2:2 and 3:3 M:L complexes of Ni(II), Pd(II) and Pt(II) derived from these bipodal *O*-alkyl-N-benzoylthiocarbamic esters, were not successfully prepared. These ligands and complexes are susceptible to base promoted hydrolysis under the reaction conditions used which results in the formation of a 'polymeric type' product. These reaction products were not easily characterised due to the exceptionally poor solubility properties of these compounds. However, in one case, poor quality crystals of the resultant copper product were obtained which provided single crystal X-ray analysis evidence of the formation of a one dimensional polymeric type hydrolysis product [as described in chapter IV section 2.7].

2. Potential Future Work

The work outlined in this thesis by no means encompasses all areas of possible investigation into variations of compounds and complexes based on the *N*-acyl(aroyl)-*N',N'*-dialkylthiourea motif and represents the tip of the iceberg at best. Some areas of further investigation include the following:

- An extension of the bipodal *O*-alkyl-*N*-benzoylthiocarbamic ester theme to the synthesis and characterisation of bipodal urea analogues.
- Exploration of further solvent combinations and other experimental variables/conditions to isolate 2:2 and 3:3 M:L metallamacrocycles derived from bipodal *O*-alkyl-*N*-benzoylthiocarbamic esters.
- Testing of the *N*-acyl(aroyl)thiocarbamic-*O*-alkyl esters and *N*-acyl(aroyl)-*N',N'*-dialkylureas in the extraction, and possible preferential extraction, of platinum group metals.
- The tethering of *N*-acyl(aroyl)thiocarbamic-*O*-alkyl esters and *N*-acyl(aroyl)-*N',N'*,-dialkyl ureas to a solid support (e.g. silica) for potential application in platinum group metals extraction.
- Investigation of the potentially photoinduced *cis trans* isomerism of *N*-acyl(aroyl)-*O*-alkylthiocarbamato complexes

One area of investigation that was not covered in this thesis is the potential synthesis of octahedral adducts of complexes derived from *N*-(acyl)aroylthiocarbamic-*O*-alkyl esters and *N*-acyl(aroyl)-*N',N'*-dialkyl ureas. An example of this is illustrated in Figure 1, where pyridine has been substituted in both of the axial positions of Bis(*N*-benzoyl-*O*-benzyl-thiocarbamato)nickel(II) [**Ni(L^2-*S,O*)$_2$** as described in chapter II], **Ni(L^2-*S,O*)$_2$(pyr)$_2$**. [note: the molecular structure and crystal lattice of **Ni(L^2-*S,O*)$_2$(pyr)$_2$** will not be discussed in any detail here as this forms part of a broader investigation of future work].

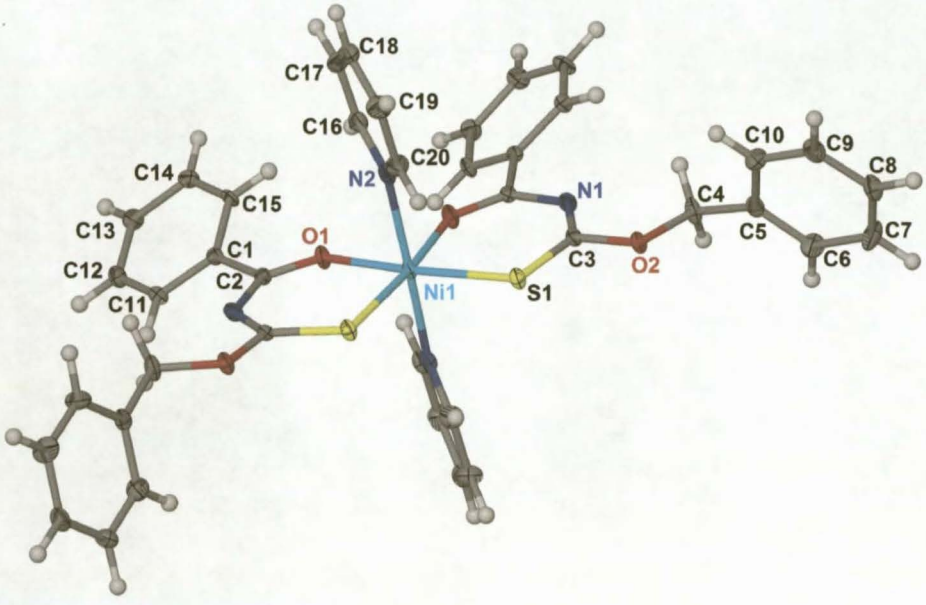

Figure 1 Molecular structure of **Ni(L^2-*S,O*)$_2$(pyr)$_2$**. Thermal ellipsoids are drawn at the 50% probability level and unlabeled atoms are generated by the symmetry operator 1-x, y, ½-z.

A logical direction for the development of investigation into the area of axial coordination of bis(*N*-acyl(aroyl)thiocarbamato-*O*-alkyl) and bis(*N*-acyl(aroyl)-*N'*,*N'*-dialkylthioureato) type complexes is the use of bidentate bridging ligands which have the potential to act as linkers between the metal centers of the complexes. This would then have the potential to allow the assembly of coordination polymers or one dimensional arrays. Several bidentate bridging ligands have frequently been used in this regard, the most common of which include 4,4'-bipyridine (bipy)[6-8] and pyrazine (pyra)[9]. Compounds such as 4,4'-bipyridine and pyrazine (pyra) are rigid, but flexible analogues such as 1,2-bis(4-pyridyl)ethane (BPE)[10, 11] may well be of use.

The expanded packing diagram of **Ni(L^2-*S,O*)$_2$(pyr)$_2$**, as viewed along [010], is illustrated in Figure 2 and gives a hint of the 'supramolecular-type' potential of complexes of this type which are substituted and in the axial position. Theoretically the equivalent complexes which are linked via bidentate bridging ligands into coordination polymers or arrays have even greater potential in this regard.

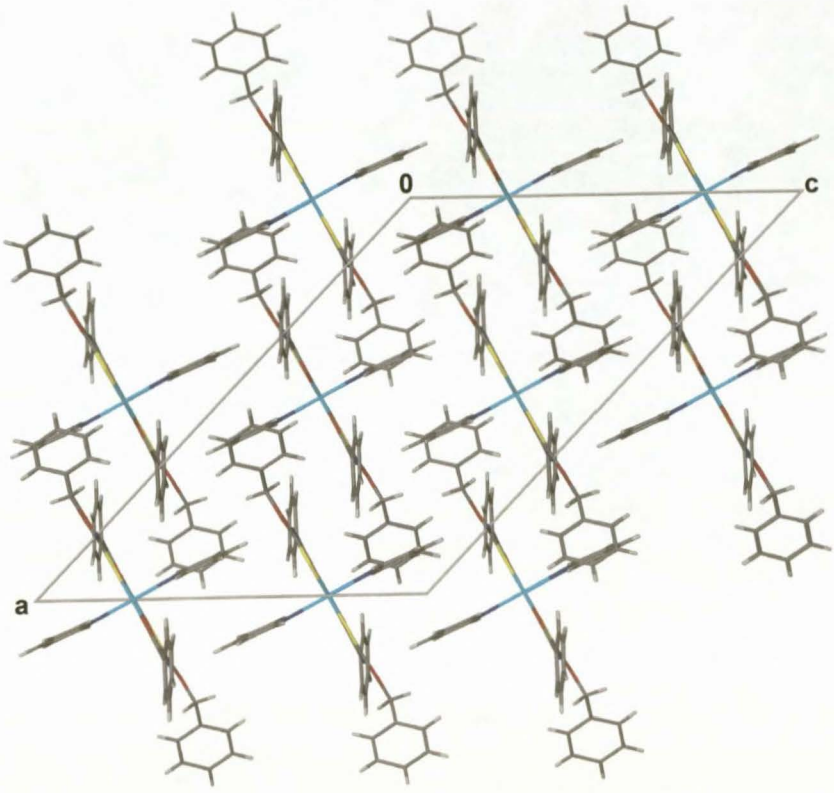

Figure 2 Extended packing diagram of **Ni(L^2-*S,O*)$_2$(pyr)$_2$** as viewed along [010].

In order for the complexes described within this thesis to be cross linked by bidentate substituents in the axial position, the metal centers would have to be able to align themselves and essentially be free from any steric hindrance in the axial positions resulting from the bis-(*S,O*) or bis-(*O,O'*) coordinated ligands. The close conformation of these complexes to overall planarity potentially makes these complexes ideal to be cross linked by rigid or flexible bidentate compounds such as 4,4'-bipyridine.

Furthermore, although the bipodal *O*-alkyl-*N*-benzoylthiocarbamic acid esters, as described in chapter IV, did not form the target 2:2 or 3:3 metallomacrocyclic complexes, it has been shown that these bipodal molecules showed some interesting 'supramolecular-type' assemblies in the solid state as the result of C-H…π, π…π and other weak intermolecular interactions. It is therefore possible that, with the use of appropriate cross linking compounds, these bipodal *O*-alkyl-*N*-benzoylthiocarbamic acid esters may form some interesting three dimensional network assemblies which may even exhibit some interesting host guest properties.

3. References.

[1] D. Hanekom, M.Sc *thesis*, Stellenbosch Univeristy, **2006**.
[2] D. Hanekom, J. M. McKenzie, N. M. Derix, K. R. Koch, *Chem. Commun.* 2005, ***6***, 767-769.
[3] G. Blewett, C. Esterhuysen, M. W. Bredenkamp, K. R. Koch, *Acta Crystallogr., Sect. E: Struct. Rep. Online* 2005, ***E61***, o4042-4044.
[4] G. Blewett, C. Esterhuysen, M. W. Bredenkamp, K. R. Koch, *Acta Crystallogr., Sect. E: Struct. Rep. Online* 2006, ***E62***, m420-m422.
[5] G. Blewett, M. W. Bredenkamp, K. R. Koch, *Acta Crystallogr., Sect. C: Cryst. Struct. Commun.* 2005, ***C61***, o469-o472.
[6] C.-D. Wu, C.-Z. Lu, S.-F. Lu, H.-H. Zhuang, J.-S. Huang, *Inorg. Chem. Commun.* 2002, ***5***, 171-174.
[7] B.-W. Sun, S. Gao, Z.-M. Wang, *Chem Lett.* 2001, ***1***, 2-3.
[8] K. Biradha, K. V. Domasevitch, C. Hogg, B. Moulton, K. N. Power, M. J. Zaworotko, *Cryst. Eng.* 1999, ***2***, 37-45.
[9] S. A. Bourne, M. Kilkenny, L. R. Nassimbeni, *J. Chem. Soc., Dalton Trans.* 2001, ***8***, 1176-1179.
[10] M. J. Plater, M. R. S. J. Foreman, R. A. Howie, J. M. S. Skakle, *Inorg. Chim. Acta* 2001, ***318***, 175-180.
[11] Y. K. Lee, S. W. Lee, *Bull. Korean Chem. Soc.* 2003, ***24***, 906-910.